

DEVELOPMENT OF LIGHT-CONTROLLED DRUG RELEASE STRATEGIES
BASED ON PHOTOLABILE NAPHTHOL DERIVATIVES. SYNTHESIS AND
AZIDE CYCLOADDITION REACTIONS OF ACTIVATED ALLENES.

by

KUN WANG

(Under the Direction of Vladimir V. Popik)

ABSTRACT

o-Quinone methide (*o*-QM) and *o*-naphthoquinone methide (*o*-NQM) are highly reactive intermediate that are widely applied in chemical, biological and engineering fields. The extraordinary reactivity of *o*-NQM towards nucleophiles (as in thiol-Michael addition) and dienophiles (as in Diels-Alder reaction), and its efficient and controllable generation through UV irradiation render *o*-NQM versatile practices in drug delivery, surface derivatization, and photolabile protecting group (PPG) development.

The first part of the research focuses on developing various *o*-naphthoquinone methide precursors (NQMPs) for photo-controlled release of cargo in a site- and time-specific manner. Due to the ease of structure modification and photoreactive feature, the NQMPs were employed in drug delivery systems, by either being attached to other vehicles such as nanoparticles or as a prodrug itself to release H₂S gasotransmitter. Particularly, comparing to the existing photo-activating H₂S donors, the light-induced H₂S release from NQMP-thiol or NQMP-disulfide showed a remarkable high yield (95%)

with the presence of simple thiols. An NQMP-thioether was also designed to generate “smart” surfaces through reversible derivatization. Additionally, NQMP-acetal was investigated as a PPG that release two equivalents of cargo molecule with 100% chemical yield and a high quantum yield of 0.26 ± 0.01 .

Azide-alkyne cycloaddition reactions have long been of great interest owing to the reaction efficiency and product stability. However, the existing methods have limitations such as rough reaction condition, use of toxic catalyst, or strenuous reactant preparation. To overcome these limitations, activated allenes were used in the cycloaddition in the second part of the research. These allenes were readily involved in cycloaddition reactions with azides. Comparing to the previous azide-alkyne cycloaddition reactions, this method worked in a catalyst free and regiospecific fashion while also benefit from convenient starting material preparation. Meanwhile, the oxidation of homopropargyl alcohols using Dess-Martin periodinane to synthesize activated allenes under mild condition also generated aryl furans with prolonged reaction time. This procedure provided a novel way of producing allenes or furans in one step without the use of organometallic catalysts.

INDEX WORDS: Light controlled drug release, *o*-Naphthoquinone methide, Photo-active hydrogen sulfide donor, Reversible thiol-Michael addition, Photolabile protecting group, Activated allenes, Catalyst-free azide-alkyne cycloaddition, Catalyst- free furan formation

DEVELOPMENT OF LIGHT-CONTROLLED DRUG RELEASE STRATEGIES
BASED ON PHOTOLABILE NAPHTHOL DERIVATIVES. SYNTHESIS AND
AZIDE CYCLOADDITION REACTIONS OF ACTIVATED ALLENES.

by

KUN WANG

BS, Beijing Institute of Fashion Technology, China, 2011

MS, University of Georgia, 2014

A Dissertation Submitted to the Graduate Faculty of The University of Georgia in Partial
Fulfillment of the Requirements for the Degree

DOCTOR OF PHILOSOPHY

ATHENS, GEORGIA

2021

© 2021

KUN WANG

All Rights Reserved

DEVELOPMENT OF LIGHT-CONTROLLED DRUG RELEASE STRATEGIES
BASED ON PHOTOLABILE NAPHTHOL DERIVATIVES. SYNTHESIS AND
AZIDE CYCLOADDITION REACTIONS OF ACTIVATED ALLENES.

by

KUN WANG

| | |
|------------------|--------------------|
| Major Professor: | Vladimir V. Popik |
| Committee: | Robert S. Phillips |
| | Richard Morrison |

Electronic Version Approved:

Ron Walcott
Dean of the Graduate School
The University of Georgia
May 2021

DEDICATION

Thank you, my dear parents, for loving me unconditionally.

Thank you, my sincere friends, for encouraging me as always.

Thank you, Daniel, for being in my life.

ACKNOWLEDGEMENTS

First, I would like to express my sincere gratitude to my advisor Dr. Popik. He not only imparted me with knowledge to comprehend the beauty of the organic chemistry, but also guided me to be an independent researcher. Next, I would like to appreciate my committee members Dr. Phillips and Dr. Morrison. It was their generous help and suggestions that made my research progressed smoothly. Also, I would like to thank former group members Dr. Nannan Lin, Dr. Christopher Mcnitt, Dr. Dewey Sutton, and Dr. Mariia Sutton for helping me and giving me suggestions when I encountered with problems. I am also thankful to all my current group members Christopher Molnar, Shubham Sharma, Chen Zhao, Zichun Ren, Ayesha Nisathar, Shrey Patel, Patrick Foster, Dinesh Balasooriya and Rohan Bhavsar. It was enjoyable to work with you all and I also learned a lot from it. Last but not the least, I want to appreciate all my other friends for continually supporting and encouraging me through the course of my Ph.D. work.

TABLE OF CONTENTS

| | Page |
|---|------|
| ACKNOWLEDGEMENTS | v |
| LIST OF SCHEMES..... | x |
| LIST OF FIGURES | xiii |
| LIST OF TABLES | xv |
| CHAPTER | |
| 1 Introduction..... | 1 |
| 1.1 Quinone Methide (<i>o</i> -QM): Stability and Reactivity | 1 |
| 1.2 Naphthoquinone Methide (NQM) and Its Photo-Generation | 3 |
| 1.3 Typical Reactions of <i>o</i> -NQM..... | 4 |
| 1.4 Applications of <i>o</i> -NQM | 7 |
| 1.5 Gold Nanoparticle Drug Delivery..... | 9 |
| 1.6 Reversible Surface Derivatization | 12 |
| 1.7 H ₂ S Releasing Agents..... | 14 |
| 1.8 <i>o</i> -NQM as Photo-Labile Protecting Group..... | 17 |
| 1.9 Azide-Alkyne Cycloaddition | 20 |
| 1.10 Synthesis of Activated Allenes and Aryl Furans | 23 |
| 1.11 Conclusions and Goals of the Projects..... | 25 |
| 1.12 References..... | 26 |
| 2 SH-NQMP-N3 Synthesis for Gold Nanoparticle Drug Delivery | 36 |

| | | |
|-----|--|----|
| 2.1 | Introduction..... | 36 |
| 2.2 | Synthesis Route 1..... | 38 |
| 2.3 | Synthesis Route 2..... | 40 |
| 2.4 | Synthesis Route 3..... | 42 |
| 2.5 | Conclusion | 43 |
| 2.6 | Experimental Section | 44 |
| 2.7 | References..... | 56 |
| 3 | N3-NQMP-SSH Synthesis for Reversible Surface Derivatization..... | 57 |
| 3.1 | Introduction..... | 57 |
| 3.2 | Design and Synthesis of N3-NQMP-SSH | 60 |
| 3.3 | Conclusion | 61 |
| 3.4 | Experimental Section | 62 |
| 3.5 | References..... | 67 |
| 4 | NQMP-Thiol and NQMP-Disulfide for H ₂ S Photo-Release | 68 |
| 4.1 | Introduction..... | 68 |
| 4.2 | Design and Synthesis of NQMP-based H ₂ S Releasing Agents | 69 |
| 4.3 | Byproducts Analysis | 72 |
| 4.4 | H ₂ S Release Condition Optimization..... | 75 |
| 4.5 | H ₂ S Release Characterization | 80 |
| 4.6 | Proposed H ₂ S Releasing Mechanism..... | 86 |
| 4.7 | Synthesis of NQMP-Persulfide..... | 89 |
| 4.8 | Conclusion | 91 |
| 4.9 | Experimental Section | 91 |

| | | |
|------|--|-----|
| 4.10 | References..... | 106 |
| 5 | NQMP-acetal as an efficient Photo-labile Protecting Group..... | 108 |
| 5.1 | Introduction..... | 108 |
| 5.2 | Synthesis of NQMP-S-acetal (NSA) and NQMP-O-acetal (NOA)... | 109 |
| 5.3 | Photolysis Patterns of NSA and NOA | 110 |
| 5.4 | Chemical Yield of NOA Photolysis..... | 112 |
| 5.5 | Quantum Yield of NOA Photolysis | 115 |
| 5.6 | Synthesis and Photolysis of NQMP-O-acetal-triazole (NOAT)..... | 119 |
| 5.7 | Conclusion | 121 |
| 5.8 | Experimental Section | 121 |
| 5.9 | References..... | 126 |
| 6 | Synthesis and Azide Cycloaddition Reactions of Activated Allenes | 127 |
| 6.1 | Introduction..... | 127 |
| 6.2 | The Synthesis Pathway | 128 |
| 6.3 | Synthesis of Activated Allenes and Aryl Furans | 130 |
| 6.4 | Triazole Formation from Activated Allenes | 132 |
| 6.5 | Conclusion | 136 |
| 6.6 | Experimental Section | 136 |
| 6.7 | References..... | 145 |

APPENDICES

| | | |
|---|---|-----|
| 1 | Ellman Reagent Test for Thiol Group of DSF..... | 147 |
| 2 | IR of DSF and RNS | 149 |
| 3 | Methylene Blue test procedure | 149 |

| | | |
|----|--|-----|
| 4 | RNS photoreaction with 2-mercaptoethanol..... | 151 |
| 5 | Photolysis of RNS (HPLC eluent 45A10M45W)..... | 152 |
| 6 | Photolysis of DSF (HPLC eluent 45A10M45W) | 153 |
| 7 | Reaction of DSF and 2-mercaptoethanol..... | 154 |
| 8 | Photolysis of (a) DSF and (b) RNS with glutathione | 155 |
| 9 | Conversion of activated allene to triazole..... | 156 |
| 10 | ¹ H and ¹³ C NMR Spectra | 157 |

LIST OF SCHEMES

| | Page |
|---|------|
| Scheme 1.1: Structures of quinone methides | 1 |
| Scheme 1.2: Generation of <i>o</i> -QM | 2 |
| Scheme 1.3: Reactions of <i>o</i> -QM | 2 |
| Scheme 1.4: Functional derivatives of NQMP | 3 |
| Scheme 1.5: Two isomeric <i>o</i> -NQM | 3 |
| Scheme 1.6: Classification of Diels–Alder reactions | 4 |
| Scheme 1.7: Diels-Alder reaction of <i>o</i> -NQM | 5 |
| Scheme 1.8: Michael addition reaction of <i>o</i> -NQM | 6 |
| Scheme 1.9: Reactivity of <i>o</i> -NQM | 6 |
| Scheme 1.10: H ₂ S photo-release from <i>o</i> -nitrobenzyl masked <i>gem</i> -dithiol | 15 |
| Scheme 1.11: H ₂ S photo-release from ketoprofenate cage | 16 |
| Scheme 1.12: H ₂ S photo-release from phenacyl cage | 16 |
| Scheme 1.13: H ₂ S photo-release from <i>o</i> -nitrobenzyl masked thiocarbamate | 16 |
| Scheme 1.14: H ₂ S photo-release from dipyrromethene-masked carbamothioate | 17 |
| Scheme 1.15: Photo-release efficiencies of <i>o</i> -NQMP caged compounds | 18 |
| Scheme 1.16: Azide–alkyne cycloaddition reactions | 20 |
| Scheme 1.17: Azide–alkyne cycloaddition accelerated by activated olefins/alkynes | 22 |
| Scheme 1.18: Site specificity of azide cycloaddition to activated alkyne/allene | 23 |
| Scheme 1.19: Isomerization of activated alkyne to allene | 23 |

| | |
|---|----|
| Scheme 1.20: Catalytic transformation of activated alkyne/allene to furan | 24 |
| Scheme 2.1: Structure of SH-NQMP-N3..... | 37 |
| Scheme 2.2: SH-NQMP-N3 for gold-nanoparticle drug delivery | 37 |
| Scheme 2.3: Synthesis route 1 for SH-NQMP-N3 | 39 |
| Scheme 2.4: Synthesis route 2 for SH-NQMP-N3 | 41 |
| Scheme 2.5: Synthesis route 3 for SH-NQMP-N3 | 43 |
| Scheme 3.1: Structures of (a) N3-NQMP-OH and (b) N3-NQMP-SSH | 57 |
| Scheme 3.2: N3-NQMP-SSH for reversible surface derivatization | 59 |
| Scheme 3.3: Synthesis of target compounds..... | 60 |
| Scheme 4.1: H ₂ S photo-release from RNS and DSF | 69 |
| Scheme 4.2: Synthesis of NQMP-based H ₂ S release agents—method 1 | 70 |
| Scheme 4.3: Synthesis of NQMP-based H ₂ S release agents—method 2 | 71 |
| Scheme 4.4: Photo-generation of the aldehyde (4.9)..... | 73 |
| Scheme 4.5: Synthesis of the thioether (4.13) | 74 |
| Scheme 4.6: Synthesis of the disulfide (4.4)..... | 74 |
| Scheme 4.7: Methylene Blue test reaction..... | 75 |
| Scheme 4.8: RNS and DSF Diels-Alder reaction with EVE | 76 |
| Scheme 4.9: Photoreaction of RNS and 2ME..... | 86 |
| Scheme 4.10: DSF and 2ME reaction..... | 87 |
| Scheme 4.11: Proposed DSF photolysis mechanism (a) without thiol (b) with thiol..... | 88 |
| Scheme 4.12: Proposed RNS photolysis mechanism (a) without thiol (b) with thiol | 88 |
| Scheme 4.13: Persulfide (a) reactivities and (b) synthesis ideas | 89 |
| Scheme 4.14: Persulfide synthesis – route 1..... | 90 |

| | |
|--|-----|
| Scheme 4.15: Persulfide synthesis – route 2..... | 90 |
| Scheme 5.1: Synthesis of (a) NQMP-S-acetal and (b) NQMP-O-acetal | 109 |
| Scheme 5.2: (a) Photolysis of NQMP-S-acetal (b) Synthesis of NQMP-S-ether..... | 111 |
| Scheme 5.3: 3,4-Dimethoxynitrobenzene photoreaction as actinometer..... | 115 |
| Scheme 5.4: Synthesis of 5.5 | 119 |
| Scheme 5.5: Synthesis of 5.7 | 119 |
| Scheme 6.1: The 3-step synthesis pathway..... | 128 |
| Scheme 6.2: Dess-Martin oxidation of homopropargyl alcohol..... | 130 |
| Scheme 6.3: Azide resonance structures and reactivity | 133 |
| Scheme 6.4: Proposed mechanism of regio-selective triazole formation | 133 |

LIST OF FIGURES

| | Page |
|--|------|
| Figure 1.1: Surface modification by DA reaction of fixed <i>o</i> -NQM | 7 |
| Figure 1.2: Surface modification by DA reaction of non-fixed <i>o</i> -NQM | 8 |
| Figure 1.3: Surface modification by <i>o</i> -NQM Michael addition | 9 |
| Figure 1.4: Protein labeling by <i>o</i> -NQM Michael addition..... | 9 |
| Figure 1.5: Reversible surface derivatization by azobenzene photochemistry..... | 13 |
| Figure 1.6: Reversible surface derivatization by disulfide photochemistry | 13 |
| Figure 1.7: Photo-release of alcohols/carboxylic acids from <i>o</i> -NQMP cage | 19 |
| Figure 1.8: <i>o</i> -NQMP as a photocage for fluorescein | 19 |
| Figure 4.1: Photolysis of DSF and RNS | 72 |
| Figure 4.2: HPLC of DSF photolysis mixture | 73 |
| Figure 4.3: DSF transformation to diol (4.1) via irradiation..... | 76 |
| Figure 4.4: HPLC analysis of DA reaction products | 76 |
| Figure 4.5: Condition test for H ₂ S photo-release from DSF..... | 78 |
| Figure 4.6: Condition test for H ₂ S photo-release from RNS | 78 |
| Figure 4.7: DSF photolysis without or with 2ME and their H ₂ S release profile | 79 |
| Figure 4.8: (a) Na ₂ S·9H ₂ O absorbance curve and (b) H ₂ S release standard curve..... | 80 |
| Figure 4.9: UV Absorbance at 663 nm from 500 μM of SH from DSF | 81 |
| Figure 4.10: UV absorbance (300 nm 0-20 min) of 250 μM DSF: (a) in AW and (b) in AP. UV absorbance at 663 nm of 250 μM DSF: (c) in AW and (d) in AP | 82 |

| | |
|--|-----|
| Figure 4.11: UV Absorbance at 663 nm from 500 μ M of RNS..... | 83 |
| Figure 4.12: UV absorbance (300 nm 0-20 min) of 500 μ M RNS: (a) in AW and (b) in AP. UV absorbance at 663 nm of 500 μ M RNS: (c) in AW and (d) in AP..... | 84 |
| Figure 4.13: Incubation of irradiation 5 min samples of (a) DSF+Cys (b) RNS+Glu | 85 |
| Figure 4.14: Control experiments (a) DSF incubate with thiols (b) 300 nm Irradiation on 10 mM 2ME, Cys and Glu (c) 300 nm Irradiation on 10 mM 2ME, Cys and Glu | 85 |
| Figure 4.15: (a) Mixture of RNS and 4.17 separated by 45A10M45W (b) UV of RNS (R.T.= 7.300 min) (c) UV of 4.17 (R.T.=7.013 min) | 86 |
| Figure 5.1: Photolysis of NQMP-S-acetal | 110 |
| Figure 5.2: Photolysis of NQMP-O-acetal..... | 111 |
| Figure 5.3: UV spectra of NOA and ALD in (a) 4:1 M/W (b) 1:1 A/W | 112 |
| Figure 5.4: ALD (in 4:1 M/W) calibration curve at 383 nm | 113 |
| Figure 5.5: ALD concentration calibration at 383nm..... | 114 |
| Figure 5.6: 6 dMNB (136 μ M in 0.5 M KOH) under irradiation (300 nm 0 and 1min) . | 116 |
| Figure 5.7: UV spectra of NOA (203 μ M) under irradiation (300 nm 0 and 1 min)..... | 116 |
| Figure 5.8: ALD calibration curve at (a) 250 nm (b) 301 nm..... | 117 |
| Figure 5.9: Photolysis of 5.7 | 120 |
| Figure 6.1: Components of reaction mixtures..... | 131 |
| Figure 6.2: NOESY spectrum of 6.10 | 134 |
| Figure 6.3: Transformation of allene to triazole | 135 |

LIST OF TABLES

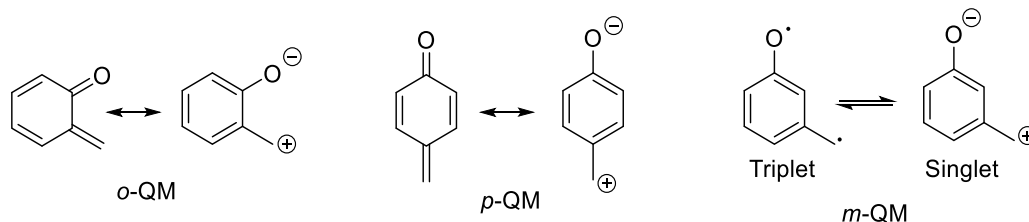
| | Page |
|---|------|
| Table 4.1: Effect of N ₂ bubbling to DSF photolysis..... | 77 |
| Table 4.2: H ₂ S Conversion from photolysis of DSF | 81 |
| Table 4.3: H ₂ S Conversion from Photolysis of RNS | 83 |
| Table 4.4: Irradiation and incubation time relationship of H ₂ S from DSF photolysis | 84 |
| Table 5.1: Conversion of NOA (29 μM in 4:1M/W) to ALD | 113 |
| Table 5.2: Conversion of NOA (29 μM in 1:1A/W) to ALD..... | 114 |
| Table 5.3: Quantum yield calculation of NOA based on HPLC analysis..... | 118 |
| Table 5.4: Quantum yield calibration of NOA | 118 |
| Table 6.1: The 3-step synthesis pathway | 129 |
| Table 6.2: GC-MS quantification of the reaction mixture in progress | 131 |
| Table 6.3: Isolated yield of furan formation | 132 |

CHAPTER 1

INTRODUCTION

1.1 Quinone Methide (*o*-QM): Stability and Reactivity

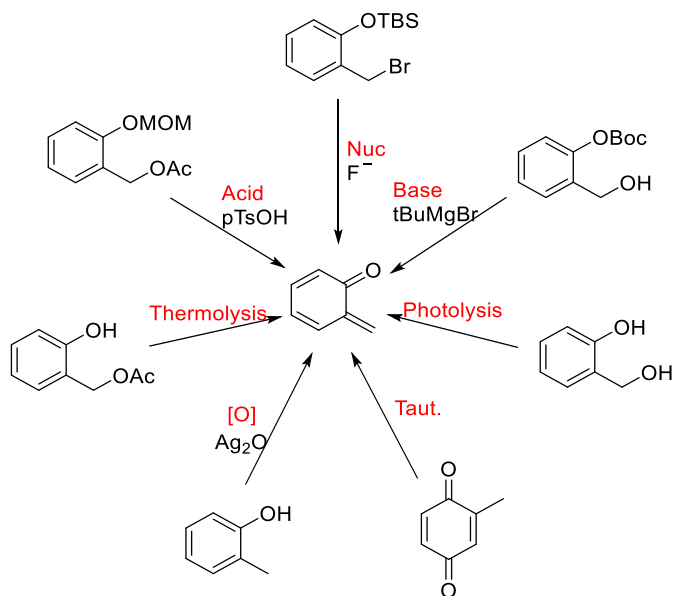
Quinone methides (QMs) are highly reactive intermediate commonly encountered in many areas of chemistry and biology^{1,2} and are widely applied in fields such as organic synthesis³, prodrug development⁴ and DNA alkylation⁵. Quinone methides consist of a cyclohexadiene core with an exocyclic carbonyl and a methylene group.⁶ Among the QM isomers, *ortho*- and *para*-QMs, as neutral molecules, are more common than the *meta*-QM which is a non Kekule structure. The zwitterionic resonance structures of the *o*- and *p*-QM reveal their polarized nature, while the neutral valence bond structure for *m*-QM is a triplet biradical (Scheme 1.1).⁷



Scheme 1.1 Structures of quinone methides

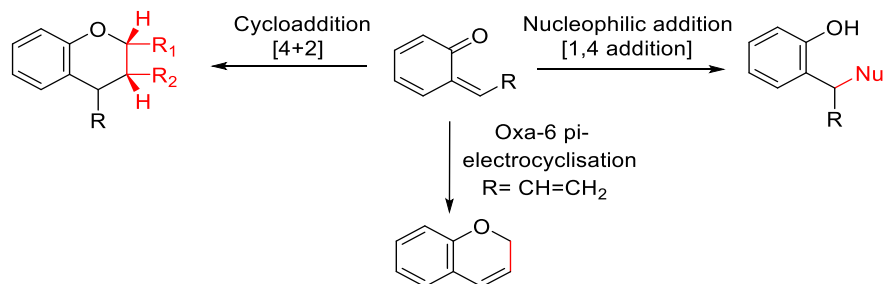
The generation of *o*-QM can be achieved through a diverse range of methods. The most common approach is the elimination of the benzylic substituent from a stable molecule, to generate the methylene and α -carbonyl functionalities with concomitant de-aromatization. This process can be induced thermally, or by addition of a nucleophile, acid, or base to facilitate the removal of the phenol-protecting group. Other *o*-QM generation routes include photolytic initiation, tautomerization, and benzylic oxidation.

Among various methods to generate *o*-QM, the photolytic approach is proved to be more efficient and controllable, though occasionally presents limitations like precursor preparation and functional group tolerance⁸ (Scheme 1.2).



Scheme 1.2 Generation of *o*-Quinone Methide

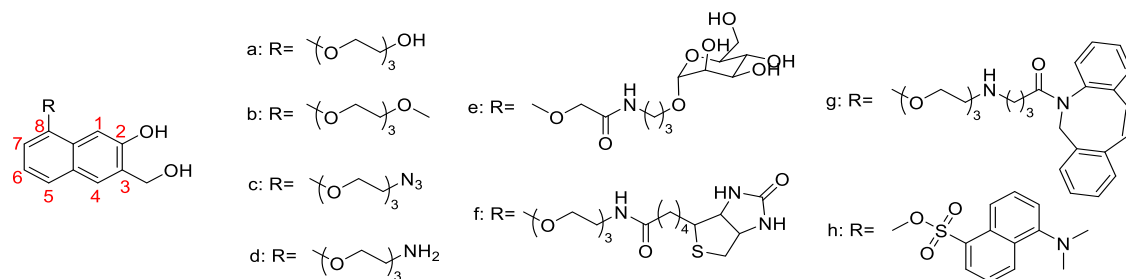
The transient nature of *o*-QMs is due to their propensity to undergo rapid reactions, such as re-aromatization either by Michael addition with nucleophiles, cycloaddition with 2p partners or, via oxa-6p-electrocyclisation to give benzopyrans (Scheme 1.3).⁹



Scheme 1.3 Reactions of *o*-QM

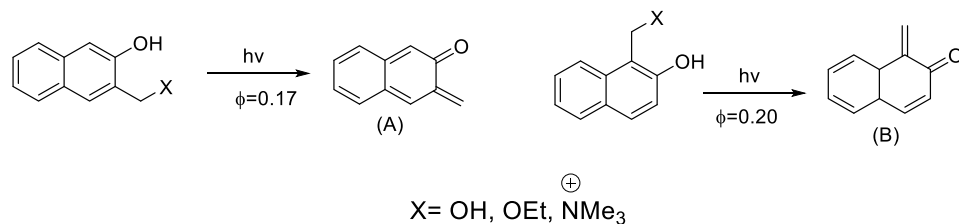
1.2 Naphthoquinone Methide (NQM) and Its Photo-Generation

Compared to the benzene-based *o*-quinone methide precursors which has little absorbance above 250 nm, *o*-naphthyl quinone methide precursors (*o*-NQMPs) absorb substantially beyond 350 nm. This red shift of absorption makes NQMPs more suitable for practical applications such as drug delivery system, surface modification and prodrug design. Additionally, the Popik group has demonstrated that various functional fragments can be introduced either directly (e, h, Scheme 1.4) or via the triethyleneglycol (TEG)-linker to the 8-position on the naphthyl ring for further molecular modification without impacting the NQMPs' photochemistry and the *o*-NQM formation (a-d,f, g, Scheme 1.4).¹⁰



Scheme 1.4 Functional derivatives of NQMP

Two isomeric *o*-NQM, 2,3-naphthoquinone-3-methide (A) and 1,2-naphthoquinone-1-methide (B), can be generated by photo-irradiation of the corresponding hydroxymethyl-, ethoxymethyl- or trimethylammonium salt precursors (Scheme 1.5).¹¹

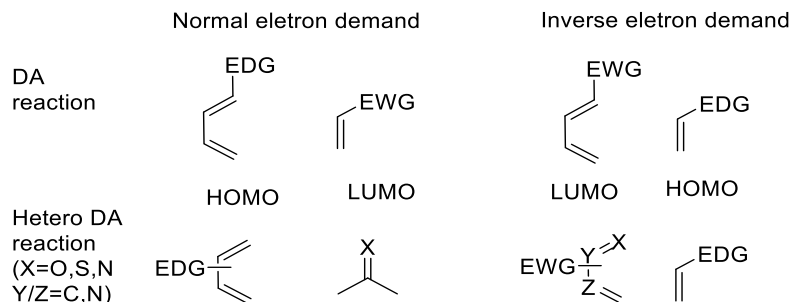


Scheme 1.5 Two isomeric *o*-NQM

The mechanism of photochemical dehydration of 3-hydroxymethyl- and 1-hydroxymethyl-2-naphthols is not yet fully understood. It is hypothesized that an excited state intramolecular proton transfer (ESIPT) occurs due to the greater acidity of the 2-naphthol at excited state ($pK_a \sim 2.8$) than in the ground state ($pK_a \sim 9.5$).^{12,13,11} This process leads to the proton transfer of a phenolic proton to an oxygen atom in the benzylic position, the concerted C-O bond heterolysis and loss of water. The loss of water from the excited state of *o*-hydroxybenzyl alcohols is very fast and the formation of *o*-QMs can usually be completed within a nanosecond laser pulse. Alternatively, there is also evidence that loss of water occurs in the ground state after proton transfer is completed.¹⁴

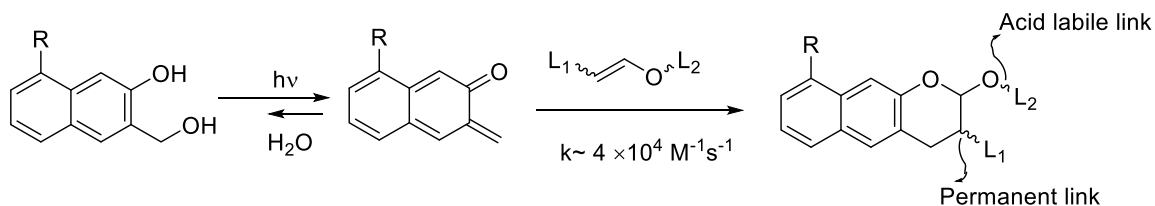
1.3 Typical Reactions of *o*-NQM

The *o*-NQMs can undergo an inverse electron demand Diels–Alder reaction (IEDDA) with electron-rich alkenes such as vinyl ethers. The IEDDA reaction involves electron-deficient diene and an electron-rich dienophile while the normal Diels–Alder reaction employs electron-deficient dienophile and an electron-rich diene. This reaction can also be classified as a hetero Diels–Alder reaction due to the oxygen atom in *o*-NQM (Scheme 1.6).¹⁵



Scheme 1.6 Classification of Diels–Alder reactions

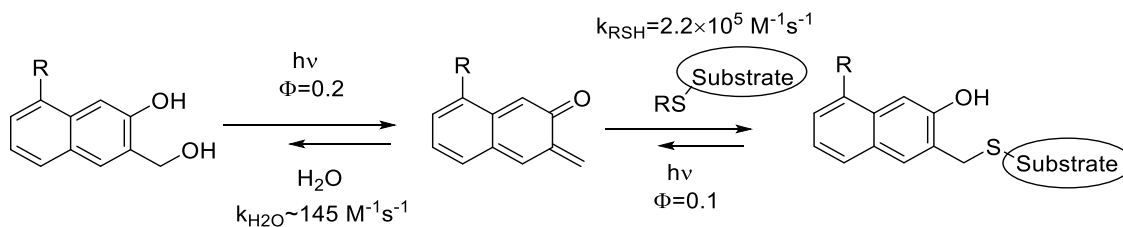
o-NQM can be efficiently generated from UV irradiation, the *o*-NQM can also hydrate back to the starting material. Because of the short lifetime of *o*-NQM in aqueous solution ($\tau \sim 7$ ms in H₂O), only a few reactions can outcompete *o*-NQM hydration, and the *o*-NQM's Diels-Alder cycloaddition with vinyl ethers and enamines is one example. The Diels-Alder adduct is photostable, but only to note that the L₂ substituent is connected to the adduct through an acid-labile link which undergoes slow hydrolysis at pH < 3 while the L₁ substituent is attached by a hydrolytically stable link. The fast rate of the *o*-NQM addition to vinyl ethers and short lifetimes of *o*-NQMs enable spatial and temporal precision of the reaction. The reaction's selectivity to electron-rich alkenes in aqueous solution and its orthogonality to alkyne-azide click chemistry make it a practical tool for ligation and labeling (Scheme 1.7).¹⁶



Scheme 1.7 Diels-Alder reaction of *o*-NQM

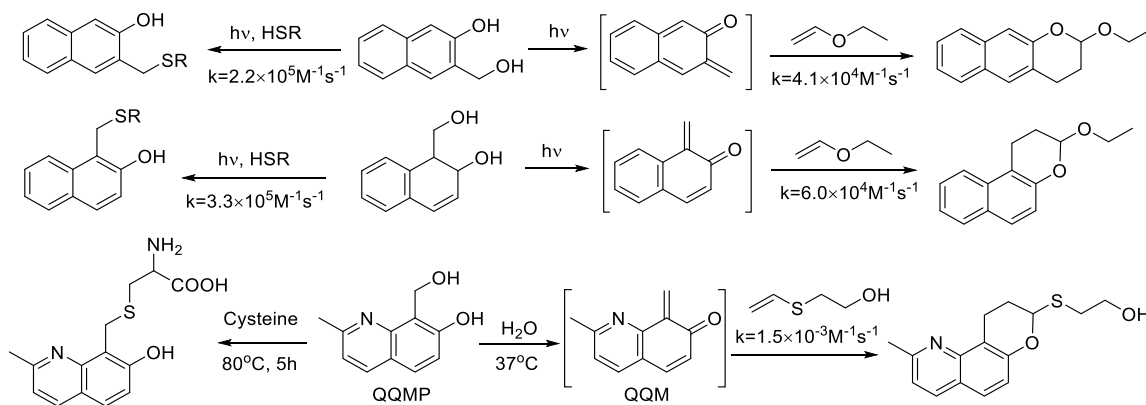
The *o*-NQMs also readily undergo reversible Michael addition. In neutral aqueous solutions, *o*-NQM's addition with thiol is another reaction that can outcompete its hydration. The thioether products are also photoreactive and can produce *o*-NQMs under 300 or 350 nm irradiation. Since the rate of *o*-NQM addition with thiol ($2.2 \times 10^5 \text{ M}^{-1} \text{ s}^{-1}$) is about three orders of magnitude higher than that of the hydration ($145 \text{ M}^{-1} \text{ s}^{-1}$), and the quantum yield for *o*-NQM generation from the NQMP-OH ($\Phi=0.2$) is two-times greater than that from NQMP-SR ($\Phi=0.1$), the equilibrium is shifted in the favor of thioether (NQMP-SR) formation (Scheme 1.8). Therefore, QM-thiol click chemistry provides great

opportunity to reversible photo-derivatization of a thiolate surface as well as selective and reversible labeling of solvent-accessible cysteine residues in peptides and proteins.¹⁰



Scheme 1.8 Michael addition reaction of *o*-NQM

The second order rate constants of photogenerated *o*-NQM reacting with various trapping agents are shown in Scheme 1.9.¹¹ Both the NQM-thiol Michael addition and the Diels-Alder reaction with ethyl vinyl ether are very fast. In comparison, the *o*-quinolinone quinone methide (*o*-QQM) generated from their precursors in aqueous solution is spontaneous and much slower to participate in similar reactions (Scheme 1.9).^{11,17} Therefore, the photogeneration of *o*-QM is a fast and efficient way to perform thiol-Michael addition and Diels-Alder reaction.



Scheme 1.9 Reactivity of *o*-NQM

1.4 Applications of *o*-NQM

In 2011, the Popik group generated 3-(hydroxymethyl)naphthalene-2-ol derivatized photoreactive polymer brushes on silicon oxide surfaces for surface functionalization. With 300 or 350 nm irradiation, NQMP efficiently produces *o*-NQM, which undergoes rapid Diels–Alder addition with vinyl ether groups attached to a substrate. Through this DA reaction ligation, the substrate was immobilized to the surface. The sequential alkyne-azide click chemistry, such as CuAAC and SPAAC reactions, enabled further derivatization of the surface with more complex functionalities (Figure 1.1).¹⁸

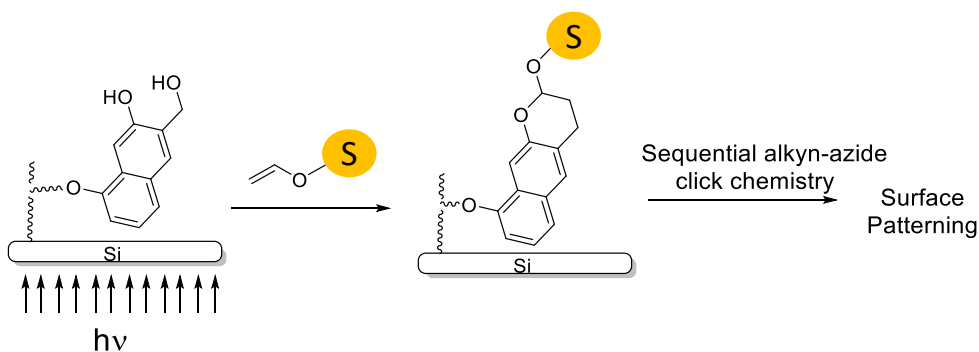


Figure 1.1 Surface modification by DA reaction of fixed *o*-NQM

Alternatively, glass surface derivatized with vinyl ether groups could be functionalized with photo-generated *o*-NQM as a substrate, where the surface itself is photochemically inert, while photoreactive component presents in the solution. The subsequent surface patterning was showcased by a biotin-streptavidin conjugation. In addition, depend on the different attaching point of the vinyl ether (the ether linkage or the β -carbon) to the surface, the photo-click immobilization technique can be tailored to produce either a hydrolytically labile linkage or a permanent one (Figure 1.2).¹⁹

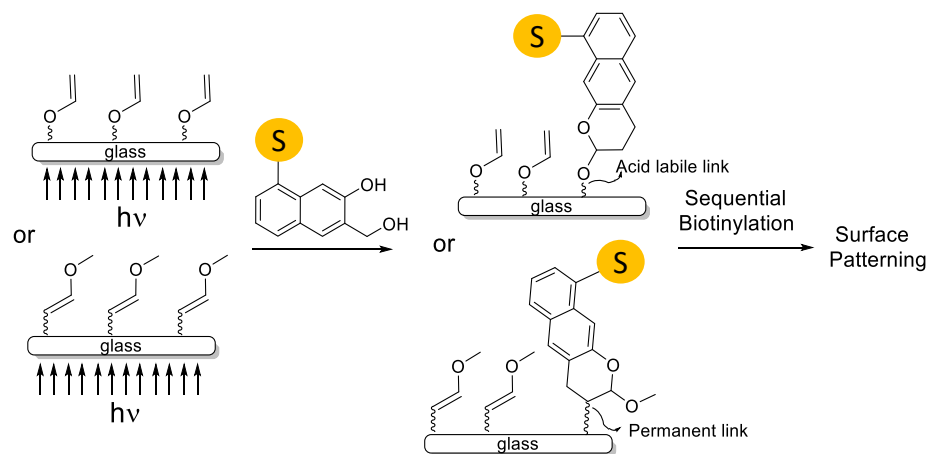


Figure 1.2 Surface modification by DA reaction of non-fixed *o*-NQM

In 2012, a reversible surface derivatization system using thiol-QM photo-click chemistry was reported by the Popik group. With the efficient reaction of photochemically generated *o*-NQMs with thiol, desired immobilization, and removal of substrates to the glass surface was achieved. Since the *o*-NQM addition with thiol is much favored than with water, the photo-generated *o*-NQM-S1 quickly reacted with thiol on the surface and the system reached the equilibrium point where *o*-NQMP-S1 was immobilized and its concentration in the solution would not further change via subsequent irradiation. Since the *o*-NQMP-S2 is two times greater than *o*-NQMP-S1 to photoelimination to form NQM, once the solution environment changes by decreasing the *o*-NQMP-S1 concentration or adding a different substituted *o*-NQMP-S2, sequential photo irradiation in the exposed area without a mask would either remove pre-immobilized *o*-NQMP-S1 or replace it with newly added *o*-NQMP-S2, until the new equilibrium is generated (Figure 1.3).²⁰

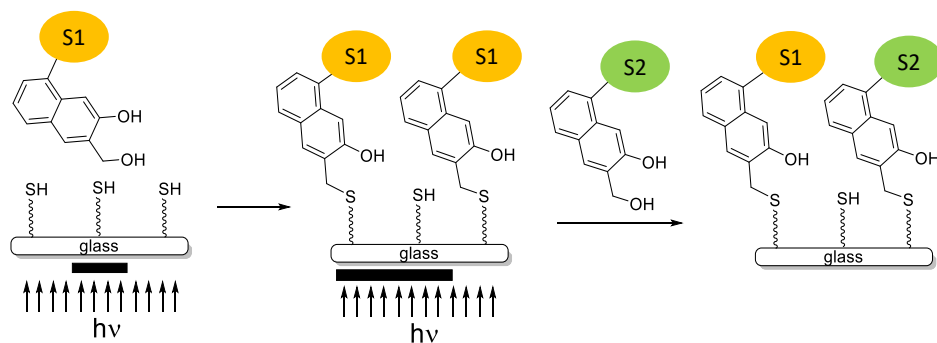


Figure 1.3 Surface modification by *o*-NQM Michael addition

In 2014, selective labeling of the solvent-exposed cysteine residues in peptides and protein (BSA) was achieved by brief irradiation of NQMP aqueous solution with 350 nm UV light. The NQMP-thioether linkage is stable under ambient conditions and protein digestion. Irradiation of an NQMP-labeled protein in aqueous solution resulted in reversible substrate release while irradiation in the presence of a vinyl ether leads to an irreversible release of substrate. The reversible modification of the cysteine residues in proteins can be employed for site-specific labeling of proteins or photo-regulation of protein activity (Figure 1.4).²¹

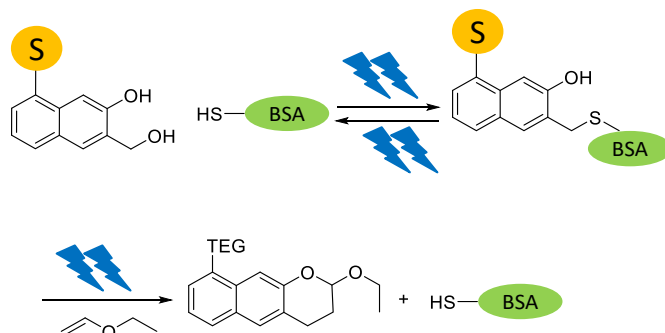


Figure 1.4 Protein labeling by *o*-NQM Michael addition

1.5 Gold Nanoparticle Drug Delivery

Drug delivery systems are designed to enhance the efficiency of conventional pharmaceuticals and medical applications. There are two major types of drug delivery

systems– the first type contains self-assembled structures including micelles and liposomes, and the second type involves the covalent attachment of drug to the carrier to generate the prodrug conjugates.²² A key attribute of drug delivery systems is their ability for the regulation of drug release. In other words, the drug delivery system should target specific tissues/cell types, remain stable in circulatory systems but labile under certain conditions to release the payload. The controlled drug release can be realized in two aspects -- spatial and temporal control.²³

For better efficiency and less chances of side-effects, wide varieties of materials have been applied to drug delivery system such as polymers and nanomaterials (*e.g.* nanotubes, nanorods, nano-shells and nanoparticles, *etc.*). Among all the nanomaterials employed, nanoparticles (NPs) are particularly useful due to their small size and large surface area, thus increased solubility, and enhanced bioavailability. Particularly, monolayer protected gold nanoparticles provide many desirable attributes for drug delivery.²⁴ First, the gold core is essentially inert and nontoxic, and can be readily fabricated with tunable core size from 1.5 to 8 nm, providing large surface area for efficient payload attachment.²⁵ Second, the payload attachment can be accomplished by either noncovalent interaction with DNA or enzymes via electrostatic interaction, or covalent conjugation with small-molecule drugs. In addition, properties of NPs can be tuned by a wide range of ligand functionality to ensure cellular uptake, specific cell targeting and controlled payload release.²⁶

The gold nanoparticles (AuNPs) have been widely applied in spatial and temporal controlled drug delivery. The spatial control of the drug release can be achieved by “passive” or “active” targeting. “Passive” targeting takes advantage of tumors cells’

enhanced permeation and retention (EPR) effect.²⁷ On the contrary, “active” targeting presents ligands on the carrier surface for specific recognition by cell surface receptors²⁸ and the transmembrane receptor-mediated endocytosis pathway, thus realize the site-specific drug delivery. The “active” targeting can be accomplished by conjugating a drug-delivery vehicle with a ligand that specifically recognizes the receptor. For example, transferrin (TF), a protein, can be employed as a ligand since many tumor cells overexpress TF receptors on their surface. The He group reported the enhanced uptake of TF-conjugated AuNPs by tumor cells.²⁹ Conjugation of folic acid would provide another strategy for targeted drug delivery since folic acid receptors are upregulated in various tumor cells. The Andres group demonstrated the specific uptake of folate-conjugated AuNPs by folate receptor-positive tumor cells.³⁰

The temporal control of the drug release can be achieved by endogenous or exogenous stimulations. Endogenous stimulation includes specific physiochemical characteristics (pH, enzyme concentration or redox gradients), providing biologically controlled release. Exogenous stimulation employs orthogonal external stimuli such as magnetic field, ultrasound intensity, electric pulses, and light.³¹ Particularly, photochemistry provides a useful orthogonal release mechanism by offering external control over payload release in a unique site- and time-specific fashion.

1.6 Reversible Surface Derivatization

Surface derivatization plays an important role in the development of novel bioanalytical, diagnostic, and sensor applications. Surface derivatization can be realized by self-assembled monolayers (SAMs) which are organic assemblies formed when molecules in solution or gaseous phase adsorb and spontaneously organize into a single layer on a surface. The surface substrate usually possesses specific affinities for the molecules constituting SAMs, such as gold bind to thiols. The gold-thiol binding has high affinity and stability; and rarely involve other side reactions.³²

Among different methods of surface derivatization, light-promoted surface derivatizations provide precise spatial control of the process. Various biomolecules have been immobilized and patterned using different photochemical methods, such as thiol-ene, azide-yne, terazole-ene, photo-triggered Diels–Alder reaction, etc. However, most of the existing photochemical methods lead to irreversible permanent surface functionalization, resulting in limited possible applications for surfaces with responsive properties or reusable functionalities.³³ Therefore, the development of photo-controlled switchable surfaces has recently drawn increasing attention. Examples of possible applications of such dynamic surfaces include rewritable surfaces, formation of complex, multi-component and gradient patterns, and surfaces with capture-and-release properties.

For example, by exploiting the trans-cis photo-isomerization of the azobenzene, a gold surface was reversibly derivatized. This system achieved lectin and carbohydrate epitope recognition by only altering orientation of the ligand (Figure 1.5).³⁴

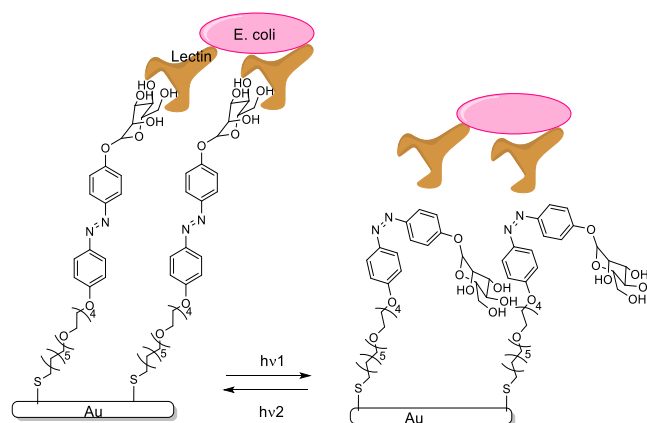


Figure 1.5 Reversible surface derivatization by azobenzene photochemistry

In 2015, Levkin et al. presented a reversible polymethacrylate surface functionalization and patterning strategy based on the photodynamic disulfide exchange reaction. This method allows exchange or removal of surface functional groups and can be used to create, erase, or modify existing surface patterns.³⁵ Disulfide bonds are known to undergo reversible cleavage under basic conditions via thiol-disulfide exchange reactions through intermediate thiolate anions.³⁶ However, disulfides can also undergo dynamic exchange reactions by homolytic photocleavage to form sulfenyl radicals. the dynamic nature of disulfide homolysis and recombination under UV irradiation could be utilized to achieve reversible dynamic functionalization of disulfide surfaces (Figure 1.6).

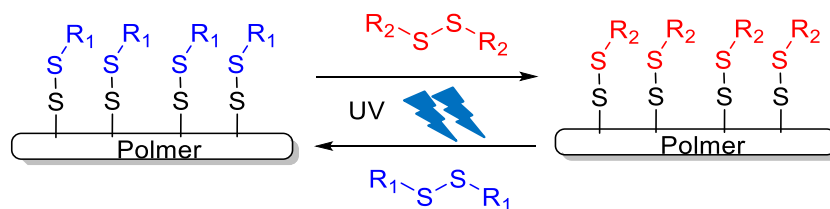


Figure 1.6 Reversible surface derivatization by disulfide photochemistry

1.7 H₂S Releasing Agents

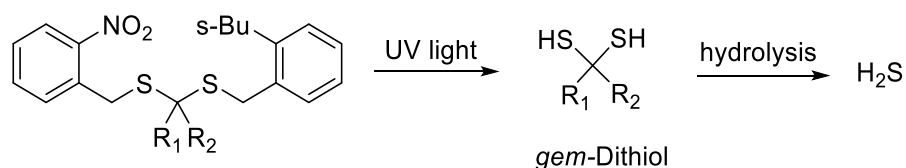
Hydrogen sulfide (H₂S) is one of the most important gasotransmitters, a family of small gaseous signaling molecules. According to recent publications, hydrogen sulfide possesses anti-inflammatory,³⁷ anti-tumor,³⁸ cardiovascular protective,³⁹ and antioxidant⁴⁰ activities. Although the mechanism is not fully understood, it is believed that abovementioned functions are due to the role of H₂S as an antioxidant, that reacts readily towards reactive oxygen and nitrogen species including hydrogen peroxide, superoxide and peroxynitrite. H₂S can also modify cysteine residues on protein to generate sulfhydrated proteins (protein-S-SH), which are believed to be a critical pathway in regulating protein functions.⁴¹

H₂S is a weak acid with pK_a values (37 °C) for the first and second dissociation steps being around 6.88 and 19, respectively. Thus, under physiological conditions (pH 7.4), H₂S largely exists in two forms: the neutral molecular form (H₂S) and the mono-ionized form (HS⁻). The H₂S generation from inorganic donors (such as NaHS and Na₂S) usually occurs spontaneously. When dissolved, these salts establish an equilibrium among S²⁻, HS⁻, and H₂S, and the ratio of them depends on temperature, pressure, and pH. Under physiological conditions, HS⁻/H₂S ratio is about 3:1.

In comparison, the organic donors release H₂S more slowly, even though such release rate may differ substantially depending on whether the process occurs with or without presence of biological material.⁴² The most widely used naturally occurring H₂S donors are the garlic constituents diallyltrisulphide (DATS) and diallyldisulphide (DADS), and their H₂S production has been characterized both *in vitro* and *in vivo*.⁴³ Among synthetic H₂S donors, two hydrolysis triggered donors such as Lawesson's

reagent and 1,2-Dithiole-3-thiones (DTTs) are extensively applied to anti-inflammation and antitumor treatments.^{44,45} Additionally, synthetic organic donors that can generate H₂S upon orthogonal external stimulus obtained great interest because of their steady and localized concentrations of H₂S release at desired timing and cellular locations. Ideally, H₂S donors should be water soluble, stable under storage conditions, and generate only innocuous byproducts, if any. They should also have a specific and well-defined release mechanism (release only in response to a specific trigger) and a tunable and controllable release rate.⁴⁶

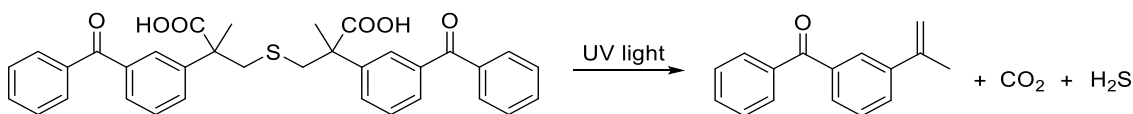
The first example of photocaged H₂S donor was based on geminal-dithiol (*gem*-dithiol) structure. In 2013, Xian's group adopted a photo-cleavable 2-nitrobenzyl group protection for the reactive *gem*-dithiol group, which readily generate H₂S in aqueous solution. Upon exposing the H₂S donor molecule to UV irradiation (365 nm), *gem*-dithiols were produced, and subsequently hydrolyzed, leading to H₂S release. Methylene Blue assay indicated that 200 μmol/L prodrugs could generate a peak concentration of 36 μmol/L (Scheme 1.10).⁴⁷



Scheme 1.10 H₂S photo-release from *o*-nitrobenzyl masked *gem*-dithiol

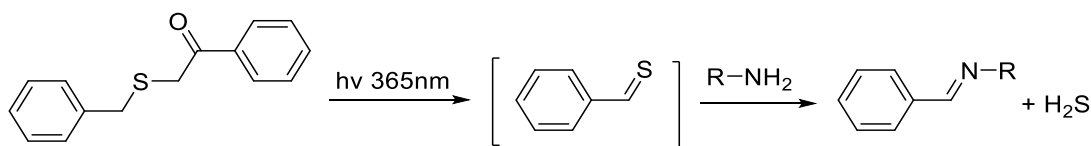
However, disadvantages of these prodrugs were also observed. Since the H₂S release rate is depending on the hydrolysis of *gem*-dithiol, it is difficult to control. Also, the reactive byproducts 2-nitrosobenzaldehyde can react with H₂S, resulting in diminishing H₂S generation. In 2014, Nakagawa's group investigated the ketoprofenate-caged photo-induced H₂S prodrugs. After 10 min of UV irradiation (300–350 nm), 500

$\mu\text{mol/L}$ of the prodrug generated $30 \mu\text{mol/L}$ of H_2S in fetal bovine serum together with 2-propenylbenzophenone and CO_2 (Scheme 1.11).⁴⁸



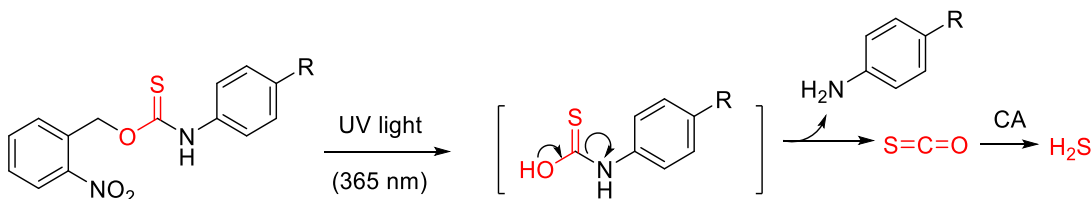
Scheme 1.11 H_2S photo-release from ketoprofenate cage

Additionally, Connal's group developed a H_2S donor with a UV-responsive phenacyl cage and produces thioaldehyde species and acetophenone upon irradiation. The thioaldehyde generated H_2S and an imine byproduct, in the presence of an amine. The authors further incorporated this donor into polymeric systems for hydrogel preparation (Scheme 1.12).⁴⁹



Scheme 1.12 H_2S photo-release from phenacyl cage

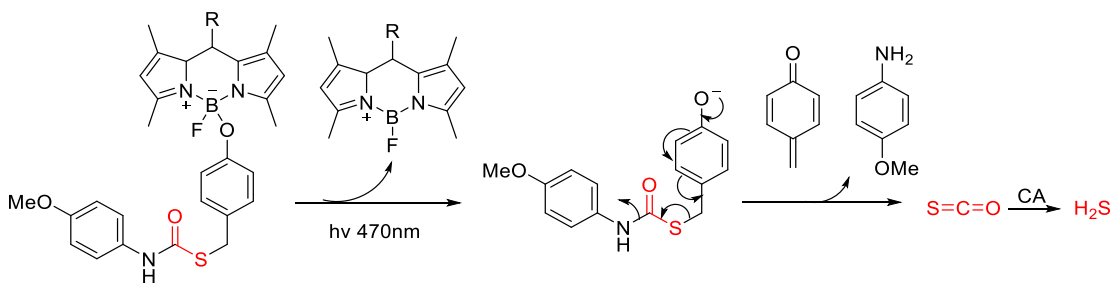
The Pluth group developed a system using an *o*-nitrobenzyl functionality that underwent UV-triggered cleavage to unmask caged thiocarbamates and selectively release carbonyl sulfide (COS) which was then converted to H_2S by carbonic anhydrase (CA). Tunable releases were also achieved by the different derivatives (Scheme 1.13).⁵⁰



Scheme 1.13 H_2S photo-release from *o*-nitrobenzyl masked thiocarbamate

In a more recent attempt, a boron dipyrromethene (BODIPY)-based H_2S cage was irradiated by visible light (470 nm) and generated a self-immolative thiocarbamate which

gives quinone methide with the formation of COS. COS was then rapidly hydrolyzed to H₂S in the presence of CA (Scheme 1.14).⁵¹

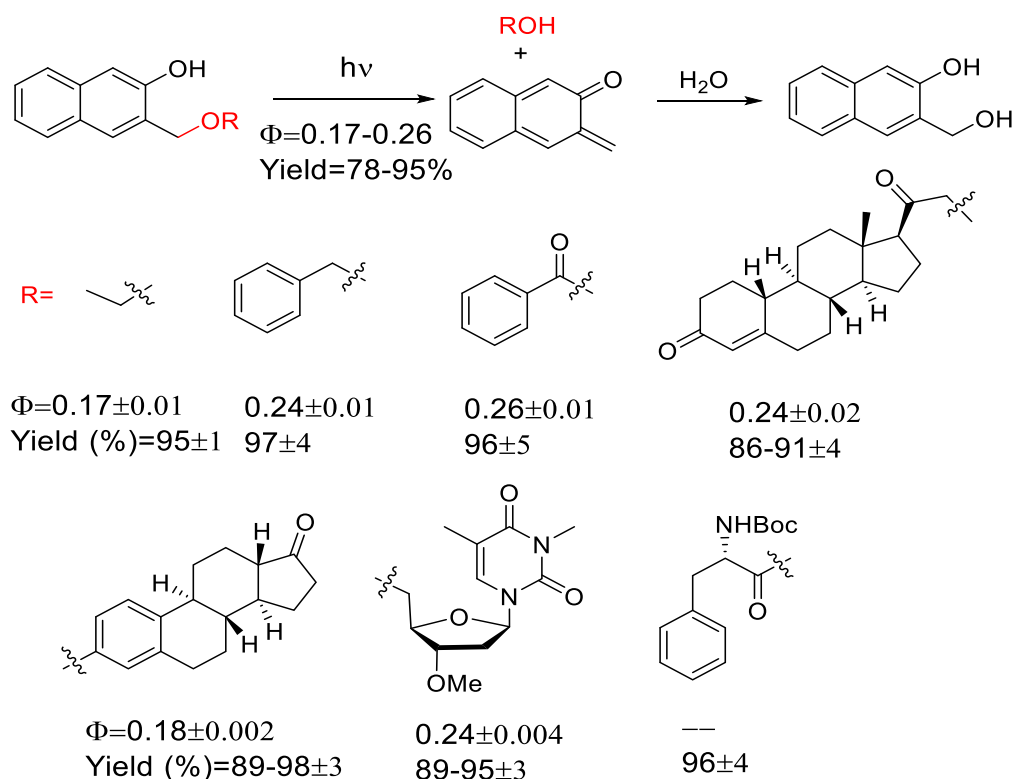


Scheme 1.14 H₂S photo-release from dipyrromethene-masked carbamothioate

1.8 *o*-NQMP as Photo-Labile Protecting Group

Photolabile protecting groups (PPG) allow for the spatial and temporal control of substrate release, as well as the “reagentless” deprotection. Ideally, a photolabile protecting group is stable in the dark and releases the caged substrate in high quantum and chemical yields upon irradiation, preferably with a high rate of release for kinetic and time-resolved studies.⁵² Additionally, PPGs with substantial absorbance above 300 nm are favored for biochemical applications. Since the deprotection reaction proceeds via heterolysis of a C-O bond, the uncaging efficiency of many common PPGs is depending on the basicity of the substrate. As a result, alcohols are difficult target for photolabile protection due to its poor leaving strength. *o*-Nitrobenzyl-based PPGs have been used to release alcohols and carbohydrates. However, the release is relatively slow because of some sluggish dark steps.⁵³ Introducing a carbonate linker improves the quantum and chemical yield of alcohol photo-release but still suffers from slow releasing rate because of the dark step --decarboxylation of the carbonate.⁵⁴

The (3-hydroxynaphthalene-2-yl) methyl (NQMP) group was shown to be a suitable PPG for caging biomolecules containing alcohol, phenol, and carboxylic acid functionalities. The photo-release utilizes bio-applicable light (300-350 nm), is fast ($k_{\text{release}} \approx 10^5 \text{ s}^{-1}$) and have good quantum ($\Phi = 0.17\text{-}0.26$) and chemical ($> 90\%$) yields. The initial byproduct of the photoreaction, 2-naphthoquinone-3-methide, reacts rapidly with water ($k_{\text{H}_2\text{O}} = 144 \pm 11 \text{ s}^{-1}$) to produce parent 3-hydroxy-2-naphthalenemethanol (Scheme 1.15).⁵⁵



Scheme 1.15 Photo-release efficiencies of *o*-NQMP caged compounds

After testing the NQMP's efficiency as a PPG, the Popik group functionalized NQMP with a fluorophore (a dansyl derivative) to achieve independent photochemical release and fluorescent imaging of caged substrates.⁵⁶ Irradiation of DNS-NQMP-caged alcohols and carboxylic acids with 300 or 350 nm light resulted in release of the

substrates. With excitation of 400 nm light, the cage revealed intense green emission but not substrate release (Figure 1.7).

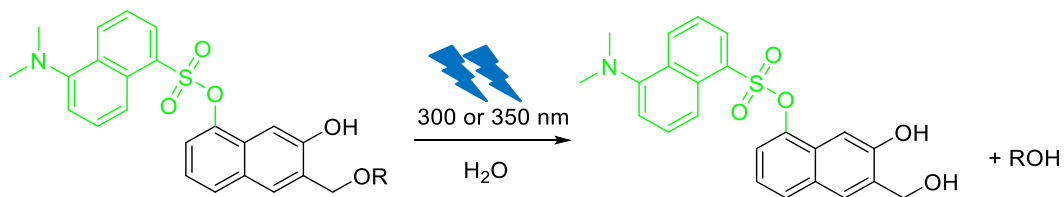


Figure 1.7 Photo-release of alcohols/carboxylic acids from *o*-NQMP cage

To better trace the release of the substrate, NQMP was used to cage the fluorescein-based dyes. Thus, irradiation of the cage with low-intensity UVA light resulted in photoactivation of the nonfluorescent cage as well as fast, efficient, and quantitative release of the substrate. The substrate showed 4-fold fluorescent increase in emission intensity (Figure 1.8).⁵⁷

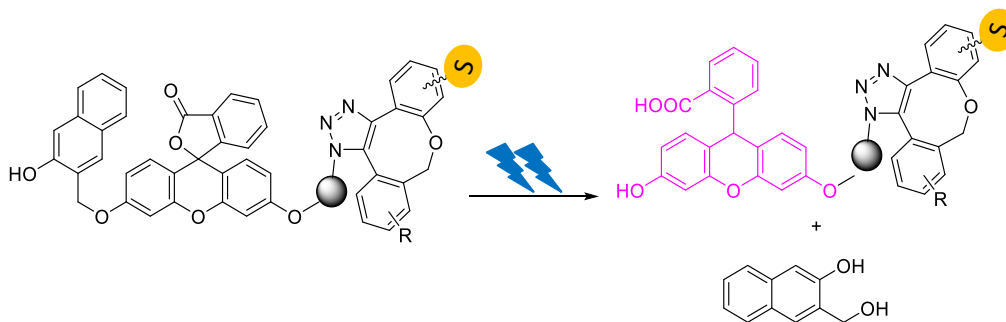


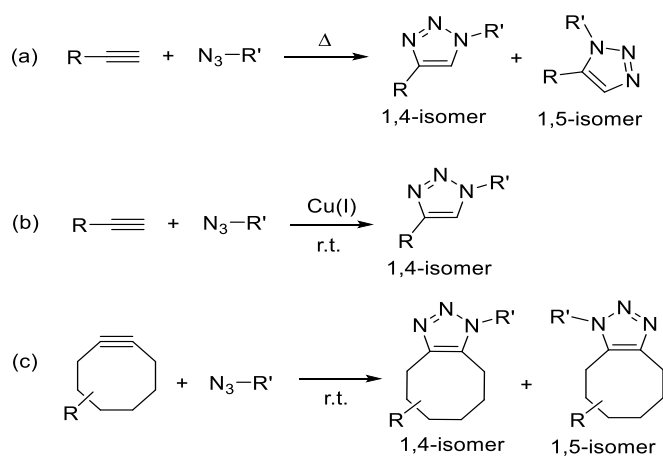
Figure 1.8 *o*-NQMP as a photocage for fluorescein

1.9 Azide-Alkyne Cycloaddition

Azide-alkyne cycloaddition (AAC) is a facile process that generate a triazole via a concerted 1,3-dipolar addition between an azide and an alkyne. Although not the most reactive 1,3-dipole, azide is known to be selective and robust for cyclization. It rarely participates in side-reactions and is remarkably stable in typical synthetic conditions.

Among different variations of the AAC reactions, Huisgen cycloaddition (Scheme 1.16 a)⁵⁸ is the first developed one which utilizes an azide and a terminal or internal alkyne to generate 1,2,3-triazole as a mixture of 1,4 and 1,5- adducts with heat.

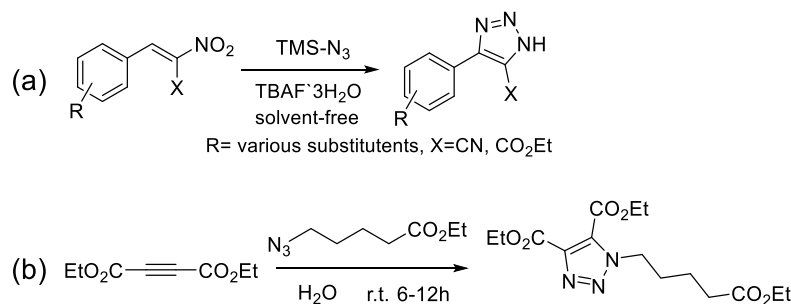
Later, copper (I) was discovered as an efficient catalyst for this reaction at room temperature with 1,4-regioisomer as the sole product. This reaction is also known as copper-catalyzed azide-alkyne cycloadditions (CuAAC) (Scheme 1.16 b). However, it is only applied to terminal alkyne and its application is also limited due to the cellular toxicity of Cu (I).⁵⁹ A solution for metal-free cycloaddition reactions is the strain-promoted azide alkyne cycloaddition (SPAAC) which significantly improved the reaction rate with mild condition (Scheme 1.16 c).⁶⁰ However, the preparation of strained alkyne substrates is usually cumbersome.

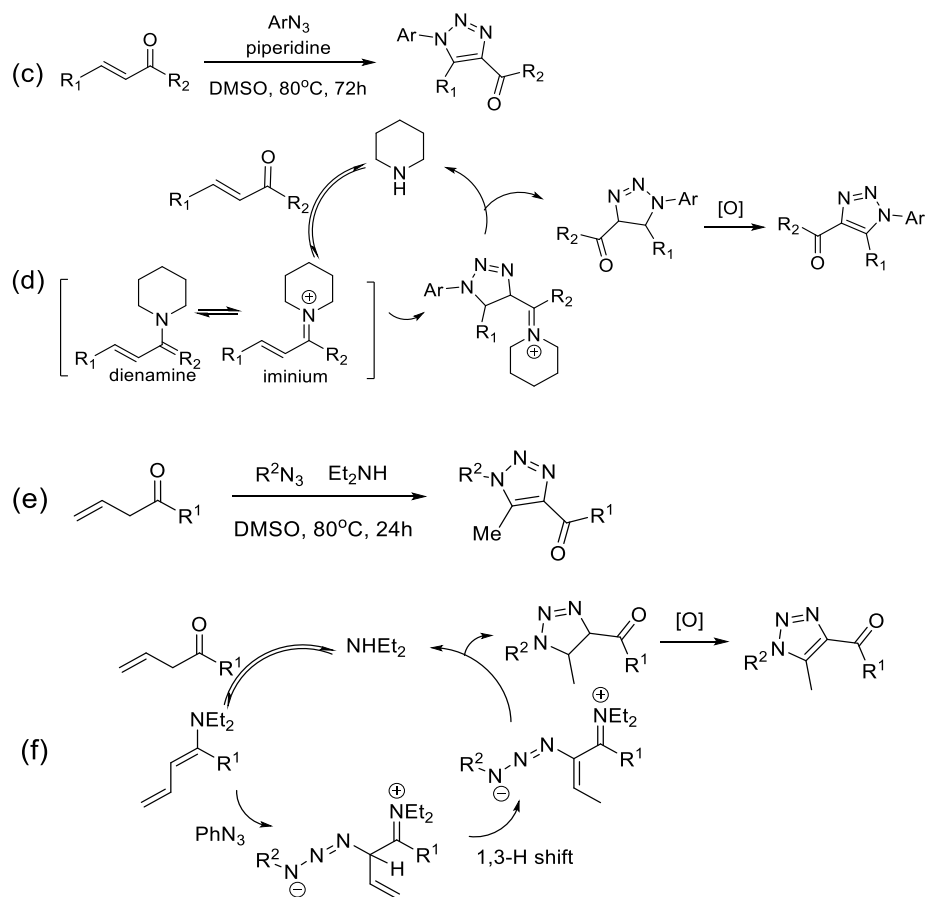


Scheme 1.16 Azide-alkyne cycloaddition reactions

Recently, it is reported that the Huisgen reaction can be accelerated by dipolarophiles such as electron-poor olefins or alkynes. Different dipolarophiles, for instance activated alkenes, enamines and enolates, have been employed to facilitate triazole formation. For example, The Vaccaro group described a triazole formation from azide and a various electron withdrawing group functionalized alkenes under mild condition (50-80 °C) (Scheme 1.17a).⁶¹ Similarly, The Ju group reported a simple synthetic protocol for the 1,3-dipolar cycloaddition of azides with electron-deficient alkynes (up to two electron-withdrawing groups) proceeds without any catalysts at room temperature in aqueous solution (Scheme 1.17b).⁶²

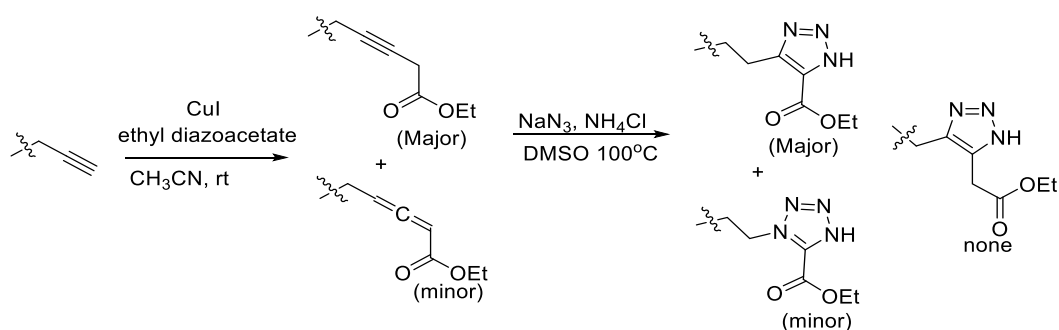
In addition, the Wang group developed a cycloaddition reaction of activated alkene (α , β -unsaturated ketones) with azides through iminium catalysis which produced only one triazole isomer (Scheme 1.17 c,d).⁶³ This reaction also applies to the non-conjugated activated alkene, where a 1,3 hydrogen shift was proposed to happen to give the triazole in conjugation with the carbonyl group (Scheme 1.17 e,f).⁶⁴ In both cases, high levels of regioselectivity was achieved with only 1,5- substituted triazole isomer formed.





Scheme 1.17 Azide–alkyne cycloaddition accelerated by activated olefins/alkynes

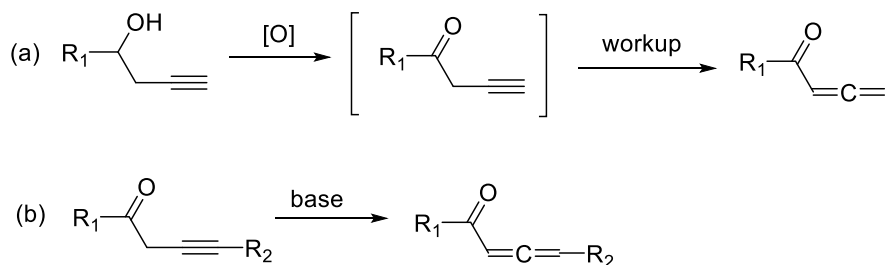
The azide cycloaddition to activated alkyne/allene is site specific. For example, alkynyl acetate was generated the Gmeiner group, and alkynyl acetate could partially isomerize to allene and formed a hardly separable mixture. Then, the alkynyl and allenyl acetate mixture was subjected to react with sodium azide for cycloaddition reaction. The reaction afforded both triazole and tetrazole with the triazole being the major product. A detailed NMR analysis suggested that both the cycloaddition products (triazole or tetrazole) are formed α , β - (instead of β , γ -) to the carbonyl moiety (Scheme 1.18).⁶⁵ This research proved the site specificity of this cycloaddition reaction and that the reaction most likely proceeded though the allenyl isomer rather than the alkynyl isomer.



Scheme 1.18 Site specificity of azide cycloaddition to activated alkyne/allene

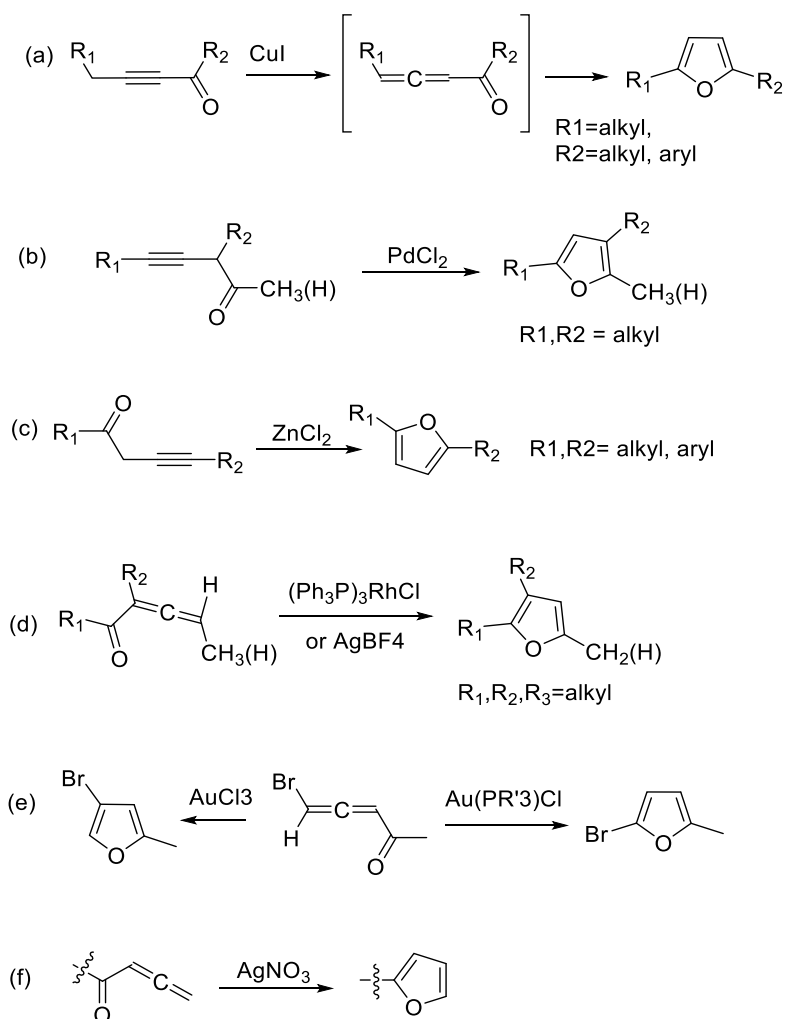
1.10 Synthesis of Activated Allenes and Aryl Furans

It was reported that with the acidic α -hydrogen of the neighboring ketone/aldehyde functional groups, terminal alkyne is easily isomerized to an allene in the presence of weak bases such as carbonate, tertiary amine, or without any base (Scheme 1.19 a).⁶⁶ For internal alkyne, such isomerization reaction rate is relatively slow compared to that of the terminal alkyne (Scheme 1.19 b), and similar slowing effect was also found for substituents to the carbonyl group.⁶⁷ But with base catalysis, the isomerization product can also be achieved with high yield.⁶⁶ Previous reports indicate that the isomerization process can also be facilitated via silica gel chromatography purification due to the separation of the acid added during oxidation of homopropargylic alcohol.⁶⁸



Scheme 1.19 Isomerization of activated alkyne to allene

It is known that activated alkynes or allenes can transform to furan with catalysts. For instance, conjugated yn-one can be converted to furan in presence of the catalysts CuI (Scheme 1.20 a)⁶⁹. Non-conjugated yn-one (propargylic ketone) can achieve similar conversion reaction using PdCl₂ (Scheme 1.20 b)⁷⁰ or ZnCl₂ (Scheme 1.20 c)⁷¹. Allenic intermediates are also capable of cyclisation to furans under Rh Au (III) or Ag (I) (Scheme 1.20 d, e, f)^{72,73,74}. However, such interesting transformation has not been done without the addition of catalyst.



Scheme 1.20 Catalytic transformation of activated alkyne/allene to furan

Conclusions and Goals of the Projects

o-Quinone methide (*o*-QM) and *o*-naphthoquinone methide (*o*-NQM) are highly reactive intermediate that finds a variety of applications in chemical, biological and engineering fields. The extraordinary *o*-NQM's reactivity towards nucleophiles and dienophiles and its efficient and controllable generation through UV irradiation render *o*-NQM versatile applications in drug delivery, surface derivatization, and photolabile protective group developments.

In the first part of the dissertation, various *o*-naphthoquinone methide precursors (NQMP) are developed for photo-controlled release of cargo in a site- and time-specific manner. Due to the ease of structure modification and photoreactive feature, the NQMPs are employed in drug delivery systems, by either attaching to other vehicles such as nanoparticles (Chapter 2) or being a prodrug itself to release H₂S gasotransmitter (Chapter 4). NQMPs are also designed to generate “smart” surfaces through reversible derivatization (Chapter 3) and explored the potential as a photolabile protecting group to release two equivalents of cargo molecule (Chapter 5).

Azide-alkyne cycloaddition reactions has long been of great interest owing to the reaction efficiency and product stability. However, the rough reaction condition, use of catalyst, or strenuous reactant preparation limit the application of the reaction.

In the second part of the dissertation (Chapter 6), activated allenes as a reactive species are synthesized and their cycloaddition reaction with azides are studied to investigate new way of generating triazole under mild condition.

1.11 References

- [1] Kupchan, S. M.; Karim, A.; Marcks, C. Tumor inhibitors. XLVIII. Taxodione and taxodone, two novel diterpenoid quinone methide tumor inhibitors from *Toxodium distichum*. *J. Org. Chem.* **1969**, 34, 3912–3918
- [2] Sarkanen, K. V.; Ludwig, C. H. Lignins, Occurrence, Formation, Structure and Reactions; Wiley-Interscience: New York, **1971**.
- [3] Nielsen, C. D. T., Abas, H., & Spivey, A. C. Stereoselective reactions of ortho-quinone methide and ortho-quinone methide imines and their utility in natural product synthesis. *Synthesis*. **2018**, 50(20), 4008-4018
- [4] Haba, K.; Popkov, M.; Shamis, M.; Lerner, R. A.; Barbas, C. F., III; Shabat, D. Singletriggered trimeric prodrugs. *Angew. Chem., Int. Ed. Engl.* **2005**, 44, 716–720
- [5] Wang, P., Song, Y., Zhang, L., He, H., & Zhou, X. Quinone methide derivatives: important intermediates to DNA alkylating and DNA cross-linking actions. *Current medicinal chemistry*. **2005**, 12(24), 2893-2913.
- [6] Rokita, Steven Edward. *Quinone methides*. Vol. 4. John Wiley & Sons, **2009**.
- [7] Toteva, M. M., & Richard, J. P. The generation and reactions of quinone methides. *Adv. Phys. Org. Chem.* **2011**, 45, 39-91.
- [8] Bai, W. J., David, J. G., Feng, Z. G., Weaver, M. G., Wu, K. L., & Pettus, T. R. The domestication of ortho-quinone methides. *Accounts of chemical research*. **2014**, 47(12), 3655-3664.
- [9] Willis, N. J., & Bray, C. D. ortho-Quinone Methides in Natural Product Synthesis. *Chemistry—A European Journal*. **2012**, 18(30), 9160-9173.

- [10] Arumugam, S., Orski, S. V., Mbua, N. E., McNitt, C., Boons, G. J., Locklin, J., & Popik, V. V. Photo-click chemistry strategies for spatiotemporal control of metal-free ligation, labeling, and surface derivatization. *Pure and Applied Chemistry*. **2013**, 85(7), 1499-1513.
- [11] Arumugam, S., & Popik, V. V. Photochemical generation and the reactivity of *o*-naphthoquinone methides in aqueous solutions. *Journal of the American Chemical Society*. **2009**, 131(33), 11892-11899.
- [12] Ireland, J. F., & Wyatt, P. A. H. Acid-base properties of electronically excited states of organic molecules. In *Advances in physical organic chemistry*. **1976**, (Vol. 12, pp. 131-221). Academic Press.
- [13] Wan, P., & Shukla, D. Utility of acid-base behavior of excited states of organic molecules. *Chemical reviews*. **1993**, 93(1), 571-584.
- [14] Wan, P., Barker, B., Diao, L., Fischer, M., Shi, Y., & Yang, C. 1995 Merck Frosst Award Lecture Quinone methides: relevant intermediates in organic chemistry. *Canadian journal of chemistry*. **1996**, 74(4), 465-475
- [15] Yang, B., & Gao, S. Recent advances in the application of Diels–Alder reactions involving *o*-quinodimethanes, *aza-o*-quinone methides and *o*-quinone methides in natural product total synthesis. *Chemical Society Reviews*, **2018**, 47(21), 7926-7953.
- [16] Arumugam, S., & Popik, V. V. Light-induced hetero-Diels–Alder cycloaddition: a facile and selective photoclick reaction. *Journal of the American Chemical Society*. **2011**, 133(14), 5573-5579.

- [17] Li, Q., Dong, T., Liu, X., & Lei, X. A bioorthogonal ligation enabled by click cycloaddition of *o*-quinolinone quinone methide and vinyl thioether. *Journal of the American Chemical Society*. **2013**, *135*(13), 4996-4999.
- [18] Arumugam, S., Orski, S. V., Locklin, J., & Popik, V. V. Photoreactive polymer brushes for high-density patterned surface derivatization using a Diels–Alder photoclick reaction. *Journal of the American Chemical Society*. **2012**, *134*(1), 179-182.
- [19] Arumugam, S., & Popik, V. V. Patterned surface derivatization using Diels–Alder photoclick reaction. *Journal of the American Chemical Society*. **2011**, *133*(39), 15730-15736.
- [20] Arumugam, S., & Popik, V. V. Attach, remove, or replace: Reversible surface functionalization using thiol–quinone methide photoclick chemistry. *Journal of the American Chemical Society*. **2012**, *134*(20), 8408-8411.
- [21] Arumugam, S., Guo, J., Mbua, N. E., Friscourt, F., Lin, N., Nekongo, E., ... & Popik, V. V. Selective and reversible photochemical derivatization of cysteine residues in peptides and proteins. *Chemical science*. **2014**, *5*(4), 1591-1598.
- [22] Cui, W., Li, J., & Decher, G. Self-assembled smart nanocarriers for targeted drug delivery. *Advanced Materials*. **2016**, *28*(6), 1302-1311.
- [23] Bansal, A., & Zhang, Y. Photocontrolled nanoparticle delivery systems for biomedical applications. *Accounts of chemical research*. **2014**, *47*(10), 3052-3060
- [24] Agasti, S. S., Chomposor, A., You, C. C., Ghosh, P., Kim, C. K., & Rotello, V. M. Photoregulated release of caged anticancer drugs from gold nanoparticles. *Journal of the American Chemical Society*. **2009**, *131*(16), 5728-5729.

- [25] Verma, A. and Rotello, V.M., Surface recognition of biomacromolecules using nanoparticle receptors. *Chemical Communications*, **2005**, (3), 303-312.
- [26] Vigderman, L., & Zubarev, E. R. Therapeutic platforms based on gold nanoparticles and their covalent conjugates with drug molecules. *Advanced drug delivery reviews*, **2013**, 65(5), 663-676.
- [27] Fomina, N., Sankaranarayanan, J. and Almutairi, A., Photochemical mechanisms of light-triggered release from nanocarriers. *Advanced drug delivery reviews*. **2012**, 64(11), 1005-1020.
- [28] Ghosh, P., Han, G., De, M., Kim, C.K. and Rotello, V.M., Gold nanoparticles in delivery applications. *Advanced drug delivery reviews*. **2008**, 60(11), 1307-1315.
- [29] Yang, P.H., Sun, X., Chiu, J.F., Sun, H. and He, Q.Y.,. Transferrin-mediated gold nanoparticle cellular uptake. *Bioconjugate chemistry*. **2005**, 16(3), pp.494-496.
- [30] Dixit, V., Van den Bossche, J., Sherman, D.M., Thompson, D.H. and Andres, R.P., Synthesis and grafting of thioctic acid– PEG– folate conjugates onto Au nanoparticles for selective targeting of folate receptor-positive tumor cells. *Bioconjugate chemistry*. **2006**, 17(3), 603-609.
- [31] Mura, S., Nicolas, J., & Couvreur, P. Stimuli-responsive nanocarriers for drug delivery. *Nature materials*, **2013**, 12(11), 991-1003.
- [32] Frasconi, M., Mazzei, F. and Ferri, T., Protein immobilization at gold–thiol surfaces and potential for biosensing. *Analytical and bioanalytical chemistry*. **2010**, 398(4), 1545-1564.
- [33] Mendes, P.M., Stimuli-responsive surfaces for bio-applications. *Chemical Society Reviews*, **2008**, 37(11), 2512-2529.

- [34] Weber, T., Chandrasekaran, V., Stamer, I., Thygesen, M.B., Terfort, A. and Lindhorst, T.K., Switching of bacterial adhesion to a glycosylated surface by reversible reorientation of the carbohydrate ligand. *Angewandte Chemie International Edition*. **2014**, 53(52), 14583-14586.
- [35] Du, X., Li, J., Welle, A., Li, L., Feng, W. and Levkin, P.A., Reversible and rewritable surface functionalization and patterning via photodynamic disulfide exchange. *Advanced Materials*, **2015**, 27(34), 4997-5001.
- [36] Fernandes, P. A., & Ramos, M. J. Theoretical insights into the mechanism for thiol/disulfide exchange. *Chemistry—A European Journal*, **2004**, 10(1), 257-266.
- [37] Li, L.; Moore, P.K. hydrogen sulfide in health and disease: a breath of not so fresh air? *Trends Pharmacol. Sci.* **2008**, 29, 84-90.
- [38] Shrotriya, S.; Kundu, J.K.; Na, H.K.; Surh, Y.J. Diallyl Trisulfide Inhibits Phorbol Ester–Induced Tumor Promotion, Activation of AP-1, and Expression of COX-2 in Mouse Skin by Blocking JNK and Akt Signaling. *Cancer Res.* **2010**, 70,1932-1940.
- [39] Sodha, N.R.; Clements, R.T.; Feng, J.; Liu, Y.; Bianchi, C.; Horvath, E.M.; Szabo, C.; Sellke, F.W. The effects of therapeutic sulfide on myocardial apoptosis in response to ischemia–reperfusion injury. *Surger Eur J Cardiothorac Surg.* **2008**, 33, 906-913.
- [40] Osborne, N.N.; Ji, D.; Majid, A.S.A.; Del Soldata, P.; Sparatore, A. Glutamate oxidative injury to RGC-5 cells in culture is necrostatin sensitive and blunted by a hydrogen sulfide (H₂S)-releasing derivative of aspirin (ACS14). *Neurochem. Int.*, **2012**, 60, 365-378.

- [41] Kang, J., Neill, D. L., & Xian, M. Phosphonothioate-based hydrogen sulfide releasing reagents: chemistry and biological applications. *Frontiers in pharmacology*. **2017**, 8, 457.
- [42] Papapetropoulos, A., Whiteman, M., & Cirino, G. Pharmacological tools for hydrogen sulphide research: a brief, introductory guide for beginners. *British journal of pharmacology*. **2015**, 172(6), 1633-1637.
- [43] Benavides, G.A., Squadrito, G.L., Mills, R.W., Patel, H.D., Isbell, T.S., Patel, R.P., Darley-USmar, V.M., Doeller, J.E. and Kraus, D.W., Hydrogen sulfide mediates the vasoactivity of garlic. *Proceedings of the National Academy of Sciences*. **2007**, 104(46), 17977-17982.
- [44] Wallace, J. L., Vong, L., McKnight, W., Dickey, M., & Martin, G. R. Endogenous and exogenous hydrogen sulfide promotes resolution of colitis in rats. *Gastroenterology*. **2009**, 137(2), 569-578.
- [45] Chattopadhyay, M., Kodela, R., Nath, N., Dastagirzada, Y. M., Velázquez-Martínez, C. A., Boring, D., & Kashfi, K. Hydrogen sulfide-releasing NSAIDs inhibit the growth of human cancer cells: a general property and evidence of a tissue type-independent effect. *Biochemical pharmacology*. **2012**, 83(6), 715-722.
- [46] Powell, C. R., Dillon, K. M., & Matson, J. B. A review of hydrogen sulfide (H₂S) donors: Chemistry and potential therapeutic applications. *Biochemical pharmacology*. **2018**, 149, 110-123.
- [47] Devarie-Baez, N.O., Bagdon, P.E., Peng, B., Zhao, Y., Park, C.M. and Xian, M., Light-induced hydrogen sulfide release from “caged” gem-dithiols. *Organic letters*, **2013**, 15(11), 2786-2789.

- [48] Fukushima, N., Ieda, N., Sasakura, K., Nagano, T., Hanaoka, K., Suzuki, T., Miyata, N. and Nakagawa, H., Synthesis of a photocontrollable hydrogen sulfide donor using ketoprofenate photocages. *Chemical communications*. **2013**, 50(5), 587-589.
- [49] Xiao, Z., Bonnard, T., Shakouri-Motlagh, A., Wylie, R.A., Collins, J., White, J., Heath, D.E., Hagemeyer, C.E. and Connal, L.A., Triggered and Tunable Hydrogen Sulfide Release from Photogenerated Thiobenzaldehydes. *Chemistry–A European Journal*. **2017**, 23(47), 11294-11300.
- [50] Zhao, Y., Bolton, S.G. and Pluth, M.D., Light-activated COS/H₂S donation from photocaged thiocarbamates. *Organic letters*. **2017**, 19(9), 2278-2281.
- [51] Venkatesh, Y., Das, J., Chaudhuri, A., Karmakar, A., Maiti, T. K., & Singh, N. P. Light triggered uncaging of hydrogen sulfide (H₂S) with real-time monitoring. *Chemical Communications*. **2018**, 54(25), 3106-3109.
- [52] Klán, P., Šolomek, T., Bochet, C. G., Blanc, A., Givens, R., Rubina, M., ... & Wirz, J. Photoremovable protecting groups in chemistry and biology: reaction mechanisms and efficacy. *Chemical reviews*. **2013**, 113(1), 119-191.
- [53] Pelliccioli, A. P., & Wirz, J. Photoremovable protecting groups: reaction mechanisms and applications. *Photochemical & photobiological sciences*. **2002**, 1(7), 441-458.
- [54] Papageorgiou, G., Barth, A., & Corrie, J. E. Flash photolytic release of alcohols from photolabile carbamates or carbonates is rate-limited by decarboxylation of the photoproduct. *Photochemical & Photobiological Sciences*. **2005**, 4(2), 216-220.

- [55] Kulikov, A., Arumugam, S., & Popik, V. V. Photolabile protection of alcohols, phenols, and carboxylic acids with 3-hydroxy-2-naphthalenemethanol. *The Journal of organic chemistry*, **2008**, 73(19), 7611-7615.
- [56] Arumugam, S., & Popik, V. V. Bichromophoric fluorescent photolabile protecting group for alcohols and carboxylic acids. *Photochemical & Photobiological Sciences*, **2012**, 11(3), 518-521.
- [57] Nekongo, E. E., & Popik, V. V. Photoactivatable fluorescein derivatives caged with a (3-hydroxy-2-naphthalenyl) methyl group. *The Journal of organic chemistry*. **2014**, 79(16), 7665-7671.
- [58] Huisgen, R. 1, 3-dipolar cycloadditions. Past and future. *Angewandte Chemie International Edition in English*. **1963**, 2(10), 565-598.
- [59] Hein, J. E., & Fokin, V. V. Copper-catalyzed azide-alkyne cycloaddition (CuAAC) and beyond: new reactivity of copper (I) acetylides. *Chemical Society Reviews*. **2010**, 39(4), 1302-1315.
- [60] Agard, N. J., Prescher, J. A., & Bertozzi, C. R. A strain-promoted [3+ 2] azide-alkyne cycloaddition for covalent modification of biomolecules in living systems. *Journal of the American Chemical Society*. **2004**, 126(46), 15046-15047.
- [61] Amantini, D., Fringuelli, F., Piermatti, O., Pizzo, F., Zunino, E., & Vaccaro, L. Synthesis of 4-aryl-1 H-1, 2, 3-triazoles through TBAF-catalyzed [3+ 2] cycloaddition of 2-aryl-1-nitroethenes with TMSN₃ under solvent-free conditions. *The Journal of organic chemistry*. **2005**, 70(16), 6526-6529.

- [62] Li, Z., Seo, T. S., & Ju, J. 1, 3-Dipolar cycloaddition of azides with electron-deficient alkynes under mild condition in water. *Tetrahedron letters*. **2004**, 45(15), 3143-3146.
- [63] Li, W., Du, Z., Zhang, K., & Wang, J. Organocatalytic 1, 3-dipolar cycloaddition reaction of α , β -unsaturated ketones with azides through iminium catalysis. *Green Chemistry*. **2015**, 17(2), 781-784.
- [64] Li, W., Du, Z., Huang, J., Jia, Q., Zhang, K., & Wang, J. Direct access to 1, 2, 3-triazoles through organocatalytic 1, 3-dipolar cycloaddition reaction of allyl ketones with azides. *Green Chemistry*. **2014**, 16(6), 3003-3006.
- [65] Paul, A., Einsiedel, J., Waibel, R., Heinemann, F. W., Meyer, K., & Gmeiner, P. Novel triazolo-peptides: chiro-specific synthesis and conformational studies of proline derived analogs. *Tetrahedron*. **2009**, 65(31), 6156-6168.
- [66] Krause, N., & Hashmi, A. S. *Modern allene chemistry*. Wiley-VCH. **2004**. p13-14.
- [67] Spencer, R. W., Tam, T. F., Thomas, E., Robinson, V. J., & Krantz, A. Ynenol lactones: synthesis and investigation of reactions relevant to their inactivation of serine proteases. *Journal of the American Chemical Society*. **1986**, 108(18), 5589-5597.
- [68] Hashmi, A.S.K. et al. 1998, *Tetrahedron Lett.* 39, pp.7491–7496
- [69] Kel'i, A. V., & Gevorgyan, V. Efficient synthesis of 2-mono-and 2, 5-disubstituted furans via the CuI-catalyzed cycloisomerization of alkynyl ketones. *The Journal of organic chemistry*. **2002**, 67(1), 95-98.
- [70] Utimoto, K. Palladium catalyzed synthesis of heterocycles. *Pure and Applied Chemistry*. **1983**, 55(11), 1845-1852.

- [71] Sniady, A., Durham, A., Morreale, M. S., Wheeler, K. A., & Dembinski, R. Room temperature zinc chloride-catalyzed cycloisomerization of alk-3-yn-1-ones: synthesis of substituted furans. *Organic letters*. **2007**, 9(7), 1175-1178.
- [72] Marshall, J. A., & Robinson, E. D. A mild method for the synthesis of furans. Application to 2, 5-bridged furano macrocyclic compounds. *The Journal of Organic Chemistry*. **1990**, 55(11), 3450-3451.
- [73] Xia, Y., Dudnik, A. S., Gevorgyan, V., & Li, Y. Mechanistic insights into the gold-catalyzed cycloisomerization of bromoallenyl ketones: ligand-controlled regioselectivity. *Journal of the American Chemical Society*. **2008**, 130(22), 6940-6941..
- [74] Cong, X., Liu, K. G., Liao, Q. J., & Yao, Z. J. Preparation of enantiomerically pure 2-(1'-aminomethyl) furan derivatives and synthesis of an unnatural polyhydroxylated piperidine. *Tetrahedron letters*. **2005**, 46(49), 8567-8571.

CHAPTER 2

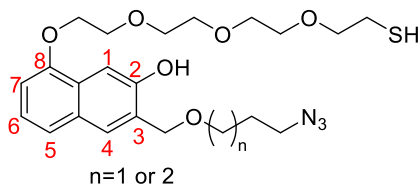
SH-NQMP-N3 SYNTHESIS FOR GOLD-NANOPARTICLE DRUG DELIVERY

2.1 Introduction

Drug delivery system (DDS) is a method to enhance the efficiency of conventional pharmaceuticals and medical applications. DDS remains stable in circulatory systems but are labile under certain conditions to release the payload.¹ Among the materials that have been used as the DDS vehicle such as polymers and nanomaterials, gold nanoparticle (AuNP) is nontoxic, possesses tunable sized core, and can be functionalized with small-molecule drugs payload via Au-S bond.^{2,3} With the efficient benzylic C-O bond cleavage ability upon photo-irradiation to release the cargo molecule, the *o*-NQMP precursors (NQMPs) have great potential to serve as temporal controlled drug delivery material.

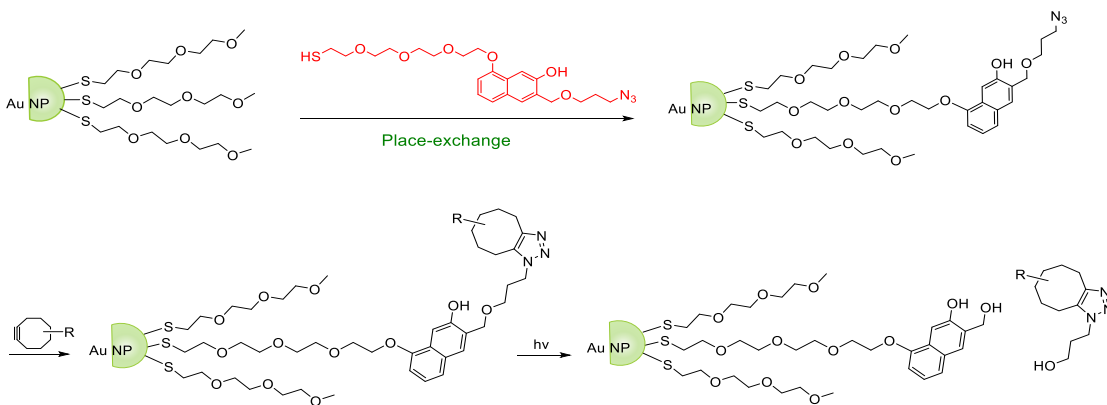
A NQMP derivative (SH-NQMP-N3) that conjugates to water soluble AuNPs was designed for the purpose of gold-nanoparticle (AuNP) drug delivery (Scheme 2.1, compound 1). The NQMP molecule is modified at 8-position with tetra ethylene glycol group linked thiol group for conjugation with the AuNPs. The tetra ethylene glycol group improves the molecule's water solubility as well as prevents AuNPs from aggregation after the photo cleavage and release of the cargo. The NQMP molecule also possesses a 3-position ether linked azide moiety to facilitate further modification through azide-alkyne click chemistry. Compared to the more common ester bond, the ether bond ensures a more stable linkage under most physiological conditions. Therefore, this

NQMP molecule is efficient to assemble functional materials onto AuNPs and release the cargo in a photochemically controlled manner.



Scheme 2.1. Structure of SH-NQMP-N3

Our research focuses on the synthesis of the NQMP-ether while the further application for modification with AuNP would be performed by our collaborator. The modification involves incorporation of the SH-NQMP-N3 onto AuNPs by direct ligand exchange (place-exchange) via the thiol moiety. A reaction between the NQMP-AuNPs and dibenzo-cyclooctyne (DIBO) based on an interfacial strain-promoted azide-alkyne cycloaddition (SPAAC) reaction would be adopted to evaluate the efficiency of the system.⁴ Upon irradiation of UV light, the modified NQMP-AuNPs undergo efficient and quantitative generation of the NQM-AuNPs which will quickly hydrate to a stable 3-(hydroxymethyl)naphthalen-2-ol derivative with the release of the triazole moiety (Scheme 2.2).

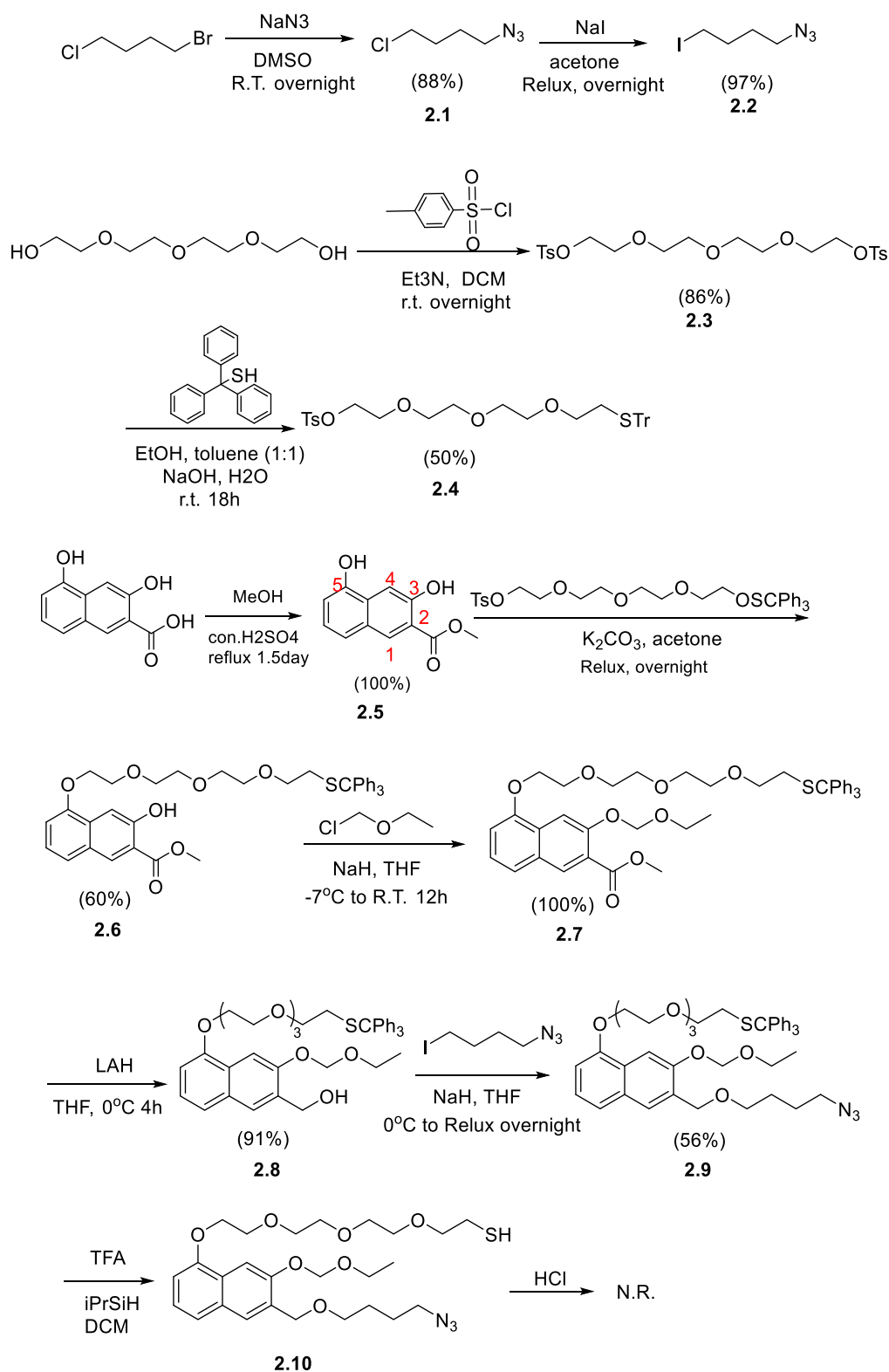


Scheme 2.2 SH-NQMP-N3 for gold-nanoparticle drug delivery

The synthesis of target compound SH-NQMP-N3 (Scheme 2.1) for drug delivery went through some trials and errors. Two synthesis routes were developed but failed before the third route finally accomplished the synthesis.

2.2 Synthesis Route 1

At the beginning of synthesis Route 1, the azide linker (compound **2.2**) was prepared from 1-bromo-4-chlorobutane — azide was installed by S_N2 replacement of bromine and the chlorine was substituted with iodine via Finkelstein reaction. The thiol linker (compound **2.4**) was prepared in its trityl protected form. The tetraethylene glycol was first tosylated on both ends, then one of the tosyl group was replaced by thiotrityl group. The NQMP backbone was generated from 3,5-dihydroxy-2-naphthoic acid — from esterification, thiol linker installment via S_N2 reaction, protection of the 3-position phenol group by ethoxymethyl ether (EOM) group, to the reduction of the ester into alcohol, and the azide linker conjugation through S_N2 reaction. Although previous steps have been demonstrated successful, failure of deprotecting EOM protecting group on the naphthalic alcohol marked the futile efforts of this route. (Scheme 2.3).



Scheme 2.3 Synthesis route 1 for SH-NQMP-N3

Although trifluoro acetic acid (TFA) is capable of removing both the EOM and trityl protecting group from the compound, only the fall-off of trityl group was observed while the EOM was quite resistant to deprotection to acidic conditions such as TFA, 5% HCl, Amberlyst-15 resin, ZnBr₂. This may be explained by the congested chemical environment that EOM group is in. Besides the failure of the last step, the S_N2 reaction to functionalize NQMP with azide linker also revealed disadvantage. Sodium hydride (NaH) was not reactive enough towards the NQMP alcohol (**2.8**) and using large equivalents of NaH greatly affected the yield due to the potential elimination of azide linker as a side-reaction.

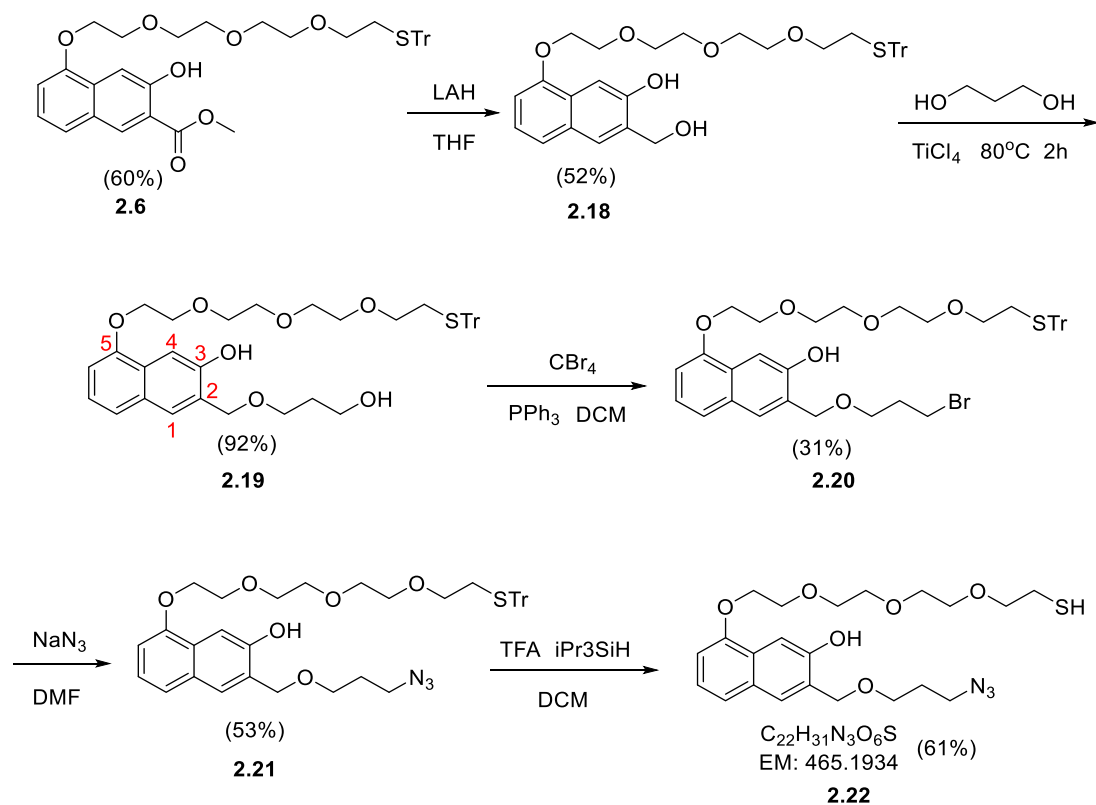
2.3 Synthesis Route 2

Since the EOM protection was not able being removed in the last step of route 1, the procedure was revised as follows. The EOM group was designed to protect both 3- and 5- position phenol allowing azide linker fitted to the 2- position, then EOM was removed for thiol linker to be installed. It was assumed that the 5- OH of compound **2.16**, was more selective towards S_N2 than the 3- OH, given that compound **2.5** was selectively equipped with thiol linker at the 5- OH in the synthesis route 1. In **2.5**, the hydrogen bonding between 3-OH hydrogen and 2-ester oxygen provides the 5-OH higher reactivity than the 3-OH. Another change of this synthesis route was the role of the S_N2 reaction for putting on the azide linker: azide linker (compound **2.11**) produced alkoxide and the NQMP (compound **2.14**) as an alkyl bromide. In this way, the elimination of alkyl halide can be avoided. However, the results demonstrated route 2 did not generate pure target compound as expected (Scheme 2.4).

The method failed because the 5- OH of compound **2.16** showed no selectivity over 3- OH. It can be explained by the weak hydrogen bonding towards an ether oxygen than an ester oxygen. Though the authenticity of product from last step was proved from ESI, the purity was questioned by NMR. With two sets of signals revealed in NMR, a mixture of two mono-substituted isomers was clearly present.

2.4 Synthesis Route 3

To improve from the previous synthesis routes, the thiol linker needs to be attached to NQMP in its ester form (compound **2.5**), therefore the azide linker can be installed onto the molecule without protecting the 3-OH. Fortunately, a related protocol was found to functionalize the 2- benzyl OH while the 3-phenol OH left unprotected.⁵ With Lewis acid such as titanium chloride under heat, the NQMP can generate *o*-NQM ready for nucleophilic attack from propane-1,3-diol to afford compound **2.19**. This reaction is a very useful tool to selectively functionalize the benzylic OH with present of the phenolic OH in NQMPs (*i.e.* **2.18**) and similar analogues. From **2.19**, the following bromination, replacement of bromine with azide, and deprotection of trityl group successfully provided the target compound **2.22** (Scheme 2.5).



Scheme 2.5 Synthesis route 3 for SH-NQMP-N3

2.5 Conclusion

Three different routes were developed and employed for SH-NQMP-N3 synthesis. The three developed routes are good explorations of the NQMPs' peculiar characters and reactivities. The routes 1 and 2 were proved unsuccessful because of steric hinderance for the EOM group deprotection, and the wrong analogy of the selectivity of 5- and 3-OH of different NQMPs, respectively. Route 3 was proved successful thanks to the convenience of addition of propane-1,3-diol to the unprotected naphthalene. With the target compound synthesized and characterized, it will be used for further research.

2.6 Experimental Section

1-azido-4-chlorobutane (2.1) 1-bromo-4-chlorobutane (4.38 g, 25.5 mmol) was added into a stirring suspension of sodium azide (2.5 g, 38.5 mmol) in dimethyl sulfoxide (25 mL). The mixture was stirred at room temperature overnight. The reaction mixture was diluted with hexane (50 mL), washed with water (50 mL), brine (50 mL), and dried over Na₂SO₄. The organic layer was then filtered, concentrated in vacuo to afford product (3.0 g, 88%) as a colorless oil. ¹H NMR (CDCl₃, 400 MHz) δ 3.57 (t, J = 6.4 Hz, 2H), 3.32 (m, 2H), 1.86 (m, 2H), 1.75 (m, 2H). ¹³C NMR (101 MHz, CDCl₃) δ 50.89, 44.38, 29.63, 26.13.

1-azido-4-iodobutane (2.2) 1-azido-4-chlorobutane (3.3 g, 24.7 mmol) in acetone (30 mL) was added to a solution of sodium iodide (7.4 g, 114 mmol) in acetone (30 mL). The reaction was reflux overnight. After cooling to room temperature, the reaction mixture was filtered to remove solid, concentrated in vacuo, re-dissolved in dichloromethane and washed with brine. The organic layer was concentrated in vacuo to afford product (4.4 g, 92%) as a colorless liquid. ¹H NMR (CDCl₃, 400 MHz) δ 3.31 – 3.22 (m, 3H), 3.14 (t, J = 6.8 Hz, 2H), 1.91 – 1.79 (m, 2H), 1.72 – 1.56 (m, 3H). ¹³C NMR (101 MHz, CDCl₃) δ 50.38, 30.45, 29.75, 5.67.

((oxybis(ethane-2,1-diyl))bis(oxy))bis(ethane-2,1-diyl) bis(4-methylbenzenesulfonate) (2.3) To a solution of *p*-toluenesulfonic acid (30 g, 0.158 mol) in CH₂Cl₂ (250 mL) at 0 °C, tetra (ethylene glycol) (14.55 g, 0.1 mol) and triethylamine (21 g, 0.208 mol) was added. The reaction was stirred at room temperature overnight. The precipitate was filtered, and the solution was washed with water, brine, and dried over Na₂SO₄ and concentrated in vacuo. The residue was purified via silica gel chromatography to provide

the product (32.1g, 86%) as a colorless oil. ^1H NMR (CDCl_3 , 400 MHz) δ 7.83 – 7.75 (m, 4H), 7.38 – 7.31 (m, 4H), 4.19 – 4.11 (m, 4H), 3.71 – 3.64 (m, 4H), 3.63 – 3.50 (m, 8H), 2.44 (s, 6H). ^{13}C NMR (101 MHz, CDCl_3) δ 144.88, 132.91, 129.87, 127.96, 70.71, 70.53, 69.32, 68.66, 21.66.

1,1,1-triphenyl-5,8,11-trioxa-2-thiatridecan-13-yl 4-methylbenzenesulfonate (2.4)

NaOH (0.6 g, 15 mmol) in H_2O (7 mL) was added to a solution of triphenylmethanethiol (2.7 g, 9.8 mmol) in EtOH /toluene (1:1, 50 mL). To this mixture was added a solution of compound **2.4** in EtOH /toluene (1:1, 50mL). The reaction was stirred at room temperature for 36 h, washed by NaHCO_3 and brine. The organic layer was dried over Na_2SO_4 and concentrated in vacuo, and purified via silica gel chromatography (ethyl acetate: hexanes 1:4 to 1:3 then 1:2) to provide the product (4.6 g, 78%) as a colorless to light yellow oil. ^1H NMR (CDCl_3 , 400 MHz) 7.86 – 7.78 (m, 2H), 7.50 – 7.40 (m, 6H), 7.37 – 7.33 (m, 2H), 7.33 – 7.27 (m, 6H), 7.26 – 7.20 (m, 3H), 4.21 – 4.13 (m, 2H), 3.73 – 3.65 (m, 2H), 3.65 – 3.52 (m, 6H), 3.51 – 3.42 (m, 2H), 3.32 (t, $J = 6.9$ Hz, 2H), 2.50 – 2.41 (m, 5H). ^{13}C NMR (101 MHz, CDCl_3) δ 144.83, 143.72, 132.99, 130.13, 129.86, 129.65, 128.01, 127.92, 127.03, 126.69, 70.74, 70.56, 70.51, 70.16, 69.62, 69.30, 68.68, 66.62, 31.67, 21.70.

Methyl 3,5-dihydroxy-2-naphthoate (2.5) Concentrated sulfuric acid (5 mL) in MeOH (50 mL) was added slowly to a stirring solution of 3,5-dihydroxy-2-naphthoic acid (4.7 g, 23 mmol) in MeOH (60 mL). The reaction was stirred under reflux for 36 h and poured into 1 L ice water. The yellow precipitate was collected and dried overnight via vacuum. The product was collected as a yellow solid (5.0 g, 100%). ^1H NMR (400 MHz, Acetone) δ 10.38 (s, 1H), 9.15 (d, $J = 0.8$ Hz, 1H), 8.52 (s, 1H), 7.64 (d, $J = 0.7$ Hz, 1H), 7.50 –

7.43 (m, 1H), 7.20 (dd, $J = 8.3, 7.5$ Hz, 1H), 6.99 (dd, $J = 7.5, 1.0$ Hz, 1H), 4.06 (s, 3H).
 ^{13}C NMR (101 MHz, Acetone) δ 205.38, 170.28, 155.76, 151.65, 132.01, 129.55, 128.46, 124.29, 120.43, 114.40, 110.55, 106.28, 52.29, 29.56, 29.36, 29.17, 28.98, 28.78, 28.59, 28.40.

methyl 3-hydroxy-5-((1,1,1-triphenyl-5,8,11-trioxa-2-thiatridecan-13-yl)oxy)-2-naphthoate (2.6) K_2CO_3 (3.8 g, 27.5 mmol) and compound **2.5** (5.6 g, 9.2 mmol) in acetone (50 mL) were added to a stirring solution of starting ester compound **2.3** (2.2 g, 10.2 mmol) in acetone (80 mL). The reaction was stirred at 70 °C overnight. The reaction mixture was filtered, concentrated in vacuo and re-dissolved in ethyl acetate, washed with water and brine, dried over Na_2SO_4 . The organic layer was concentrated in vacuo, purified by the silica gel chromatography (ethyl acetate: hexane 1:3 to 1:2) to provide the product (3.6 g, 60%) (M.P. = 102-103°C) as a yellow solid. ^1H NMR (CDCl_3 , 400 MHz) δ 10.41 (s, 1H), 8.42 (s, 1H), 7.73 (s, 1H), 7.39 (d, $J = 4.5$ Hz, 5H), 7.36 (s, 1H), 7.26 (t, $J = 7.6$ Hz, 6H), 7.19 (t, $J = 7.5$ Hz, 4H), 6.79 (d, $J = 7.5$ Hz, 1H), 4.24 (t, $J = 4.9$ Hz, 2H), 3.98 (d, $J = 17.8$ Hz, 5H), 3.77 (t, $J = 4.7$ Hz, 2H), 3.67 (dd, $J = 5.6, 3.8$ Hz, 2H), 3.59 (t, $J = 4.9$ Hz, 2H), 3.45 (t, $J = 4.7$ Hz, 2H), 3.29 (t, $J = 6.9$ Hz, 2H), 2.42 (t, $J = 7.0$ Hz, 2H).
 ^{13}C NMR (101 MHz, CDCl_3) δ 170.34, 156.16, 153.27, 144.86, 131.86, 130.56, 129.65, 127.99, 127.90, 126.66, 123.82, 121.45, 114.39, 107.31, 107.04, 77.41, 77.09, 76.78, 71.04, 70.73, 70.55, 70.18, 69.77, 69.60, 68.00, 66.60, 52.61, 31.65.

methyl 3-(ethoxymethoxy)-5-((1,1,1-triphenyl-5,8,11-trioxa-2-thiatridecan-13-yl)oxy)-2-naphthoate (2.7) To a suspension of NaH (0.08 g, 3.48 mmol) in THF (5 mL) at -7 °C, a solution of compound **2.6** in THF was added and stirred for 15 min in -7 °C. Then, (chloromethoxy)ethane (0.08 g, 0.85 mmol) was slowly added slowly warmed up

to room temperature and stirred for 5 h. The reaction was quenched by NH₄Cl solution, separated between ethyl acetate and water. The organic layer was washed with brine, dried over Na₂SO₄, concentrated in vacuo, purified by silica gel chromatography (ethyl acetate: hexanes 1:2) to afford the product (0.33 g, 100%) as a colorless oil. ¹H NMR (400 MHz, CDCl₃) δ 8.17 (d, *J* = 7.9 Hz, 1H), 7.81 (d, *J* = 5.1 Hz, 1H), 7.33 (d, *J* = 7.8 Hz, 7H), 7.20 (d, *J* = 7.3 Hz, 6H), 7.11 (t, *J* = 7.2 Hz, 3H), 6.77 (d, *J* = 7.5 Hz, 1H), 5.31 (d, *J* = 2.2 Hz, 2H), 4.21 (t, *J* = 5.0 Hz, 2H), 3.95 – 3.85 (m, 4H), 3.79 – 3.68 (m, 4H), 3.59 (dd, *J* = 5.7, 3.8 Hz, 2H), 3.49 (hept, *J* = 5.3 Hz, 3H), 3.40 – 3.31 (m, 2H), 3.21 (t, *J* = 6.9 Hz, 2H), 2.34 (t, *J* = 6.9 Hz, 2H), 1.17 (p, *J* = 9.1, 8.1 Hz, 9H), 0.85 – 0.71 (m, 4H). ¹³C NMR (101 MHz, CDCl₃) δ 166.80, 153.53, 152.82, 144.83, 132.08, 129.63, 128.16, 127.90, 126.66, 124.78, 120.97, 107.09, 106.61, 94.06, 77.38, 77.06, 76.75, 71.09, 70.80, 70.53, 70.16, 69.74, 69.61, 68.16, 66.59, 64.60, 52.26, 31.64, 29.74, 15.18.

(3-(ethoxymethoxy)-5-((1,1,1-triphenyl-5,8,11-trioxa-2-thiatridecan-13-yl)oxy)naphthalen-2-yl)methanol (2.8) A suspension of LAH (16 mL 2.4 M, 38 mmol) in anhydrous THF (150 mL) was stirred at 0 °C, and a solution of compound **2.7** (8.9 g, 12.5 mmol) in anhydrous THF (50 mL) was slowly added to the mixture. The reaction was stirring in 0 °C for 1.5 h, quenched by adding water dropwise until no gas was formed, extracted by ethyl acetate. The organic layer was washed with brine and dried over Na₂SO₄, filtered, concentrated in vacuo to afford the product (7.7 g, 91%) as a colorless oil. ¹H NMR (CDCl₃, 400 MHz) δ 7.71 (s, 1H), 7.64 (s, 1H), 7.37 – 7.24 (m, 7H), 7.24 – 7.06 (m, 10H), 6.70 (dd, *J* = 7.7, 1.0 Hz, 1H), 5.31 (s, 2H), 4.75 (d, *J* = 5.2 Hz, 2H), 4.20 (dd, *J* = 5.7, 4.2 Hz, 2H), 3.90 (dd, *J* = 5.6, 4.3 Hz, 2H), 3.80 – 3.61 (m, 4H), 3.61 – 3.55 (m, 2H), 3.55 – 3.46 (m, 2H), 3.40 – 3.32 (m, 2H), 3.21 (t, *J* = 6.9 Hz,

2H), 2.34 (t, $J = 6.9$ Hz, 2H), 1.16 (t, $J = 7.1$ Hz, 4H). ^{13}C NMR (101 MHz, CDCl_3) δ 153.72, 153.14, 144.84, 131.31, 130.25, 129.64, 127.90, 127.22, 126.67, 126.03, 124.21, 120.25, 105.54, 103.95, 93.58, 77.41, 77.09, 76.77, 71.06, 70.81, 70.53, 70.17, 69.80, 69.62, 68.08, 66.61, 64.77, 62.25, 31.65, 15.22.

13-((6-((4-azidobutoxy)methyl)-7-(ethoxymethoxy)naphthalen-1-yl)oxy)-1,1,1-

triphenyl-5,8,11-trioxa-2-thiatridecane (2.9) A solution of compound **2.8** (3.8 g, 2.9 mmol) in THF (50 mL) was added to a suspension of NaH (3.2 g, 14.3 mmol) in THF (5 mL) at 0 °C under N_2 protection. The reaction mixture was stirred at 80 °C for 1 h and cooled down to room temperature. Then a solution of 1-azido-4-iodobutane (1.95 g, 8.7 mmol) in THF (3 mL) was added dropwise and reaction was stirred under reflux overnight. The reaction was quenched with NH_4Cl solution and extracted by ethyl acetate. The organic layer was washed with brine, dried and concentrated in vacuo, purified by silica gel chromatography (ethyl acetate: hexanes 1:2) to afford the product (2.5 g, 58%) as a colorless oil as well as recovered starting material (1.1 g, 28%). ^1H NMR (CDCl_3 , 400 MHz) δ 7.69 (d, $J = 2.3$ Hz, 2H), 7.36 – 7.24 (m, 7H), 7.21 – 7.04 (m, 10H), 6.67 (dd, $J = 7.7, 0.9$ Hz, 1H), 5.27 (s, 2H), 4.60 (d, $J = 1.0$ Hz, 2H), 4.17 (dd, $J = 5.6, 4.3$ Hz, 2H), 3.88 (dd, $J = 5.6, 4.3$ Hz, 2H), 3.76 – 3.60 (m, 4H), 3.60 – 3.54 (m, 2H), 3.54 – 3.44 (m, 4H), 3.38 – 3.31 (m, 2H), 3.25 – 3.15 (m, 4H), 2.33 (t, $J = 6.9$ Hz, 2H), 1.71 – 1.59 (m, 4H), 1.23 – 1.10 (m, 4H). ^{13}C NMR (101 MHz, CDCl_3) δ 153.71, 152.79, 144.87, 130.16, 129.67, 129.12, 127.94, 127.12, 126.70, 125.90, 124.00, 120.30, 105.34, 103.50, 93.31, 77.51, 77.19, 76.87, 71.10, 70.83, 70.54, 70.19, 70.04, 69.83, 69.63, 68.23, 68.11, 66.63, 64.53, 51.36, 31.68, 27.04, 25.96, 15.28.

2-(2-(2-(2-((6-((4-azidobutoxy)methyl)-7-(ethoxymethoxy)naphthalen-1-

yl)oxy)ethoxy)ethoxy)ethoxy)ethane-1-thiol (2.10) Triisopropylsilane (0.1 mL, 0.49 mmol) was added to a solution of compound **2.9** (0.15 g, 0.19 mmol) and trifluoroacetic acid (0.2 mL, 2.6 mmol) in CH₂Cl₂ (5 mL). The reaction was stirred under room temperature under N₂ for 3 hours, concentrated in vacuo and purified via silica gel chromatography (ethyl acetate: hexanes 1:2 to 1:1) to provide the product (trace amount) as a yellow oil. ¹H NMR (400 MHz, CDCl₃) δ 7.61 (s, 1H), 7.49 (s, 1H), 7.26 (d, *J* = 8.2 Hz, 1H), 7.17 – 7.08 (m, 1H), 6.78 – 6.67 (m, 1H), 4.77 – 4.71 (m, 2H), 4.59 (s, 2H), 4.24 – 4.17 (m, 2H), 3.93 – 3.86 (m, 2H), 3.79 – 3.45 (m, 14H), 3.25 (t, *J* = 6.3 Hz, 2H), 2.74 (t, *J* = 6.9 Hz, 2H), 1.66 (dddd, *J* = 11.8, 9.0, 4.8, 2.4 Hz, 4H), 1.12 (t, *J* = 7.0 Hz, 3H). ¹³C NMR (101 MHz, CDCl₃) δ 153.54, 153.51, 129.30, 127.27, 127.03, 125.65, 123.38, 120.31, 105.85, 105.65, 77.36, 77.05, 76.73, 73.80, 71.46, 71.05, 70.72, 70.31, 69.98, 69.81, 68.23, 63.60, 51.20, 30.32, 26.83, 25.73, 14.81.

3-azidopropan-1-ol (2.11) 3-Bromo-1-propanol (5 g, 36 mmol) and sodium azide (5 g, 77 mmol) were dissolved in a mixture of acetone (60 mL) and water (10 mL) and the resulting solution was heated to reflux overnight. After removing acetone under reduced pressure, 40 mL of water were added and the mixture was extracted with diethyl ether (4 × 40 mL). The organic layers collected were dried over Na₂SO₄, filtered, and concentrated in vacuo to give the product (3.6g 100%) as a colorless liquid. ¹H NMR (400 MHz, Chloroform-*d*) δ 3.57 (td, *J* = 10.4, 9.8, 5.4 Hz, 2H), 3.30 (dq, *J* = 12.4, 6.4 Hz, 2H), 1.68 (dp, *J* = 12.7, 6.3 Hz, 2H). ¹³C NMR (101 MHz, CDCl₃) δ 78.09, 77.76, 77.44, 59.56, 48.59, 31.81, 0.22.

methyl 3,5-bis(ethoxymethoxy)-2-naphthoate (2.12) To a stirring solution of NaH (2.5 g 60% weight in oil, 62 mmol) in THF (90 mL) at -7 °C was added solution of starting

ester compound **2.3** (3.3 g, 15 mmol) in THF (90 mL) dropwise. Then, (chloromethoxy)ethane (3.5 g, 37.6 mmol) was slowly added. The reaction was stirred in 0 °C for 2 h, quenched with saturated NH₄Cl, extracted by ethyl acetate. The organic layer was washed with water, brine, dried over Na₂SO₄, filtered, concentrated in vacuo and purified by silica gel chromatography (ethyl acetate: hexanes 1:9) to yield the product (3.8 g, 78%) as a yellow oil. ¹H NMR (400 MHz, Chloroform-*d*) δ 8.27 (d, *J* = 4.1 Hz, 1H), 7.88 (s, 1H), 7.46 (d, *J* = 8.2 Hz, 1H), 7.43 – 7.24 (m, 1H), 7.18 (d, *J* = 7.6 Hz, 1H), 5.43 (d, *J* = 1.5 Hz, 4H), 3.95 (s, 3H), 3.83 (dp, *J* = 11.8, 6.9 Hz, 4H), 1.35 – 1.19 (m, 7H). ¹³C NMR (101 MHz, CDCl₃) δ 166.74, 152.81, 152.09, 133.46, 132.17, 132.03, 129.20, 128.37, 125.93, 124.84, 123.42, 122.72, 121.78, 113.05, 110.13, 106.03, 100.78, 94.29, 93.80, 93.58, 77.38, 77.06, 76.74, 65.93, 64.61, 64.58, 52.23, 15.18, 15.11, -0.00.

(3,5-bis(ethoxymethoxy)naphthalen-2-yl)methanol (2.13) A solution of compound **2.12** in THF (25 mL) was added dropwise to a stirring suspension of LAH (9.5 mL 2.4 M LAH in THF, 22.8 mmol) in THF (40 mL) at 0 °C. The reaction was stirred under room temperature for 1 h, quenched with NH₄Cl solution, and separated between ethyl acetate and water. The organic layer was washed with brine, dried over Na₂SO₄, filtered, concentrated under vacuum, and purified by silica gel chromatography (ethyl acetate: hexanes 1:9) to yield the product (2 g, 57%) as a pale-yellow oil. ¹H NMR (400 MHz, Chloroform-*d*) δ 7.71 (dd, *J* = 17.8, 4.2 Hz, 2H), 7.35 (d, *J* = 8.1 Hz, 1H), 7.21 (d, *J* = 8.0 Hz, 1H), 7.10 – 7.03 (m, 1H), 5.37 (d, *J* = 12.4 Hz, 5H), 4.79 (s, 2H), 3.74 (dq, *J* = 26.6, 7.0 Hz, 5H), 1.21 (td, *J* = 7.0, 6.0 Hz, 7H). ¹³C NMR (101 MHz, CDCl₃) δ 152.98,

152.21, 131.36, 130.25, 126.95, 126.14, 124.15, 121.04, 108.38, 103.27, 93.52, 93.22, 77.48, 77.16, 76.84, 64.64, 64.47, 61.66, 15.17, 15.10, 0.00.

6-(bromomethyl)-1,7-bis(ethoxymethoxy)naphthalene (2.14) Bromine (3.6 g, 1.2 mL, 22 mmol) was added to a stirring solution of triphenylphosphine (6.9 g, 26 mmol) and imidazole (1.8 g, 26 mmol) in DCM (250 mL) at 0 °C and stirred for 10 min. Then, a solution of compound **2.13** (5.4 g, 17.6 mmol) in CH₂Cl₂ (150 mL) was added to the mixture. The reaction was stirred for 15 min and filtered. The filtrate was washed by sodium thiosulfate solution, water, and brine, dried over Na₂SO₄. The organic layer was filtered, concentrated in vacuo, purified by silica gel chromatography (ethyl acetate: hexanes 1:9) to provide the product as a white solid (4.6 g, 71%). ¹H NMR (400 MHz, Chloroform-*d*) δ 7.77 (dd, *J* = 7.7, 3.2 Hz, 2H), 7.45 – 7.29 (m, 1H), 7.25 (t, *J* = 7.9 Hz, 1H), 7.10 (dd, *J* = 7.7, 1.0 Hz, 1H), 5.48 – 5.38 (m, 4H), 4.69 (s, 2H), 3.95 (s, 1H), 3.81 (dq, *J* = 16.2, 7.1 Hz, 4H), 1.24 (dt, *J* = 10.0, 7.1 Hz, 7H). ¹³C NMR (101 MHz, CDCl₃) δ 152.59, 152.19, 130.07, 129.96, 129.89, 128.19, 126.99, 124.39, 124.30, 120.97, 119.86, 108.99, 104.67, 103.75, 103.70, 93.51, 92.95, 92.92, 77.37, 77.05, 76.74, 64.75, 64.67, 64.47, 55.43, 29.41, 29.38, 15.18, 15.14, -0.00.

6-((3-azidopropoxy)methyl)-1,7-bis(ethoxymethoxy)naphthalene (2.15) 3-azidopropan-1-ol (2.7 g, 27 mmol) in THF (50 mL) was added to a stirring solution of NaH (3.2 g 60% wt in oil, 80 mmol) in THF (100 mL) under N₂ at 0 °C and stirred for 5 min. Then, compound **2.14** (5.1 g, 13.8 mmol) in THF (70 mL) was added to the mixture and the reaction was warmed to room temperature and stirred 24 h. The reaction mixture was quenched by ammonium chloride solution and separated between ethyl acetate and water. The organic layer was washed by brine and dried over Na₂SO₄, concentrated in

vacuo, purified by silica gel chromatography (ethyl acetate: hexanes 1:9) to afford the product (2 g, 37%) as a colorless oil as well as recovered starting material (1.5 g, 30%). ¹H NMR (400 MHz, Chloroform-*d*) δ 7.86 – 7.71 (m, 2H), 7.42 (d, *J* = 8.2 Hz, 1H), 7.28 – 7.19 (m, 1H), 7.08 (dd, *J* = 7.8, 1.0 Hz, 1H), 5.40 (d, *J* = 2.9 Hz, 4H), 4.69 (s, 2H), 3.77 (dq, *J* = 10.2, 7.1 Hz, 4H), 3.64 (t, *J* = 6.0 Hz, 2H), 3.44 (t, *J* = 6.8 Hz, 2H), 1.91 (p, *J* = 6.4 Hz, 2H), 1.34 – 1.18 (m, 7H). ¹³C NMR (101 MHz, CDCl₃) δ 152.80, 152.25, 130.15, 128.81, 127.30, 126.19, 124.05, 121.03, 108.34, 103.11, 93.56, 93.10, 77.47, 77.15, 76.83, 68.33, 67.26, 64.48, 64.44, 48.54, 29.29, 15.20, 15.16, 0.00.

6-((3-azidopropoxy)methyl)naphthalene-1,7-diol (2.16) Amberlyst-15 resin (1 g) was added to a solution of compound **2.15** (1.6 g, 4.1 mmol) in methanol (40 mL). The reaction was stirred under room temperature for 8 h, filtered, concentrated in vacuo, and purified by silica gel chromatography (ethyl acetate: hexanes 1:3) to give the product (0.8 g, 73%) as a red-brown liquid. ¹H NMR (400 MHz, Chloroform-*d*) δ 7.57 (s, 1H), 7.51 (s, 1H), 7.29 (d, *J* = 8.1 Hz, 1H), 7.10 (t, *J* = 7.8 Hz, 1H), 6.84 – 6.66 (m, 1H), 4.79 (s, 2H), 3.61 (t, *J* = 6.0 Hz, 2H), 3.38 (t, *J* = 6.6 Hz, 2H), 1.87 (p, *J* = 6.4 Hz, 2H), 1.25 (dt, *J* = 18.0, 7.0 Hz, 1H). ¹³C NMR (101 MHz, CDCl₃) δ 153.23, 150.48, 129.72, 127.91, 125.68, 125.27, 123.72, 120.25, 109.30, 105.42, 77.45, 77.13, 76.81, 71.99, 67.56, 48.38, 28.92, 0.07.

3-(hydroxymethyl)-8-((1,1,1-triphenyl-5,8,11-trioxa-2-thiatridecan-13-yl)oxy)naphthalen-2-ol (2.18) A solution of compound **2.6** (1 g, 1.5 mmol) in THF (8 mL) was slowly added to a stirring suspension of LAH (solid, 0.2 g, 4.5 mmol) in THF (7 mL) at 0 °C. The reaction was stirred under room temperature for 2 h, quenched by NH₄Cl solution and extracted by ethyl acetate. The organic layer was washed by water,

dried over Na₂SO₄, concentrated in vacuo, and purified by silica gel chromatography (ethyl acetate: hexanes 1:2) to yield (0.5 g, 52%) product as yellow oil. ¹H NMR (400 MHz, Chloroform-*d*) δ 8.01 (s, 1H), 7.62 (s, 1H), 7.47 (s, 1H), 7.43 – 7.33 (m, 6H), 7.31 – 7.19 (m, 7H), 7.19 – 7.06 (m, 4H), 6.69 (d, *J* = 7.5 Hz, 1H), 4.81 (s, 2H), 4.27 – 4.03 (m, 2H), 3.88 – 3.79 (m, 2H), 3.70 (dd, *J* = 5.8, 3.3 Hz, 2H), 3.63 (dd, *J* = 5.7, 3.3 Hz, 2H), 3.61 – 3.53 (m, 2H), 3.50 – 3.40 (m, 2H), 3.28 (t, *J* = 6.9 Hz, 3H), 2.41 (t, *J* = 6.9 Hz, 2H), 1.19 (d, *J* = 7.1 Hz, 1H). ¹³C NMR (101 MHz, CDCl₃) δ 153.29, 144.70, 129.54, 129.32, 128.72, 127.84, 126.84, 126.82, 126.61, 123.16, 120.50, 106.03, 105.12, 77.38, 77.06, 76.74, 70.81, 70.57, 70.49, 70.05, 69.67, 69.62, 68.18, 66.58, 63.40, 60.44, 31.46, 0.00.

3-((3-hydroxypropoxy)methyl)-8-((1,1,1-triphenyl-5,8,11-trioxa-2-thiatridecan-13-yl)oxy)naphthalen-2-ol (2.19) Titanium tetrachloride (0.5 g, 2.6 mmol) was added to a stirring mixture of compound **2.18** (1.3 g, 2.08 mmol) and 1,3 propanediol (25 mL, 1.06g/ml, 349 mmol). The reaction mixture was stirred at 80 °C for 2 h. After cooling to room temperature, the reaction mixture was partitioned between ethyl acetate (30ml) and water (30ml). The organic layer was dried over Na₂SO₄, filtered, evaporated, and purified by silica gel chromatography (ethyl acetate: hexanes 1:1) to afford the product (1.3 g, 92%). ¹H NMR (400 MHz, Chloroform-*d*) δ 7.84 – 7.09 (m, 19H), 6.74 (d, *J* = 7.6 Hz, 1H), 4.78 (s, 2H), 4.23 (q, *J* = 5.0, 4.2 Hz, 2H), 3.90 (q, *J* = 4.7, 4.0 Hz, 2H), 3.84 – 3.71 (m, 6H), 3.64 (ddd, *J* = 19.8, 5.3, 3.1 Hz, 4H), 3.47 (dd, *J* = 5.8, 3.8 Hz, 2H), 3.31 (t, *J* = 6.9 Hz, 2H), 2.43 (t, *J* = 7.0 Hz, 2H), 1.88 (h, *J* = 6.1 Hz, 2H), 1.35 – 1.12 (m, 2H). ¹³C NMR (101 MHz, CDCl₃) δ 153.46, 153.38, 144.78, 129.59, 129.26, 127.86, 127.62,

127.07, 126.62, 125.82, 123.29, 120.32, 105.90, 105.56, 77.36, 77.04, 76.72, 71.26, 70.95, 70.67, 70.57, 70.14, 69.73, 69.63, 69.03, 68.18, 66.58, 61.10, 31.93, 31.53, 0.00.

3-((3-bromopropoxy)methyl)-8-((1,1,1-triphenyl-5,8,11-trioxa-2-thiatridecan-13-yl)oxy)naphthalen-2-ol (2.20) Carbontetrabromide (0.18 g, 0.54 mmol) was added to a solution of triphenylphosphine (0.14 g, 0.5 mmol) in CH₂Cl₂ (2 mL), at 0 °C and stirred for 5min. Then, Compound **2.19** (0.15 g, 0.22 mmol) in CH₂Cl₂ (3 mL) was slowly added to the mixture. The reaction was warmed up to room temperature and stirred for 6-10 h. The reaction mixture was concentrated in and purified by silica gel chromatography (ethyl acetate: hexanes 1:1) to yield product (very nonpolar, the minor product, 0.05 g, 31%) as a colorless oil. ¹H NMR (400 MHz, Chloroform-*d*) δ 7.62 (d, *J* = 37.1 Hz, 2H), 7.51 – 7.09 (m, 18H), 6.77 (dd, *J* = 10.3, 7.5 Hz, 1H), 4.80 (s, 2H), 4.24 (dd, *J* = 5.6, 3.9 Hz, 2H), 3.91 (dd, *J* = 5.6, 3.8 Hz, 2H), 3.76 (dd, *J* = 5.8, 3.4 Hz, 2H), 3.73 – 3.65 (m, 4H), 3.62 (dd, *J* = 5.8, 3.8 Hz, 2H), 3.52 (t, *J* = 6.5 Hz, 2H), 3.50 – 3.42 (m, 2H), 3.31 (t, *J* = 6.9 Hz, 2H), 2.43 (t, *J* = 6.9 Hz, 2H), 2.17 (p, *J* = 6.2 Hz, 2H), 1.25 (s, 1H). ¹³C NMR (101 MHz, CDCl₃) δ 153.55, 153.35, 144.82, 129.64, 129.34, 127.95, 127.90, 127.39, 127.11, 126.66, 125.67, 123.40, 120.39, 106.04, 105.64, 77.39, 77.07, 76.76, 71.37, 71.01, 70.71, 70.61, 70.19, 69.78, 69.68, 68.31, 68.13, 66.63, 32.60, 31.57, 30.25, 0.04.

3-((3-azidopropoxy)methyl)-8-((1,1,1-triphenyl-5,8,11-trioxa-2-thiatridecan-13-yl)oxy)naphthalen-2-ol (2.21) Sodium azide (0.1 g, 1.5 mmol) was added to a stirring solution of compound **2.20** (0.1 g, 0.13 mmol) in DMF (3 mL). The reaction was stirring at 80 °C for 12 h, redissolved in ethyl acetate (100 mL). The organic layer was washed by water (5 mL×10), brine (10 mL), evaporated and purified by silica gel chromatography

(ethyl acetate: hexanes 1:2 to 1:1) to yield the product (0.5 g, 53%) as a light green oil.

^1H NMR (400 MHz, Chloroform-*d*) δ 7.73 – 7.27 (m, 12H), 7.25 – 7.09 (m, 9H), 6.74 (d, $J = 7.5$ Hz, 1H), 4.78 (s, 2H), 4.23 (t, $J = 4.8$ Hz, 2H), 3.90 (dd, $J = 5.7, 3.8$ Hz, 2H), 3.75 (dd, $J = 5.8, 3.5$ Hz, 2H), 3.71 – 3.58 (m, 6H), 3.47 (dd, $J = 5.8, 3.7$ Hz, 2H), 3.41 (t, $J = 6.7$ Hz, 2H), 3.31 (t, $J = 6.9$ Hz, 2H), 2.43 (t, $J = 7.0$ Hz, 2H), 1.89 (t, $J = 6.3$ Hz, 2H), 0.08 (s, 1H). ^{13}C NMR (101 MHz, CDCl_3) δ 153.54, 153.33, 144.83, 129.65, 129.35, 127.96, 127.91, 127.42, 127.28, 127.09, 126.68, 125.71, 123.40, 120.38, 105.99, 105.64, 77.44, 77.13, 76.81, 71.26, 71.00, 70.72, 70.62, 70.19, 69.79, 69.68, 68.27, 67.42, 66.64, 48.44, 31.59, 29.07.

3-((3-azidopropoxy)methyl)-8-(2-(2-(2-

mercaptoethoxy)ethoxy)ethoxy)ethoxy)naphthalen-2-ol (2.22) Triisopropylsilane (0.03 mL) was added to a stirring solution of compound **2.21** (0.05 g, 0.07 mmol) in CH_2Cl_2 (1.5 mL). Then, trifluoroacetic acid (0.05 mL) in CH_2Cl_2 (1.5 mL) was added dropwise to the mixture. The reaction was stirred for 5 h, quenched with NaHCO_3 solution. The organic layer was washed by water, brine. evaporated, and purified by silica gel chromatography (ethyl acetate: hexanes 1:1) to afford the product (0.2 g, 61%) as a light yellow oil. ^1H NMR (400 MHz, Chloroform-*d*) δ 7.67 (s, 1H), 7.65 (s, 1H), 7.58 (s, 1H), 7.33 (d, $J = 8.2$ Hz, 1H), 7.18 (t, $J = 7.9$ Hz, 1H), 6.75 (d, $J = 7.6$ Hz, 1H), 4.77 (s, 2H), 4.24 (dd, $J = 5.6, 3.8$ Hz, 2H), 3.96 – 3.88 (m, 2H), 3.78 (dd, $J = 5.8, 3.2$ Hz, 2H), 3.75 – 3.57 (m, 10H), 3.42 (t, $J = 6.7$ Hz, 2H), 2.66 (dt, $J = 8.4, 6.5$ Hz, 3H), 1.90 (p, $J = 6.4$ Hz, 2H), 1.59 (t, $J = 8.3$ Hz, 1H). ^{13}C NMR (101 MHz, CDCl_3) δ 171.24, 153.31, 153.14, 129.25, 127.39, 126.80, 126.10, 123.22, 120.35, 105.75, 105.13, 77.56, 77.24, 76.93, 72.85, 70.85, 70.57, 70.53, 70.48, 70.10, 69.69, 68.02, 67.32, 60.41, 48.38, 28.98,

24.07, 21.01, 14.16, -0.00. ESI, m/z: calcd. for C₂₂H₃₁N₃O₆S calcd. [M – H]⁻ 464.2, found 464.1. calcd. [M+Na]⁺ 488.2, found 488.3.

2.7 References

- [1] Wang, A. Z., Langer, R., & Farokhzad, O. C. Nanoparticle delivery of cancer drugs. *Annual review of medicine*. **2012**, *63*, 185-198
- [2] Han, Gang, Partha Ghosh, and Vincent M. Rotello. Functionalized gold nanoparticles for drug delivery. *Future Medicine*. **2007**, 113-123.
- [3] Gibson, J. D., Khanal, B. P., & Zubarev, E. R. Paclitaxel-functionalized gold nanoparticles. *Journal of the American Chemical Society*. **2007**, *129*(37), 11653-11661.
- [4] Luo, W., Gobbo, P., McNitt, C.D., Sutton, D.A., Popik, V.V. and Workentin, M.S., “Shine & Click” Photo-Induced Interfacial Unmasking of Strained Alkynes on Small Water-Soluble Gold Nanoparticles. *Chemistry–A European Journal*. **2017**, *23*(5), 1052-1059.
- [5] Holakovský, R., Hovorka, M., & Stibor, I. Preparation of New Binaphthol-Based Tridentate Ligands for Enantioselective Synthesis. *Collection of Czechoslovak Chemical Communications*. **2000**, *65*(5), 805-815.

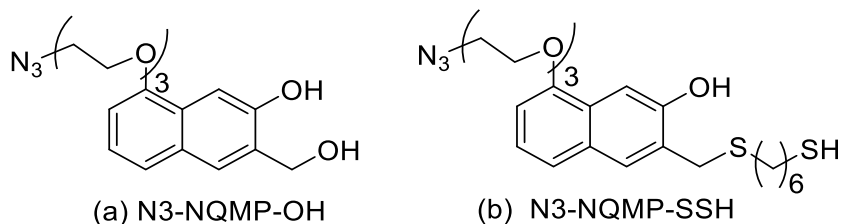
CHAPTER 3

N3-NQMP-SSH SYNTHESIS FOR REVERSIBLE SURFACE DERIVATIZATION

3.1 Introduction

Surface derivatization finds wide applications in bio-analysis, diagnoses, and sensor development.^{1,2} A common way to achieve surface derivatization is through self-assembled monolayers (SAMs) via gold-thiol linkage.³ The Au-S binding has high affinity and stability; and rarely participate in other side reactions. To develop surface with switchable properties, which is also known as smart surfaces, external stimuli such as chemical/biochemical, thermal, electric, and optical stimuli are often employed.⁴ In particular, light stimuli provide precise spatial and temporal control of the process and can also achieve reversible modifications.

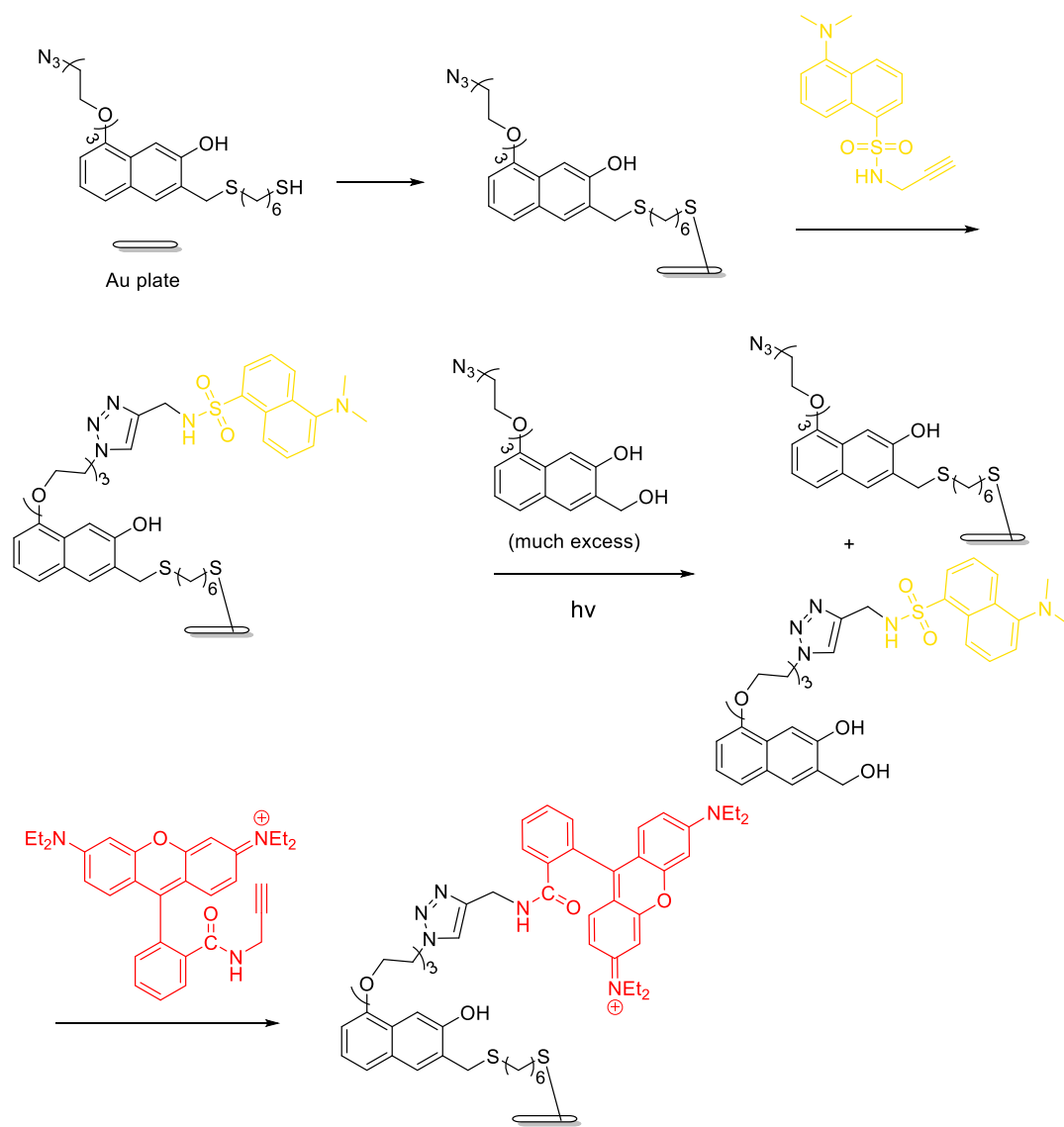
The NQMP derivatives (N3-NQMP-OH and N3-NQMP-SSH) designed for reversible surface derivatization purpose are shown below (Scheme 3.1). Such NQMP derivatives can be used as photo-controllable labeling tools to reversibly derivatize gold surfaces.



Scheme 3.1 Structures of (a) N3-NQMP-OH and (b) N3-NQMP-SSH

The thiol group on compound N3-NQMP-SSH enables the initial attachment of the molecule to Au plate through stable Au-S bond. The two NQMPs both can produce *o*-NQMP upon UV irradiation. They are equipped with azide group as an efficient handle for further modification and triethylene glycol group helps with water solubility. Our focus was to synthesize the target compounds for subsequent applications performed by our collaborators.

To test the potential of this method for reversible surface derivatization, N3-NQMP-SSH would be first applied to gold plate for adsorption to form a monolayer. Then, dansyl-alkyne as a fluorescent compound would be introduced to the plate (through CuAAC reaction) as an example payload for convenient visualization (fluorescence-on) to confirm the NQMP attachment. Then, excess of N3-NQMP-OH would be added to the system and subjected to UV light (300 nm) irradiation. Since the *o*-NQMP formation from N3-NQMP-OH ($\Phi = 0.2$) is twice than that from N3-NQMP-SSH ($\Phi = 0.1$), and *o*-NQMP's reaction for thiol-Michael addition reaction ($k_{\text{RSH}} \approx 2.2 \times 10^5 \text{ M}^{-1}\text{s}^{-1}$) is much faster than its hydration with water ($k_{\text{H}_2\text{O}} \approx 145 \text{ M}^{-1}\text{s}^{-1}$).⁵ Therefore, the first modification on surface would be removed via *o*-NQMP formation and the resultant benzylic C-S bond cleavage. Meanwhile, the *o*-NQMP formed from N3-NQMP-OH is readily available and immediately undergoes thiol-Michael addition to attach to the gold surface. As a result, the dansyl-NQMP would be completely replaced by the new NQMP, leading to the fluorescence-off of the gold plate. After removing the solution containing dansyl-NQMP from the gold surface, the plate would be treated with rhodamine B-alkyne so that the fluorescence is regenerated due to the formation of rhodamine B-NMQP (Scheme 3.2).

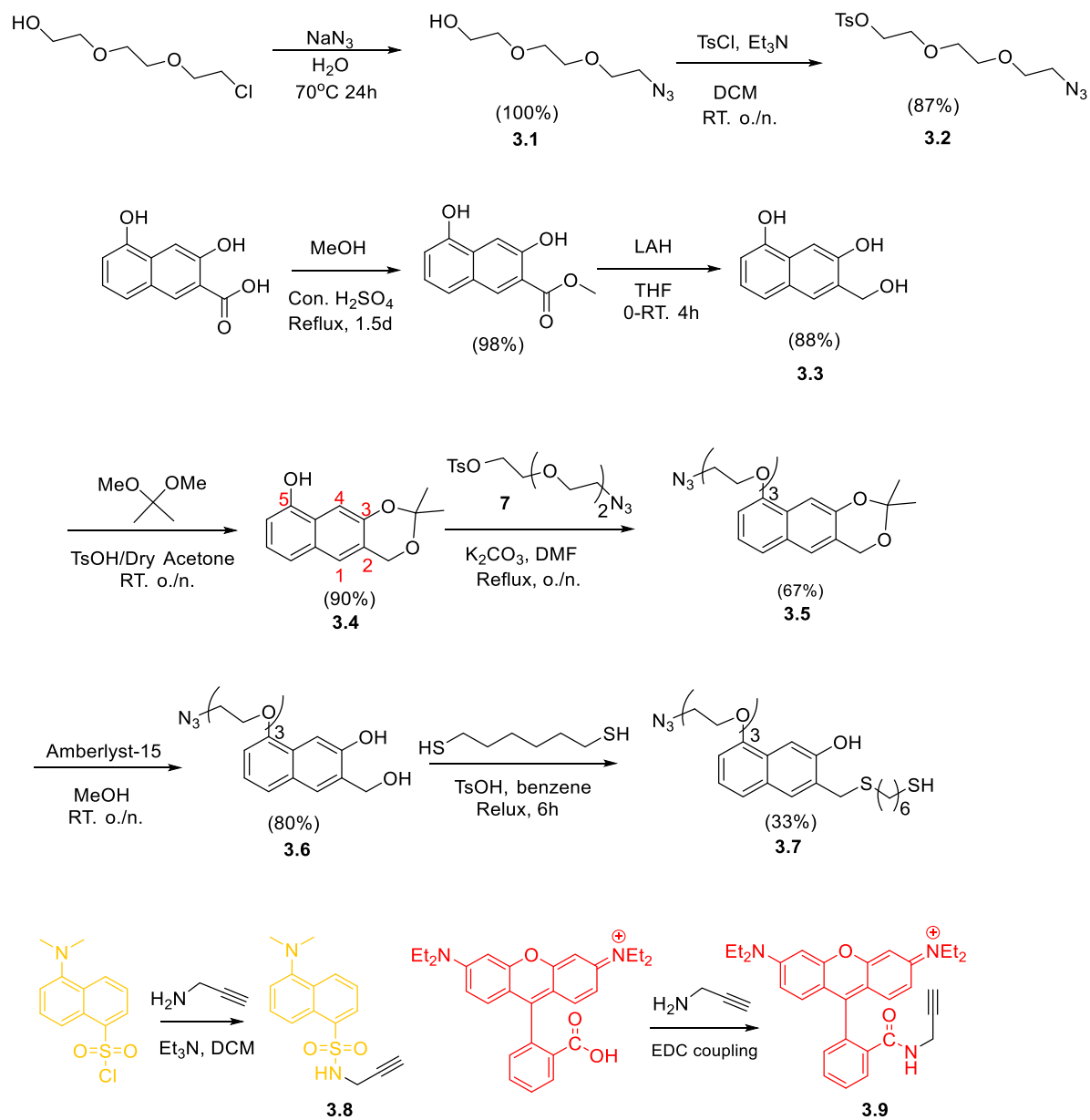


Scheme 3.2 N3-NQMP-SSH for reversible surface derivatization

This method can achieve reversible derivatization of gold surface and spatial and temporal control of the derivatization. The uniqueness of this pathway is that the NQMP derivatives also act as temporary protecting groups to the gold surface from free thiol group's back attack after first modification was removed, because NQMP outcompetes gold to react with the thiol group.

3.2 Design and Synthesis of N3-NQMP-SSH

The synthesis of target compounds for the application of reversible surface derivatization are shown below (Scheme 3.3).



Scheme 3.3 Synthesis of target compounds

The azide linker was prepared from 2-(2-(2-chloroethoxy)ethoxy)ethan-1-ol, of which the chlorine was replaced with azide and alcohol was tosylated. The NQMP backbone was built from 3,5-dihydroxy-2-naphthoic acid's esterification, reduction, and protection of the 1,3-diol using acetal. This made the 5-OH ready to be derivatized with the azide linker via S_N2 reaction. Removal of acetal in acidic condition generated N3-NQMP-OH (compound **3.6**). The **3.6** was ready for addition of hexane-1,6-dithiol with acid catalysis under heat through generation of quinone methide *in situ* to afford N3-NQMP-SSH (compound **3.7**). Compounds **3.8** and **3.9** were then obtained by alkyne derivatization of dansyl and rhodamine-B through amine nucleophilic addition and EDC coupling reaction, respectively.

3.3 Conclusion

The synthesis of compound NQMP-OH was proved successful although the step for preparing NQMP-SSH did not have a quantitative yield (33%). However, the NQMP-SSH preparation showcased the feasibility of modification of the benzylic alcohol without protecting the phenolic OH. Also, since it is the last step of the synthetic pathway, the low yield did not affect the viability of the whole synthetic route. With all the target compounds synthesized and characterized, the reversible surface derivatization will be performed by the collaborator.

3.4 Experimental Section

2-(2-(2-azidoethoxy)ethoxy)ethan-1-ol (3.1) Sodium azide (12 g, 178 mmol) was added to a stirring solution of 2-(2-(2-chloroethoxy)ethoxy)ethan-1-ol (15 g, 89 mmol) in DI water (45 mL). The reaction was heated to 75 °C for 48 h, evaporated by air flow. The crude product was extracted by ether and concentrated in vacuo to yield the product (14 g, 89%) as a colorless oil. IR: 2100 cm⁻¹ (N3 stretch) and 3300cm⁻¹ (OH stretch). ¹H NMR (400 MHz, cdcl₃) δ 3.78 – 3.71 (m, 2H), 3.71 – 3.64 (m, 6H), 3.64 – 3.59 (m, 2H), 3.46 – 3.35 (m, 2H), 2.30 (t, *J* = 6.2 Hz, 1H).

2-(2-(2-azidoethoxy)ethoxy)ethyl 4-methylbenzenesulfonate (3.2) To a solution of *p*-toluenesulfonyl chloride (22.9 g, 120 mmol) in CH₂Cl₂ (150 mL) at 0 °C, was added compound **3.1** (14 g, 80 mmol) and dry triethyl amine (16.2 g, 160 mmol). The reaction was then stirred at room temperature overnight. The precipitate was filtered, and the solution was concentrated in vacuo. The residue was purified via silica gel chromatography (ethyl acetate: hexanes 1:2) to afford the product (22.4 g, 85%) as a light yellow liquid. ¹H NMR (400 MHz, cdcl₃) δ 7.80 – 7.59 (m, 2H), 7.35 – 7.20 (m, 2H), 4.17 – 3.94 (m, 2H), 3.65 – 3.59 (m, 2H), 3.56 (dd, *J* = 5.5, 4.5 Hz, 2H), 3.51 (s, 4H), 3.34 – 3.22 (m, 2H), 2.36 (s, 3H).

6-(hydroxymethyl)naphthalene-1,7-diol (3.3) A solution of methyl 3,5-dihydroxy-2-naphthoate (2 g, 9.16 mmol) in dry THF (40 mL) was slowly added to a stirring suspension of LAH (1.04 g, 29.5 mmol) in dry THF (30 mL) at 0 °C. The reaction was warmed up to room temperature and stirred for 4 h, quenched with saturated NH₄Cl, extracted with ether. The organic layer was washed with saturated sodium bicarbonate, brine, dried over Na₂SO₄, filtered, concentrated in vacuo to provide the product (1 g,

57%) as a grey solid. ^1H NMR (400 MHz, Acetone- d_6) δ 8.75 (s, 1H), 8.70 (s, 1H), 7.78 (s, 1H), 7.57 (s, 1H), 7.29 (d, J = 8.1 Hz, 1H), 7.09 (dd, J = 8.2, 7.5 Hz, 1H), 6.82 (dd, J = 7.5, 1.0 Hz, 1H), 4.90 (dd, J = 5.6, 1.2 Hz, 2H), 4.51 (t, J = 5.6 Hz, 1H). ^{13}C NMR (101 MHz, Acetone) δ 205.60, 152.84, 151.72, 130.78, 129.97, 125.81, 125.35, 123.10, 118.95, 107.75, 103.79, 60.73, 29.58, 29.39, 29.20, 29.00, 28.81, 28.62, 28.43.

2,2-dimethyl-4H-naphtho[2,3-d][1,3]dioxin-9-ol (3.4)

2,2-Dimethoxypropane (4.9 g, 47 mmol) and catalytic amount of *p*-toluenesulfonic acid (50 mg) were added to a solution of compound **3.3** (3 g, 16 mmol) in dry acetone.

Reaction mixture was stirred at room temperature overnight, quenched with triethylamine (3 mL) and evaporated. The residue was re-dissolved in ethyl acetate, washed with brine, dried over sodium sulfate, filtered, concentrated in vacuo, and purified by silica gel chromatography (ethyl acetate: hexanes 1:4) to give product (3.2 g, 87%) as a yellow solid. ^1H NMR (400 MHz, cdCl_3) δ 7.58 (s, 1H), 7.42 (s, 1H), 7.27 (d, J = 15.4 Hz, 1H), 7.12 (t, J = 7.8 Hz, 1H), 6.73 (d, J = 7.4 Hz, 1H), 5.06 (d, J = 1.2 Hz, 2H), 2.19 (d, J = 0.9 Hz, 1H), 1.60 (s, 6H).

9-(2-(2-(2-azidoethoxy)ethoxy)ethoxy)-2,2-dimethyl-4H-naphtho[2,3-d][1,3]dioxine (3.5)

Potassium carbonate (5.8 g, 42 mmol) was added to a solution of acetal **3.4** (3.2 g, 14 mmol) in DMF (200 mL), followed by dropwise addition of compound **3.2** (6.9 g, 21 mmol) in DMF (20 mL). The reaction was heated at 95 °C for 8 h, cooled to room temperature and extracted with ethyl acetate. The organic layer was washed with water (200 mL \times 10), dried over sodium sulfate, evaporated, and purified by silica gel chromatography (ethyl acetate: hexanes 1:4) to yield the product (3.4 g, 64%) as an off white solid. ^1H NMR (400 MHz, cdCl_3) δ 7.66 (s, 1H), 7.42 (d, J = 1.4 Hz, 1H), 7.30 (d, J

= 8.3 Hz, 1H), 7.20 (t, $J = 7.9$ Hz, 1H), 6.72 (dd, $J = 7.6, 1.0$ Hz, 1H), 5.05 (d, $J = 1.3$ Hz, 2H), 4.27 (dd, $J = 5.7, 4.0$ Hz, 2H), 4.06 – 3.92 (m, 2H), 3.87 – 3.76 (m, 2H), 3.76 – 3.61 (m, 4H), 3.39 (t, $J = 5.0$ Hz, 2H), 1.60 (s, 6H). ^{13}C NMR (101 MHz, cdCl_3) δ 153.59, 149.36, 129.43, 126.12, 123.69, 123.09, 121.45, 119.83, 107.07, 104.52, 99.76, 77.36, 77.04, 76.73, 71.07, 70.72, 70.09, 69.90, 67.74, 61.19, 50.69, 24.96.

8-(2-(2-(2-azidoethoxy)ethoxy)ethoxy)-3-(hydroxymethyl)naphthalen-2-ol (3.6)

Amberlyst-15 resin (3 g) was added to a solution of compound **3.5** (3.5 g, 9 mmol) in methanol (80 mL) and stirred for 24 h. The reaction mixture was filtered, concentrated and purified by silica gel chromatography (ethyl acetate: hexanes 1:1) to afford the product (3.1 g, 100%) as a yellow liquid. ^1H NMR (400 MHz, cdCl_3) δ 7.66 (s, 1H), 7.54 (d, $J = 12.0$ Hz, 2H), 7.32 (d, $J = 8.2$ Hz, 1H), 7.19 (t, $J = 7.9$ Hz, 1H), 6.76 (d, $J = 7.6$ Hz, 1H), 4.93 (d, $J = 5.8$ Hz, 2H), 4.35 – 4.19 (m, 2H), 4.03 – 3.90 (m, 2H), 3.86 – 3.75 (m, 2H), 3.76 – 3.64 (m, 4H), 3.39 (t, $J = 5.0$ Hz, 2H), 2.73 (t, $J = 6.1$ Hz, 1H). ^{13}C NMR (101 MHz, cdCl_3) δ 153.25, 129.35, 128.35, 126.97, 126.64, 123.32, 120.40, 105.63, 105.23, 103.10, 77.38, 77.07, 76.75, 70.93, 70.64, 70.08, 69.91, 67.84, 63.66, 50.65. IR: 2104.68 medium sharp (N_3). 3317.07 broad (OH).

8-(2-(2-(2-azidoethoxy)ethoxy)ethoxy)-3-(((6-

mercaptohexyl)thio)methyl)naphthalen-2-ol (3.7) Dithiol (0.9 g, 5.9 mmol) and *p*-toluenesulfonic acid (10 mg) were added to a solution of Compound **3.6** (0.23 g, 0.66 mmol) in benzene (25 mL). The reaction mixture was heated to 80 °C for 6 h, washed by NaHCO_3 and brine. The organic layer was concentrated in vacuo, purified by chromatography column (1:3 ethyl acetate: hexanes 1:3) to afford the product (0.17 g, 53%) as a yellow liquid. ^1H NMR (400 MHz, CDCl_3) δ 7.63 (s, 1H), 7.48 (s, 1H), 7.25

(d, $J = 8.2$ Hz, 1H), 7.22 – 7.08 (m, 2H), 6.82 (s, 1H), 6.70 (d, $J = 7.5$ Hz, 1H), 4.21 (t, $J = 4.7$ Hz, 2H), 3.90 (dd, $J = 5.7, 3.8$ Hz, 2H), 3.87 (s, 2H), 3.74 (dd, $J = 5.8, 3.2$ Hz, 2H), 3.67 (q, $J = 4.6, 4.0$ Hz, 4H), 3.34 (t, $J = 5.1$ Hz, 2H), 2.37 (dt, $J = 21.2, 7.4$ Hz, 4H), 1.48 (dd, $J = 13.8, 6.6$ Hz, 4H), 1.25 (p, $J = 3.6$ Hz, 4H). ^{13}C NMR (101 MHz, CDCl_3) δ 153.54, 152.96, 129.67, 129.09, 126.66, 125.73, 123.67, 120.02, 106.57, 105.58, 77.35, 77.03, 76.72, 71.17, 70.78, 70.24, 69.92, 68.09, 50.78, 33.78, 32.69, 30.79, 28.91, 28.12, 27.82, 24.50. HRMS (ESI), m/z : calcd. for $\text{C}_{23}\text{H}_{33}\text{N}_3\text{O}_4\text{S}_2$ $[\text{M}+\text{Na}]^+$ 502.1810, found 502.1808. IR: 2103.64 medium sharp. (N_3), 2600-2550 cm^{-1} weak (SH), 3360.26 broad (OH).

5-(dimethylamino)-N-(prop-2-yn-1-yl)naphthalene-1-sulfonamide (3.8)

Propargylamine (0.3 mL, 4.4 mmol) and triethylamine (0.45 g, 4.4 mmol) were added to a solution of 5-(dimethylamino) naphthalene-1-sulfonyl chloride (1 g, 3.7 mmol) in dry CH_2Cl_2 (10 mL). The reaction was stirred at room temperature for 6 h, quenched by water (6 mL). The mixture was further extracted by CH_2Cl_2 (10 mL \times 2). The organic layer was concentrated in vacuo and purified by silica gel chromatography to obtain the product (0.6 g, 56%) as a yellow solid. ^1H NMR (400 MHz, Chloroform- d) δ 8.53 (dt, $J = 8.6, 1.1$ Hz, 1H), 8.33 – 8.23 (m, 2H), 7.51 (ddd, $J = 17.9, 8.6, 7.5$ Hz, 2H), 7.20 – 7.12 (m, 1H), 3.76 (d, $J = 2.5$ Hz, 2H), 2.86 (s, 6H), 1.89 (t, $J = 2.5$ Hz, 1H). ^{13}C NMR (101 MHz, CDCl_3) δ 151.89, 134.31, 130.68, 129.76, 129.72, 128.50, 128.32, 123.12, 118.65, 115.17, 77.93, 77.44, 77.12, 76.81, 72.60, 45.36, 32.85, -0.00.

N-(6-(diethylamino)-9-(2-(prop-2-yn-1-ylcarbamoyl)phenyl)-3H-xanthen-3-ylidene)-N-ethylethanaminium (3.9) Rhodamine B (0.2 g, 0.45 mmol) was added a solution of N-hydroxysuccinimide (0.08 g, 0.7 mmol) in CH_2Cl_2 (10 mL). Then, N-(3-

Dimethylaminopropyl)-N'-ethylcarbodiimide hydrochloride (EDC-HCl) (0.13 g, 0.68 mmol) and catalytic amount 4-Dimethylaminopyridine (DMAP) (12 mg) were added to the mixture. The reaction mixture was kept stirring under room temperature overnight. Then, a solution of propargylamine (0.06 g, 1.1 mmol) in CH₂Cl₂ (8 mL) was added to the reaction over 10 min and the reaction was again stirred overnight. The reaction mixture was partitioned between water and CH₂Cl₂. The organic layer was washed by brine and dried by sodium sulfate, concentrated in vacuo. The crude product was purified by silica gel chromatography (ethyl acetate: hexane 1:3) to get the product (0.1 g, 50%) as a yellow oil. ¹H NMR (400 MHz, CDCl₃) δ 7.98 – 7.88 (m, 1H), 7.48 – 7.37 (m, 2H), 7.15 – 7.05 (m, 1H), 6.47 (d, *J* = 8.8 Hz, 2H), 6.39 (d, *J* = 2.5 Hz, 2H), 6.27 (dd, *J* = 8.9, 2.6 Hz, 2H), 3.95 (d, *J* = 2.5 Hz, 2H), 3.33 (q, *J* = 7.1 Hz, 8H), 1.76 (d, *J* = 5.0 Hz, 1H), 1.15 (t, *J* = 7.0 Hz, 12H). ¹³C NMR (101 MHz, CDCl₃) δ 167.37, 153.75, 153.46, 148.83, 132.63, 130.39, 129.07, 127.99, 123.77, 122.97, 107.97, 105.03, 97.76, 78.27, 77.42, 77.10, 76.78, 70.03, 64.78, 44.36, 28.49, 12.56, -0.00.

3.5 References

- [1] Liu, Y., Mu, L., Liu, B., & Kong, J. Controlled switchable surface. *Chemistry–A European Journal*. **2005**, *11*(9), 2622-2631.
- [2] Zhou, F., & Huck, W. T. Surface grafted polymer brushes as ideal building blocks for “smart” surfaces. *Physical Chemistry Chemical Physics*. **2006**, *8*(33), 3815-3823.
- [3] Schreiber, F. Self-assembled monolayers: from ‘simple’ model systems to biofunctionalized interfaces. *Journal of Physics: Condensed Matter*. **2004**, *16*(28), R881
- [4] Mendes, P. M. Stimuli-responsive surfaces for bio-applications. *Chemical Society Reviews*. **2008**, *37*(11), 2512-2529.
- [5] Arumugam, S., & Popik, V. V. Attach, remove, or replace: Reversible surface functionalization using thiol–quinone methide photoclick chemistry. *Journal of the American Chemical Society*. **2012**, *134*(20), 8408-8411

CHAPTER 4

NQMP-THIOL AND NQMP-DISULFIDE FOR HYDROGEN SULFIDE PHOTO- RELEASE

4.1 Introduction

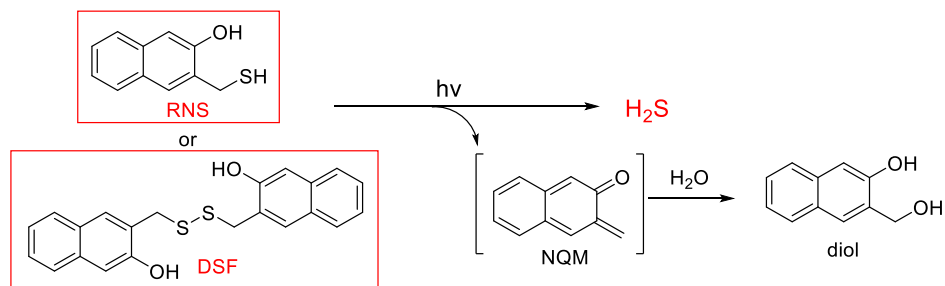
Hydrogen sulfide (H_2S) is commonly known as a poisonous gas with the foul smell like rotten eggs. However, researches recently have convincingly demonstrated the role of H_2S as an endogenous gasotransmitter with important functions such as anti-inflammation¹, antitumor², ion channel regulation³, cardiovascular protection⁴ and antioxidation effects⁵. With these biological functions, H_2S is emerging as a valuable therapeutic agent.

Some chemical and biochemical catabolic reactions of H_2S can help explain H_2S 's above-mentioned biological functions. For example, H_2S is a powerful reducing agent which reacts with endogenous oxidants such as peroxynitrite, superoxide and hydrogen peroxide. H_2S reacts readily with methemoglobin to form sulfhemoglobin and this pathway serves as a metabolic sink for H_2S . H_2S can also cause protein S-sulfhydration (*i.e.* to form $-\text{S}-\text{SH}$) which provides a way to protein or enzyme modifications.⁶

Due to the medical values of H_2S , there has been a growing interest in developing H_2S -based therapeutics. The key aspect of H_2S -based therapeutics is the ability to deliver hydrogen sulfide of proper concentrations, to the desired location(s) and with the suitable pharmacokinetics.⁷ The H_2S generation from inorganic donors (such as NaHS and Na_2S) usually occurs spontaneously at the time the solution is prepared, making it difficult to

precisely control the H₂S concentration which is an important factor for *in vivo* applications. Given the problems of sulfide salts, synthetic and the ‘controllable’ H₂S donors have received considerable attention in recent years. Particularly, synthetic organic donors that can generate steady and localized concentrations of H₂S upon external stimulus gained extensive interest.⁸

The molecules 3-(mercaptomethyl)naphthalen-2-ol (RNS) and its disulfide (DSF) can form NQM with the release of hydrogen sulfide upon UV irradiation and serve as effective photo-activate H₂S donors. In aqueous solution, NQM quickly reacts with water to form 3-(hydroxymethyl)naphthalen-2-ol (Scheme 4.1). The detailed mechanism of H₂S release from these two donors can be found later (section 4.6, page 88) in this text.



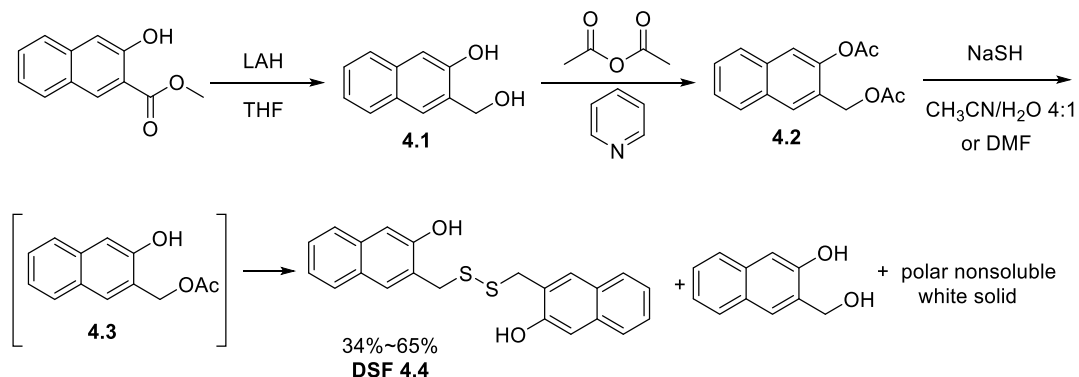
Scheme 4.1 H₂S photo-release from RNS and DSF

The two NQMP compounds are very stable at ambient environment, possess good water solubility, and can achieve high yield of H₂S release in a controllable fashion upon UV irradiation.

4.2 Design and Synthesis of NQMP-based H₂S Releasing Agents

The synthesis of RNS and DSF was achieved by a few methods. In the first method, commercially available methyl 3-hydroxy-2-naphthoate was first reduced by lithium aluminum hydride and then the alcohol groups were protected by acetate. The

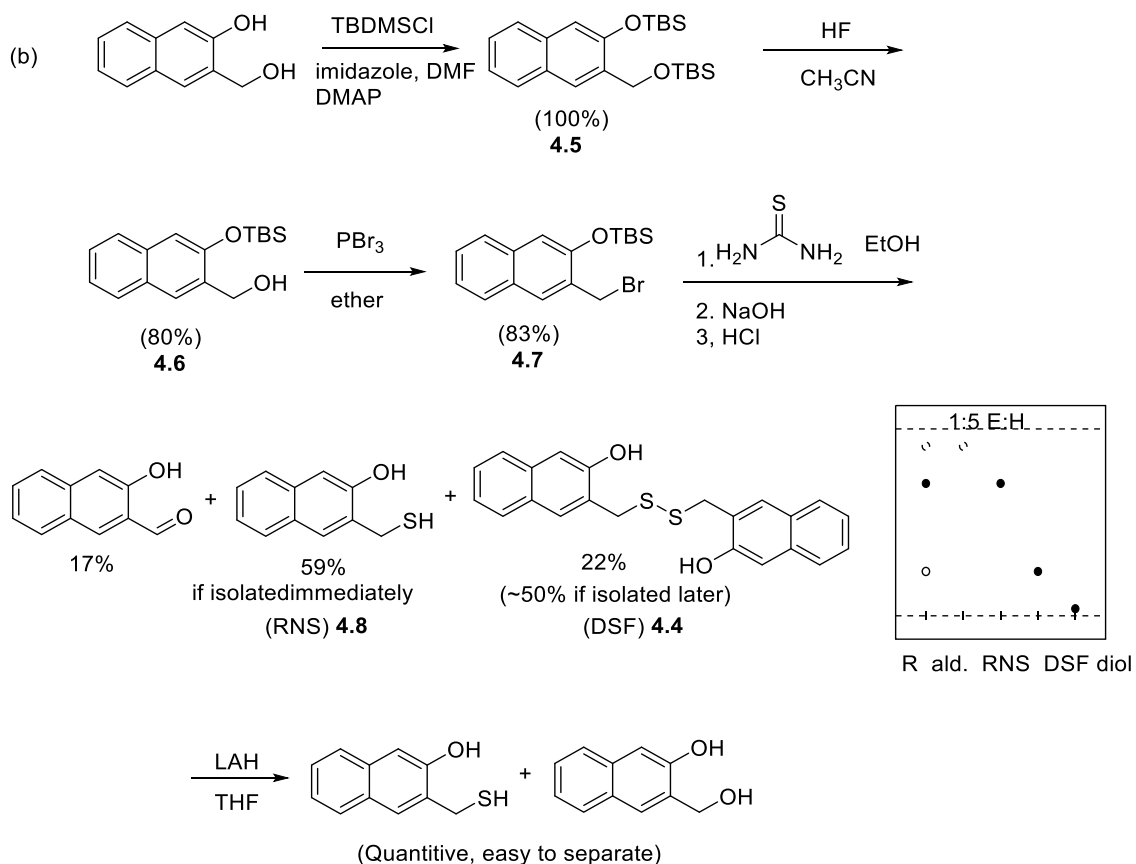
diacetate (compound **4.2**) was then reacted with sodium hydrosulfide to generate DSF through formation of monoacetate (compound **4.3**). However, the reaction also generated other byproducts due to the basicity of the NaSH (Scheme 4.2).



Scheme 4.2 Synthesis of NQMP-based H₂S release agents--method 1

A more common way to synthesize thiol is through reaction of alkyl bromide and thiourea. Therefore, the NQMP-bromide was designed for this purpose. However, this compound was not obtained under different bromination conditions due to its rapid decomposition upon formation (Scheme 4.3 a). Therefore, it is necessary to protect the 2-position phenolic OH of the NQMP-bromide to increase its stability. By protecting both the 2- and 3- position alcohol, and subsequent selective deprotection of the 3- OH, compound **4.6** was obtained before undergoing bromination to afford compound **4.7**. The reaction of **4.7** with thiourea provided RNS as the major product (Scheme 4.3 b).





Scheme 4.3. Synthesis of NQMP-based H₂S release agents--method 2

If the organic extract of the thiolation reaction was not purified immediately after the reaction, the RNS would partially turn to DSF, leaving DSF as the major product. At the early stage of research DSF was erroneously identified as the RNS since it is more polar than its precursors (compound **4.2** and **4.7**). The identity of DSF was only revealed until Ellman reagent test (Appendix 1) suggesting no free thiol group as well as the successful reduction of DSF using LAH⁹. The DSF is quite stable under reducing conditions such as TCEP, LiCl/NaBH₄, Mg, and LTBA (Lithium tri-tert-butoxyaluminum hydride). It was also found that DSF exhibits higher polarity (with lower R_f value on TLC) than RNS. The IR spectra of DSF and RNS can be found in Appendix 2.

4.3 Byproducts Analysis

after synthesis of DSF and RNS was achieved, the photolysis of the two compounds was studied. Photolysis was conducted using a Rayonet photoreactor equipped with sixteen 4W 300 or 350 nm fluorescent lamps. The typical patterns of DSF and RNS upon irradiation with 300 nm UV for 0-8 min are shown in Figure 4.1. With HPLC 75MeOH/25H₂O as eluting system, both the DSF and RNS transformed to diol (compound **4.1**) eventually, although with various amounts of same byproducts formed during the process.

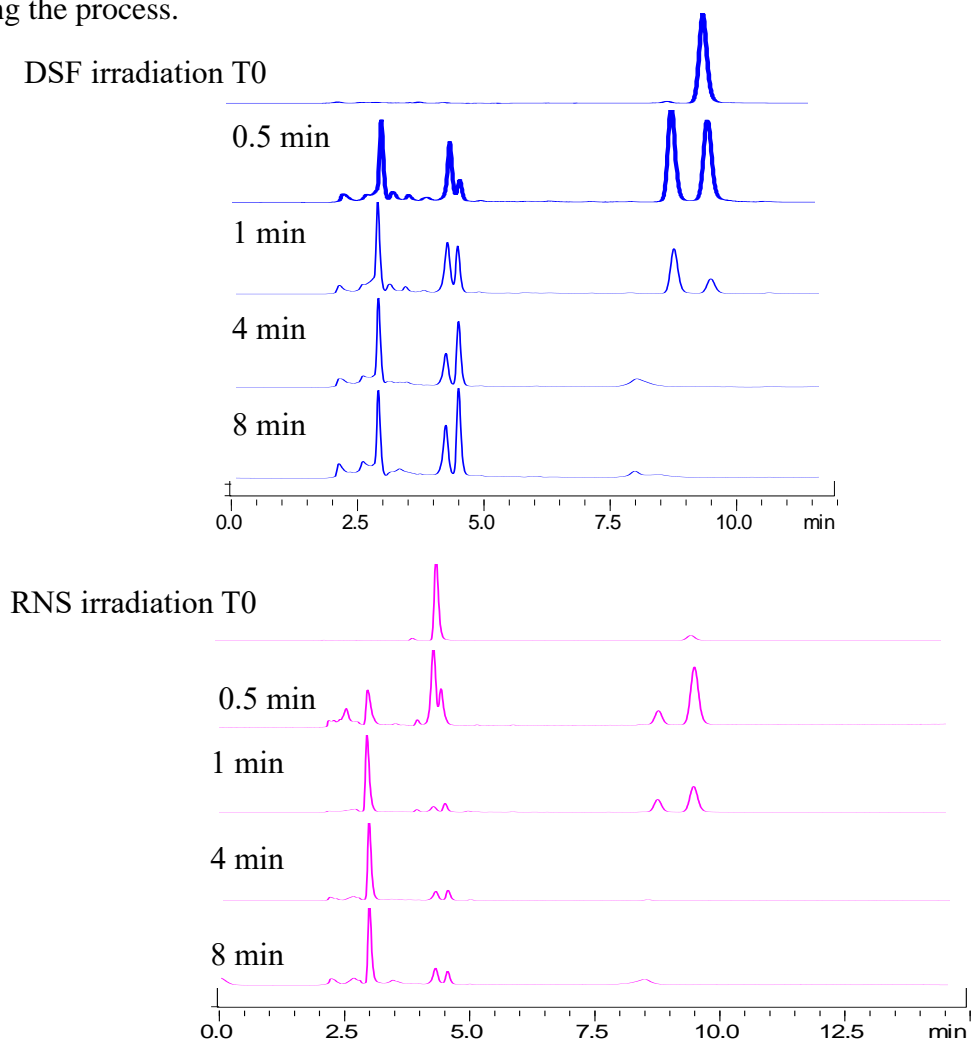


Figure 4.1 Photolysis of DSF and RNS

Particularly, the DSF with 300 nm UV for 1 min is shown in Figure 4.2. The mixture from DSF photolysis (300 nm for 1 min irradiation) was studied by HPLC analysis (eluting system 75% MeOH + 25% Water). The mixture contains several compounds which were later characterized as aldehyde (**4.9**), bypdt158 (**4.17**) and thioether (**4.13**). The thioether as intermediate byproduct disappears in the final irradiation mixture while the aldehyde, bypdt158 survived for longer irradiation time (over 5 min). In comparison, the photolysis of RNS exhibits similar pattern as DSF but much less thioether formation with shorter irradiation time. The amount of aldehyde and bypdt158 formed from UV irradiation of RNS over 5 min were also much less than that formed from DSF photolysis.

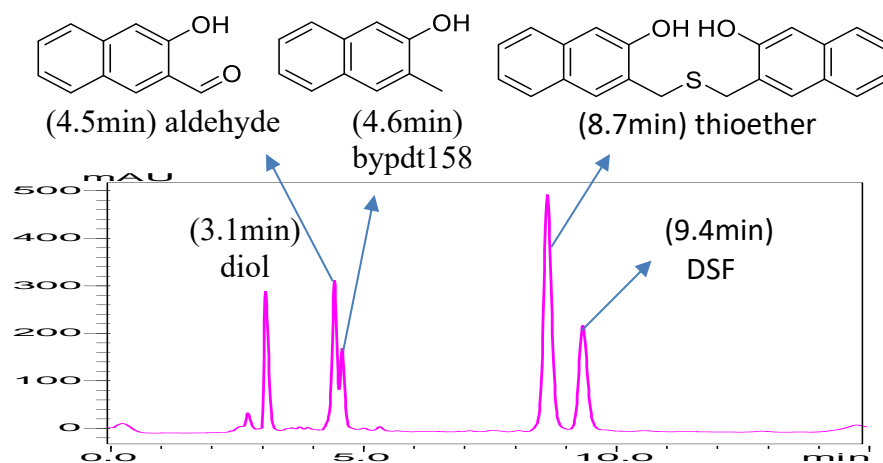
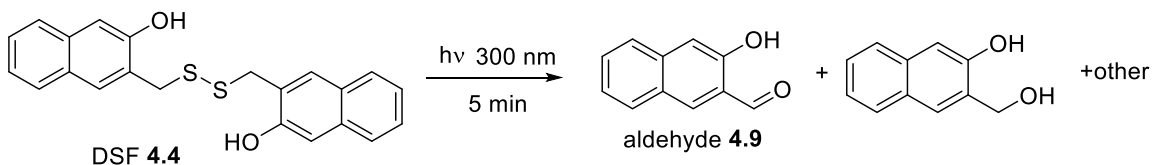


Figure 4.2 HPLC analysis of DSF photolysis mixture

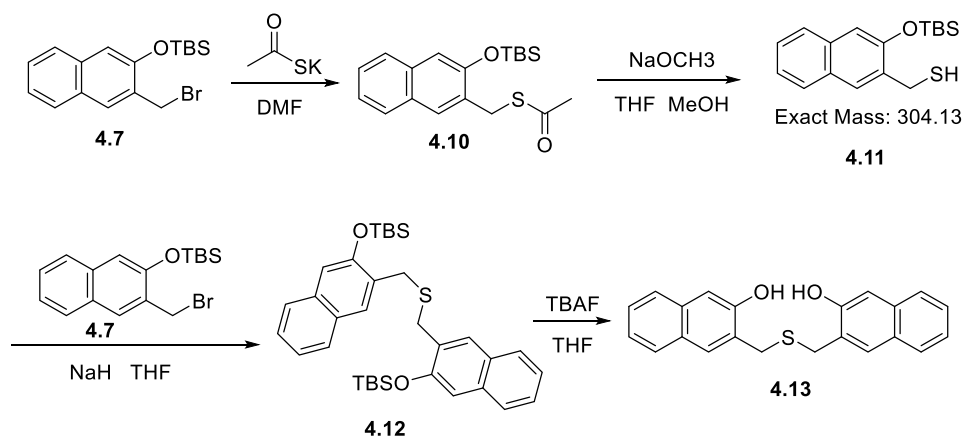


Scheme 4.4 Photo-generation of the aldehyde (**4.9**)

The aldehyde (**4.9**) was successfully isolated and characterized from the DSF photolysis (300 nm irradiation for 5 min) sample (Scheme 4.4). The bypdt158 (**4.17**) was

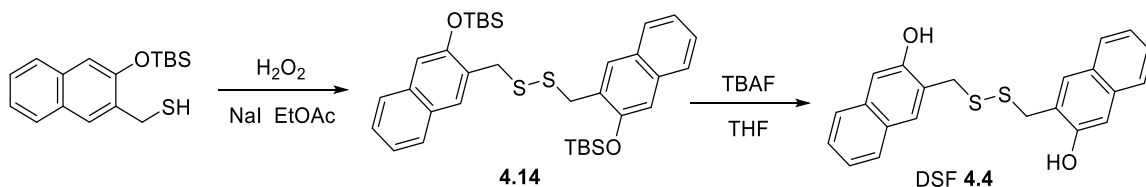
isolated and characterized later in the final irradiation mixture of RNS + 2ME (2-mercaptoethanol) in which bypdt158 was the major byproduct (section 4.6, page 86).

Since the thioether (**4.13**) was unable to be isolated from any mixture, it was synthesized instead (Scheme 4.5) to confirm its identity. From NQMP-bromide (**4.7**) thioacetate (**4.10**) was obtained and then the acetate was removed to form thiol (**4.11**). **4.11** underwent S_N2 reaction with **4.7** to generate a thioether **4.12**, leading to **4.13** after TBS removal. **4.13** was characterized by NMR and mass spectroscopy. Compound **4.13** also matched and intensified the thioether peak from the “DSF 300 nm 1 min photolysis mixture” from HPLC analysis.



Scheme 4.5 Synthesis of the thioether (**4.13**)

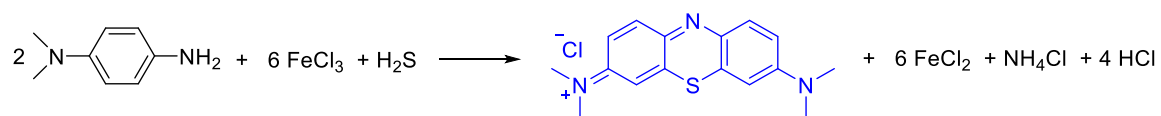
The DSF (**4.4**) was also synthesized from another route (Scheme 4.6) which again confirmed its identity as a disulfide, not the RNS.



Scheme 4.6 Synthesis of the disulfide (**4.4**)

4.4 H₂S Release Condition Optimization

To quantify the H₂S formation, Methylene Blue (MB) test was carried out. The method requires iron (III) chloride, N,N, dimethyl-p-phenylenediamine sulfate and zinc acetate solutions mixed *in situ*, and upon reaction with hydrogen sulfide, generates a blue colored compound with the maximum absorption of light at 663 nm after over 15 minutes incubation (Scheme 4.7).



Scheme 4.7 Methylene Blue test reaction

However, the first attempt to quantify the H₂S release from DSF proved to be unsuccessful. The transparent solution turned turbid yellow after irradiation, and no peak absorption of methylene blue at 663 nm was observed. The turbid yellow solution suggested the formation of byproduct particles; therefore, it is important to evaluate and quantify the NQM formed *in situ* as well as to minimize the formation of byproducts from NQM.

The formation and quantification of NQM from DSF were verified by using two methods through HPLC analysis. The first method is to analyze the formation of the NQM hydration product diol (**4.1**). The other method is to trap the NQM by Diels-Alder reaction using ethyl vinyl ether. In the first method, after generating calibration curves for authentic samples of DSF and diol, respectively, the contents of DSF solution under 350 nm irradiation for 0-120 min were quantified (Figure 4.3). The result indicated the conversion of DSF to diol is as high as 36%.

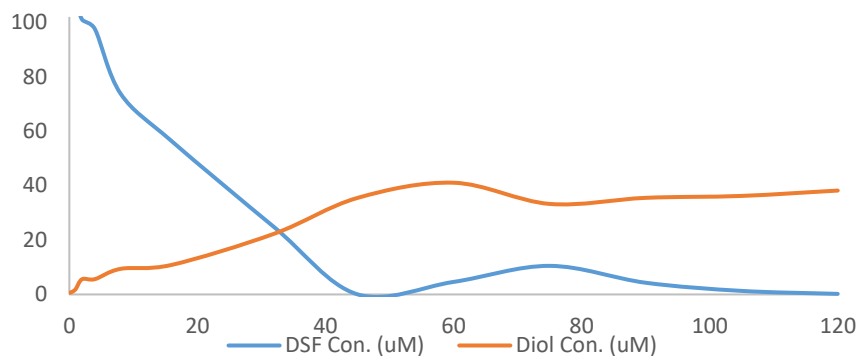
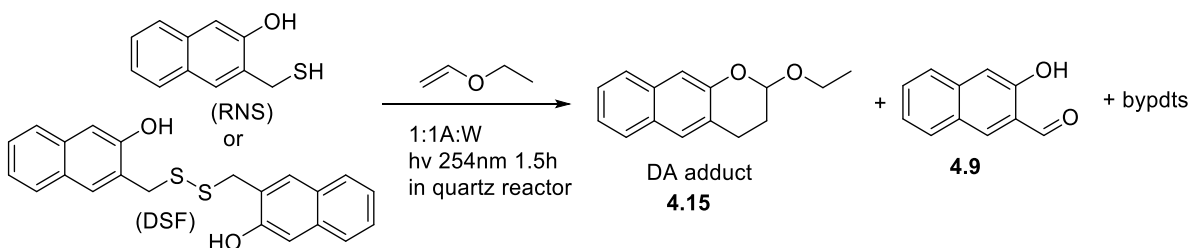


Figure 4.3 DSF transformation to diol (**4.1**) via irradiation

For the second method, the reaction of RNS and DSF were performed with ethyl vinyl ether (EVE), respectively. The DA adduct (**4.15**) was observed and characterized by HPLC (Scheme 4.8, Figure 4.4). The yield of the reaction was also measured. With 100 equivalent EVE, the DA adduct yield from RNS or DSF is 12%, while with 200 equivalent EVE, the yield increased to 20%. The results of the two methods showed that formation of NQM is not quantitative.



Scheme 4.8 RNS and DSF Diels-Alder reaction with EVE

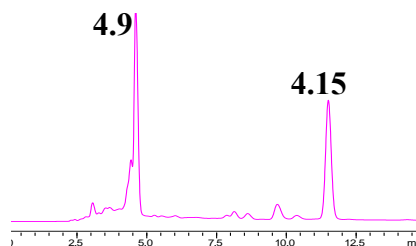


Figure 4.4 HPLC analysis of DA reaction products

After the study of NQM formation during irradiation, measures were taken to improve the NQM yield and suppress the byproduct formation. The first attempt was to deprive the sample solution of oxygen by degassing. The DSF sample was subjected to N₂ bubbling for 10 min and immediately sealed with cap. Then, the sample was irradiated (350 nm) for different time duration, and the ratio of byproduct to starting material in the mixture was compared to that of sample without degassing (Table 4.1). The results demonstrated that with degassing, the formation of diol and aldehyde only decreased a small amount (except for “aldehyde:SM” ratio for “100 min” irradiation), while the amount of thioether increased compared to those without degassing. Therefore, the removal of oxygen reduced the formation of diol and aldehyde to a degree but encouraged the formation of thioether. This suggested that solution degassing did not impede the byproducts formation from NQM.

| Irradiation time Ratio | 0.5 h | 1 h | 100 min |
|---------------------------|------------------------------------|-------------|-------------|
| | *N ₂ bubbling: Yes (No) | | |
| Diol: SM | 0.08 (0.14) | 0.26 (0.38) | 0.70 (0.86) |
| Aldehyde: SM | 0.11 (0.20) | 0.48 (0.51) | 1.25 (1.12) |
| Thioether: SM | 0.64 (0.61) | 1.93 (1.30) | 2.69 (1.87) |

Table 4.1 Effect of N₂ bubbling to DSF photolysis

Then, we hypothesized that large excess of competing thiol, such as 2-mercaptoethanol (2ME) can readily react with the NQM and compete with other side reactions, thus enhancing the H₂S release. So, the UV absorbance of 250 μM DSF (should produce 500 μM SH) solutions without or with 2ME were recorded. As we expected, the addition of 2ME greatly enhanced the featured Methylene Blue (MB) band (blue vs. red line, green vs. yellow line in Figure 4.5). It is also interesting that when

2ME was not added, the water as co-solvent helped the MB band formation compared to phosphate buffer as the co-solvent. The 1:1 acetonitrile: water solvent mixture helped the revelation of the MB band comparing to the 1:1 acetonitrile: phosphate buffer solvent mixture (red vs. yellow line in Figure 4.5).

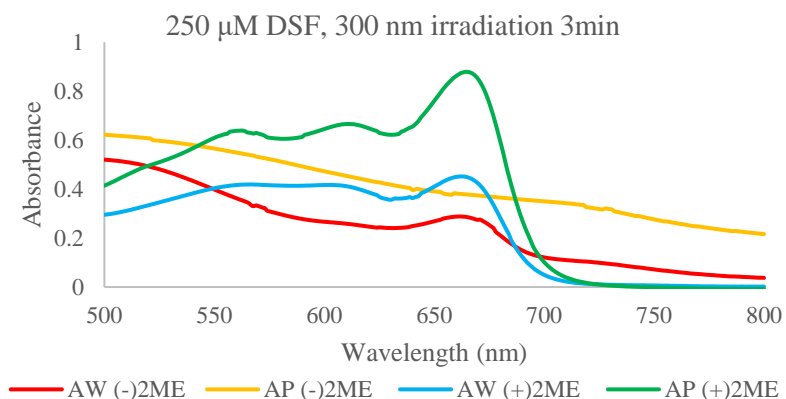


Figure 4.5 Condition test for H₂S photo-release from DSF

The same improving effect was found in 500 μM RNS (provided 500 μM SH) solutions (Figure 4.6) as to addition of 2ME. Using water instead of buffer in the mixture improved the MB band formation when without 2ME (red vs. yellow line) and made comparable MB bands when with 2ME (blue vs. green line).

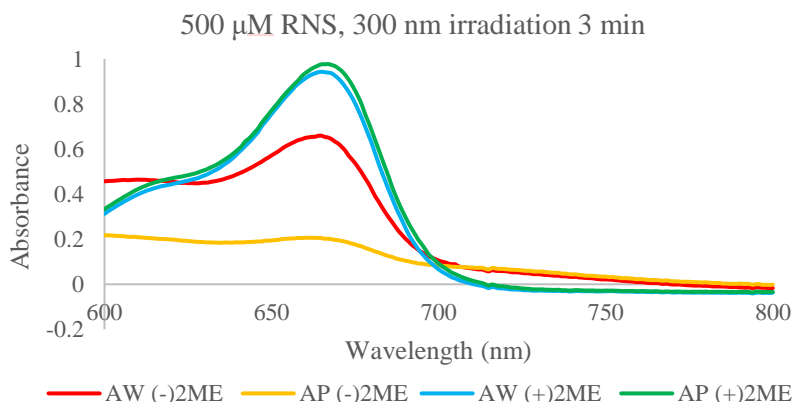


Figure 4.6 Condition test for H₂S photo-release from RNS

Further, the relationship of H₂S release with irradiation time was studied. 300 nm light with different duration of irradiation was applied to DSF in 1:1 acetonitrile/buffer solution without (Figure 4.7 a) or with (Figure 4.7 b) 2ME. It was also worth noting that without the presence of 2ME, the solution turned yellow after irradiation while the one in presence of 2ME remained colorless transparent after irradiation. The relation of absorbance values at 663 nm and irradiation time was recorded and plotted for the two samples (Figure 4.7 c). It was found that higher absorbance was observed (indicating higher H₂S yield) with the addition of 2ME; while in absence of 2ME, the achieved absorbance even decreased after the peak value at 3 min irradiation.

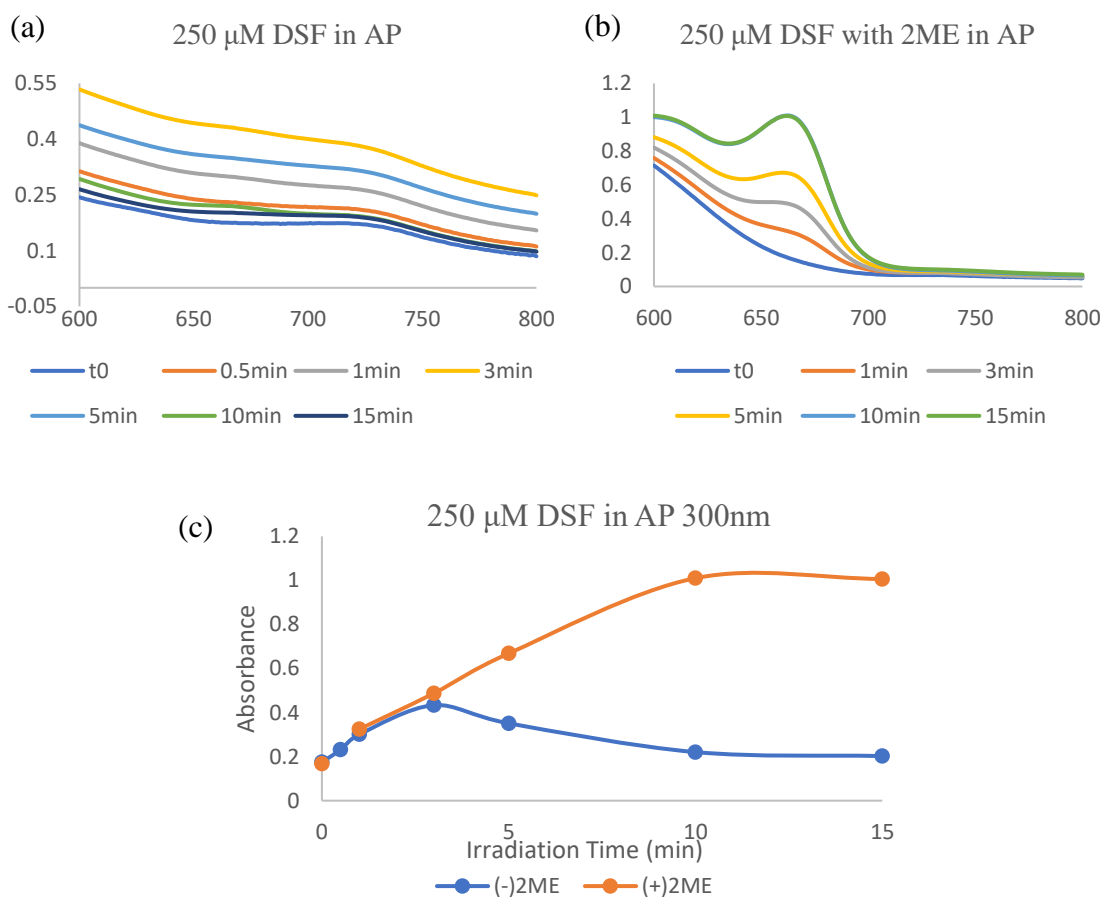


Figure 4.7 DSF photolysis (a) Without or (b) With 2ME and (c) their H₂S release profile

4.5 H₂S Release Characterization

Different concentrations of Na₂S·9H₂O in 1:1 acetonitrile/phosphate buffer were applied to Methylene Blue (MB) working solutions, then the measured UV absorbance at 663 nm after incubating over 15 minutes was used to generate an MB test standard curve (Appendix 3). Based on the UV absorbance of the samples (Figure 4.8 a) at 663 nm, the H₂S Release Standard curve was obtained (Figure 4.8 b).

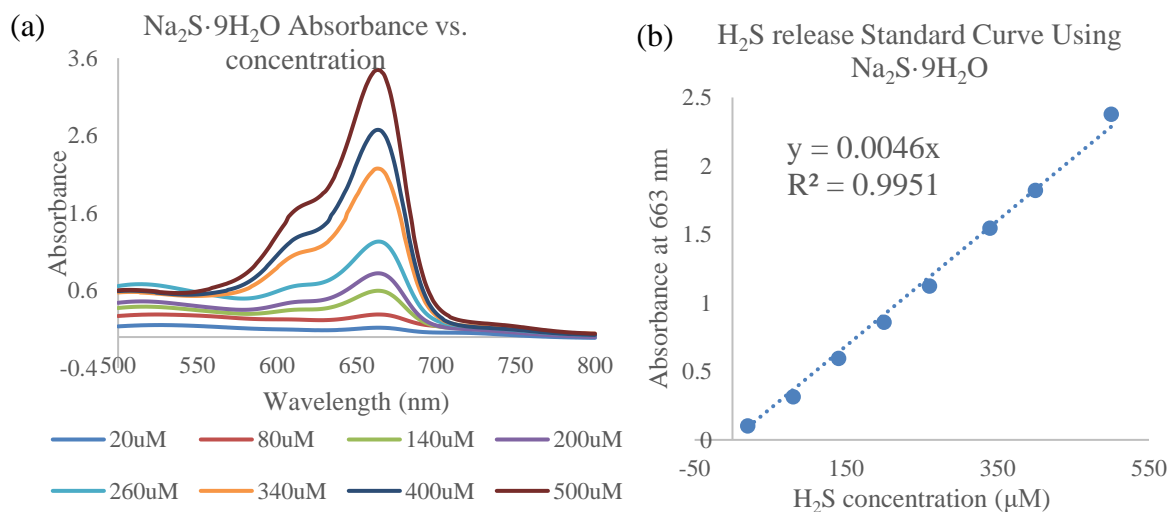


Figure 4.8 (a) Na₂S·9H₂O absorbance curve and (b) H₂S release standard curve

With the irradiation conditions optimized, H₂S photo-release from 250 μM DSF was measured using Methylene Blue test (Appendix 3). Samples were irradiated by 300 nm UV light for certain period of time, then MB reagents and incubation were applied. A sample could only be used for one certain irradiation period once MB reagents were added, and not for further accumulation of irradiation. Besides 2ME, cysteine and glutathione were also evaluated to assist H₂S release due to their abundance in the biological environment. The absorbance values of the samples at 663 nm were recorded and each data point comes from the average of three repetitions. The H₂S photo-releasing curve is thus plotted versus irradiation period (Figure 4.9). The three solutions with thiols

(2ME, cysteine, glutathione) added were all performed in 1:1 acetonitrile/ buffer while the result of DSF alone was the averaged result of in 1:1 acetonitrile/water and acetonitrile/buffer.

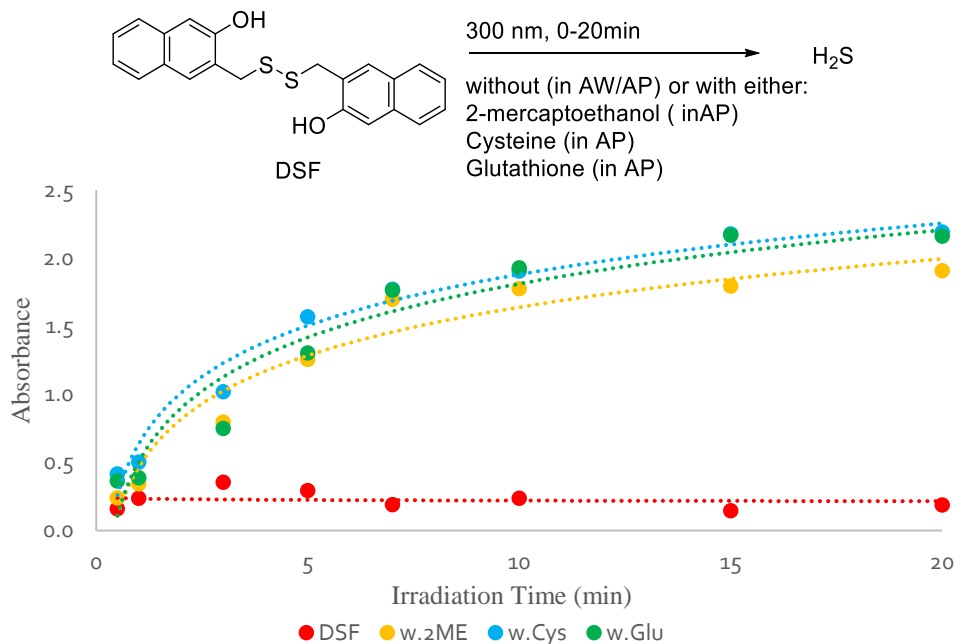


Figure 4.9 UV Absorbance at 663 nm from 500 μ M of SH from DSF

| H ₂ S Yield (%) | DSF | w.2ME | w.Cys | w.Glu |
|----------------------------|------|-------|-------|-------|
| 0 | 3.1 | 2.5 | 2.3 | 3.5 |
| 0.5min | 6.9 | 10.4 | 18.1 | 15.8 |
| 1 min | 10.3 | 14.9 | 21.8 | 16.9 |
| 3 min | 15.4 | 34.6 | 44.3 | 32.6 |
| 5 min | 12.7 | 54.6 | 68.2 | 56.6 |
| 7 min | 8.3 | 73.8 | 77.0 | 76.7 |
| 10 min | 10.3 | 77.2 | 82.8 | 83.8 |
| 15 min | 6.3 | 78.0 | 94.6 | 94.2 |
| 20 min | 8.1 | 83.0 | 95.2 | 93.9 |

Table 4.2 H₂S Conversion from photolysis of DSF

The yield of H₂S was then calculated based on the standard curve and listed in Table 4.2. It was concluded that the competing thiols greatly enhanced the H₂S

generation from DSF, achieved up to 95% conversion, which is much higher than other existing photocages.

The MB analysis results of DSF in 1:1 acetonitrile/water (AW) and 1:1 acetonitrile/phosphate buffer (AP) samples are compared (Figure 4.10). The results from the two groups demonstrate similar maximum absorbance at 663 nm. However, the AW group formed MB band while the AP group did not. When MB band was not formed, the absorbance at 663 nm also fluctuated with high uncertainties.

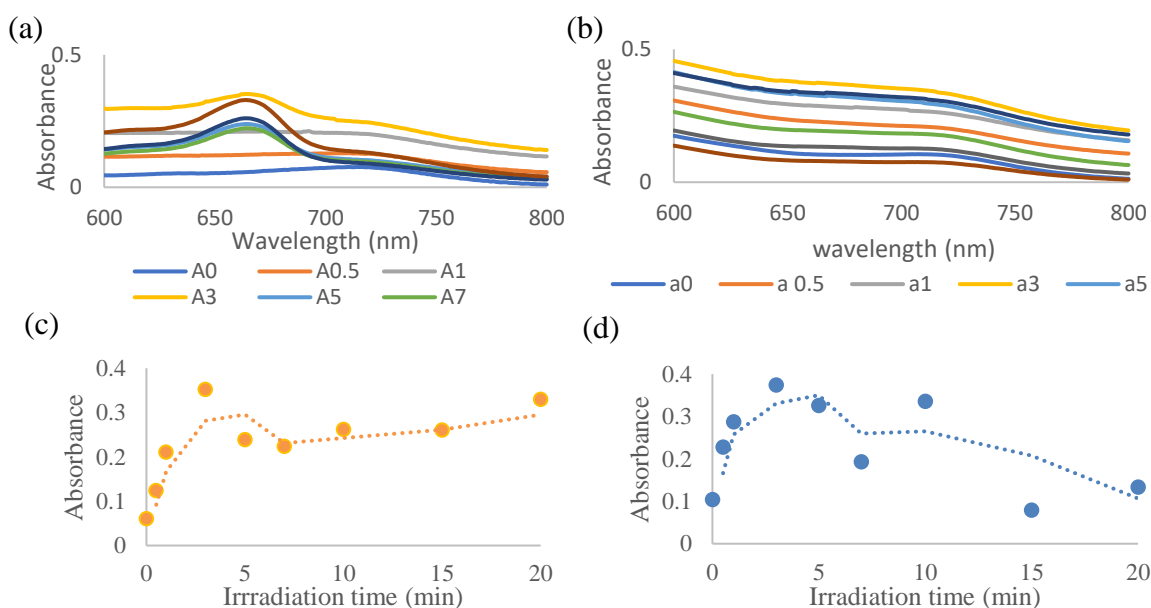


Figure 4.10 UV absorbance (300 nm 0-20 min) of 250 μM DSF: (a) in AW and (b) in AP. UV absorbance at 663 nm of 250 μM DSF: (c) in AW and (d) in AP

Similarly, H₂S photo-release by 500 μM RNS was also measured by MB test (Figure 4.11, Table 4.3). Each RNS solution was freshly prepared (instead of prepared from stock solution) for the experiment because they are prone to oxidation in solution over time. The RNS is a superior H₂S photo-releasing agent without or with the presence of competing thiols. The H₂S yield from irradiation of RNS solution reaches 43% with no additional thiols, and as high as 94% when additional thiols were added.

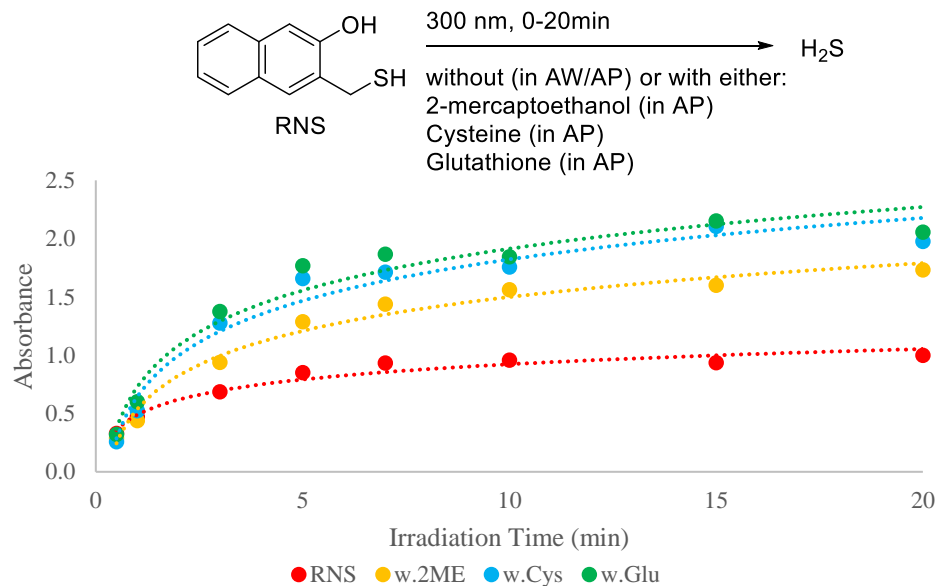


Figure 4.11 UV Absorbance at 663 nm from 500 μ M of RNS

| H ₂ S Yield (%) | RNS | w.2ME | w.Cys | w.Glu |
|----------------------------|------|-------|-------|-------|
| 0 | 5.2 | 0.0 | 0.0 | 0.0 |
| 0.5min | 14.4 | 12.5 | 11.3 | 13.9 |
| 1 min | 20.5 | 19.1 | 22.8 | 26.1 |
| 3 min | 29.9 | 40.8 | 55.5 | 59.7 |
| 5 min | 36.9 | 56.0 | 72.1 | 76.8 |
| 7 min | 40.5 | 62.5 | 74.5 | 81.1 |
| 10 min | 41.7 | 67.9 | 76.3 | 80.2 |
| 15 min | 40.7 | 69.6 | 91.5 | 93.5 |
| 20 min | 43.4 | 75.3 | 85.9 | 89.4 |

Table 4.3 H₂S Conversion from Photolysis of RNS

The MB analysis results of RNS in 1:1 acetonitrile/water (AW) and 1:1 acetonitrile/buffer (AP) samples were also plotted (Figure 4.12). The AW group formed a significant MB band and exhibited high absorbance, demonstrating high H₂S yield, which was retained for over 20 min. In comparison, a fluctuating low-yield H₂S release pattern was observed from the AP group.

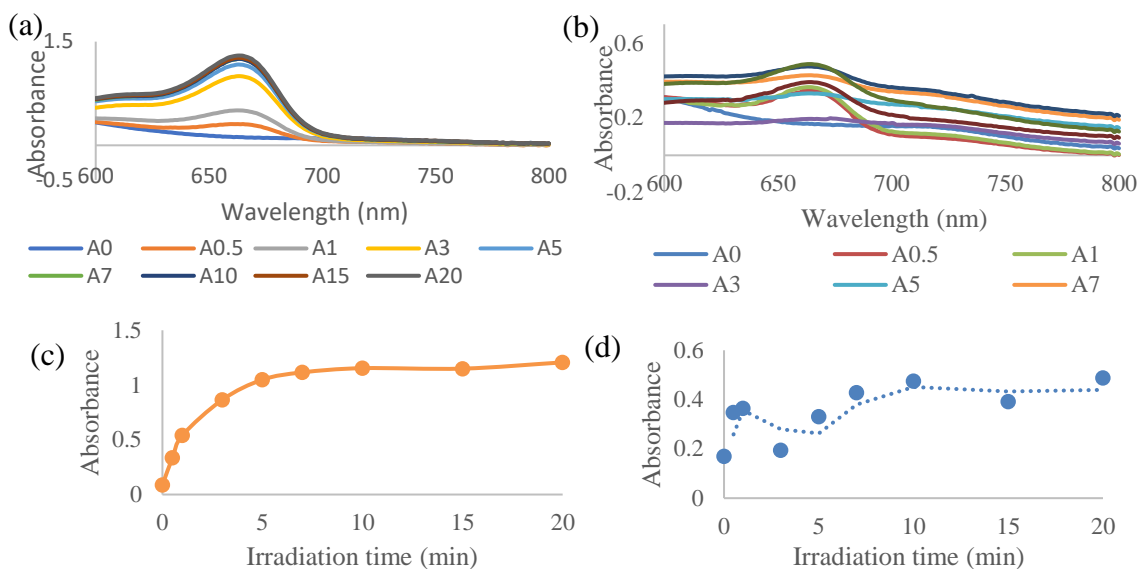


Figure 4.12 UV absorbance (300 nm 0-20 min) of 500 μ M RNS: (a) in AW and (b) in AP. UV absorbance at 663 nm of 500 μ M RNS: (c) in AW and (d) in AP

The relationship between irradiation time and incubation time of DSF was also studied (Table 4.4). The results show that irradiating (300 nm light) for 5 min with 20 min incubation achieved fully H₂S release, and with irradiation less than 5 min, incubation resulted in more percentage of H₂S release comparing to the over irradiated (irradiated more than 5 min) samples.

| | | | | | | | | | |
|---|------|------|------|------|------|-------|------|------|------|
| Irradiation time_ incubation time (min) | 1_0 | 1_5 | 1_20 | 3_0 | 3_5 | 3_20 | 5_0 | 5_5 | 5_20 |
| Absorbance | 0.32 | 0.56 | 0.64 | 0.66 | 0.86 | 1.27 | 1.42 | 1.68 | 1.72 |
| increase% from Incubate 0 min | | 72 | 98 | | 31 | 94 | | 19 | 21 |
| | 7_0 | 7_5 | 7_20 | 10_0 | 10_5 | 10_20 | | 20_0 | |
| Absorbance | 1.37 | 1.35 | 1.68 | 1.63 | 1.58 | 1.63 | | 1.75 | |
| increase% from Incubate 0 min | | -1 | 23 | | -3 | 0 | | | |

Table 4.4 Irradiation and incubation time relationship of H₂S from DSF photolysis

Then, solutions of DSF with cysteine and RNS with glutathione were tested for 5 min irradiation and 0-20 min incubation for the H₂S release ability (Figure 4.13), which indicated that incubate 5 min can easily drive the release to completion.

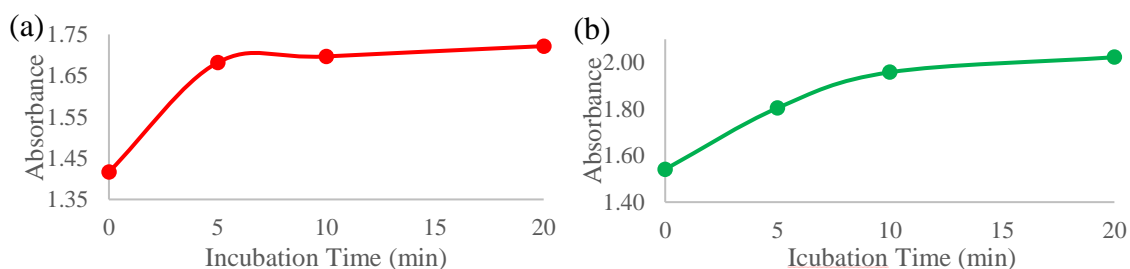


Figure 4.13 Incubation of irradiation 5 min samples of (a) DSF+Cys (b) RNS+Glu

The DSF is a yellow solid and RNS as a white crystal, they are both stable under ambient environment and exhibited reasonable to excellent water solubility. The RNS aqueous solution may undergo disulfide formation overtime, while DSF solution is stable in dark over a month. It was found that both UV irradiation and the RNS or DSF are necessary for H₂S release. MB test of DSF and RNS solution incubation together with 2-mecaptoethanol (2ME), cystine (Cys) and glutathione (Glu) (each 10 mM) for 30 minutes showed no MB band formation (Figure 4.14 a, b). UV irradiation of the thiols' mixture in absence of RNS or DSF also showed no MB band (Figure 4.14 c).

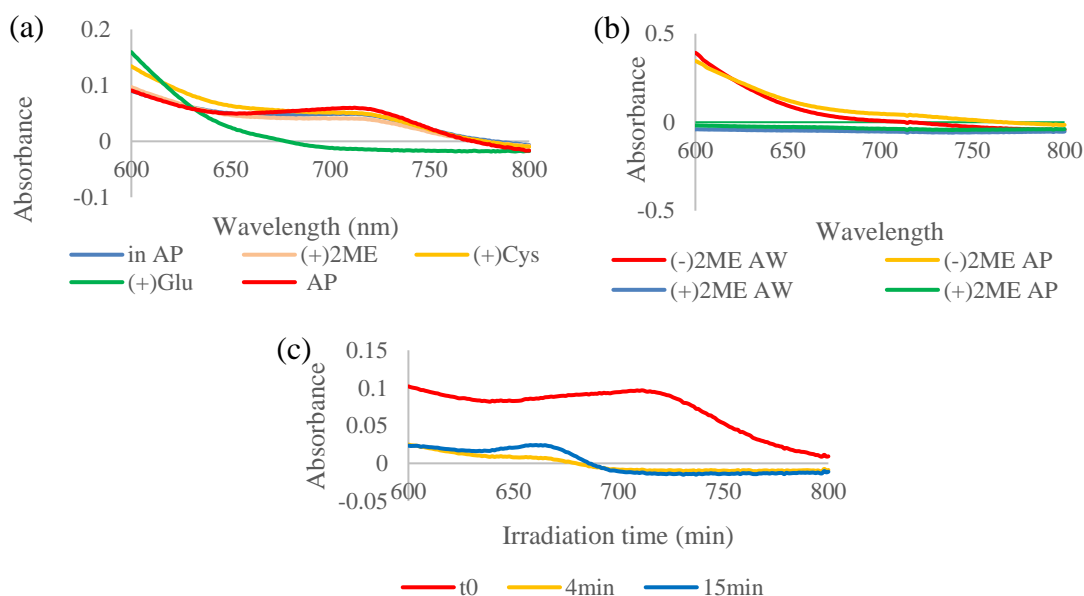
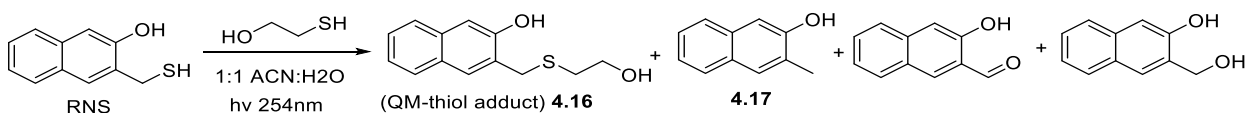


Figure 4.14 Control experiments (a) DSF incubate with thiols (b) RNS incubate with thiols (c) 300 nm Irradiation on 10 mM 2ME, Cys and Glu

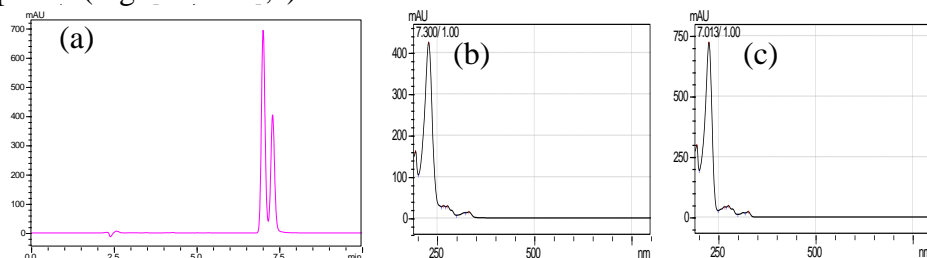
4.6 Proposed H₂S Releasing Mechanism

To understand the mechanism of why the addition of thiols such as 2-mercaptoethanol (2ME) can improve the H₂S release yield of RNS and DSF, the reactions of RNS and DSF with 2ME were studied using HPLC (Appendix 4). For RNS, 2ME can capture the QM generated to form QM-thiol adduct (**4.16**, Scheme 4.9) and prevent QM from converting to other byproducts (such as thioether **4.13**). Compound **4.16** was formed within 254 nm 20 min irradiation then decreased after 0.5 hours. In comparison, compound **4.17** was formed as the major product with 1.5 hours of irradiation. **4.17** is also a common byproduct of RNS photolysis without the addition of 2ME.



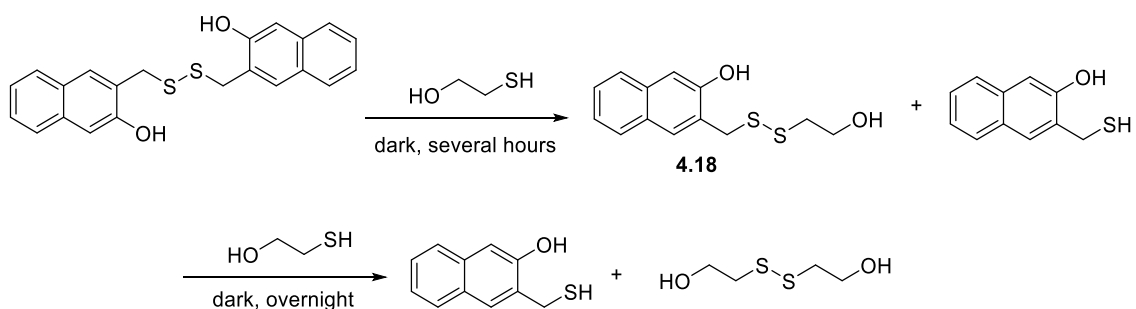
Scheme 4.9 Photoreaction of RNS and 2ME

The **4.17** and RNS have the same retention time (R.T.=4.6 min) in HPLC with many different eluting systems such as 75% MeOH + 25% Water (75M25W). By carefully tuning HPLC eluent, they were separated under 45% MeCN + 10%MeOH + 45% Water (45A10M45W) (Figure 4.15 a), even though they have the same UV absorptions (Figure 4.15 b,c).



The photolysis of RNS and DSF were again analyzed under 45A10M45W system. It was found that in RNS photolysis (300 nm irradiation), RNS disappeared in 3 min irradiation and **4.17** appeared from 3 min (Appendix 5). The DSF photolysis produced no RNS but only **4.17** (Appendix 6).

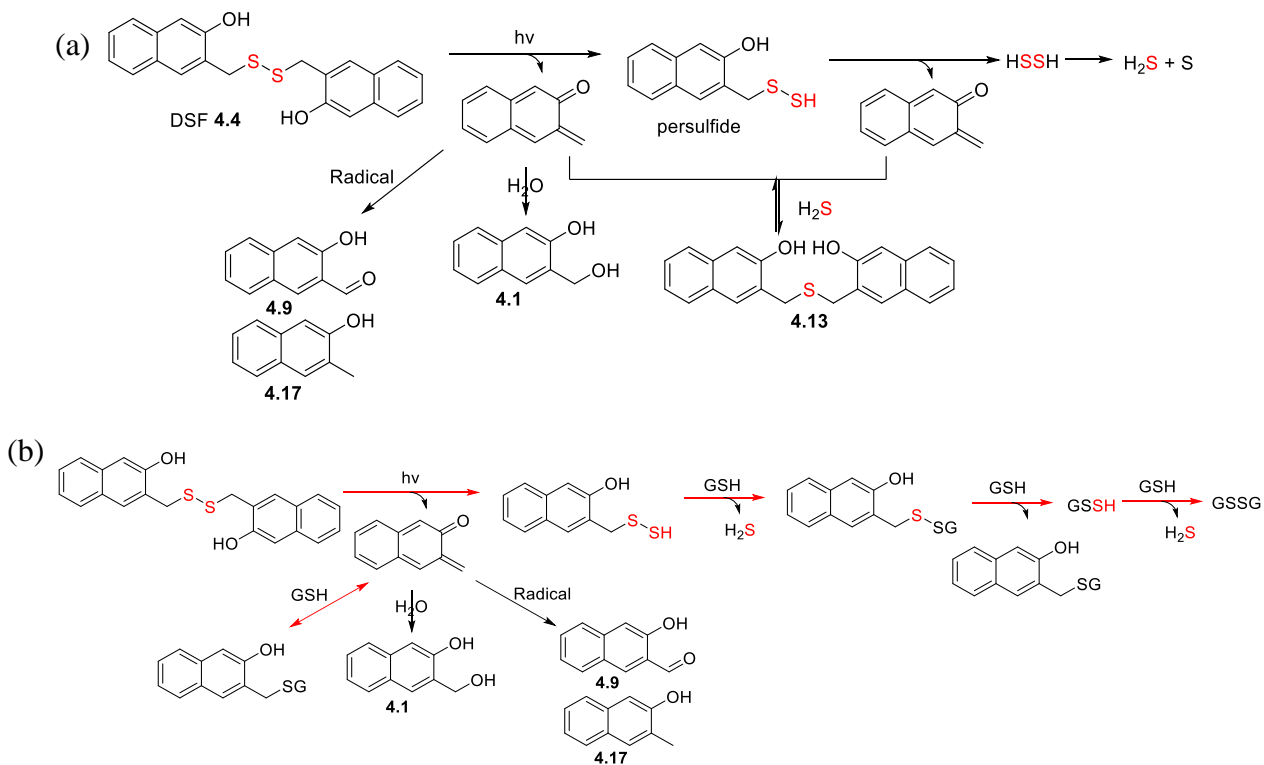
Besides competition reaction with QM which is formed by UV irradiation, 2ME can also react readily with DSF even without irradiation. Through the thiol-disulfide exchange, the 2ME and eventually reduces DSF to RNS (Scheme 4.10) therefore suppressed the formation of the “thioether” **4.13**. The HPLC analysis of the reaction was also studied (Appendix 7).



Scheme 4.10 DSF and 2ME reaction

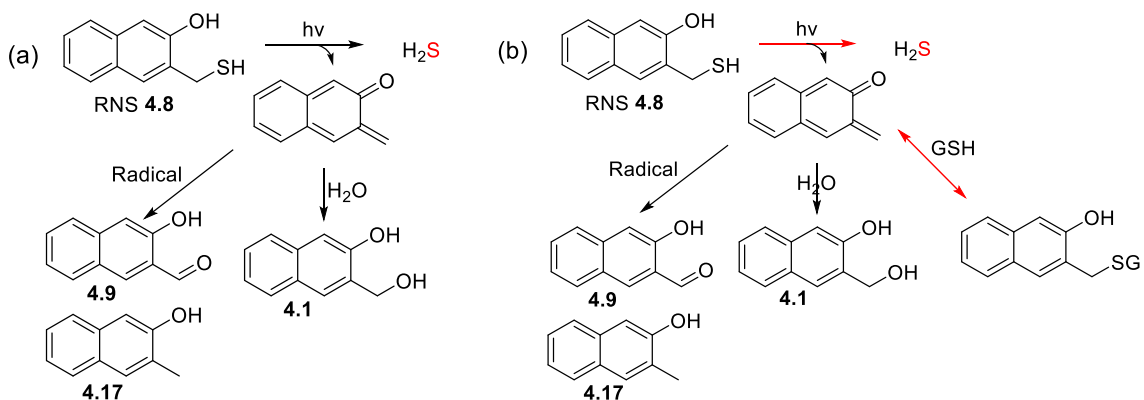
With the byproduct of photolysis characterized, the mechanisms of the H₂S release from DSF and RNS without or with excess thiols addition are proposed (Scheme 4.11). When thiols are not added, the photolysis of DSF results in NQM and persulfide, which produces HSSH. The HSSH undergoes a disproportionation reaction to give one equivalent of H₂S and sulfur. The sulfur was probably the reason why the DSF solution turned turbid yellow upon photolysis. The NQM can consume some H₂S formed to reversibly form thioether (**4.13**). Eventually, the NQM undergoes addition with water and forms aldehyde (**4.9**) and methyl naphthalenol (**4.17**) probably through radical reactions. With excess thiols (such as glutathione, GSH) added, GSH reacts readily with NQM to

release two equivalents of H₂S and suppressed the thioether formation. The HPLC analysis of DSF photolysis in presence of GSH is shown in Appendix 8 (a).



Scheme 4.11 Proposed DSF photolysis mechanism (a) without thiol (b) with thiol

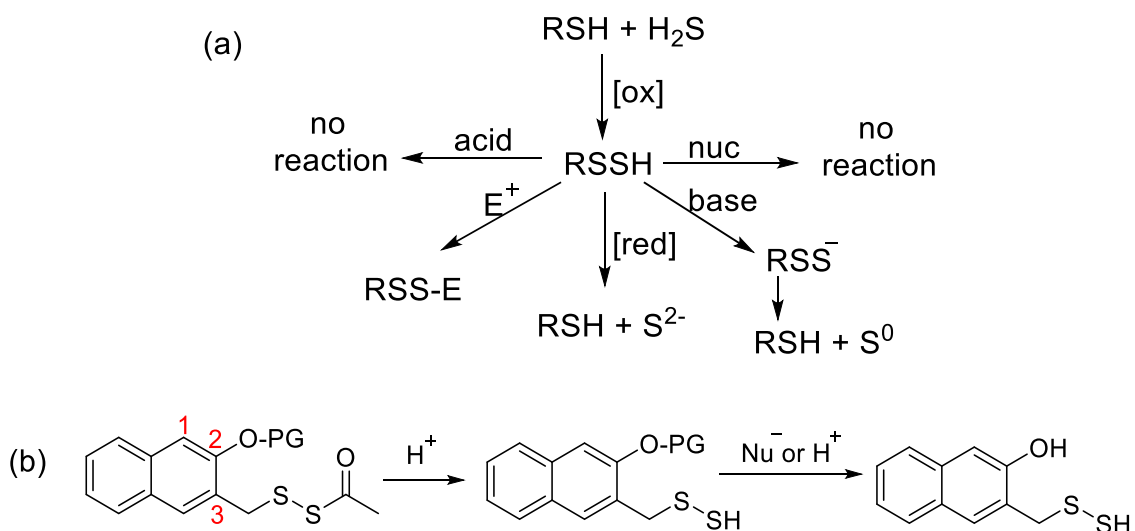
Similarly, with addition of excess thiol (GSH) to the RNS solution, GSH out-competes water to react with NQM to achieve fully release of H₂S. The HPLC analysis of RNS with GSH is shown in Appendix 8 (b).



Scheme 4.12 Proposed RNS photolysis mechanism (a) without thiol (b) with thiol

4.7 Synthesis of NQMP-Persulfide

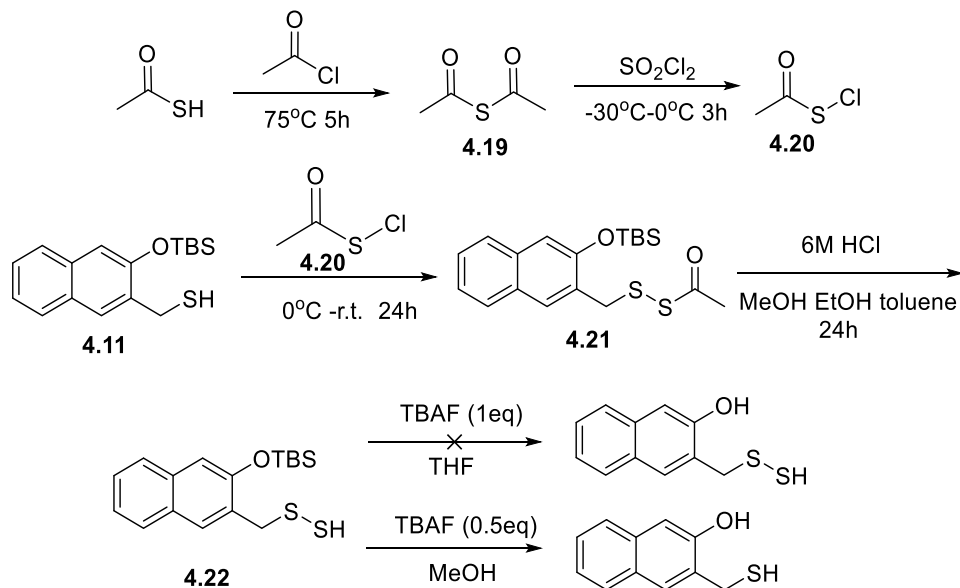
The transient persulfide produced in the process of H₂S release from DSF photolysis is an interesting compound and potentially another H₂S releasing agent. Persulfides are reactive towards base, reduction, and electrophiles conditions, but are stable under nucleophile or acid conditions (Scheme 4.13 a).¹⁰ Persulfide usually forms from the oxidation of thiol and H₂S, but this does not serve as a viable method for synthesis. The NQMP-persulfide (**4.29**) can be obtained from the corresponding persulfide acetate, with removal of nucleophilic or acid-labile protecting group at the 2-position OH (Scheme 4.13 b).



Scheme 4.13 Persulfide (a) reactivities and (b) synthesis ideas

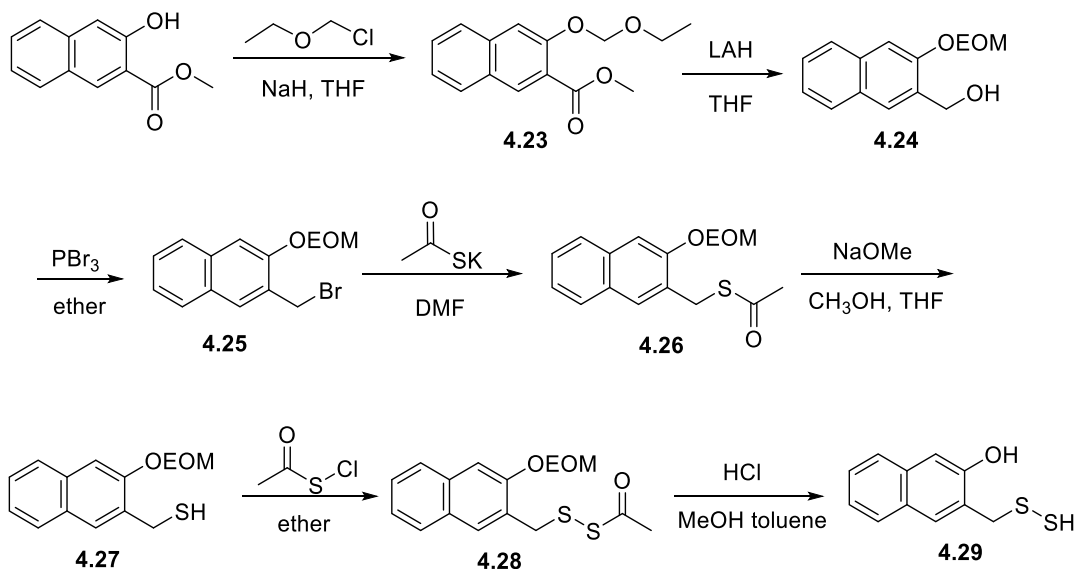
To synthesize the persulfide, acetyl sulfonylchloride (**4.20**) was made from diacetylsulfide (**4.19**). Then, TBS- protected NQMP thiol (**4.11**) was treated with **4.20** to form persulfide acetate **4.21**, which led to TBS- protected NQMP persulfide (**4.22**) after acid removal of the acetate group. However, fluoride ion as nucleophile towards **4.22** failed to generate the desired product. This was because fluoride ion in aprotic solvents,

is considered un-solvated, or “naked”, and naked fluoride is a very strong Lewis base (Scheme 4.14).



Scheme 4.14 Persulfide synthesis – route 1

Then, the acid-labile protecting group ethoxymethyl ether (EOM) was used to make the persulfide acetate (**4.28**). The acid deprotection removed both the acetate and the EOM group to afford the target persulfide **4.29**.



Scheme 4.15 Persulfide synthesis – route 2

4.8 Conclusion

In this chapter, two hydrogen sulfide photo-releasing agents (RNS and DSF), which are based on *o*-naphthoquinone methide precursors (NQMPs) were synthesized and analyzed. The hydrogen sulfide releasing conditions were optimized and the release from the two H₂S donors was characterized by Methylene Blue method. The photo-release showed quantitative yield. the yield was boosted to 95% with addition of simple thiols. Such yields are remarkable comparing to previous photo-activating H₂S donors in literature (30-40%). The reaction intermediate and byproducts were thoroughly studied to understanding the mechanism.

4.9 Experimental Section

3-(hydroxymethyl)naphthalen-2-ol (4.1) A solution of methyl 3-hydroxy-2-naphthoate (10 g, 49 mmol) in THF (200 mL) was added to a suspension of LAH (4 g, 98 mmol) in THF (100 mL) at 0 °C. Reaction was stirred at room temperature for 1 h, quenched with 1M HCl, extracted by ethyl acetate. The organic layer was washed with water, brine, dried with Na₂SO₄, filtered, and concentrated in vacuo to obtain the product (8.6 g, 100%) as a pale yellow solid. ¹H NMR (400 MHz, Acetone-d₆) δ 8.81 (s, 1H), 7.85 (s, 1H), 7.79 (dd, J = 8.2, 1.2 Hz, 1H), 7.67 (dd, J = 8.3, 1.2 Hz, 1H), 7.37 (ddd, J = 8.2, 6.8, 1.4 Hz, 1H), 7.28 (ddd, J = 8.1, 6.8, 1.3 Hz, 1H), 7.20 (s, 1H), 4.93 – 4.87 (m, 2H), 4.51 (t, J = 5.6 Hz, 1H). ¹³C NMR (101 MHz, Acetone) δ 205.39, 153.67, 134.15, 130.79, 128.56, 127.50, 125.99, 125.77, 125.63, 122.96, 108.80, 60.71, 29.56, 29.37, 29.17, 28.98, 28.79, 28.59, 28.40.

3-(acetoxymethyl)naphthalen-2-yl acetate (4.2) Acetic anhydride (7.1 ml) was added to a solution of compound **4.1** (3.2 g, 18.3 mmol) in pyridine (7.3 ml). The reaction was stirred under room temperature for 2 h, evaporated solvent overnight. the residual solid was re-dissolved with CH₂Cl₂, washed with 1M HCl, water, brine, dried over Na₂SO₄, CH₂Cl₂ was stripped to give the product (4.0 g, 100%) as a pale yellow solid. NMR showing that the product is pure, so no column is needed. This compound is known, only H-NMR is needed. ¹H NMR (400 MHz, Chloroform-*d*) δ 7.91 (s, 1H), 7.81 (ddd, *J* = 20.0, 6.8, 2.6 Hz, 2H), 7.57 (s, 1H), 7.54 – 7.43 (m, 2H), 5.24 (s, 2H), 2.37 (s, 3H), 2.10 (s, 3H). ¹³C NMR (101 MHz, CDCl₃) δ 170.67, 169.55, 146.75, 133.65, 131.34, 130.16, 127.86, 127.41, 127.16, 126.98, 126.14, 120.08, 77.35, 77.04, 76.72, 62.03, 20.97, 20.92, -0.00.

(3-hydroxynaphthalen-2-yl)methyl acetate (4.3)

NaSH (2.25 g, 40 mmol) was added to a solution of compound **4.2** (2 g, 7.7 mmol) in acetonitrile/water (40 mL :10 mL). the reaction was heated at 40 °C for 1 h, the intermediate (compound **4.3**) was formed. ¹H NMR (400 MHz, Chloroform-*d*) δ 7.80 (s, 1H), 7.75 (d, *J* = 8.2 Hz, 1H), 7.67 (d, *J* = 8.3 Hz, 1H), 7.44 (s, 1H), 7.43 – 7.38 (m, 1H), 7.32 (ddd, *J* = 8.2, 6.8, 1.2 Hz, 1H), 7.28 (s, 1H), 5.31 (s, 2H), 2.13 (s, 3H). ¹³C NMR (101 MHz, CDCl₃) δ 173.21, 152.60, 135.28, 131.80, 128.49, 127.78, 126.99, 126.26, 124.00, 123.88, 111.97, 77.34, 77.03, 76.71, 63.28, 20.97, 0.00.

3,3'-(disulfanediybis(methylene))bis(naphthalen-2-ol) (4.4)

A solution of **4.7** (5.1 g, 14.5 mmol) in EtOH (40 mL) was added to a solution of thiourea (1.2 g, 15.8 mmol) in warm EtOH (40 mL). Then the mixture was heated to reflux for 2.5 h. A NaOH solution (1.5 g, 37.5 mmol) in H₂O (20 mL) was slowly added and white

solid precipitates formed. Another 50 mL EtOH was added to the mixture and a light-yellow homogeneous solution was formed. The mixture was heated to 80 °C for 30 min. Then, 2M HCl (20.5 mL, 1:5 dilution of concentrated HCl) was added to acidify the solution. Partitioned the mixture between ethyl acetate and water washed the organic layer with brine and dried with sodium sulfate and concentrated in vacuo. The crude product was purified by column chromatography (ethyl acetate: hexanes 1:3) to obtain the product (1.5g, 54%), with the major byproduct was RNS (compound **4.8**).

(Alternative protocol) tetra-n-butylammonium fluoride (TBAF) (0.16 mL of 1M in THF solution, 0.16 mmol) was added to a solution of compound **4.14** (0.1 g, 0.16 mmol) in THF (4 mL) and at 0 °C for 5 min, poured into brine (30 mL), extracted with ethyl acetate. The organic layer was dried over Na₂SO₄. The crude product was purified by column chromatography (ethyl acetate: hexanes 1:3) to obtain the product (0.01 g, 17%) as a light yellow solid. ¹H NMR (400 MHz, CD₃OD_SPE) δ 7.60 (dd, *J* = 21.5, 8.2 Hz, 3H), 7.40 (s, 1H), 7.27 (dddd, *J* = 35.1, 8.1, 6.9, 1.3 Hz, 3H), 7.09 (s, 1H), 3.77 (s, 2H), 1.20 (t, *J* = 7.1 Hz, 1H). ¹³C NMR (101 MHz, CD₃OD_SPE) δ 153.48, 134.62, 130.01, 128.19, 127.27, 126.30, 125.64, 125.39, 122.68, 108.39, 38.13 HRMS (ESI), *m/z*: calcd. for C₁₁H₁₀OS [M-H]⁻ 189.0374, found 189.0379.

tert-butyl((3-(((tert-butyl)dimethylsilyloxy)methyl)naphthalen-2-

yl)oxy)dimethylsilane (4.5) Tert-butylchlorodimethylsilane (2.9 g, 19 mmol), imidazole (1.3 g, 19 mmol) and DMAP (10 mg) were added to a stirring solution of compound **4.1** (1 g, 5.74 mmol) in DMF (20 mL). The reaction was stirred at room temperature overnight, extracted with ethyl acetate, washed with water (50 mL×3) and purified by a silica flash chromatography (ethyl acetate: hexanes 1:4) to obtain the product (2.3 g, 100%) as a yellow oil. ¹H NMR (400 MHz, Chloroform-*d*) δ 7.89 (s, 1H), 7.78 (d, *J* = 8.0

Hz, 1H), 7.66 (d, $J = 8.0$ Hz, 1H), 7.42 – 7.27 (m, 2H), 7.08 (s, 1H), 4.90 (t, $J = 1.3$ Hz, 2H), 1.04 (d, $J = 1.1$ Hz, 9H), 1.00 (d, $J = 1.2$ Hz, 9H), 0.29 (d, $J = 1.1$ Hz, 6H), 0.15 (d, $J = 1.2$ Hz, 6H). ^{13}C NMR (101 MHz, CDCl_3) δ 150.97, 133.79, 133.41, 129.25, 127.71, 126.26, 125.56, 125.50, 123.72, 112.72, 77.40, 77.08, 76.76, 61.29, 26.11, 25.83, 18.65, 18.35, 0.08, -4.13, -5.23.

(3-((tert-butyldimethylsilyl)oxy)naphthalen-2-yl)methanol (4.6) HF (0.4 ml, 20 mmol) was added to a stirring solution of compound **4.5** (2 g, 5 mmol) in acetonitrile (30 mL) at 50 °C for 15 min. The reaction was quenched by NaHCO_3 solid, filtered, and concentrated in vacuo, extracted with ethyl acetate. The organic layer was washed with water and brine, evaporated, purified by silica gel chromatography (ethyl acetate: hexanes 1:4) to afford the product (1.14 g, 80%) as a yellow oil. ^1H NMR (400 MHz, CDCl_3) δ 7.76 (d, $J = 8.9$ Hz, 2H), 7.67 (dd, $J = 8.1, 1.2$ Hz, 1H), 7.41 (ddd, $J = 8.2, 6.8, 1.3$ Hz, 1H), 7.34 (ddd, $J = 8.0, 6.8, 1.3$ Hz, 1H), 7.14 (s, 1H), 4.82 (d, $J = 5.9$ Hz, 2H), 2.38 – 2.25 (m, 1H), 1.05 (s, 9H), 0.33 (s, 6H). ^{13}C NMR (101 MHz, CDCl_3) δ 171.20, 151.82, 133.92, 132.82, 129.05, 127.63, 127.38, 126.29, 126.09, 124.03, 113.29, 77.35, 77.03, 76.71, 62.40, 60.41, 25.78, 21.06, 18.24, 14.19, -0.00, -4.16.

((3-(bromomethyl)naphthalen-2-yl)oxy)(tert-butyl)dimethylsilane (4.7) PBr_3 (0.47 g, 1.73 mmol) was added dropwise to a solution of compound **4.6** (1 g, 3.47 mmol) in anhydrous ether (6 mL). The reaction was stirred at room temperature for 0.5 h, quenched by of saturated sodium bicarbonate solution (50 mL), extracted by ethyl ether. The organic layer was dried over sodium sulfate, concentrated in vacuo. The residue was purified by chromatography (ethyl acetate: hexanes 1:30) to afford the (1 g, 83%) as a white solid. ^1H NMR (400 MHz, CDCl_3) δ 7.95 (s, 1H), 7.87 (dd, $J = 8.2, 4.5$ Hz, 2H),

7.60 (ddd, $J = 8.2, 6.8, 1.2$ Hz, 1H), 7.51 (ddd, $J = 8.0, 6.9, 1.2$ Hz, 1H), 4.86 (s, 2H), 1.34 (s, 9H), 0.59 (s, 6H). ^{13}C NMR (101 MHz, CDCl_3) δ 151.98, 135.00, 130.85, 130.16, 129.05, 127.94, 127.00, 126.58, 124.37, 113.61, 77.69, 77.37, 77.05, 29.91, 26.18, 18.59, -3.82.

3-(mercaptomethyl)naphthalen-2-ol (4.8) The solution of compound **4.4** (0.1 g, 0.26 mmol) in THF (1 mL) was added dropwise to a stirring solution of LAH (0.3 mL 2.4 M LAH in THF, 0.72 mmol) in THF (1 mL). The reaction was stirred at room temperature for 30 min, quenched by adding water and 1M HCl dropwise, extracted by ethyl acetate. The organic layer was combined and washed with brine, dried by Na_2SO_4 , filtered, purified by silica gel chromatography (ethyl acetate: hexanes 1:3) to afford the product (0.1 g, 100%) as a colorless to light yellow crystal. ^1H NMR (400 MHz, CDCl_3) δ 7.67 (d, $J = 8.1$ Hz, 1H), 7.57 (d, $J = 12.0$ Hz, 2H), 7.40 – 7.33 (m, 1H), 7.29 (td, $J = 7.5, 6.9, 1.4$ Hz, 1H), 6.19 (s, 1H), 3.86 (d, $J = 7.5$ Hz, 2H), 1.97 (td, $J = 7.6, 1.3$ Hz, 1H). ^{13}C NMR (101 MHz, CDCl_3) δ 151.92, 133.99, 129.12, 128.85, 128.31, 127.40, 126.30, 126.01, 123.90, 110.92, 77.37, 77.05, 76.73, 25.18, 0.00. ESI, m/z : calcd. for $\text{C}_{22}\text{H}_{18}\text{O}_2\text{S}_2$ $[\text{M-H}]^-$ 377.1, found 377.0.

3-hydroxy-2-naphthaldehyde (4.9) Compound **4.4** (28 mg, 0.5 mmol) was dissolved in 290 mL 1:1 acetonitrile: water solution in quartz photoreactor and was irradiated by 300 nm light for 5 min. A more nonpolar spot than starting material was formed and extracted from the reaction using ethyl acetate. The organic layer was washed with brine, evaporated, purified by column chromatography to provide the product as a yellow solid. ^1H NMR (400 MHz, CDCl_3) δ 10.26 (s, 1H), 10.02 (d, $J = 0.6$ Hz, 1H), 8.09 (s, 1H), 7.81 (dd, $J = 8.4, 1.2$ Hz, 1H), 7.65 (dd, $J = 8.4, 1.1$ Hz, 1H), 7.50 (ddd, $J = 8.3, 6.8, 1.3$ Hz,

1H), 7.31 (ddd, $J = 8.2, 6.8, 1.2$ Hz, 1H), 7.22 (s, 1H). ^{13}C NMR (101 MHz, CDCl_3) δ 196.76, 155.87, 138.23, 137.94, 130.34, 129.41, 127.44, 126.73, 124.47, 122.32, 111.98, 77.38, 77.06, 76.74.

S-((3-((tert-butyldimethylsilyl)oxy)naphthalen-2-yl)methyl) ethanethioate (4.10)

Compound **4.7** (1 g, 2.8 mmol) was added to a green solution of potassium thioacetate (0.65 g, 5.6 mmol) in DMF (10 mL) at 0 °C. The mixture was stirred at 0 °C for 10 min, diluted with diethyl ether. The organic layer was washed with water, brine, dried over Na_2SO_4 , evaporated, and purified by flash silica chromatography (ethyl acetate: hexanes 1:30) to afford the product (0.75 g, 76%) as a colorless oil. ^1H NMR (400 MHz, Chloroform- d) δ 7.63 (s, 1H), 7.53 (d, $J = 8.1$ Hz, 1H), 7.43 (s, 1H), 7.19 (ddd, $J = 8.2, 6.8, 1.3$ Hz, 1H), 7.11 (ddd, $J = 8.1, 6.9, 1.2$ Hz, 1H), 6.93 (s, 1H), 4.07 (s, 2H), 2.12 (s, 3H), 0.87 (s, 9H), 0.15 (s, 6H). ^{13}C NMR (101 MHz, CDCl_3) δ 195.59, 151.96, 134.03, 129.80, 129.73, 128.93, 127.55, 126.26, 126.17, 123.99, 113.01, 77.41, 77.09, 76.78, 30.46, 29.34, 25.90, 18.36, -4.06.

(3-((tert-butyldimethylsilyl)oxy)naphthalen-2-yl)methanethiol (4.11) NaOCH_3 (0.16 g, 3 mmol) was added to a stirred solution of compound **4.10** (0.35 g, 1 mmol) in THF (4 mL)/ CH_3OH (4 mL) at 0 °C was added. The mixture was stirred at 0 °C for 5 min, quenched by saturated NH_4Cl , extracted by ethyl acetate (30 mL x 3). The organic layer was washed with brine, dried over Na_2SO_4 , evaporated, and purified by silica gel chromatography (ethyl acetate: hexanes 1:30) to afford the product (0.2 g, 65%) as a colorless to light yellow liquid. Under TLC using 1:9 ethyl acetate: hexanes eluent, there are 2 spots formed: (Top: R_f 0.9 and bottom: R_f 0.25) while the S.M. has R_f 0.5. Separated the two products by column chromatography (1:9 ethyl acetate: hexanes)

obtained 0.2g top spot (colorless to light yellow liquid) and 0.1g bottom spot (yellow liquid). To my surprise, the top spot is the product, according to nmr (65%). Notably, the product is made of two extremely close spots which can be seen using 1:30 ethyl acetate: hexane. ^1H NMR (400 MHz, CDCl_3) δ 7.52 (d, $J = 7.7$ Hz, 2H), 7.46 (d, $J = 8.2$ Hz, 1H), 7.19 (dd, $J = 8.3, 6.8$ Hz, 1H), 7.16 – 7.08 (m, 1H), 6.94 (s, 1H), 3.66 (d, $J = 7.9$ Hz, 2H), 1.72 (t, $J = 8.0$ Hz, 1H), 1.36 (s, 1H), 0.88 (d, $J = 2.1$ Hz, 9H), 0.15 (d, $J = 2.6$ Hz, 6H). ^{13}C NMR (101 MHz, CDCl_3) δ 151.64, 133.87, 133.54, 129.11, 128.35, 127.36, 126.28, 126.02, 123.99, 113.43, 77.37, 77.05, 76.73, 25.91, 24.83, 18.36, -4.08. ESI, m/z : calcd. for $\text{C}_{17}\text{H}_{24}\text{OSSi}$ $[\text{M}+\text{H}]^+$ 305.1, found 305.1.

bis((3-((tert-butyl)dimethylsilyloxy)naphthalen-2-yl)methyl)sulfane (4.12) sodium hydride (0.1 g 60% dispersion in oil, 3 mmol) was added to a solution of compound **4.11** (0.3 g, 1 mmol) in THF (6 mL) at 0 °C. Then, compound **4.7** (0.35 g, 1 mmol) was added to the stirring solution. The mixture was stirred at 0 °C for 30 min, quenched by saturated NH_4Cl , extracted by ethyl acetate. The organic layer was washed with brine, dried over Na_2SO_4 , evaporated, purified by silica gel chromatography (ethyl acetate: hexanes 1:30) to afford the product (0.3 g, 64%) as a colorless oil. ^1H NMR (400 MHz, Chloroform- d) δ 7.65 – 7.57 (m, 6H), 7.31 (dd, $J = 8.2, 6.8$ Hz, 3H), 7.24 (dd, $J = 8.2, 6.7$ Hz, 2H), 7.08 (s, 2H), 3.79 (s, 4H), 0.93 (s, 18H), 0.22 (d, $J = 1.0$ Hz, 12H). ^{13}C NMR (101 MHz, CDCl_3) δ 152.30, 133.95, 130.48, 129.24, 129.01, 127.51, 126.31, 125.94, 123.90, 113.51, 77.49, 77.17, 76.85, 31.66, 25.97, 18.40, -4.02. ESI, m/z : calcd. for $\text{C}_{34}\text{H}_{46}\text{O}_2\text{SSi}_2$ $[\text{M}+\text{H}]^+$ 575.3, found 575.2.

3,3'-(thiobis(methylene))bis(naphthalen-2-ol) (4.13) tetra-*n*-Butylammonium fluoride (TBAF) (0.52 mL of 1M in THF solution, 0.52 mmol) was added to a stirring solution of

compound **4.12** (0.3 g, 0.52 mmol) in THF (4 mL) at 0 °C for 5 min, extracted with ethyl acetate. The organic layer was washed with brine, dried over Na₂SO₄, evaporated. The crude product was purified by column chromatography (ethyl acetate: hexanes 1:3) to afford the product (0.05 g, 27%) as a light yellow solid. ¹H NMR (400 MHz, CDCl₃) δ 7.71 (d, *J* = 8.1 Hz, 2H), 7.65 (dd, *J* = 13.8, 8.2 Hz, 2H), 7.54 (s, 1H), 7.47 (s, 1H), 7.42 (dd, *J* = 8.2, 6.8 Hz, 2H), 7.40 – 7.30 (m, 2H), 7.23 (s, 1H), 7.17 (s, 1H), 6.76 (s, 1H), 6.29 (s, 1H), 4.19 (d, *J* = 7.2 Hz, 1H), 3.94 (s, 2H), 3.89 (s, 2H), 1.31 (s, 2H). ¹³C NMR (101 MHz, CDCl₃) δ 152.78, 152.05, 134.35, 130.66, 130.05, 128.84, 128.70, 127.62, 127.40, 126.51, 126.45, 126.25, 126.19, 125.58, 124.88, 124.00, 123.96, 111.47, 110.88, 77.43, 77.11, 76.79, 39.11, 32.29. HRMS (ESI), *m/z*: calcd. for C₂₂H₁₈O₂S [M-H]⁻ 345.0949, found 345.0953.

1,2-bis((3-((tert-butyldimethylsilyl)oxy)naphthalen-2-yl)methyl)disulfane (4.14) 30% hydrogen peroxide solution (0.34 mL, 3 mmol) was added to a solution of compound **4.11** (0.2 g, 0.66 mmol) in ethyl acetate (3 mL). Then, sodium iodide (0.02 g, 0.13 mmol) was added to the stirring solution as bubbling was observed. The mixture was stirred at room temperature for 3 days, extracted by ethyl acetate. The organic layer was washed by water and brine, dried over Na₂SO₄, evaporated. The crude product was purified by column chromatography (ethyl acetate: hexanes 1:30) to provide the product (quantitative) as a yellow solid. ¹H NMR (400 MHz, Chloroform-*d*) δ 7.82 (dt, *J* = 19.6, 6.6 Hz, 4H), 7.63 (d, *J* = 5.0 Hz, 2H), 7.51 (dq, *J* = 20.6, 6.7 Hz, 4H), 7.33 – 7.26 (m, 2H), 3.92 (dd, *J* = 6.4, 3.6 Hz, 4H), 1.27 – 1.19 (m, 18H), 0.49 (dd, *J* = 6.3, 3.4 Hz, 12H). ¹³C NMR (101 MHz, CDCl₃) δ 152.09, 134.33, 134.30, 130.37, 130.34, 129.56, 128.92,

128.90, 127.68, 126.50, 126.25, 124.06, 113.23, 77.58, 77.27, 77.24, 76.95, 39.72, 26.13, 18.51, -3.88.

2-ethoxy-3,4-dihydro-2H-benzo[g]chromene (4.15) A solution of diol (50 mg, 0.29 mmol) and ethyl vinyl ether (2.8 mL, 29 mmol) in acetonitrile/water (1:1, 290 mL) was stirred in a 500 mL glass RBF and irradiated using mini-Rayonet photochemical reactor equipped with 8 fluorescent UV lamps (254 nm) for 1.5 h. Photolysate was extracted with ethyl acetate, dried over sodium sulfate, evaporated. The residue was separated by chromatography (ethyl acetate: hexanes 1:3) to give the Diels Alder adduct (quantitative) as a colorless oil. ^1H NMR (400 MHz, Chloroform-*d*) δ 7.71 – 7.63 (m, 2H), 7.52 (s, 1H), 7.34 (ddd, $J = 8.3, 6.8, 1.3$ Hz, 1H), 7.27 (ddd, $J = 8.1, 6.8, 1.3$ Hz, 1H), 5.32 (t, $J = 3.0$ Hz, 1H), 3.93 (dq, $J = 9.7, 7.1$ Hz, 1H), 3.67 (dq, $J = 9.7, 7.1$ Hz, 1H), 3.19 (dddd, $J = 17.6, 11.6, 6.3, 1.5$ Hz, 1H), 2.90 – 2.79 (m, 1H), 2.08 (dddd, $J = 15.8, 11.6, 5.9, 3.0$ Hz, 2H), 1.18 (t, $J = 7.1$ Hz, 3H). ^{13}C NMR (101 MHz, CDCl_3) δ 150.97, 133.45, 128.90, 127.59, 127.03, 126.31, 125.40, 124.61, 123.54, 111.67, 97.16, 77.34, 77.02, 76.70, 63.70, 26.77, 21.01, 15.14, 0.00.

3-(((2-hydroxyethyl)thio)methyl)naphthalen-2-ol (4.16) A solution of compound **4.7** (27.5 mg, 0.145 mmol) and ethyl vinyl ether (1.13 g, 14.5 mmol) in acetonitrile/water (1:1, 145 mL) was stirred in a quartz container and irradiated using Rayonet photochemical reactor equipped with 15 fluorescent UV lamps (254 nm) for 20min. Photolysate was extracted with ethyl acetate, dried over sodium sulfate, concentrated in vacuo. The product was separated by column chromatography (ethyl acetate: hexanes 1:5). ^1H NMR (400 MHz, Chloroform-*d*) δ 7.71 (d, $J = 7.7$ Hz, 1H), 7.66 (d, $J = 8.2$ Hz, 1H), 7.62 (s, 1H), 7.40 (ddd, $J = 8.2, 6.8, 1.3$ Hz, 1H), 7.32 (ddd, $J = 8.1, 6.8, 1.2$ Hz,

1H), 7.26 (s, 1H), 7.23 (s, 1H), 3.99 (s, 2H), 3.79 (t, $J = 5.9$ Hz, 2H), 2.68 (t, $J = 5.8$ Hz, 2H). ^{13}C NMR (101 MHz, CDCl_3) δ 152.79, 134.31, 129.66, 128.66, 127.36, 126.36, 126.16, 125.52, 123.86, 111.43, 77.35, 77.03, 76.72, 61.11, 60.37, 41.16, 33.82, 32.23, -0.00.

3-methylnaphthalen-2-ol (4.17) A solution of diol (25 mg, 0.13 mmol) and ethyl vinyl ether (1.0 g, 13 mmol) in acetonitrile/water (1:1, 130 mL) was stirred in a quartz container and irradiated using Rayonet photochemical reactor equipped with 16 fluorescent UV lamps (254 nm) for 1.5 h. Photolysate was extracted with ethyl acetate, dried over sodium sulfate, concentrated in vacuo. The crude was purified by chromatography (ethyl acetate: hexanes 1:30) to afford the product (10 mg, 48%) as a white crystal. ^1H NMR (400 MHz, Chloroform-*d*) δ 7.70 (d, $J = 8.1$ Hz, 1H), 7.64 (d, $J = 8.2$ Hz, 1H), 7.59 (s, 1H), 7.40 – 7.33 (m, 1H), 7.29 (ddd, $J = 8.1, 6.8, 1.3$ Hz, 1H), 7.10 (s, 1H), 5.06 (s, 1H), 2.42 (s, 3H). ^{13}C NMR (101 MHz, CDCl_3) δ 152.71, 133.35, 129.35, 129.15, 126.99, 126.36, 125.84, 125.55, 123.52, 108.97, 77.34, 77.02, 76.70, 16.51, -0.00.

3-(((2-hydroxyethyl)disulfaneyl)methyl)naphthalen-2-ol (4.18) A solution of compound **4.13** (1 mM, 3 mL) and 2-mercaptoethanol (36 mg, 150 mmol) in acetonitrile/water (1:1) solution was left in dark for 10 h, extracted with ethyl acetate, dried over sodium sulfate, concentrated in vacuo. The residue was separated by chromatography (ethyl acetate: hexanes 1:3) to get the product. ^1H NMR (400 MHz, Chloroform-*d*) δ 7.78 – 7.67 (m, 2H), 7.64 – 7.58 (m, 1H), 7.39 (ddd, $J = 8.2, 6.9, 1.3$ Hz, 1H), 7.31 (ddd, $J = 8.1, 6.8, 1.3$ Hz, 1H), 7.13 (s, 1H), 6.95 (s, 1H), 4.12 (s, 2H), 3.84 (t, $J = 5.7$ Hz, 2H), 2.60 (t, $J = 5.6$ Hz, 2H). ^{13}C NMR (101 MHz, CDCl_3) δ 152.26,

152.19, 134.27, 130.48, 128.69, 127.52, 126.48, 126.05, 125.59, 123.87, 110.77, 110.44, 110.25, 77.34, 77.02, 76.70, 60.79, 40.63, 38.86, -0.00.

acetic thioanhydride (4.19) Acetyl chloride (13.4 g, 170 mmol) was added dropwise to a stirring solution of thioacetic acid (6.5 g, 85 mmol). The reaction was heat to 75 °C for 5 h, cooled to room temperature and concentrated in vacuo to afford the product (8 g, 80%) as a yellow liquid. The product must be stored under -20 °C immediately to prevent decomposition. ¹H NMR (400 MHz, Chloroform-d) δ 2.54 (s, 6H). ¹³C NMR (101 MHz, CDCl₃) δ 191.91, 32.66.

acetic hypochlorous thioanhydride (4.20) Sulfuryl chloride (3.73 mL, 46.2 mmol) was added dropwise to diacetyl sulfide (5.3 g, 45 mmol) at -30 °C and was allowed to warm to 0 °C over a course of 3 h, during which time the color of the solution changed from pale yellow to orange. The reaction mixture was concentrated in vacuo to yield the product (4 g, 80%) as a yellow liquid. The product must be stored under -20°C immediately to avoid decomposition. ¹H NMR (400 MHz, Chloroform-d) δ 2.43 (s, 3H). ¹³C NMR (101 MHz, CDCl₃) δ 190.15, 26.37.

SS-((3-((tert-butyldimethylsilyl)oxy)naphthalen-2-yl)methyl)

ethane(dithioperoxoate) (4.21) Acetyl sulfenyl chloride (0.28 g, 2.55 mmol) in 4 mL ether was added dropwise to a solution of compound **4.9** (0.5 g, 1.7 mmol) in ether (9 mL) in an ice bath. The reaction mixture stirred at room temperature for 24 h, quenched by saturated NaHCO₃ and stirred for 1 h until the bubbling subsided, extracted by ethyl acetate. The organic layer was washed by saturated NaHCO₃ twice, dried over Na₂SO₄, concentrated in vacuo, purified by silica gel chromatography (ethyl acetate: hexanes 1:20) to afford the product (0.8 g, 100% yield) as a yellow oil. ¹H NMR (400 MHz,

Chloroform-*d*) δ 7.72 (d, $J = 8.9$ Hz, 1H), 7.65 (d, $J = 8.3$ Hz, 2H), 7.62 (s, 1H), 7.44 – 7.37 (m, 2H), 7.32 (t, $J = 7.5$ Hz, 2H), 7.14 (s, 2H), 5.41 – 5.26 (m, 1H), 4.06 (s, 2H), 2.27 (s, 3H), 1.07 (s, 9H), 0.36 (s, 6H). ^{13}C NMR (101 MHz, CDCl_3) δ 195.70, 151.86, 134.29, 130.55, 130.20, 128.55, 128.30, 127.52, 126.36, 124.08, 113.19, 77.43, 77.12, 76.80, 38.88, 28.50, 25.97, 18.41, 0.09, -4.05.

tert-butyl((3-(disulfaneylmethyl)naphthalen-2-yl)oxy)dimethylsilane (4.22)

Compound **4.21** (0.6 g, 1.58 mmol) was dissolved in EtOH: toluene solvent (7:5, 3.3 mL EtOH and 2.4 mL toluene) in 0 °C under stirring. Then, a 3M HCl in MeOH solution (3.3 mL) was chilled to 0 °C and added dropwise. The reaction mixture was stirred at room temperature for 24 h, extracted by ethyl acetate. The organic layer was washed with brine and dried over Na_2SO_4 , concentrated in vacuo, purified by silica gel chromatography (ethyl acetate: hexanes 1:20) to afford the product (0.4 g, 75%) as a yellow oil. ^1H NMR (400 MHz, Chloroform-*d*) δ 7.73 (s, 2H), 7.64 (s, 1H), 7.39 (d, $J = 7.0$ Hz, 1H), 7.31 (d, $J = 7.3$ Hz, 1H), 7.13 (s, 1H), 4.28 (s, 2H), 1.86 (d, $J = 1.8$ Hz, 1H), 1.05 (d, $J = 2.5$ Hz, 9H), 0.33 (dt, $J = 6.0, 2.4$ Hz, 6H). ^{13}C NMR (101 MHz, CDCl_3) δ 151.87, 134.41, 130.68, 130.55, 128.77, 128.10, 127.65, 126.39, 124.11, 113.28, 77.45, 77.13, 76.81, 39.95, 26.06, 18.44, 0.14, -3.93.

methyl 3-(ethoxymethoxy)-2-naphthoate (4.23) A solution of methyl 3-hydroxy-2-naphthoate (3.3 g, 16.3 mmol) in THF (50 mL) was slowly added to a stirring suspension of NaH (2.2 g, 23.7 mmol 60% weight in oil) in THF (100 mL) at -7 °C and kept stirring for 15 min. Then, the chloromethyl ethyl ether (2.2 g, 24.3 mmol) was slowly added to the solution. The reaction mixture was stirred room temperature overnight, quenched with water, extracted by ethyl acetate. The organic layer was washed with brine, dried

over sodium sulfate, evaporated, and purified by silica gel chromatography (ethyl acetate: hexanes 1:5) to afford the product (3.9 g, 100%) as a yellow liquid. ^1H NMR (400 MHz, Chloroform-*d*) δ 8.29 (s, 1H), 7.81 (d, $J = 8.2$ Hz, 1H), 7.74 (d, $J = 8.2$ Hz, 1H), 7.54 – 7.45 (m, 2H), 7.42 – 7.33 (m, 1H), 5.41 (s, 2H), 3.95 (s, 3H), 3.82 (q, $J = 7.1$ Hz, 2H), 1.25 (t, $J = 7.1$ Hz, 3H). ^{13}C NMR (101 MHz, CDCl_3) δ 166.70, 153.14, 135.93, 132.48, 128.60, 128.31, 128.11, 126.83, 124.80, 122.39, 111.27, 93.79, 77.44, 77.12, 76.80, 64.66, 52.25, 15.15, 0.02.

(3-(ethoxymethoxy)naphthalen-2-yl)methanol (4.24) Compound **4.23** (4 g, 16 mmol) was added to a stirring solution of LAH (18 mL, 41 mmol 2.4 M LAH in THF solution) in THF (30ml). The reaction was stirred at room temperature for 4 h, quenched with water, extracted by ethyl acetate. The organic layer was washed with brine, dried over sodium sulfate, evaporated, purified by silica gel chromatography (ethyl acetate: hexanes 1:3) to afford the product (3.6 g, 100%) as a colorless oil. ^1H NMR (400 MHz, Chloroform-*d*) δ 7.75 – 7.67 (m, 3H), 7.45 – 7.28 (m, 3H), 5.33 (s, 2H), 4.80 (s, 2H), 3.71 (q, $J = 7.1$ Hz, 2H), 1.21 (t, $J = 7.1$ Hz, 3H). ^{13}C NMR (101 MHz, CDCl_3) δ 153.35, 133.97, 130.97, 129.18, 127.66, 127.32, 126.82, 126.26, 124.27, 108.87, 93.26, 77.50, 77.18, 76.86, 64.72, 61.97, 15.18, 0.08.

2-(bromomethyl)-3-(ethoxymethoxy)naphthalene (4.25) To a stirring solution of PPh_3 (19.1 g, 73 mmol) and imidazole (5 g, 73 mmol) in CH_2Cl_2 (250 mL) at 0 °C, was added Br_2 (9.2 g~3 mL, 58 mmol) dropwise and stirred for another 10 min. Then, the compound **4.24** (10.1 g, 48.6 mmol) in CH_2Cl_2 (50 mL) was added. The reaction was warmed up to room temperature and reacted for 0.5 h, filter, washed with sodium thiosulfate solution, extracted by ethyl acetate. The organic layer was washed with water, brine, dried over

sodium sulfate, evaporated, purified by silica gel chromatography (ethyl acetate: hexane 1:9 to 1:3) to afford the product (9.9 g, 72%) as a yellow liquid. ^1H NMR (400 MHz, Chloroform-*d*) δ 7.81 (s, 1H), 7.77 – 7.69 (m, 2H), 7.47 – 7.38 (m, 2H), 7.34 (ddd, J = 8.1, 6.9, 1.2 Hz, 1H), 5.40 (s, 2H), 4.78 (s, 2H), 3.79 (q, J = 7.0 Hz, 2H), 1.24 (td, J = 7.1, 1.0 Hz, 4H). ^{13}C NMR (101 MHz, CDCl_3) δ 152.97, 134.65, 130.00, 128.88, 127.74, 127.61, 126.89, 126.87, 124.41, 109.20, 93.10, 77.44, 77.13, 76.81, 64.69, 42.37, 15.21, 0.08.

S-((3-(ethoxymethoxy)naphthalen-2-yl)methyl) ethanethioate (4.26) Compound **4.25** (9.9 g, 3 mmol) in DMF (10 mL) was added to a stirring solution of potassium thioacetate (6 g, 53 mmol) in DMF (25 mL) at 0 °C. The solution was stirred for 20 min at 0 °C. Then the mixture, extracted by ethyl acetate. The organic layer was washed with water (30 mL \times 10), brine, dried over sodium sulfate, filtered, concentrated in vacuo, and purified by silica gel chromatography (ethyl acetate: hexanes 1:9) to afford the product (8.8 g, 91%) as a light-yellow liquid. ^1H NMR (400 MHz, Chloroform-*d*) δ 7.79 (s, 1H), 7.68 (t, J = 7.9 Hz, 2H), 7.40 – 7.33 (m, 2H), 7.32 – 7.26 (m, 1H), 5.33 (s, 2H), 4.27 (s, 2H), 3.74 (q, J = 7.1 Hz, 2H), 2.27 (s, 3H), 1.23 (td, J = 7.1, 1.0 Hz, 3H). ^{13}C NMR (101 MHz, CDCl_3) δ 195.40, 153.22, 134.05, 129.59, 129.04, 127.78, 127.57, 126.81, 126.37, 124.27, 108.75, 93.04, 77.62, 77.30, 76.98, 64.66, 30.45, 29.19, 15.28.

(3-(ethoxymethoxy)naphthalen-2-yl)methanethiol (4.27) Sodium methoxide (5.2 g, 96 mmol) was added to a stirring solution of compound **4.26** (8.8 g, 32 mmol) in THF (20 mL) and methanol (20 mL) at 0 °C. The reaction was stirred for 20 min at 0 °C, extracted by ethyl acetate. The organic layer was washed with water, brine, dried over sodium sulfate, filtered, evaporated and purified by silica gel chromatography (ethyl acetate:

hexanes 1:19) to afford the product (6.1 g, 82%) as a colorless to white liquid. ^1H NMR (400 MHz, Chloroform-*d*) δ 7.70 (dd, $J = 8.2, 4.3$ Hz, 2H), 7.66 (s, 1H), 7.45 – 7.35 (m, 2H), 7.35 – 7.27 (m, 1H), 5.39 (s, 2H), 3.86 (d, $J = 8.0$ Hz, 2H), 3.78 (q, $J = 7.1$ Hz, 2H), 1.96 (tt, $J = 8.0, 1.1$ Hz, 1H), 1.24 (t, $J = 7.1$ Hz, 3H). ^{13}C NMR (101 MHz, CDCl_3) δ 153.04, 133.92, 131.56, 129.19, 128.17, 127.38, 126.85, 126.23, 124.28, 109.08, 93.15, 77.51, 77.19, 76.87, 64.72, 24.73, 15.27.

SS-((3-(ethoxymethoxy)naphthalen-2-yl)methyl) ethane(dithioperoxoate) (4.28)

Acetylsulfenyl chloride (2 g, 18 mmol) in ether (5 mL) and was added dropwise to a stirring solution of compound **4.27** (0.7 g, 3 mmol) in ether (10 mL) in at 0 °C. The reaction was stirred at room temperature for 15 h, quenched by sodium bicarbonate solution and stirring for 10 min. The mixture was then separated between ethyl acetate and sodium bicarbonate. The organic layer was washed with water and brine, and dried over sodium sulfate, filtered, evaporated, and purified by silica gel chromatography (ethyl acetate: hexanes 1:19) to afford (0.46 g, 50%) product as yellow oil. ^1H NMR (400 MHz, CDCl_3) δ 7.74 (d, $J = 7.9$ Hz, 2H), 7.60 (s, 1H), 7.45 – 7.41 (m, 2H), 7.39 – 7.34 (m, 1H), 5.45 – 5.36 (m, 2H), 4.30 (d, $J = 2.9$ Hz, 2H), 3.86 – 3.74 (m, 2H), 2.50 (s, 3H), 1.31 – 1.20 (m, 3H). ^{13}C NMR (101 MHz, CDCl_3) δ 195.53, 153.14, 134.28, 130.02, 128.64, 127.47, 126.90, 126.50, 124.32, 109.05, 93.18, 77.43, 77.12, 76.80, 64.69, 38.87, 28.49, 15.22, 0.08. ESI, m/z : calcd. for $\text{C}_{16}\text{H}_{18}\text{O}_3\text{S}_2$ $[\text{M}+\text{Na}]^+$ 345.1, found 345.0.

3-(disulfaneylmethyl)naphthalen-2-ol (4.29) Compound **4.28** (0.23 g, 0.71 mmol) was dissolved in EtOH: toluene (4:3) solvent (1.5 mL EtOH and 1.1 ml toluene) in 0 °C under stirring. Then, a 3M HCl in MeOH solution (1.2 mL) was chilled to 0 °C and added dropwise. The reaction mixture was stirred at room temperature for 24 h, extracted by

ethyl acetate. The organic layer was washed by brine, dried over Na₂SO₄, filtered, evaporated, and purified by silica gel chromatography (ethyl acetate: hexanes 1:19) to afford the product (0.08 g, 51%) as a yellow oil. ¹H NMR (400 MHz, Chloroform-*d*) δ 7.77 – 7.68 (m, 2H), 7.66 – 7.58 (m, 1H), 7.44 – 7.37 (m, 1H), 7.36 – 7.29 (m, 1H), 7.17 – 7.07 (m, 1H), 5.66 (d, *J* = 19.1 Hz, 1H), 4.39 – 4.27 (m, 2H), 1.77 (s, 1H). ¹³C NMR (101 MHz, CDCl₃) δ 151.87, 134.40, 130.90, 128.86, 127.68, 126.62, 126.08, 124.69, 124.02, 110.66, 77.39, 77.07, 76.76, 39.70, 39.21. ESI, *m/z*: calcd. for C₁₁H₁₀OS₂ [M-H]⁻ 221.0, found 221.0.

4.10 References

- [1] Wallace, J. L., & Wang, R. Hydrogen sulfide-based therapeutics: exploiting a unique but ubiquitous gasotransmitter. *Nature Reviews Drug Discovery*. **2015**, *14*(5), 329-345.
- [2] Hellmich, M. R., Coletta, C., Chao, C., & Szabo, C. The therapeutic potential of cystathionine β-synthetase/hydrogen sulfide inhibition in cancer. *Antioxidants & redox signaling*. **2015**, *22*(5), 424-448.
- [3] Zhao, W., Zhang, J., Lu, Y., & Wang, R. The vasorelaxant effect of H₂S as a novel endogenous gaseous KATP channel opener. *The EMBO journal*. **2001**, *20*(21), 6008-6016.
- [4] Liu, M. H., Zhang, Y., He, J., Tan, T. P., Wu, S. J., Guo, D. M., ... & Jiang, Z. S. Hydrogen sulfide protects H9c2 cardiac cells against doxorubicin-induced cytotoxicity through the PI3K/Akt/FoxO3a pathway. *International journal of molecular medicine*. **2016**, *37*(6), 1661-1668.

- [5] Xie, L., Feng, H., Li, S., Meng, G., Liu, S., Tang, X., ... & Ji, Y. SIRT3 mediates the antioxidant effect of hydrogen sulfide in endothelial cells. *Antioxidants & redox signaling*. **2016**, 24(6), 329-343.
- [6] Devarie-Baez, N.O., Bagdon, P.E., Peng, B., Zhao, Y., Park, C.M. and Xian, M., Light-induced hydrogen sulfide release from “caged” gem-dithiols. *Organic letters*, **2013**, 15(11), 2786-2789.
- [7] Zheng, Y., Yu, B., De La Cruz, L. K., Roy Choudhury, M., Anifowose, A., & Wang, B. Toward hydrogen sulfide based therapeutics: critical drug delivery and developability issues. *Medicinal research reviews*. **2018**, 38(1), 57-100.
- [8] Kang, J., Neill, D. L., & Xian, M. Phosphonothioate-based hydrogen sulfide releasing reagents: chemistry and biological applications. *Frontiers in pharmacology*. **2017**, 8, 457.
- [9] Arnold, R. C., Lien, A. P., & Alm, R. M. The action of lithium aluminum hydride on organic disulfides. *Journal of the American Chemical Society*. **1950**, 72(2), 731-733.
- [10] Bailey, T. S., Zakharov, L. N., & Pluth, M. D. Understanding hydrogen sulfide storage: probing conditions for sulfide release from hydrodisulfides. *Journal of the American Chemical Society*. **2014**, 136(30), 10573-10576.

CHAPTER 5

NQMP-ACETAL FOR HIGH-EFFICIENCY CARGO PHOTO-RELEASE

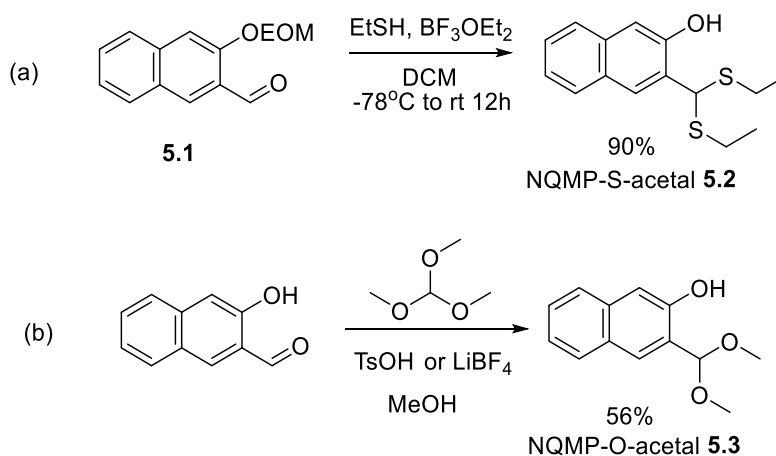
5.1 Introduction

Photolabile protecting groups (PPG), known as “cages” in biochemistry, allow for “reagentless” deprotection and spatial and temporal control of a substrate release. PPGs found numerous applications in biochemistry, organic synthesis, and material sciences. Although there exist varieties of PPGs, few of them are suitable for the direct protection of alcohols or carboxylic acids. A majority of PPGs have quantum yield (Φ) at or below 0.1, *e.g.* the well-known *o*-nitrobenzyl group (*o*-NB).¹ Additionally, most PPGs usually carry and release only one equivalent of cargo molecule.

In this project, NQMP-acetals were designed as efficient photocages. NQMP as a PPG can protect various substrates including alcohols, and has a generally high quantum yield range from 0.1 (*i.e.* NQMP-thioether) to 0.2 (*i.e.* NQMP-alcohol).² Moreover, the NQMP-acetals can carry and release two equivalents of cargo molecule, which greatly enhanced the releasing efficiency. These photoreactive precursors, if further coupled with other functionalities by click chemistry, will find a wide range of applications such as drug delivery, supramolecular, and material chemistry.

5.2 Synthesis of NQMP-S-acetal (NSA) and NQMP-O-acetal (NOA)

NQMP-acetals are designed as photocages by installing NQM with two equivalents of potential cargo molecules on the benzylic position. NQMP-S-acetal and NQMP-O-acetal were synthesized to explore the feasibility of this strategy (Scheme 5.1). The two compounds were obtained from NQMP-aldehyde precursors with or without the phenolic group protection using reported protocols.^{3,4}



Scheme 5.1 Synthesis of (a) NQMP-S-acetal and (b) NQMP-O-acetal

Then the two acetals were tested for the ability to release the thiol or alcohol upon 300 nm wavelength UV irradiation. The two compounds have different photolysis mechanisms. Upon irradiation, the NQMP-S-acetal first converted to monosubstituted NQMP-S-ether and then decomposed to the diol and some other byproducts (Figure 5.1, Scheme 5.2 a). Specifically, to confirm the identity of the intermediate, the authentic NQMP-S-ether was obtained from the reaction of diol photo-addition with ethanethiol (Scheme 5.2 b) and the HPLC peak of the reaction adduct matched that of the intermediate (procedure for **5.4**, page 126).

5.3 Photolysis Patterns of NSA and NOA

The photolysis of the NQMP-S-acetal (**5.2**) was analyzed by HPLC (Figure 5.1) and ESI (-MS) of reaction mixture of irradiation 300 nm for 5 min found 276.9 (E), 216.8 (D), 170.8 (B) and the irradiation of 25 min mixture found 156.8 (C) and 172.8 (A).

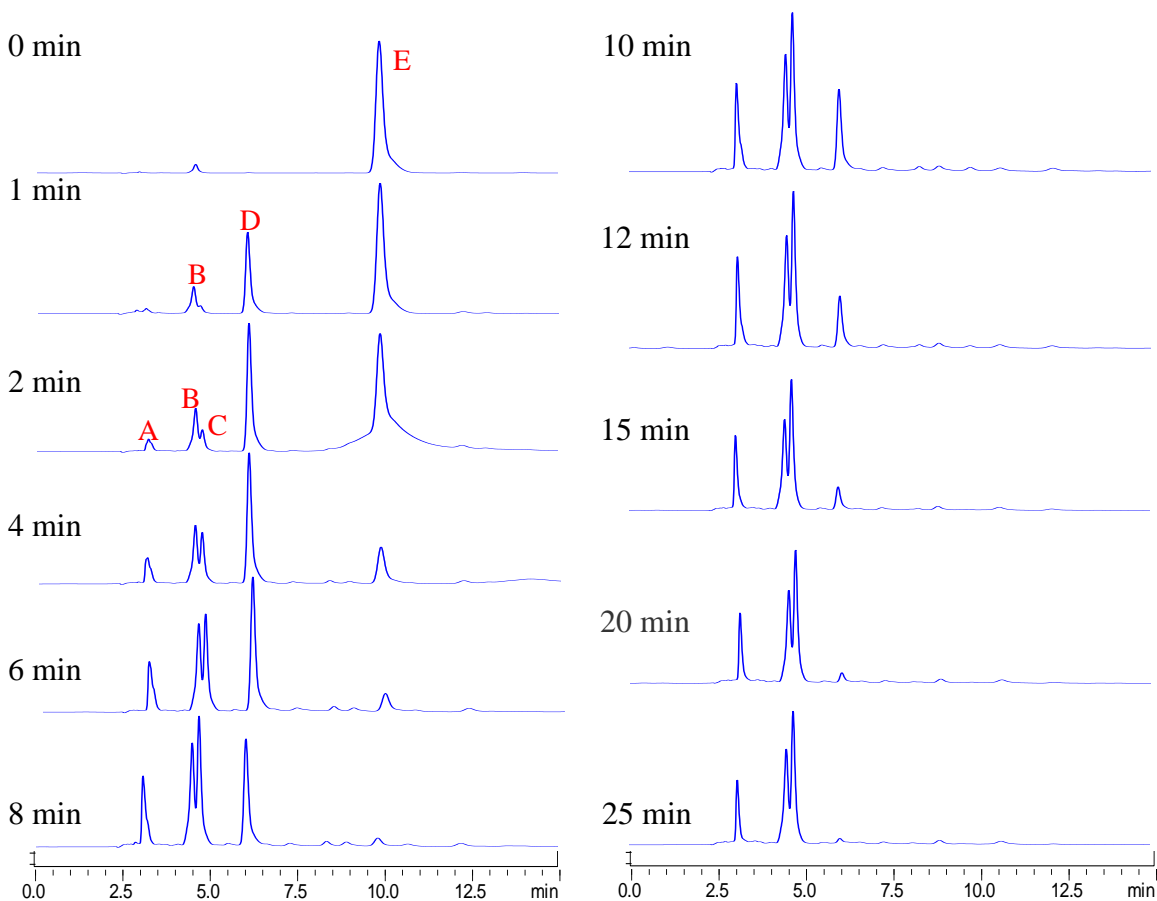
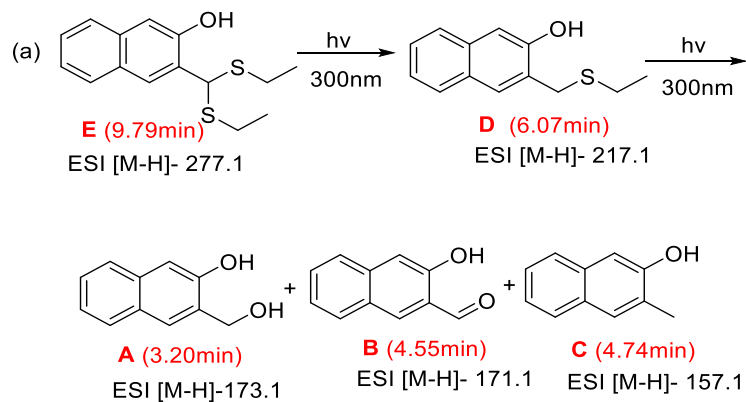
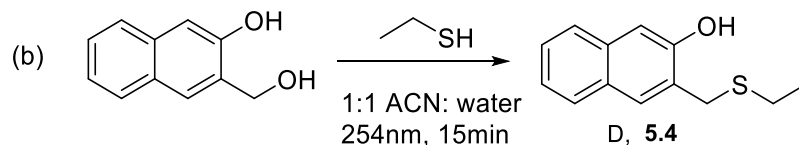


Figure 5.1 Photolysis of NQMP-S-acetal





Scheme 5.2 (a) Photolysis of NQMP-S-acetal (b) Synthesis of NQMP-S-ether

Compared to that of NQMP-S-acetal, the photolysis reaction of NQMP-O-acetal (NOA) (in 1:1 acetonitrile/water) was much cleaner, with the NQMP-aldehyde (ALD) as the only product from 300 nm UV irradiation for 22 min. With HPLC eluting system of 45A15M40W, the NOA (R.T.= 5.51 min) turned completely to ALD (R.T. = 6.05 min) (Figure 5.2). Therefore, NQMP-O-acetal is a better photocage than NQMP-S-acetal and deserves further evaluation.

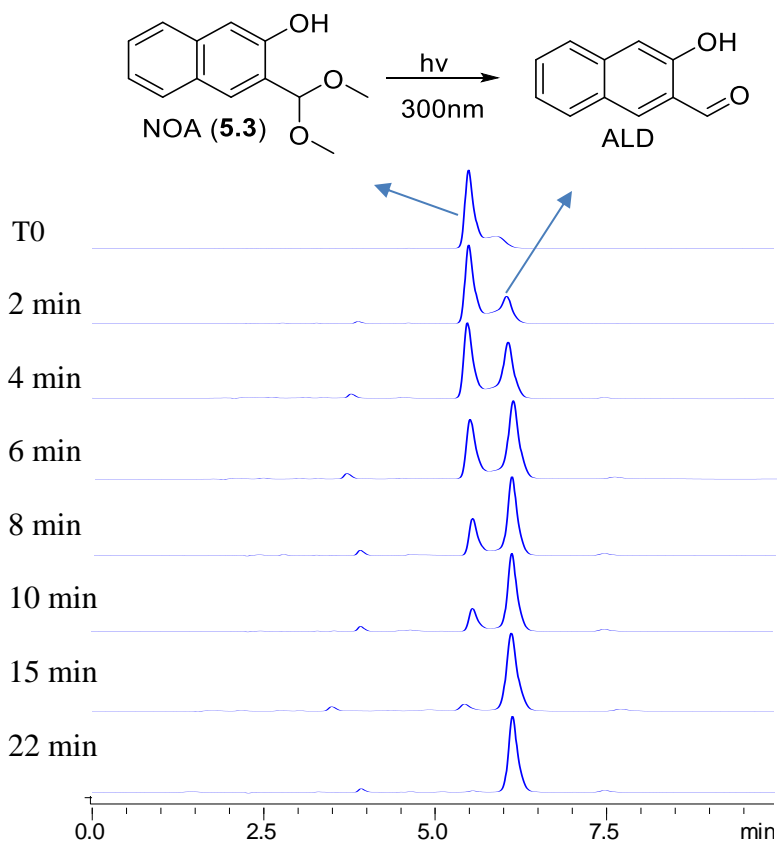


Figure 5.2 Photolysis of NQMP-O-acetal

5.4 Chemical Yield of NOA Photolysis

To study the chemical yield of the NOA photolysis reaction, the UV spectra of same concentrations of NOA and ALD in 4:1 methanol/water (4:1 MW) and 1:1 acetonitrile/water (1:1AW) were taken, respectively and shown below (Figure 5.3). NOA has characteristic absorption bands at 226, 276, and 333 nm while the ALD has characteristic absorption bands at 250, 301, and 383 nm.

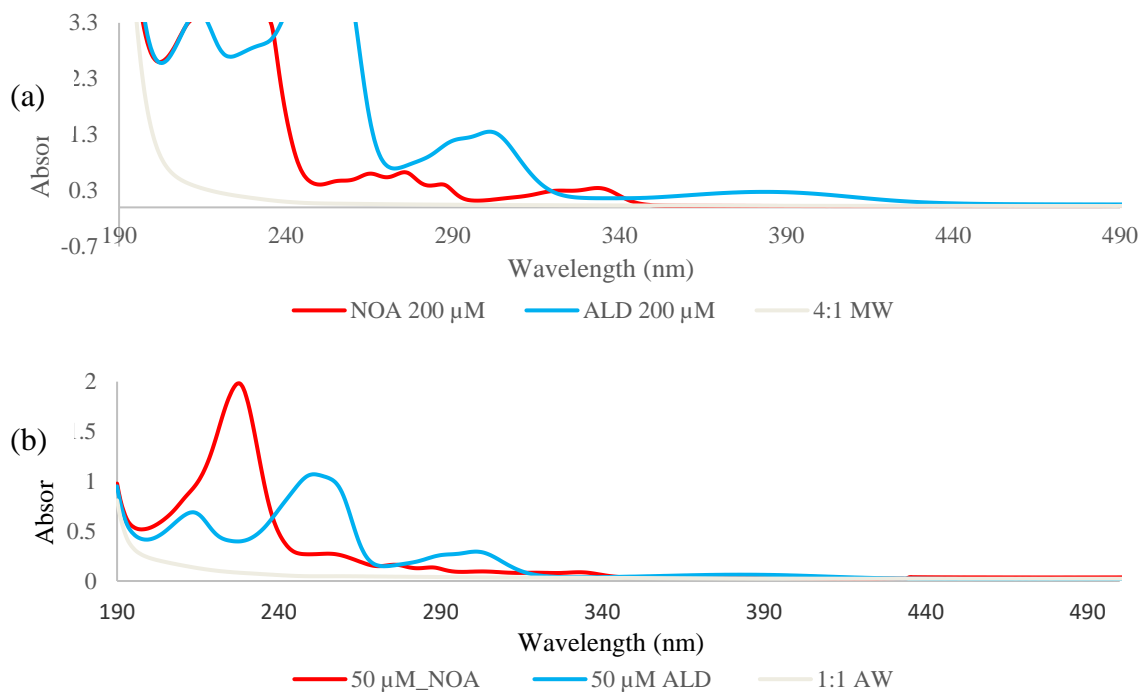


Figure 5.3 UV spectra of NOA and ALD in (a) 4:1 M/W (b) 1:1 A/W

The reaction was monitored by HPLC area change of the two compounds' peaks in relation to the irradiation duration. To calculate the reaction's chemical yield, calibration curves were generated for ALD. First, the concentration and HPLC peak area relationship for ALD sample in 4:1 methanol/water at 383 nm was characterized. The resulted calibration curve is $y = 1E+09x + 32408$ $R^2 = 0.999$ (Figure 5.4).

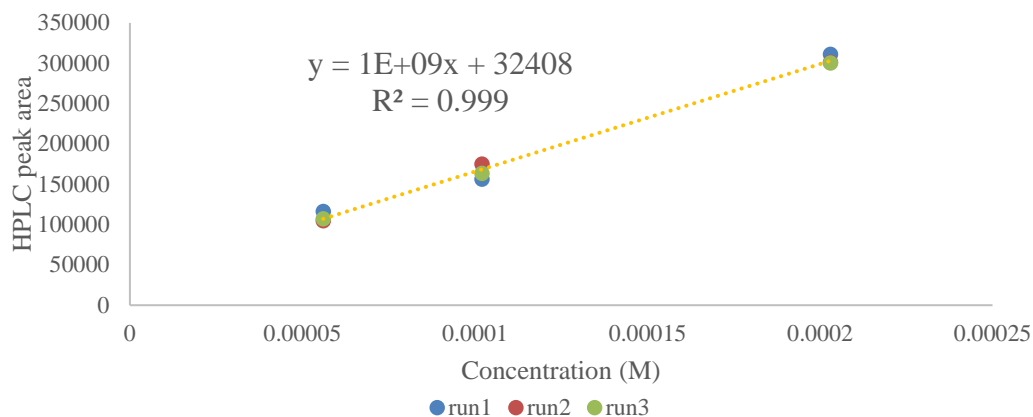


Figure 5.4 ALD (in 4:1 M/W) calibration curve at 383 nm

UV light (300 nm) was applied to a 29 μM NOA sample in 4:1 MW for up to 75 min, and the area integration was recorded at 383 nm channel. The concentration was calculated using the above calibration curve equation (Table 5.1). The concentration of ALD in the sample irradiated for 75 min was calculated to be 29 μM , indicating the photolysis reaction of NOA completed at 75 min with 100% conversion.

| Irradiation time (min) | HPLC peak area (observe at 383 nm) | Concentration of ALD (M) |
|------------------------|------------------------------------|--------------------------|
| 30 | 41537 | 9.13E-06 |
| 47 | 54767 | 2.24E-05 |
| 61 | 56027 | 2.36E-05 |
| 75 | 61297 | 2.89E-05 |

Table 5.1 Conversion of NOA (29 μM in 4:1M/W) to ALD

Then, the concentration and HPLC peak area relationship for ALD sample in 1:1 Acetonitrile/water at 383 nm was characterized. The resulted calibration curve is $y = 1.2251\text{E}+09x + 69085$ $R^2 = 0.999$ (Figure 5.5).

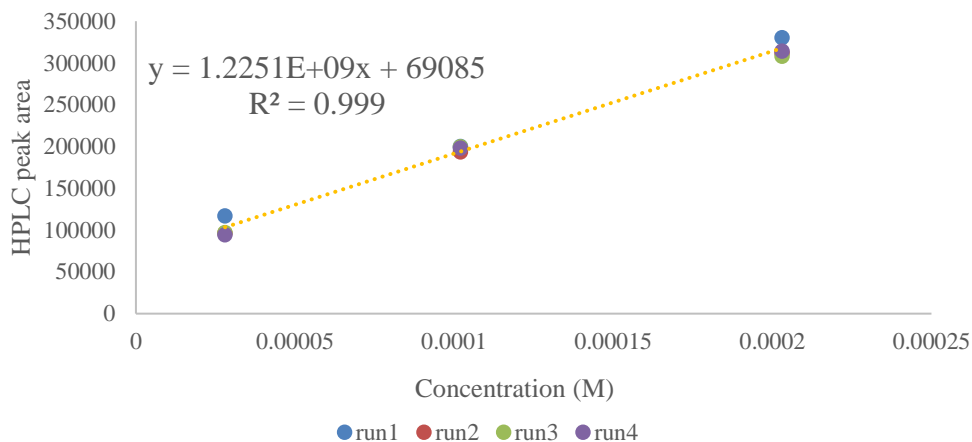


Figure 5.5 ALD concentration calibration at 383nm

UV light (300 nm) was applied to 29 μM NOA in 1:1 AW samples for up to 10 min, and the peak area integration was recorded under 383 nm channel. Then, the concentration was calculated using the above calibration curve equation (Table 5.2). The concentration of ALD in the sample irradiated for 10 min was calculated as 29 μM , indicating the photolysis reaction of NOA completed at 10 min with 100% conversion.

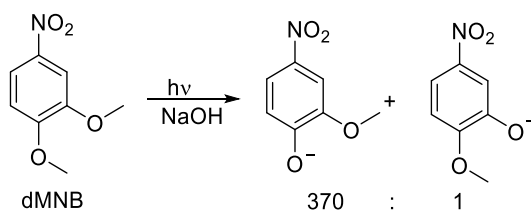
| Irradiation time (min) | HPLC peak area (observe at 383 nm) | Concentration of ALD (M) |
|------------------------|------------------------------------|--------------------------|
| 5 | 94629 | 2.09E-05 |
| 10 | 105251 | 2.95E-05 |

Table 5.2 Conversion of NOA (29 μM in 1:1A/W) to ALD

For both NOA solutions (29 μM in 4:1 MW or 1:1AW), the reaction chemical was 100%. Compared to the reaction in 4:1 MW, the photolysis reaction in 1:1AW was much faster. Therefore, the 1:1AW solution was adopted for the following quantum yield study.

5.5 Quantum Yield of NOA Photolysis

Quantum yield (Φ) is a measure of the efficiency of photon emission. It is the ratio of the number of photons emitted (or compound molecules decomposed) to the number of photons absorbed. To measure quantum yield, an actinometer is required. Actinometer is a system that can be used for the determination of the excitation light intensity. 3,4-Dimethoxynitrobenzene (dMNB) was used as the actinometer in this research since it has similar quantum yield to many photocages and uses the same type of analytical procedures (*e.g.*, chromatography, spectroscopy) for measurements. The photohydrolysis of dMNB in alkaline media yields 2-methoxy-5-nitrophenolate as the main product (Scheme 5.3), making a UV absorbance increase at 450 nm.⁵



Scheme 5.3 3,4-Dimethoxynitrobenzene photoreaction as actinometer

The actinometer (dMNB) and the sample (NOA) were irradiated under the same conditions to ensure that the two compounds absorb same numbers of photons. Therefore, for the actinometer and NOA, the ratio of the number of the molecule decomposed to the quantum yield should be the same. It is known that the quantum yield of dMNB is 0.116.⁵ The number of dMNB decomposed could be calculated by UV absorbance change, while the number of NOA decomposed was to be obtained from NOA's HPLC peak area change.

First, a 136 μ M dMNB in 0.5 M KOH aqueous solution was prepared. Then, 3 mL such solution in quartz cuvette was treated with 300 nm (in photo-reactor with 15

lamps) for 1 min. The absorbance changes at 450 nm before and after irradiation were recorded (Figure 5.7).

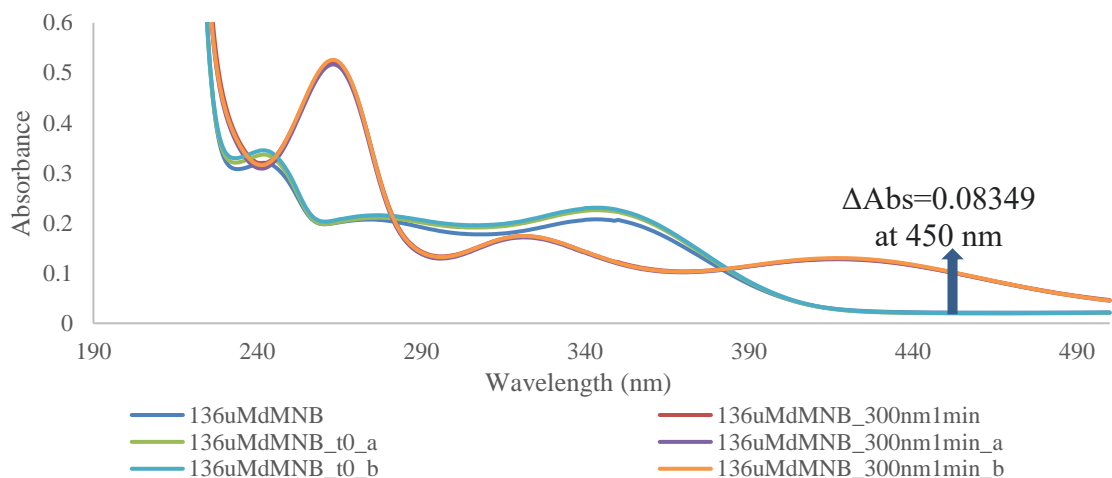


Figure 5.7 dMNB (136 μM in 0.5 M KOH) under irradiation (300 nm 0 and 1 min)

Next, 3 mL 203 μM NOA in 1:1AW solution in quartz cuvette was tested for the number of molecules decomposed by the same conditions of UV irradiation (300 nm 1 min). The UV absorbance at 250 nm, 301 nm, and 383 nm displayed a prominent increase, indicating the transformation of NOA to ALD (Figure 5.8).

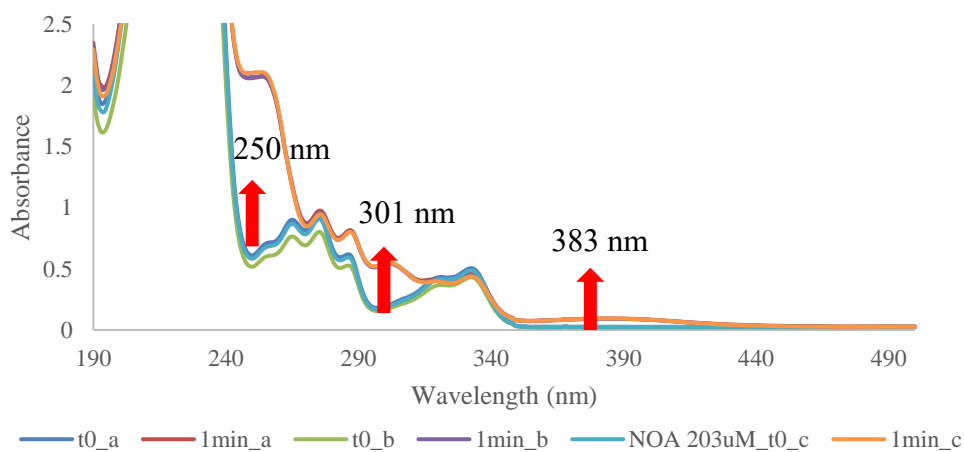


Figure 5.8 UV spectra of NOA (203 μM) under irradiation (300 nm 0 and 1 min)

For dMNB: $\Delta A = \epsilon l \Delta c$, $\Delta A = 0.08349$, $l = 1$ cm, $\epsilon = 3040$ L/(mol · cm).

Therefore, $\Delta c_{\text{dMNB}} = \Delta A_{\text{dMNB}} / (\epsilon l) = 0.08349 / 3040$ mol/L

$\Delta N = \Delta c \times V$, $V = 3$ mL = 0.003 L, $\Delta N_{\text{dMNB}} = (0.08349 / 3040) \times 0.003$ mol

Since $\Delta N_{\text{dMNB}} / \Phi_{\text{dMNB}} = \Delta N_{\text{NOA}} / \Phi_{\text{NOA}}$, and $\Phi_{\text{dMNB}} = 0.116$,

$\Delta N_{\text{NOA}} = \Delta c_{\text{NOA}} \times V = (\Delta \text{area} / \text{slope}) \times 0.003$ mol

Therefore, $\Phi_{\text{NOA}} = \Phi_{\text{dMNB}} \times \Delta N_{\text{NOA}} / \Delta N_{\text{dMNB}}$

$= 0.116 \times ((\Delta \text{area} / \text{slope}) \times 0.003) / ((0.08349 / 3040) \times 0.003)$ **Equation 1**

From the standard curves for ALD (concentration and HPLC peak area relationship) at 250 nm and 301 nm (Figure 5.9), the slope at 250 nm is 2.8681E10, the slope at 301 nm is 7.0119E9, and that at 383 nm is 1.2251E9 (Figure 5.5).

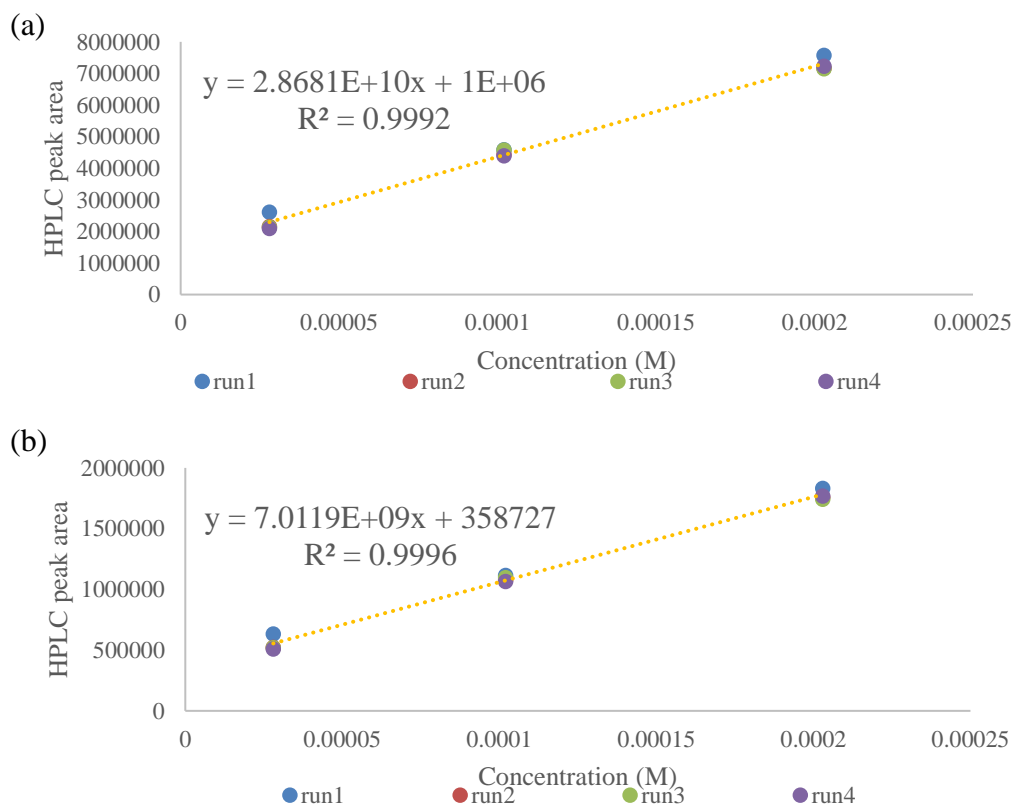


Figure 5.9 ALD calibration curve at (a) 250 nm (b) 301 nm

The HPLC peak area increase observe at 250 nm, 301 nm, and 383 nm before and after NOA (203 μ M in 1:1 AW) was irradiated (300 nm UV light for 1 min) was analyzed, and the area difference was recorded. Then the quantum yield of each data point was calculated based on **Equation 1** and the results are listed below (Table 5.3).

| | Area difference (Δ area) | QY calculate by HPLC |
|----------|-------------------------------------|-------------------------|
| 250 nm | 1653351 | 0.243 |
| | 1683550 | 0.248 |
| | 1700720 | 0.250 |
| 301 nm | 371995 | 0.224 |
| | 410768 | 0.247 |
| | 404263 | 0.244 |
| 383 nm | 73878 | 0.255 |
| | 74917 | 0.258 |
| | 76345 | 0.263 |
| average | | 0.248 |
| σ | | 0.010 |

Table 5.3 Quantum yield calculation of NOA based on HPLC analysis

To accurately apply **Equation 1**, the actinometer and substrate solutions should have the same initial optical density (same absorbance) at irradiation wavelength (300 nm). Since there was an absorbance difference between the dMNB and NOA (Table 5.4), the quantum yield need to be calibrated using **Equation 2** to adjust this difference.

| Φ Calibration | run1 | run2 | run3 | average |
|--------------------------------------|----------|----------|----------|----------|
| dMNB (136 μ M) | | | | |
| absorbance at 300 nm | 0.180256 | 0.192746 | 0.197439 | 0.190147 |
| 203 μ M NOA | | | | |
| absorbance at 300 nm | 0.191962 | 0.164992 | 0.180639 | 0.179198 |

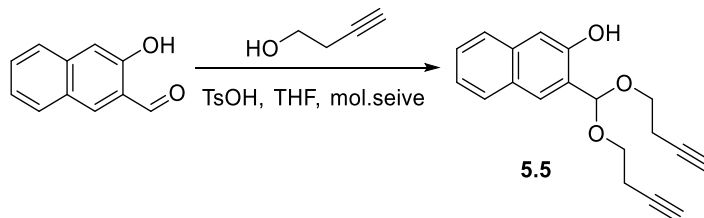
Table 5.4 Quantum yield calibration of NOA

$$\Phi(\text{NOA})_{\text{calibrated}} = \Phi(\text{NOA}) * \frac{1-10^{-\text{Abs}(\text{dMNB})}}{1-10^{-\text{Abs}(\text{NOA})}} \quad \text{Equation 2}$$

Therefore, $\Phi(\text{NOA})_{\text{calibrated}} = 0.248 * (1-10^{-0.190147}) / (1-10^{-0.179198}) = 0.248 * 1.0487 = 0.260$, and the result of the quantum yield Φ for NOA is 0.26 ± 0.01 .

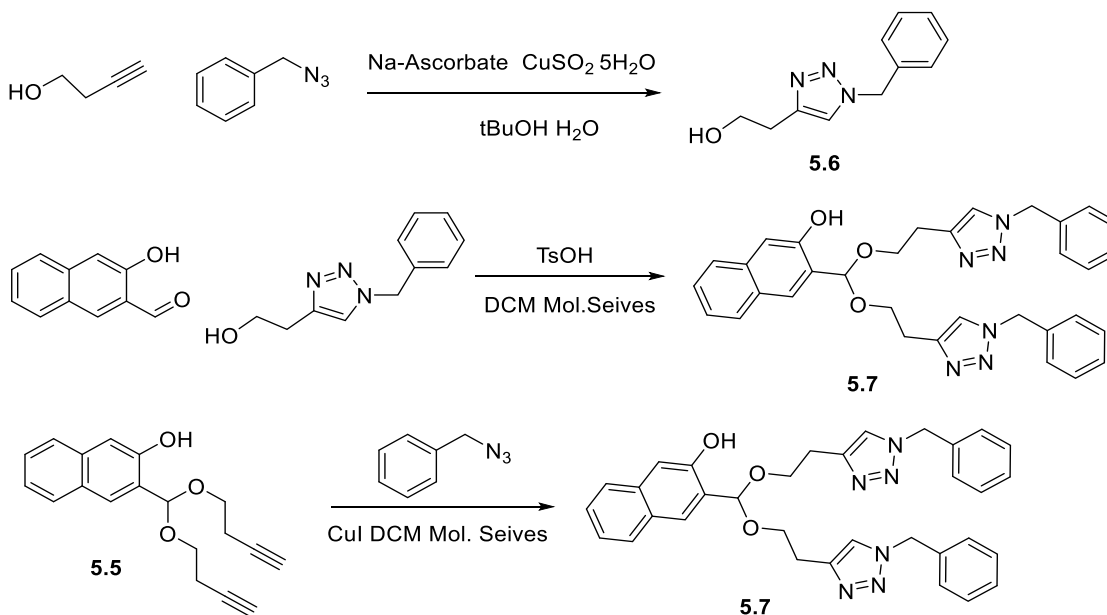
5.6 Synthesis and Photolysis of NQMP-O-acetal-triazole (NOAT)

With the features of NQMP-O-acetal thoroughly studied, the acetal **5.5** with an alkyne functional group was synthesized based on a similar acetal formation protocol reported previously⁶ (Scheme 5.4). The alkyne group provides a handle for further cargo conjugation with the NQMP-O-acetal photocage via click chemistry.



Scheme 5.4 Synthesis of **5.5**

The target compound **5.7** can be synthesized in two ways, either by first synthesizing the triazole **5.6** and then forming the acetal with the aldehyde or by click chemistry of **5.5** and benzyl azide (Scheme 5.5).



Scheme 5.5 Synthesis of **5.7**

The photolysis of **5.6** was then performed. 300 nm UV light was applied to **5.6** for 40 min and the sample composition change was analyzed by HPLC. The HPLC result indicated that **5.6** was fully converted to aldehyde and triazole **5.5** (Figure 5.9).

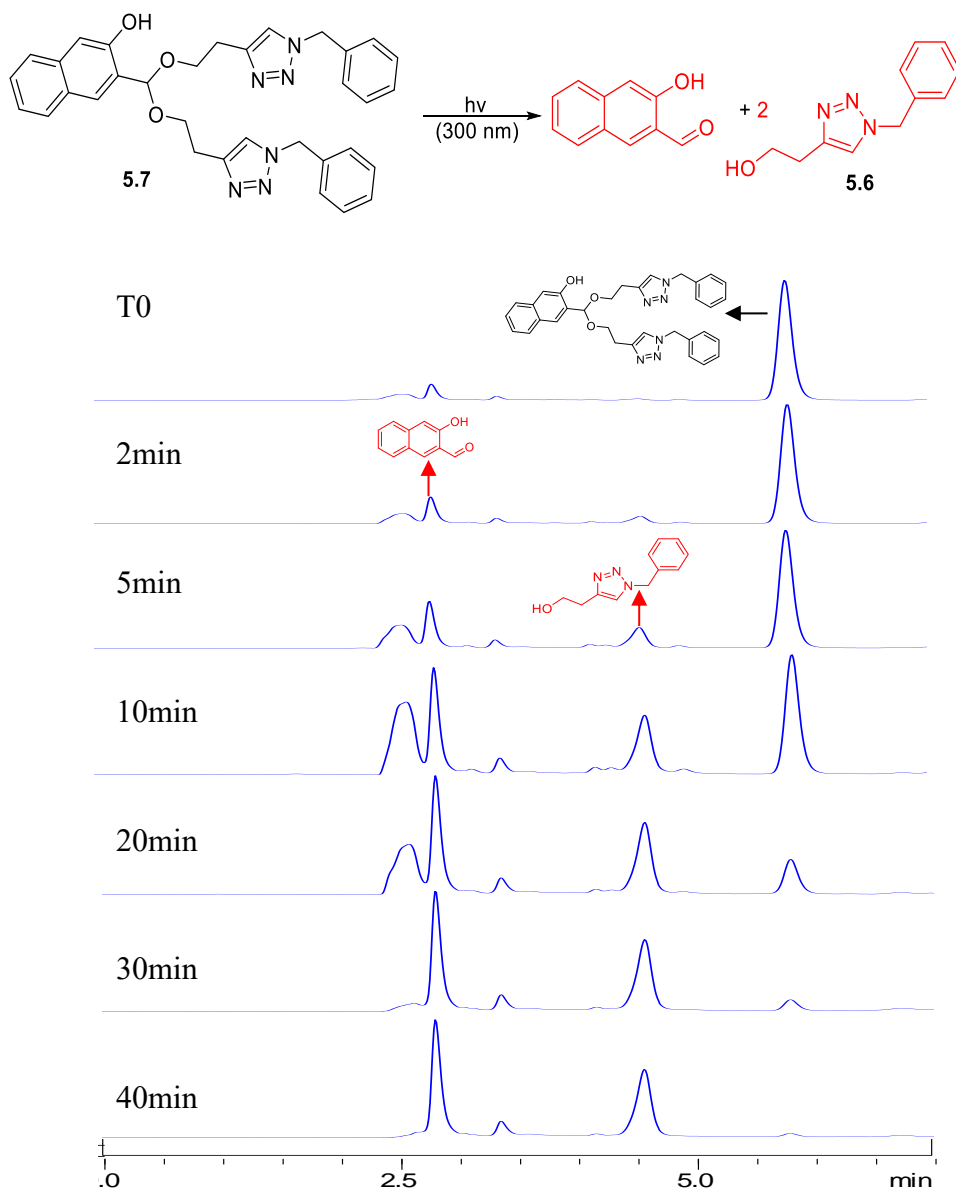


Figure 5.9 Photolysis of **5.7**

5.7 Conclusion

The NQMP-acetals (such as NQMP-S-acetal and NQMP-O-acetal) were designed as photocages and their photolysis features were studied. The NQMP-S-acetal photolysis first converted to monosubstituted NQMP-S-ether and then decomposed to several products. The photolysis of NQMP-O-acetal (NOA) is much cleaner, with aldehyde (ALD) as the only product. The NQMP-O-acetal showed a 100% chemical yield and a high quantum yield of 0.26 ± 0.01 . The click chemistry was also used to showcase the potential modifications of such acetal photocage. The ability of NQMP-acetal carrying and releasing two equivalents of cargo molecules greatly enhanced its releasing efficiency.

5.8 Experimental Section

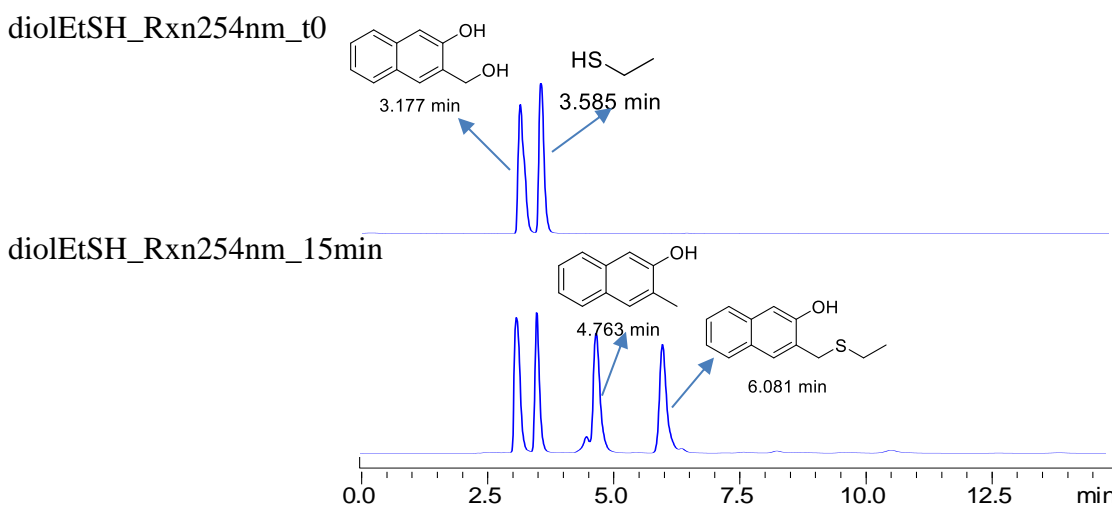
3-(ethoxymethoxy)-2-naphthaldehyde (5.1) Pyridinium chlorochromate (PCC) (5.3 g, 24.7 mmol) was added slowly to a stirring solution of (3-(ethoxymethoxy)naphthalen-2-yl)methanol (3.6 g, 16.5 mmol) in CH_2Cl_2 (50 mL) at 0 °C. The reaction was stirred at room temperature for 2 h, extracted by ethyl acetate. The organic layer was washed by brine and dried over Na_2SO_4 , evaporated, purified by silica gel chromatography (ethyl acetate: hexanes 1:3) to afford the product (3.2 g, 84%) as an off-white crystal. ^1H NMR (400 MHz, Chloroform-*d*) δ 10.60 (s, 1H), 8.39 (s, 1H), 7.93 – 7.85 (m, 1H), 7.80 – 7.73 (m, 1H), 7.59 – 7.49 (m, 2H), 7.40 (ddd, $J = 8.1, 6.8, 1.2$ Hz, 1H), 5.47 (s, 2H), 3.83 (q, $J = 7.1$ Hz, 2H), 1.27 (t, $J = 7.0$ Hz, 3H). ^{13}C NMR (101 MHz, CDCl_3) δ 190.30, 155.28, 137.47, 130.69, 129.89, 129.18, 128.27, 127.00, 125.84, 125.03, 110.12, 93.55, 77.37, 77.05, 76.73, 64.94, 15.18.

3-(bis(ethylthio)methyl)naphthalen-2-ol (5.2) Ethanethiol (0.62 g, 10 mmol) and boron trifluoride etherate (0.43 uL, 0.3 mmol) were added successively to a solution of compound **5.1** (0.23 g, 1 mmol) in CH₂Cl₂ (10 mL) at -78 °C. The reaction was stirred for 12 h at room temperature, quenched by saturated NaHCO₃ solution, extracted by ethyl acetate. The organic layer was washed by water, brine, dried over sodium sulfate and evaporated. The crude product as purified by silica gel chromatography (ethyl acetate: hexanes 1:9) and generat the product (0.25 g, 90%) as a colorless to light yellow liquid. ¹H NMR (400 MHz, Chloroform-*d*) δ 7.77 (s, 1H), 7.75 – 7.71 (m, 1H), 7.64 (dd, *J* = 8.2, 1.1 Hz, 1H), 7.39 (ddd, *J* = 8.2, 6.8, 1.3 Hz, 1H), 7.34 – 7.24 (m, 2H), 7.09 (s, 1H), 5.34 (s, 1H), 2.65 – 2.52 (m, 4H), 1.23 (t, *J* = 7.4 Hz, 6H). ¹³C NMR (101 MHz, CDCl₃) δ 152.47, 134.51, 128.74, 128.41, 127.73, 126.76, 126.24, 126.17, 124.02, 112.47, 77.50, 77.19, 76.87, 49.23, 26.58, 14.33.

3-(dimethoxymethyl)naphthalen-2-ol (5.3) Trimethyl orthoformate (0.8 mL, 8 mmol) and tosyl sulfonic acid (10 mg) were added to a stirring solution of 3-hydroxy-2-naphthaldehyde (0.14 g, 0.81 mmol) in methanol (8 mL). The reaction was refluxed at 50 °C for 24 h. The reaction was quenched by saturated sodium bicarbonate solution and extracted by ethyl acetate with triethylamine (0.5 mL). The extract was washed with water and brine, dried over sodium sulfate and evaporated. The crude product as purified by silica gel chromatography (ethyl acetate: hexanes 1:9) to generate the product (0.1 g, 56%) as a yellow oil. The product needs to be stored in fridge to avoid decomposition to aldehyde. (R.T. over a week resulted in mostly decomposing.) ¹H NMR (400 MHz, Chloroform-*d*) δ 7.89 (s, 1H), 7.74 (d, *J* = 7.0 Hz, 2H), 7.67 (d, *J* = 8.3 Hz, 1H), 7.40 (ddd, *J* = 8.2, 6.8, 1.2 Hz, 1H), 7.32 – 7.25 (m, 2H), 5.65 – 5.60 (m, 1H), 3.41 (s, 6H).

^{13}C NMR (101 MHz, CDCl_3) δ 153.08, 135.08, 128.41, 128.03, 126.91, 126.31, 123.81, 123.67, 111.42, 104.10, 77.48, 77.16, 76.84, 53.22. HRMS (ESI), m/z : calcd. for $\text{C}_{13}\text{H}_{13}\text{O}_3$ $[\text{M}-\text{H}]^-$ 217.0865, found 217.0871.

3-((ethylthio)methyl)naphthalen-2-ol (5.4) In a quartz photoreaction vessel was placed starting material (46 mg, 0.261 mmol, 1 mM) and ethanethiol (1.6 g, 26.1 mmol, 100 mM). Then acetonitrile (130.5 ml), water (130.5 ml) and a stir bar were added with 5 min stirring to dissolve the reagents. The vessel was then put in photoreactor irradiated with 254 nm UV light for 15 min. The sample of mixture components were tested by HPLC using eluting system: 75MeOH/25H₂O.



The peak of 6.08 min in mixture of irradiation 254 nm 15 min sample matches the intermediate formed from photolysis of compound **5.2**. ESI, m/z : calcd. for $\text{C}_{13}\text{H}_{14}\text{OS}$ $[\text{M}-\text{H}]^-$ 217.1, found 216.8, matches what found in the mixture.

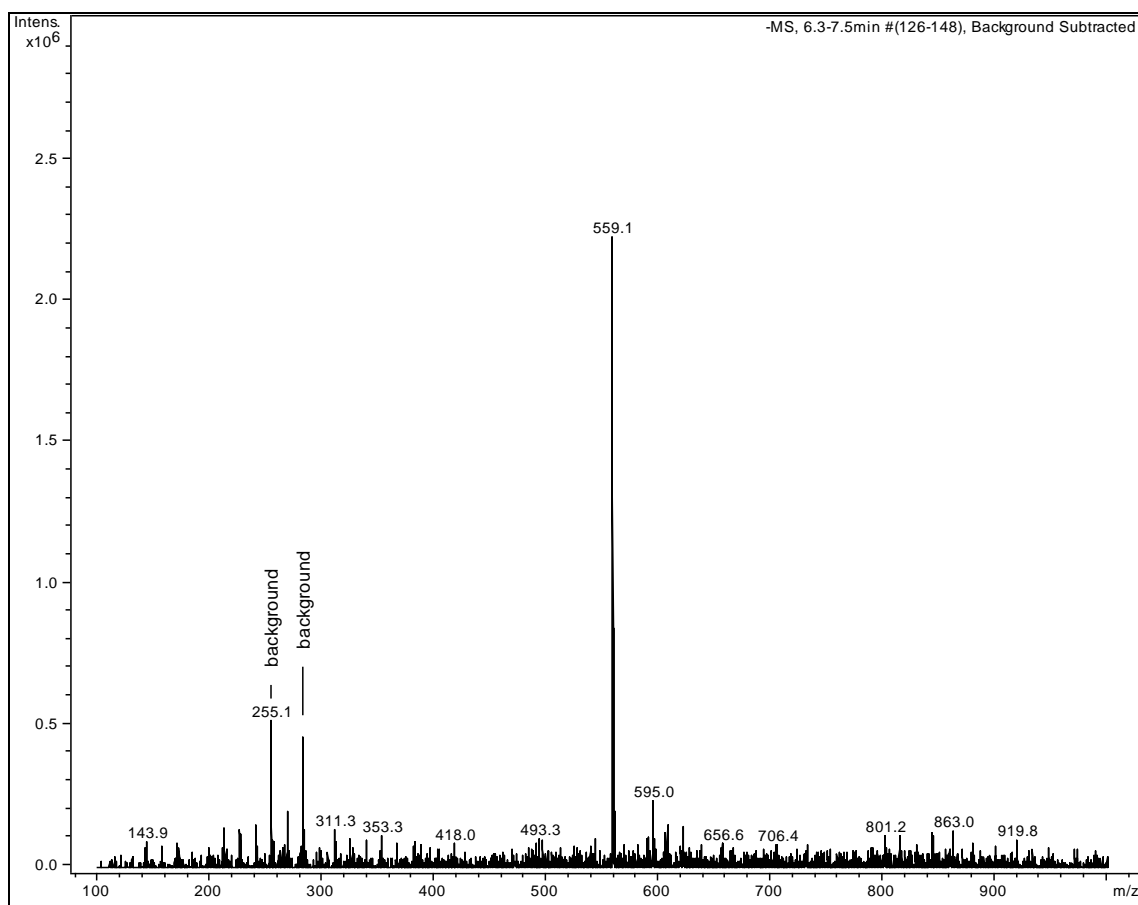
3-(bis(but-3-yn-1-yloxy)methyl)naphthalen-2-ol (5.5) 3-butyn-1-ol (0.94 g, 13.4 mmol), *p*-toluenesulfonic acid (20 mg) and molecular sieves (1 g) were added to a stirring solution of 3-hydroxy-2-naphthaldehyde (0.192 g, 1.12 mmol) in dry CH_2Cl_2 (6 mL) and the reaction was stirred at room temperature for 24 h, quenched by saturated sodium

bicarbonate solution and extracted by ethyl acetate. The extract was washed with water and brine, dried over sodium sulfate, and concentrated by vacuum evaporation. The crude product as purified by silica gel chromatography (ethyl acetate: hexanes 1:9 with triethylamine) to afford the product (0.06 g, 18%) as a light-yellow oil. ^1H NMR (400 MHz, Chloroform-*d*) δ 7.79 (s, 1H), 7.78 – 7.73 (m, 2H), 7.72 – 7.66 (m, 1H), 7.43 (ddd, $J = 8.2, 6.8, 1.3$ Hz, 1H), 7.27 (s, 1H), 5.92 (d, $J = 0.9$ Hz, 1H), 3.87 – 3.71 (m, 4H), 2.56 (td, $J = 6.6, 2.7$ Hz, 4H), 2.05 (t, $J = 2.6$ Hz, 2H). ^{13}C NMR (101 MHz, CDCl_3) δ 152.81, 135.04, 128.23, 127.96, 127.91, 126.94, 126.27, 123.69, 123.59, 111.71, 102.37, 80.78, 77.34, 77.02, 76.71, 69.94, 63.92, 19.83, -0.00. HRMS (ESI), m/z : calcd. for $\text{C}_{19}\text{H}_{18}\text{O}_3$ $[\text{M}-\text{H}]^-$ 293.1178, found 293.1180.

2-(1-benzyl-1H-1,2,3-triazol-4-yl)ethan-1-ol (5.6) Freshly prepared 1M sodium ascorbate (0.3 mmol, 300 μL) in water was added to a solution of 3-butynol (0.29 g, 3 mmol) and benzyl azide (0.4 g, 3 mmol) in 1:1 *t*BuOH and water (12 mL). Then, copper (II) sulfate (7.5 mg, 0.03 mmol) in water (100 μL) was added. the reaction was stirred vigorously for 2 days. The reaction mixture was purified by chromatography (ethyl acetate: hexanes 2:1) to afford the product (0.76 g, 90%) as a colorless oil. ^1H NMR (400 MHz, Chloroform-*d*) δ 7.35 – 7.27 (m, 3H), 7.26 (s, 1H), 7.19 (d, $J = 8.0$ Hz, 2H), 5.42 (s, 2H), 3.88 – 3.80 (m, 2H), 2.84 (t, $J = 6.0$ Hz, 2H), 2.77 (s, 1H). ^{13}C NMR (101 MHz, CDCl_3) δ 145.99, 134.67, 129.14, 128.78, 128.12, 121.60, 77.41, 77.09, 76.78, 61.53, 54.14, 28.71. ESI, m/z : calcd. for $\text{C}_{11}\text{H}_{13}\text{N}_3\text{O}$ $[\text{M}+\text{H}]^+$ 204.1, found 204.1. $[\text{M}+\text{Na}]^+$ 226.1, found 226.1.

3-(bis(2-(1-benzyl-1H-1,2,3-triazol-4-yl)ethoxy)methyl)naphthalen-2-ol (5.7) Benzyl azide (0.5 g, 3.8 mmol), CuI (10 mg, 0.05 mmol) and molecular sieves (0.2 g) were

added a stirring solution of starting acetal (0.07 g, 0.24 mmol) in dry CH_2Cl_2 (4 mL). The reaction was stirred at room temperature for 48 h, quenched by saturated sodium bicarbonate solution and extracted by ethyl acetate. The extract was washed with water and brine, dried over sodium sulfate, and concentrated by in vacuo. The crude product as purified by silica gel chromatography (ethyl acetate: hexanes 1:3 with 2 mL triethylamine) to afford the product (quantitative) as a pale-yellow oil. ^1H NMR (400 MHz, CDCl_3) δ 7.85 – 7.63 (m, 5H), 7.42 (ddd, $J = 8.2, 6.8, 1.3$ Hz, 2H), 7.31 (ddd, $J = 4.8, 3.6, 1.6$ Hz, 6H), 7.26 (s, 1H), 7.25 – 7.12 (m, 4H), 5.80 (s, 1H), 5.45 (d, $J = 5.7$ Hz, 2H), 3.64 (ddt, $J = 24.7, 9.3, 6.5$ Hz, 2H), 2.47 (td, $J = 6.5, 2.5$ Hz, 2H). ESI, m/z : calcd. for $\text{C}_{33}\text{H}_{32}\text{N}_6\text{O}_3$ $[\text{M}-\text{H}]^-$ 559.2, found 559.1.



5.9 References

- [1] Klán, P., Šolomek, T., Bochet, C. G., Blanc, A., Givens, R., Rubina, M., ... & Wirz, J. Photoremovable protecting groups in chemistry and biology: reaction mechanisms and efficacy. *Chemical reviews*. **2013**, *113*(1), 119-191.
- [2] Arumugam, S., Orski, S. V., Mbua, N. E., McNitt, C., Boons, G. J., Locklin, J., & Popik, V. V. Photo-click chemistry strategies for spatiotemporal control of metal-free ligation, labeling, and surface derivatization. *Pure and Applied Chemistry*. **2013**, *85*(7), 1499-1513.
- [3] Tran, V., & Minehan, T. G. Lewis acid catalyzed intramolecular condensation of ynol ether-acetals. Synthesis of alkoxycycloalkene carboxylates. *Organic letters*. **2012**, *14*(23), 6100-6103.
- [4] Kang, J., Lee, J. H., & Lim, D. S. Stereoselective conjugate addition of diethylzinc to enones and nitroalkenes. *Tetrahedron: Asymmetry*. **2003**, *14*(3), 305-315.
- [5] Pavlíčková, L., Kuzmič, P., & Souček, M. Chemical actinometry in the UV range based on the photohydrolysis of 3, 4-dimethoxynitrobenzene. *Collection of Czechoslovak chemical communications*. **1986**, *51*(2), 368-374.
- [6] Lee, K., Rafi, M., Wang, X., Aran, K., Feng, X., Sterzo, C. L., ... & Murthy, N. In vivo delivery of transcription factors with multifunctional oligonucleotides. *Nature materials*. **2015**, *14*(7), 701-706.

CHAPTER 6
SYNTHESIS AND AZIDE CYCLOADDITION REACTIONS OF
ACTIVATED ALLENES

6.1 Introduction

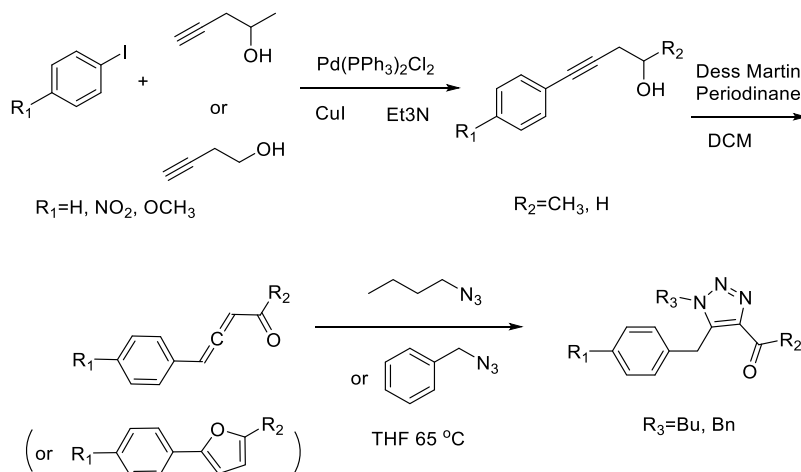
Azide-alkyne cycloaddition is a robust reaction between alkyne and azide to generate 1,2,3-triazole. This reaction was studied by Huisgen in the 1960s¹ and soon gained popularity due to the superior stability of the product. However, the lack of regioselectivity as well as the need for elevated temperature limit its application. In 2002, the copper-catalyzed azide-alkyne cycloaddition (CuAAC) was reported. It is implemented under room temperature and is regiospecific (only 1,4-adduct was formed).² But its narrow substrate scope (only applicable to terminal alkyne) and the cellular toxicity of Cu (I) were the major drawbacks. The strain promoted azide-alkyne cycloaddition (SPAAC) developed in 2004³ alleviated the need for Cu but suffered from demanding reactant preparation due to the unstable nature of the reactants.

Recently, it is discovered that the electron-poor olefins or alkynes as dipolarophiles can achieve metal-free and regioselective triazole synthesis. Different dipolarophiles, such as enamines, enolates and activated alkenes, have been employed to facilitate triazole formation.^{4,5} However, as shown before (section 1.9), a base catalyst is usually required to facilitate the cycloaddition. Activated allene as a dipolarophile is an attractive substrate that has not yet been tested in cycloaddition with azides. Therefore, such reaction would be a good supplement to the toolbox of the azide cycloaddition.

As previously mentioned in the first chapter, the activated alkynes or allenes can undergo cyclization to form furan with organometallic catalysts. In this project, Dess-Martin oxidation of homopropargyl alcohols generated the highly reactive activated alkynes *in situ*. These activated alkynes undergo potential isomerization to activated allenes or aryl furans with different reaction time duration is provided without the addition of metal catalyst.

6.2 The Synthesis Pathway

The synthesis pathway of this project is composed of three steps. Initially, a series of phenyl homopropargyl alcohols were prepared via Sonogashira coupling reaction. Next, the homopropargyl alcohols were oxidized using Dess-Martin periodinane (DMP) under room temperature to give activated alkyne. By separating the acidic DMP during column purification, the activated alkynes isomerized to the more stable activated allenes. The DMP oxidation was also able to generate aryl furans with a longer reaction time. Activated allenes then reacted with butyl azide or benzyl azide in cycloaddition reaction to yield triazoles (Scheme 6.1).



Scheme 6.1 The 3-step synthesis pathway

The above-mentioned synthesis pathway generated a variety of compounds. The different functional group variations further broadened the product scope. With R₁ being hydrogen, nitro, or methoxy group, aromatic rings with different electronic characters were made; by tuning R₂ into methyl or hydrogen, ketone or aldehyde were formed; the R₃ group's choice of butyl or benzyl group makes two different triazoles. The compounds synthesized in the pathway are listed below (Table 6.1).

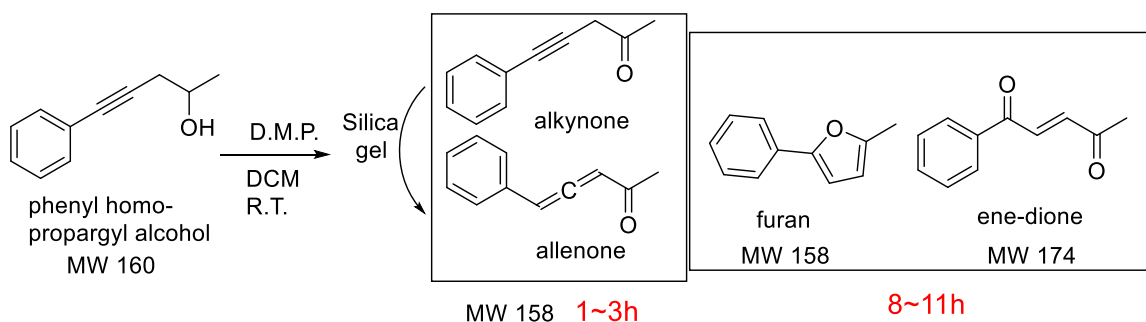
| | Alkyn alcohol | Allene-ketone (aldehyde) | Furan |
|---------------------|--|---|--|
| Compound Structure: | | | |
| Compound labeling: | 6.1 R ₁ =H; R ₂ =CH ₃ 6.6 R ₁ =NO ₂ ; R ₂ =CH ₃ 6.11 R ₁ =OCH ₃ ; R ₂ =CH ₃ 6.16 R ₁ =H; R ₂ =H 6.21 R ₁ =NO ₂ ; R ₂ =H 6.26 R ₁ =OCH ₃ ; R ₂ =H | 6.2 R ₁ =H; R ₂ =CH ₃ 6.7 R ₁ =NO ₂ ; R ₂ =CH ₃ 6.12 R ₁ =OCH ₃ ; R ₂ =CH ₃ 6.17 R ₁ =H; R ₂ =H 6.22 R ₁ =NO ₂ ; R ₂ =H 6.27 R ₁ =OCH ₃ ; R ₂ =H | 6.3 R ₁ =H; R ₂ =CH ₃ 6.8 R ₁ =NO ₂ ; R ₂ =CH ₃ 6.13 R ₁ =OCH ₃ ; R ₂ =CH ₃ 6.18 R ₁ =H; R ₂ =H 6.23 R ₁ =NO ₂ ; R ₂ =H 6.28 R ₁ =OCH ₃ ; R ₂ =H |
| | Butyl-triazole | Benzyl-triazole | |
| Compound Structure: | | | |
| Compound labeling: | 6.4 R ₁ =H; R ₂ =CH ₃ 6.9 R ₁ =NO ₂ ; R ₂ =CH ₃ 6.14 R ₁ =OCH ₃ ; R ₂ =CH ₃ 6.19 R ₁ =H; R ₂ =H 6.24 R ₁ =NO ₂ ; R ₂ =H 6.29 R ₁ =OCH ₃ ; R ₂ =H | 6.5 R ₁ =H; R ₂ =CH ₃ 6.10 R ₁ =NO ₂ ; R ₂ =CH ₃ 6.15 R ₁ =OCH ₃ ; R ₂ =CH ₃ 6.20 R ₁ =H; R ₂ =H 6.15 R ₁ =NO ₂ ; R ₂ =H 6.30 R ₁ =OCH ₃ ; R ₂ =H | |

Table 6.1 Compounds synthesized in the pathway

6.3 Synthesis of Activated Allenes and Aryl Furans

During the Dess-Martine periodinane oxidation step, activated alkynes were typically generated as the major product within room temperature to 35 °C for 15 min. Then, the reaction was quenched by saturated sodium bicarbonate solution. The following column chromatography purification achieved the transformation from activated alkynes to allenes. Literature suggested that alkyne with neighboring groups such as ketone/aldehyde undergo isomerization to allene under base catalysis. The isomerization in this reaction occurred more conveniently once the DMP was neutralized and separated. It was also found that the nitro-substituted activated alkynes were easier to convert to the allenes compared to their methoxy-substituted counterparts (Scheme 6.2).

If a longer reaction time was provided such as room temperature overnight, a rearrangement spontaneously occurred to form furan without additional catalyst. Besides, the “ene-dione” was also found as a byproduct. This method provides an efficient way to prepare aryl furans from simple starting materials (Scheme 6.2).



Scheme 6.2 Dess-Martin oxidation of homopropargyl alcohol

Gas chromatography-mass spectrometry (GC-MS) was used to follow the progress of the reaction shown in Scheme 6.2. The relationship of reaction mixture contents to reaction time lengths is listed below (Table 6.2, Figure 6.1). Table 6.2

indicated that under room temperature, with longer reaction times, the tendency to form allenone decreases while that to form furan increases.

| percentage in mixture (%) | 0 | .67h | 1h | 2h | 3h | 5h | 6h | 11h | 23h | 24h | 32h |
|-----------------------------|-------|-------|-------|-------|-------|-------|-------|-------|-------|-------|-------|
| furan (4.88min MS 158) | | 18.5 | 18.5 | 24.7 | 43.5 | 51.2 | 47.7 | 50.9 | 67.6 | 78.5 | 92.9 |
| alkynone (5.31 min MS 158) | | | | 9.4 | | | 10.3 | 2.3 | | | |
| SM (5.36 min, MS 160) | | | 26.7 | 21.8 | 13.0 | 15.6 | 11.5 | 4.1 | | | |
| allenone (5.46 min, MS 158) | 81.5 | 54.9 | 38.4 | 36.8 | 28.4 | 21.3 | 2.5 | 2.8 | 3.1 | 1.4 | |
| 5.94 min MS 220 | | | | 2.3 | 6.7 | 3.1 | 4.8 | | | | 2.2 |
| 6.12 min MS 174 | | | | 3.4 | | 1.6 | 4.3 | 7.9 | 20.5 | 18.4 | 3.4 |
| 6.13 min MS 248 | | | | | | | | 32.3 | 9.1 | | |
| total | 100.0 | 100.1 | 100.0 | 100.0 | 100.0 | 100.0 | 100.0 | 100.0 | 100.0 | 100.0 | 100.0 |
| ratio of furan/allenone | | 0.2 | 0.3 | 0.6 | 1.2 | 1.8 | 2.2 | 20.3 | 24.4 | 24.9 | 64.8 |

Table 6.2 GC-MS quantification of the reaction mixture in progress

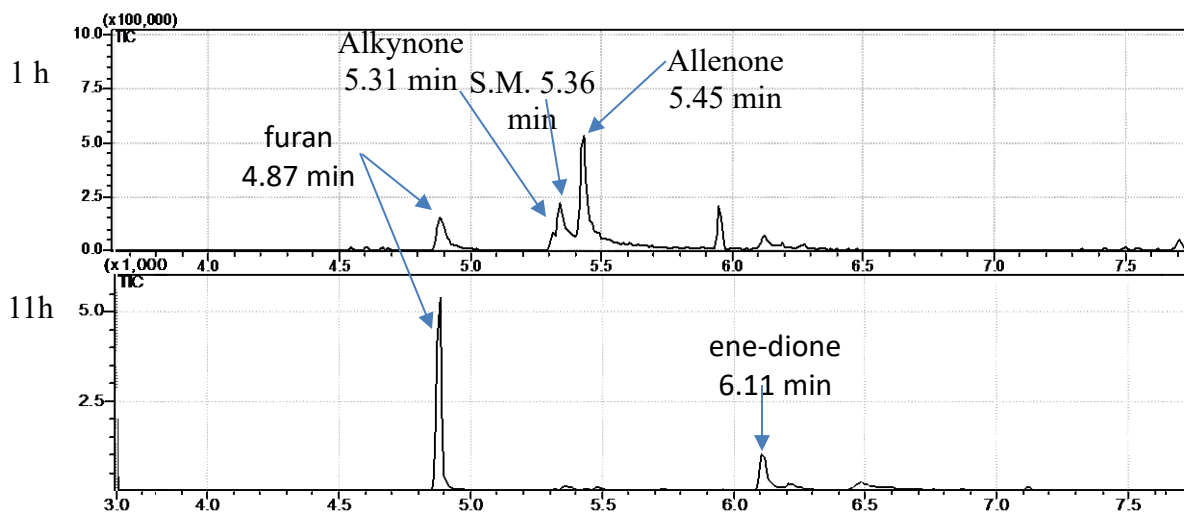


Figure 6.1 Components of reaction mixtures

The condition that favors the formation of furan was applied to all the DMP oxidation reactions in preparative scales (Table 6.3). However, the isolated yield was not as good as the GC-MS analysis. Particularly, the reactions with $R_2 = \text{CH}_3$ are more likely to form furan than those $R_2 = \text{H}$. Although the yield for synthesizing aryl furan from this

reaction was not very satisfactory, some aryl furans could be produced quantitatively in a catalyst-free manner. It is hypothesized that the furan was formed due to the acidic condition of the Dess-Martin oxidation.

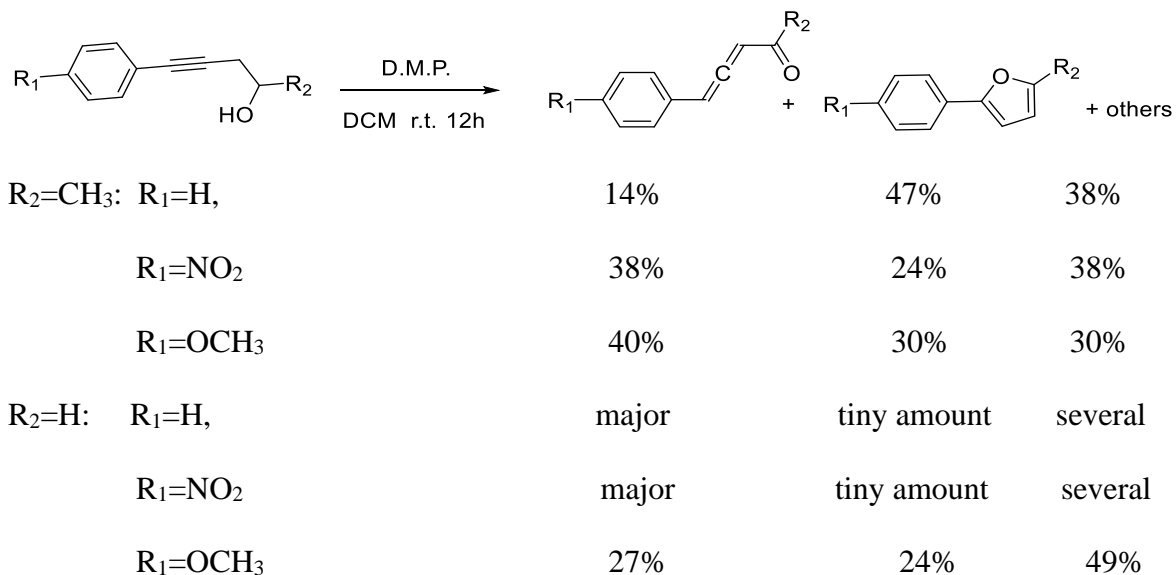


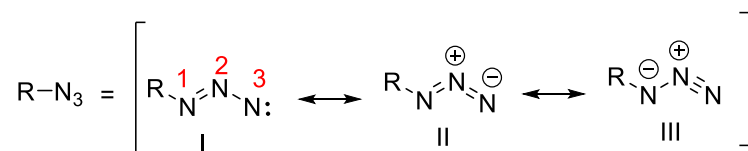
Table 6.3 Isolated yield of furan formation

6.4 Triazole Formation from Activated Allenes

To our surprise, the azide cycloaddition to activated allene was regioselective, and only one isomer formed and isolated. To determine the product structure, we first need to know which double bond of allene is involved in the reaction. It is known that the addition of nucleophiles to electron-deficient allenes occurs at the electrophilic α,β - (not β,γ -) carbon-carbon double bond to give Michael type adduct. This was indeed verified by ¹H NMR spectra of the triazoles. Then, the question was whether the 1,4- or 1,5-adduct (1,4- or 1,5-substituting 1,2,3-triazole) was formed.

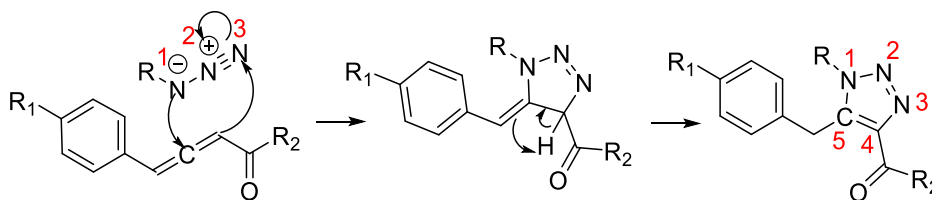
Azide act as the dipole in the azide-alkyne cycloaddition reaction. Therefore, the regio-specificity of the reaction can be partially explained by a consideration of different

azide isomeric structures (Scheme 6.3).⁶ Azides react differently in various types of reactions based on the dipolar structures of II and III (proposed by Pauling).⁷ The azides' activity and regioselectivity in the cycloaddition reaction are usually explained by resonance structure III.^{8,9}



Scheme 6.3 Azide resonance structures and reactivity

For allenes substituted with electron-donating groups, the central carbon is nucleophilic in nature, while the central carbon of allenes with electron-withdrawing substitutions shows electrophilic activity.¹⁰ Quantum chemistry calculation also supports that N¹ of azide nucleophilic attack onto the allene's central carbon and suggests that 1,5-adduct is favored over the 1,4-adduct.^{11,12} Therefore, the mechanism for azide cycloaddition with activated allene is proposed as below (Scheme 6.4). First, the cyclization of azide and activated allene occurred at the unsaturated carbons α,β - to the carbonyl due to the inductive effect of the carbonyl group. Then, the following 1,3-hydrogen shift affords the 1,5-adduct as the product.



Scheme 6.4 Proposed mechanism of regio-selective triazole formation

The triazole structure was then confirmed by the nuclear Overhauser effect spectroscopy (NOESY) of a representative triazole **6.10** (Figure 6.2).

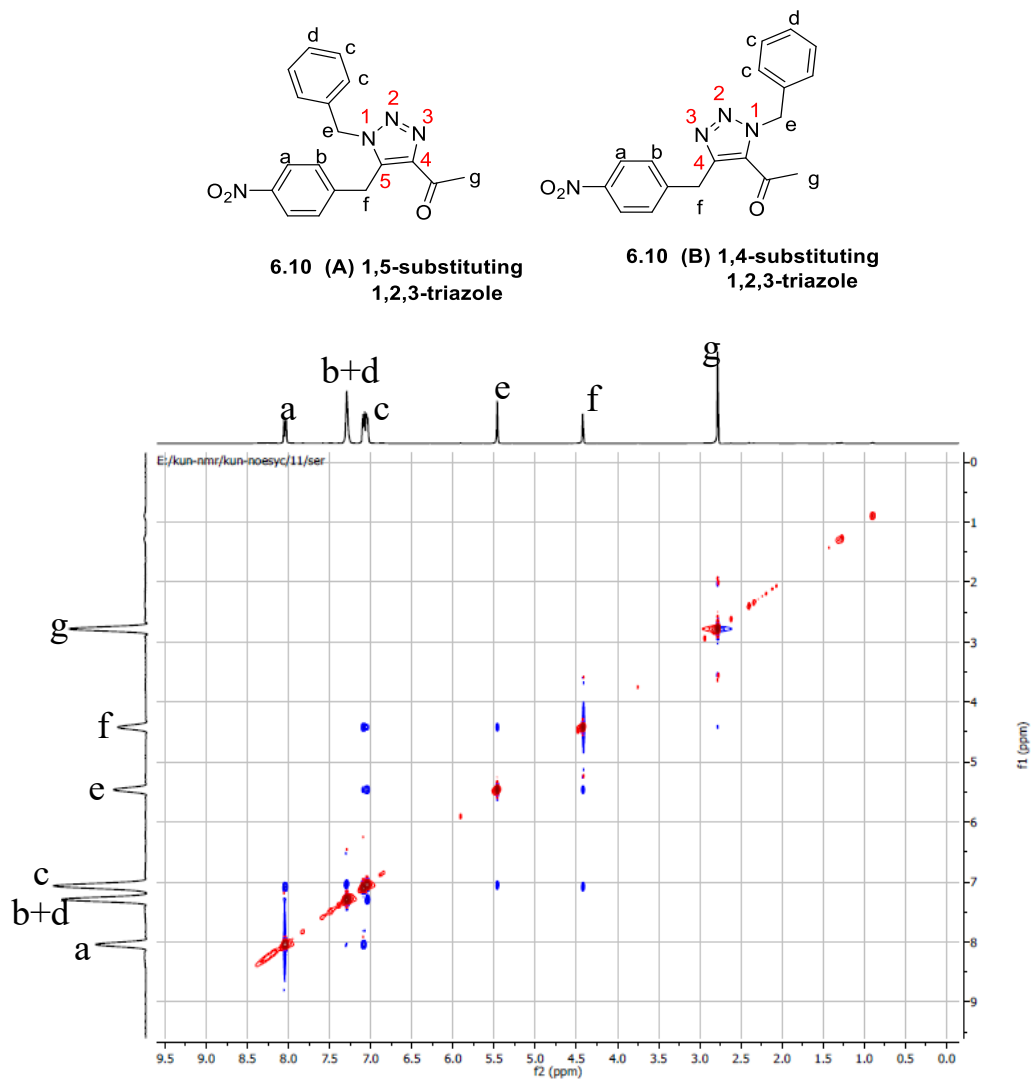


Figure 6.2 NOESY spectrum of **6.10**

The NOESY spectrum of the compound **6.10** clearly showed cross peak of H (f) and H (e) but no cross peak of H (g) with H (e), meaning that H (e) is of closer inter-atomic distance with H (f) than with H (g). Therefore, compound **6.10** should be isomer (A), the 1,5-substituting 1,2,3-triazole.

The transformation of a representative activated allene (**6.2**) reacting with butyl azide to form triazole (**6.4**) was quantitatively analyzed by HPLC (Appendix 9). First, calibration curves of the starting material (Aln) and product (Trz) from authentic samples were generated, respectively. Then, a ALN (10 mM) and BuN₃ (400 mM) in dioxane solution was heated in water bath (78 °C). The reaction mixture contents were monitored and analyzed using HPLC. Then the consumption of the reactant and the formation of the product are plotted by their concentration changes (Figure 6.3). The figure demonstrated that 10 mM Aln was consumed with 10 mM Trz formed, namely a 100% conversion of the reaction.

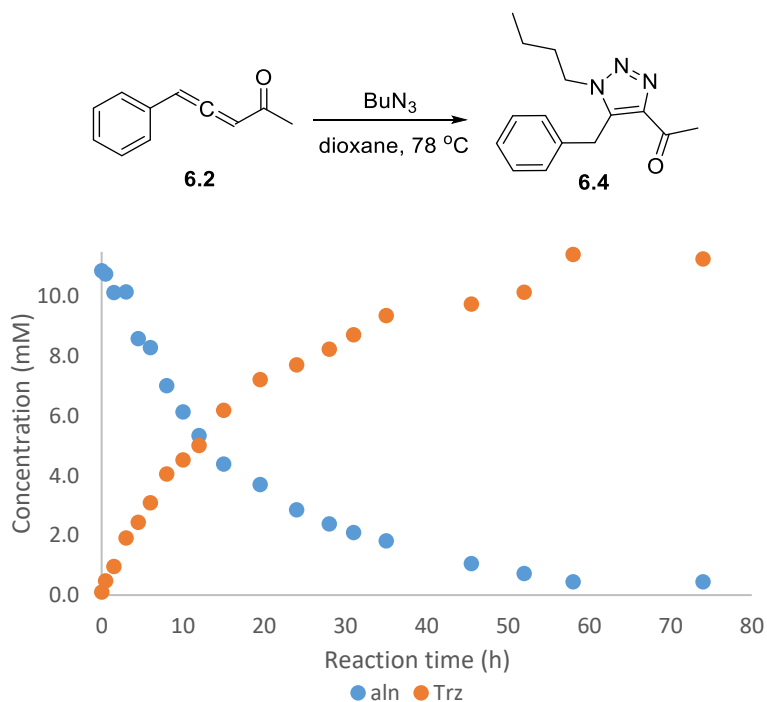


Figure 6.3 Transformation of allene to triazole

6.5 Conclusion

Activated allenes were efficiently synthesized from oxidation of homopropargyl alcohols using Dess-Martin periodinane under mild condition with quantitative yield. These allenes readily participated in cycloaddition reactions with azides to provide 1,5-substituted 1,2,3-triazoles. Comparing to the earlier azide-alkyne cycloaddition reactions, this reaction proceeds in a catalyst-free and regiospecific fashion while also benefit from convenient preparation of the starting materials.

Meanwhile, the DMP oxidation of homopropargyl alcohols also generated aryl furans with a longer reaction time, especially for ketone (compared to aldehyde) substituted allenes. Since previous conversions from activated alkynes/allenes to aryl furans require metal catalysts, this DMP oxidation procedure provided a novel way of producing allene or furan in one step without the use of organometallic catalysts.

6.6 Experimental Section

General procedure for synthesizing homopropargyl alcohols (compound **6.1**, **6.6**, **6.11**, **6.16**, **6.21**, **6.26**): iodobenzene (2 g, 10 mmol) and pent-4-yn-2-ol (1 g, 12 mmol) were dissolved in triethylamine (50 mL) and bis(triphenylphosphine)palladium (II) dichloride (0.14 g, 0.2 mmol) and CuI (0.02 g, 0.1 mmol) were added to the stirring reaction mixture. The reaction was stirred under 50 °C for 40 min. The mixture was extracted by ethyl acetate and washed by water and brine. the organic layer was dried by sodium sulfate and the solvent was removed. The crude mixture was purified by column using 1:3 E:H to afford 1.6 g (100%) product as yellow oil. Typical yield 100%.

General procedure for synthesizing allene-ketones/allene-aldehydes (compound **6.2**, **6.7**, **6.12**, **6.17**, **6.22**, **6.27**): Dess-Martin periodinane (2.1 g, 5.0 mmol) was added to a stirring solution of 5-phenylpent-4-yn-2-ol (0.6 g, 3.75 mmol) in CH₂Cl₂ (100 mL). The reaction was stirred at 35 °C for 15 min, quenched by saturated NaHCO₃ solution (100 mL) and stirred for 15 min, extracted by ether (100 mL). The organic layer was washed by brine wash (200 mL), dried by Na₂SO₄ and concentrated in vacuo. The crude product was purified by column chromatography 1:4 ethyl acetate: hexane during which the activated alkyne partially or fully converted to allenes (allenes have slightly higher R_f than the alkynes). Typical yield 30-60%.

General procedure for synthesizing furans (compound **6.3**, **6.8**, **6.13**, **6.18**, **6.23**, **6.28**): Dess-Martin periodinane (0.8 g, 1.9 mmol) was added to a stirring solution of 5-phenylpent-4-yn-2-ol (0.2 g, 1.25 mmol) in CH₂Cl₂ (30 mL). The reaction was stirred at room temperature for 12 h, quenched by saturated NaHCO₃ solution (30 mL) and stirred for 15 min. The organic layer was washed by brine wash (50 mL), dried by Na₂SO₄ and concentrated in vacuo. The crude product was purified by column chromatography 1:4 ethyl acetate: hexane to separate the top spot. Typical yield 20-50%.

General procedure for synthesizing butyl-triazoles (compound **6.4**, **6.9**, **6.14**, **6.19**, **6.24**, **6.29**): Butyl azide (0.75 g, 7.5 mmol) was added to a solution of 5-phenylpenta-3,4-dien-2-one (0.2 g, 1.3 mmol) in THF (5 mL) and the reaction was stirring under 65 °C for 4 days, the progress of the reaction was monitored by GC-MS until done. The reaction was concentrated in vacuo and purified by column chromatography. Typical yield 80-90%.

General procedure for synthesizing benzyl-triazoles (compound **6.5**, **6.10**, **6.15**, **6.20**, **6.25**, **6.30**): Butyl azide (0.76 g, 5.7 mmol) was added to a solution of 5-phenylpenta-3,4-

dien-2-one (0.3 g, 1.9 mmol) in THF (5 mL) and the reaction was stirring under 65 °C for 4 days, the progress of the reaction was monitored by GC-MS. The reaction was concentrated in vacuo and purified by column chromatography. Typical yield 80-90%.

5-phenylpent-4-yn-2-ol (6.1) ^1H NMR (400 MHz, Chloroform-*d*) δ 7.46 – 7.36 (m, 2H), 7.34 – 7.23 (m, 3H), 4.03 (h, $J = 6.1$ Hz, 1H), 2.66 – 2.49 (m, 2H), 1.31 (d, $J = 6.2$ Hz, 3H). ^{13}C NMR (101 MHz, CDCl_3) δ 131.64, 128.26, 127.93, 123.35, 86.22, 82.98, 77.40, 77.08, 76.76, 66.55, 29.97, 22.39, -0.00.

5-phenylpenta-3,4-dien-2-one (6.2) ^1H NMR (400 MHz, Chloroform-*d*) δ 7.41 – 7.29 (m, 5H), 6.65 (d, $J = 6.2$ Hz, 1H), 6.15 (d, $J = 6.2$ Hz, 1H), 2.28 (s, 3H). ^{13}C NMR (101 MHz, CDCl_3) δ 215.92, 198.11, 130.95, 129.06, 128.30, 127.31, 101.17, 98.59, 77.35, 77.04, 76.72, 26.85.

2-methyl-5-phenylfuran (6.3) ^1H NMR (400 MHz, Chloroform-*d*) δ 7.66 – 7.58 (m, 2H), 7.35 (t, $J = 7.8$ Hz, 2H), 7.24 – 7.16 (m, 1H), 6.54 (d, $J = 3.2$ Hz, 1H), 6.08 – 6.02 (m, 1H), 2.37 (s, 3H). ^{13}C NMR (101 MHz, CDCl_3) δ 152.26, 151.95, 131.15, 128.59, 126.73, 123.27, 107.67, 105.83, 77.34, 77.02, 76.70, 13.73, -0.00.

1-(5-benzyl-1-butyl-1H-1,2,3-triazol-4-yl)ethan-1-one (6.4) ^1H NMR (400 MHz, Chloroform-*d*) δ 7.19 (dd, $J = 8.2, 5.1$ Hz, 4H), 7.07 – 6.94 (m, 2H), 4.38 (s, 2H), 4.06 (t, $J = 7.5$ Hz, 2H), 2.68 (s, 3H), 1.58 (ddt, $J = 9.0, 7.6, 3.7$ Hz, 2H), 1.18 (h, $J = 7.4$ Hz, 2H), 0.78 (t, $J = 7.3$ Hz, 3H). ^{13}C NMR (101 MHz, CDCl_3) δ 194.57, 143.69, 138.38, 135.76, 128.93, 128.20, 127.18, 77.37, 77.06, 76.74, 47.86, 31.56, 28.62, 27.92, 19.73, 13.43. HRMS (ESI), m/z : calcd. for $\text{C}_{15}\text{H}_{19}\text{N}_3\text{O}$ $[\text{M}+\text{H}]^+$ 258.1601, found 258.1602.

1-(1,5-dibenzyl-1H-1,2,3-triazol-4-yl)ethan-1-one (6.5) ^1H NMR (400 MHz, Chloroform-*d*) δ 7.27 – 7.20 (m, 3H), 7.20 – 7.10 (m, 3H), 6.96 (ddd, $J = 14.0, 7.4, 2.6$

Hz, 4H), 5.27 (s, 2H), 4.23 (s, 2H), 2.69 (s, 3H). ^{13}C NMR (101 MHz, CDCl_3) δ 194.50, 144.27, 138.77, 135.31, 133.90, 129.07, 128.94, 128.59, 128.25, 127.22, 127.20, 77.39, 77.07, 76.75, 51.92, 28.44, 27.96. HRMS (ESI), m/z : calcd. for $\text{C}_{18}\text{H}_{17}\text{N}_3\text{O}$ $[\text{M}+\text{H}]^+$ 292.1444, found 292.1447.

5-(4-nitrophenyl)pent-4-yn-2-ol (6.6) ^1H NMR (400 MHz, Chloroform-*d*) δ 8.19 – 8.11 (m, 2H), 7.57 – 7.50 (m, 2H), 4.09 (h, $J = 6.1$ Hz, 1H), 2.72 – 2.56 (m, 2H), 1.35 (d, $J = 6.2$ Hz, 3H). ^{13}C NMR (101 MHz, CDCl_3) δ 146.78, 132.40, 130.51, 123.52, 92.58, 81.28, 77.43, 77.11, 76.79, 66.39, 30.00, 22.60.

5-(4-nitrophenyl)penta-3,4-dien-2-one (6.7) ^1H NMR (400 MHz, Chloroform-*d*) δ 8.27 – 8.20 (m, 2H), 7.52 – 7.45 (m, 2H), 6.75 (d, $J = 6.3$ Hz, 1H), 6.26 (d, $J = 6.3$ Hz, 1H), 2.31 (s, 3H). ^{13}C NMR (101 MHz, CDCl_3) δ 216.64, 196.75, 147.36, 138.15, 127.87, 124.39, 101.40, 97.48, 77.40, 77.08, 76.77, 27.31.

2-methyl-5-(4-nitrophenyl)furan (6.8) ^1H NMR (400 MHz, Chloroform-*d*) δ 8.15 (d, $J = 8.9$ Hz, 2H), 7.66 (d, $J = 9.0$ Hz, 2H), 6.71 (d, $J = 3.4$ Hz, 1H), 6.08 (dd, $J = 3.4, 1.1$ Hz, 1H), 2.34 (s, 3H). ^{13}C NMR (101 MHz, CDCl_3) δ 154.66, 150.13, 136.73, 124.37, 124.09, 123.27, 110.29, 108.82, 77.35, 77.03, 76.71, 13.88.

1-(1-butyl-5-(4-nitrobenzyl)-1H-1,2,3-triazol-4-yl)ethan-1-one (6.9) ^1H NMR (400 MHz, Chloroform-*d*) δ 8.09 (d, $J = 8.7$ Hz, 2H), 7.21 (d, $J = 8.3$ Hz, 3H), 4.47 (s, 2H), 4.11 (t, $J = 7.4$ Hz, 2H), 2.68 (s, 3H), 1.67 (s, 1H), 1.35 – 1.13 (m, 2H), 0.81 (t, $J = 7.4$ Hz, 3H). ^{13}C NMR (101 MHz, CDCl_3) δ 194.60, 147.16, 143.91, 143.23, 136.70, 129.01, 124.16, 77.36, 77.04, 76.73, 47.95, 31.73, 28.57, 27.84, 19.73, 13.43. HRMS (ESI), m/z : calcd. for $\text{C}_{15}\text{H}_{18}\text{N}_4\text{O}_3$ $[\text{M}-\text{H}]^-$ 303.1306, found 303.1304.

1-(1-benzyl-5-(4-nitrobenzyl)-1H-1,2,3-triazol-4-yl)ethan-1-one (6.10) ¹H NMR (400 MHz, CDCl₃) δ 8.07 – 8.00 (m, 2H), 7.32 – 7.25 (m, 3H), 7.08 (d, *J* = 8.6 Hz, 2H), 7.04 (dd, *J* = 7.2, 2.4 Hz, 2H), 5.46 (s, 2H), 4.42 (s, 2H), 2.78 (s, 3H). ¹³C NMR (101 MHz, CDCl₃) δ 194.48, 146.96, 144.54, 142.70, 137.14, 133.47, 129.18, 128.98, 128.82, 127.09, 123.90, 77.38, 77.06, 76.75, 52.23, 28.56, 27.88. Melting point 120-122 °C. HRMS (ESI), *m/z*: calcd. for C₁₈H₁₆N₄O₃ [M-H]⁻ 335.1150, found 335.1148.

5-(4-methoxyphenyl)pent-4-yn-2-ol (6.11) ¹H NMR (400 MHz, Chloroform-*d*) δ 7.32 – 7.23 (m, 2H), 6.79 – 6.71 (m, 2H), 3.96 (ddd, *J* = 9.8, 6.6, 5.0 Hz, 1H), 3.73 (s, 3H), 2.50 (qd, *J* = 16.6, 5.9 Hz, 2H), 1.99 (d, *J* = 4.6 Hz, 1H), 1.24 (d, *J* = 6.2 Hz, 3H). ¹³C NMR (101 MHz, CDCl₃) δ 159.32, 133.04, 115.46, 113.89, 84.49, 82.88, 77.37, 77.05, 76.73, 66.61, 55.29, 30.06, 22.40.

5-(4-methoxyphenyl)penta-3,4-dien-2-one (6.12) ¹H NMR (400 MHz, Chloroform-*d*) δ 7.23 – 7.13 (m, 3H), 6.87 – 6.80 (m, 2H), 6.54 (d, *J* = 6.3 Hz, 1H), 6.05 (d, *J* = 6.2 Hz, 1H), 3.75 (s, 3H), 2.20 (s, 3H). ¹³C NMR (101 MHz, CDCl₃) δ 215.81, 198.42, 159.73, 128.55, 123.02, 114.57, 101.25, 98.09, 77.35, 77.24, 77.03, 76.72, 55.39, 26.77.

2-(4-methoxyphenyl)-5-methylfuran (6.13) ¹H NMR (400 MHz, Chloroform-*d*) δ 7.49 – 7.41 (m, 2H), 6.82 – 6.73 (m, 2H), 6.28 (d, *J* = 3.2 Hz, 1H), 5.90 (dd, *J* = 3.1, 1.2 Hz, 1H), 3.67 (s, 3H), 2.23 (s, 3H). ¹³C NMR (101 MHz, CDCl₃) δ 158.67, 152.39, 151.21, 127.48, 124.78, 124.44, 114.12, 113.80, 107.60, 104.28, 77.47, 77.15, 76.84, 55.30, 13.73.

1-(1-butyl-5-(4-methoxybenzyl)-1H-1,2,3-triazol-4-yl)ethan-1-one (6.14) ¹H NMR (400 MHz, Chloroform-*d*) δ 6.99 – 6.91 (m, 2H), 6.77 – 6.69 (m, 2H), 4.30 (s, 2H), 4.07 (t, *J* = 7.5 Hz, 2H), 3.69 (s, 3H), 2.67 (s, 3H), 1.67 – 1.54 (m, 2H), 1.20 (h, *J* = 7.4 Hz,

2H), 0.80 (t, $J = 7.3$ Hz, 3H). ^{13}C NMR (101 MHz, CDCl_3) δ 194.56, 158.67, 143.56, 138.76, 129.24, 127.71, 114.28, 77.38, 77.27, 77.06, 76.75, 55.29, 47.82, 31.58, 27.92, 27.77, 19.75, 13.46. HRMS (ESI), m/z : calcd. for $\text{C}_{16}\text{H}_{21}\text{N}_3\text{O}_2$ $[\text{M}+\text{H}]^+$ 288.1707, found 288.1711.

1-(1-benzyl-5-(4-methoxybenzyl)-1H-1,2,3-triazol-4-yl)ethan-1-one (6.15) ^1H NMR (400 MHz, Chloroform- d) δ 7.23 (dd, $J = 7.2, 3.1$ Hz, 3H), 6.99 (dt, $J = 5.9, 3.4$ Hz, 2H), 6.87 (d, $J = 8.3$ Hz, 2H), 6.71 (d, $J = 8.5$ Hz, 2H), 5.28 (s, 2H), 4.16 (s, 2H), 3.70 (s, 3H), 2.69 (s, 3H). ^{13}C NMR (101 MHz, CDCl_3) δ 194.52, 158.68, 139.16, 133.98, 129.31, 129.06, 128.55, 127.25, 127.18, 114.30, 113.98, 77.36, 77.04, 76.72, 55.30, 51.88, 27.97, 27.61. HRMS (ESI), m/z : calcd. for $\text{C}_{19}\text{H}_{19}\text{N}_3\text{O}_2$ $[\text{M}+\text{H}]^+$ 322.1550, found 322.1552.

4-phenylbut-3-yn-1-ol (6.16) ^1H NMR (400 MHz, Chloroform- d) δ 7.45 – 7.38 (m, 2H), 7.29 (dp, $J = 5.1, 1.9$ Hz, 3H), 3.81 (t, $J = 6.3$ Hz, 2H), 2.69 (t, $J = 6.3$ Hz, 2H), 2.02 (dt, $J = 9.9, 5.7$ Hz, 1H). ^{13}C NMR (101 MHz, CDCl_3) δ 131.66, 128.26, 127.96, 123.30, 86.35, 82.46, 77.36, 77.04, 76.72, 61.15, 23.81, -0.00.

4-phenylbuta-2,3-dienal (6.17) ^1H NMR (400 MHz, CDCl_3) δ 9.59 (dd, $J = 7.6, 2.8$ Hz, 1H), 7.39 – 7.32 (m, 5H), 6.78 (d, $J = 6.1$ Hz, 1H), 6.24 (t, $J = 6.6$ Hz, 1H). ^{13}C NMR (101 MHz, CDCl_3) δ 221.47, 191.09, 130.30, 129.09, 128.63, 127.55, 101.78, 99.66, 77.35, 77.23, 77.03, 76.71.

2-phenylfuran (6.18) ^1H NMR (400 MHz, Chloroform- d) δ 7.60 – 7.54 (m, 2H), 7.35 (d, $J = 1.8$ Hz, 1H), 7.30 – 7.25 (m, 2H), 7.15 (d, $J = 7.4$ Hz, 1H), 6.54 (dd, $J = 3.3, 0.7$ Hz, 1H), 6.35 (dd, $J = 3.4, 1.8$ Hz, 1H). ^{13}C NMR (101 MHz, CDCl_3) δ 154.07, 142.14, 130.98, 128.76, 127.41, 123.87, 111.73, 105.05, 77.46, 77.14, 76.82.

5-benzyl-1-butyl-1H-1,2,3-triazole-4-carbaldehyde (6.19) ^1H NMR (400 MHz, Chloroform-*d*) δ 10.13 (s, 1H), 7.23 – 7.05 (m, 4H), 7.00 – 6.93 (m, 2H), 4.29 (s, 2H), 4.01 (t, $J = 7.5$ Hz, 2H), 1.60 – 1.47 (m, 3H), 1.13 (hept, $J = 7.2$ Hz, 2H), 0.72 (t, $J = 7.4$ Hz, 3H). ^{13}C NMR (101 MHz, CDCl_3) δ 186.60, 143.95, 138.68, 135.20, 129.07, 128.19, 127.44, 77.37, 77.05, 76.74, 47.89, 31.49, 28.49, 19.73, 13.42. HRMS (ESI), m/z : calcd. for $\text{C}_{14}\text{H}_{17}\text{N}_3\text{O}$ $[\text{M}+\text{H}]^+$ 244.1444, found 244.1446.

1,5-dibenzyl-1H-1,2,3-triazole-4-carbaldehyde (6.20) ^1H NMR (400 MHz, CDCl_3) δ 10.20 (s, 1H), 7.27 – 7.23 (m, 3H), 7.19 (q, $J = 5.3, 4.7$ Hz, 3H), 7.01 – 6.97 (m, 2H), 6.95 (dd, $J = 7.5, 2.0$ Hz, 2H), 5.29 (s, 2H), 4.21 (s, 2H). ^{13}C NMR (101 MHz, CDCl_3) δ 186.51, 144.50, 139.05, 134.76, 133.60, 129.14, 129.07, 128.73, 128.25, 127.44, 127.29, 77.37, 77.05, 76.73, 51.97, 28.34. HRMS (ESI), m/z : calcd. for $\text{C}_{17}\text{H}_{15}\text{N}_3\text{O}$ $[\text{M}+\text{H}]^+$ 278.1288, found 278.1291.

4-(4-nitrophenyl)but-3-yn-1-ol (6.21) ^1H NMR (400 MHz, Chloroform-*d*) δ 8.12 – 8.04 (m, 2H), 7.51 – 7.42 (m, 2H), 3.79 (q, $J = 6.0$ Hz, 2H), 2.67 (t, $J = 6.3$ Hz, 2H), 2.06 – 1.98 (m, 1H). ^{13}C NMR (101 MHz, CDCl_3) δ 146.82, 132.43, 130.46, 123.54, 92.73, 80.74, 77.40, 77.08, 76.76, 60.87, 23.88.

4-(4-nitrophenyl)buta-2,3-dienal (6.22) ^1H NMR (400 MHz, Chloroform-*d*) δ 9.65 (d, $J = 6.7$ Hz, 1H), 8.28 – 8.20 (m, 2H), 7.53 – 7.40 (m, 2H), 6.86 (d, $J = 6.2$ Hz, 1H), 6.34 (t, $J = 6.4$ Hz, 1H). ^{13}C NMR (101 MHz, CDCl_3) δ 221.67, 189.78, 147.58, 137.44, 128.13, 124.37, 101.97, 98.54, 77.35, 77.03, 76.71, 0.00.

2-(4-nitrophenyl)furan (6.23) ^1H NMR (400 MHz, Chloroform-*d*) δ 8.28 – 8.23 (m, 2H), 7.82 – 7.76 (m, 2H), 7.58 (d, $J = 1.8$ Hz, 1H), 6.88 (d, $J = 3.5$ Hz, 1H), 6.56 (dd, $J =$

3.5, 1.8 Hz, 1H). ^{13}C NMR (101 MHz, CDCl_3) δ 151.77, 146.43, 144.20, 136.48, 124.38, 123.98, 112.49, 109.02, 77.37, 77.05, 76.73.

1-butyl-5-(4-nitrobenzyl)-1H-1,2,3-triazole-4-carbaldehyde (6.24) ^1H NMR (400 MHz, Chloroform-*d*) δ 10.26 (s, 1H), 8.21 – 8.14 (m, 2H), 7.29 (d, $J = 8.5$ Hz, 2H), 4.52 (s, 2H), 4.20 (t, $J = 7.4$ Hz, 2H), 1.76 (p, $J = 7.5$ Hz, 2H), 1.34 – 1.27 (m, 2H), 0.89 (t, $J = 7.3$ Hz, 3H). ^{13}C NMR (101 MHz, CDCl_3) δ 186.64, 147.30, 144.10, 142.56, 136.90, 129.02, 124.27, 77.34, 77.02, 76.70, 47.95, 31.66, 28.36, 19.73, 13.41, 0.00. HRMS (ESI), m/z : calcd. for $\text{C}_{14}\text{H}_{16}\text{N}_4\text{O}_3$ $[\text{M}+\text{H}]^+$ 289.1295, found 289.1297.

1-benzyl-5-(4-nitrobenzyl)-1H-1,2,3-triazole-4-carbaldehyde (6.25) ^1H NMR (400 MHz, Chloroform-*d*) δ 10.27 (s, 1H), 8.04 (d, $J = 8.7$ Hz, 2H), 7.32 – 7.25 (m, 3H), 7.08 (d, $J = 8.5$ Hz, 2H), 7.05 – 7.01 (m, 2H), 5.46 (s, 2H), 4.38 (s, 2H). ^{13}C NMR (101 MHz, CDCl_3) δ 186.51, 147.11, 144.71, 142.03, 137.32, 133.19, 129.24, 128.98, 128.95, 127.11, 124.00, 77.34, 77.03, 76.71, 52.25, 28.35, 0.00. HRMS (ESI), m/z : calcd. for $\text{C}_{17}\text{H}_{14}\text{N}_4\text{O}_3$ $[\text{M}-\text{H}]^-$ 321.0993, found 321.0991.

4-(4-methoxyphenyl)but-3-yn-1-ol (6.26) ^1H NMR (400 MHz, Chloroform-*d*) δ 7.31 – 7.23 (m, 2H), 6.78 – 6.69 (m, 2H), 3.71 (m, 5H), 2.59 (t, $J = 6.3$ Hz, 2H), 2.09 (s, 1H). ^{13}C NMR (101 MHz, CDCl_3) δ 159.30, 133.04, 115.45, 113.89, 84.79, 82.25, 77.41, 77.09, 76.77, 61.23, 55.28, 23.82.

4-(4-methoxyphenyl)buta-2,3-dienal (6.27) ^1H NMR (400 MHz, Chloroform-*d*) δ 9.57 (d, $J = 7.1$ Hz, 1H), 7.26 (s, 2H), 6.90 (d, $J = 8.7$ Hz, 2H), 6.74 (d, $J = 6.0$ Hz, 1H), 6.22 (s, 1H), 3.83 (s, 3H). ^{13}C NMR (101 MHz, CDCl_3) δ 221.59, 191.34, 159.94, 128.79, 122.26, 114.56, 101.87, 99.14, 77.34, 77.02, 76.70, 55.37, 0.00.

2-(4-methoxyphenyl)furan (6.28) ^1H NMR (400 MHz, Chloroform-*d*) δ 7.65 – 7.51 (m, 2H), 7.43 (d, $J = 1.7$ Hz, 1H), 6.99 – 6.88 (m, 2H), 6.51 (d, $J = 3.4$ Hz, 1H), 6.44 (dd, $J = 3.5, 1.8$ Hz, 1H), 3.83 (s, 3H). ^{13}C NMR (101 MHz, CDCl_3) δ 158.99, 154.02, 141.38, 125.22, 124.03, 114.10, 111.53, 103.36, 77.33, 77.02, 76.70, 55.31, -0.00.

1-butyl-5-(4-methoxybenzyl)-1H-1,2,3-triazole-4-carbaldehyde (6.29) ^1H NMR (400 MHz, Chloroform-*d*) δ 10.26 (d, $J = 1.0$ Hz, 1H), 7.03 (d, $J = 8.3$ Hz, 2H), 6.82 (d, $J = 8.3$ Hz, 2H), 4.35 (s, 2H), 4.16 (t, $J = 7.5$ Hz, 2H), 3.78 (s, 3H), 1.71 (q, $J = 7.5$ Hz, 2H), 1.32 – 1.24 (m, 2H), 0.88 (t, $J = 7.4$ Hz, 3H). ^{13}C NMR (101 MHz, CDCl_3) δ 186.59, 158.84, 143.82, 139.06, 129.24, 127.11, 114.40, 77.34, 77.02, 76.70, 55.30, 47.84, 31.51, 27.65, 19.75, 13.44, 0.00. HRMS (ESI), m/z : calcd. for $\text{C}_{15}\text{H}_{19}\text{N}_3\text{O}_2$ $[\text{M}+\text{H}]^+$ 274.1550, found 274.1552.

1-benzyl-5-(4-methoxybenzyl)-1H-1,2,3-triazole-4-carbaldehyde (6.30) ^1H NMR (400 MHz, CDCl_3) δ 10.27 (s, 1H), 7.36 – 7.30 (m, 3H), 7.06 (dd, $J = 6.7, 2.8$ Hz, 2H), 6.94 (d, $J = 8.4$ Hz, 2H), 6.79 (d, $J = 8.6$ Hz, 2H), 5.37 (s, 2H), 4.21 (s, 2H), 3.77 (s, 3H). ^{13}C NMR (101 MHz, CDCl_3) δ 186.47, 158.82, 144.36, 139.45, 133.67, 129.30, 129.10, 128.66, 127.22, 126.63, 114.39, 77.35, 77.03, 76.71, 55.29, 51.90, 27.49, 0.00. HRMS (ESI), m/z : calcd. for $\text{C}_{18}\text{H}_{17}\text{N}_3\text{O}_2$ $[\text{M}+\text{H}]^+$ 308.1394, found 308.1395.

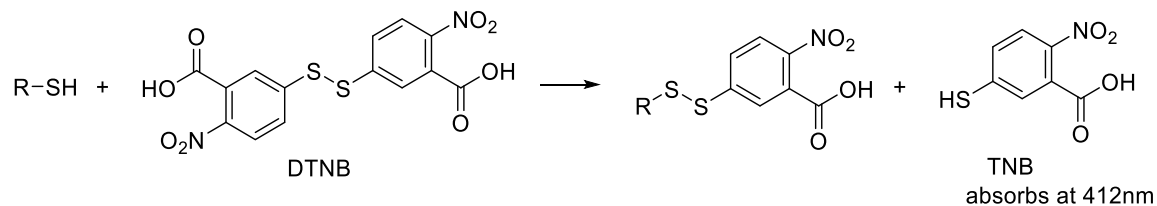
(E)-1-phenylpent-2-ene-1,4-dione (6.31) ^1H NMR (400 MHz, CDCl_3) δ 7.92 – 7.86 (m, 2H), 7.57 – 7.51 (m, 1H), 7.46 – 7.39 (m, 2H), 6.82 (d, $J = 12.0$ Hz, 1H), 6.54 (d, $J = 12.0$ Hz, 1H), 2.23 (s, 3H). ^{13}C NMR (101 MHz, CDCl_3) δ 199.65, 193.62, 136.44, 135.84, 135.45, 133.74, 128.81, 128.60, 77.65, 77.34, 77.02, 29.88. ESI, m/z : calcd. for $\text{C}_{11}\text{H}_{10}\text{O}_2$ $[\text{M}+\text{H}]^+$ 197.1, found 197.1.

6.7 References

- [1] Huisgen, R. 1, 3-dipolar cycloadditions. Past and future. *Angewandte Chemie International Edition in English*. **1963**, 2(10), 565-598.
- [2] Rostovtsev, V. V., Green, L. G., Fokin, V. V., & Sharpless, K. B. A stepwise huisgen cycloaddition process: copper (I)-catalyzed regioselective “ligation” of azides and terminal alkynes. *Angewandte Chemie*. **2002**, 114(14), 2708-2711.
- [3] Agard, N. J., Prescher, J. A., & Bertozzi, C. R. A strain-promoted [3+ 2] azide–alkyne cycloaddition for covalent modification of biomolecules in living systems. *Journal of the American Chemical Society*. **2004**, 126(46), 15046-15047.
- [4] Lima, C. G., Ali, A., van Berkel, S. S., Westermann, B., & Paixão, M. W. Emerging approaches for the synthesis of triazoles: beyond metal-catalyzed and strain-promoted azide–alkyne cycloaddition. *Chemical Communications*. **2015**, 51(54), 10784-10796.
- [5] Jalani, H. B., Karagöz, A. Ç., & Tsogoeva, S. B. Synthesis of substituted 1, 2, 3-triazoles via metal-free click cycloaddition reactions and alternative cyclization methods. *Synthesis*. **2017**, 49(01), 29-41.
- [6] (a) Scriven, E. F. V, Turnbull K. *Chem. Rev.* **1988**, 88, 297. (b) L'abbe, G. Decomposition and addition reactions of organic azides. *Chemical Reviews*. **1969**, 69(3), 345-363.
- [7] (a) Pauling, L., & Brockway, L. O. The adjacent charge rule and the structure of methyl azide, methyl nitrate, and fluorine nitrate. *Journal of the American Chemical Society*. **1937**, 59(1), 13-20. (b) Brockway, L. O., & Pauling, L. The electron-diffraction investigation of the structure of molecules of methyl azide and carbon

- suboxide. *Proceedings of the National Academy of Sciences of the United States of America*. **1933**, *19*(9), 860.
- [8] Bräse, S., Gil, C., Knepper, K., & Zimmermann, V. Organic azides: an exploding diversity of a unique class of compounds. *Angewandte Chemie International Edition*. **2005**, *44*(33), 5188-5240.
- [9] (a) Ding, P. G., Hu, X. S., Zhou, F., & Zhou, J. Catalytic enantioselective synthesis of α -chiral azides. *Organic Chemistry Frontiers*. **2018**, *5*(9), 1542-1559. (b) Carlson, A. S., & Topczewski, J. J. Allylic azides: synthesis, reactivity, and the Winstein rearrangement. *Organic & biomolecular chemistry*. **2019**, *17*(18), 4406-4429.
- [10] Krause, N., & Hashmi, A. S. **2004**, *Modern allene chemistry*. Wiley-VCH. P390
- [11] Yu, S., Vermeeren, P., van Dommelen, K., Bickelhaupt, M., & Hamlin, T. A. Understanding the 1, 3-Dipolar Cycloadditions of Allenes. *Chemistry—A European Journal*. **2020**. doi.org/10.1002/chem.202000857
- [12] Molteni, G., & Ponti, A. The Azide-Allene Dipolar Cycloaddition: Is DFT Able to Predict Site-and Regio-Selectivity?. *Molecules*. **2021**, *26*(4), 928.

Appendix 1: Ellman Reagent Test for Thiol Group of DSF



Can test for as low as 2-10uM free thiols.

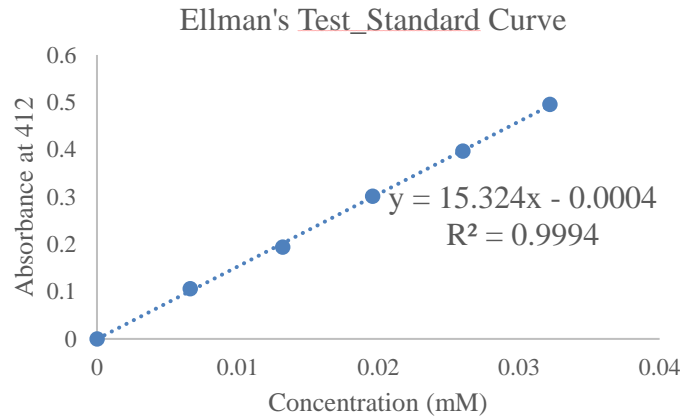
Working solution

- 1) Stock: DTNB (MW396.3) 79.3mg (2mM) and NaAc (MW 82.0) 410mg (50mM) were dissolve in DI water to 100mL.
- 2) Tris: tris base (MW 121.1) 12.1g (1M) first dissolve in 80mL DI water then add about 4.2 ml concentrated HCl and measured by pH meter to adjust pH to 8, then add water till 100mL.
- 3) Working solution: 10ml working solution = 0.5ml stock + 1ml tris + 8.5ml water

To make standard curve using acetyl cysteine:

- 1) 50mM acetyl cysteine stock: 81.5mg acetylcysteine in water to 10ml.
Dilute 50 times to make 1mM acetyl cysteine: take 1mL dilute with water to 50mL.
- 2) To a quartz cuvette: 3mL Ellman's working solution, add 20,40, 60, 80, 100uL 1mM acetyl cysteine solution separately to get 5 samples with different concentrations: 0.00662, 0.0132, 0.0196, 0.026, 0.0322mM accordingly.
- 3) Record absorption at 412nm, plot Beer Lambert plot, calculate extinction coefficient (EC).

Standard curve is plotted as bellow. EC=15.324. (EC reference values: 14.150 for dilute buffers, 13.700 for high salt concentrations)



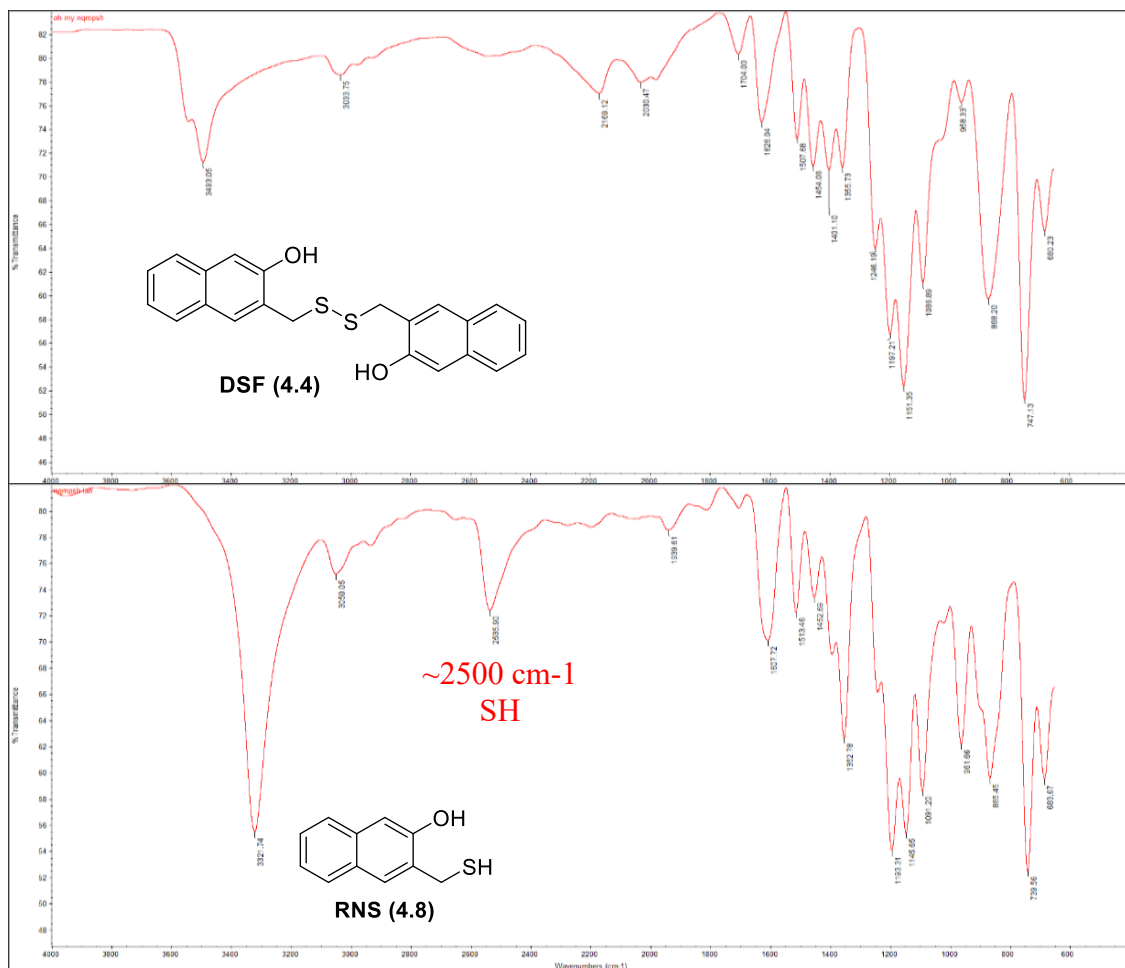
1mM DSF in 1to1 AW solution:

20uL in 3ml (0.00662mM) absorbs at 412nm: 0.004605, so SH concentration is 0.0003mM, therefore 4% of the sample has SH group.

1ml in 2ml (0.03mM) absorbs at 412nm: 0.244307, so SH concentration is 0.0159mM, therefore 5% of the sample has SH group.

From the above 2 samples, we can see that the DSF sample is a disulfide.

Appendix 2: IR of DSF and RNS



Appendix 3: Methylene Blue test procedure

1. Calibration curve for the methylene blue method

A 10 mM solution of Na₂S in sodium phosphate buffer (20 mM, pH 7.4)/acetonitrile (HPLC grade) (1:1) was prepared (Na₂S.9H₂O, 240 mg in 100 mL volumetric flask) and used as the stock solution. Aliquots of 100, 400, 700, 1000, 1300, 1700, 2000, 2500 μL of the Na₂S stock solution were added into a 50 mL volumetric flask and dissolved in a mixture of sodium phosphate buffer/acetonitrile to obtain the standard solutions in 20, 80, 140, 200, 260, 340, 400, 500 μM, respectively. 2 ml aliquot of the respective solution was

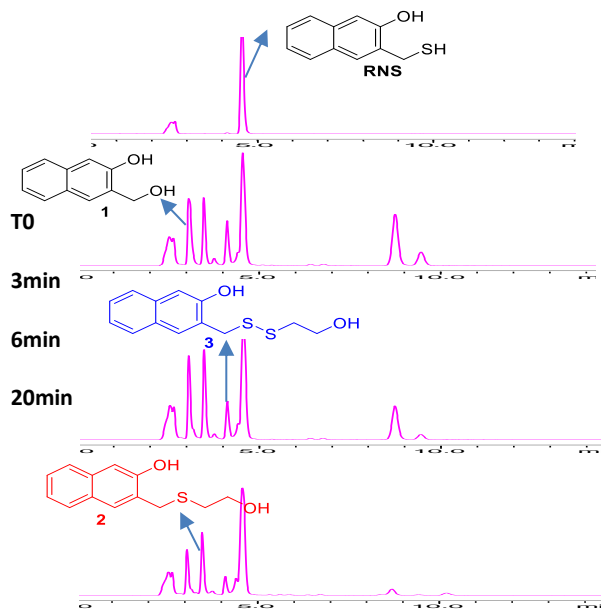
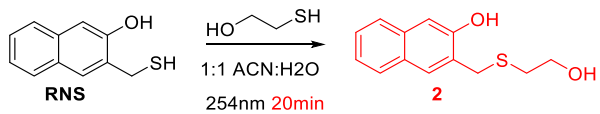
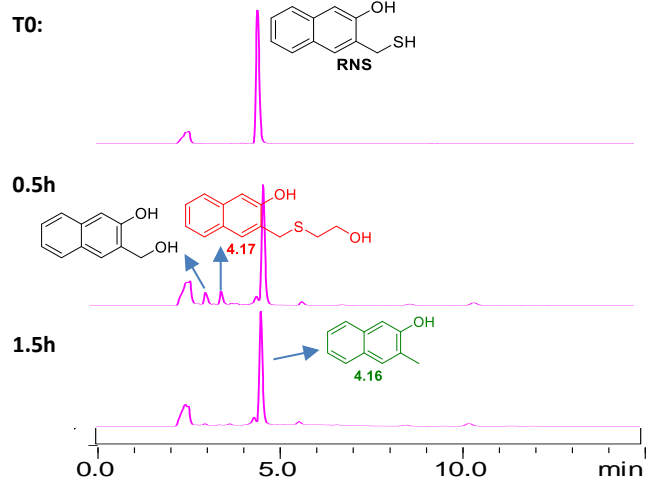
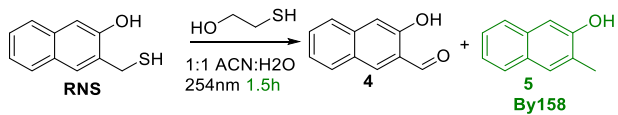
reacted with the methylene blue (MB+) cocktail: 30 mM FeCl₃ (400 μL) in 1.2 M HCl, 20 mM of N,N-dimethyl-1,4-phenylenediamine sulfate (400 μL) in 7.2 mM HCl, 1% w/v of Zn(OAc)₂ (200 μL) in H₂O at room temperature for at least 15 min (each reaction was performed in triplicate). The absorbance of methylene blue was measured at λ_{max}= 663 nm in a Cary 300 Bio UV-Vis spectrophotometer.

2. Determination of H₂S release of donors

Sample preparation: 250 μM DSF was prepared by dilute 3.125 mL of 4 mM DSF stock solution (76.1 mg in 50 mL 1:1 buffer/acetonitrile) into 50 mL 1:1 water/acetonitrile or buffer/acetonitrile. 500 μM RNS was prepared by dissolving 4.8 mg RNS in 1:1 water/acetonitrile or buffer/acetonitrile. The donor samples with excess thiols (10 mM) were made by adding either 39 mg 2-mercaptoethanol, 88 mg cysteine or 154 mg glutathione into the above mentioned DSF or RNS in 1:1 buffer/acetonitrile.

Photo-irradiation: Photo-irradiation was performed in a Rayonet Photochemical reactor (15 300 nm lamps). 2 mL aliquots was taken from the irradiated samples and mixed immediately with the methylene blue cocktail: 30 mM FeCl₃ (400 μL) in 1.2 M HCl, 20 mM of N,N-dimethyl-1,4-phenylenediamine sulfate (400 μL) in 7.2 mM HCl, 1% w/v of Zn(OAc)₂ (200 μL) in H₂O at room temperature for at least 20 min. The absorbance of methylene blue was measured at λ_{max}= 663 nm against a blank: 2 mL 1:1 buffer/ACN treated with same volumes of the three methylene blue cocktail reagents in a Cary 300 Bio UV-Vis spectrophotometer. Experiments performed in the absence of UV-light were executed in a similar fashion.

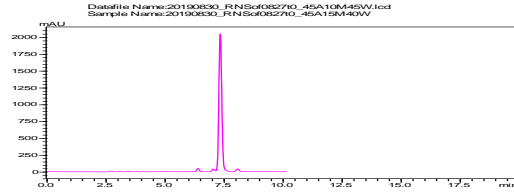
Appendix 4: RNS photoreaction with 2-mercaptoethanol



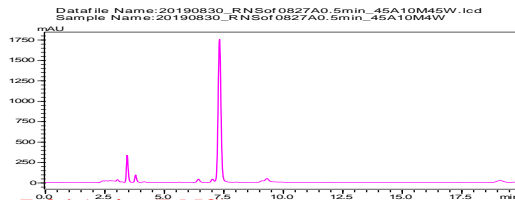
Appendix 5: Photolysis of RNS (HPLC eluent 45A10M45W)

300 nm irradiation for 0-7 min

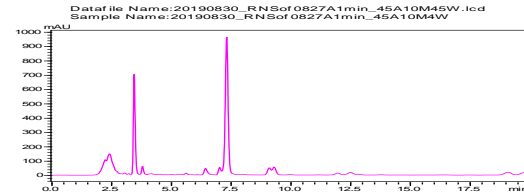
T0: 7.367min (RNS)



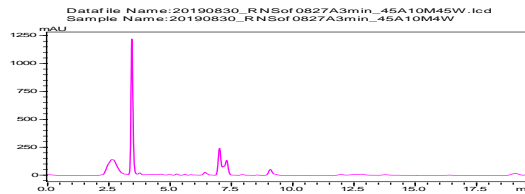
0.5min: 3.469 (diol), 7.351min (RNS)



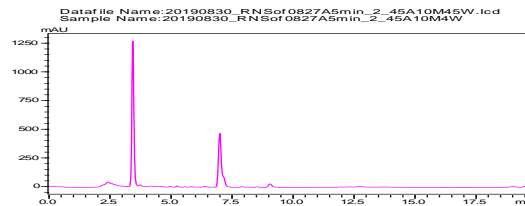
1min: 3.473 (diol), 7.345min (RNS)



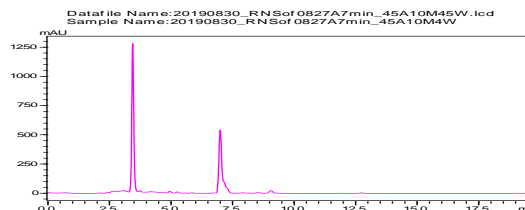
3min: 3.470 (diol), 7.048 (by158), 7.338 (RNS)



5min: 3.464 (diol), 7.029min (by158)



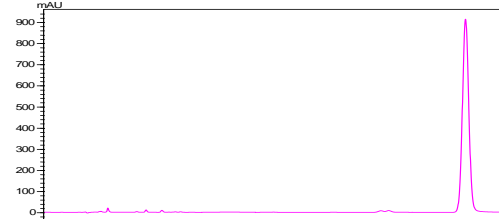
7min: 3.475(diol), 7.032min (by158)



Appendix 6: Photolysis of DSF (HPLC eluent 45A10M45W)

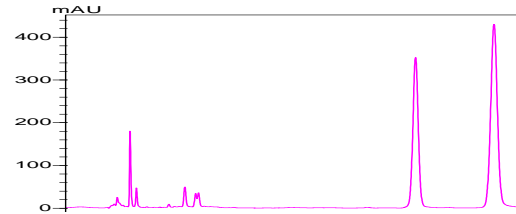
300 nm irradiation for 0-15 min

T0: 22.842 (DSF)

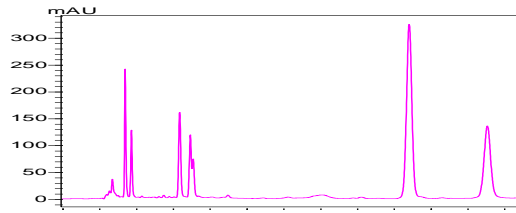


0.5min: 3.469 (diol), 3.812, 6.432, 7.013(by158), 7.169(aldehyde), 18.916 (thioether),

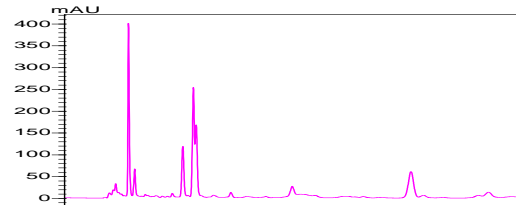
23.160 (DSF)



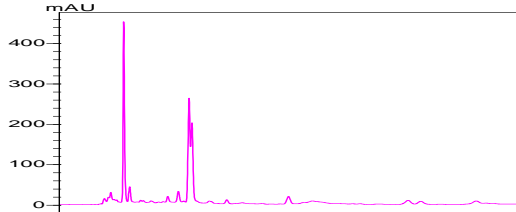
1min: 3.457, 3.800, 6.419, 6.997, 7.152, 18.889, 23.136



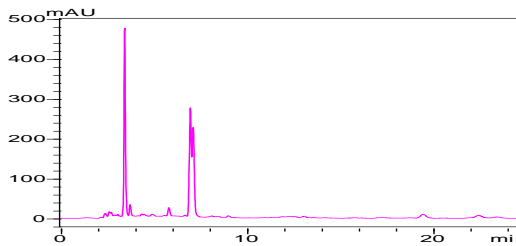
3min



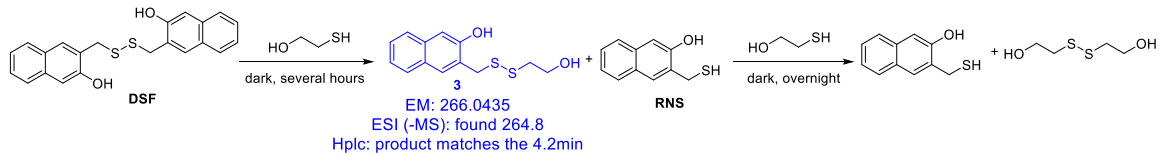
5min



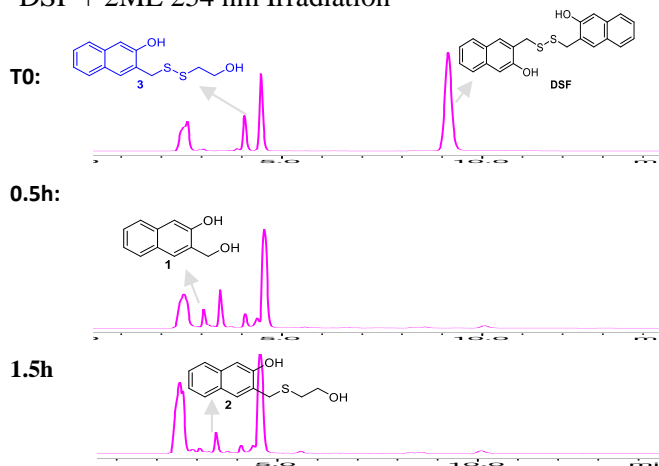
15min



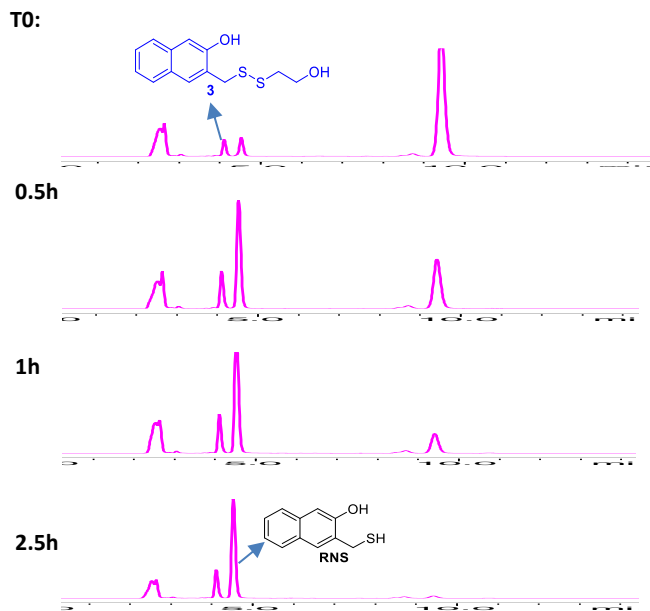
Appendix 7: Reaction of DSF and 2-mercaptoethanol



DSF + 2ME 254 nm Irradiation

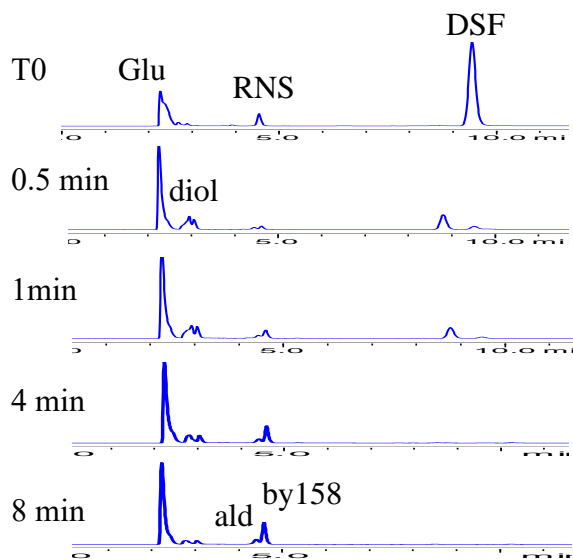


DSF + 2ME in dark

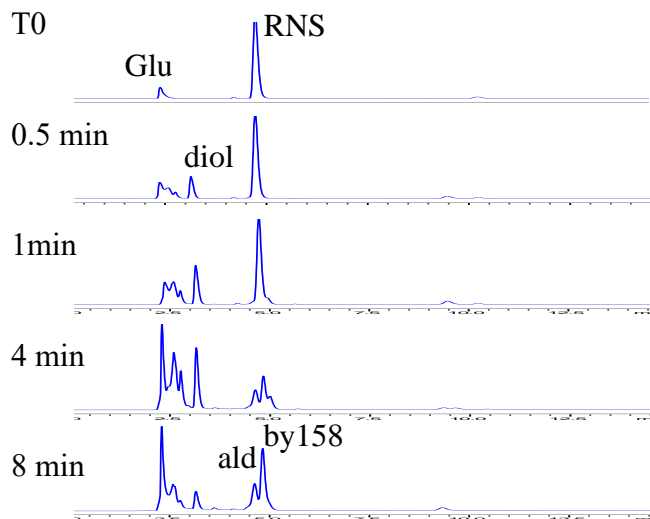


Appendix 8: Photolysis of (a) DSF and (b) RNS with glutathione

(a) DSF+Glu: 300 nm irradiation for 0, 0.5, 1, 4, 8 min (HPLC eluent: 75M25W)



(b) RNS+Glu: 300 nm irradiation for 0, 0.5, 1, 4, 8 min (HPLC eluent: 75M25W)



Appendix 9: Conversion of activated allene to triazole

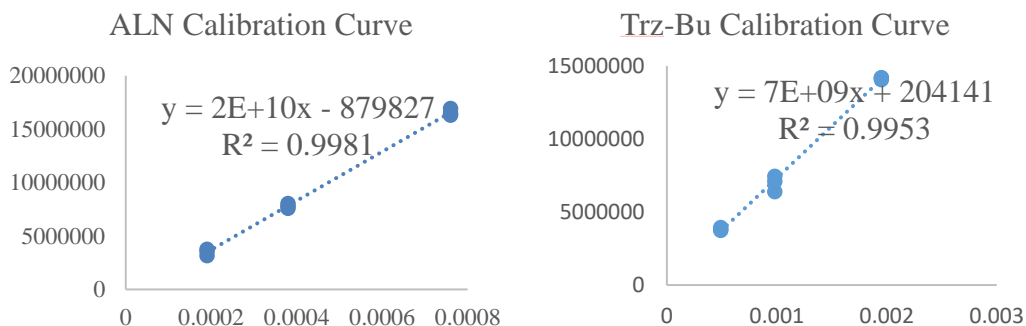
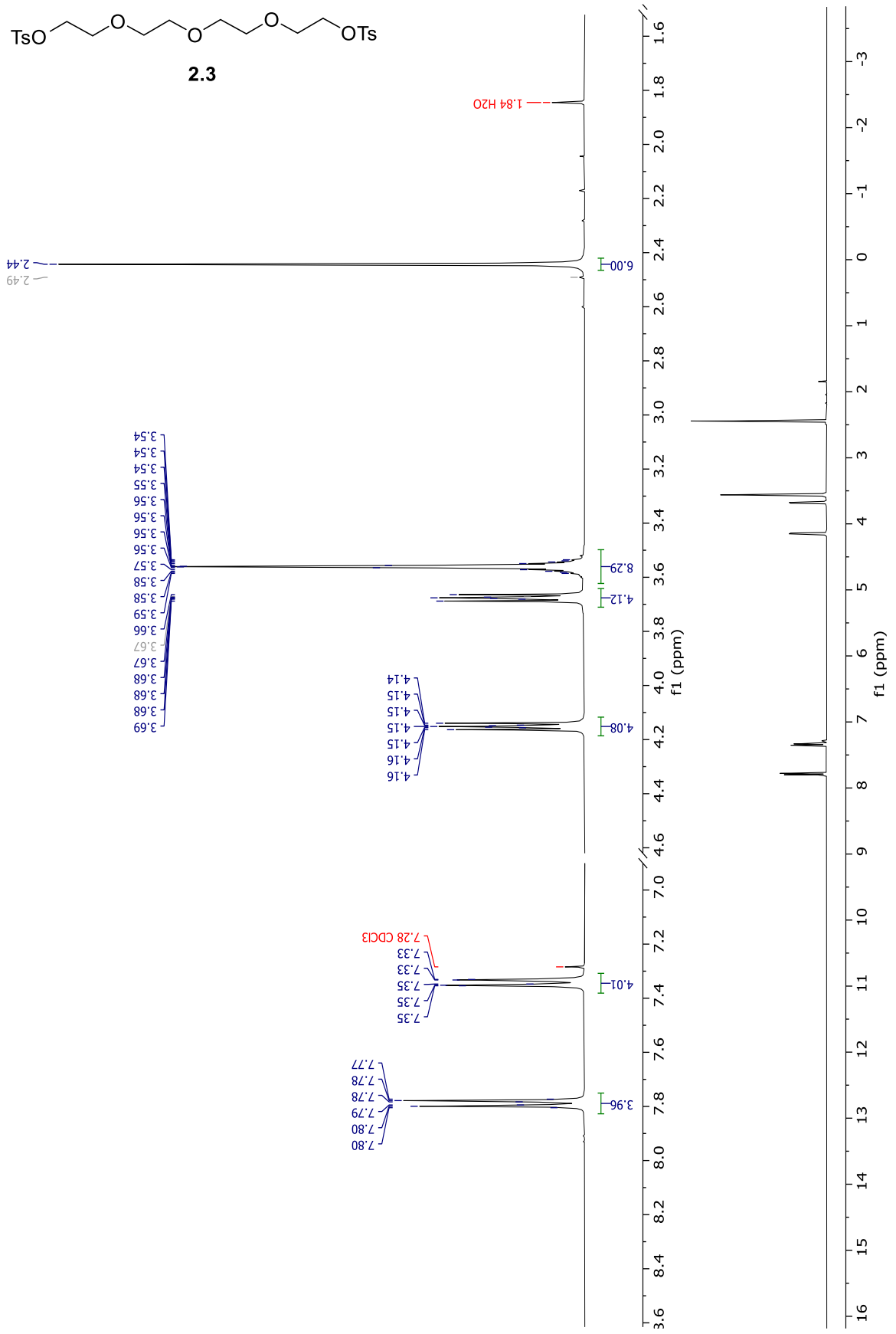
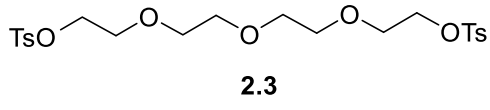


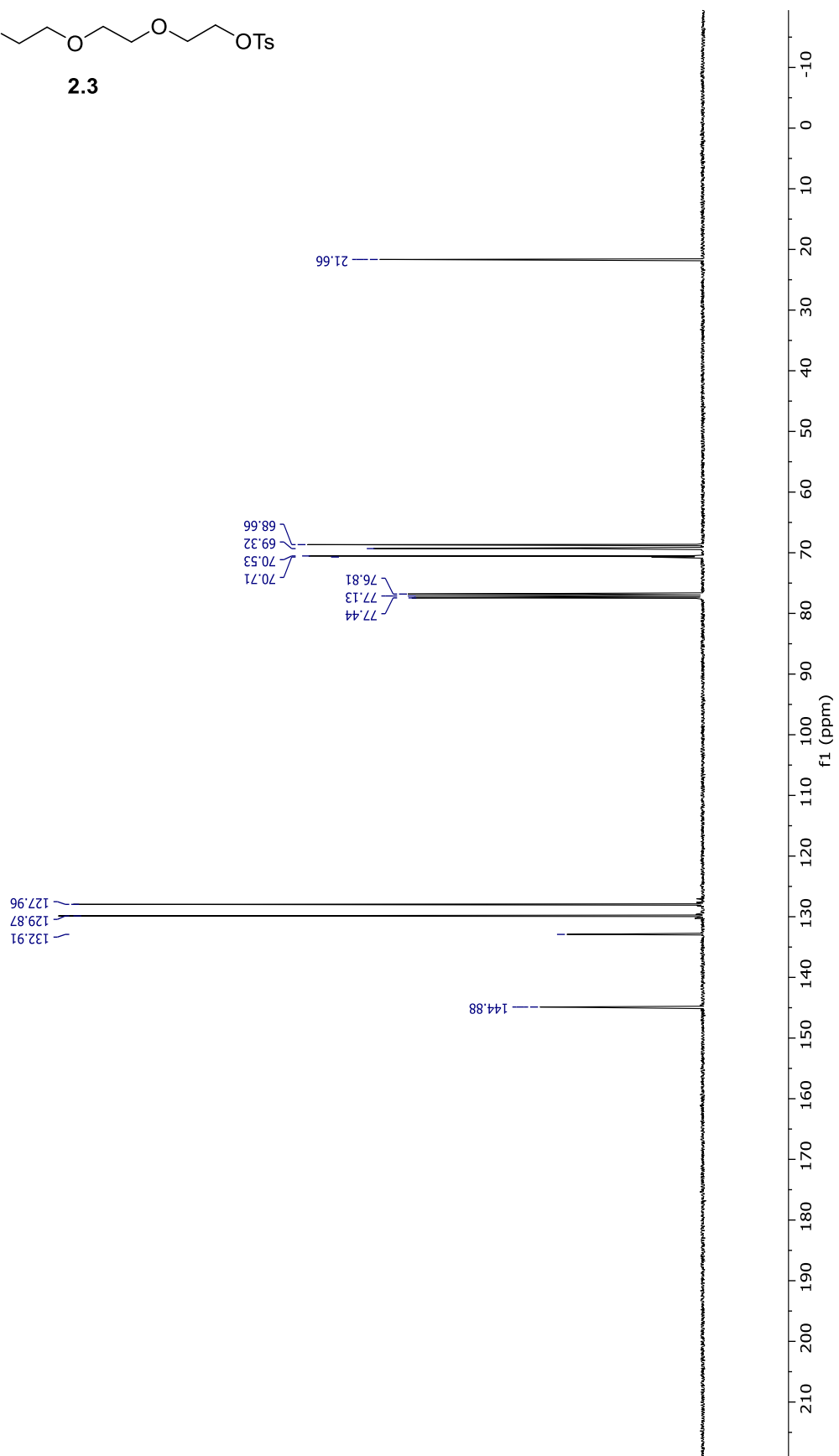
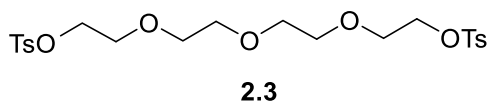
Figure. Calibration curves for the reactant and the product.

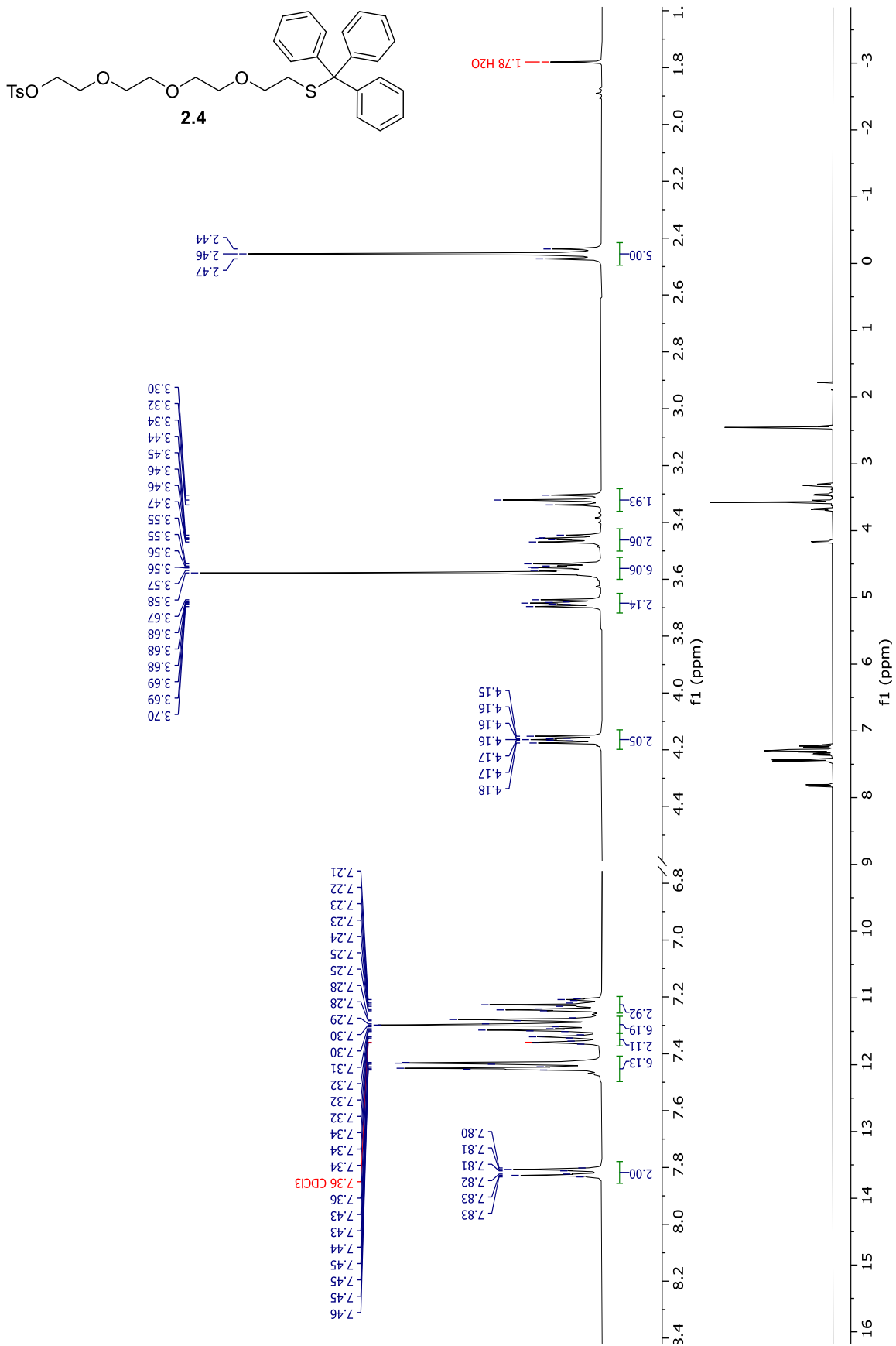
The butyl azide (400 mM) in dioxane solution was prepared preheat in water bath for 15 min before the calculated amount of reactant was added to the solution. The HPLC was using 65Acetonitrile/35 water eluting system observing at 205 nm channel. Samples were taken from reaction mixture and diluted 10 times with methanol for HPLC measurement. The reactant and product peak area were corrected based on the reaction azide concentration of the solution at time zero.

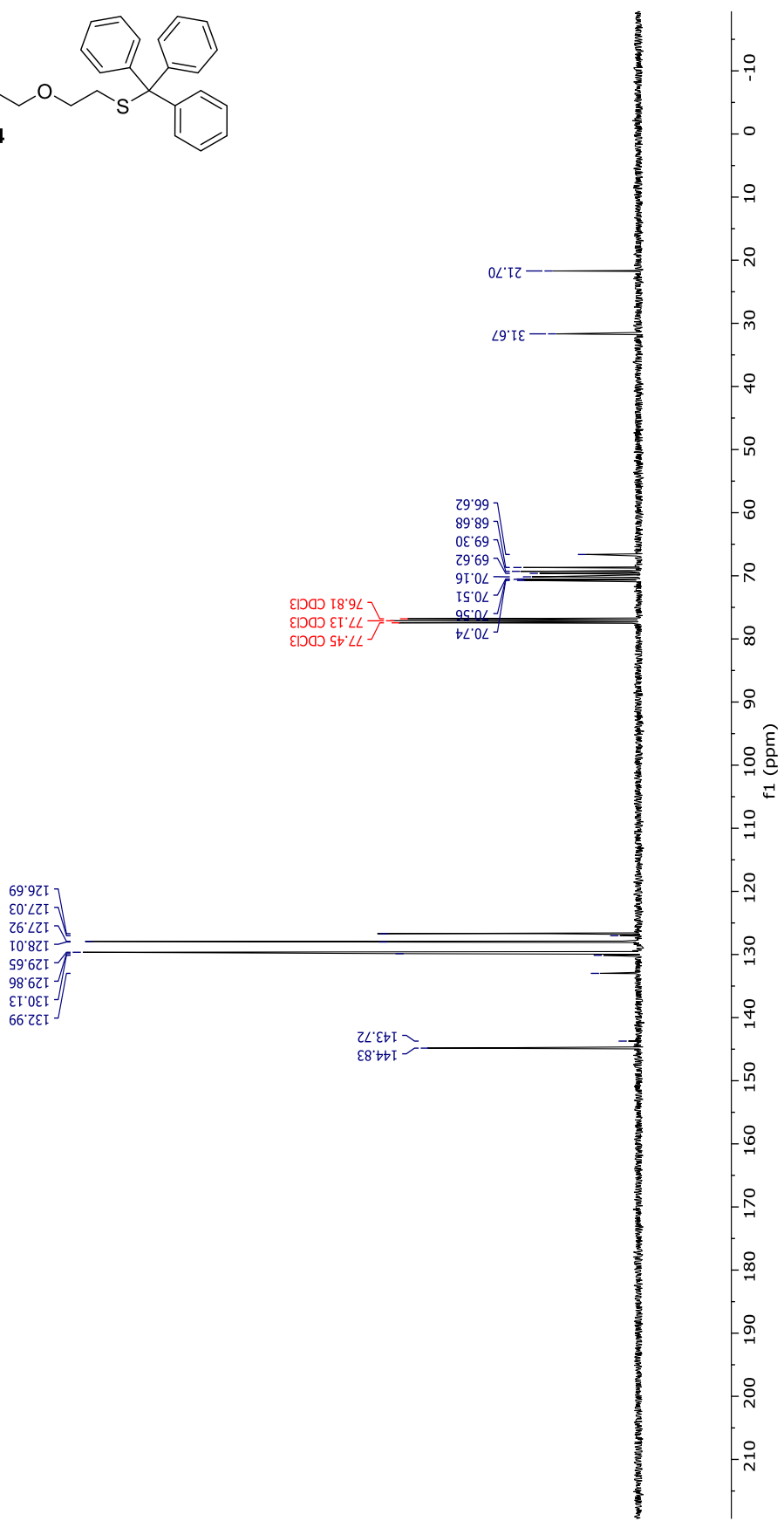
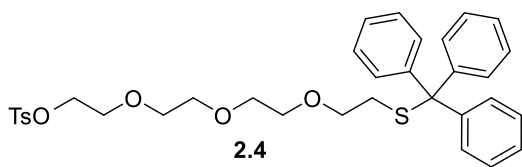
| | ALN 3 (10mM) | ALN corrected | BuN3 (400mM) | Trz | Trz corrected | aln consumed% |
|------|-----------------|------------------|-----------------|---------|------------------|------------------|
| 0 | 20850117 | 20850117 | 16394641 | 0 | 0 | 0.0 |
| 0.5 | 20042955 | 20642673 | 15918338 | 524313 | 540001 | 1.0 |
| 1.5 | 18984961 | 19398177 | 16045406 | 854079 | 872668 | 7.0 |
| 3 | 17207906 | 19442574 | 14510293 | 1367001 | 1544524 | 6.8 |
| 4.5 | 17072467 | 16295707 | 17176117 | 2002964 | 1911833 | 21.8 |
| 6 | 15521985 | 15701529 | 16207171 | 2344740 | 2371862 | 24.7 |
| 8 | 12988184 | 13149547 | 16193456 | 3003109 | 3040419 | 36.9 |
| 10 | 10909133 | 11402017 | 15685937 | 3225014 | 3370723 | 45.3 |
| 12 | 9860315 | 9817187 | 16466664 | 3730906 | 3714588 | 52.9 |
| 15 | 8257789 | 7899647 | 17137916 | 4743578 | 4537848 | 62.1 |
| 19.5 | 5768828 | 6528113 | 14487780 | 4647296 | 5258966 | 68.7 |
| 24 | 4885622 | 4827081 | 16593470 | 5669030 | 5601102 | 76.8 |
| 28 | 3701388 | 3888229 | 15606829 | 5682999 | 5969869 | 81.4 |
| 31 | 2875784 | 3319301 | 14204029 | 5466608 | 6309694 | 84.1 |
| 35 | 2861297 | 2760524 | 16993126 | 7002908 | 6756271 | 86.8 |
| 45.5 | 1173626 | 1220705 | 15762351 | 6759345 | 7030489 | 94.1 |
| 52 | 505741 | 569976.6 | 14546987 | 6483426 | 7306904 | 97.3 |
| 58 | 0 | 0 | 13051727 | 6523424 | 8194256 | 100.0 |
| 74 | 0 | 0 | 12447831 | 6142052 | 8089501 | 100.0 |

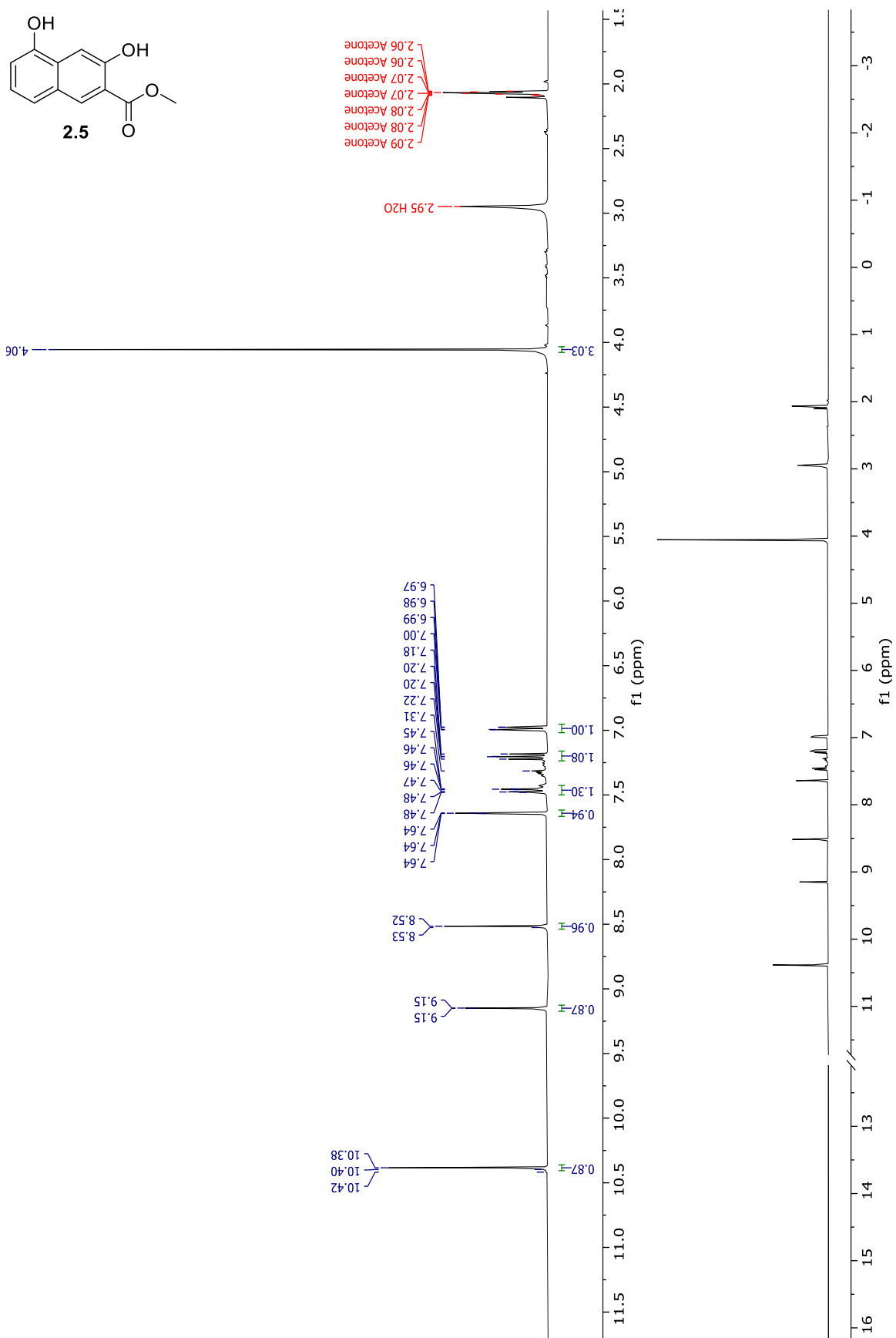
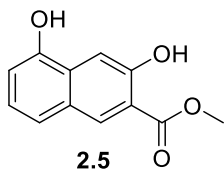
APPENDIX 10
 ^1H And ^{13}C NMR Spectra

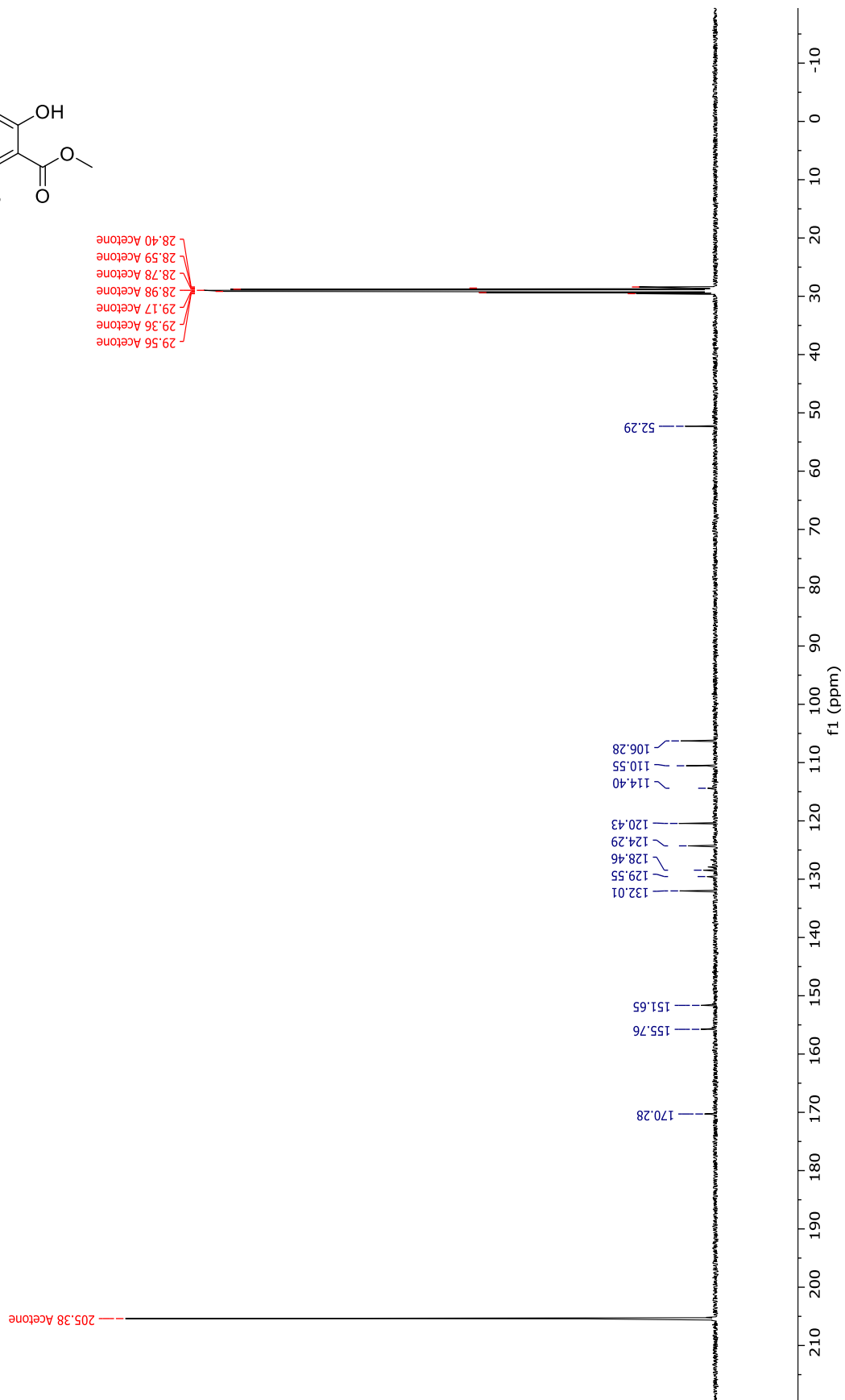
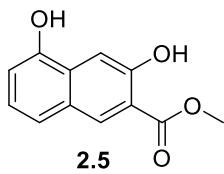


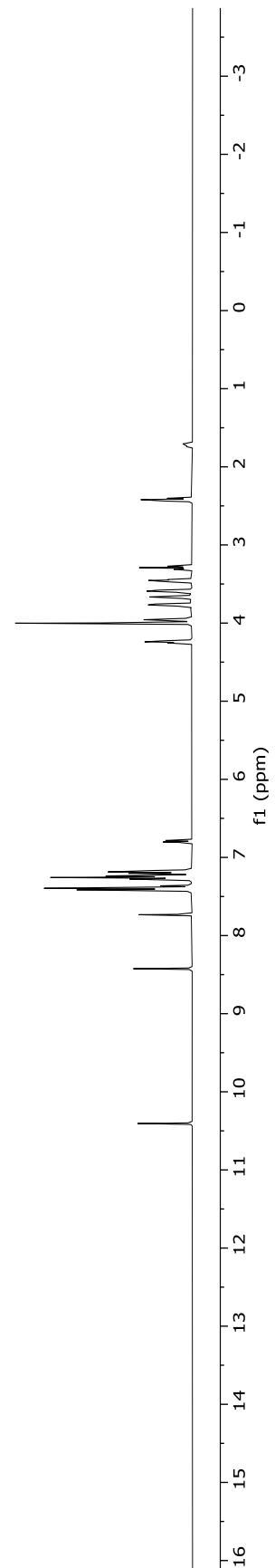
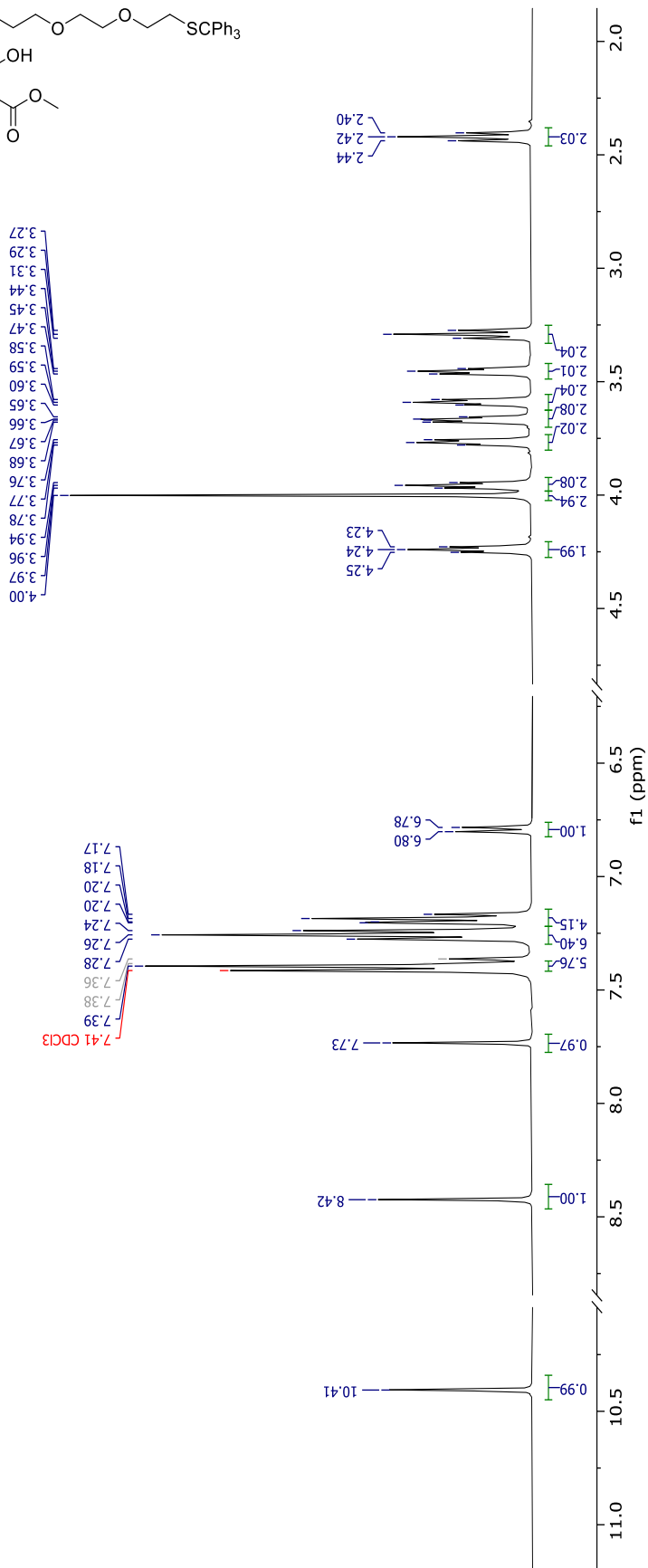
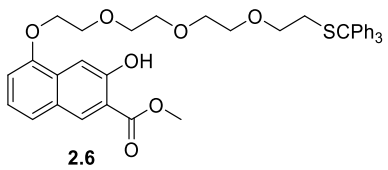


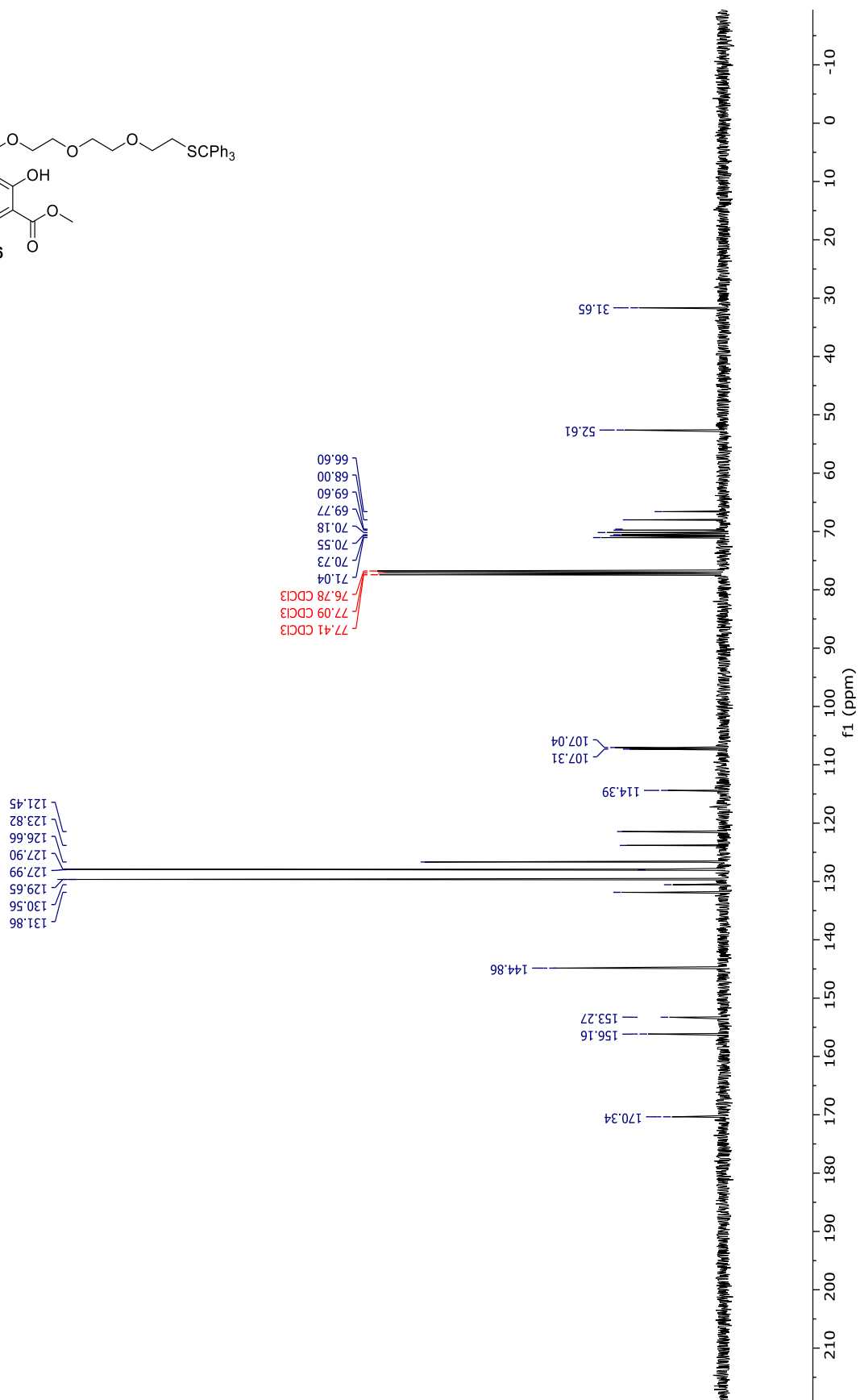
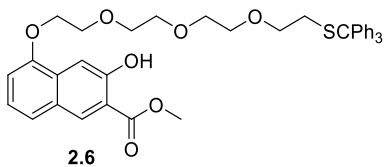


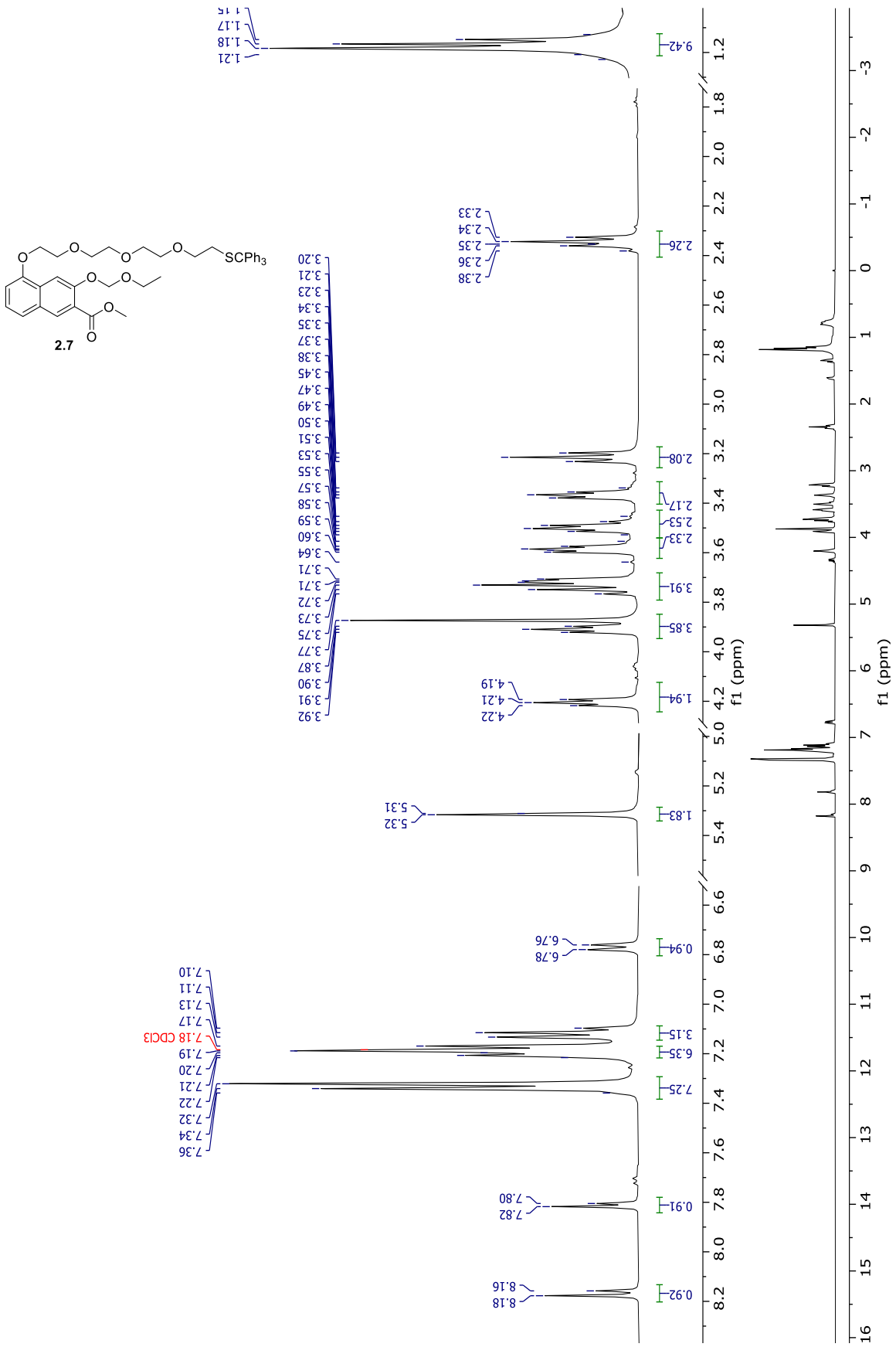


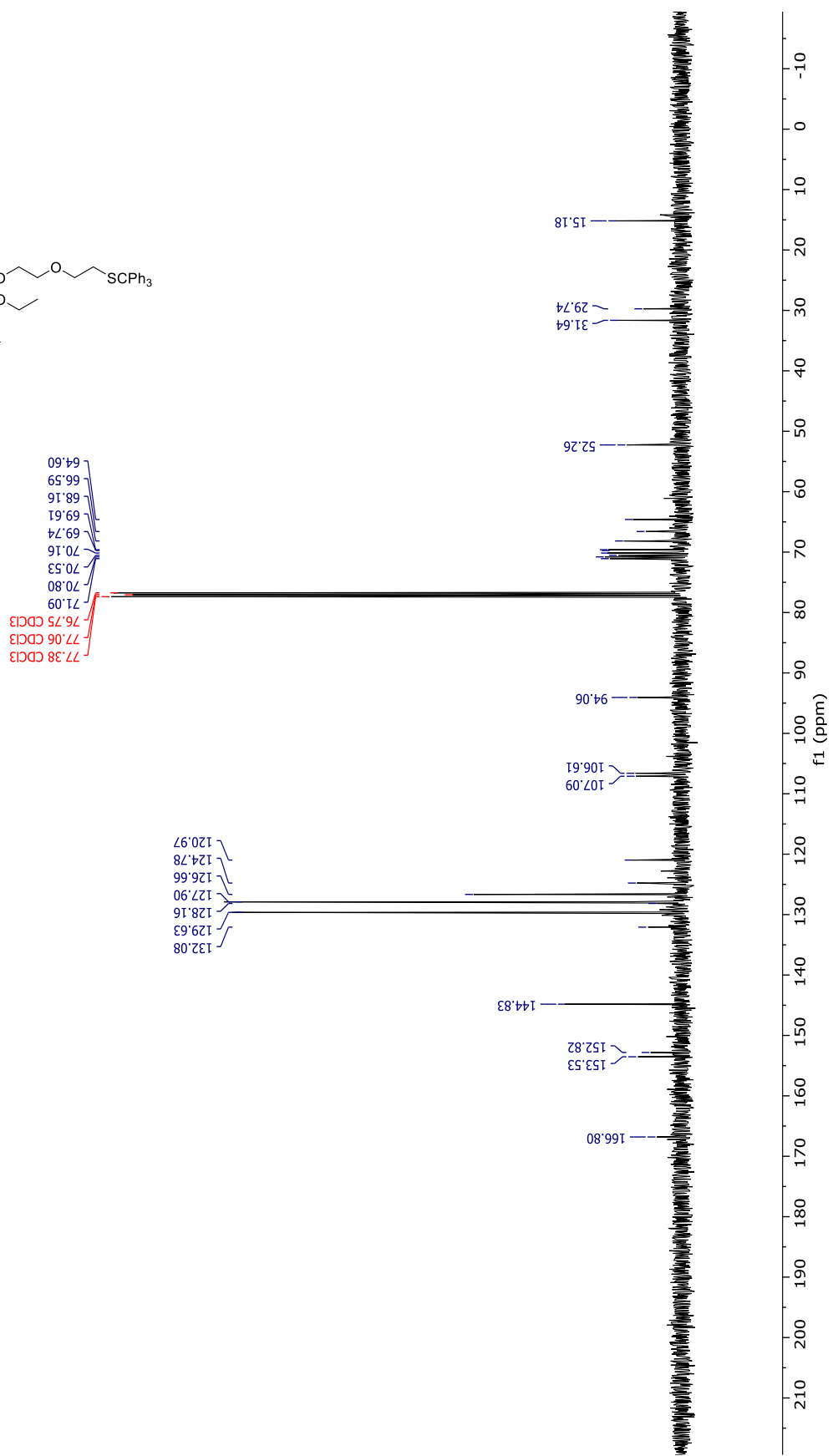
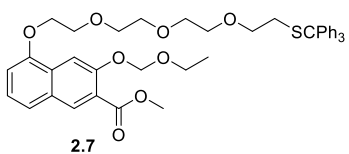


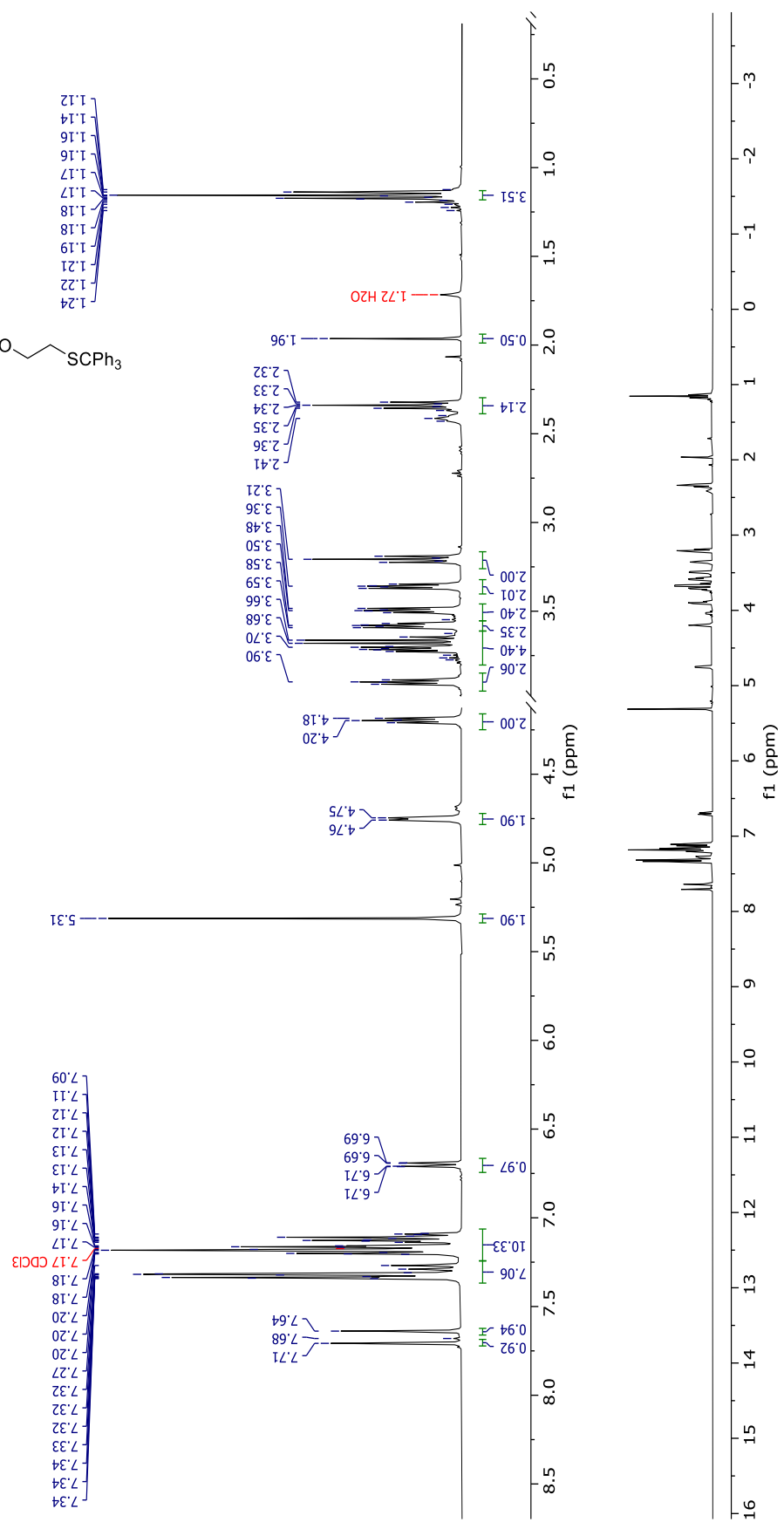
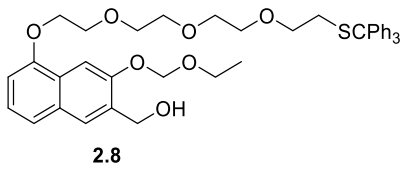


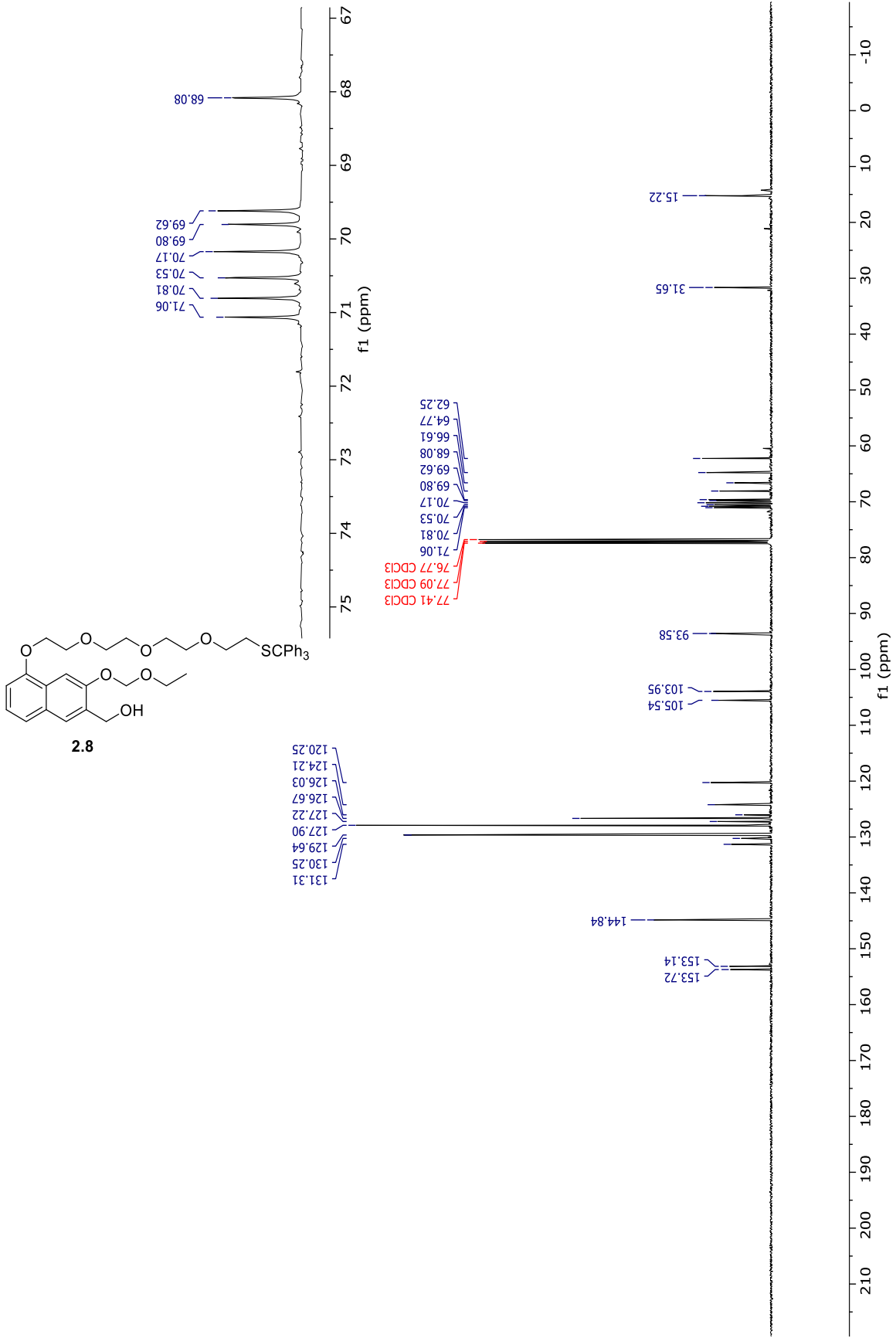


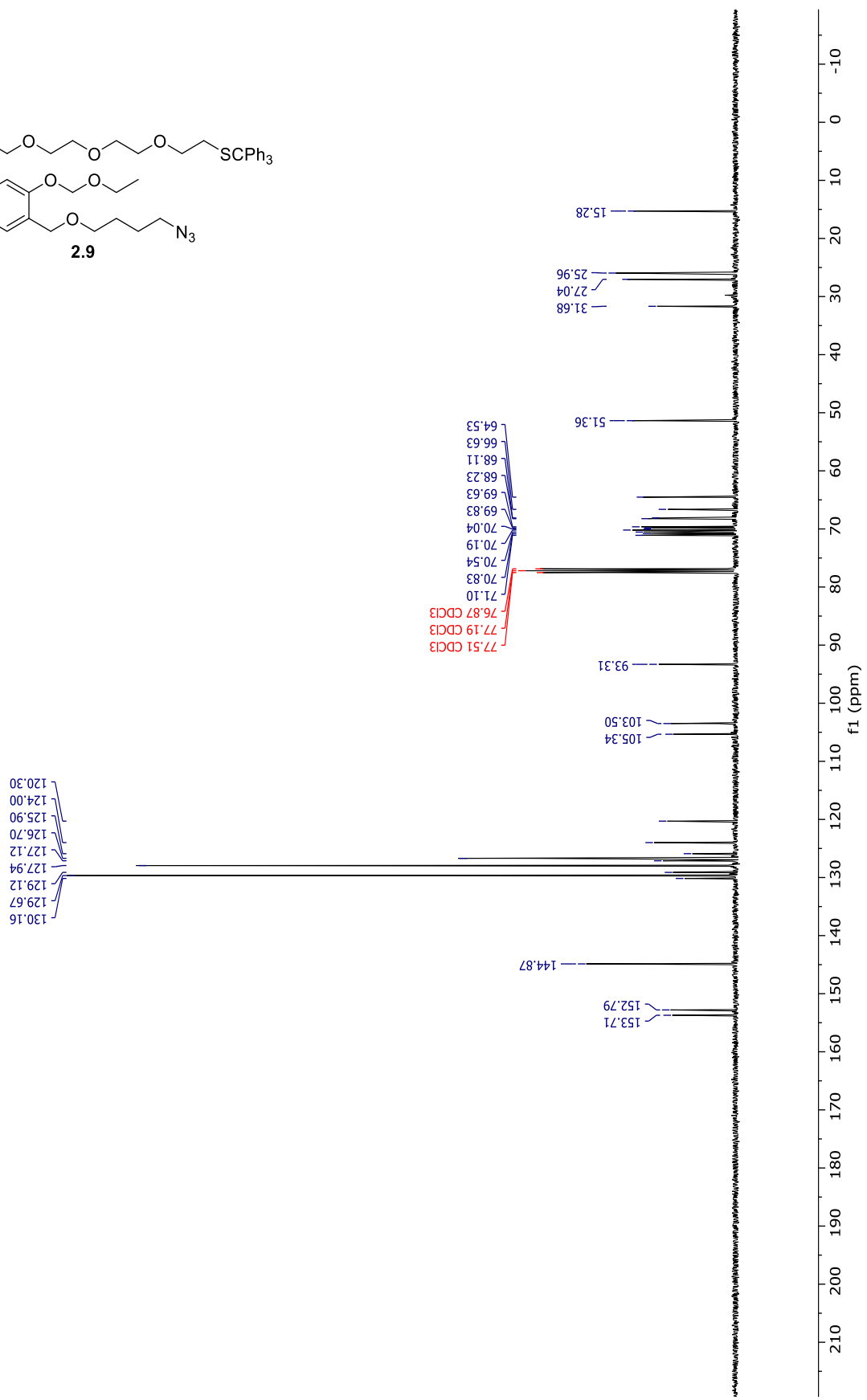
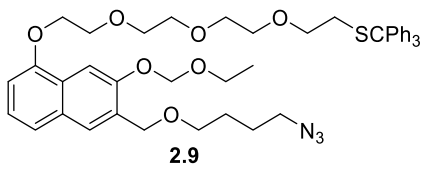


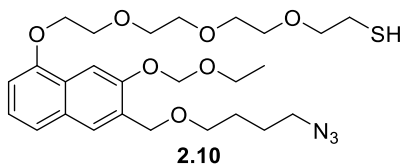




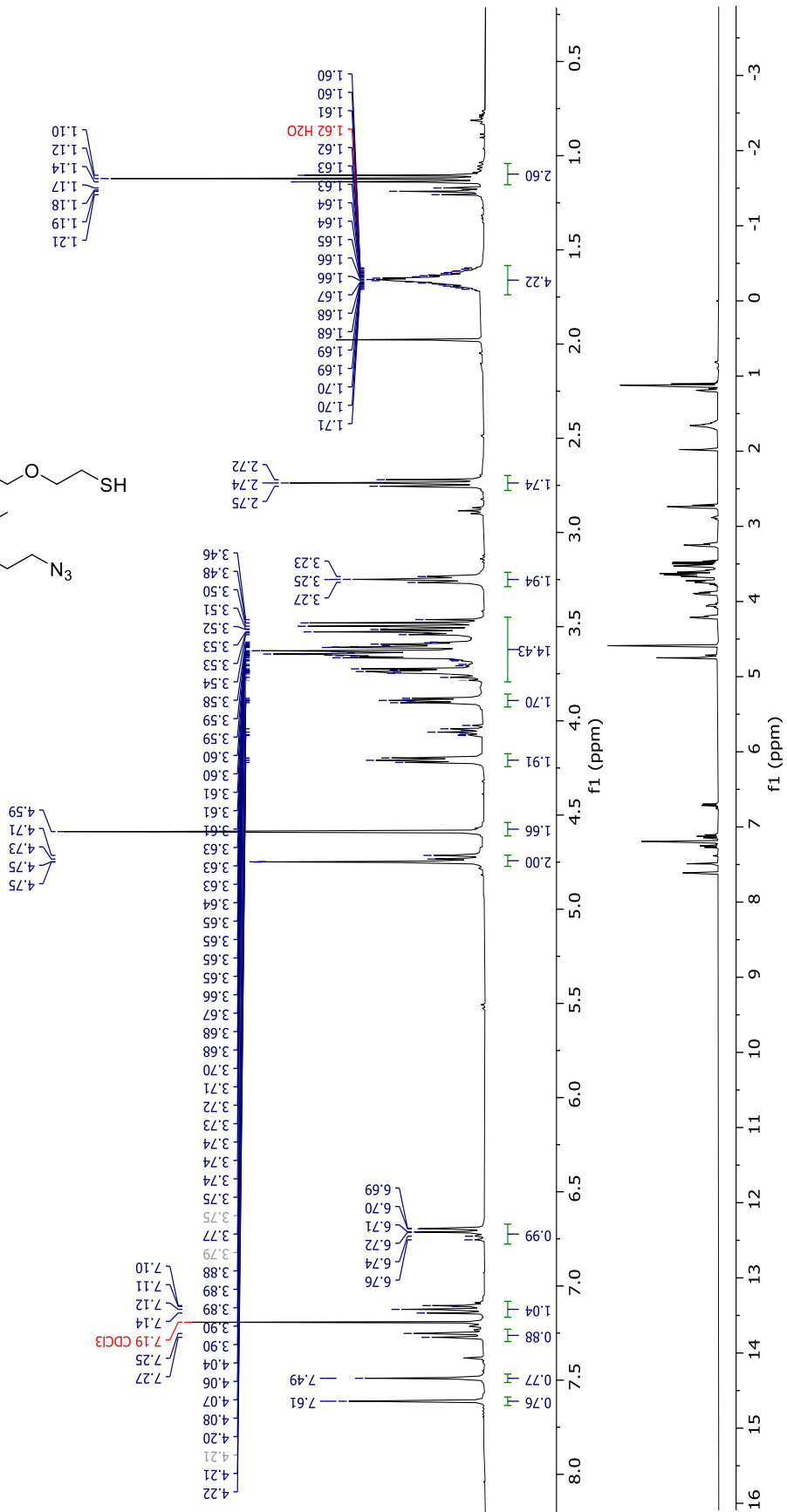


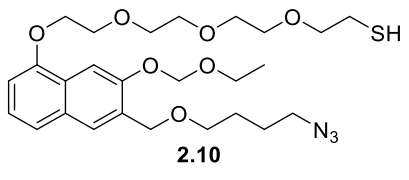






2.10





Chemical shift values (ppm) for the aromatic region of the spectrum:

- 63.60
- 68.23
- 69.81
- 69.98
- 70.31
- 70.72
- 71.05
- 71.46
- 73.80
- 76.73 CDCl₃
- 77.05 CDCl₃
- 77.36 CDCl₃

Chemical shift values (ppm) for the aliphatic region of the spectrum:

- 14.81
- 25.73
- 26.83
- 30.32

Chemical shift value (ppm) for the azide group:

- 51.20

Chemical shift values (ppm) for the carbonyl region:

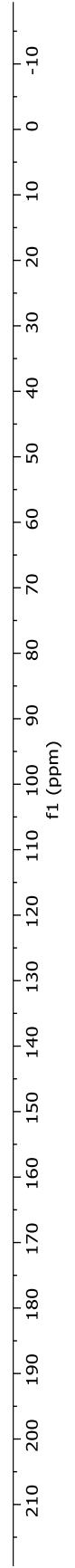
- 105.65
- 105.85

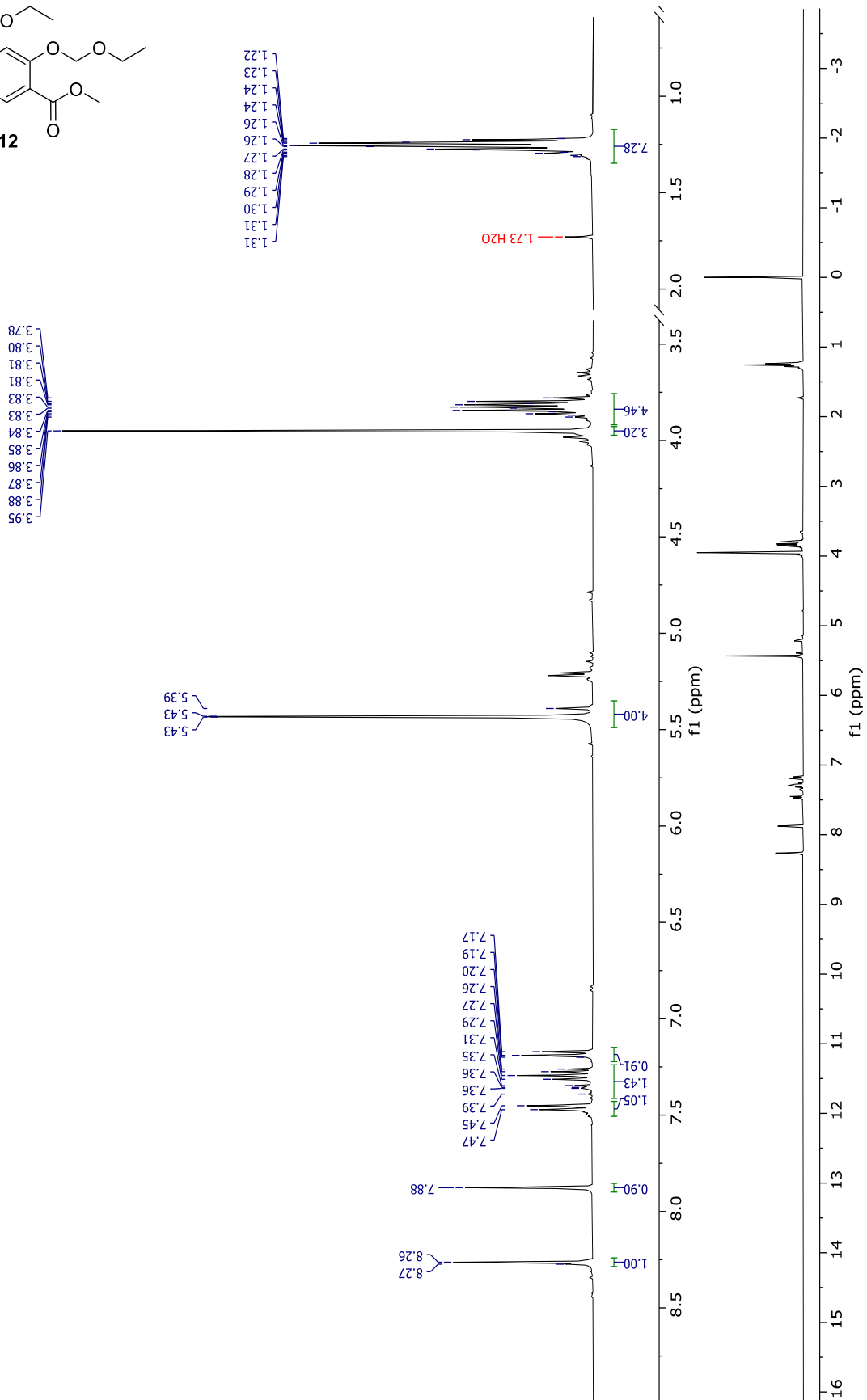
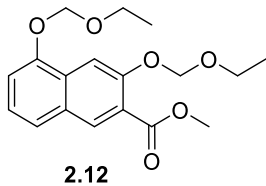
Chemical shift values (ppm) for the aromatic region (continued):

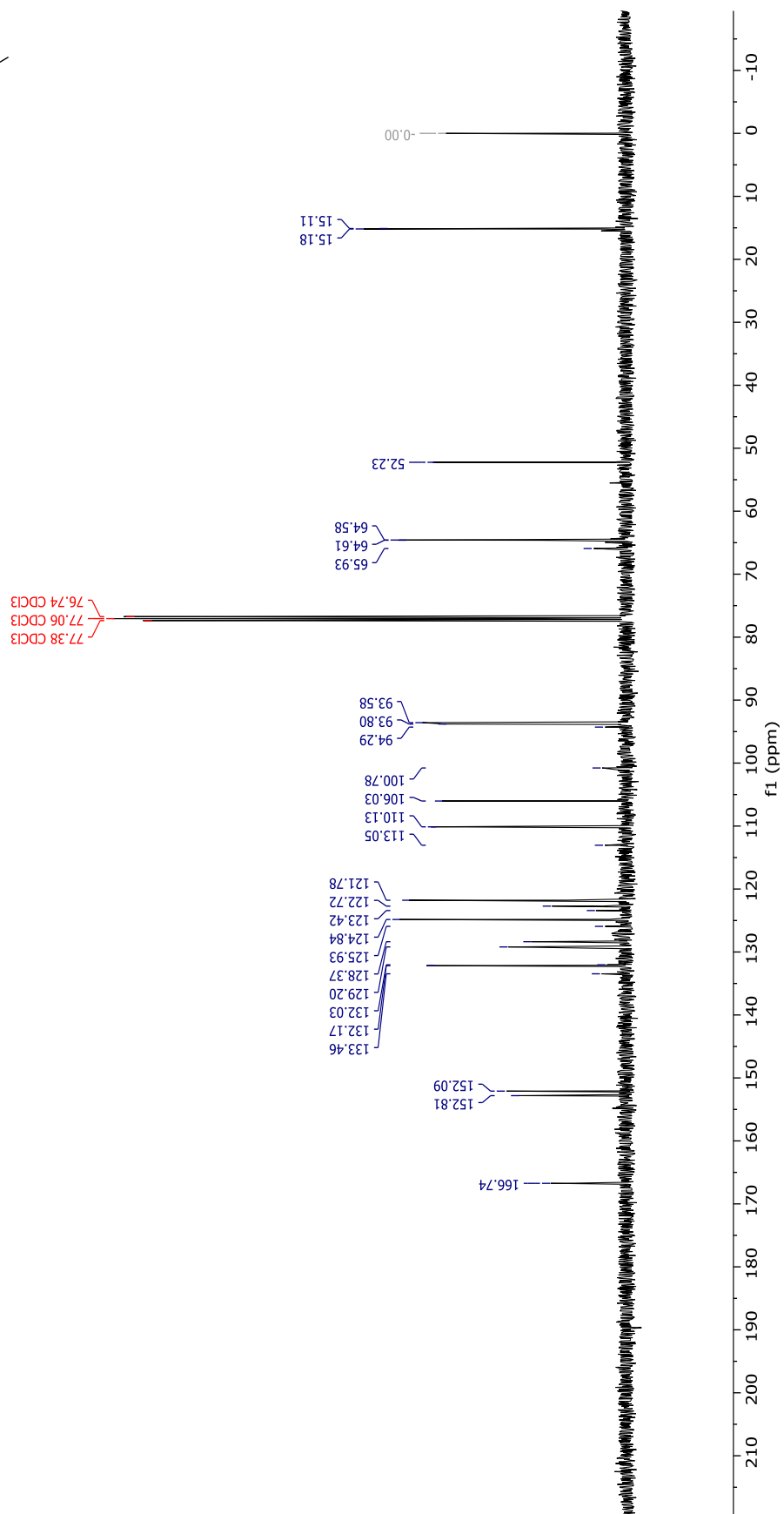
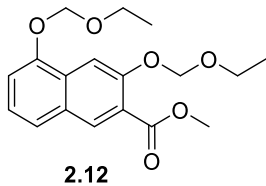
- 120.31
- 123.38
- 125.65
- 127.03
- 127.27
- 129.30

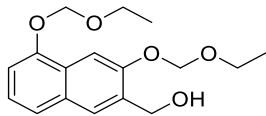
Chemical shift values (ppm) for the carbonyl region (continued):

- 153.51
- 153.54

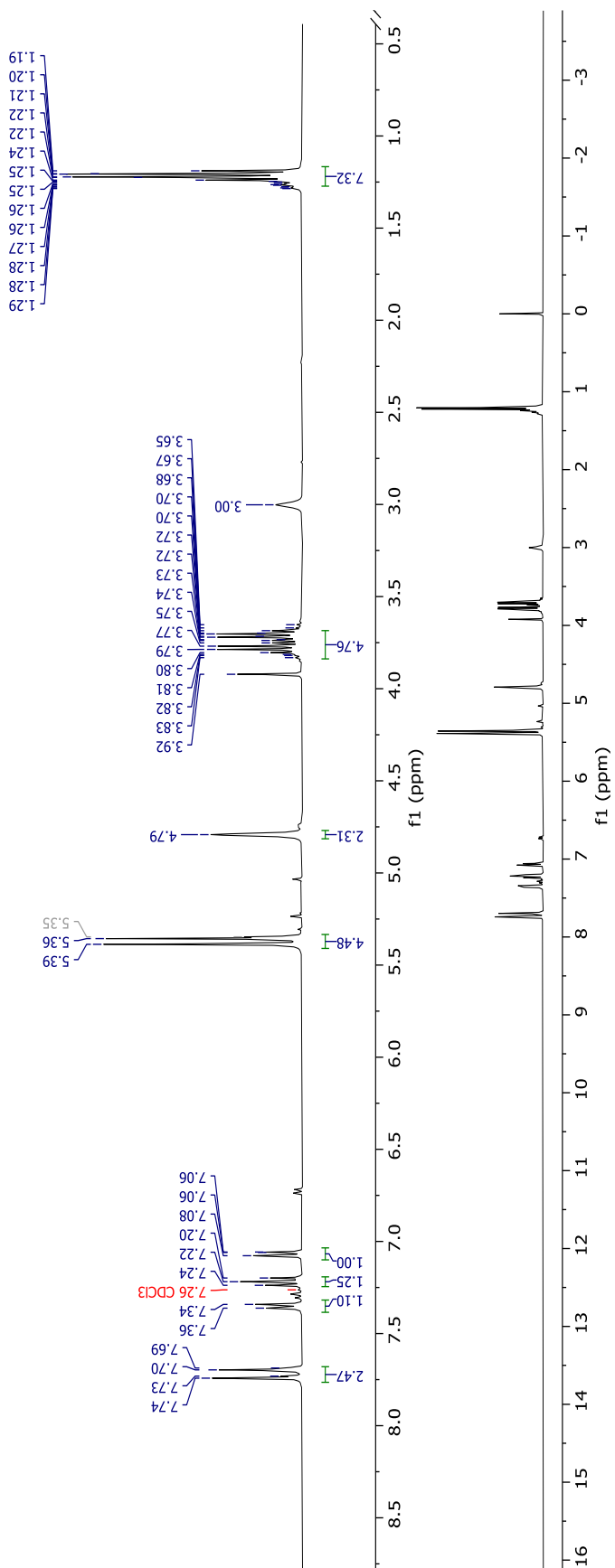


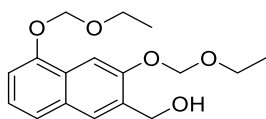




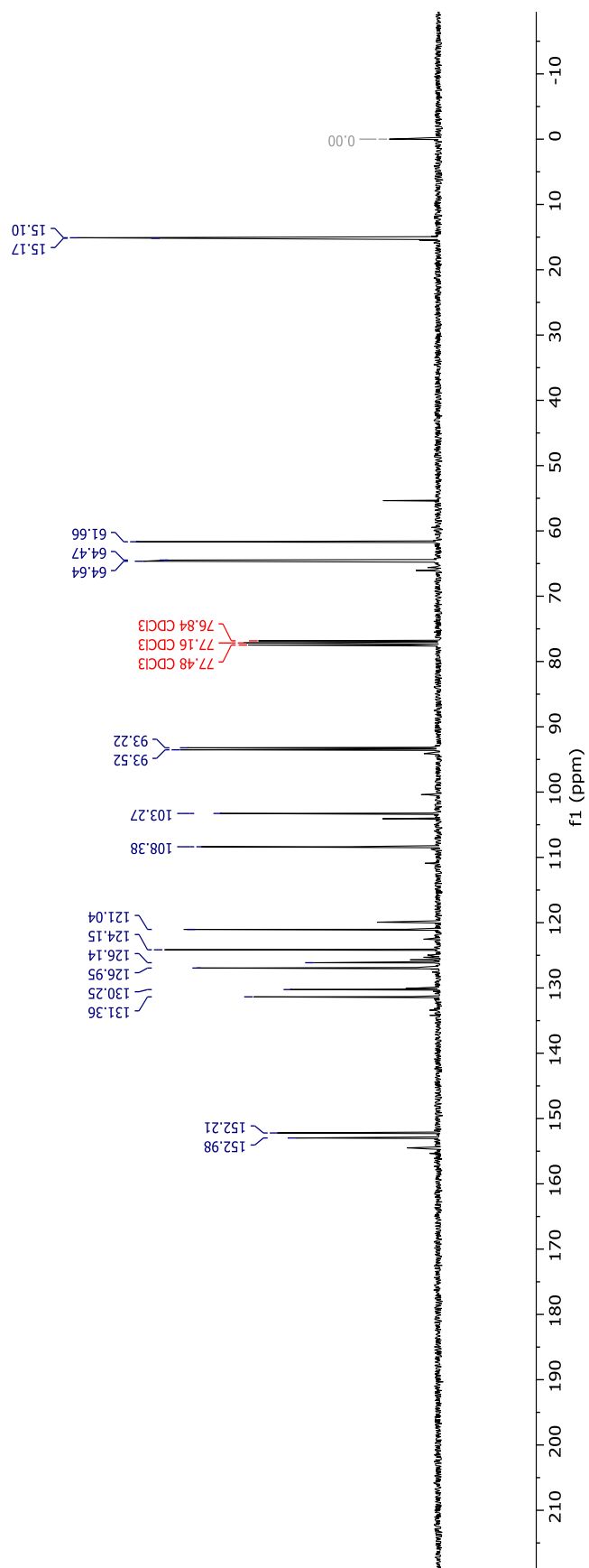


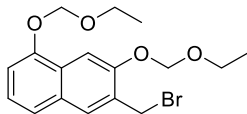
2.13



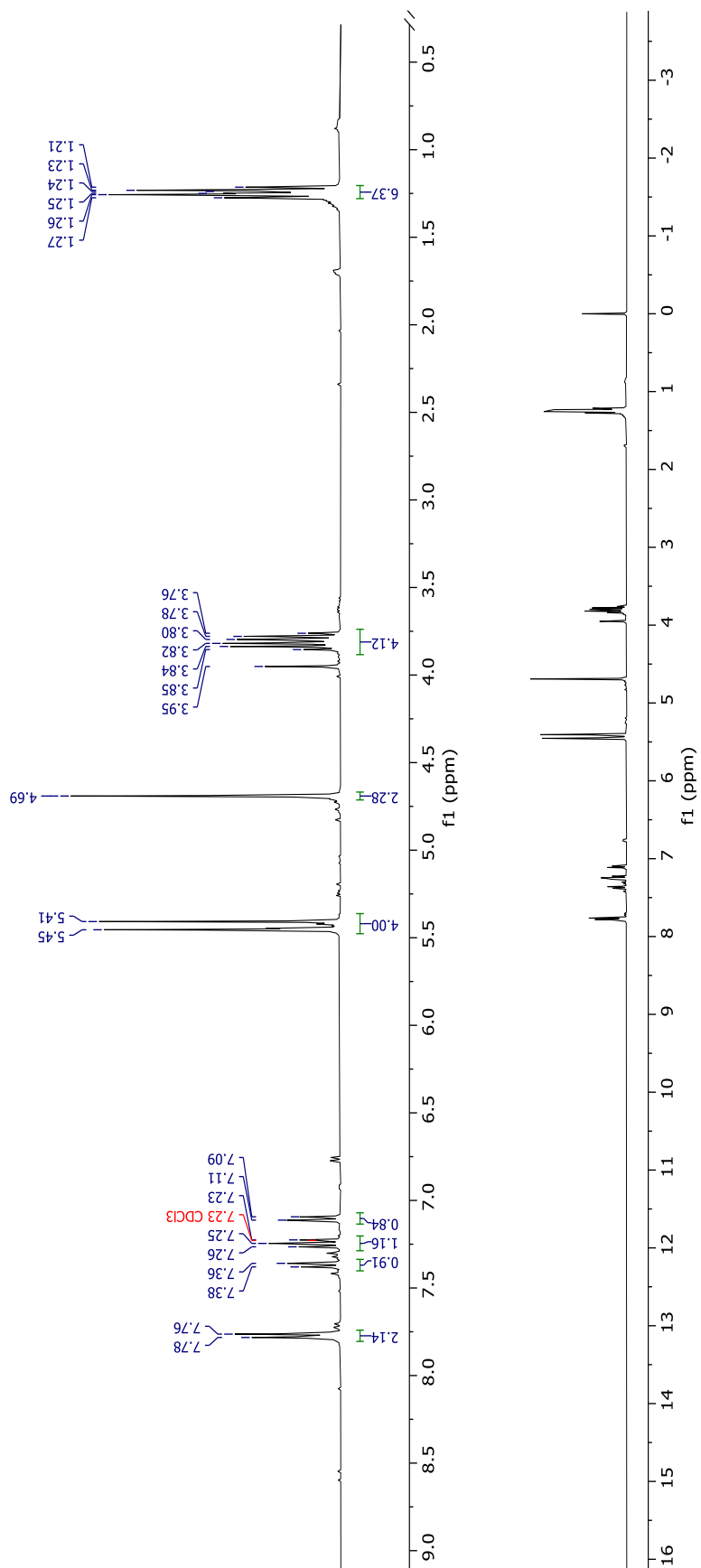


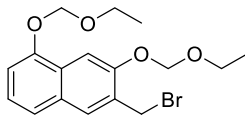
2.13



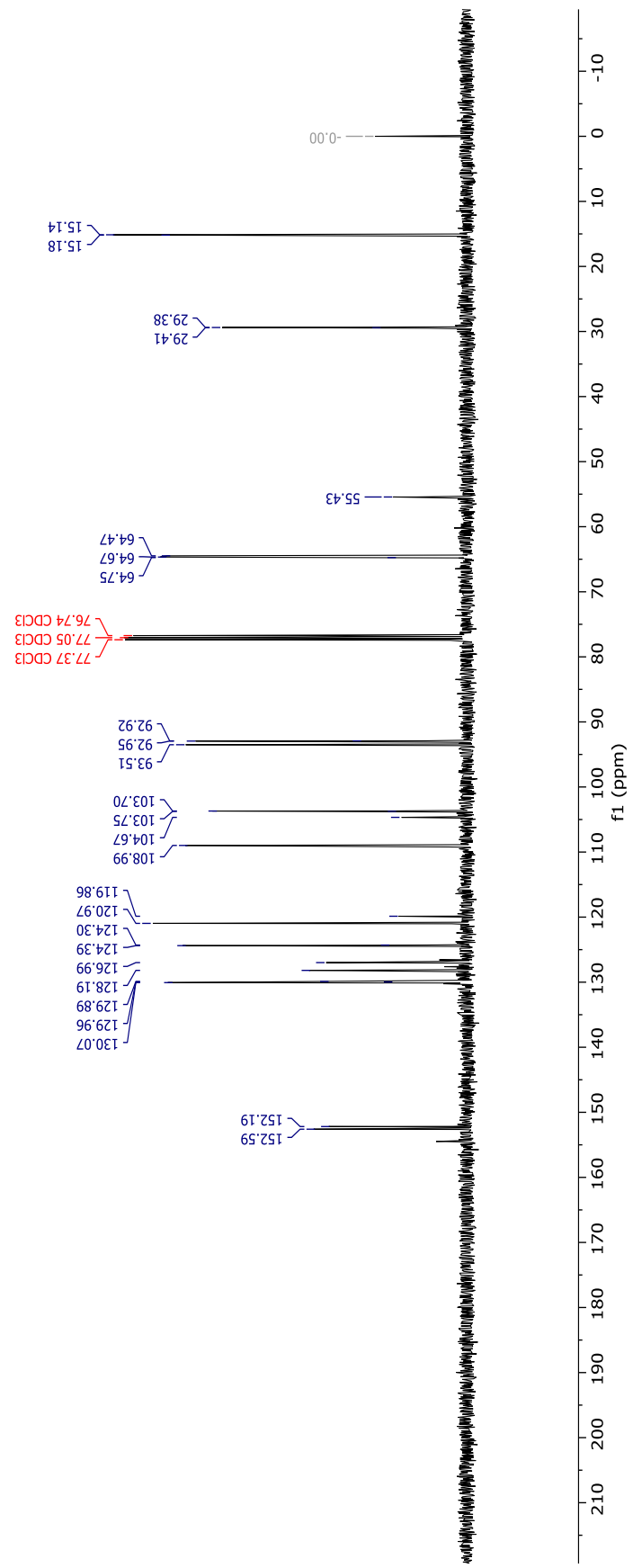


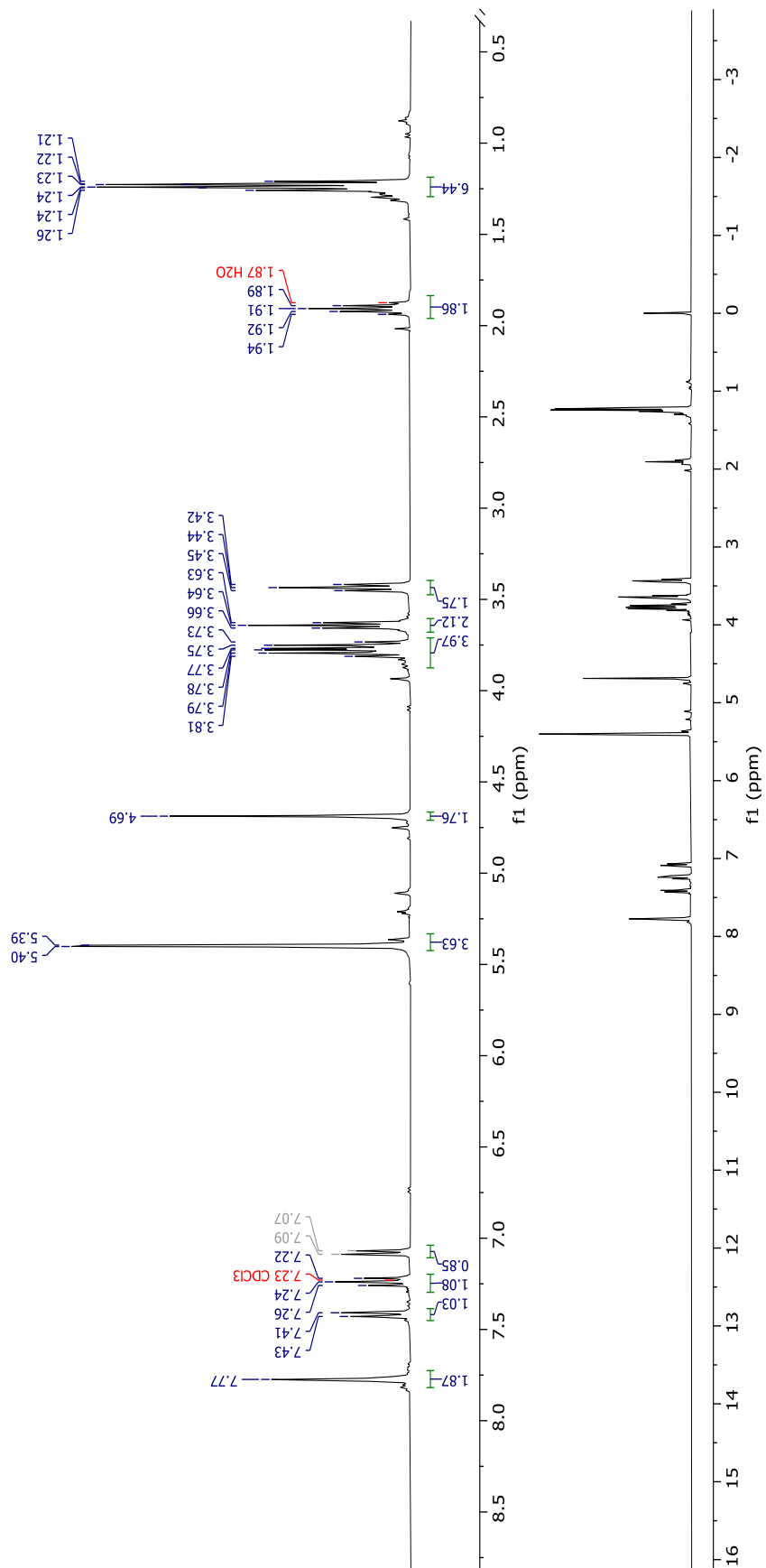
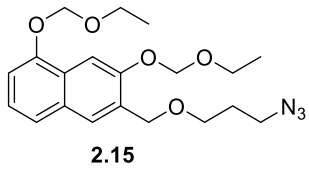
2.14

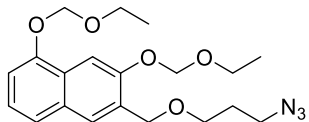




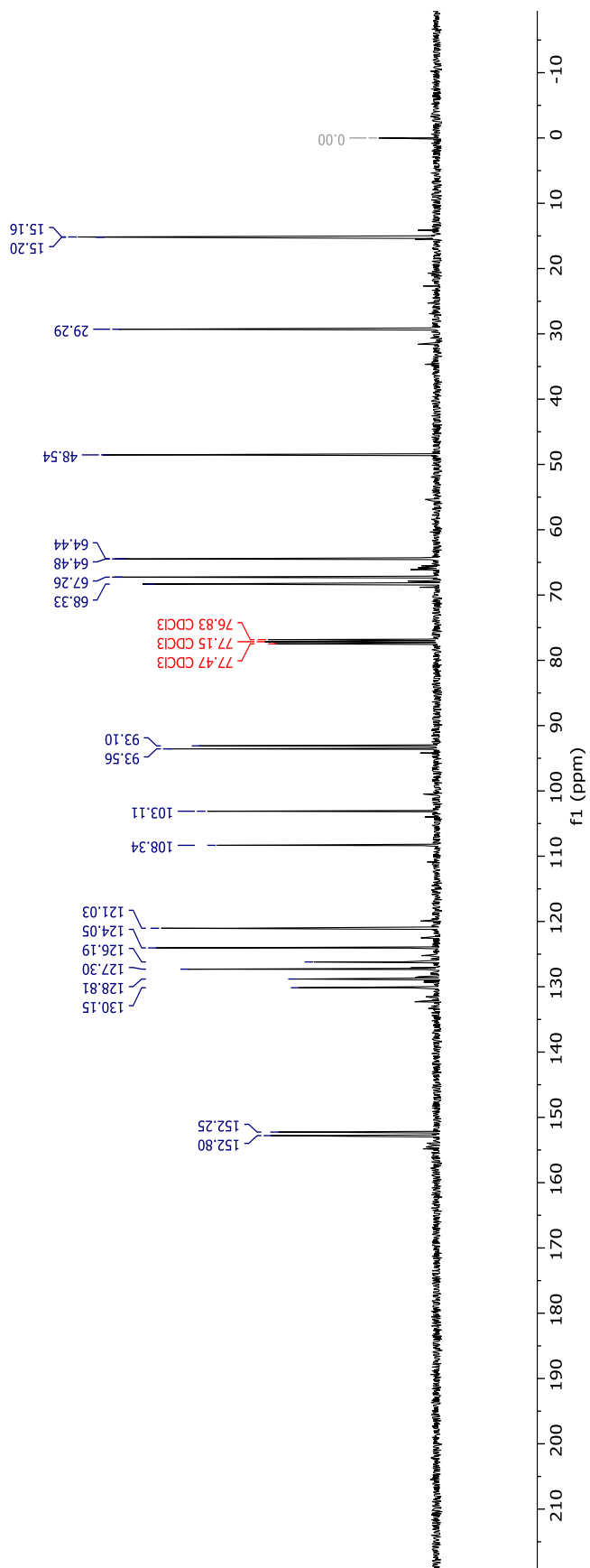
2.14

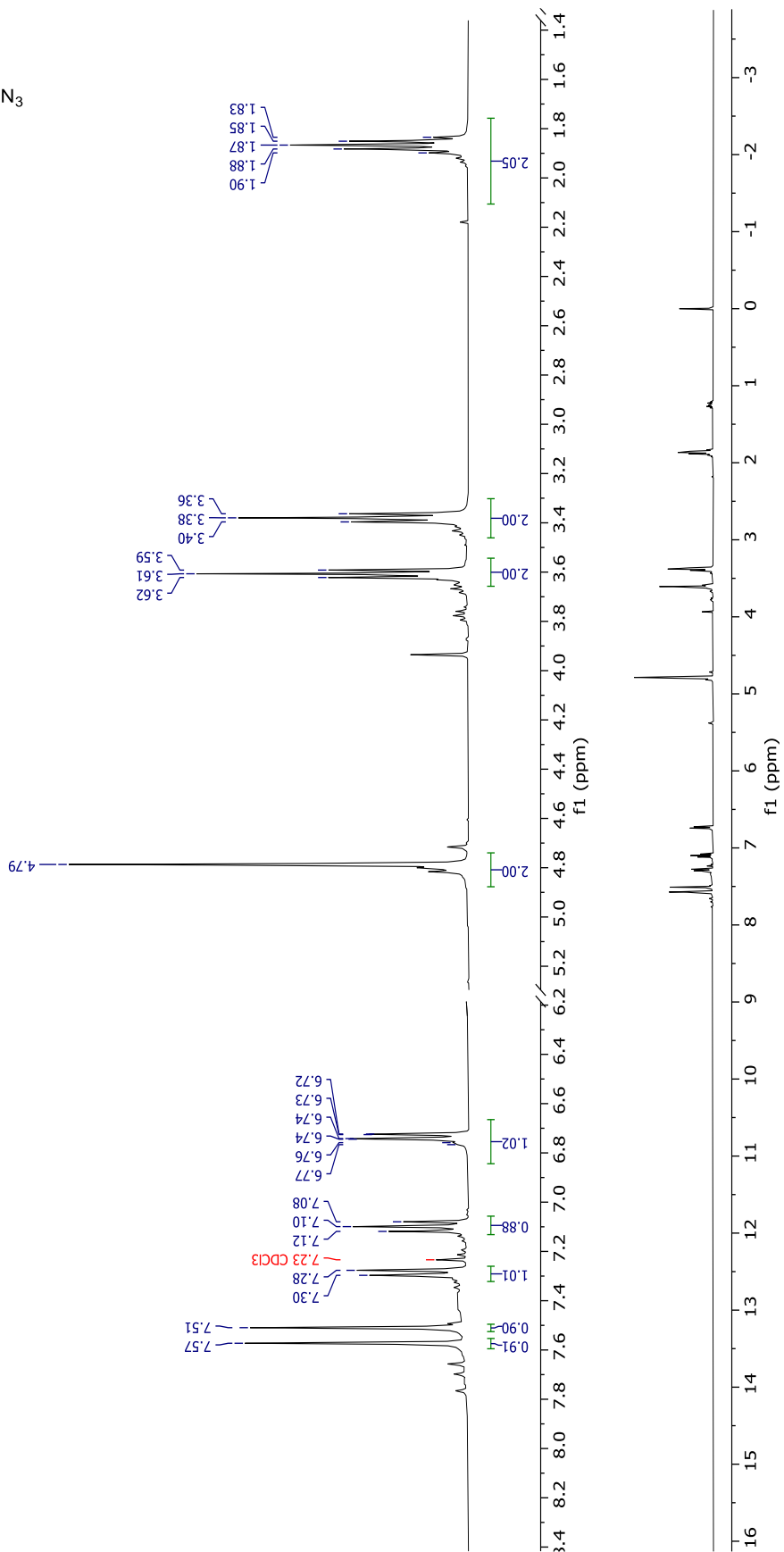
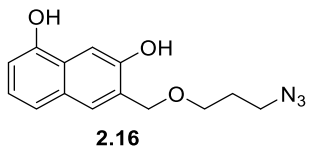


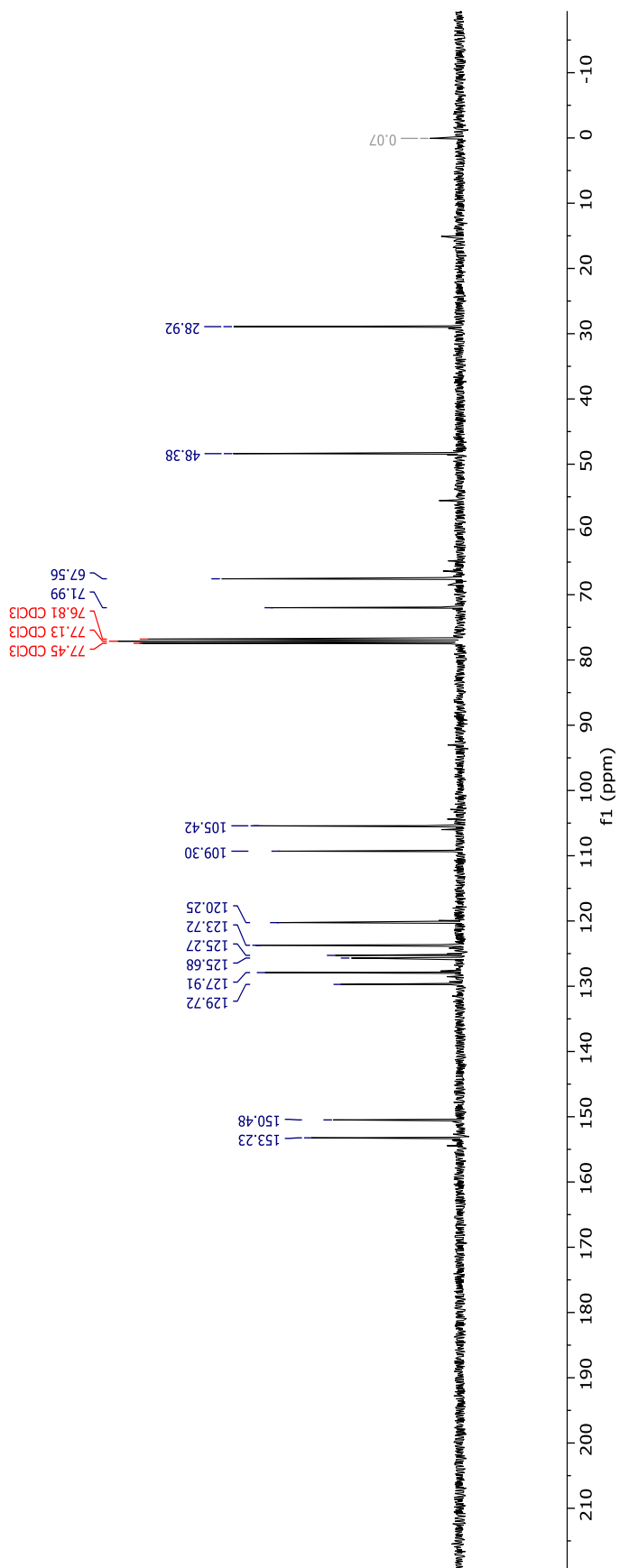
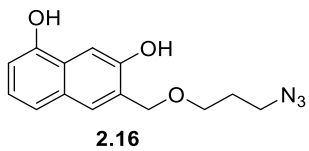


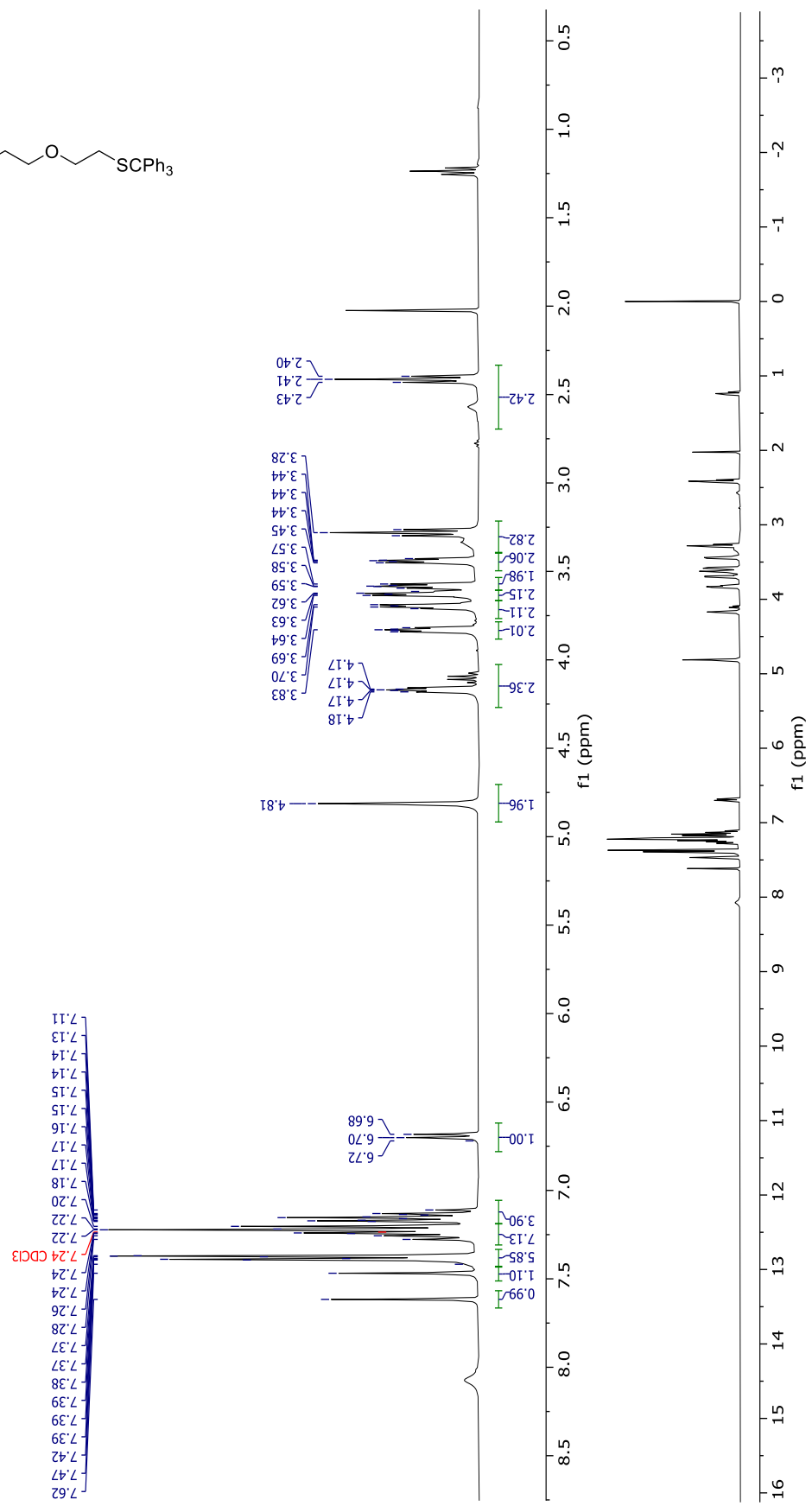
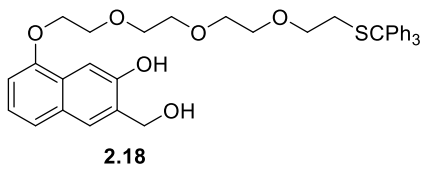


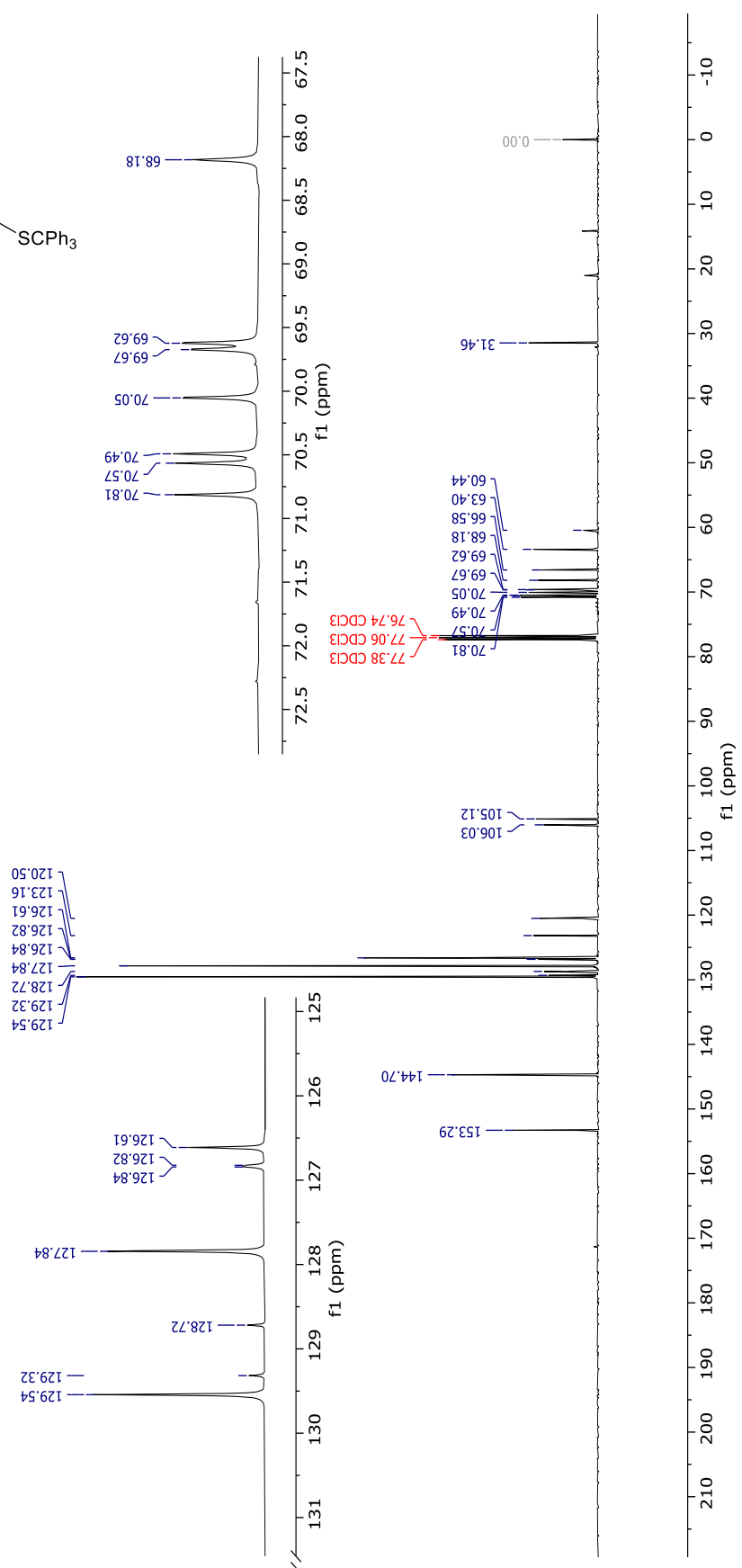
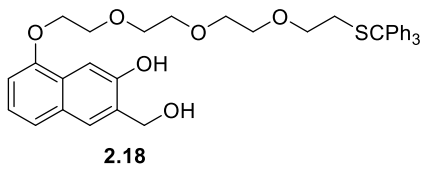
2.15

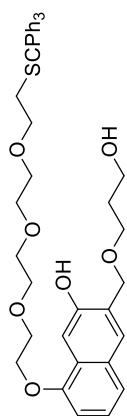




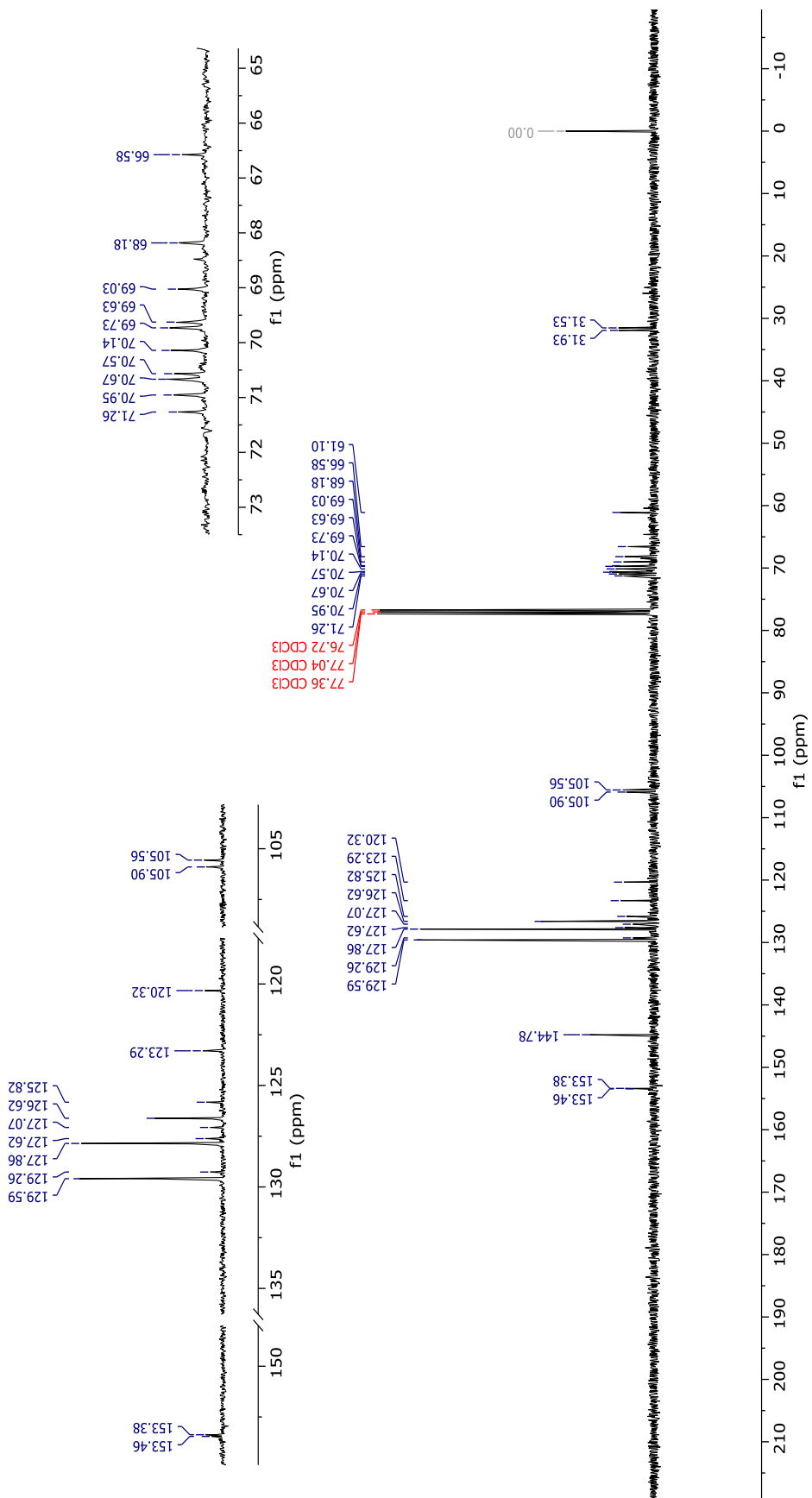


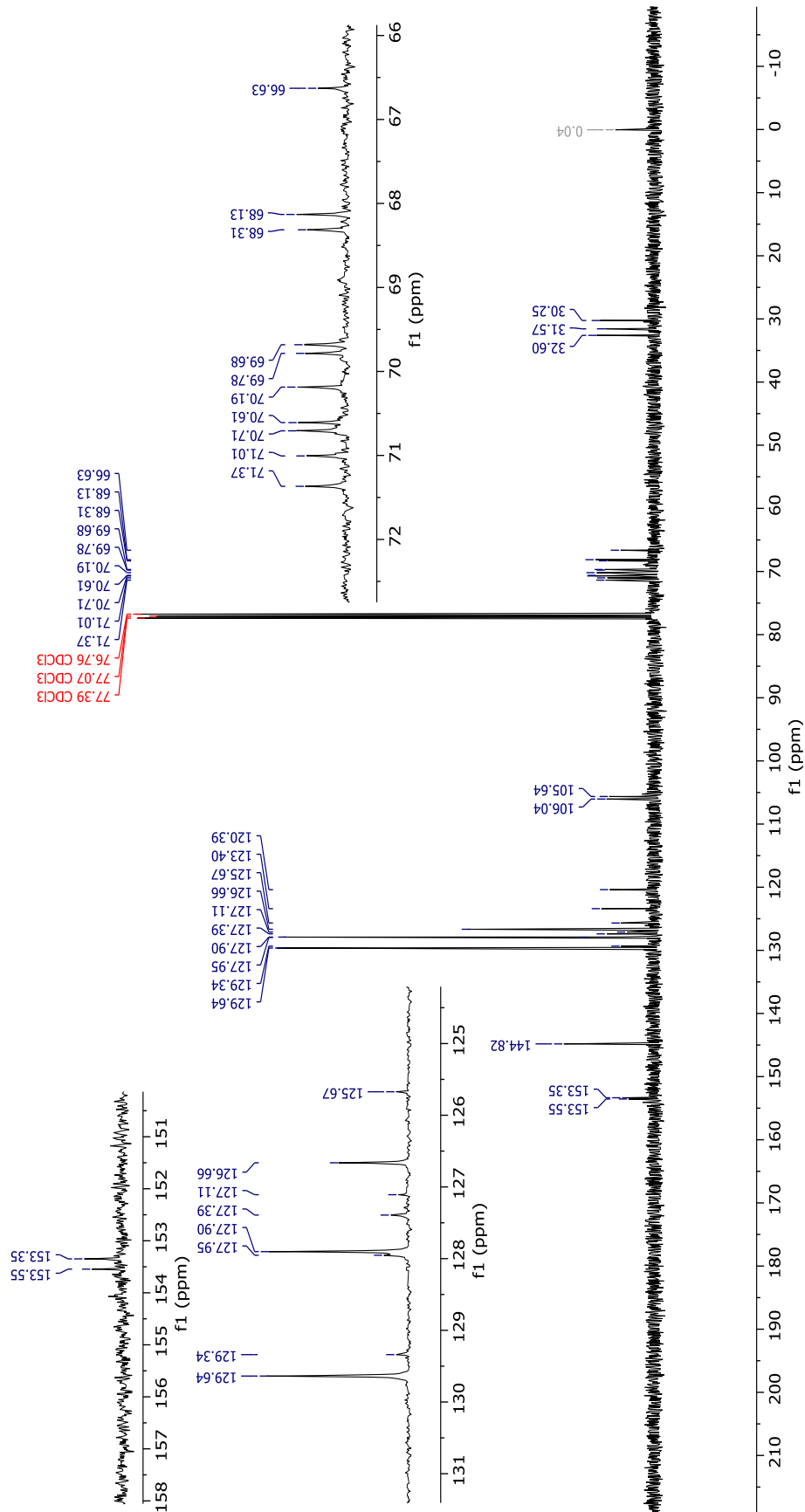
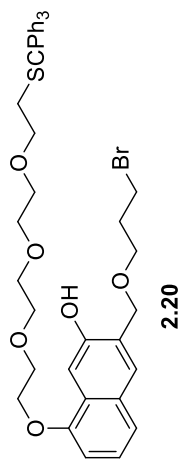


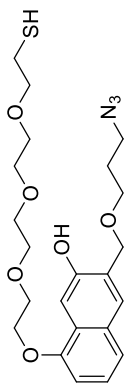




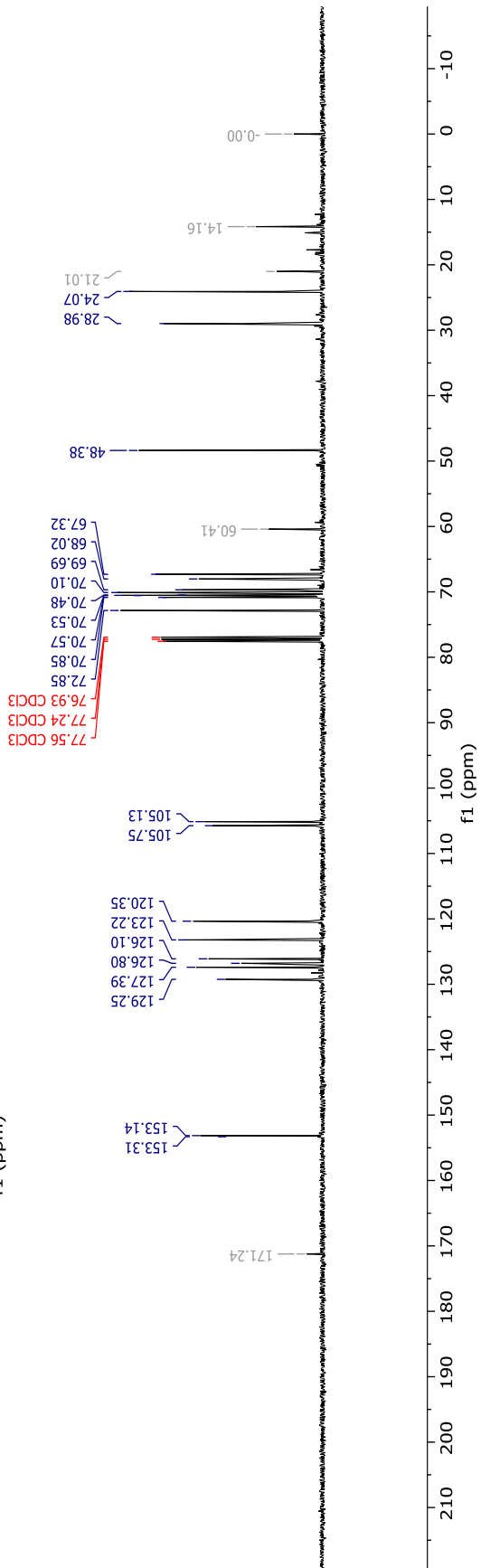
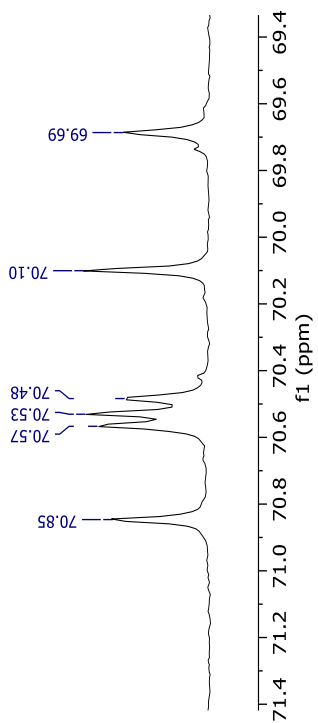
2.19

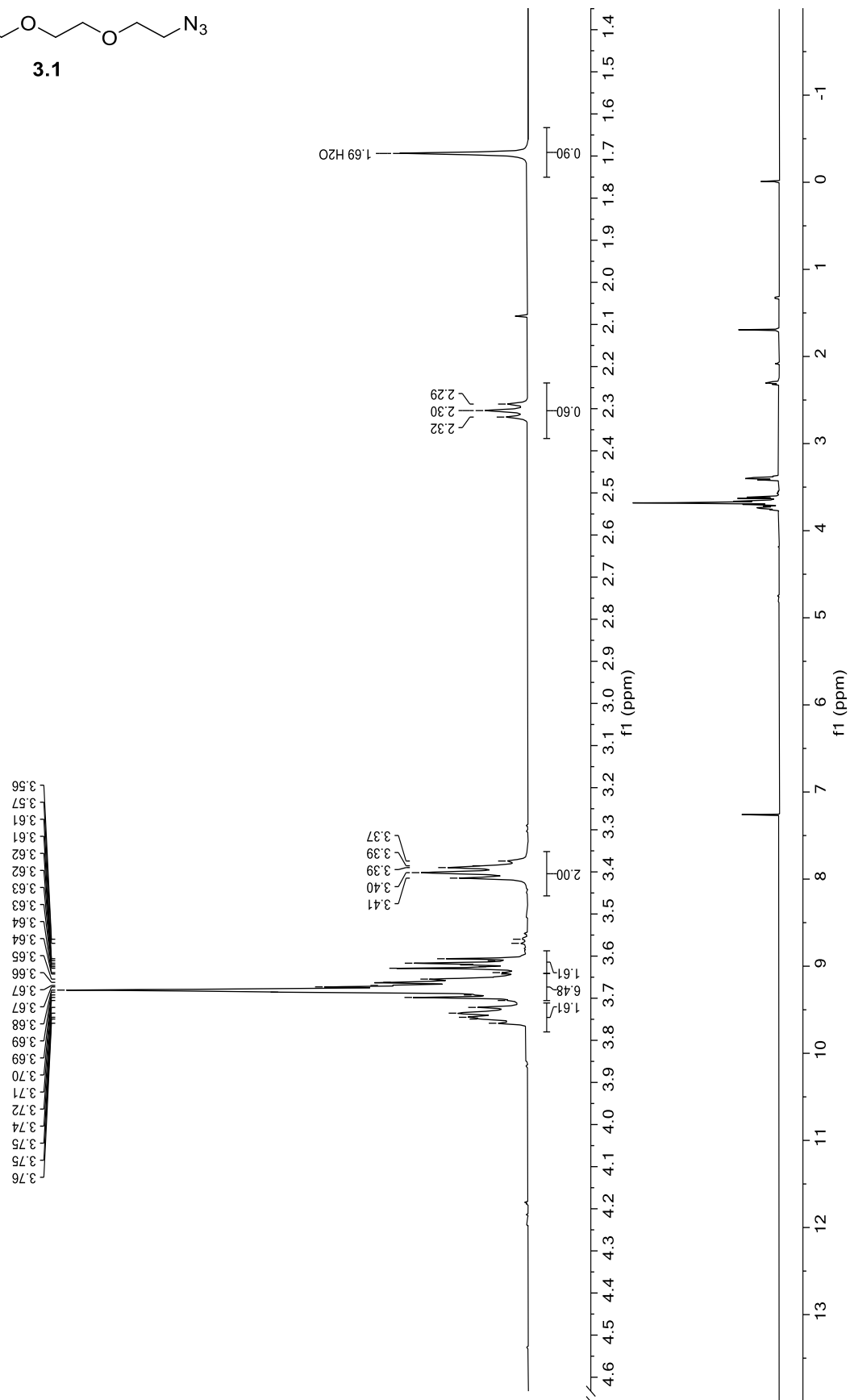
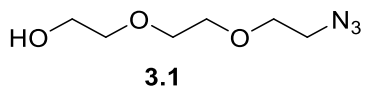


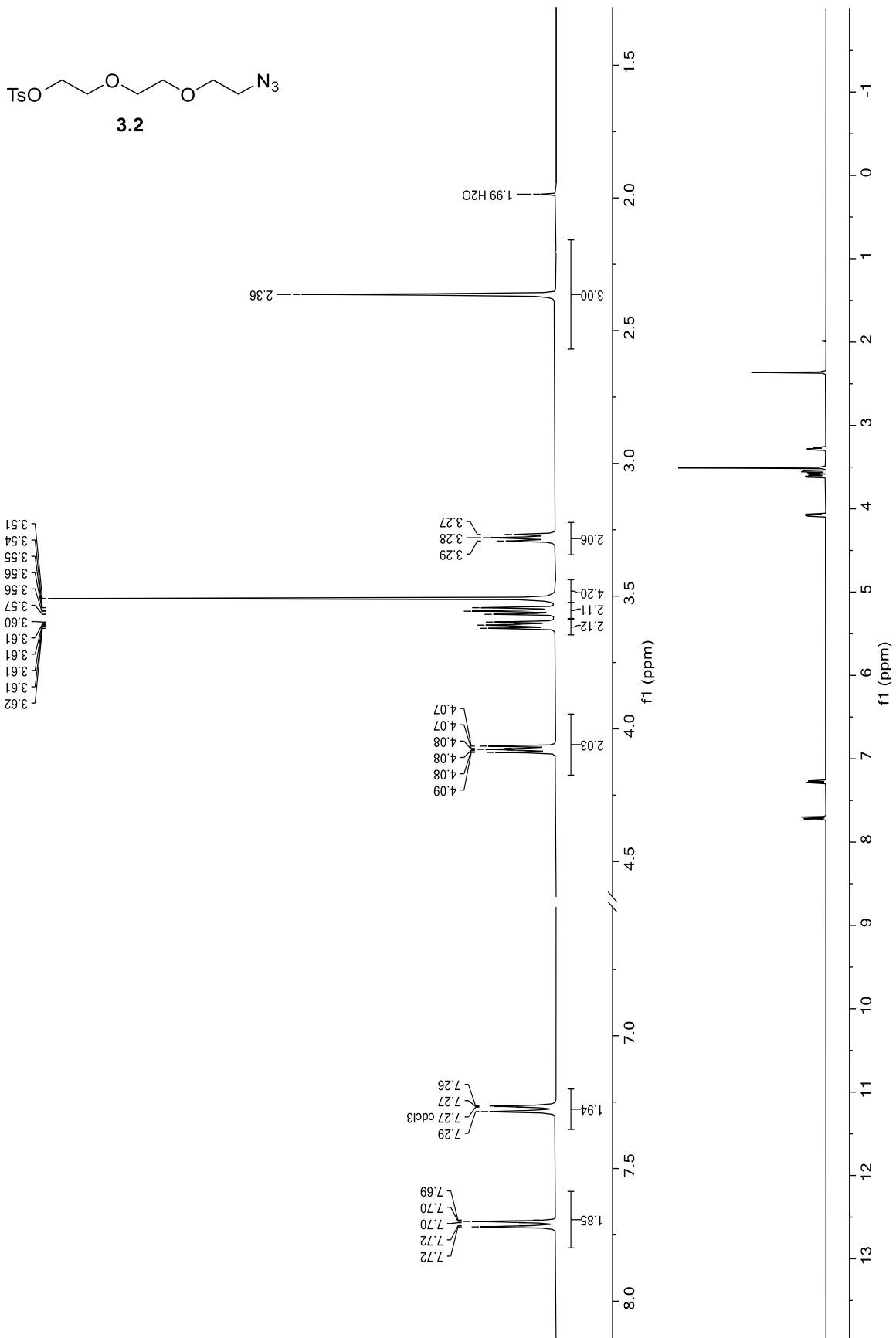


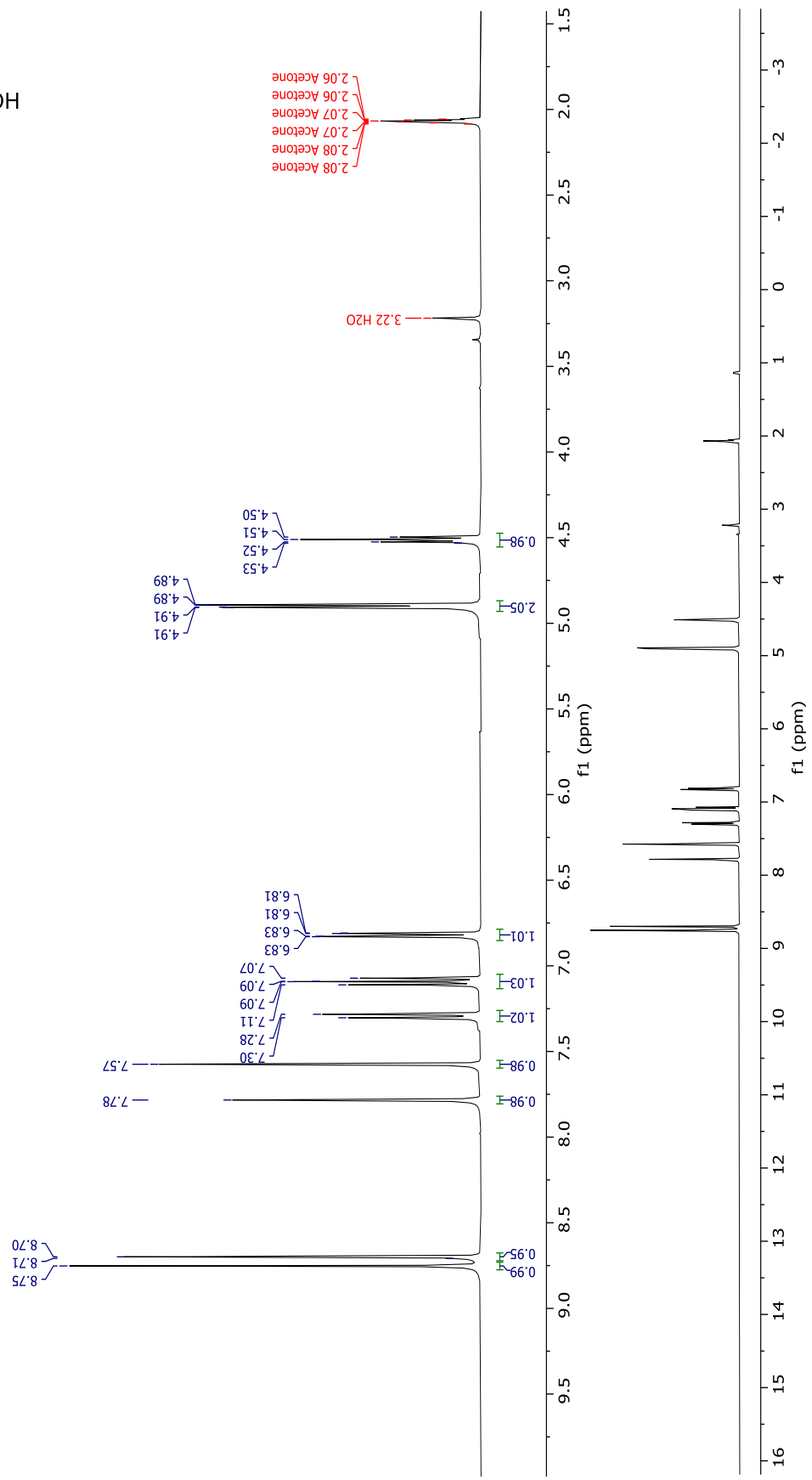
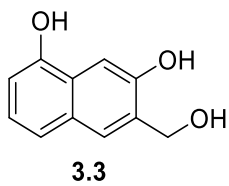


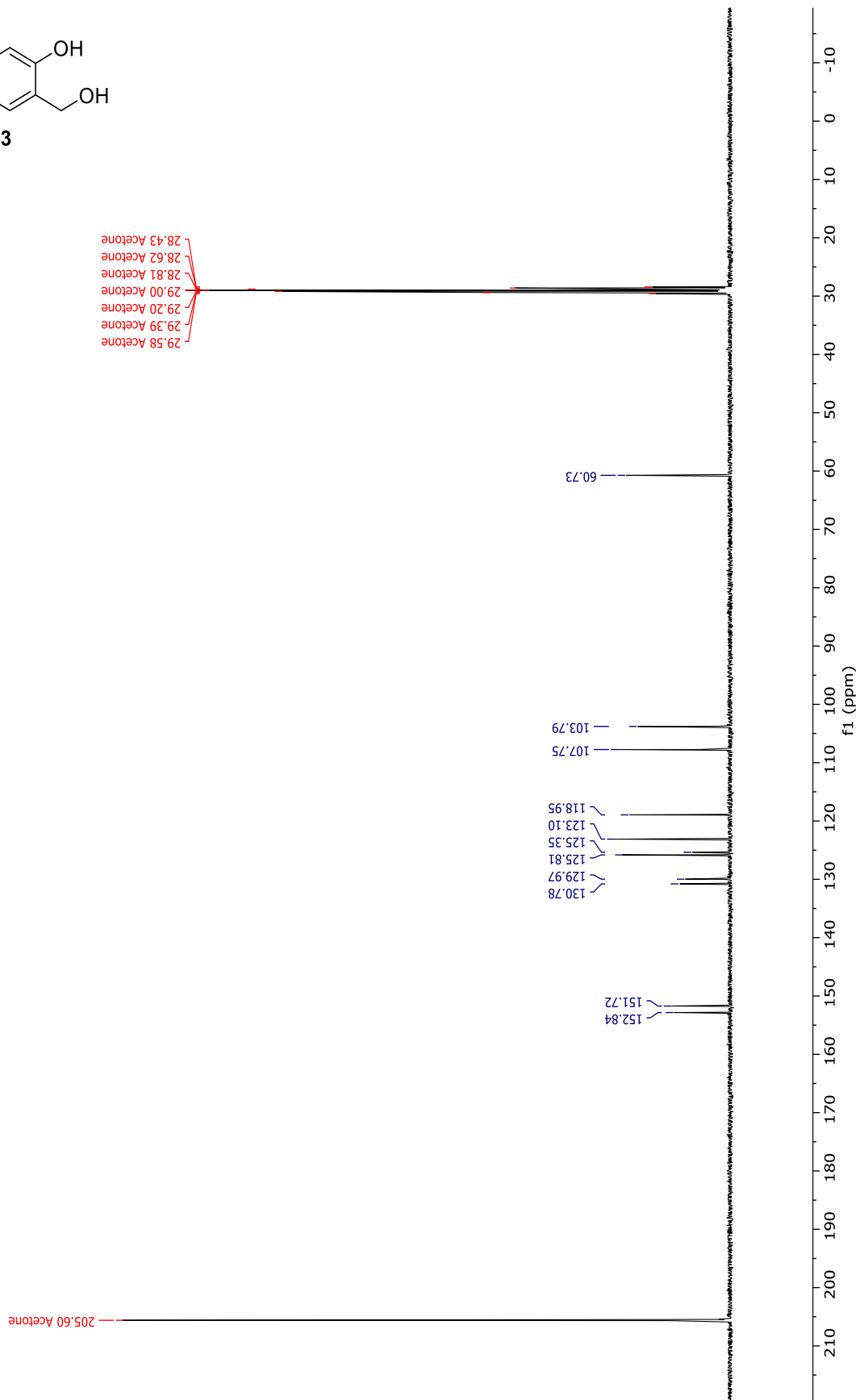
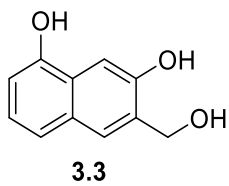
2.22

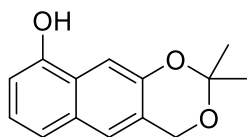




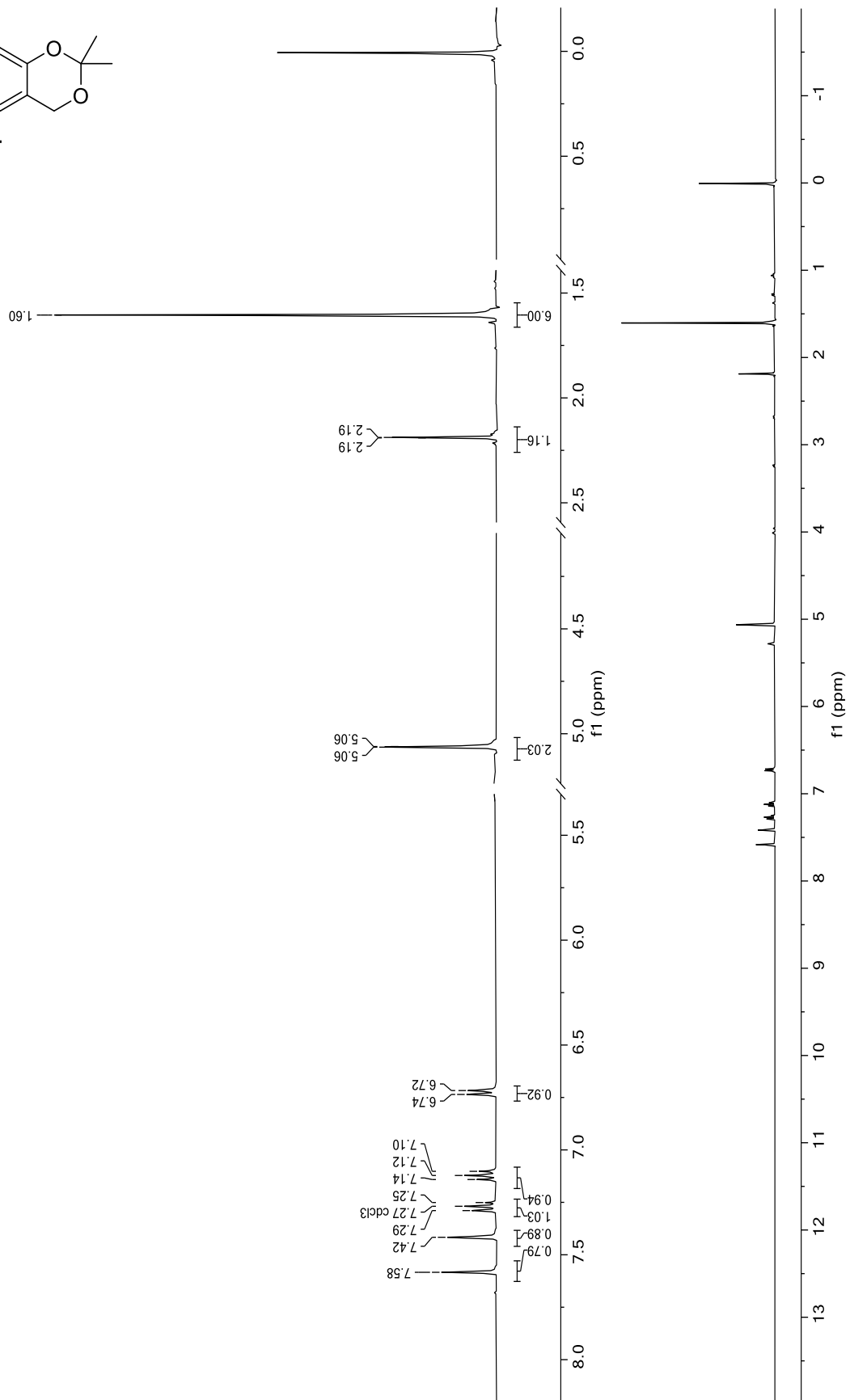


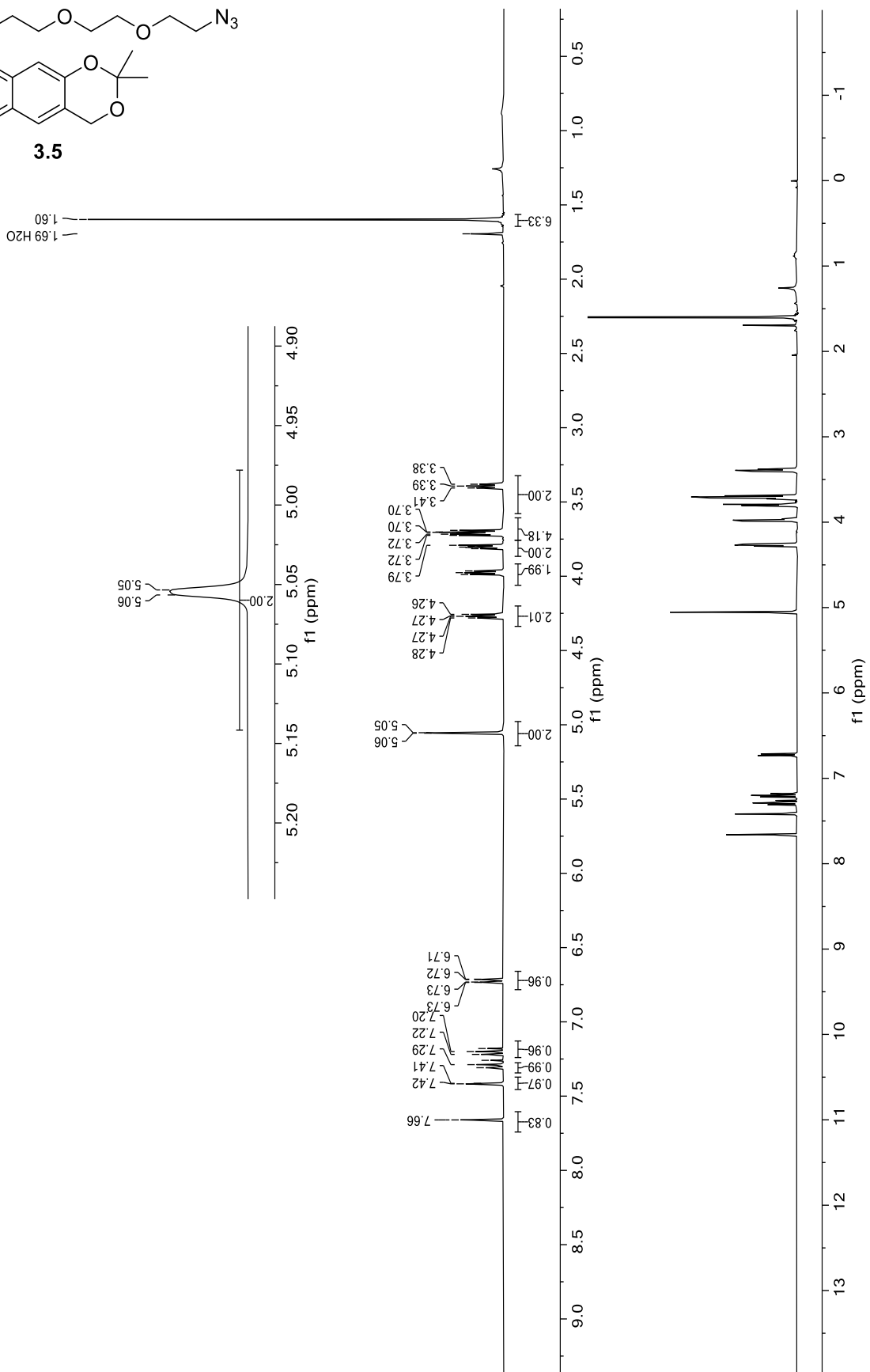
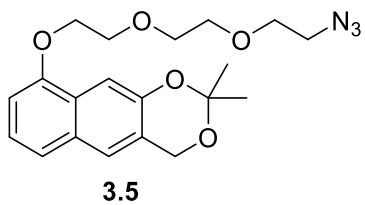


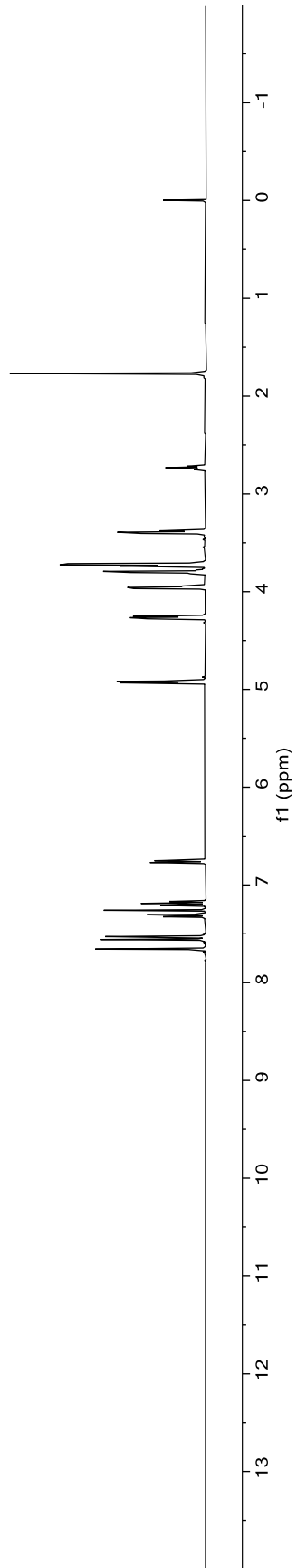
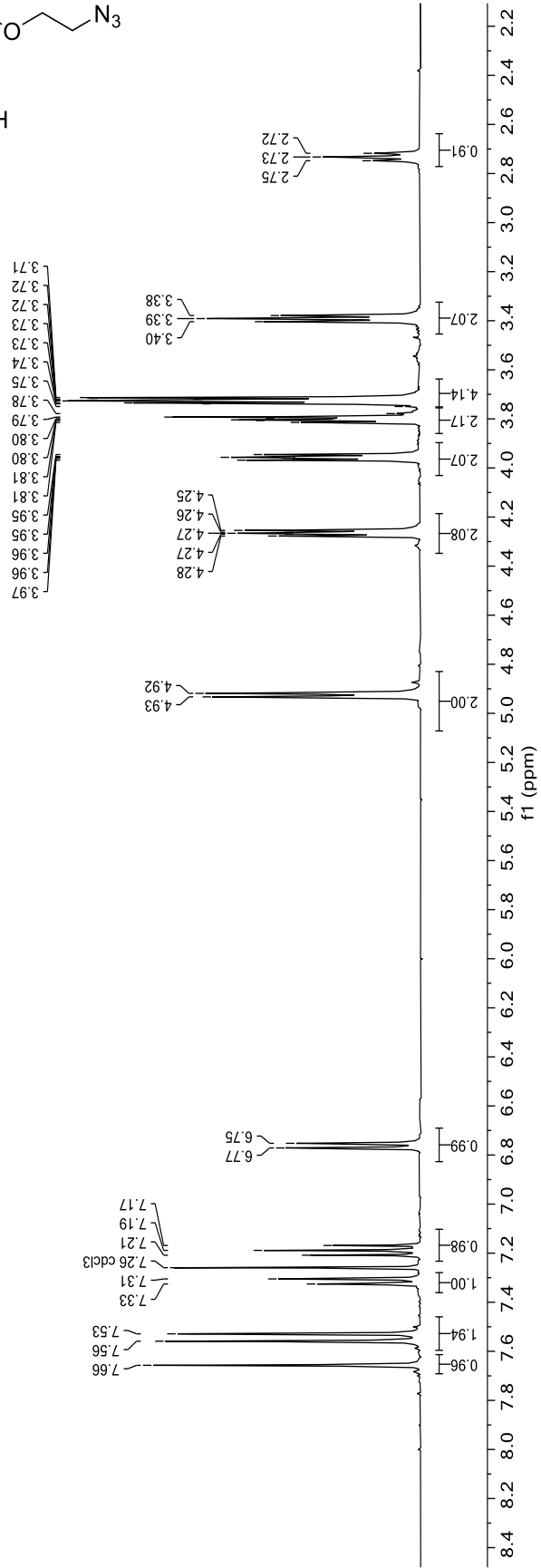
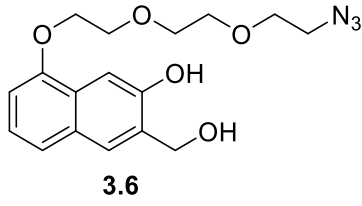


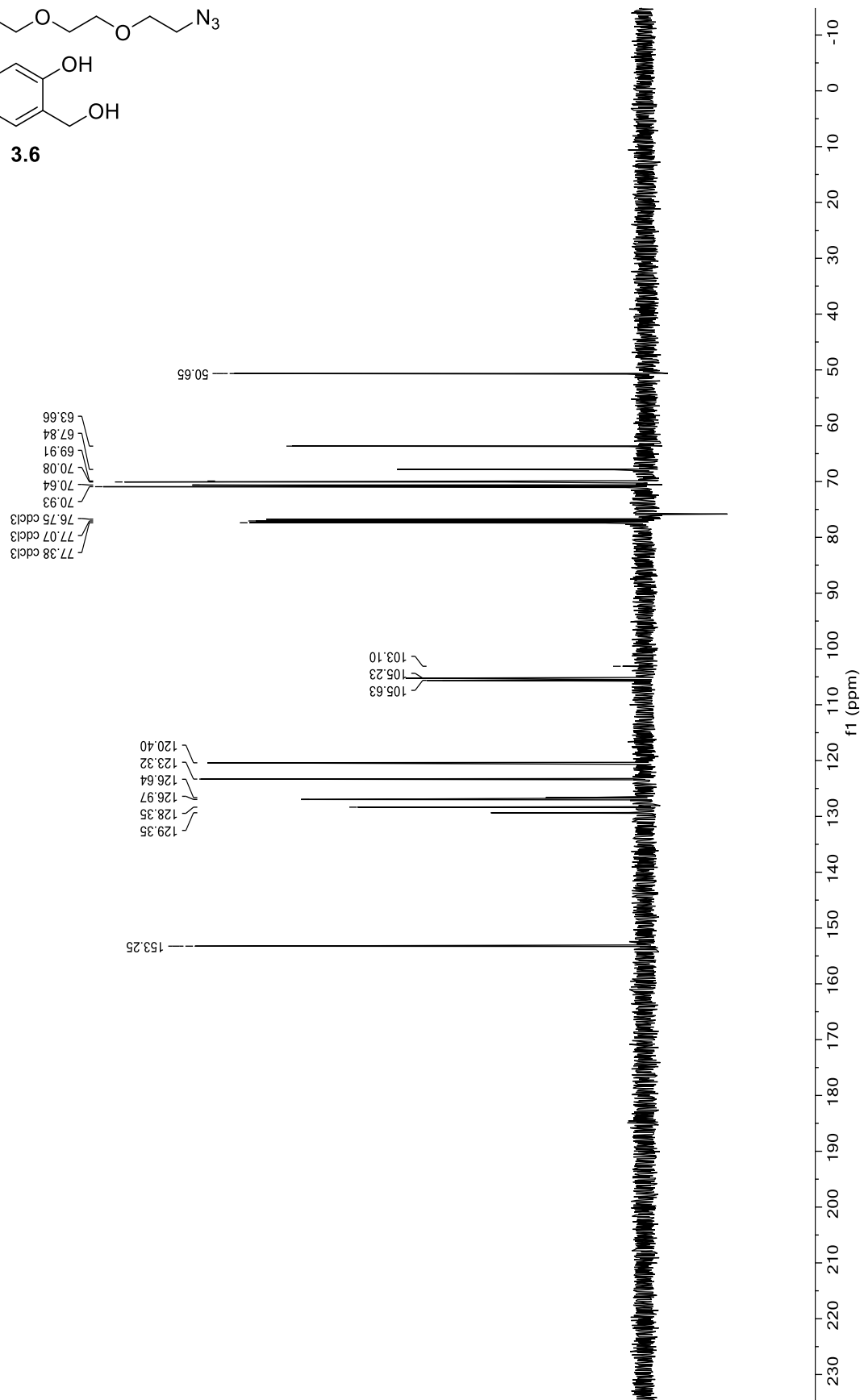
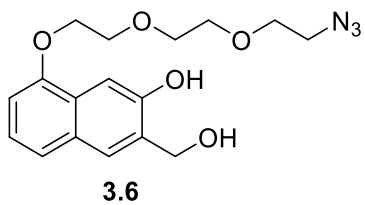


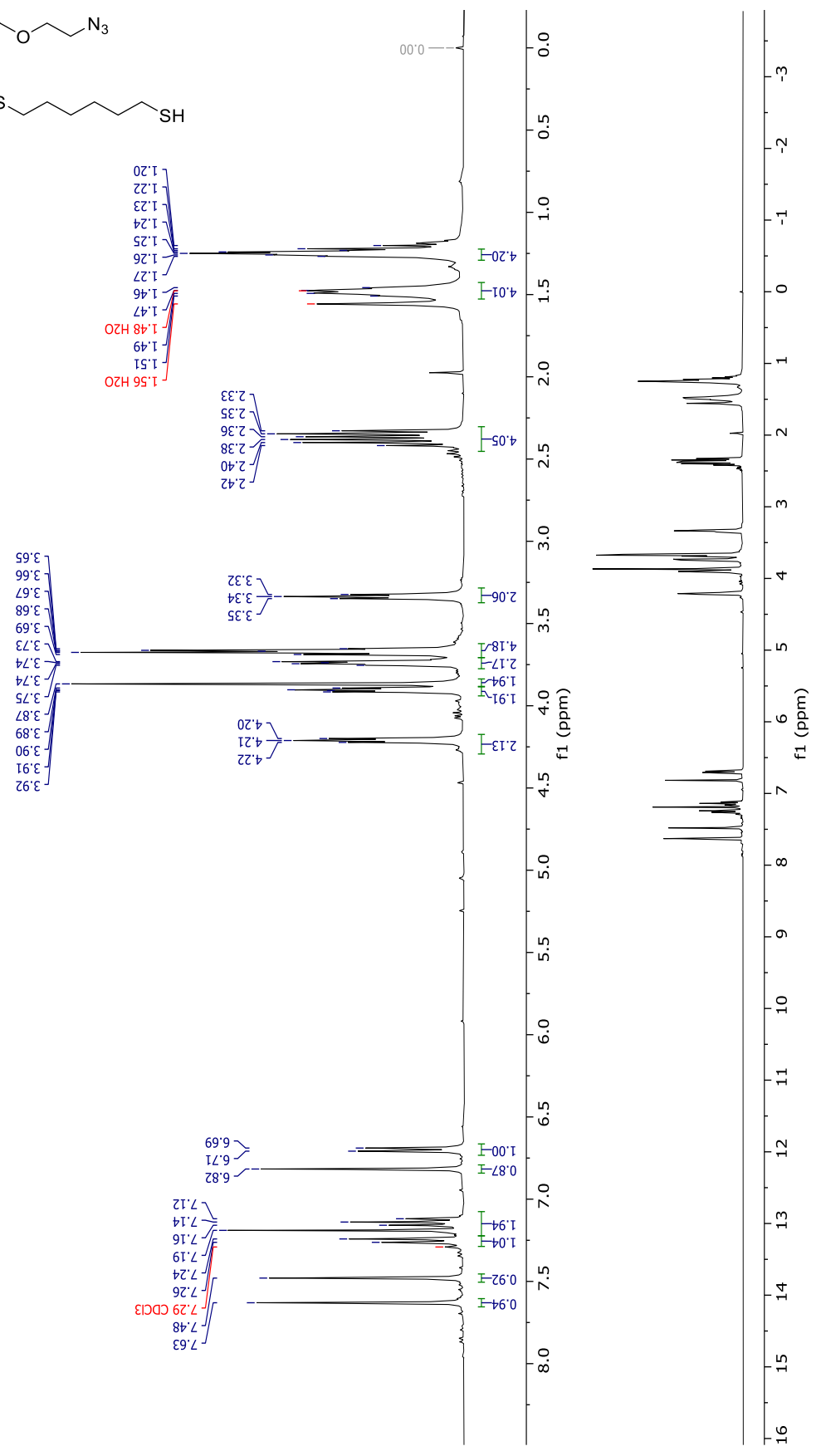
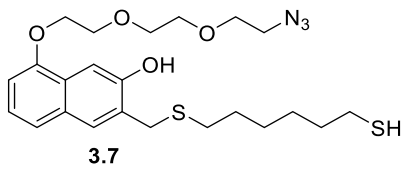
3.4

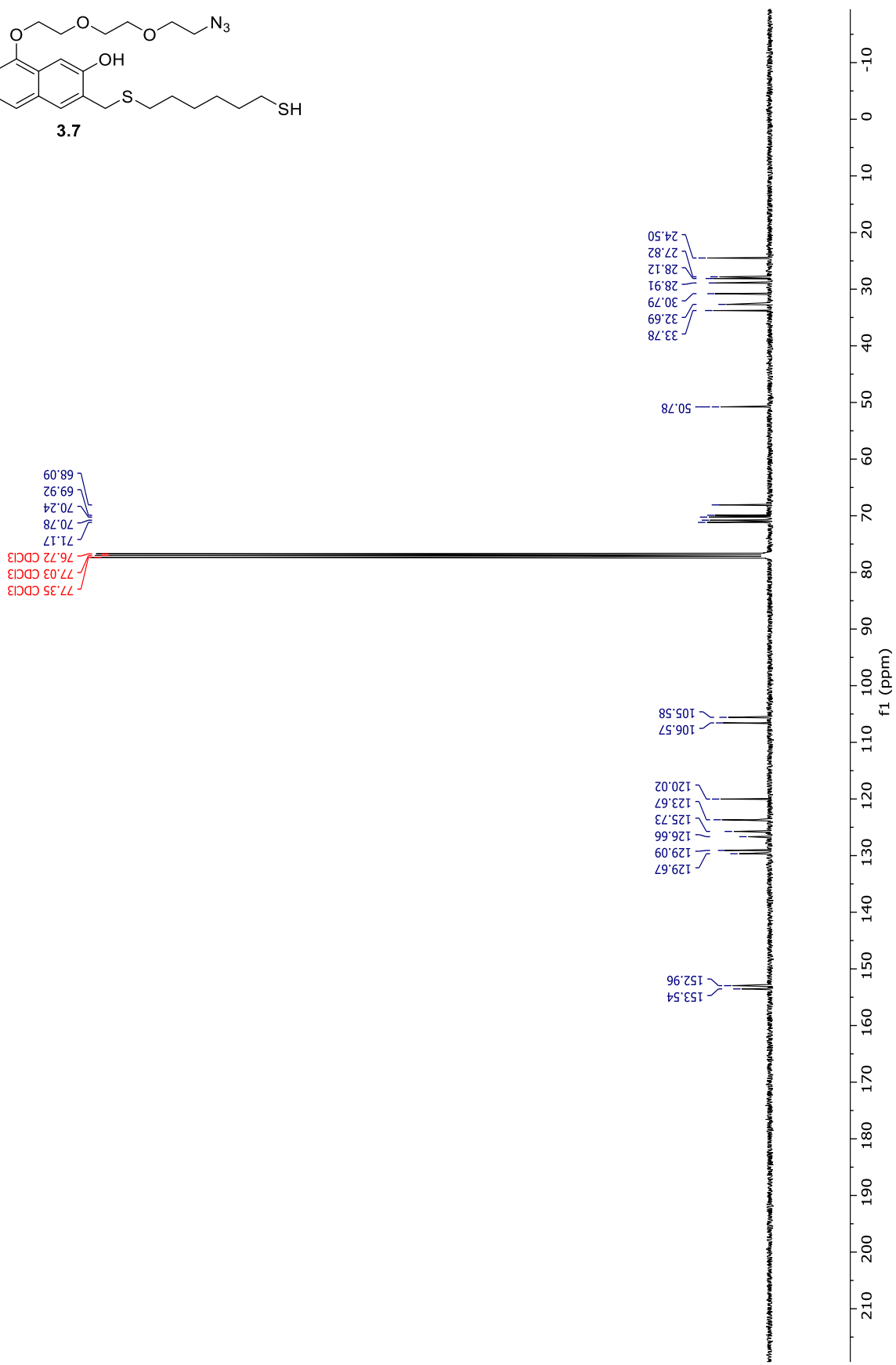
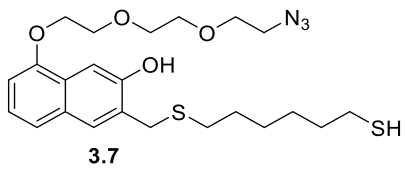


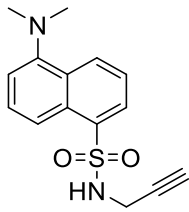




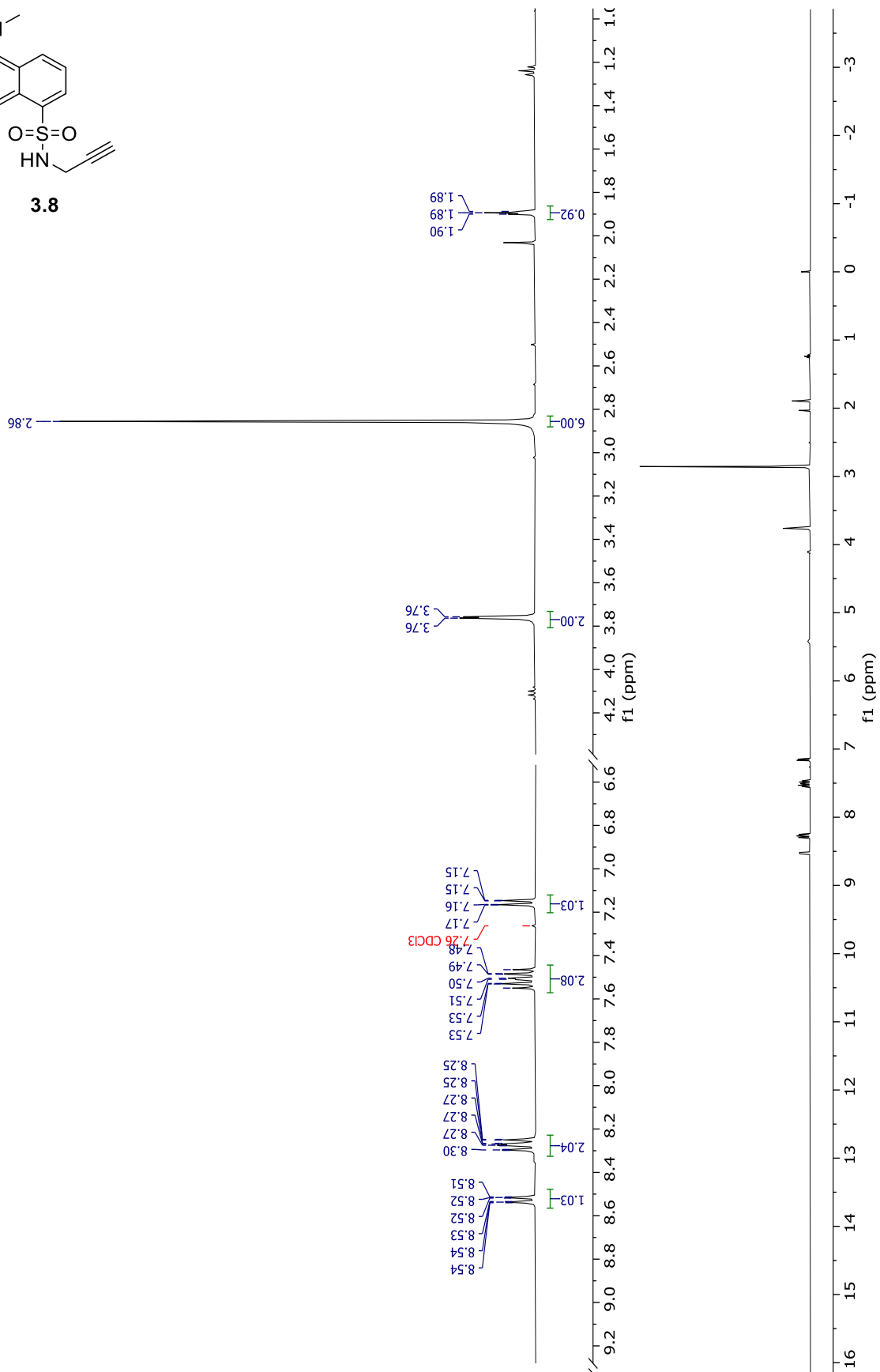


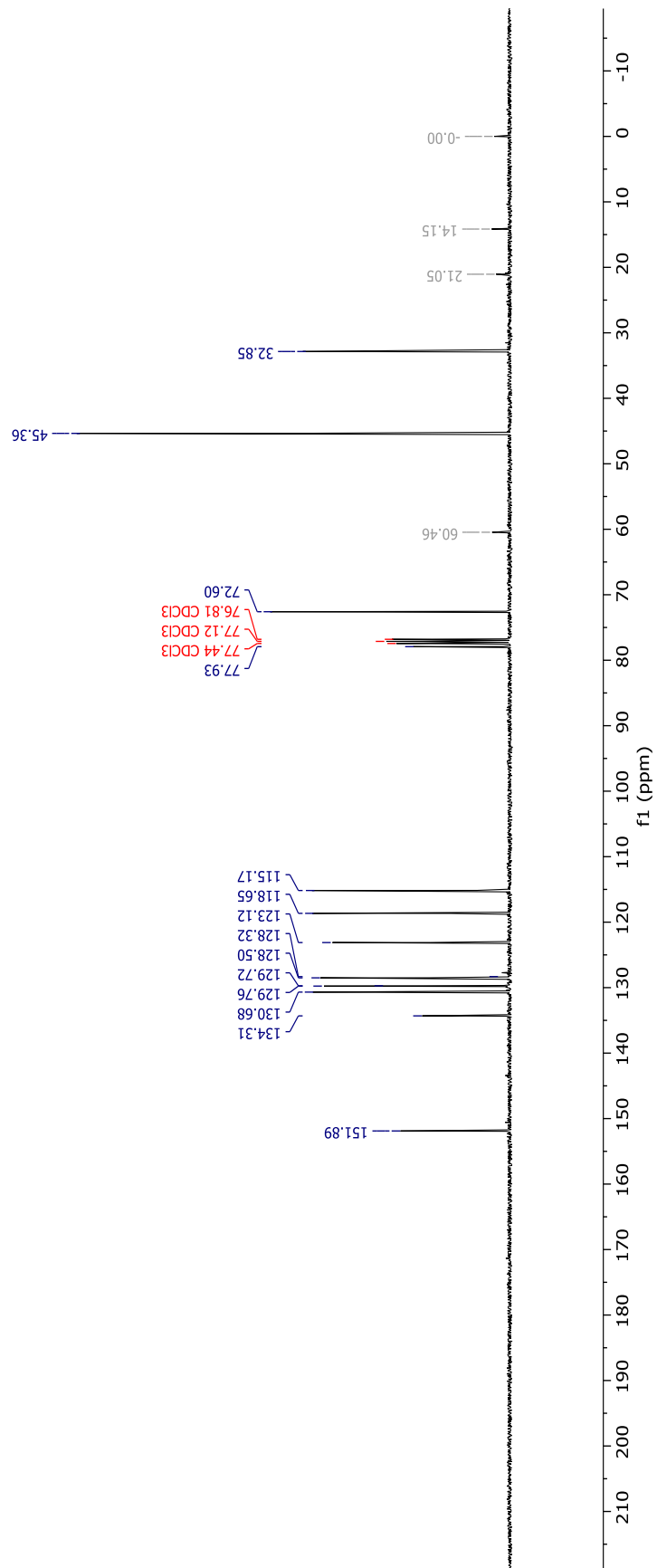
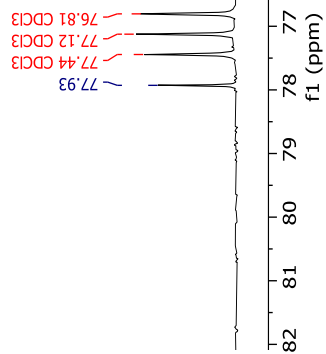
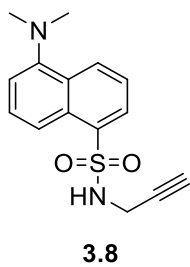


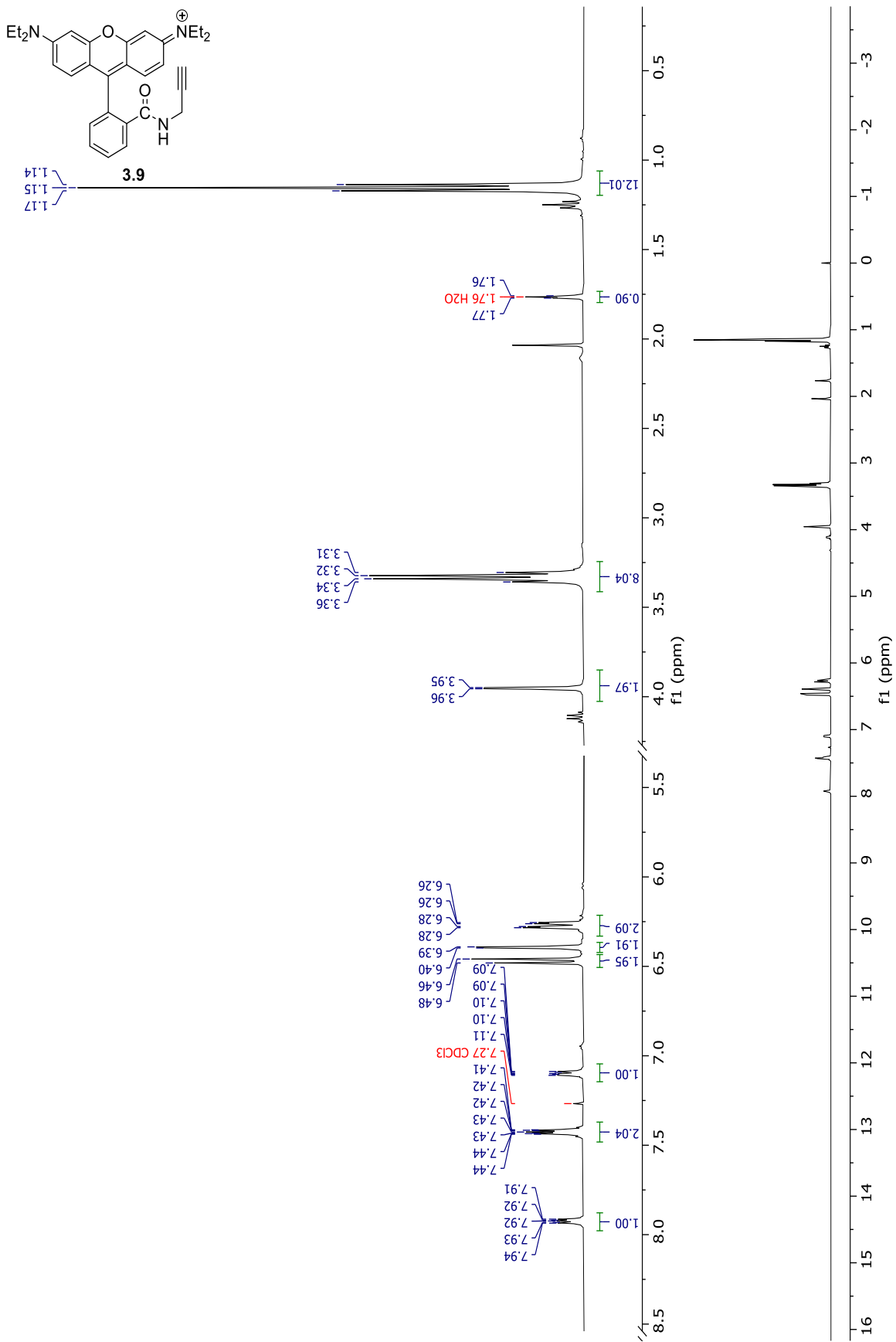


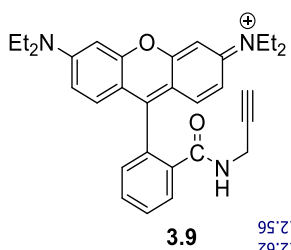


3.8

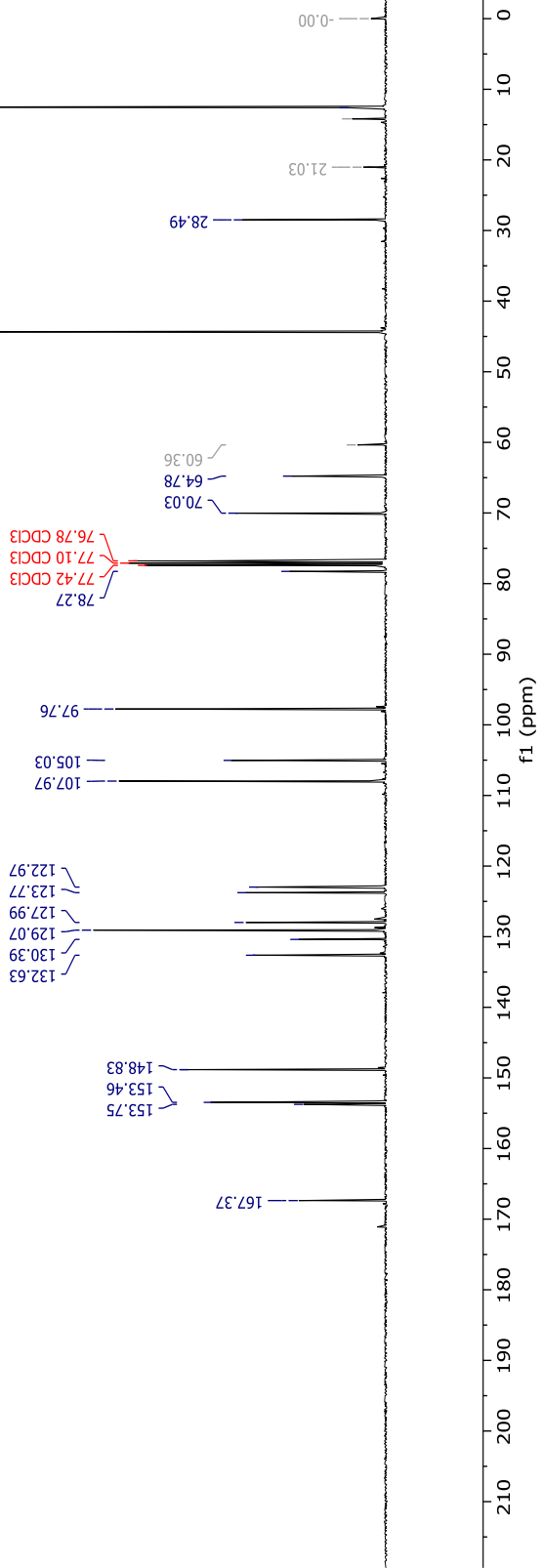


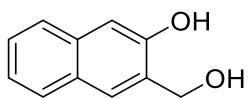






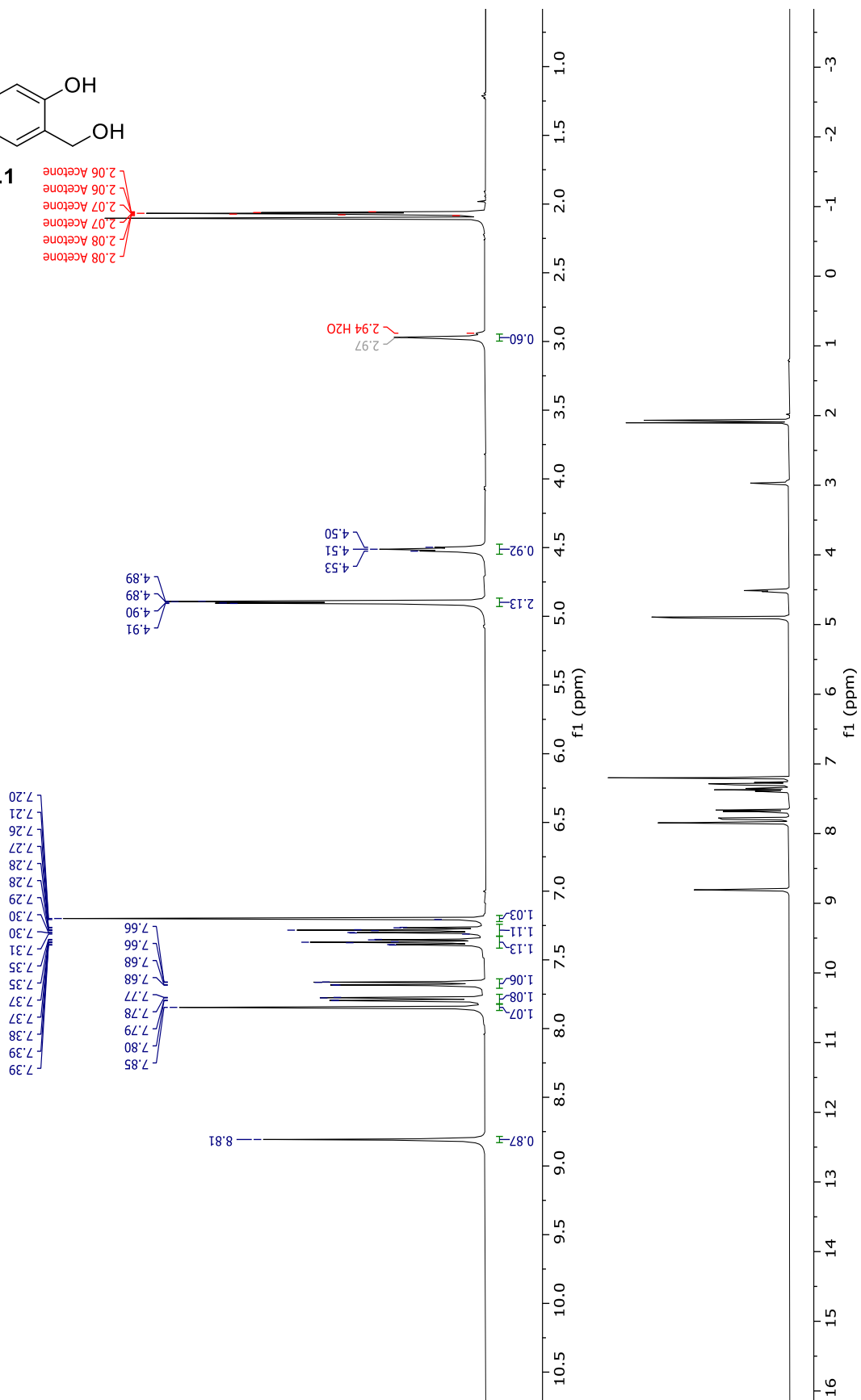
14.19
12.62
12.56

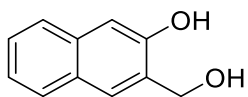




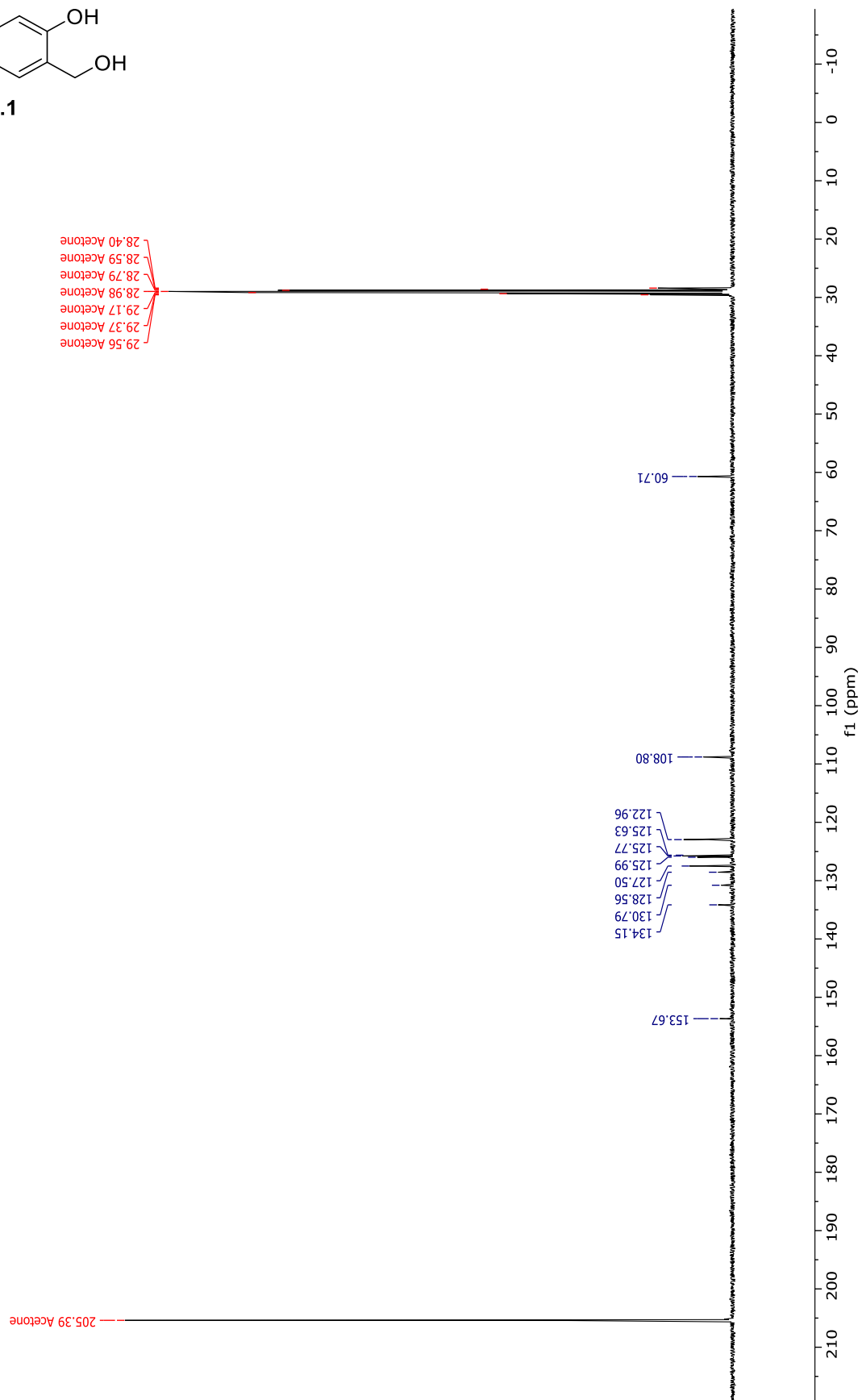
4.1

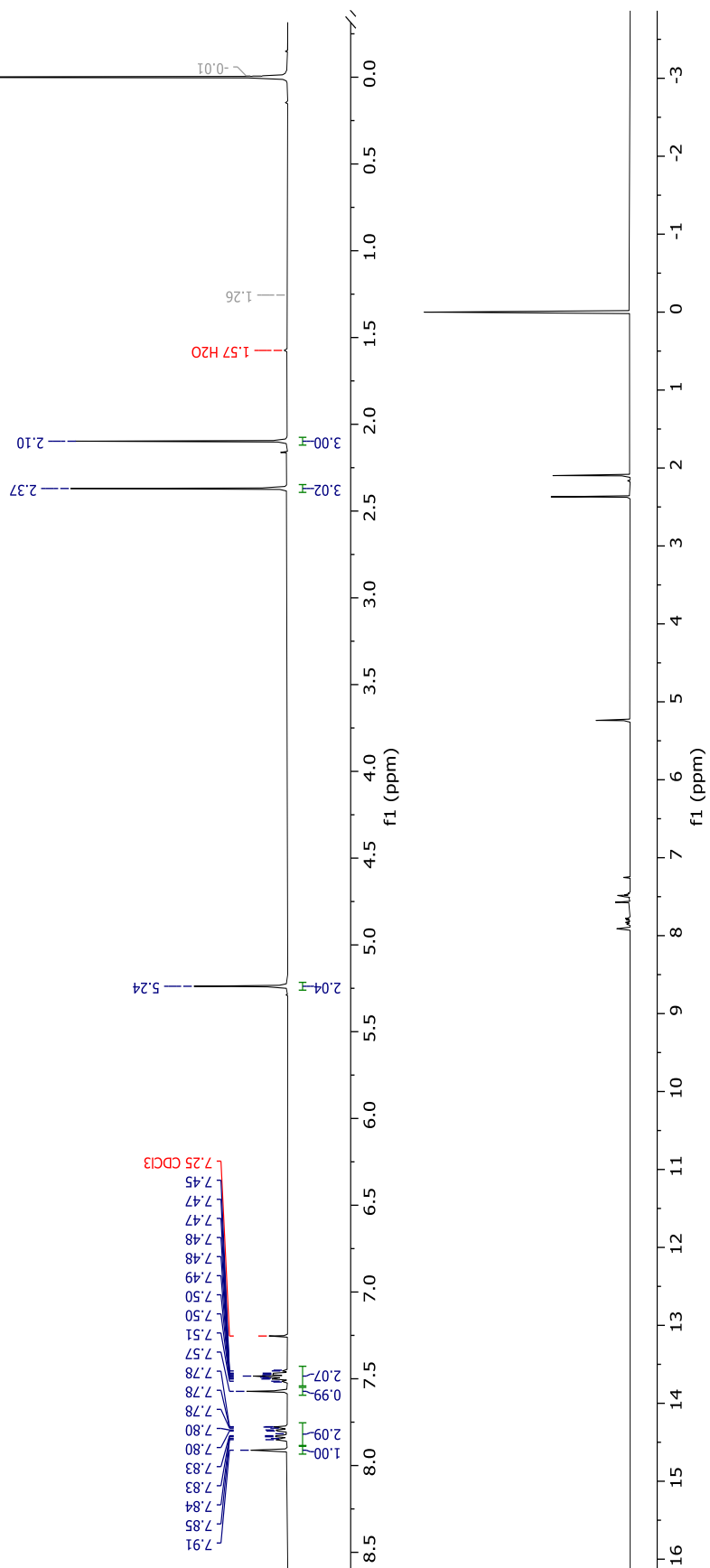
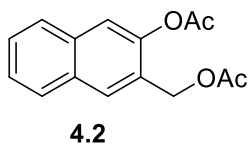
2.06 Acetone
2.07 Acetone
2.07 Acetone
2.08 Acetone
2.08 Acetone

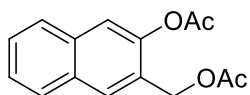




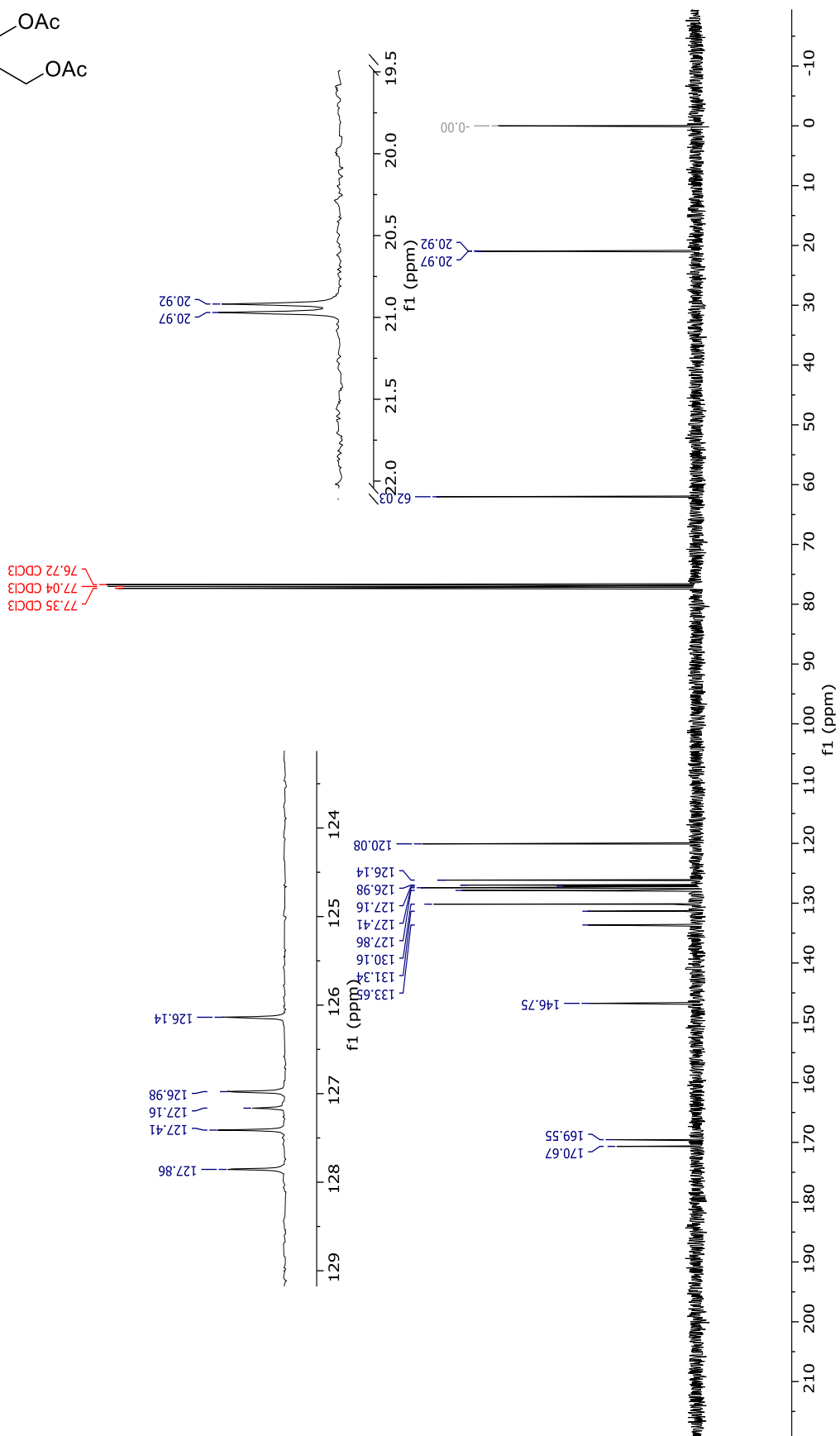
4.1

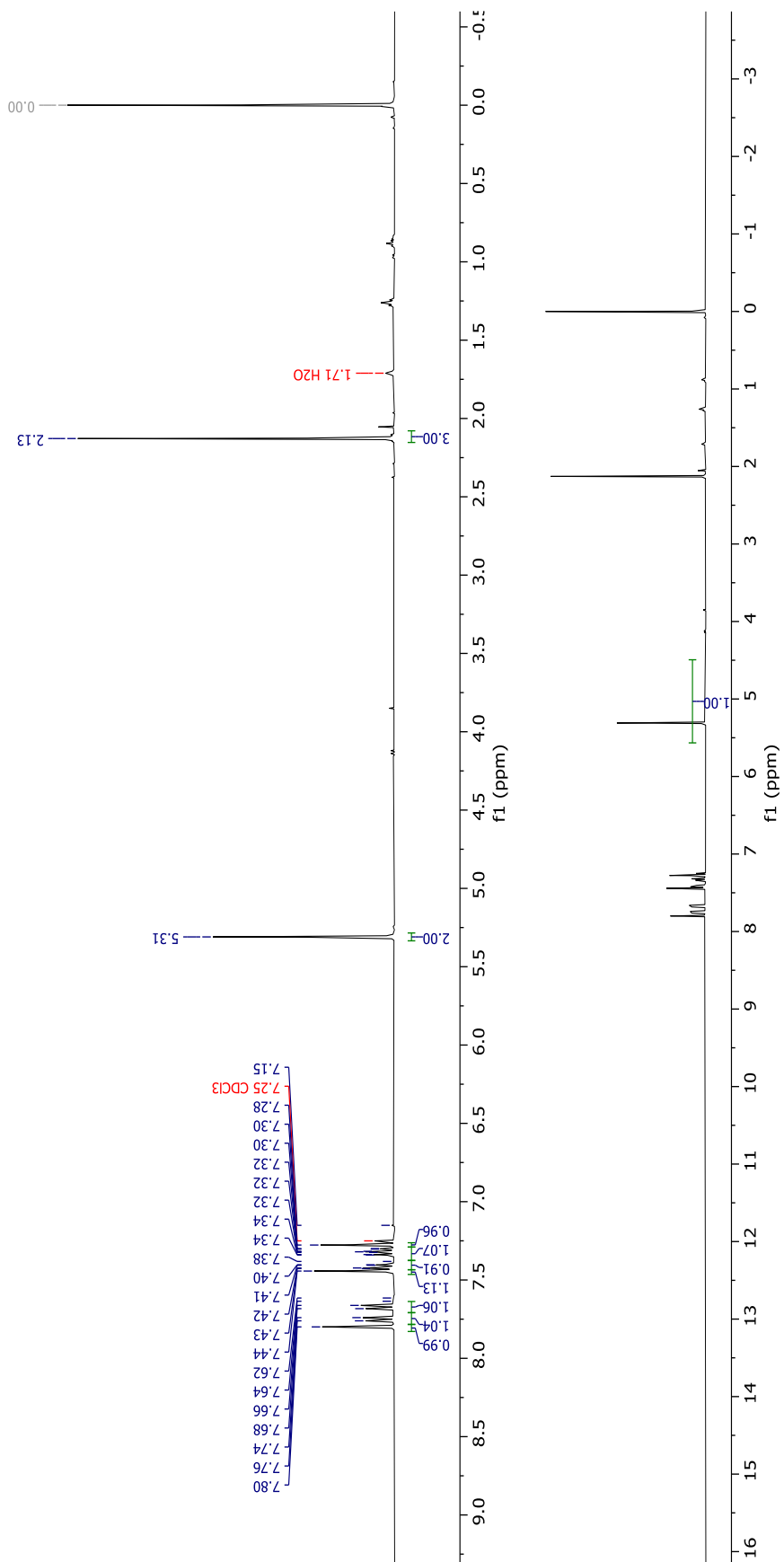
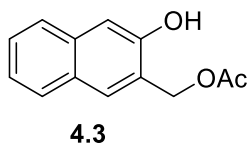


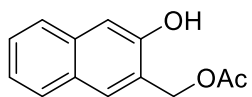




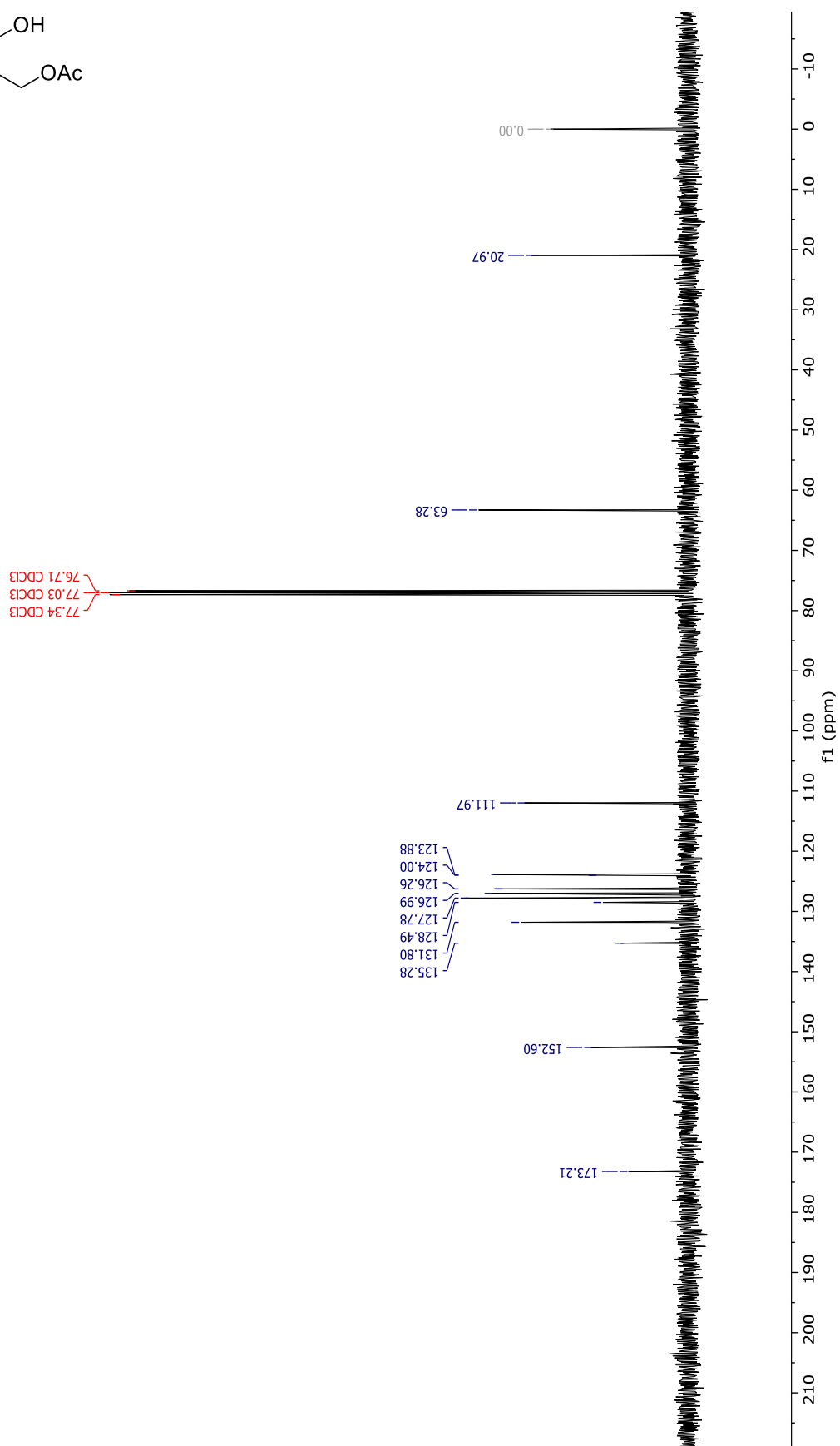
4.2

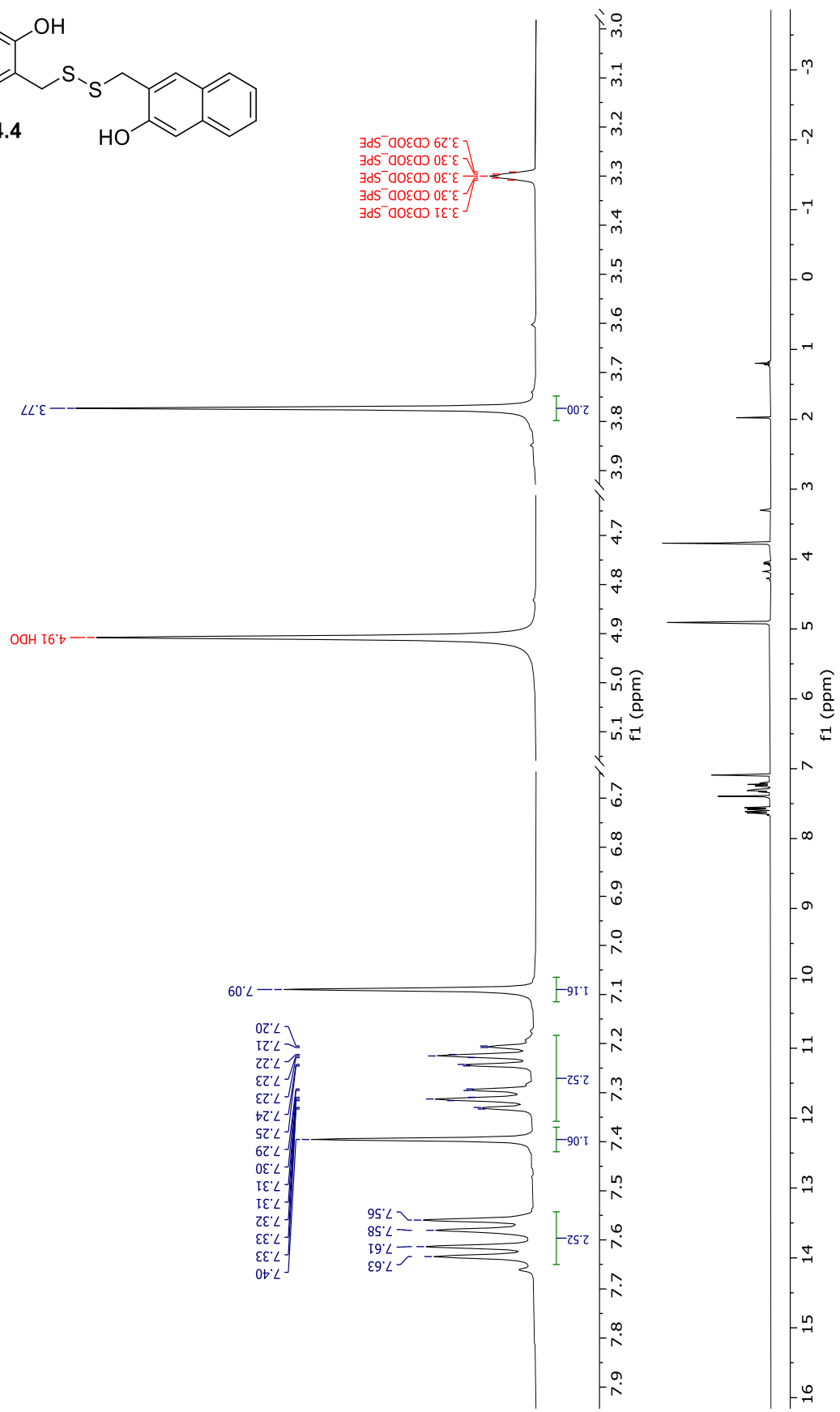
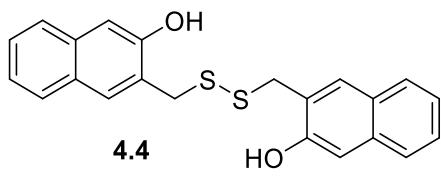


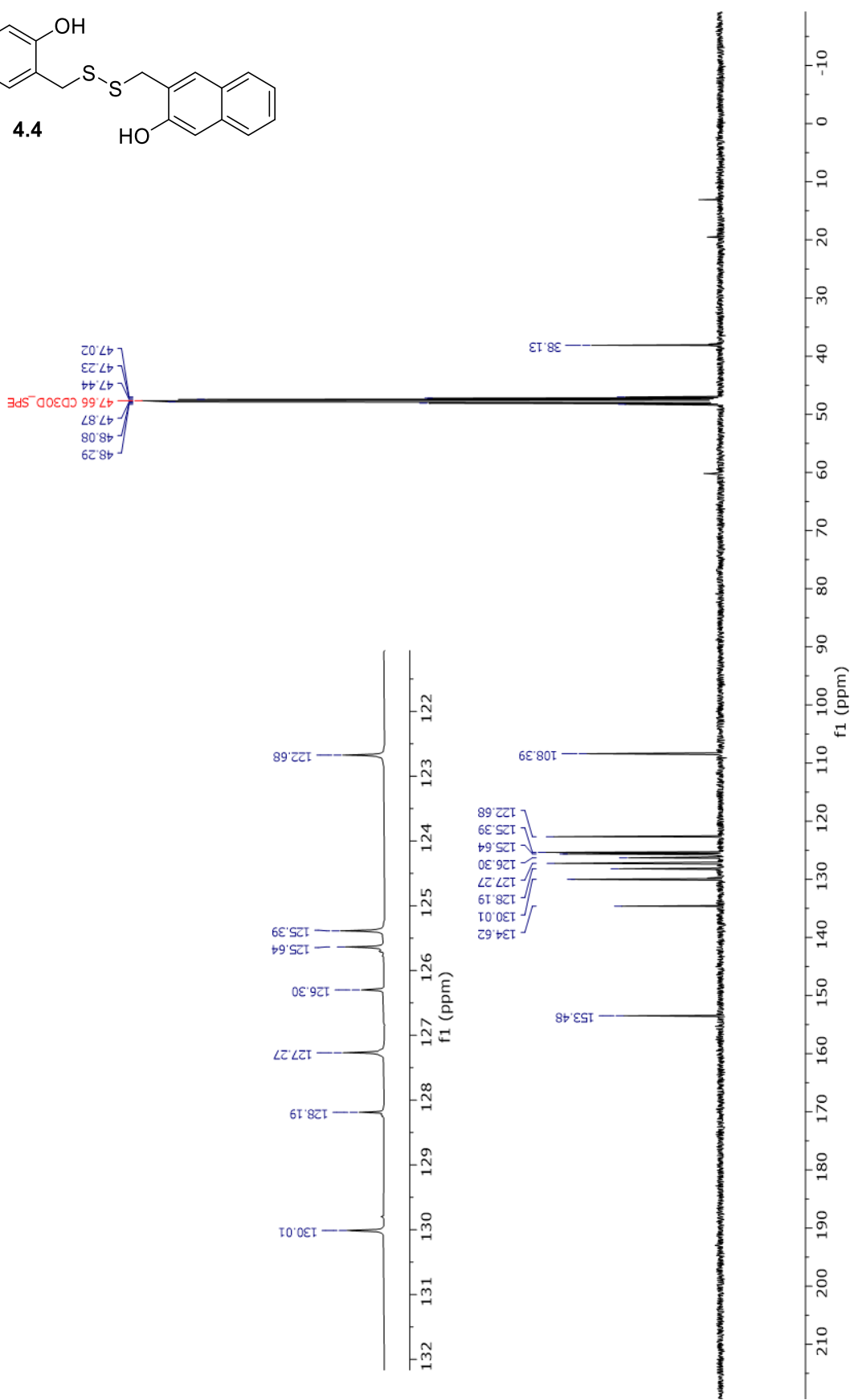
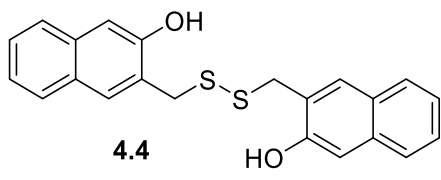


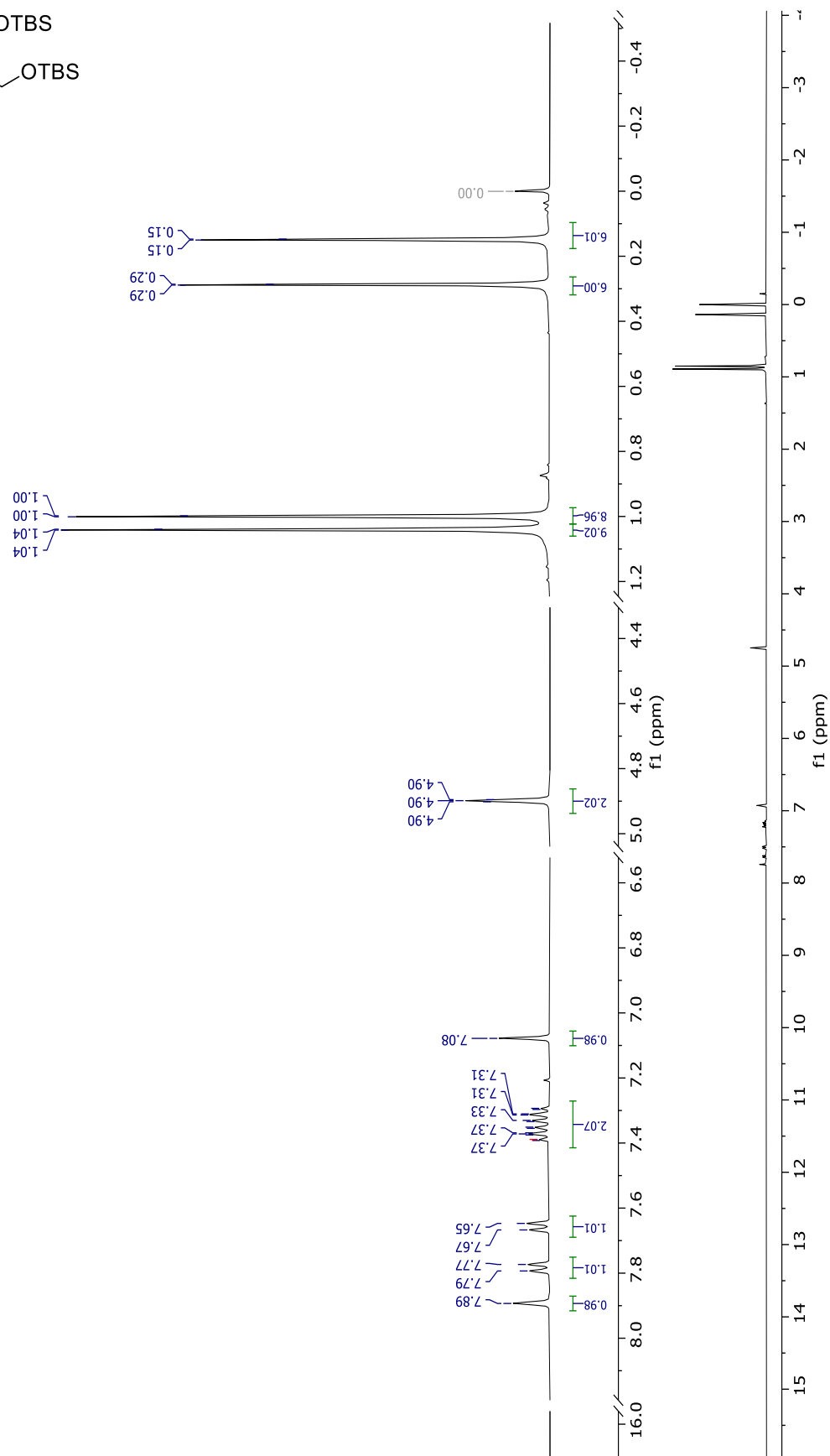
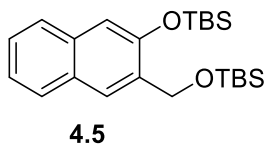


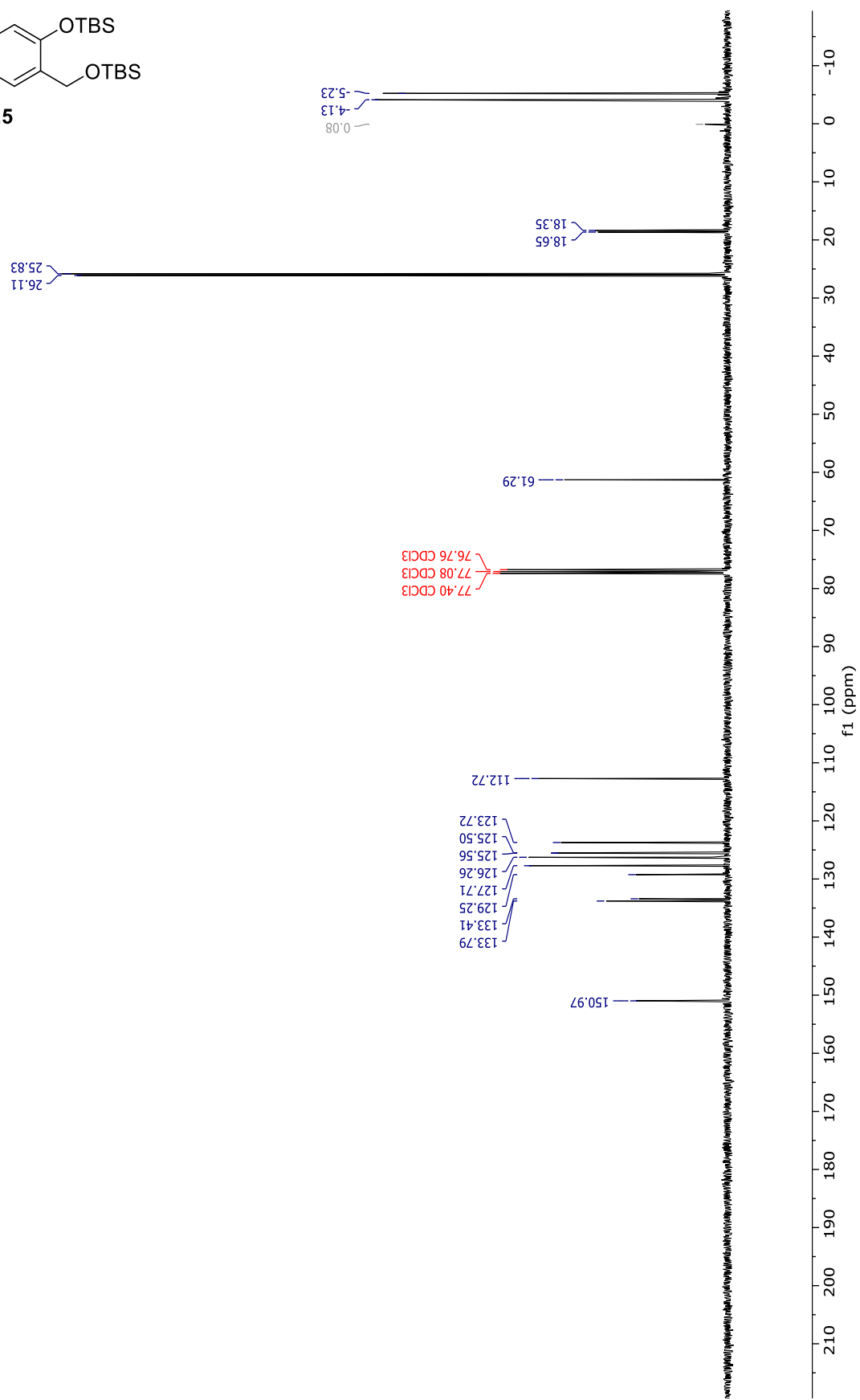
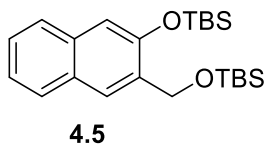
4.3

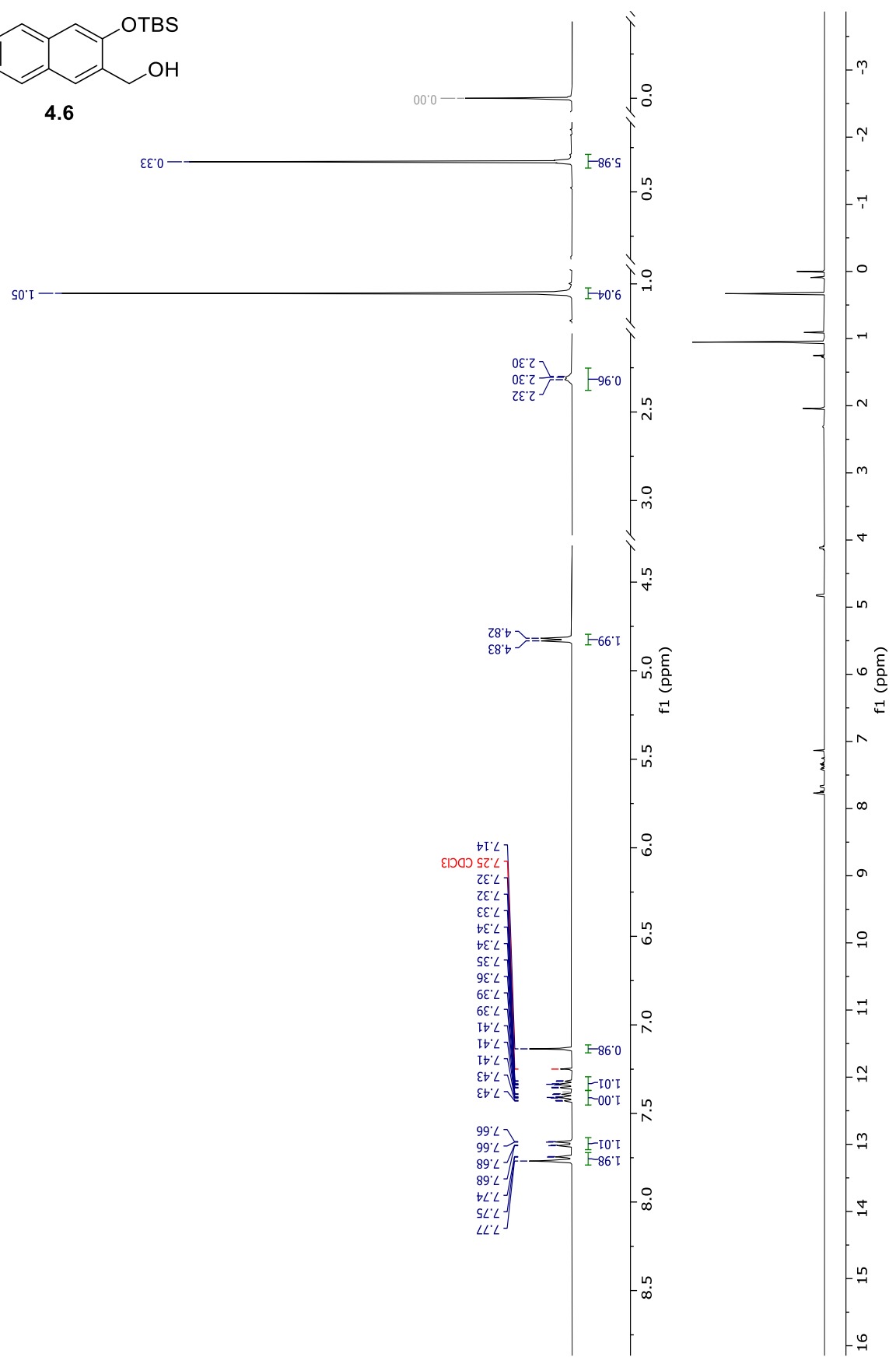
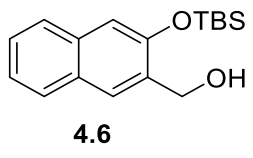


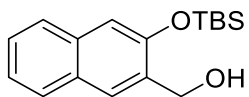












4.6

25.78
21.06
18.24
14.19

77.35 CDCl₃
77.03 CDCl₃
76.71 CDCl₃

-4.16
-0.00

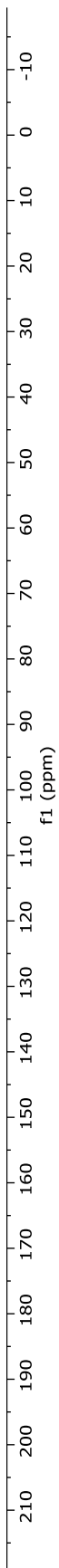
62.40
60.41

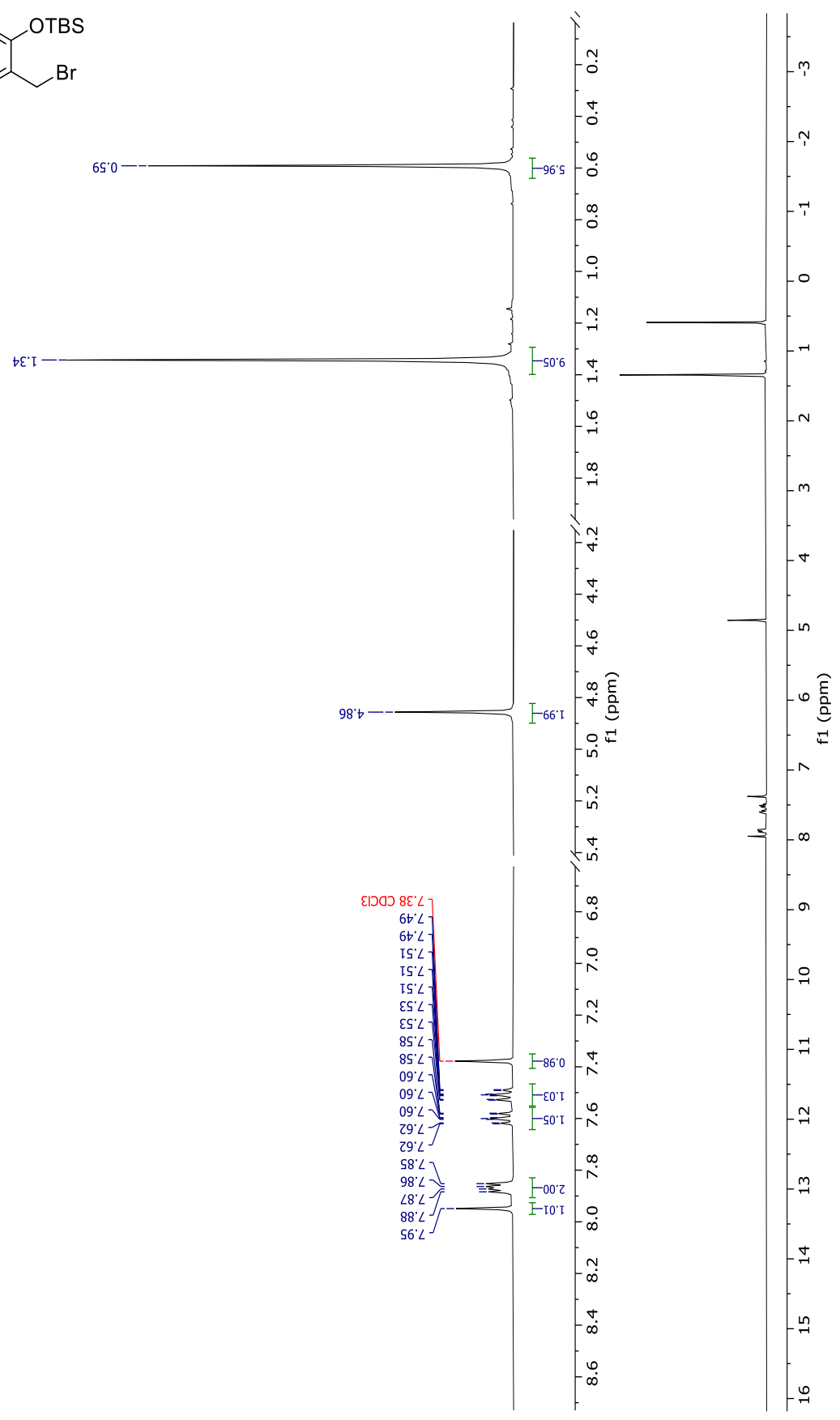
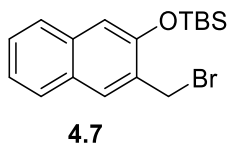
133.92
132.82
129.05
127.63
127.38
126.29
126.09
124.03

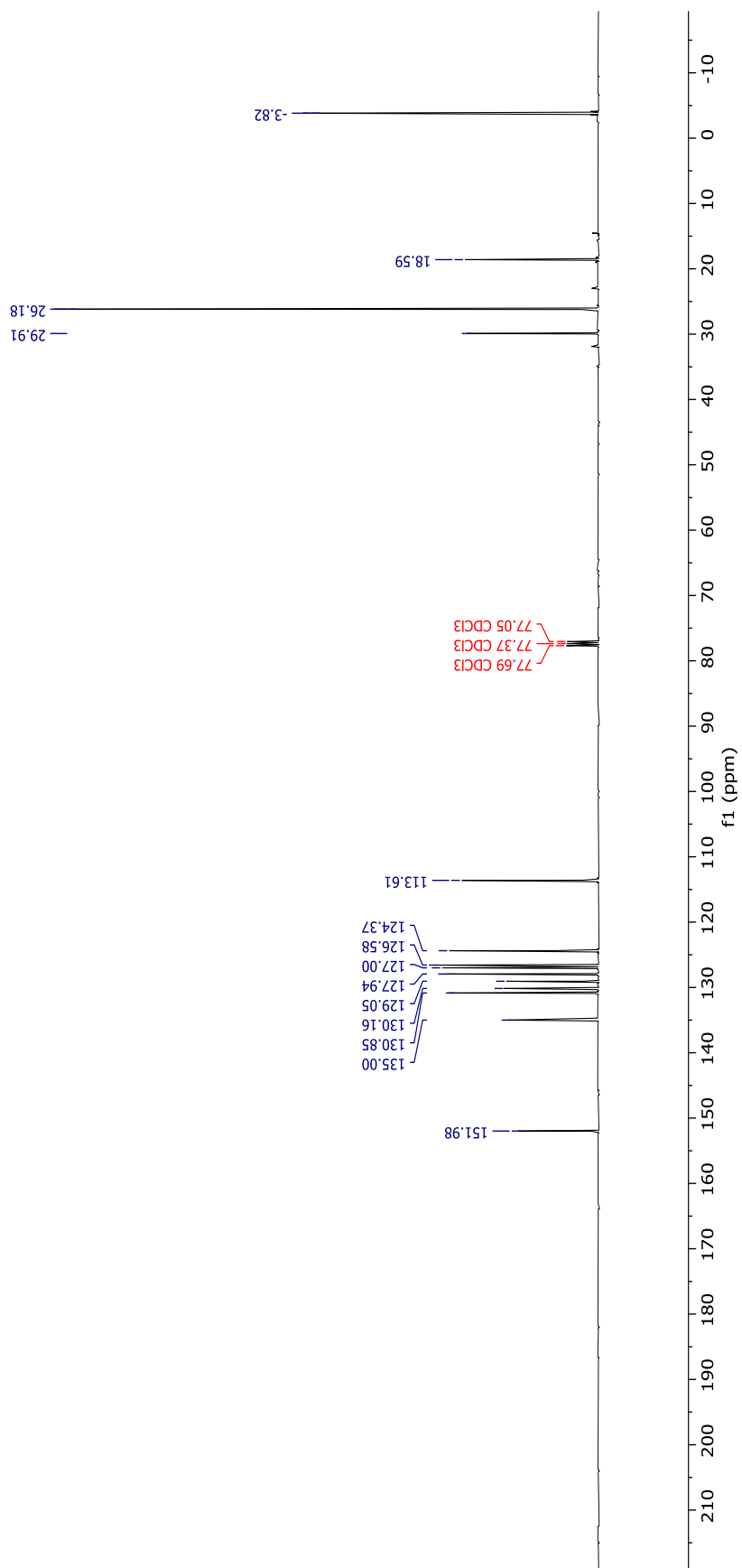
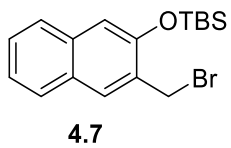
151.82

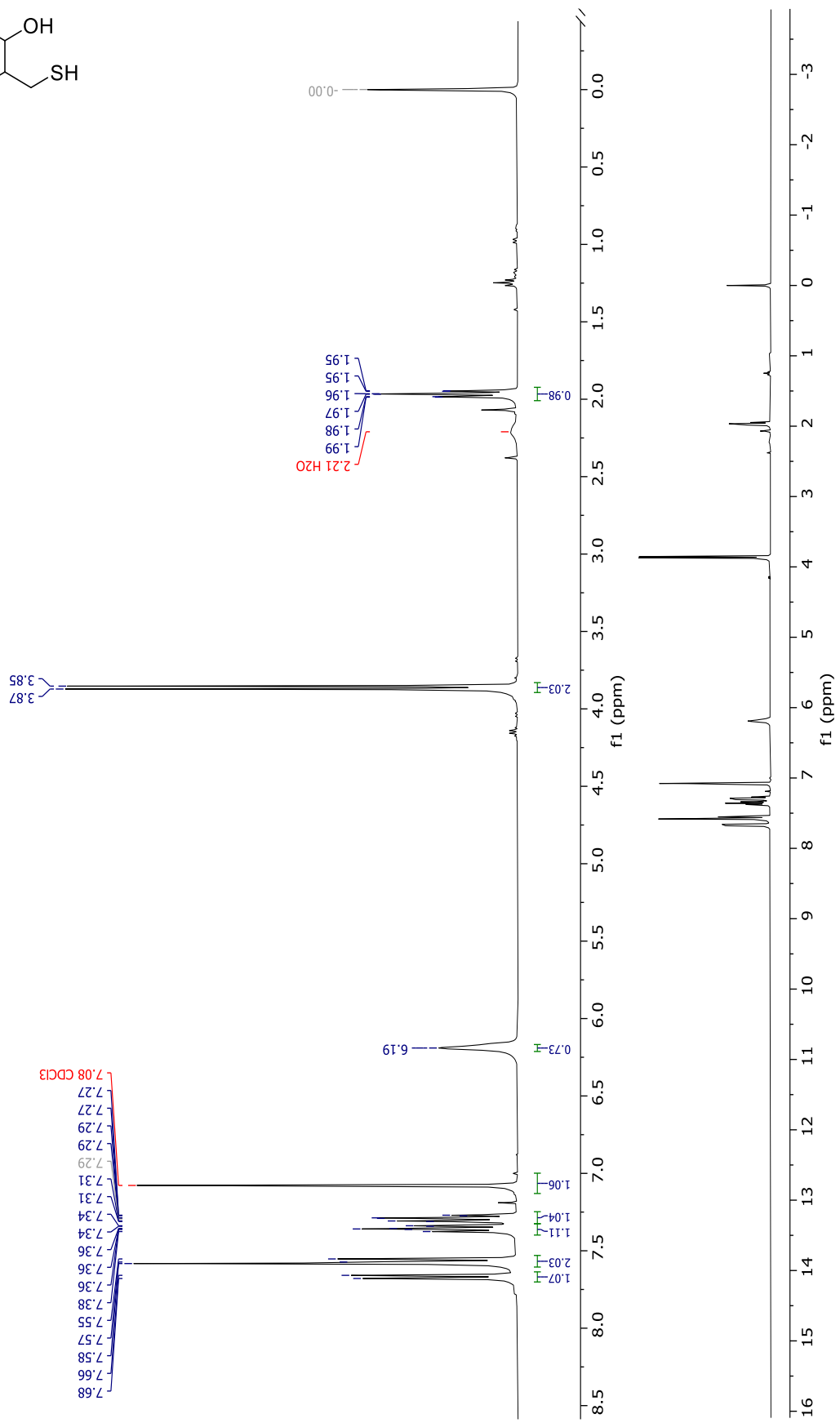
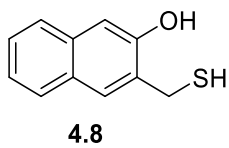
171.20

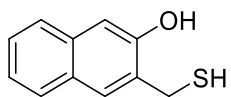
113.29



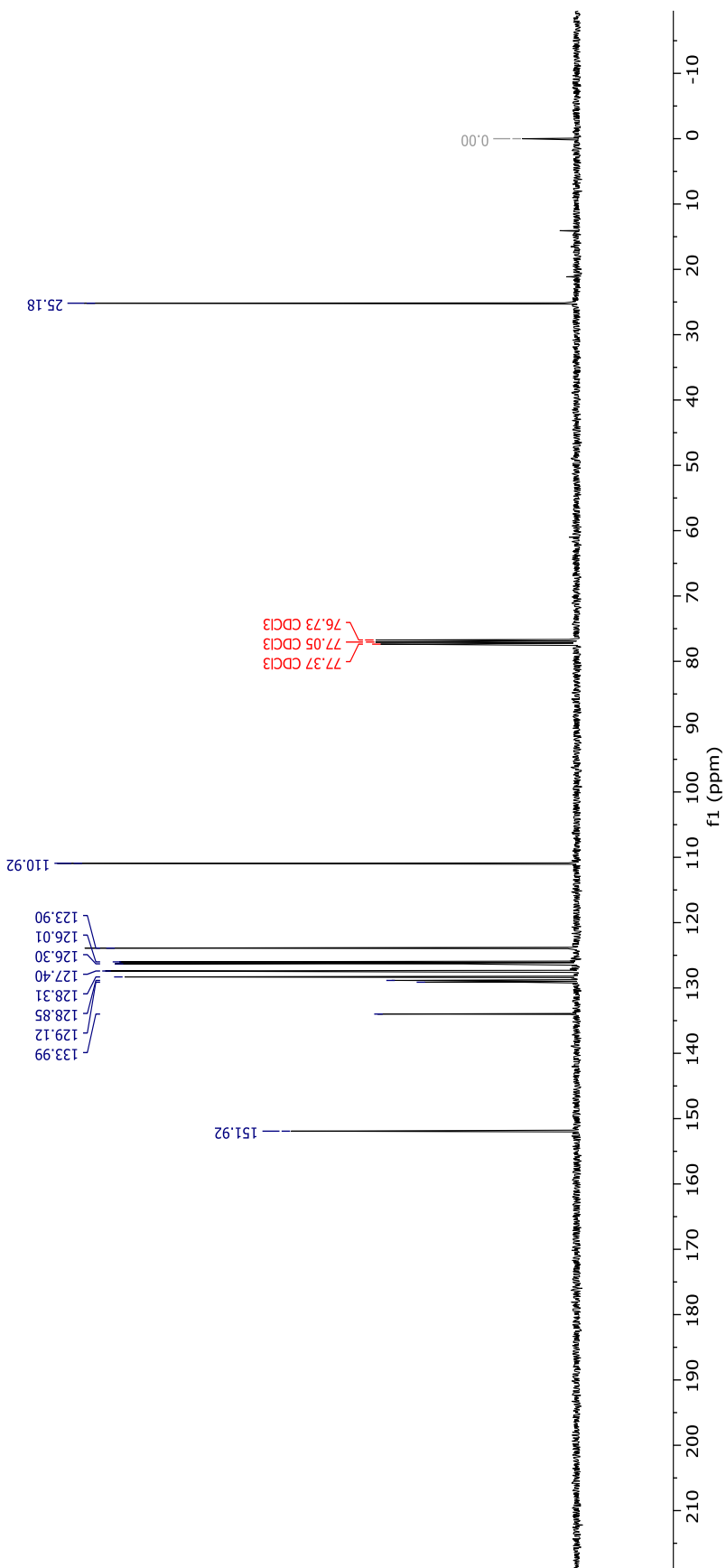


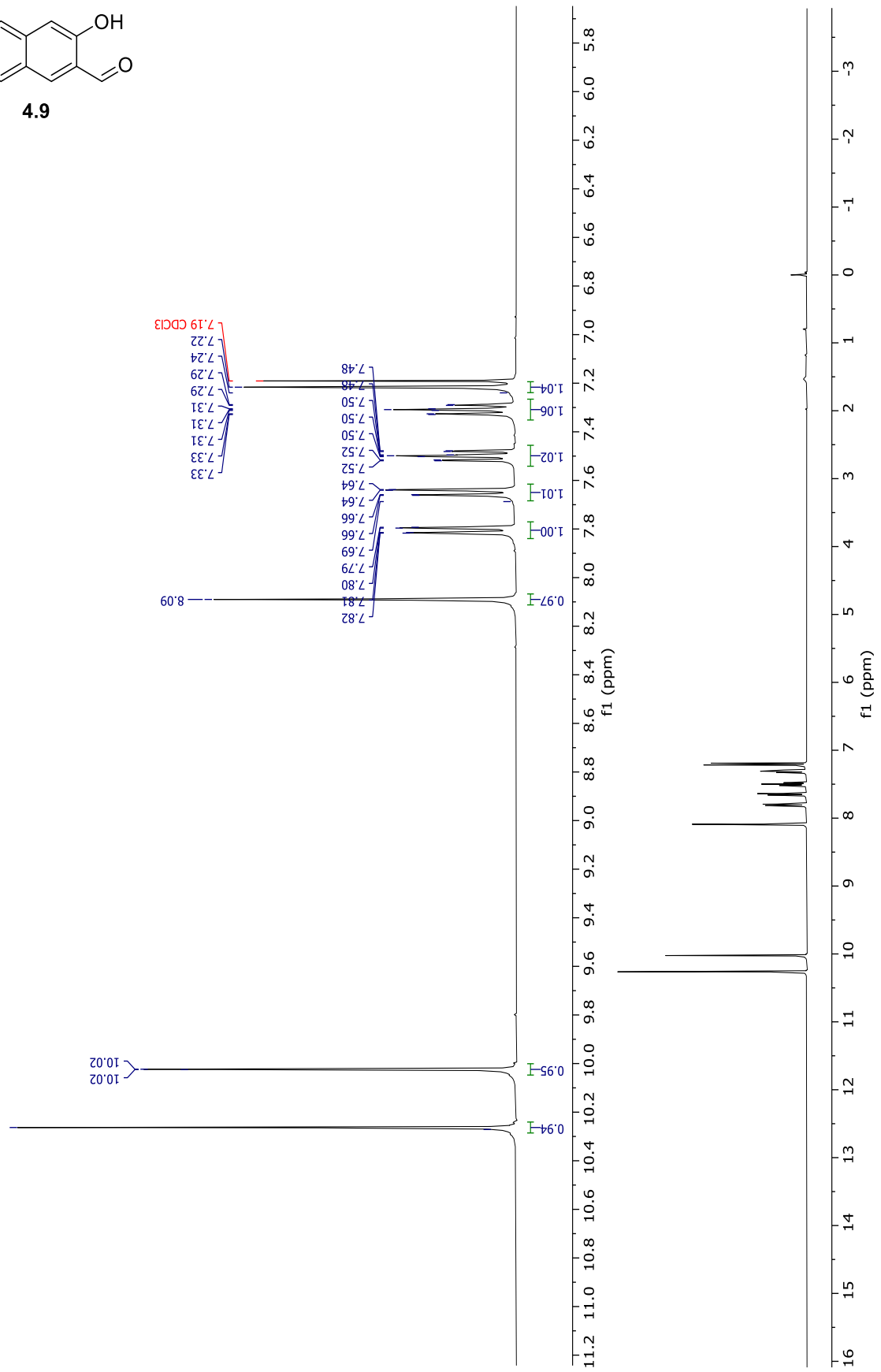
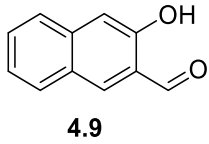


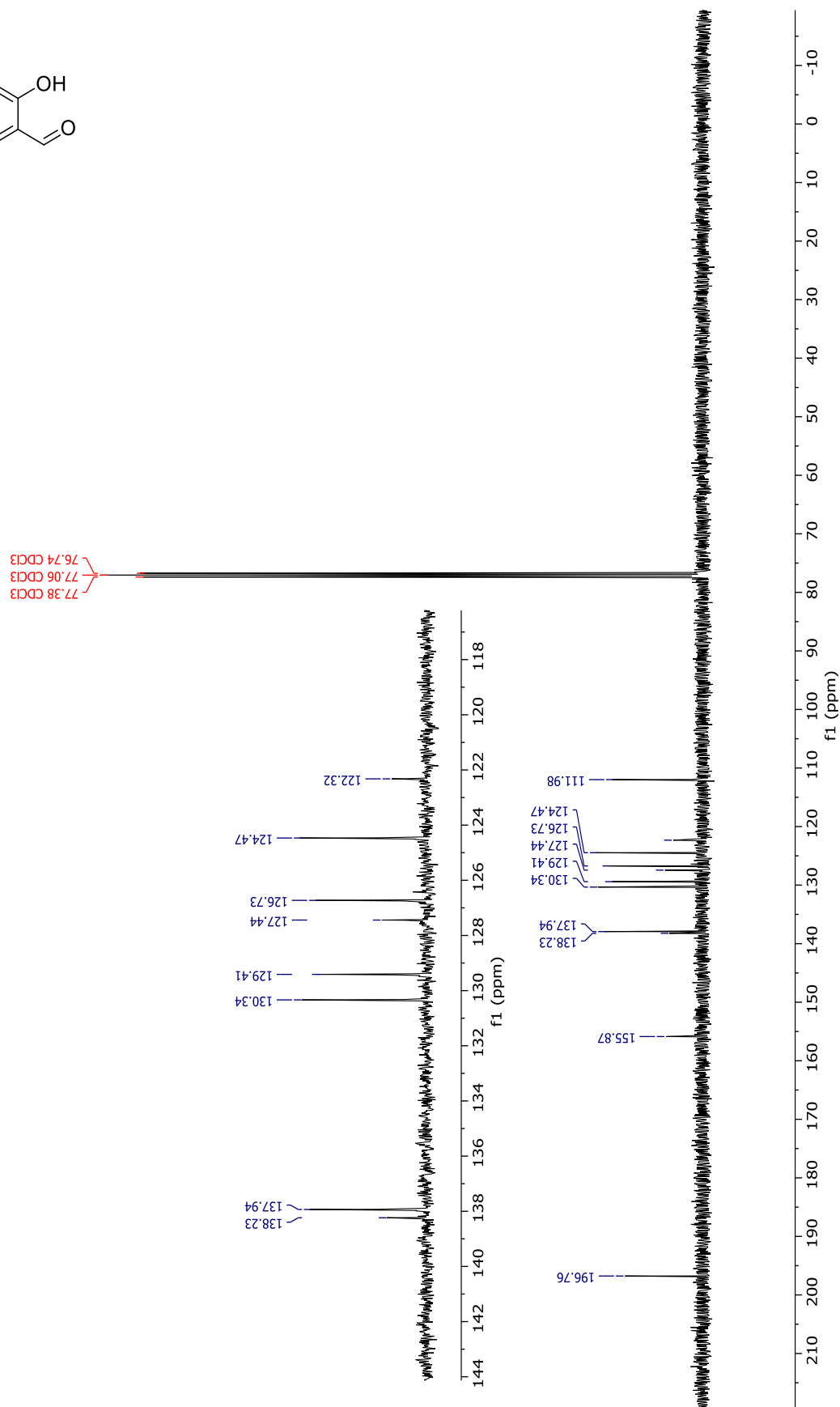
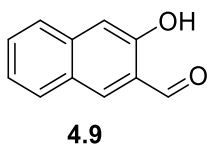


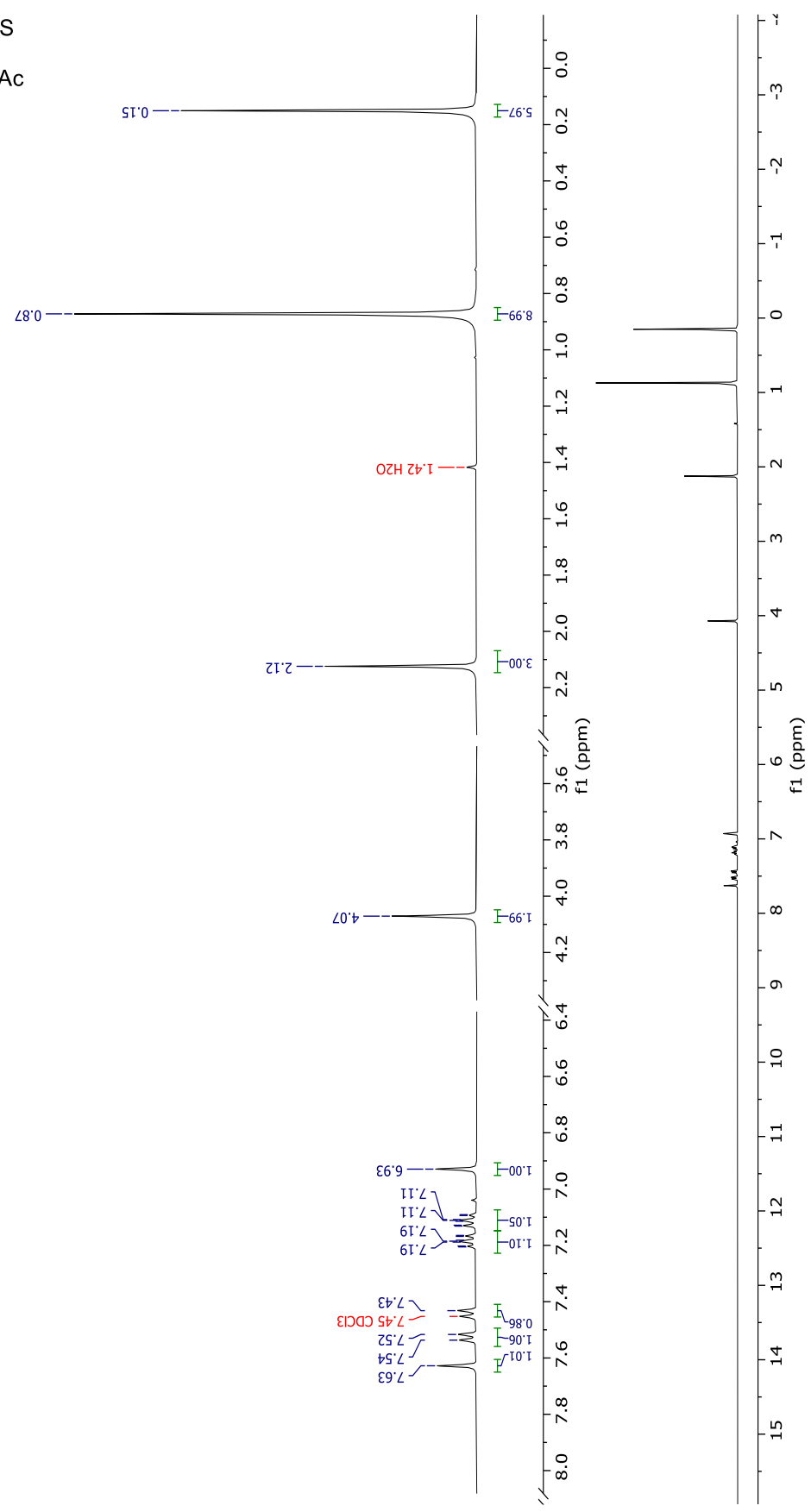
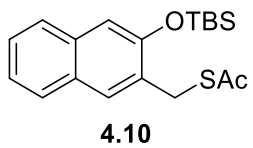


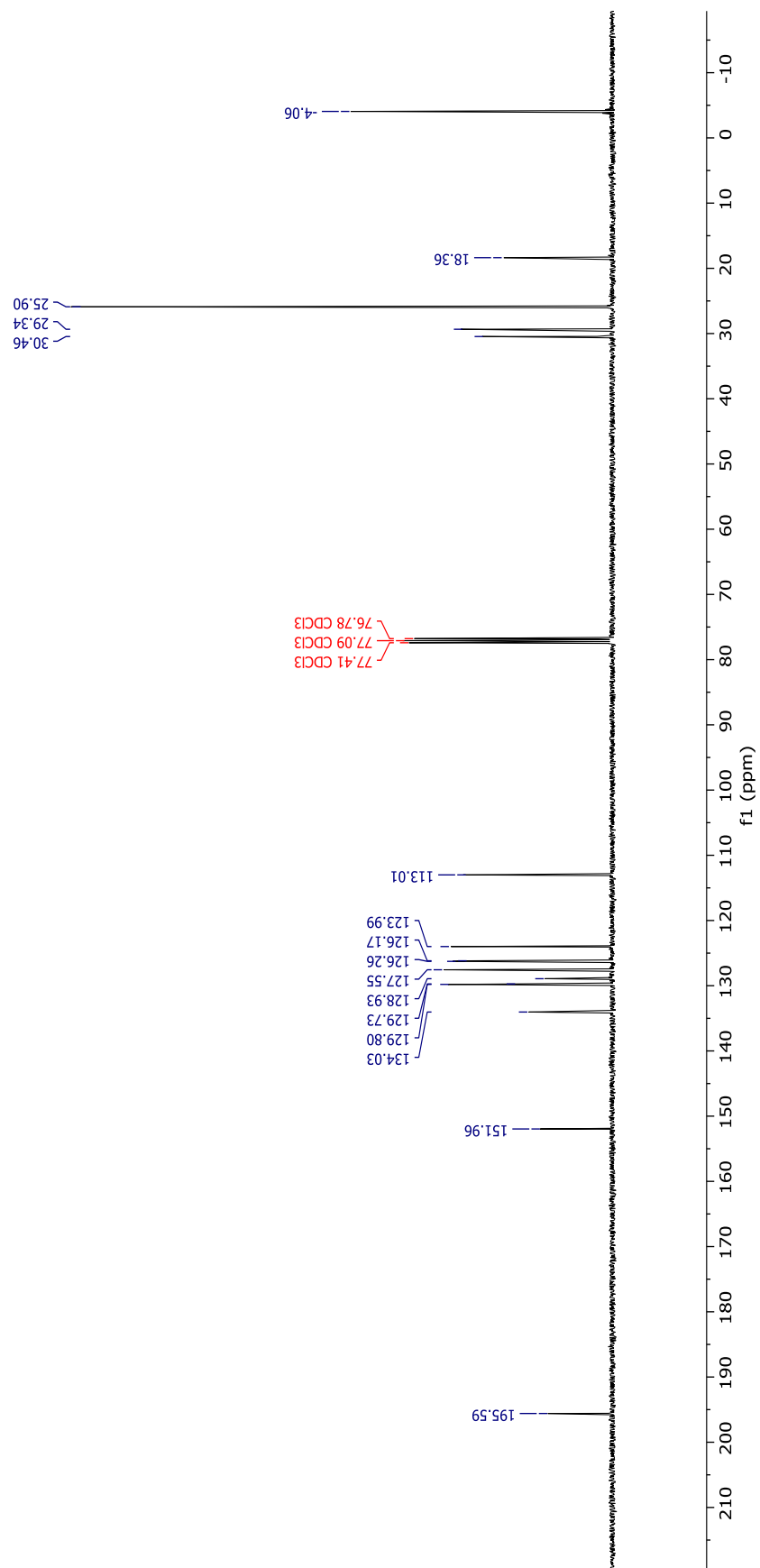
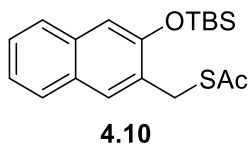
4.8

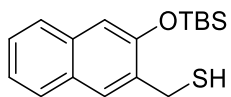




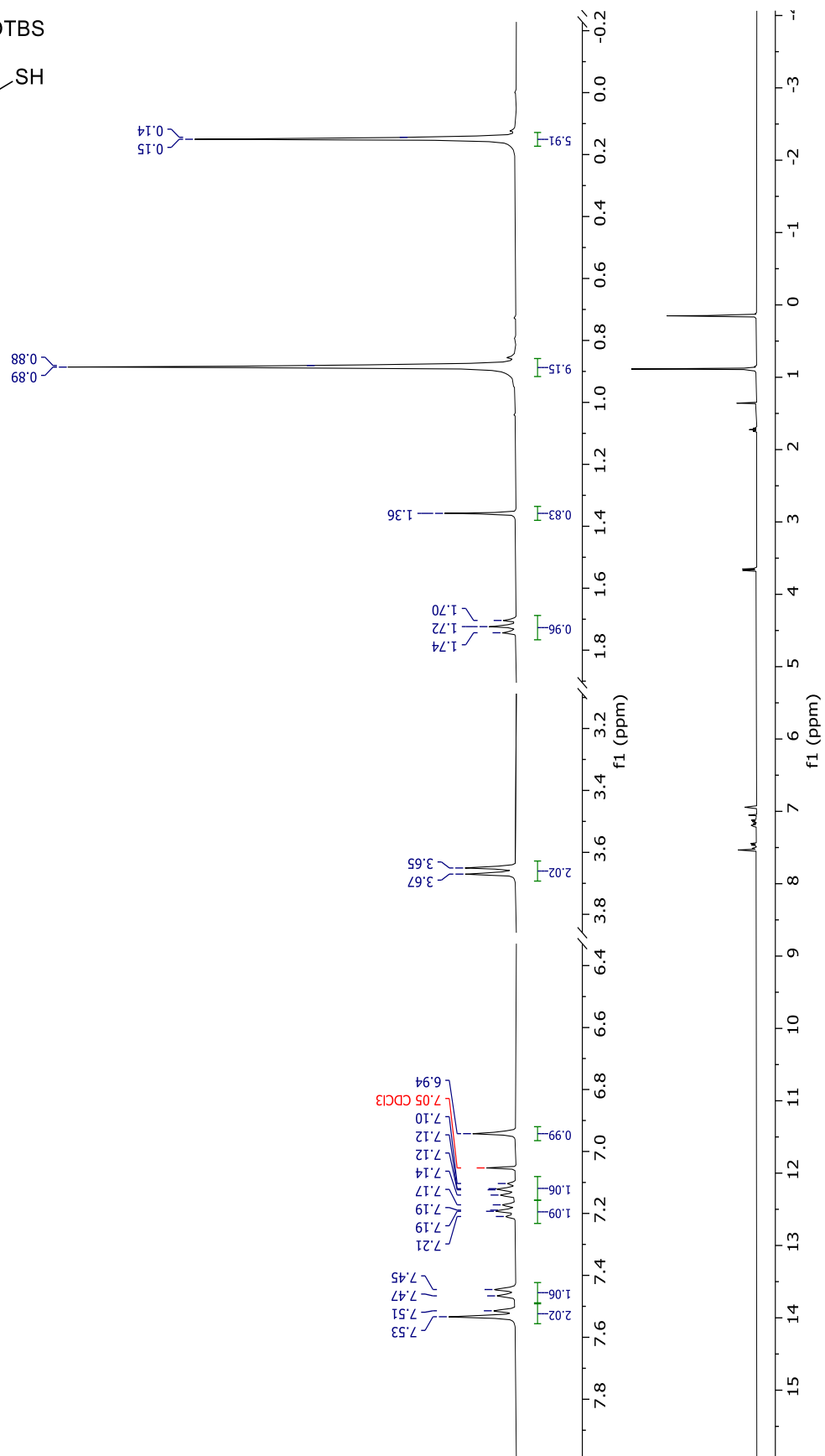


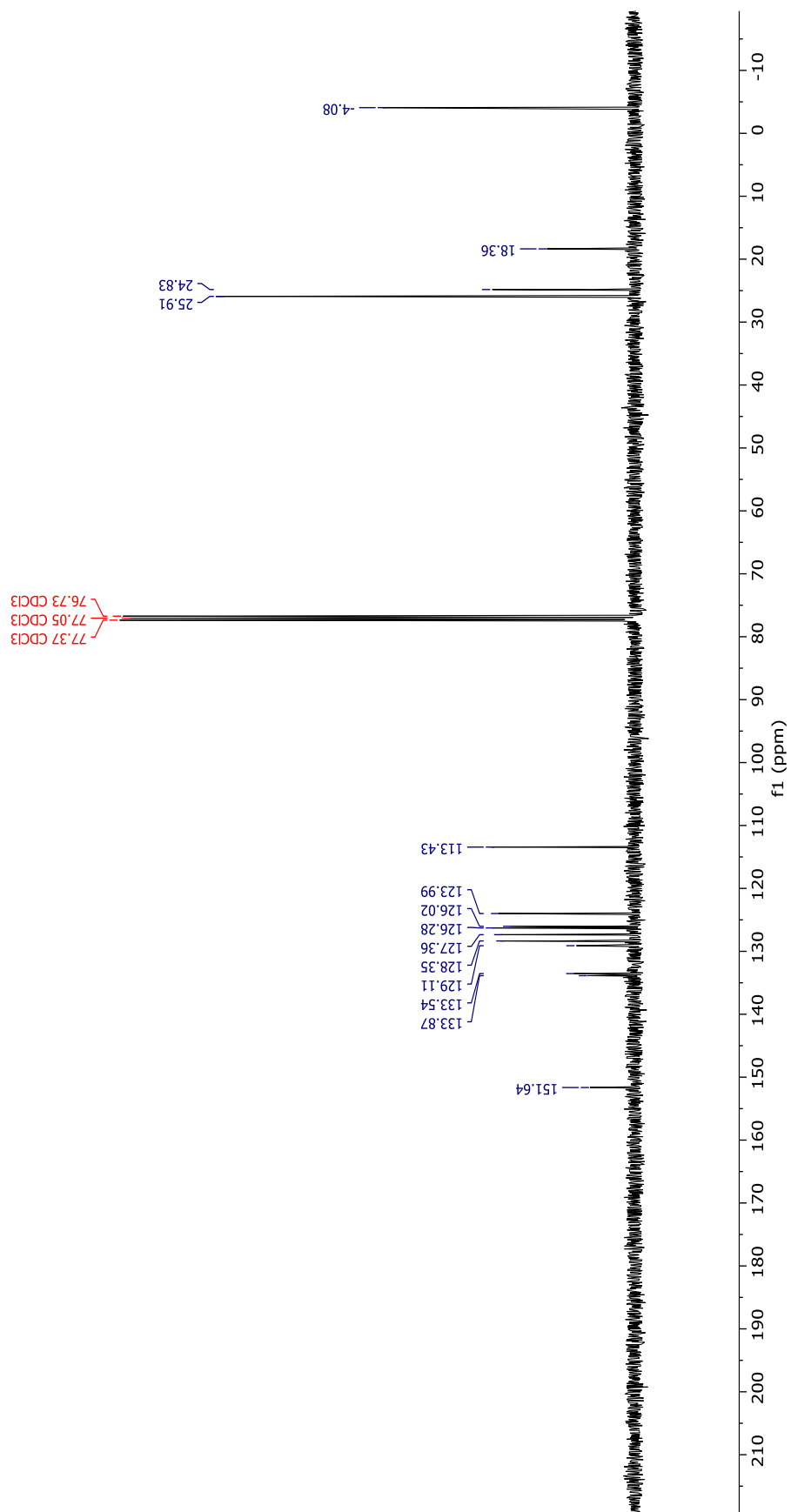
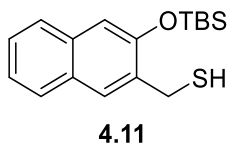


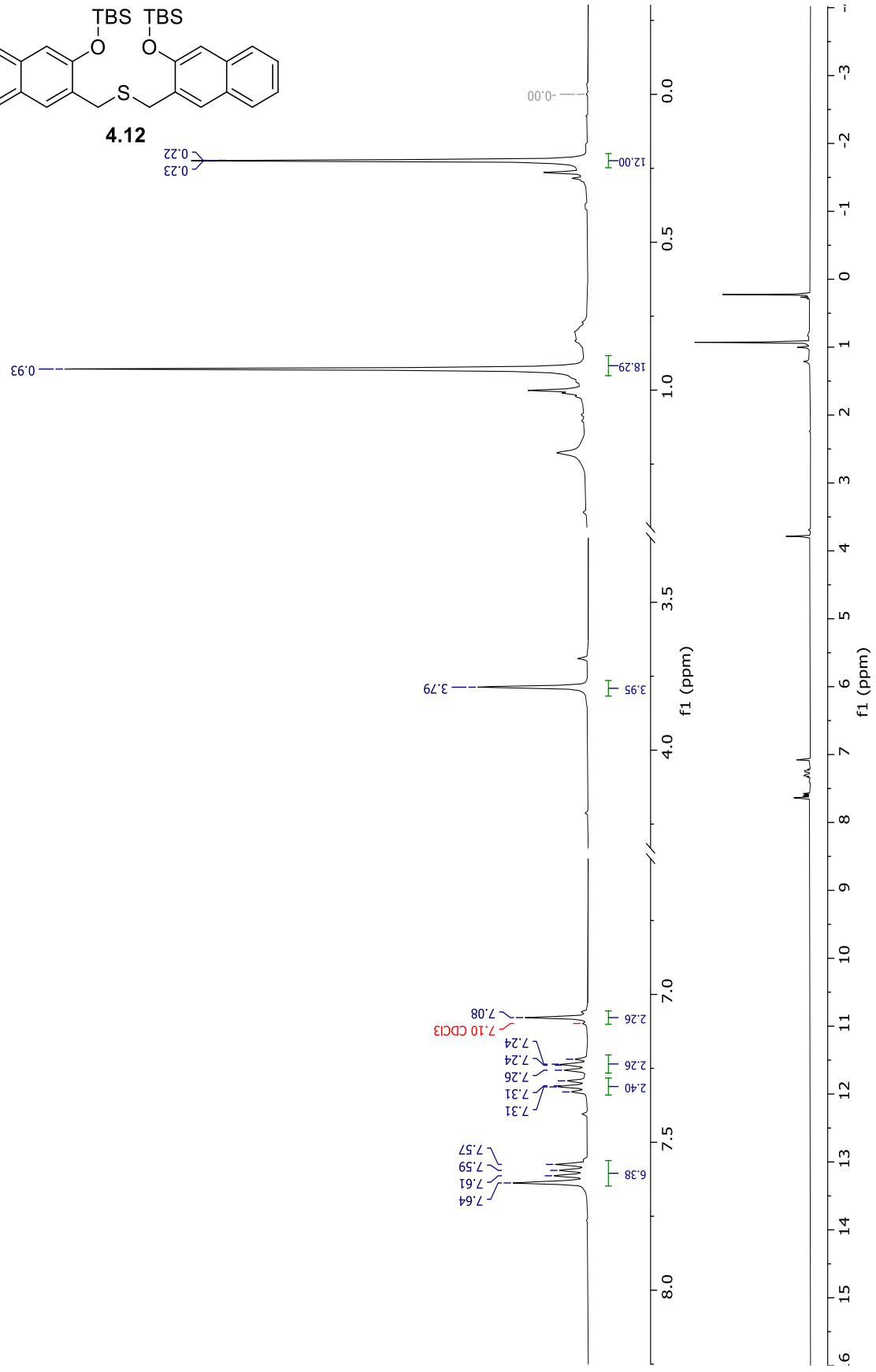
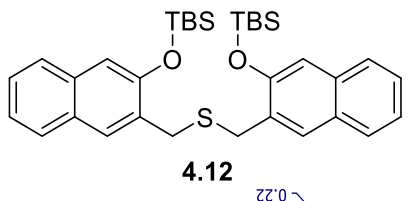


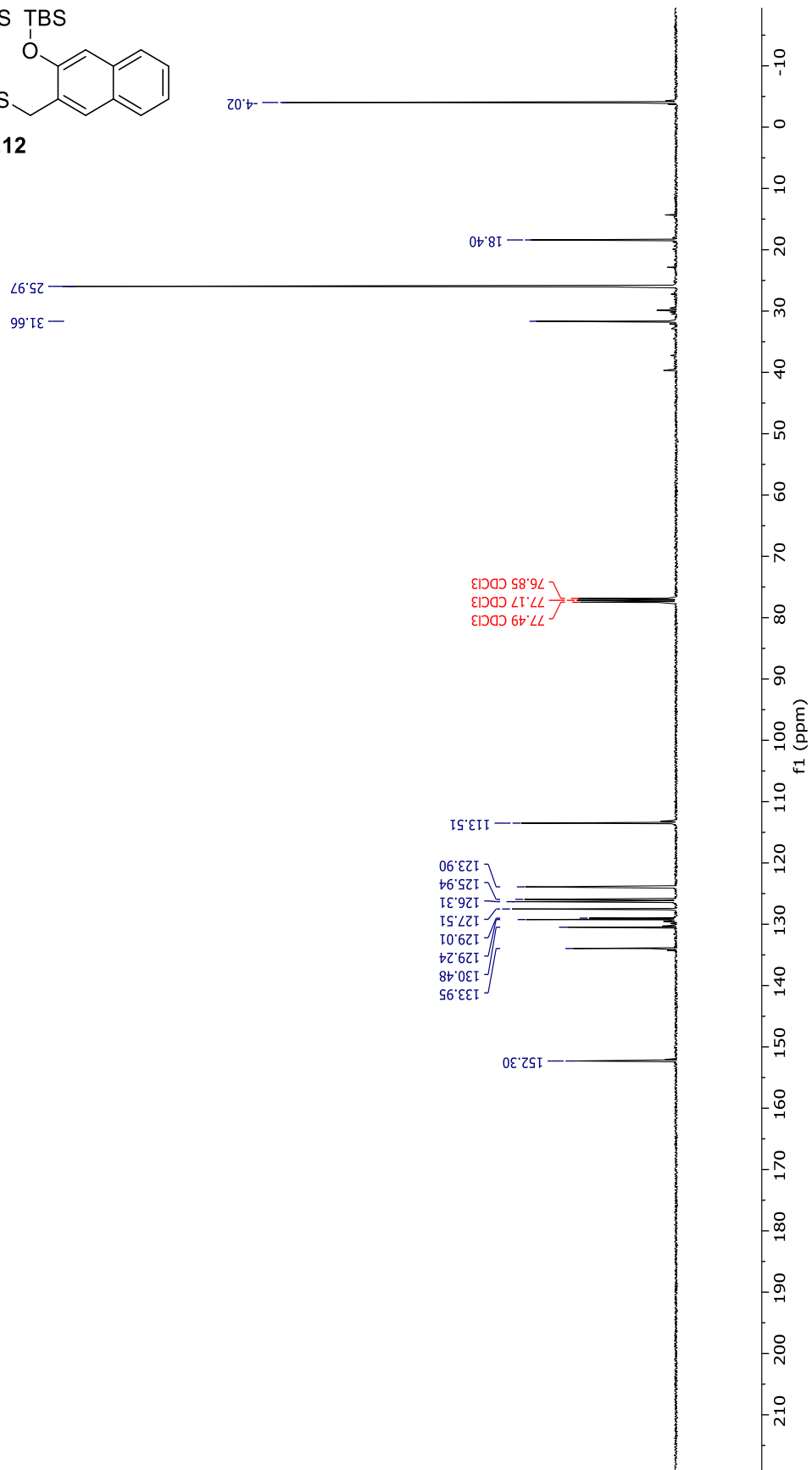
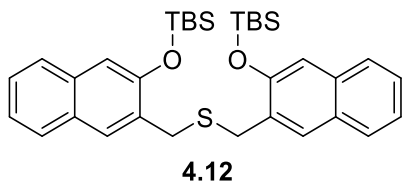


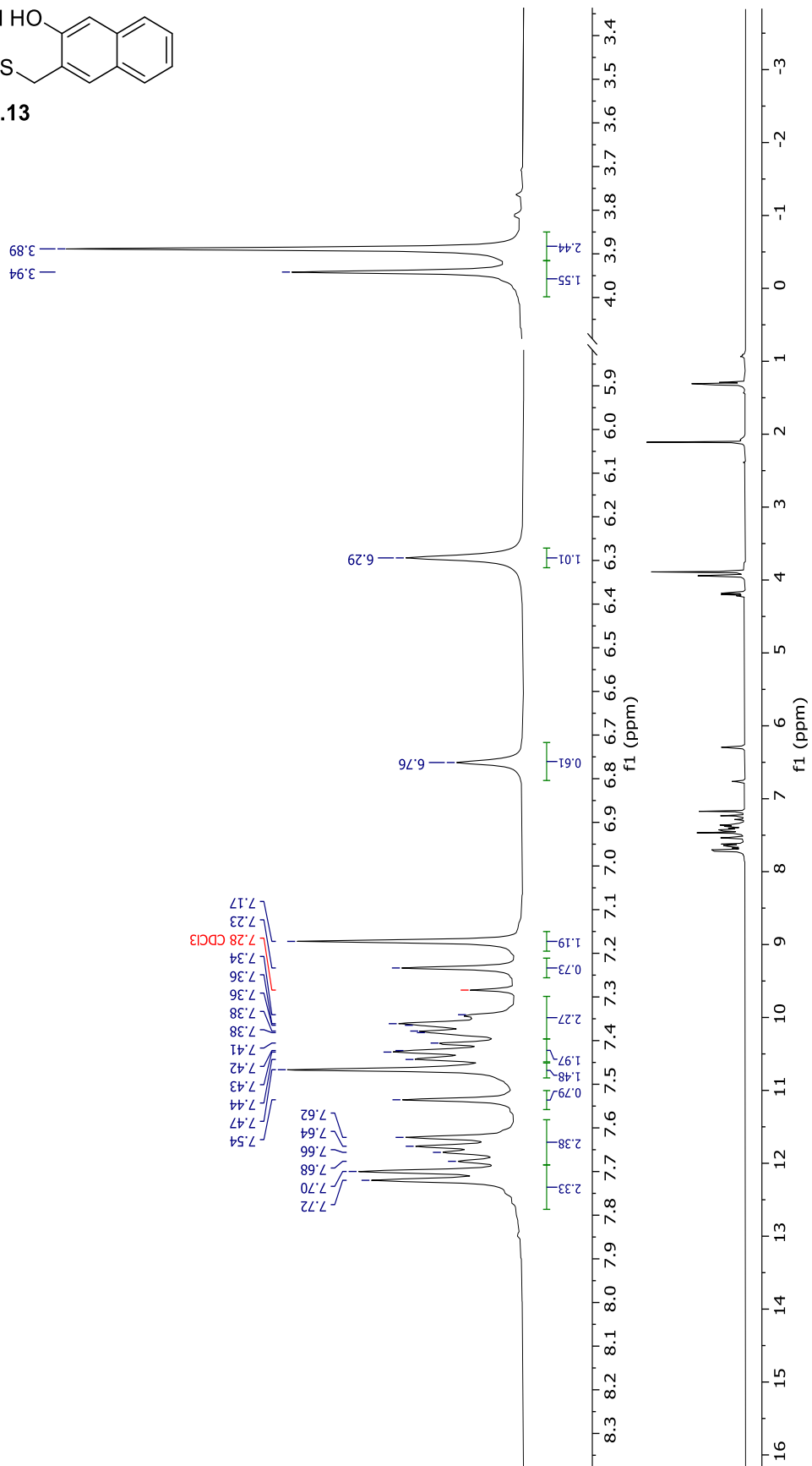
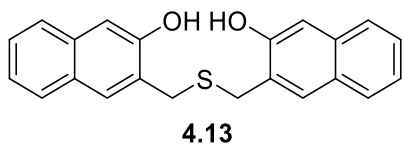
4.11

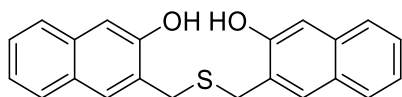




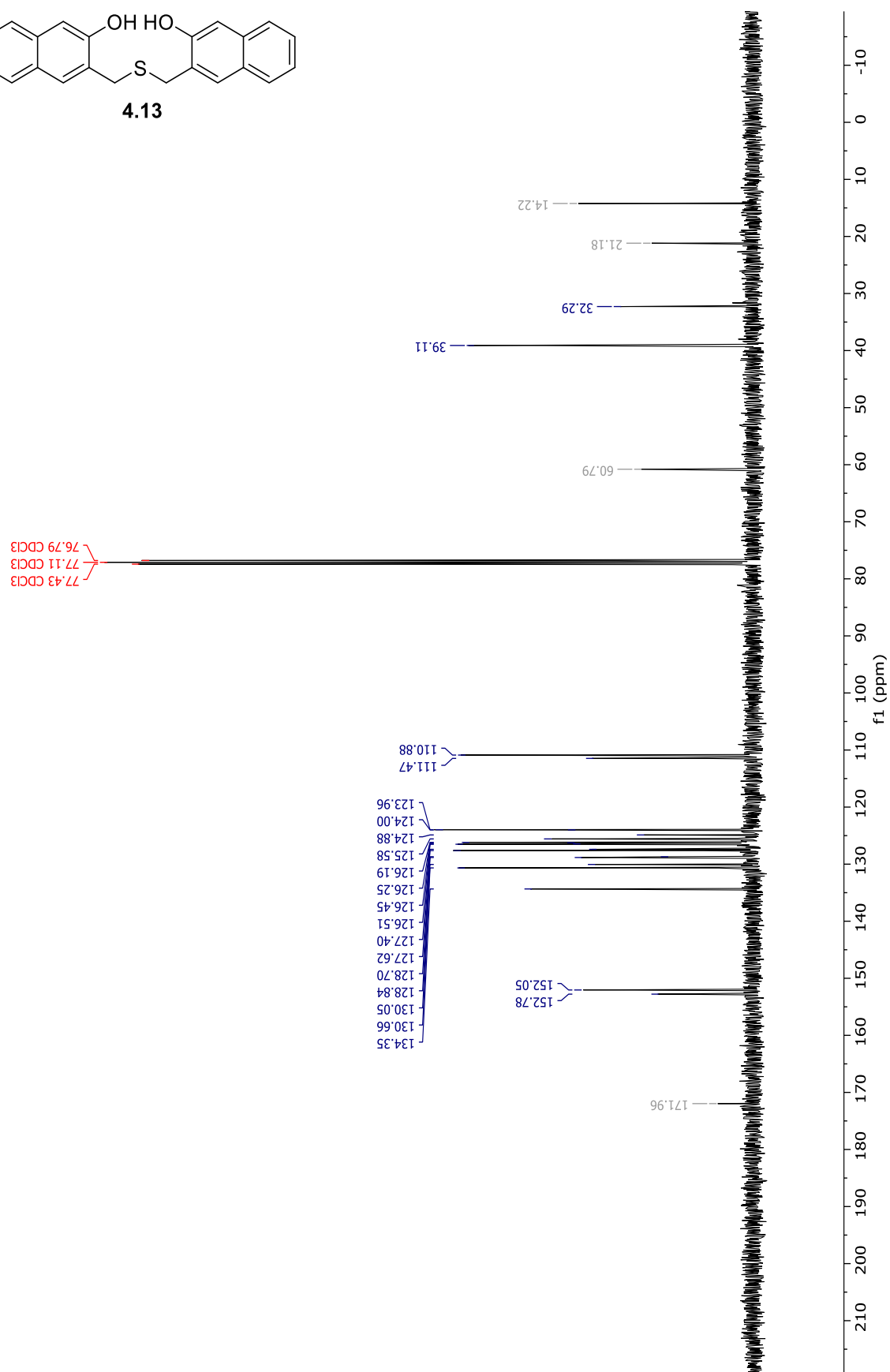


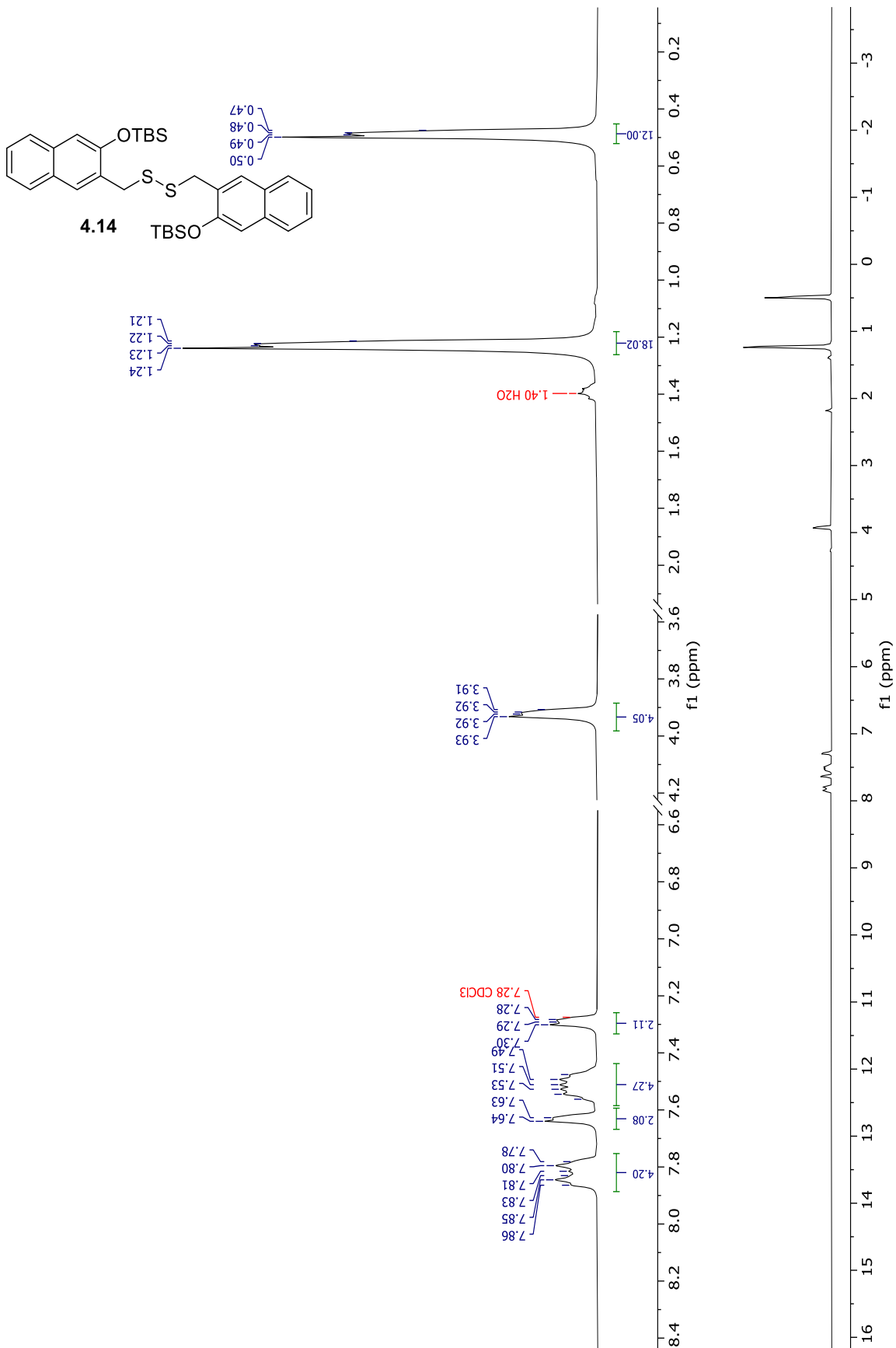


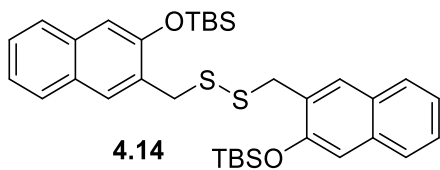




4.13







14.40
 18.51
 21.20
 26.13

-3.88

39.72

60.52

76.95 CDCl₃
 77.24
 77.27 CDCl₃
 77.58 CDCl₃

113.23

124.06

126.25

126.50

127.68

129.56

130.34

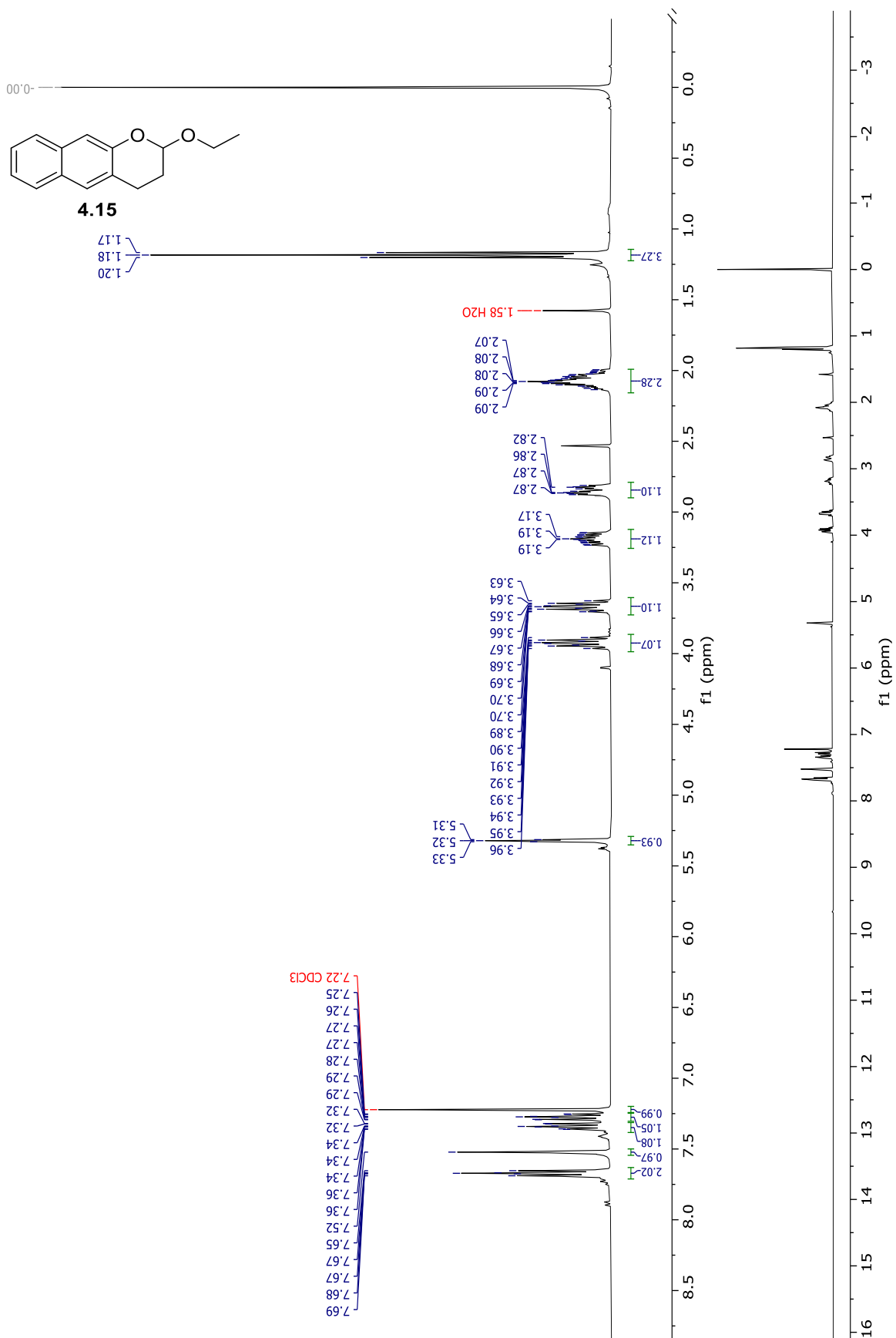
130.37

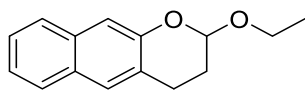
134.33

152.09

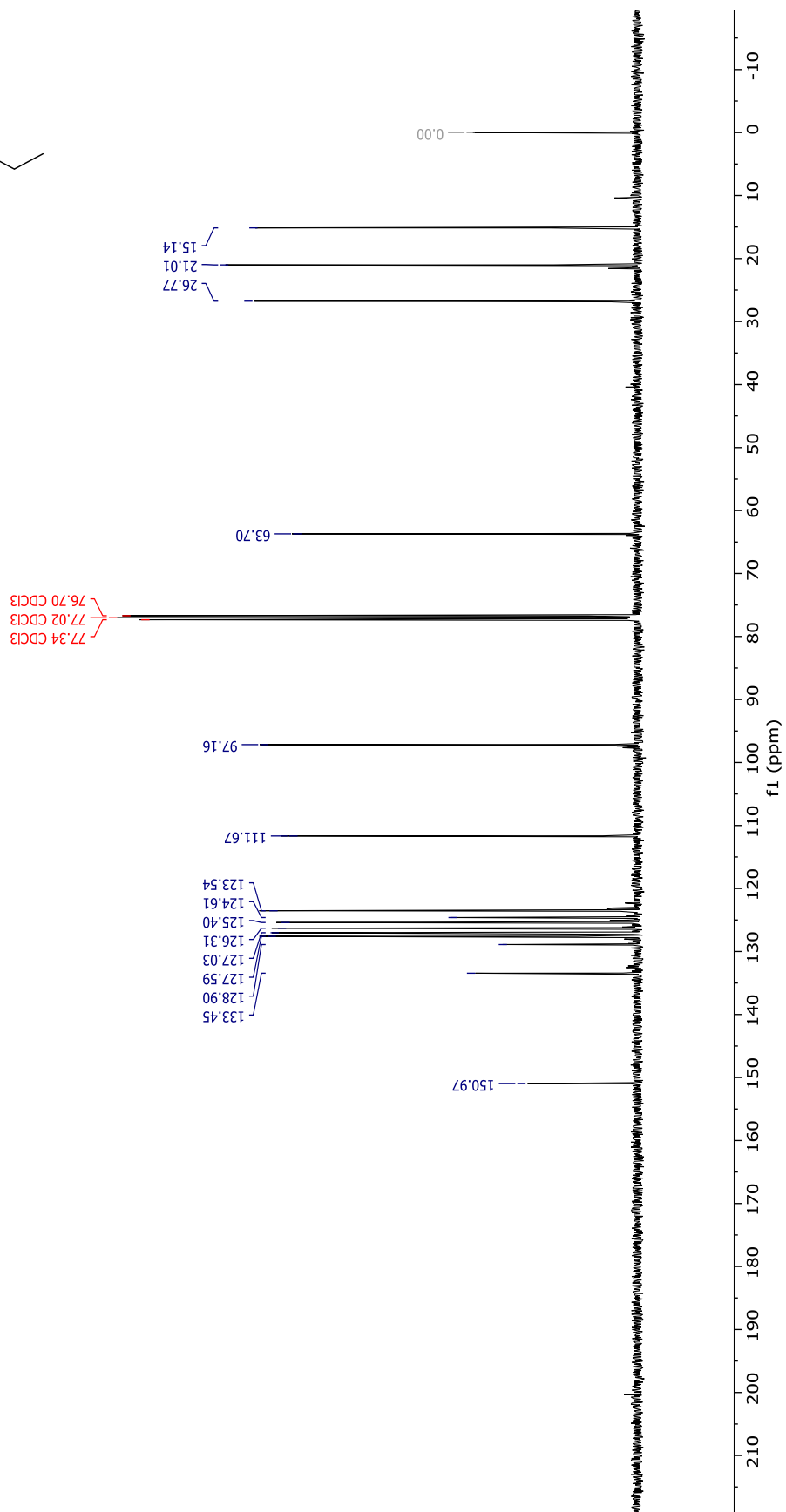
171.20

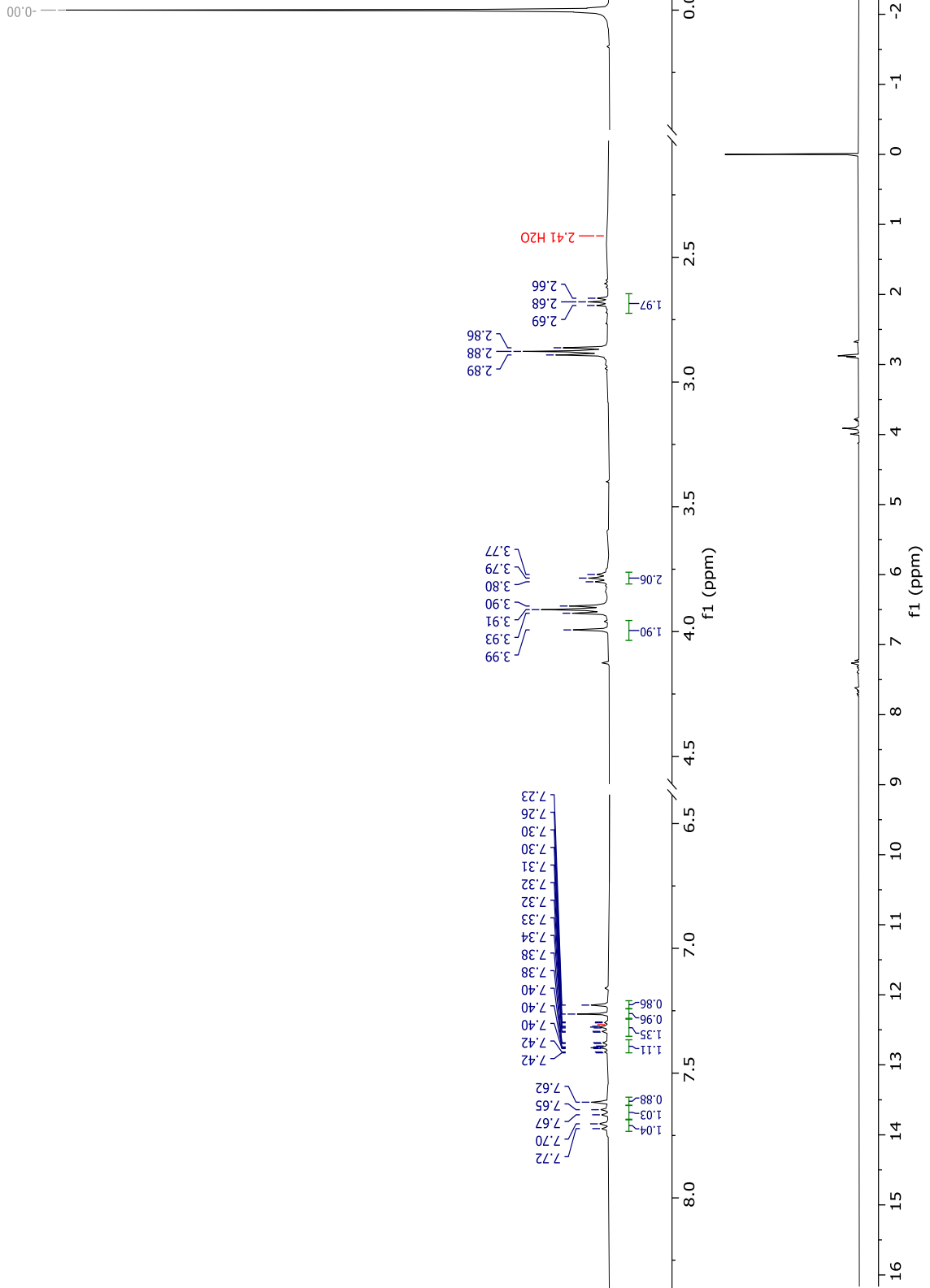
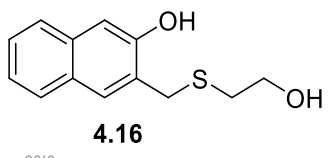
f1 (ppm)

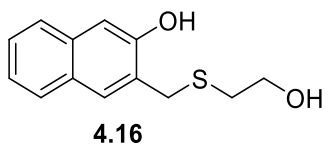




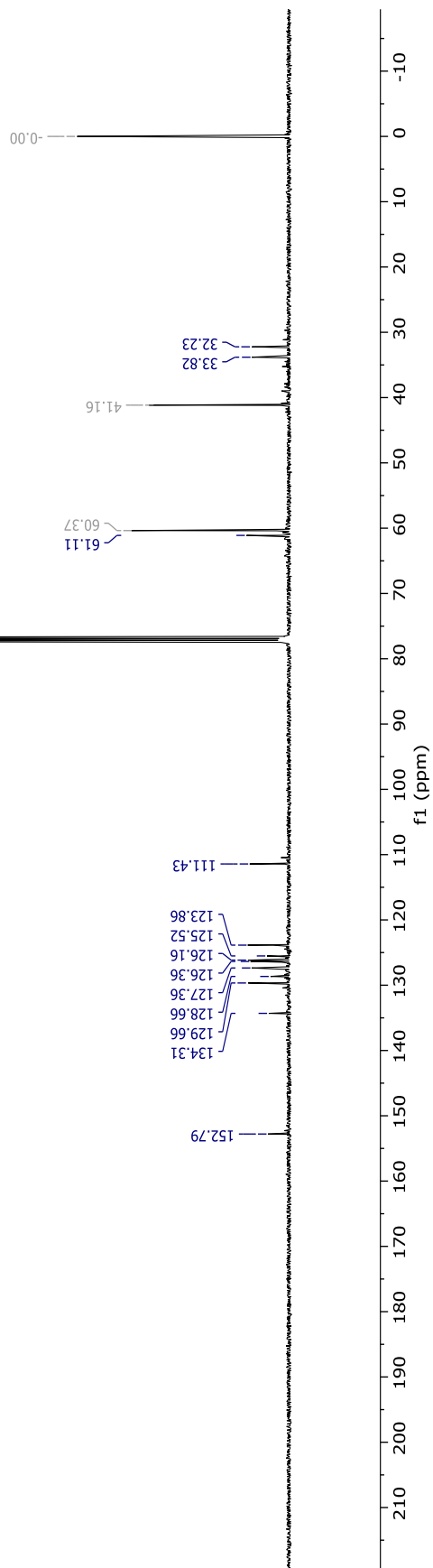
4.15

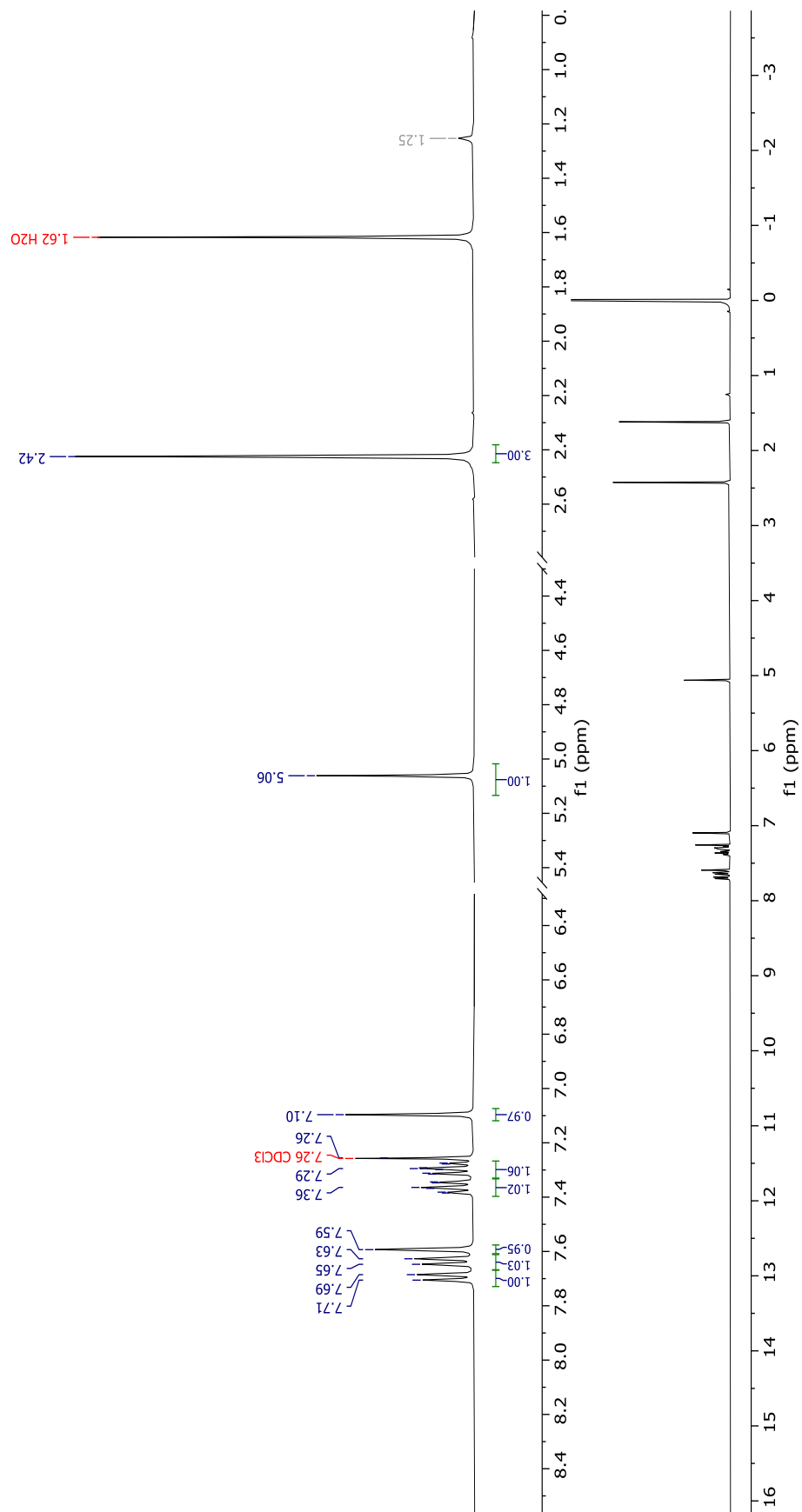
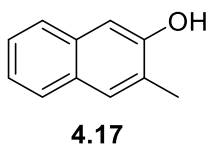


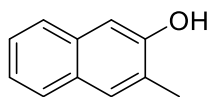




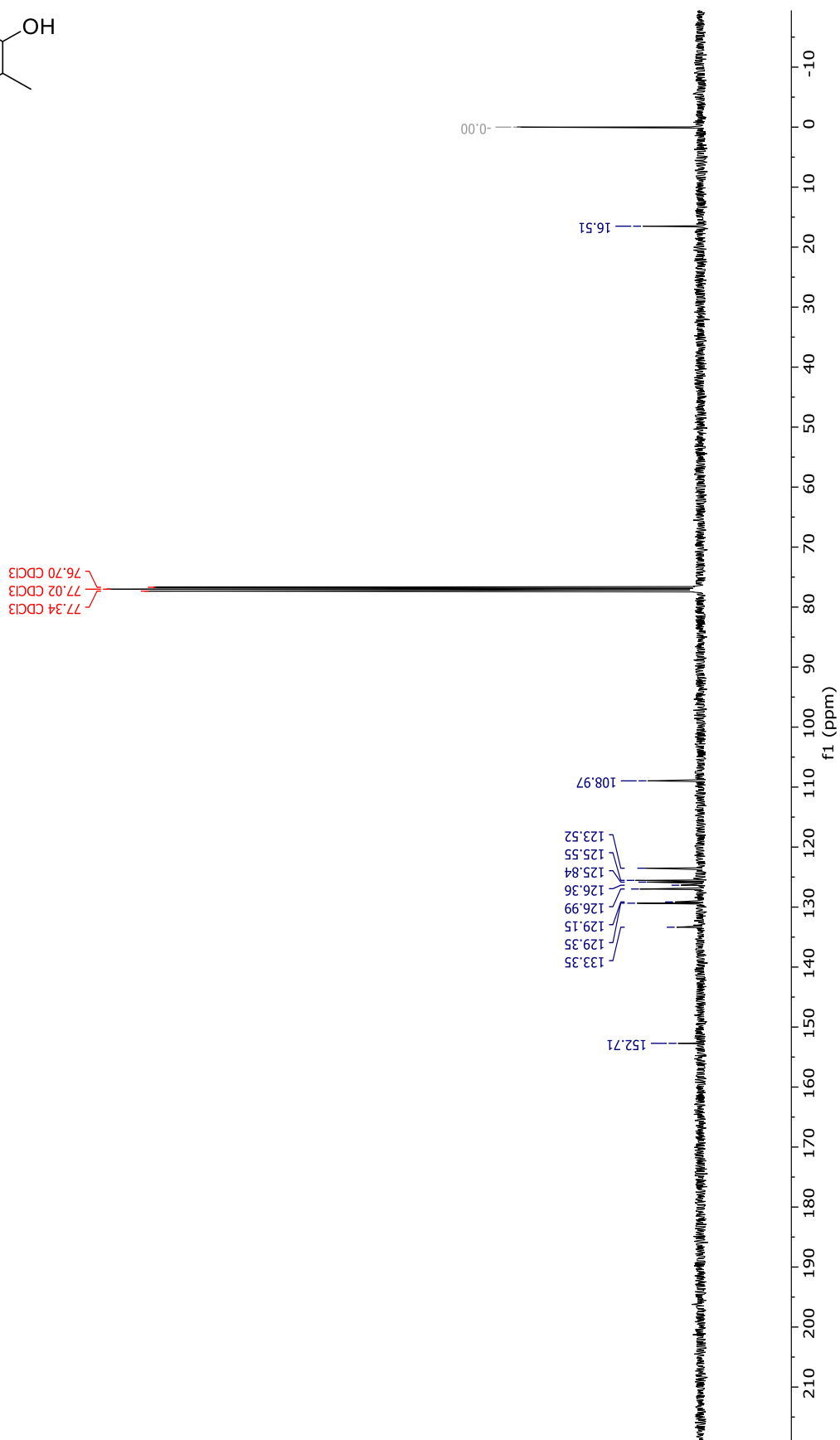
76.72 CDCl₃
77.03 CDCl₃
77.35 CDCl₃

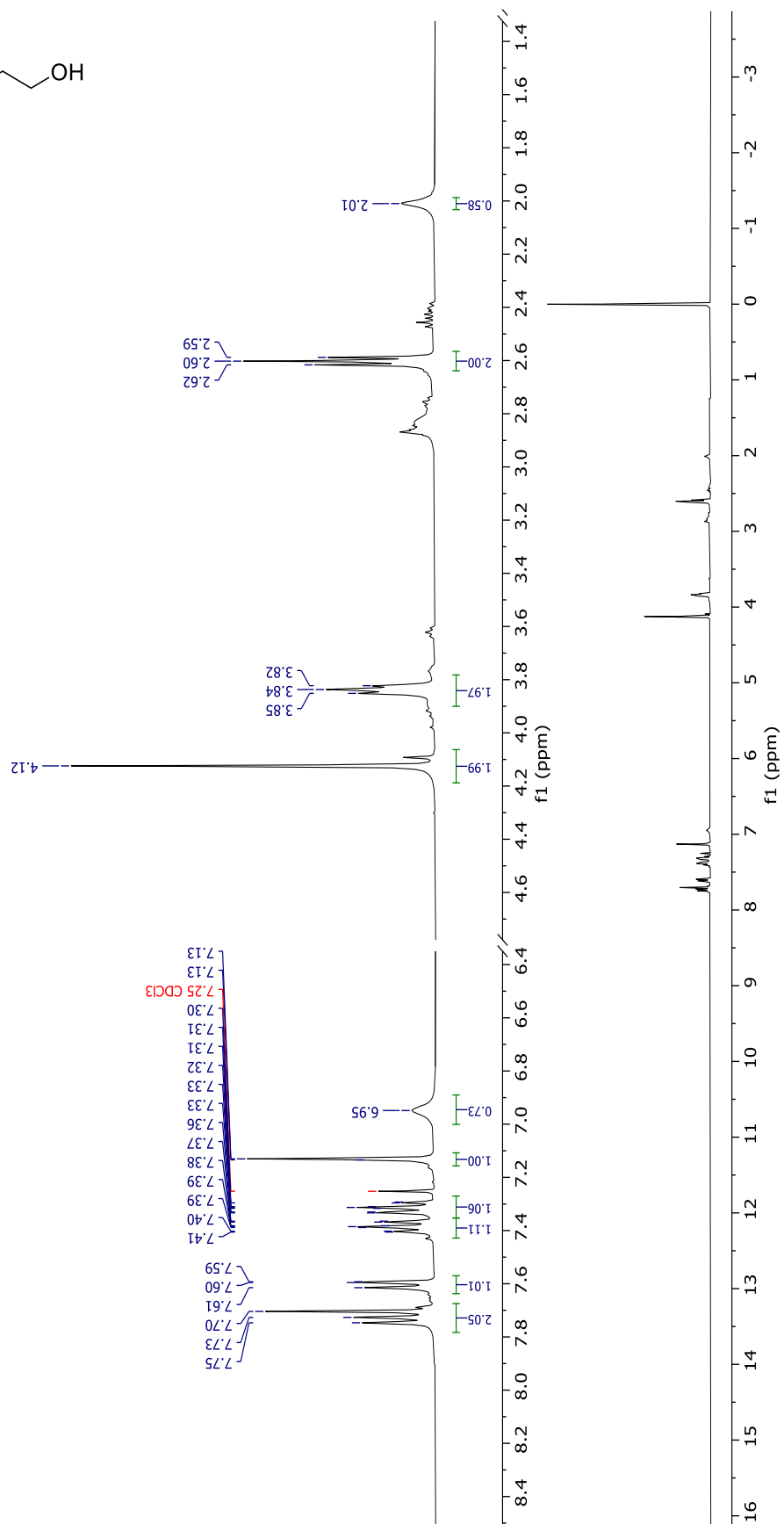
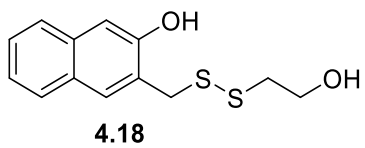


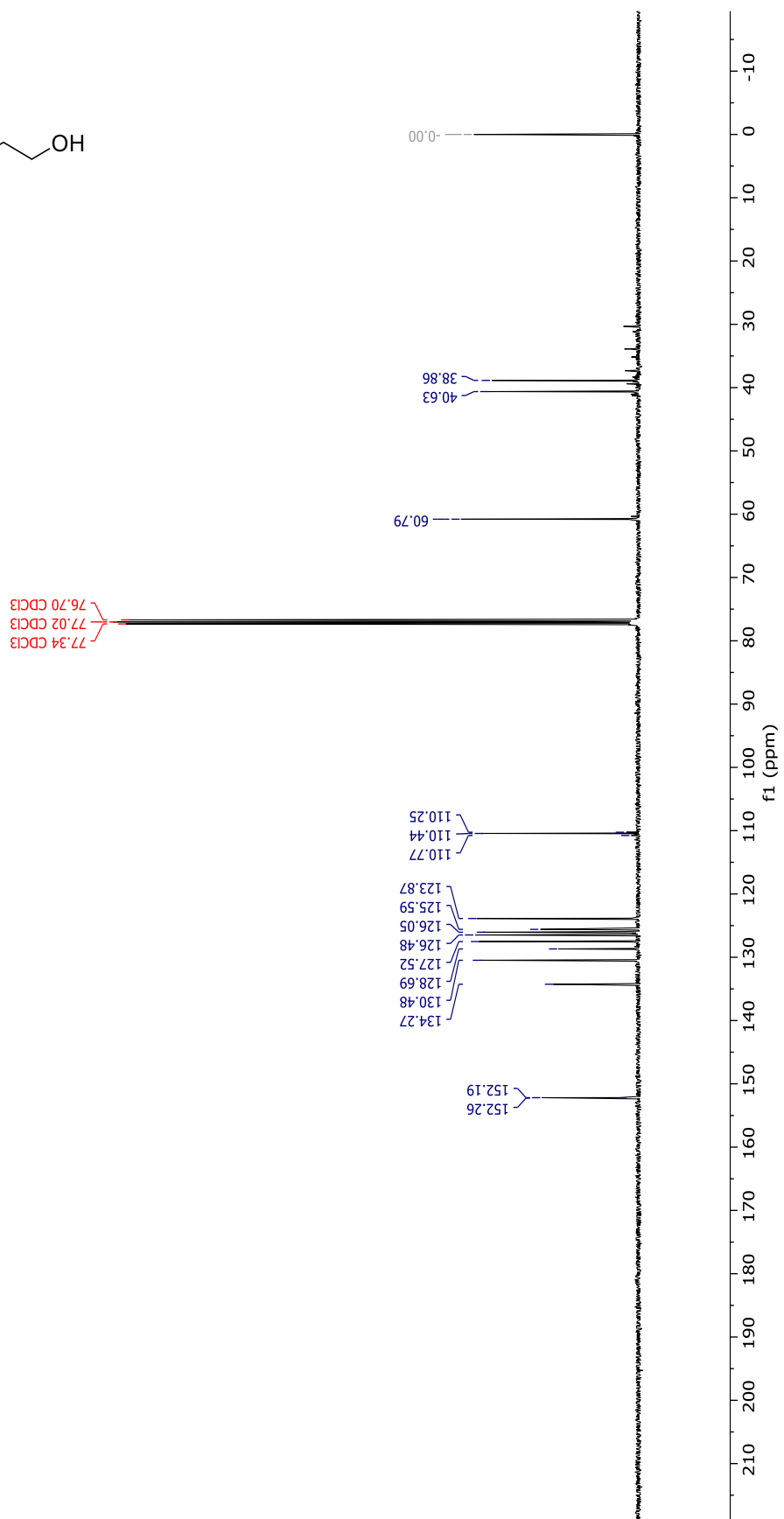
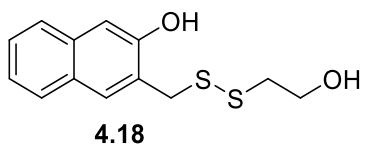


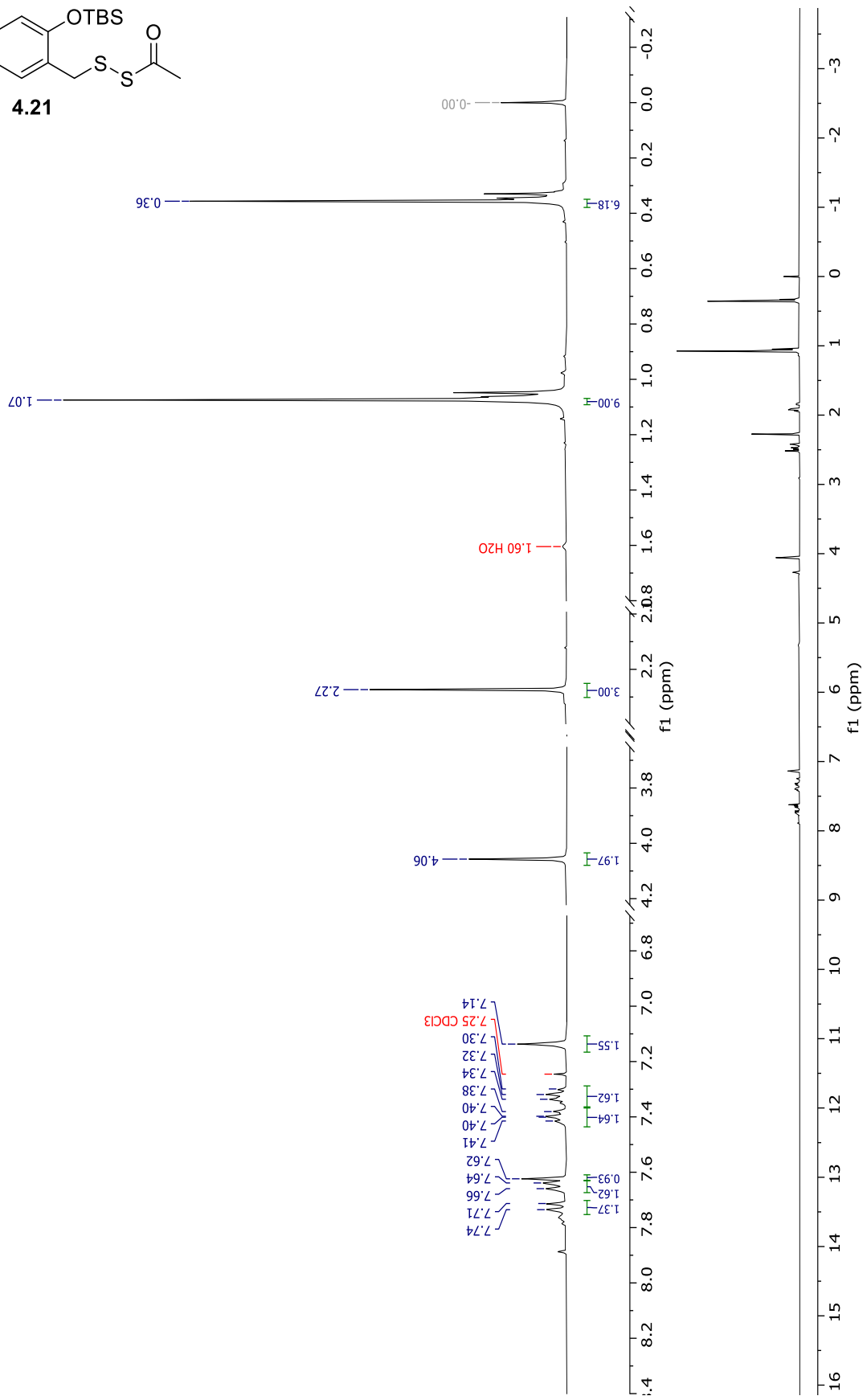
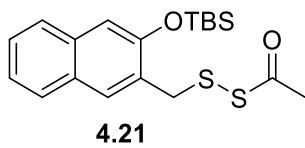


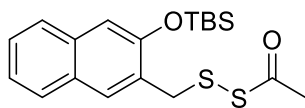
4.17



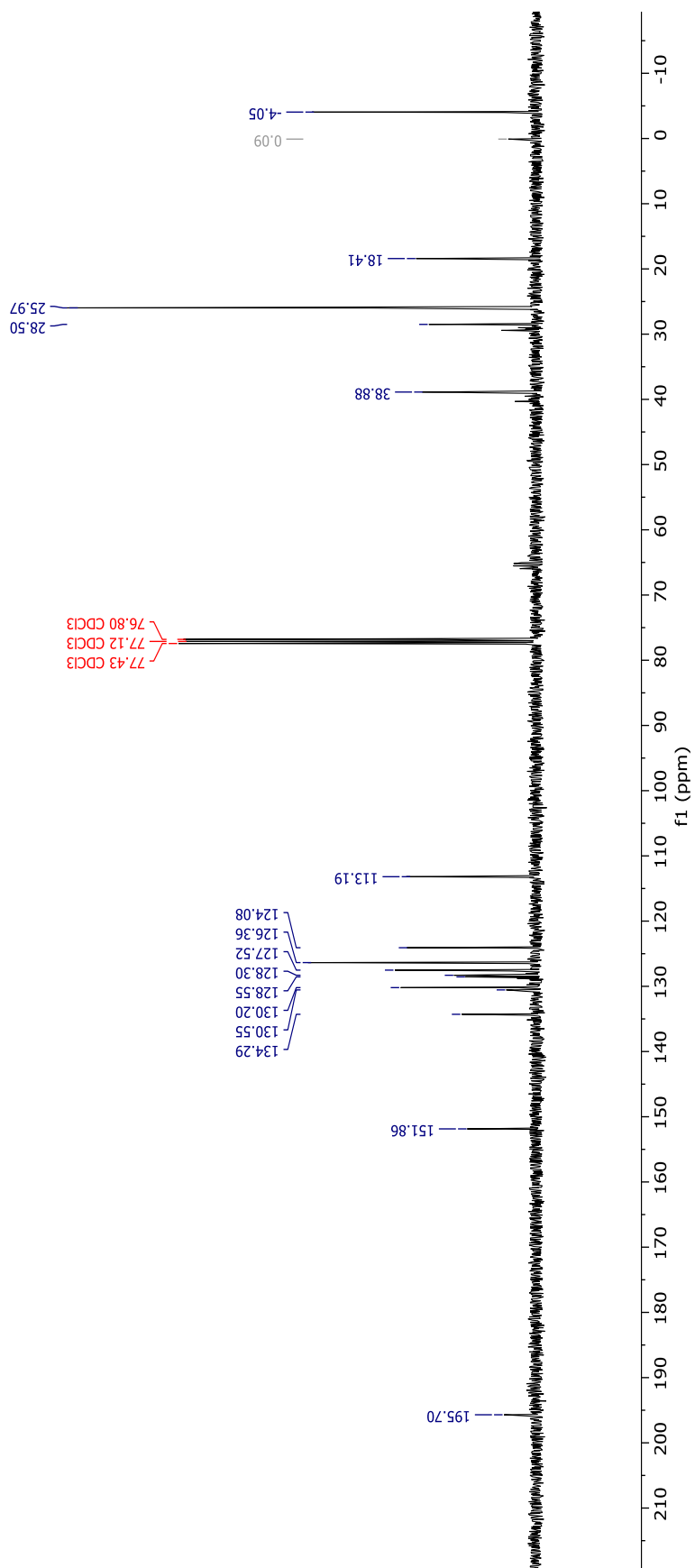


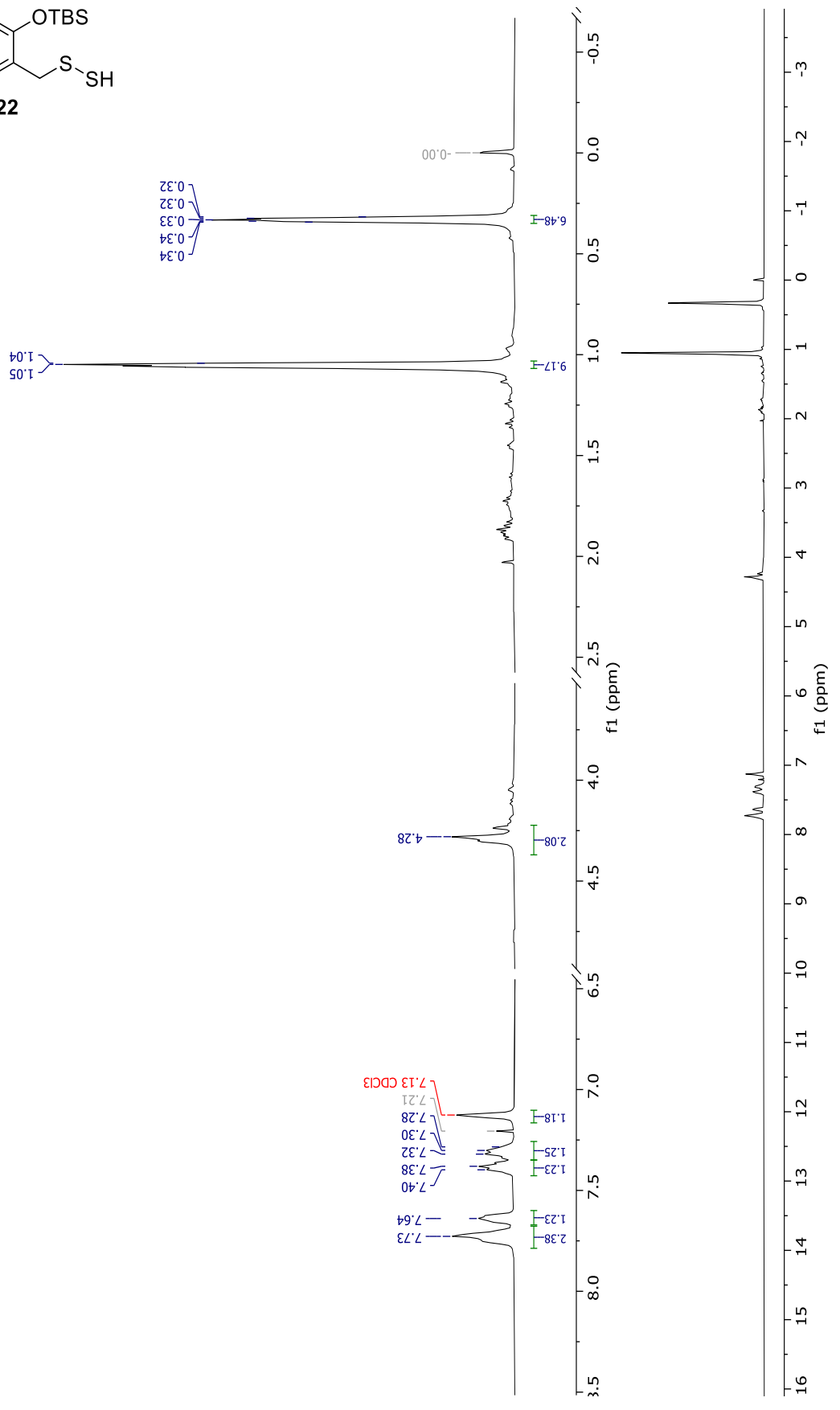
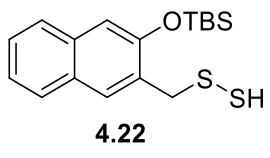


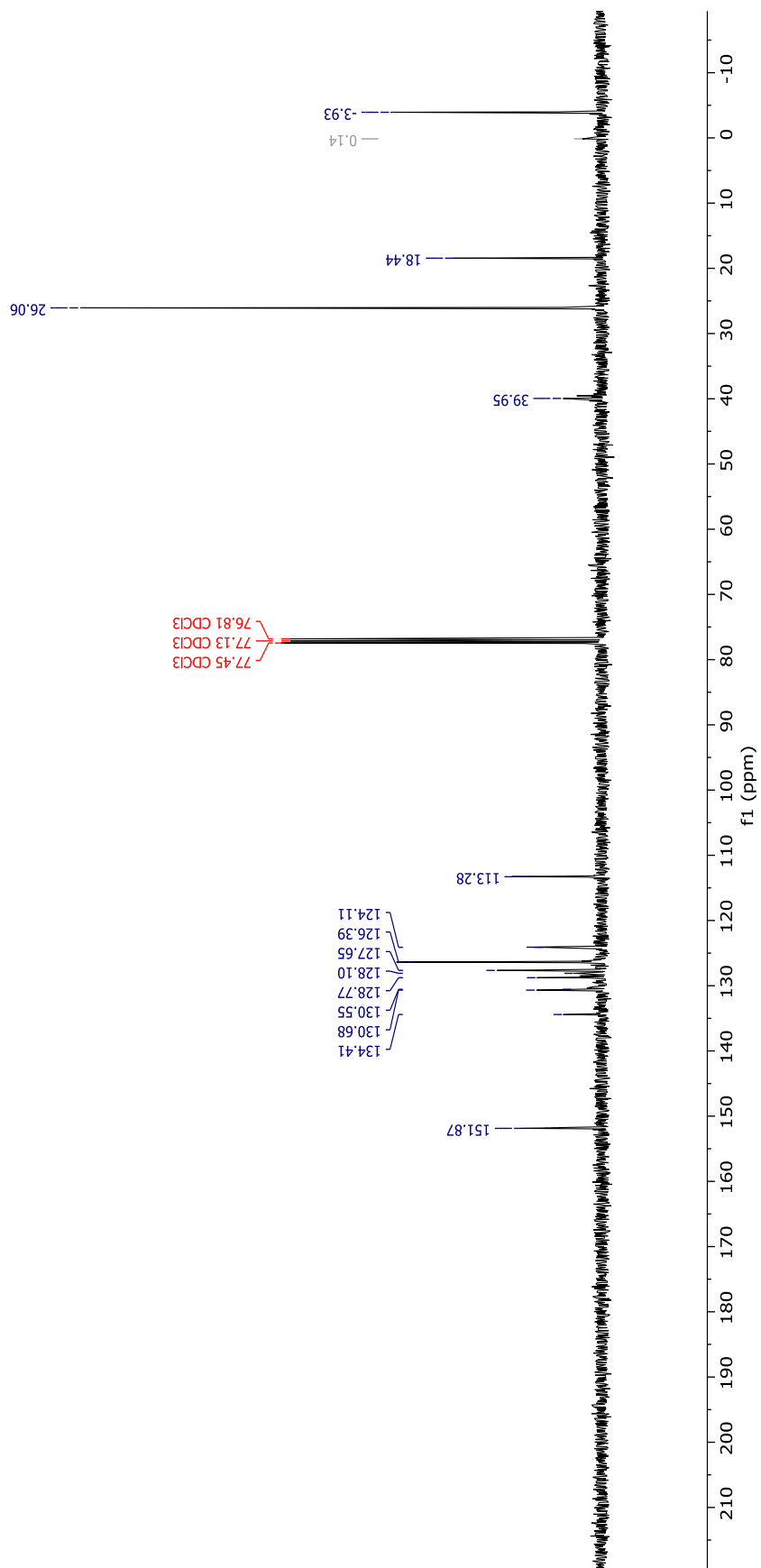
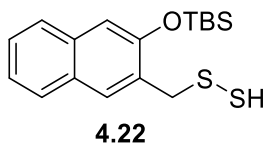


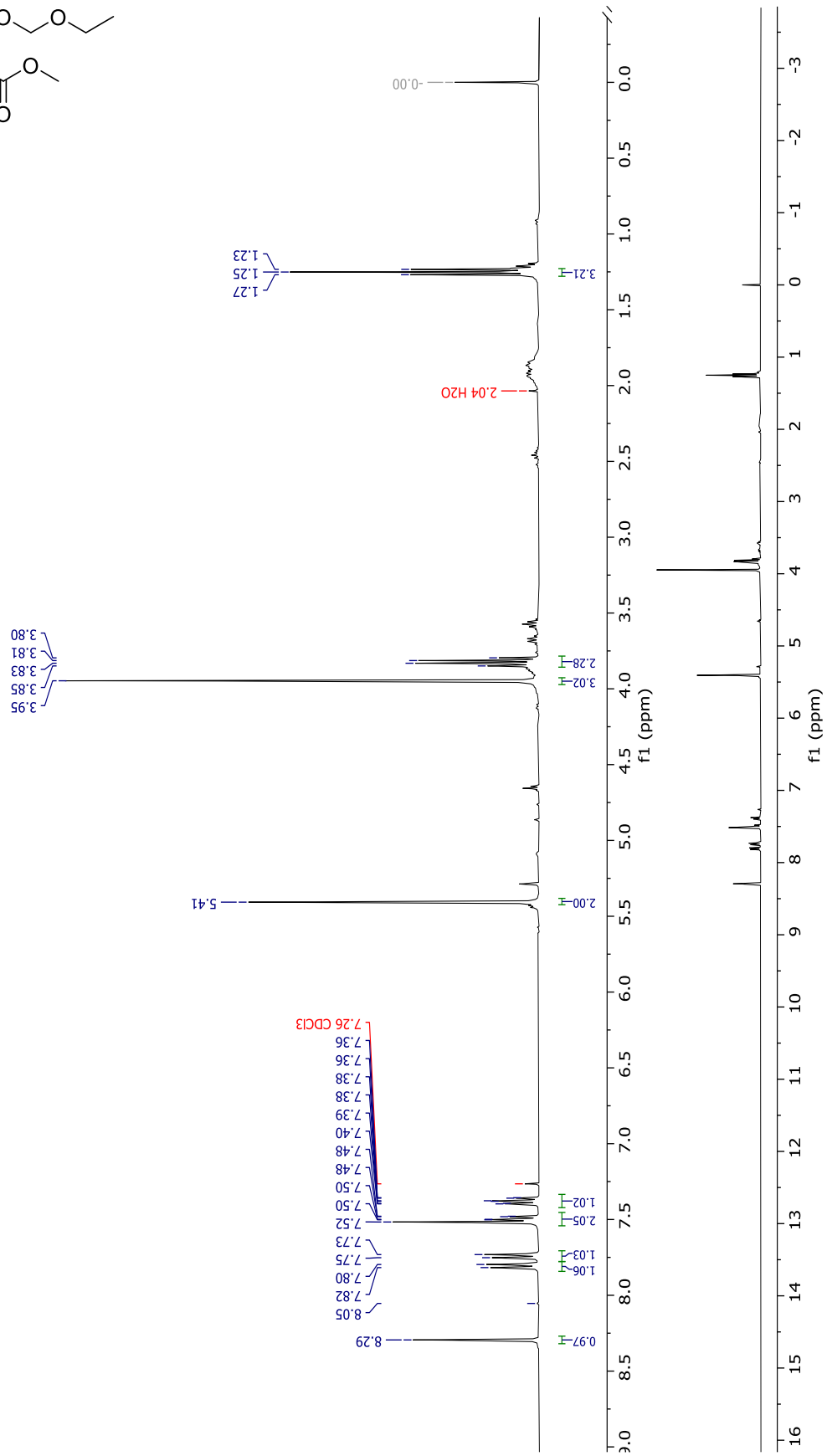
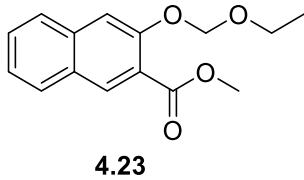


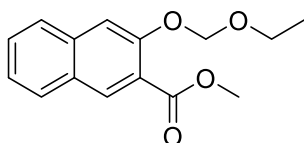
4.21



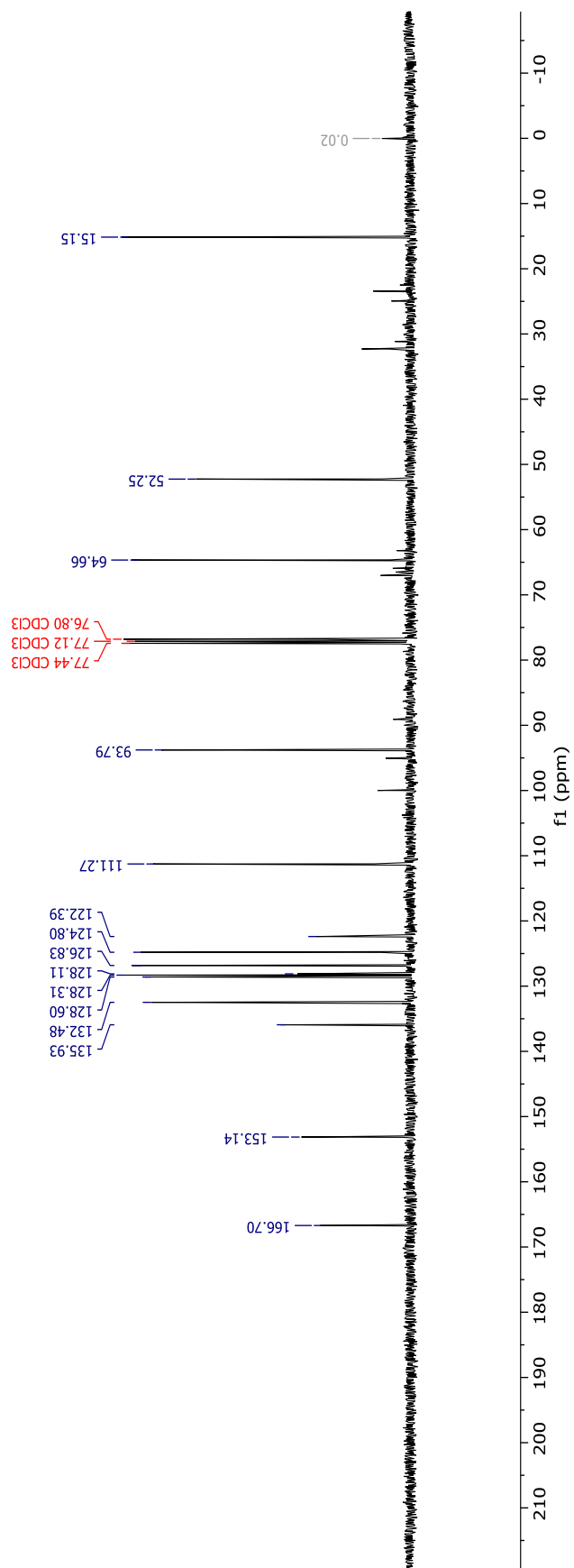


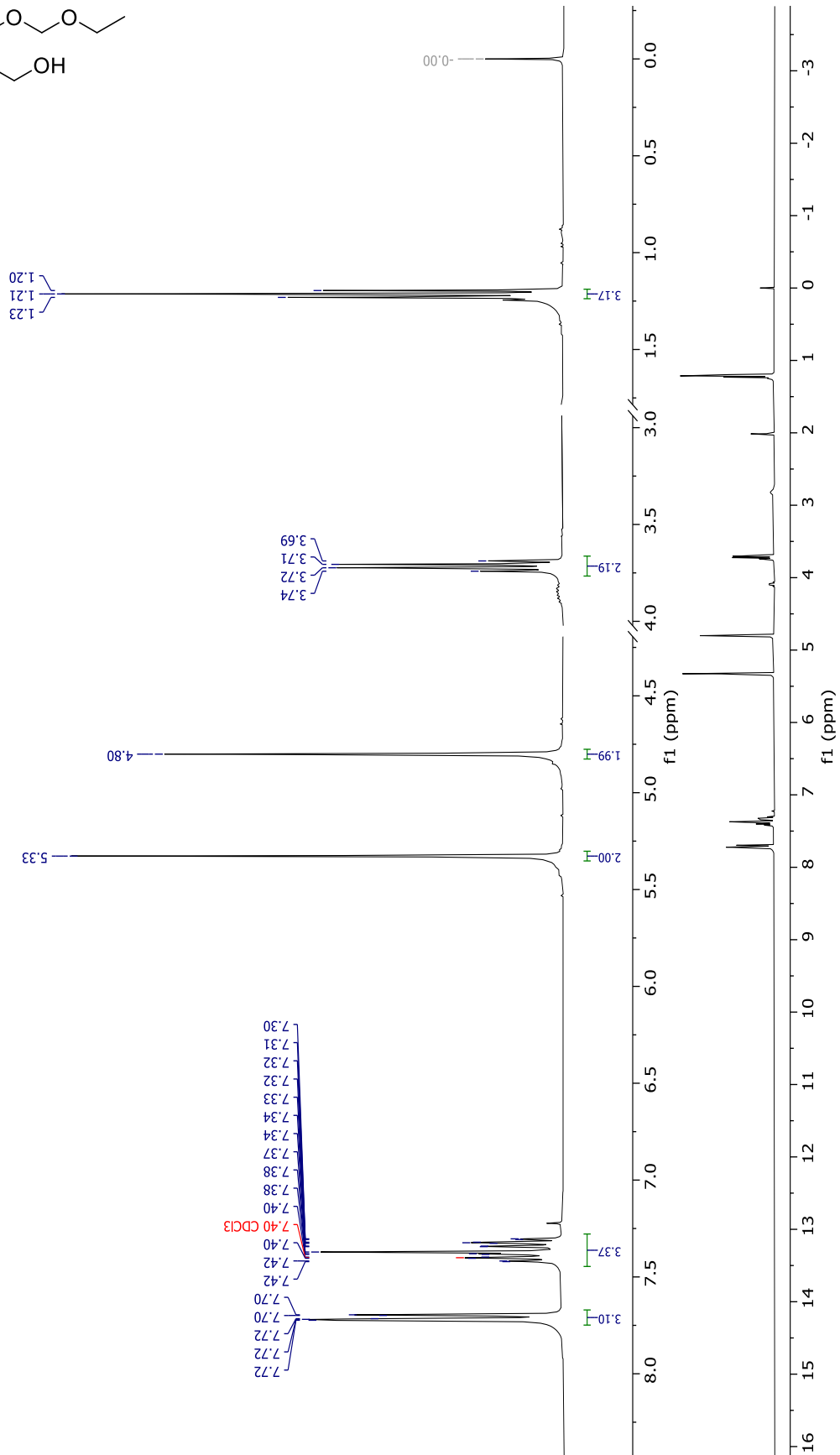
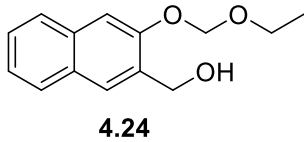


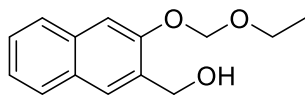




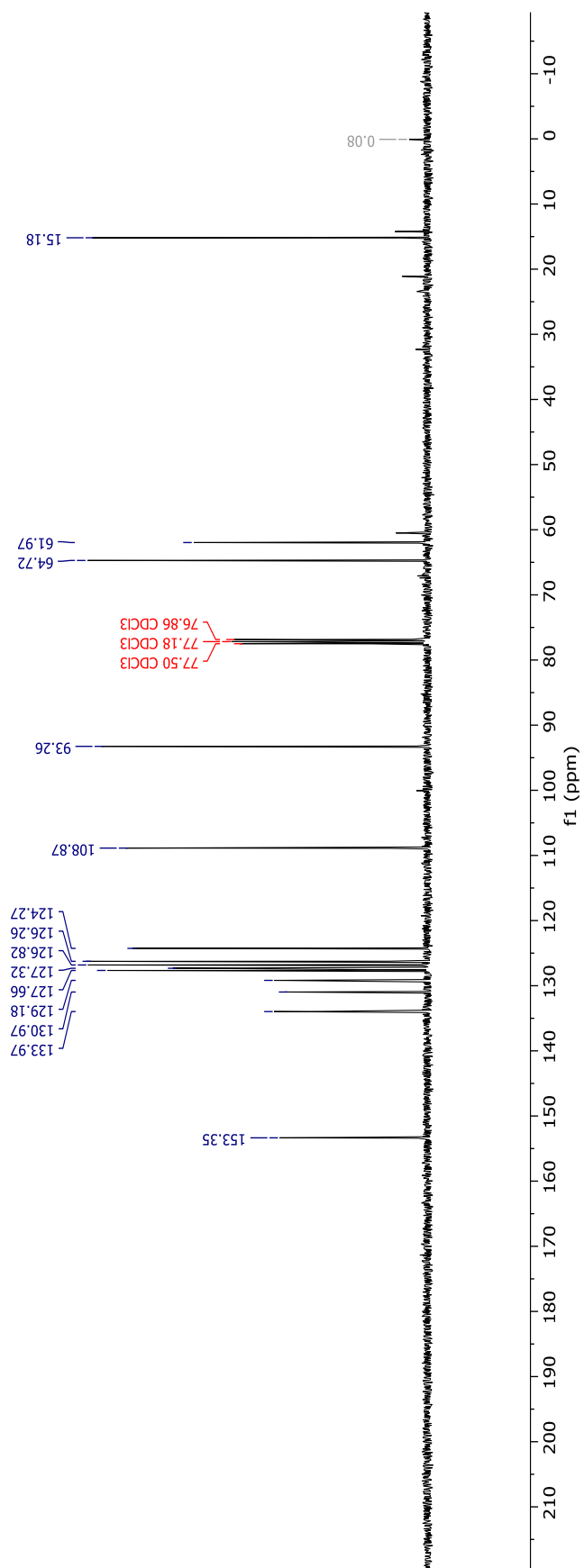
4.23

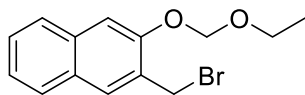




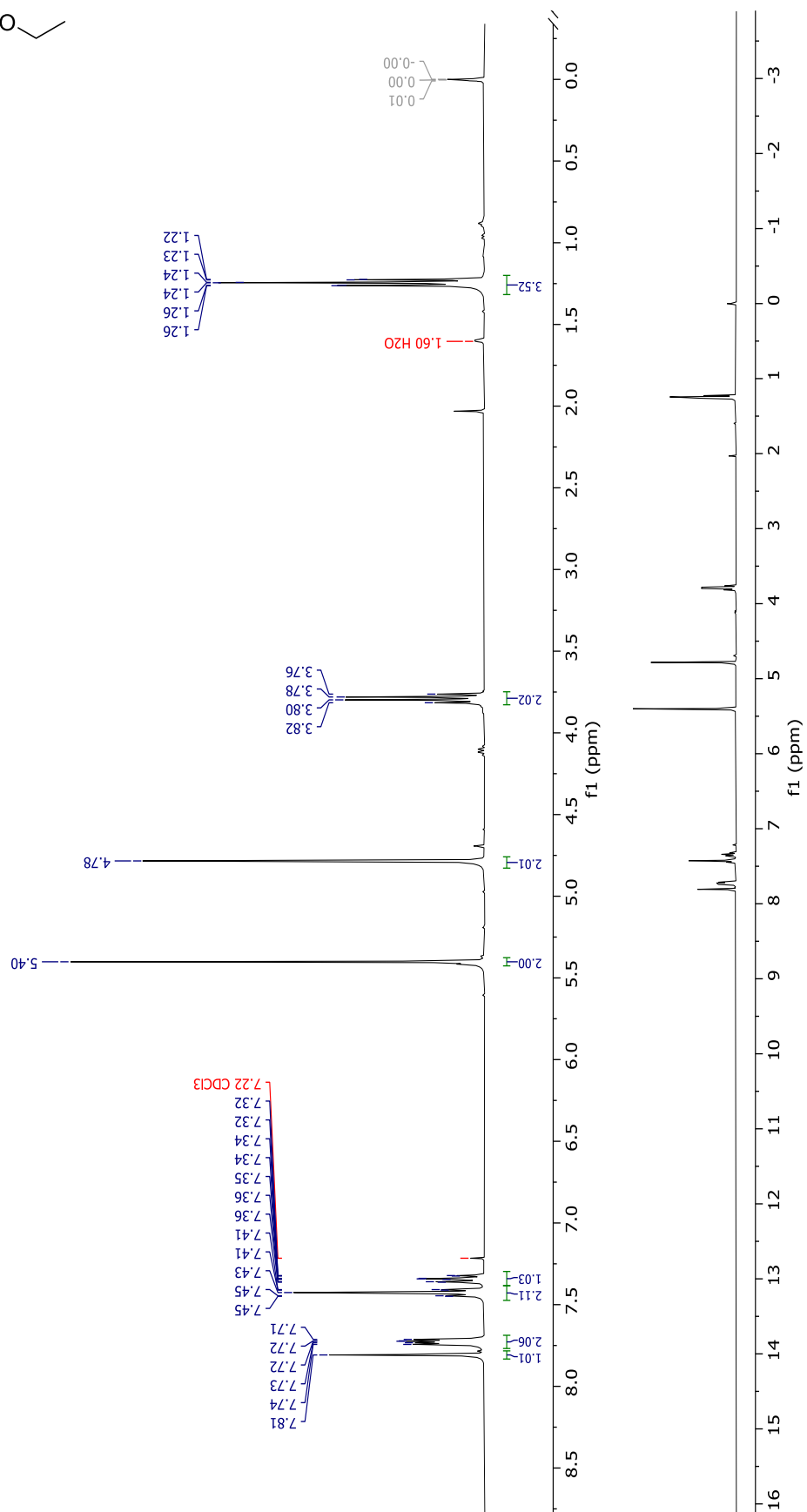


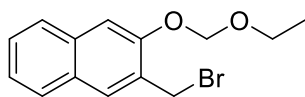
4.24



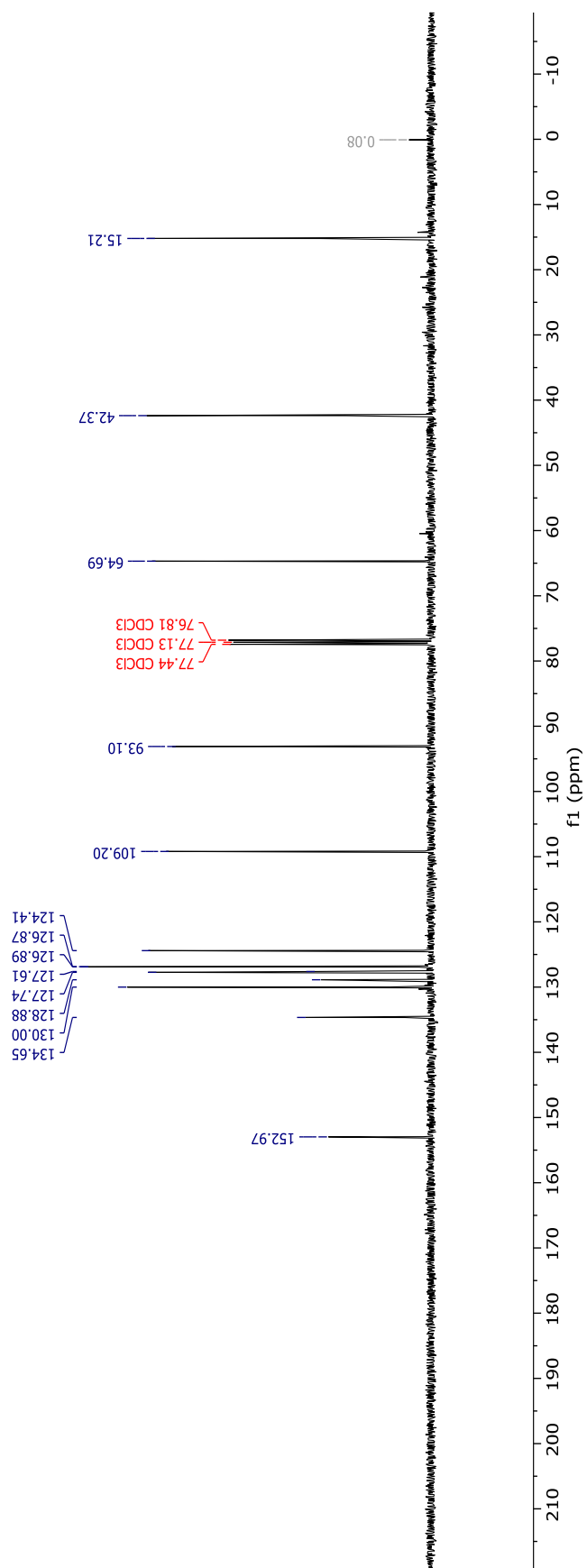


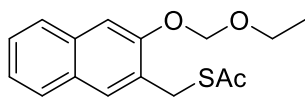
4.25



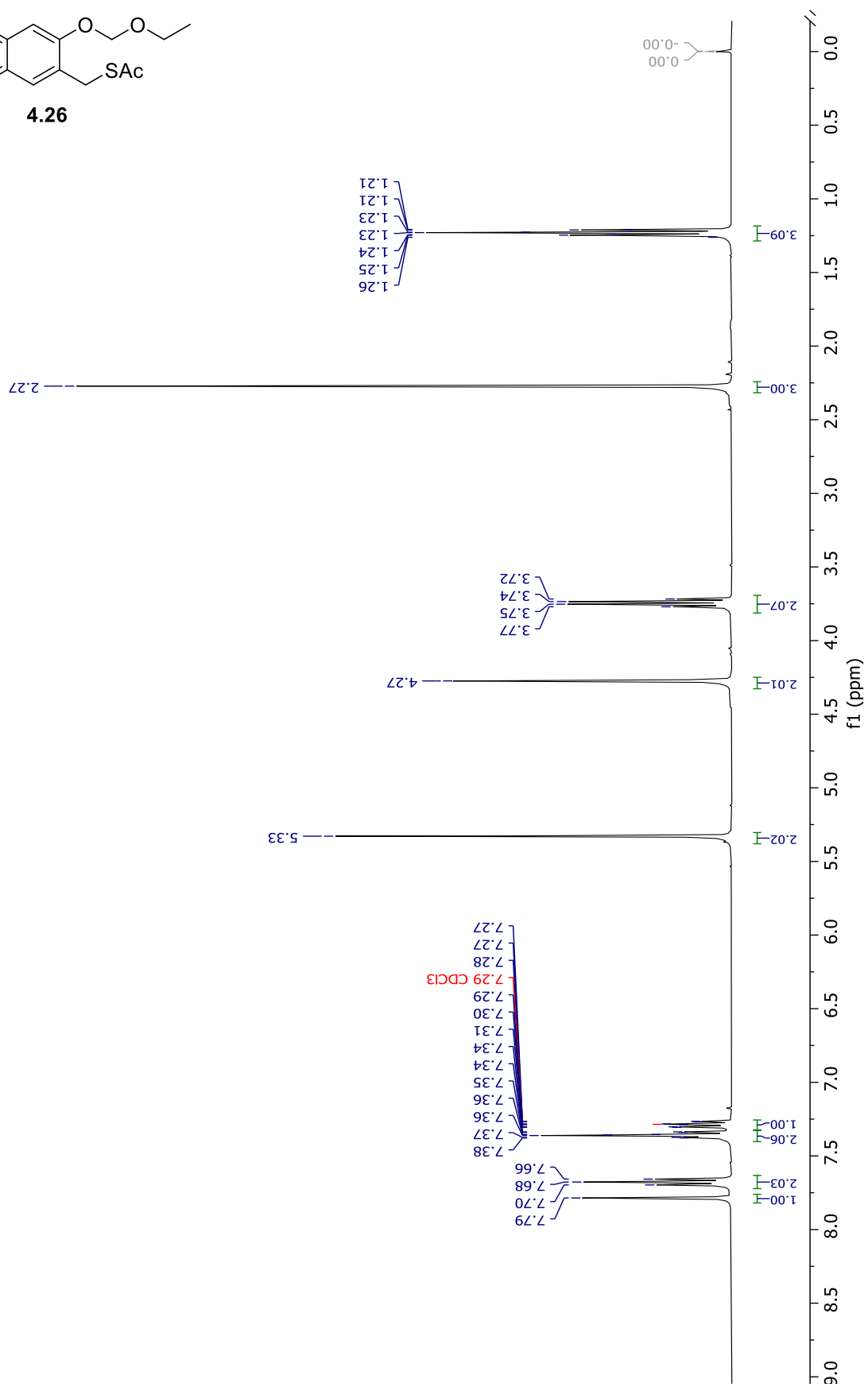


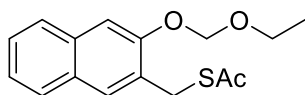
4.25



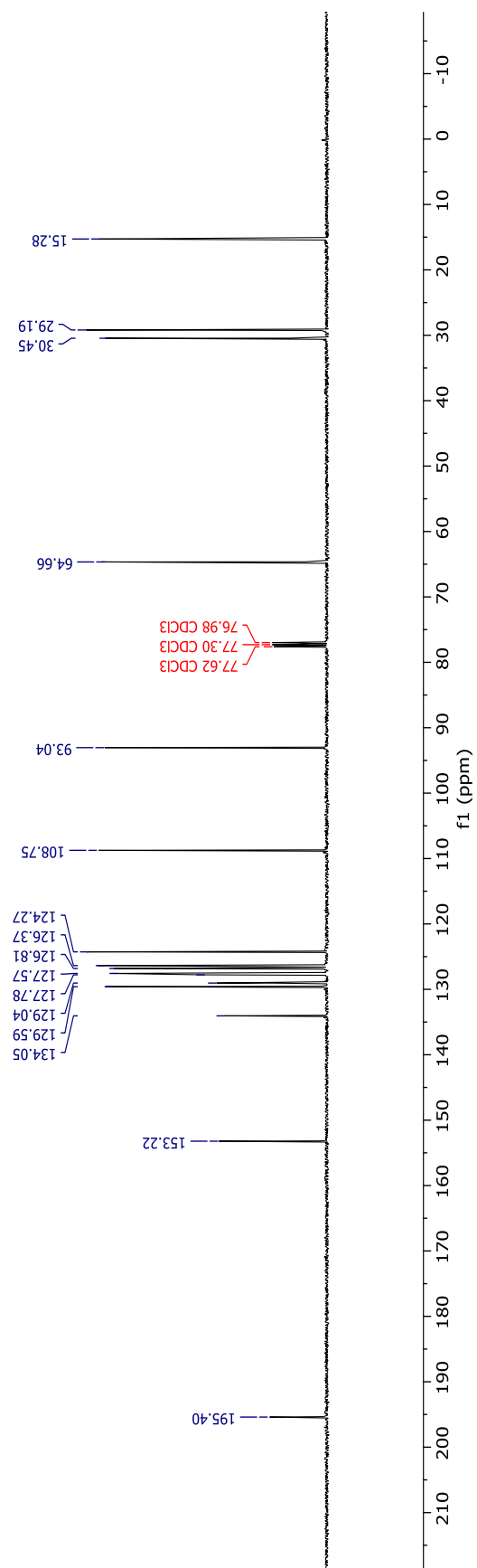


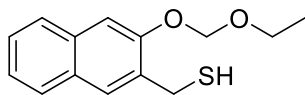
4.26



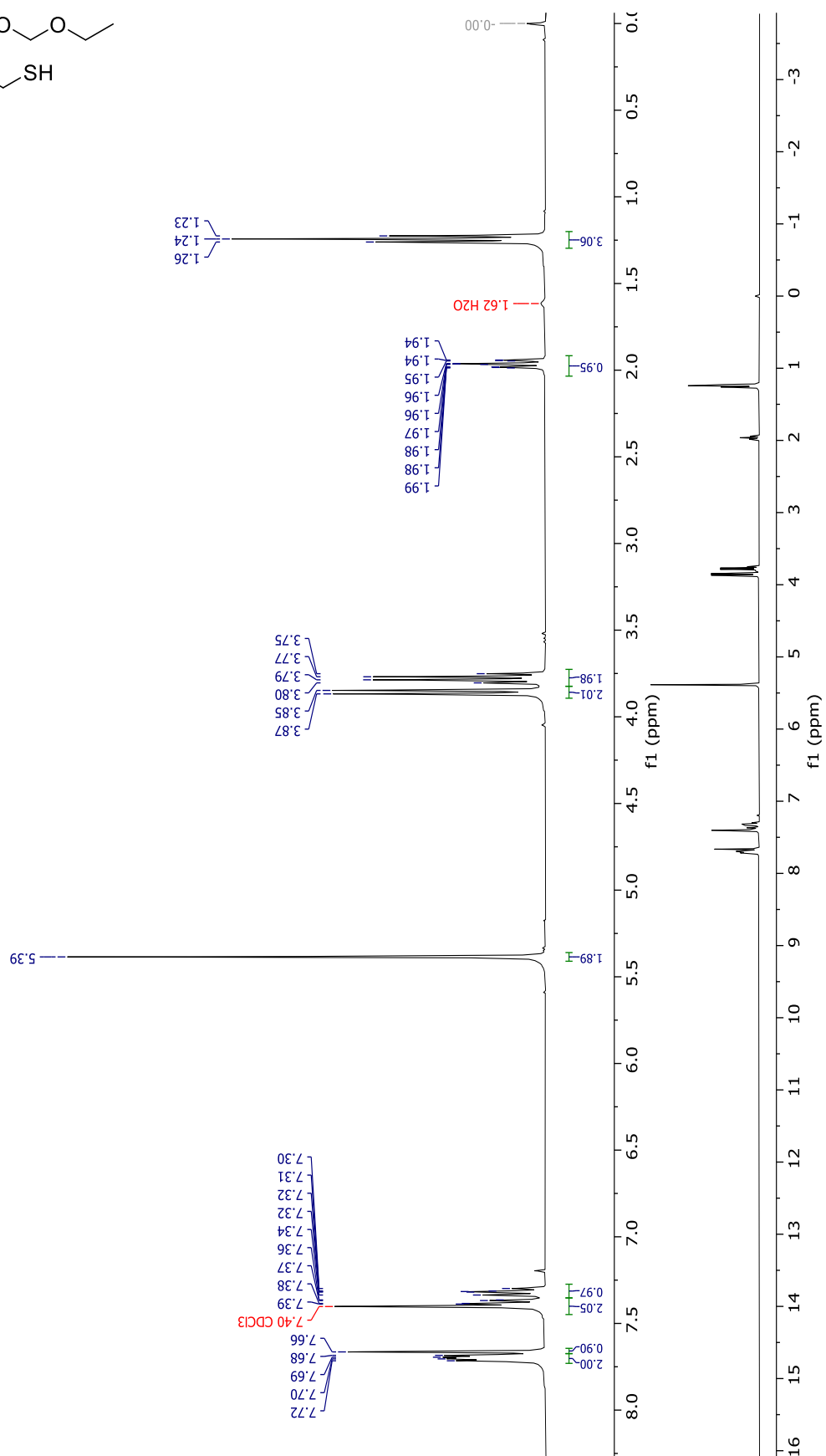


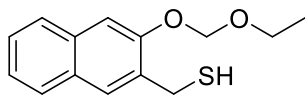
4.26



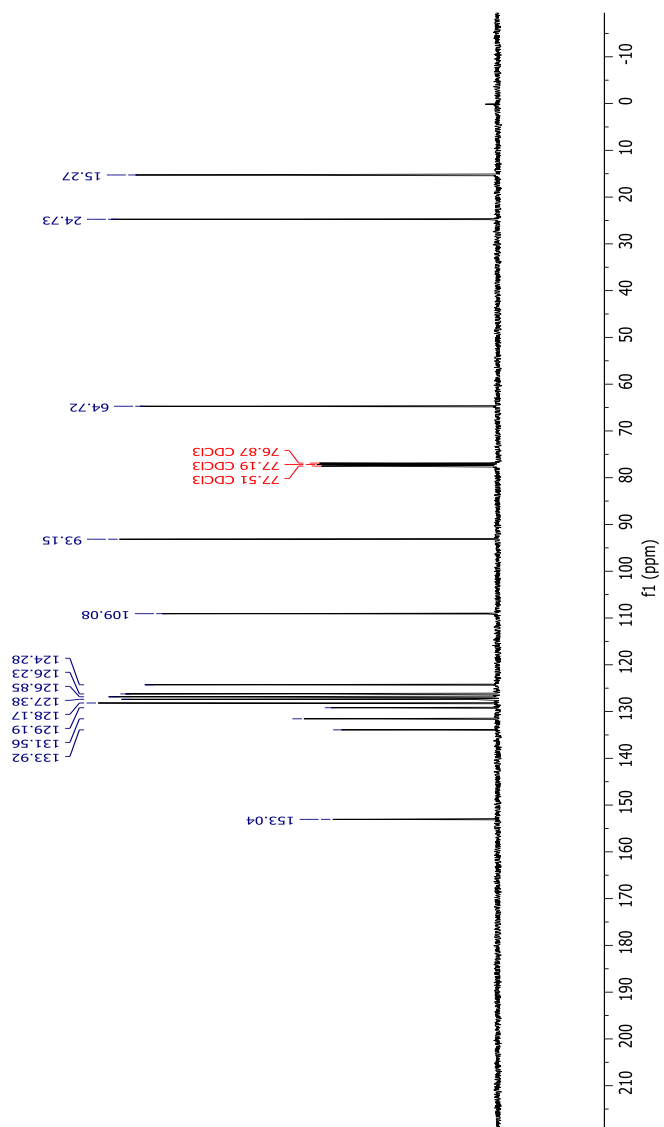


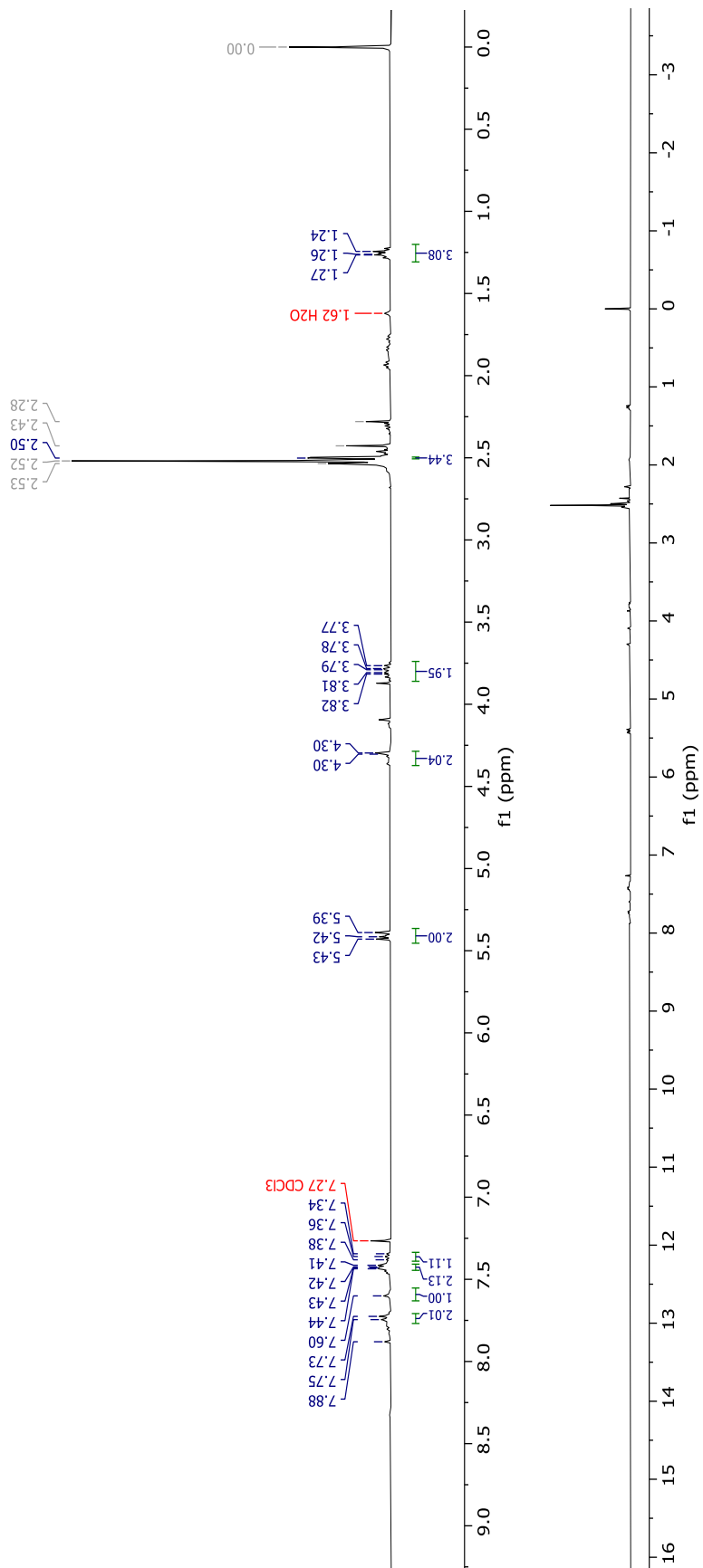
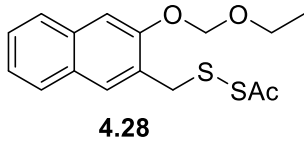
4.27

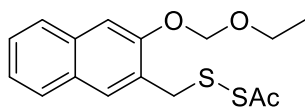




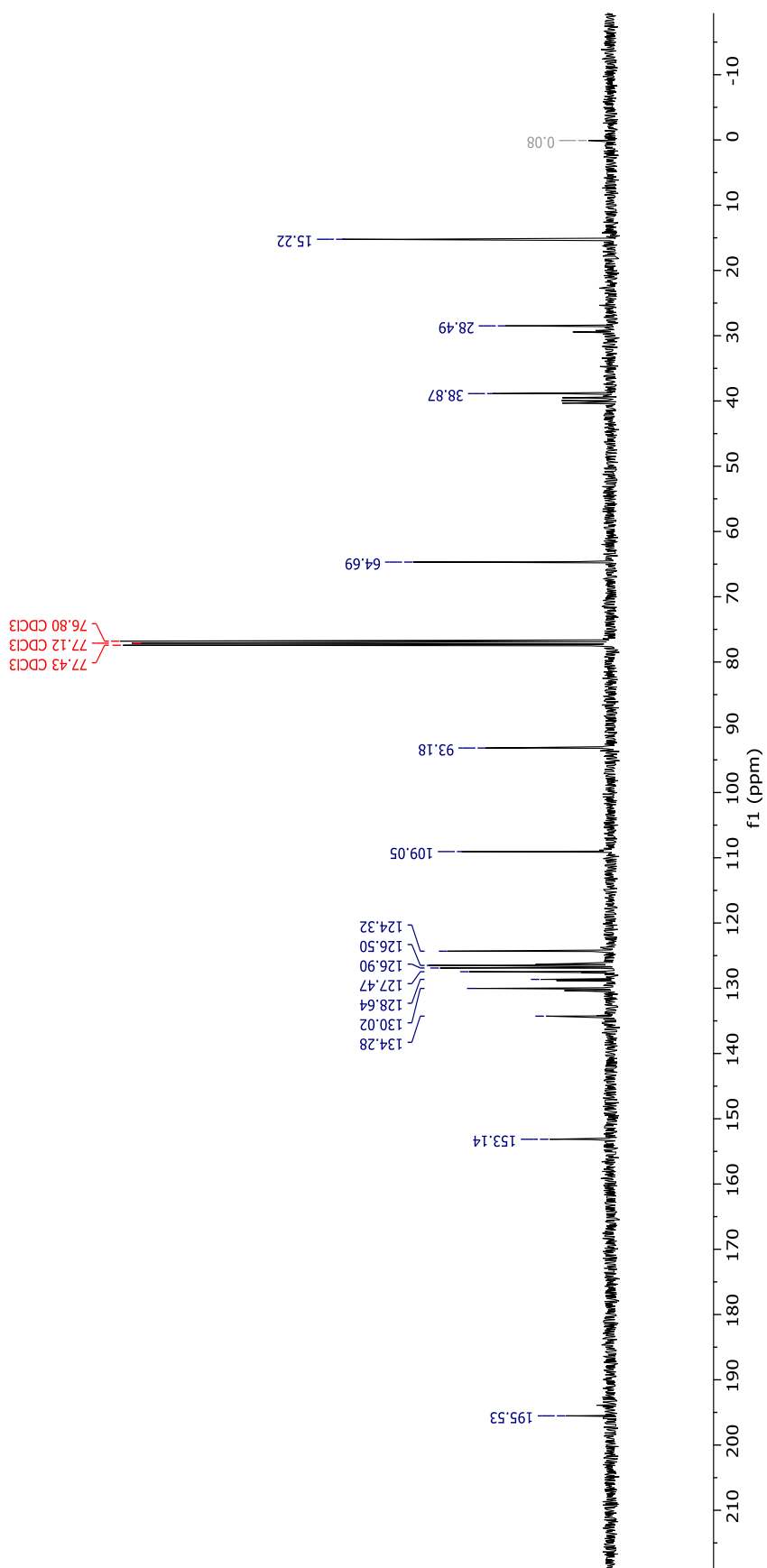
4.27

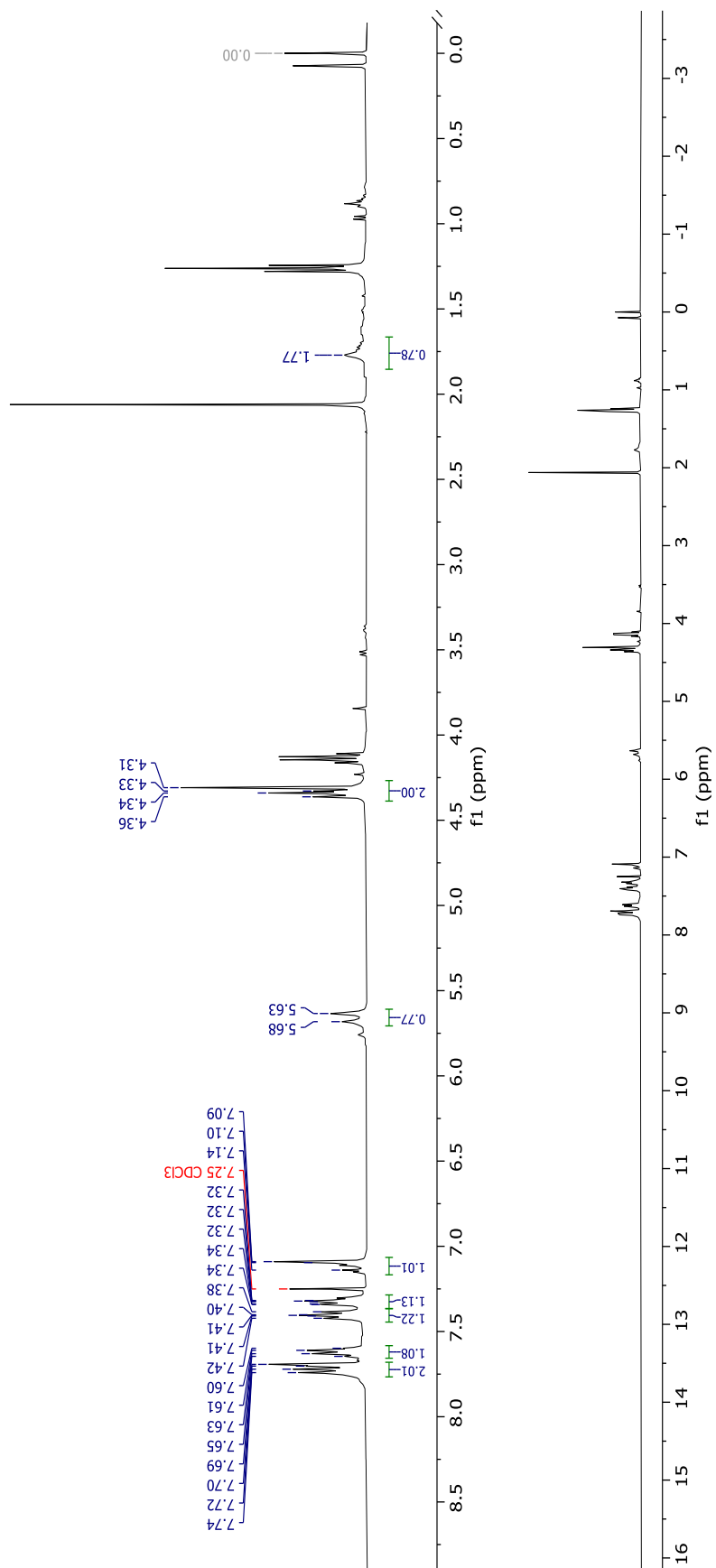
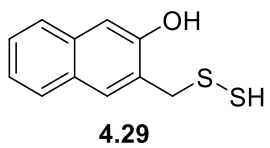


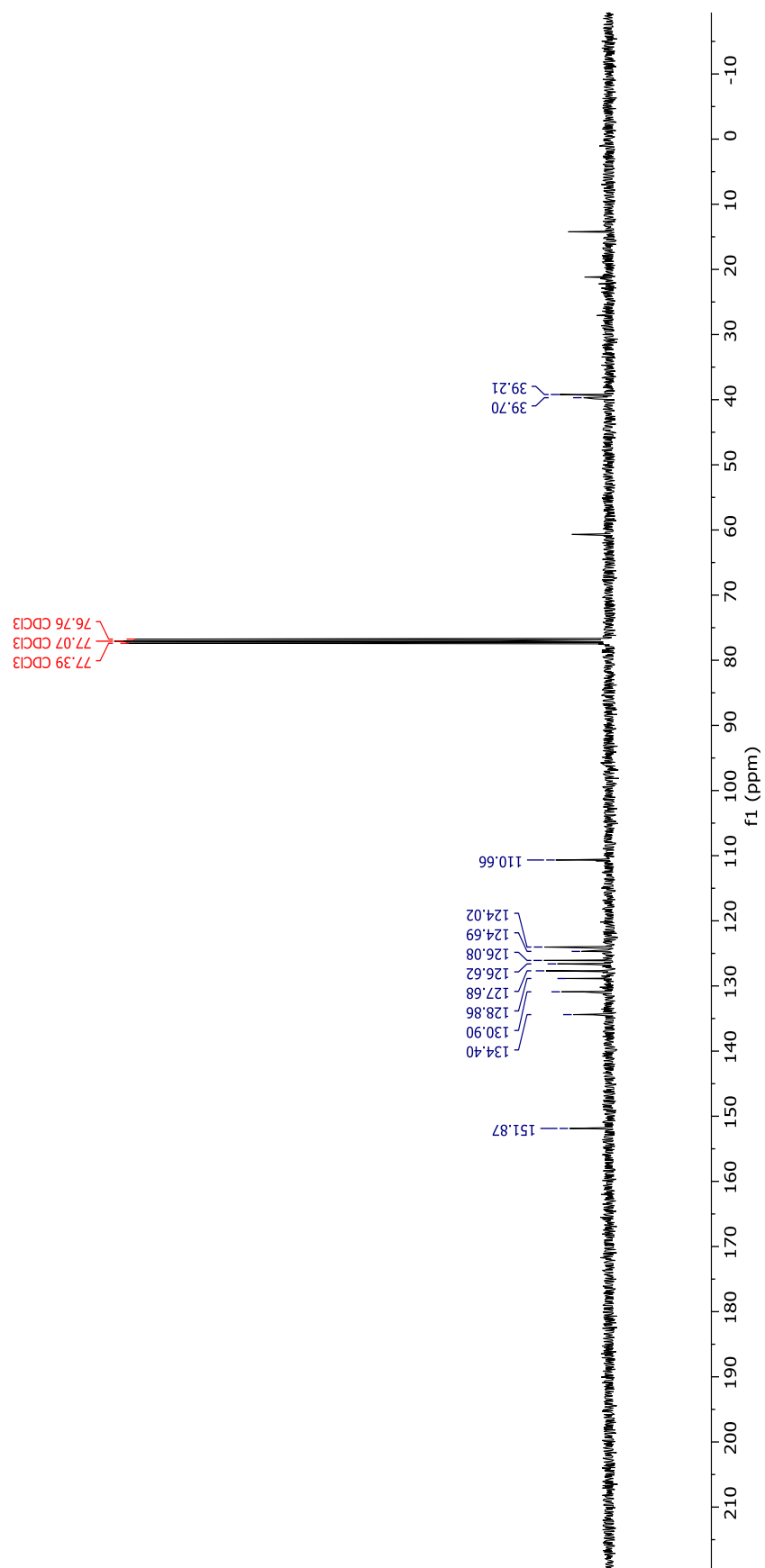
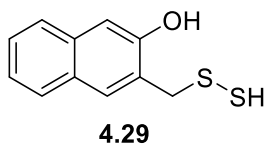


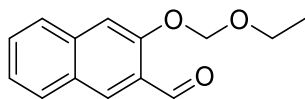


4.28

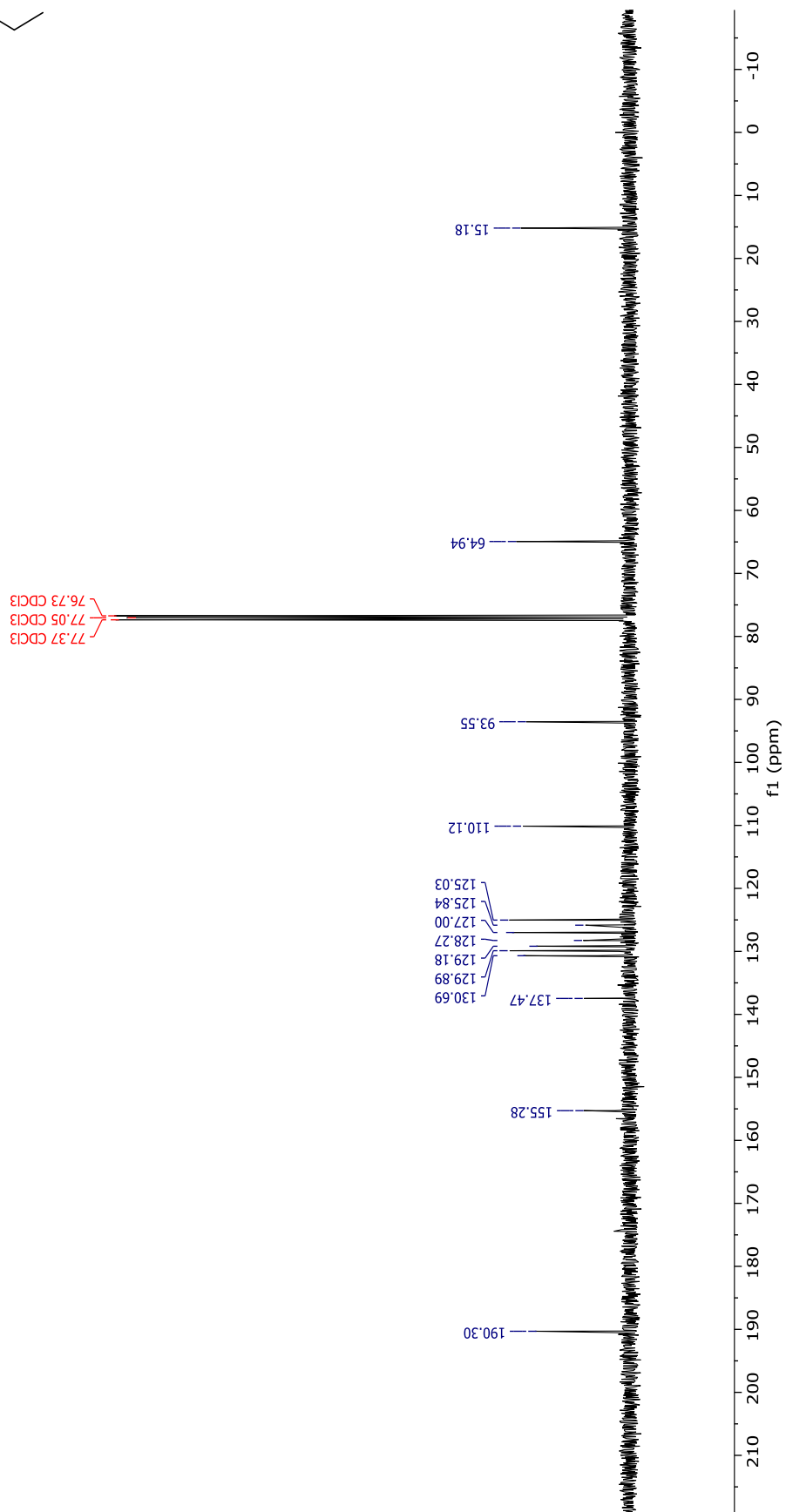


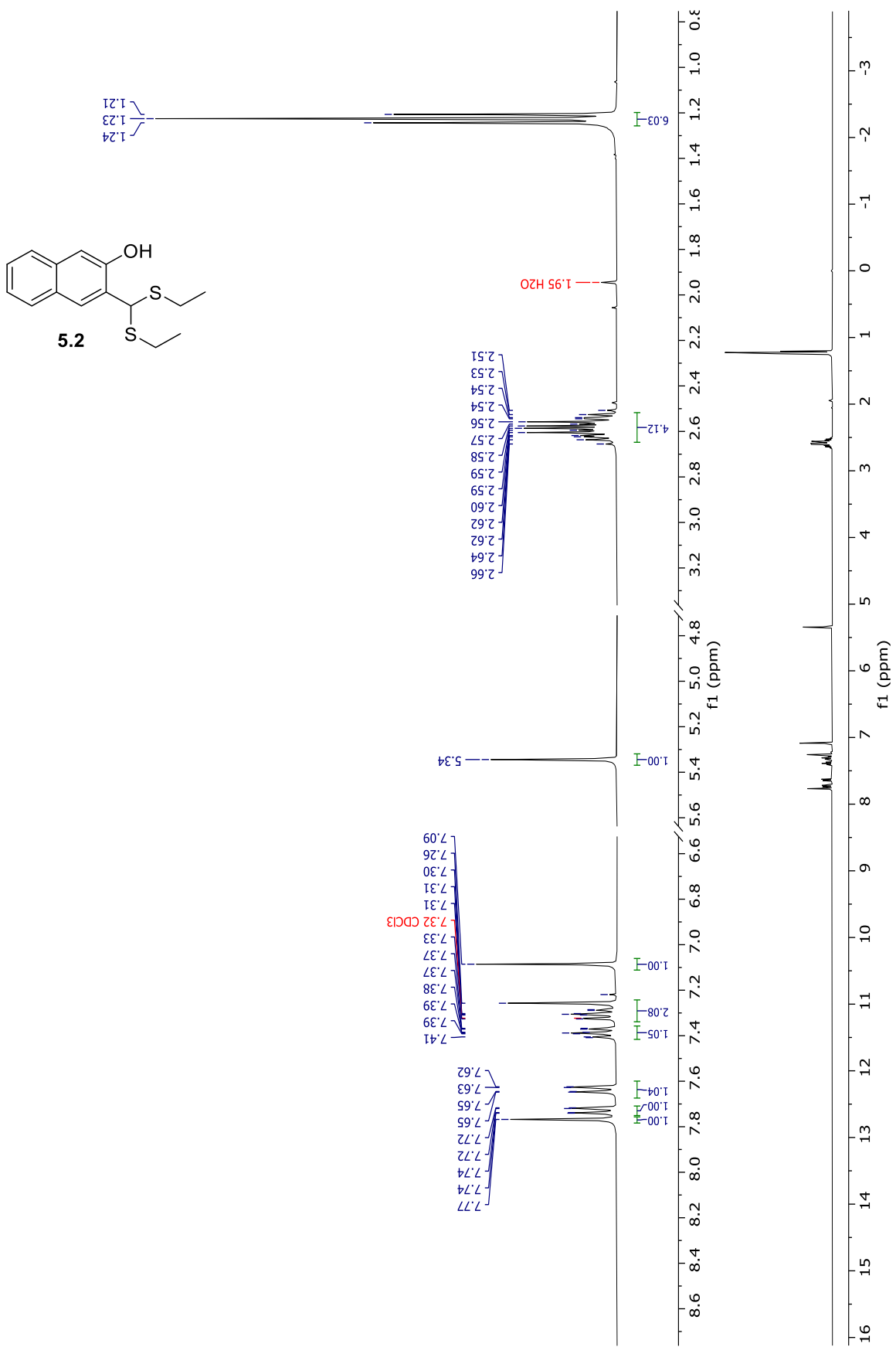


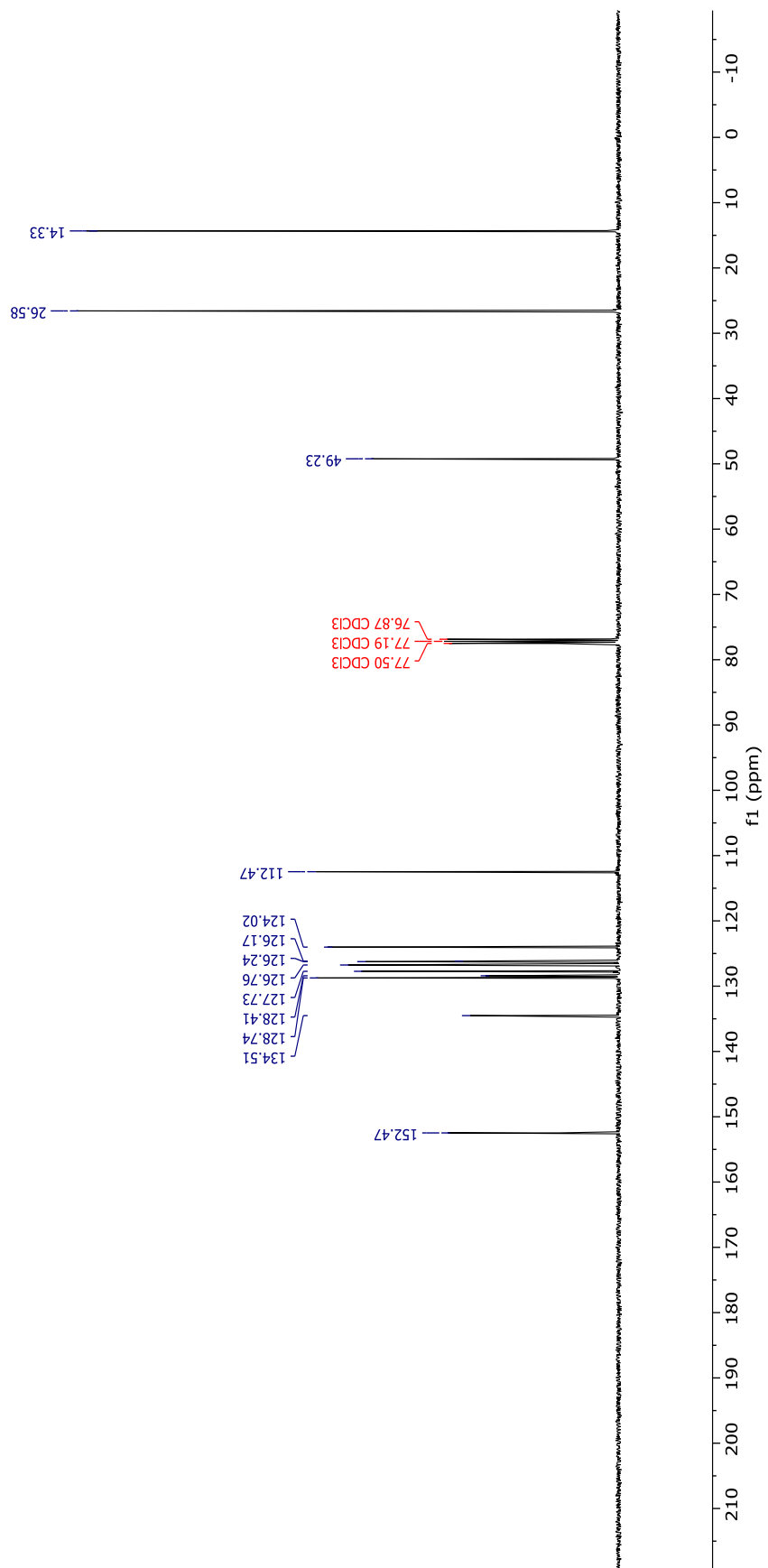
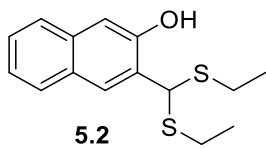


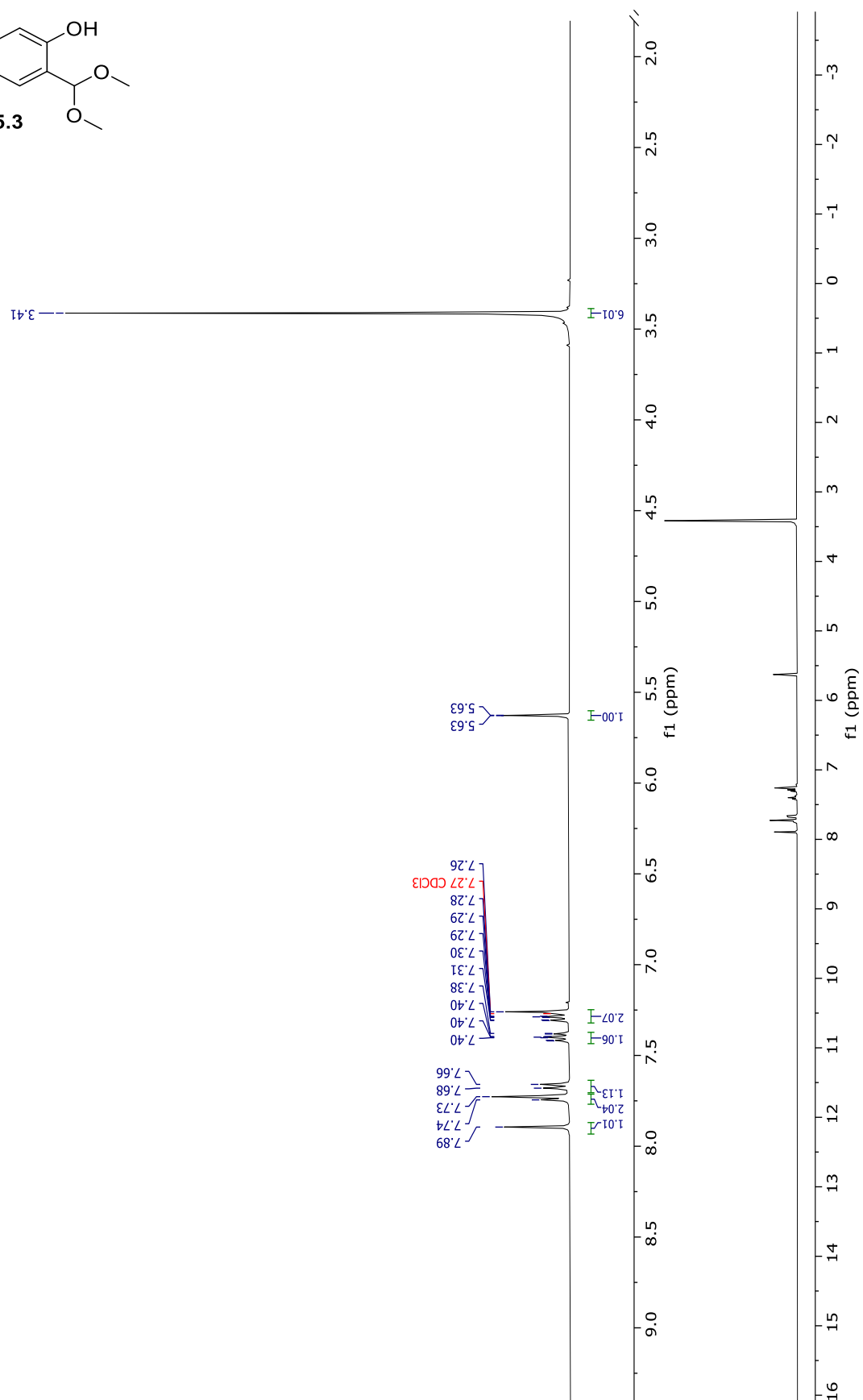
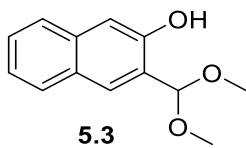


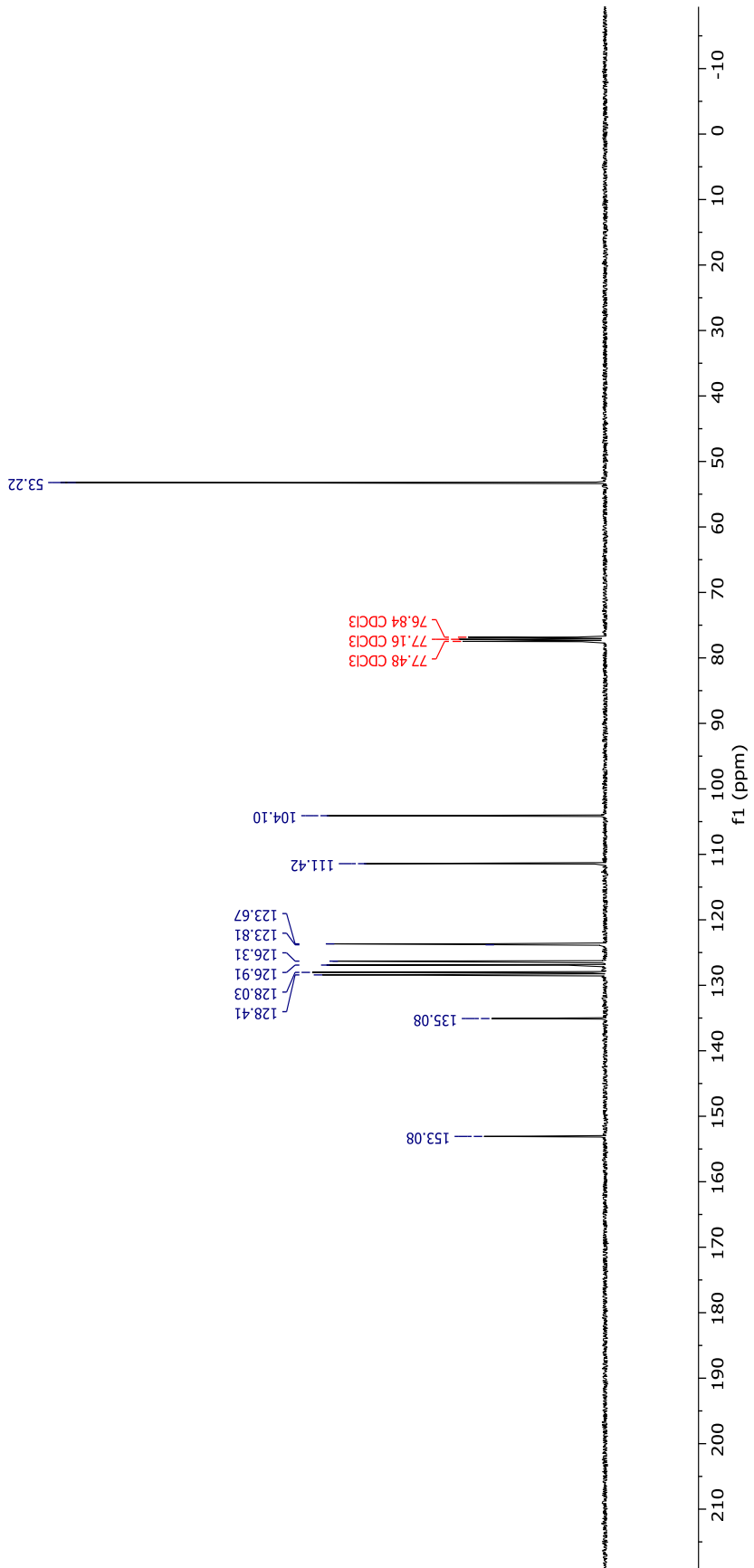
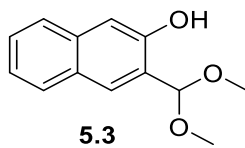
5.1

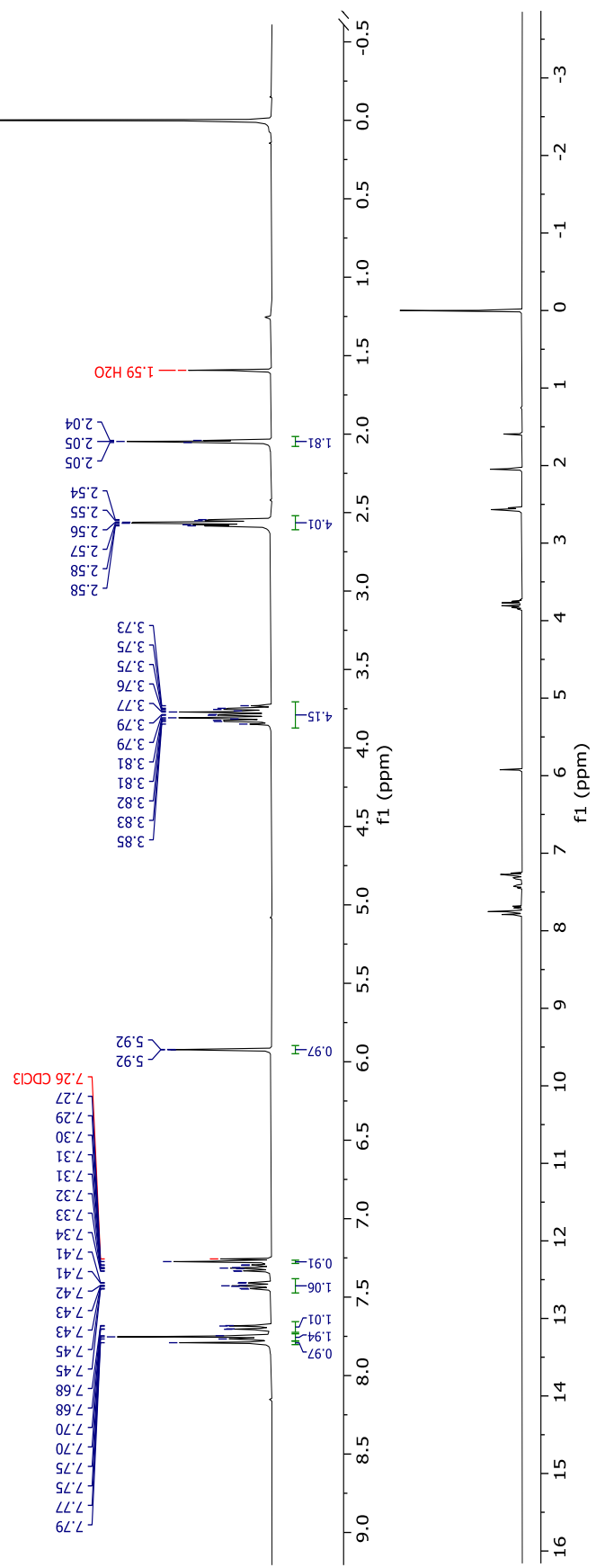
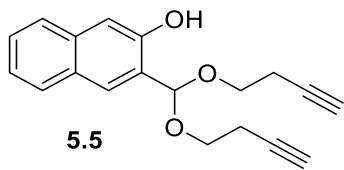


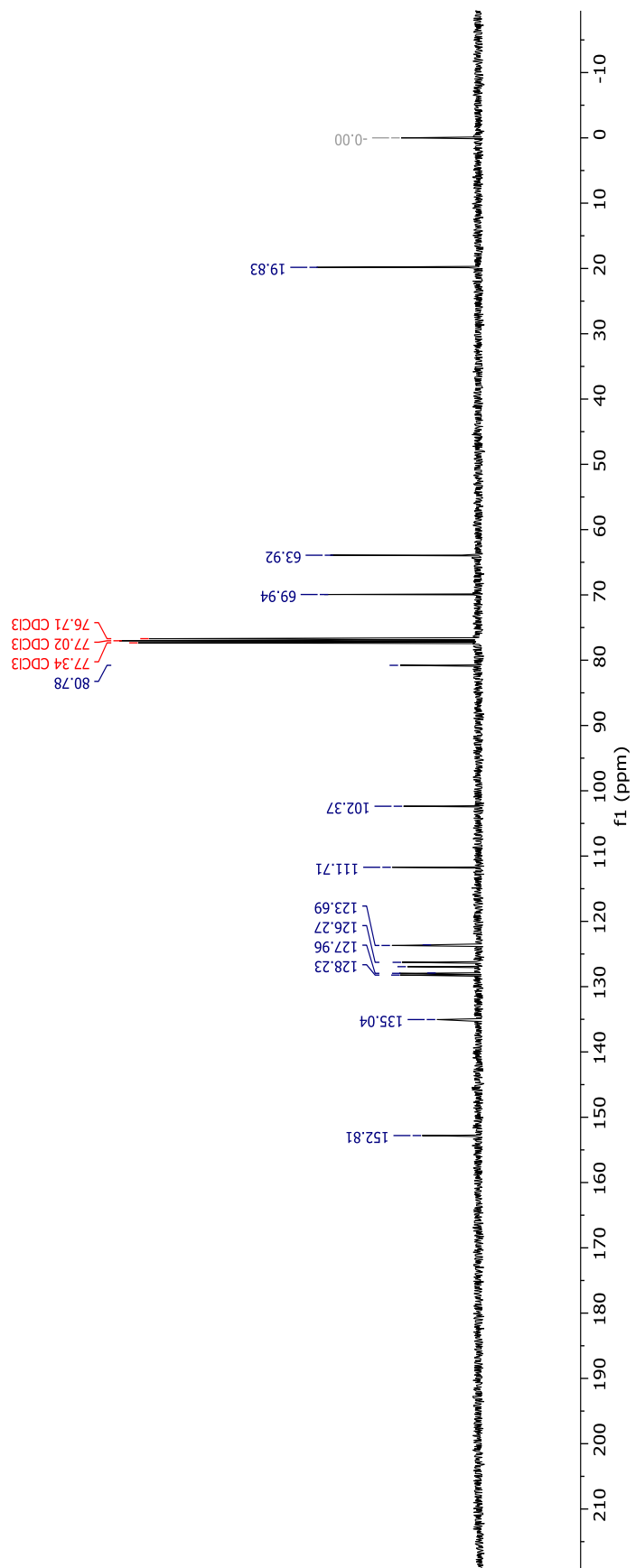
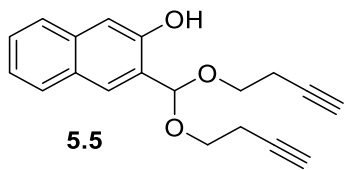


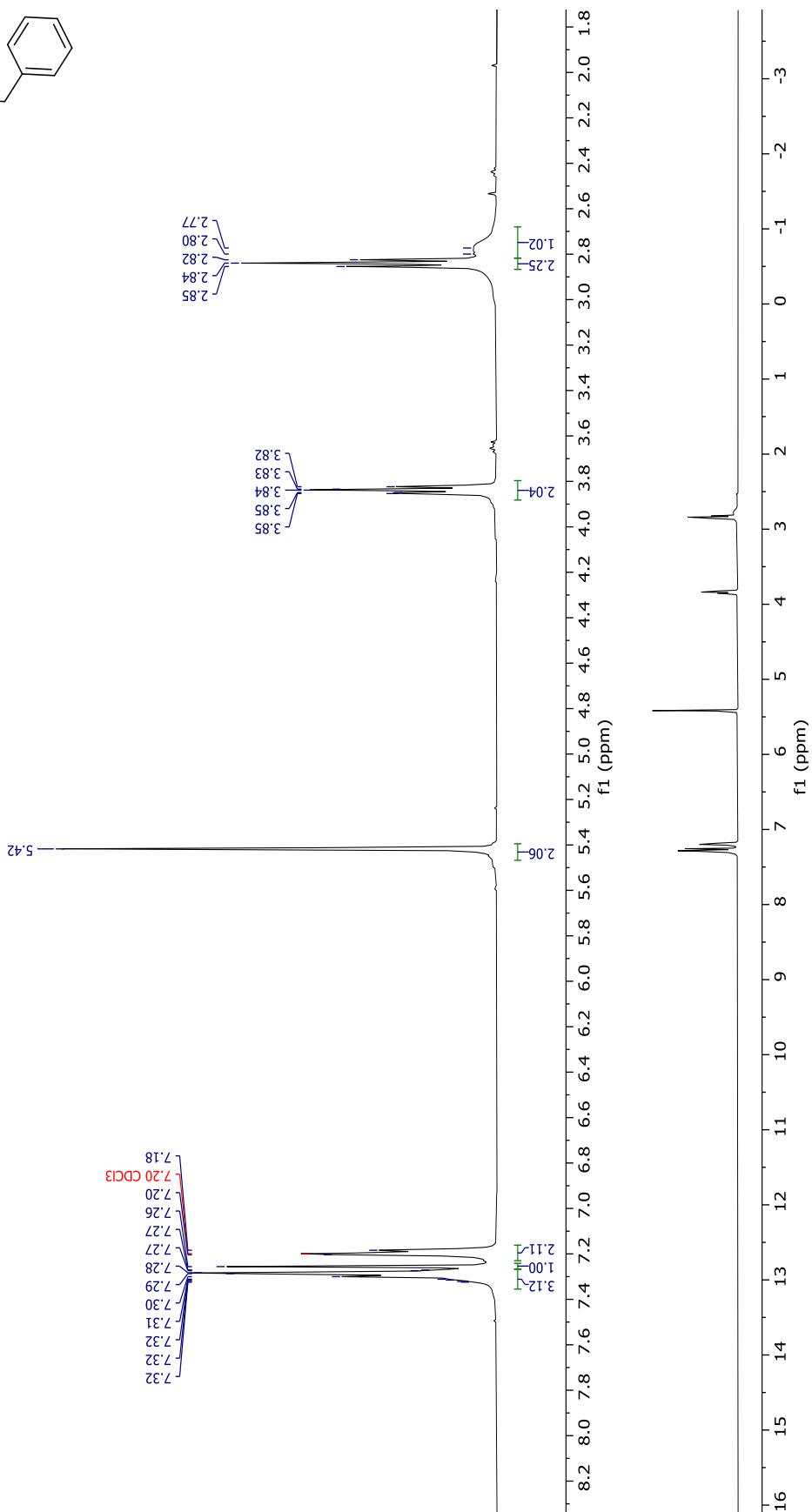
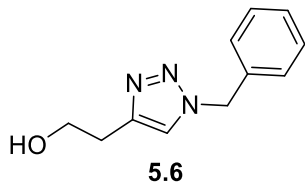


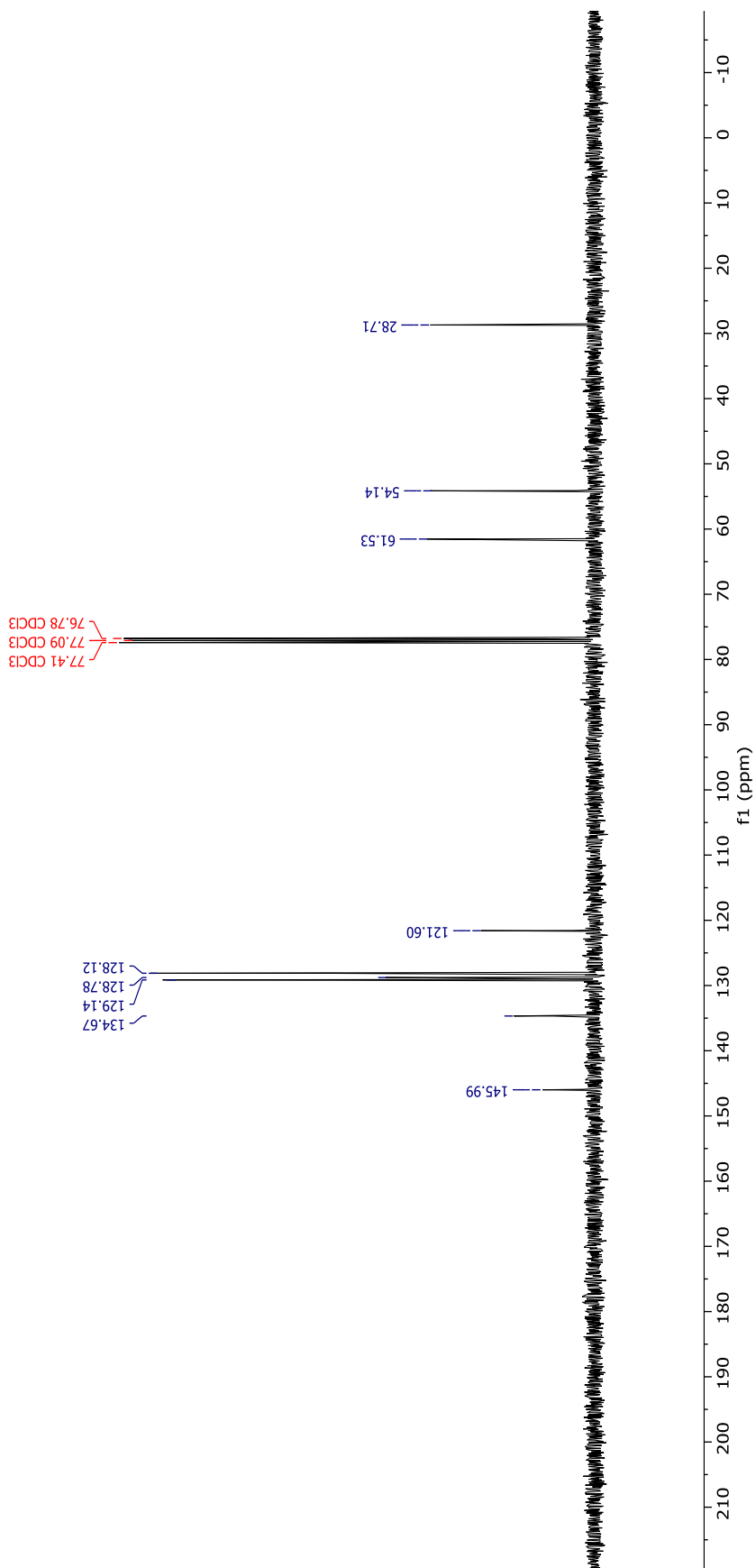
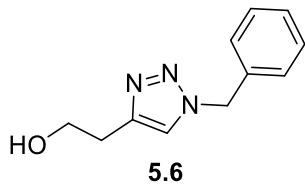


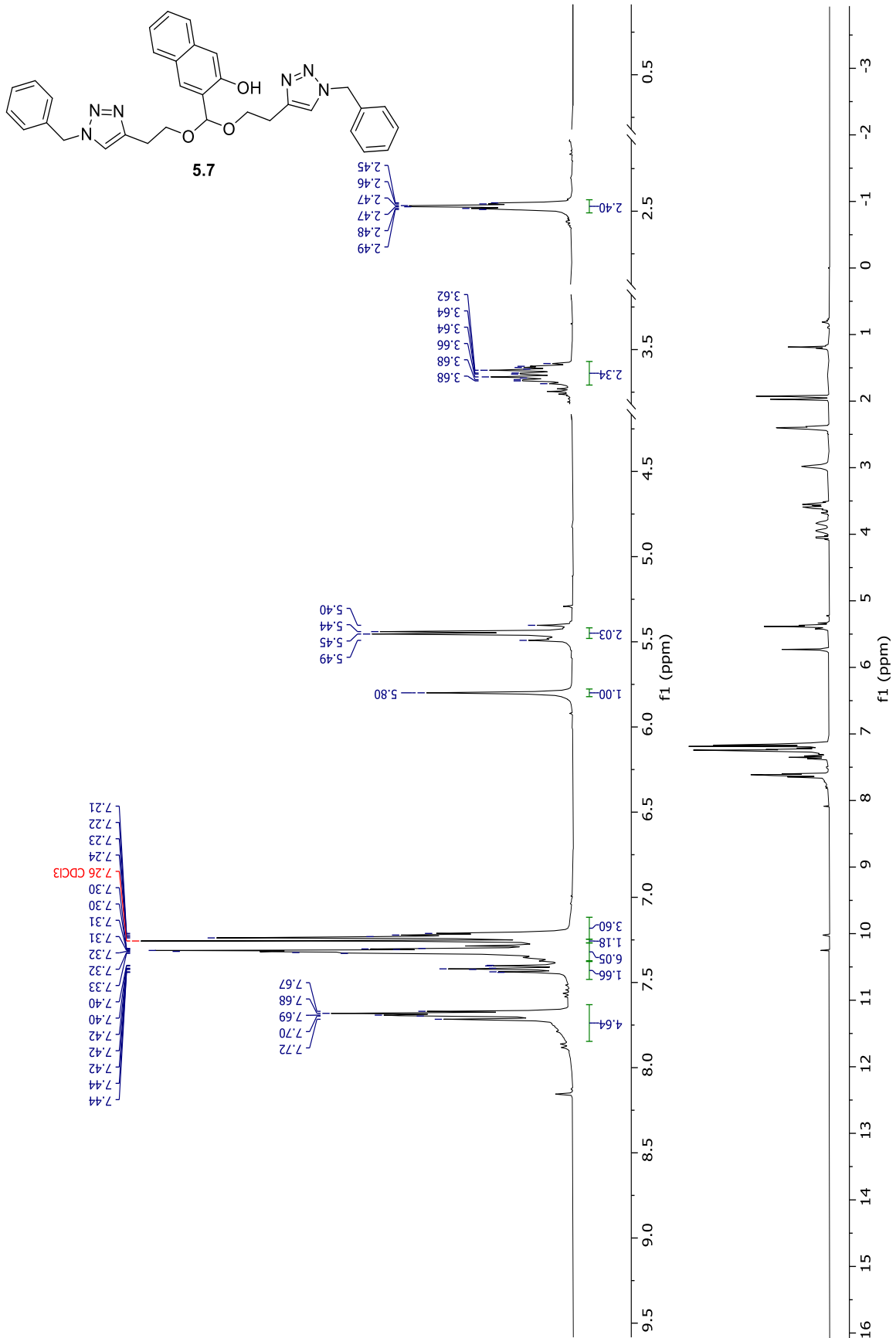


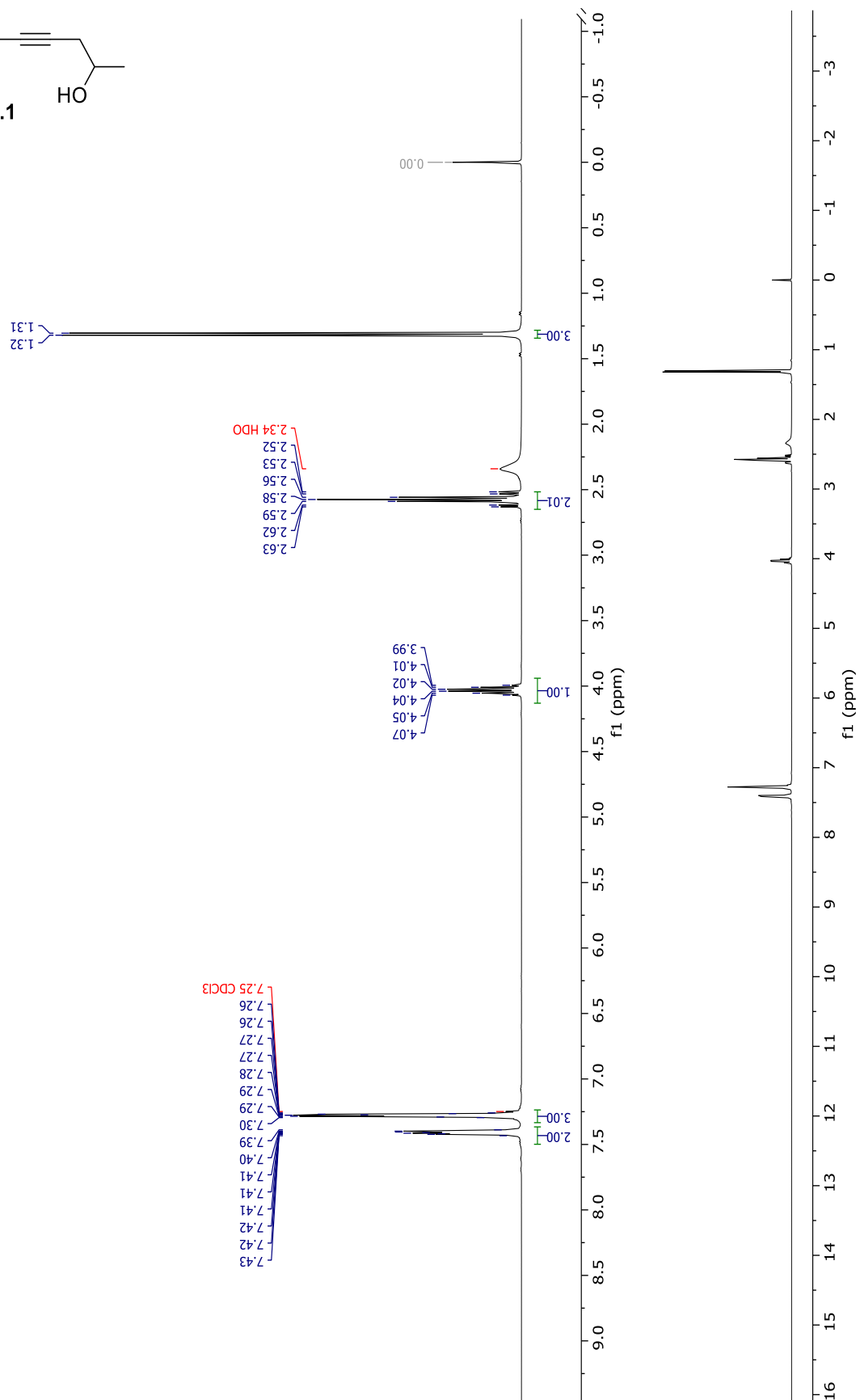
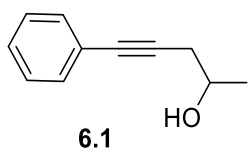


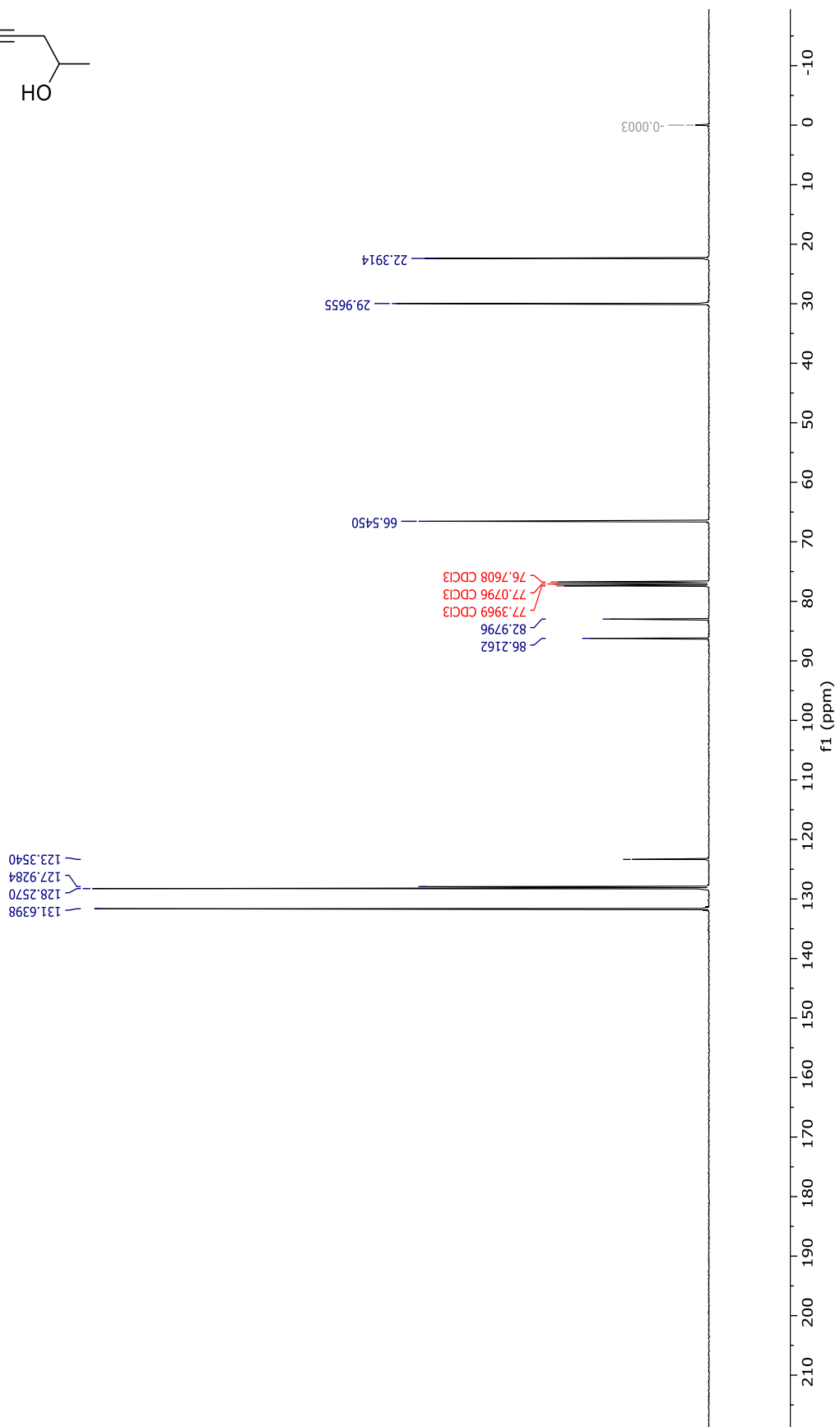
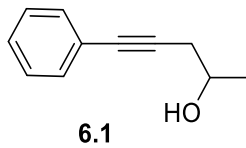


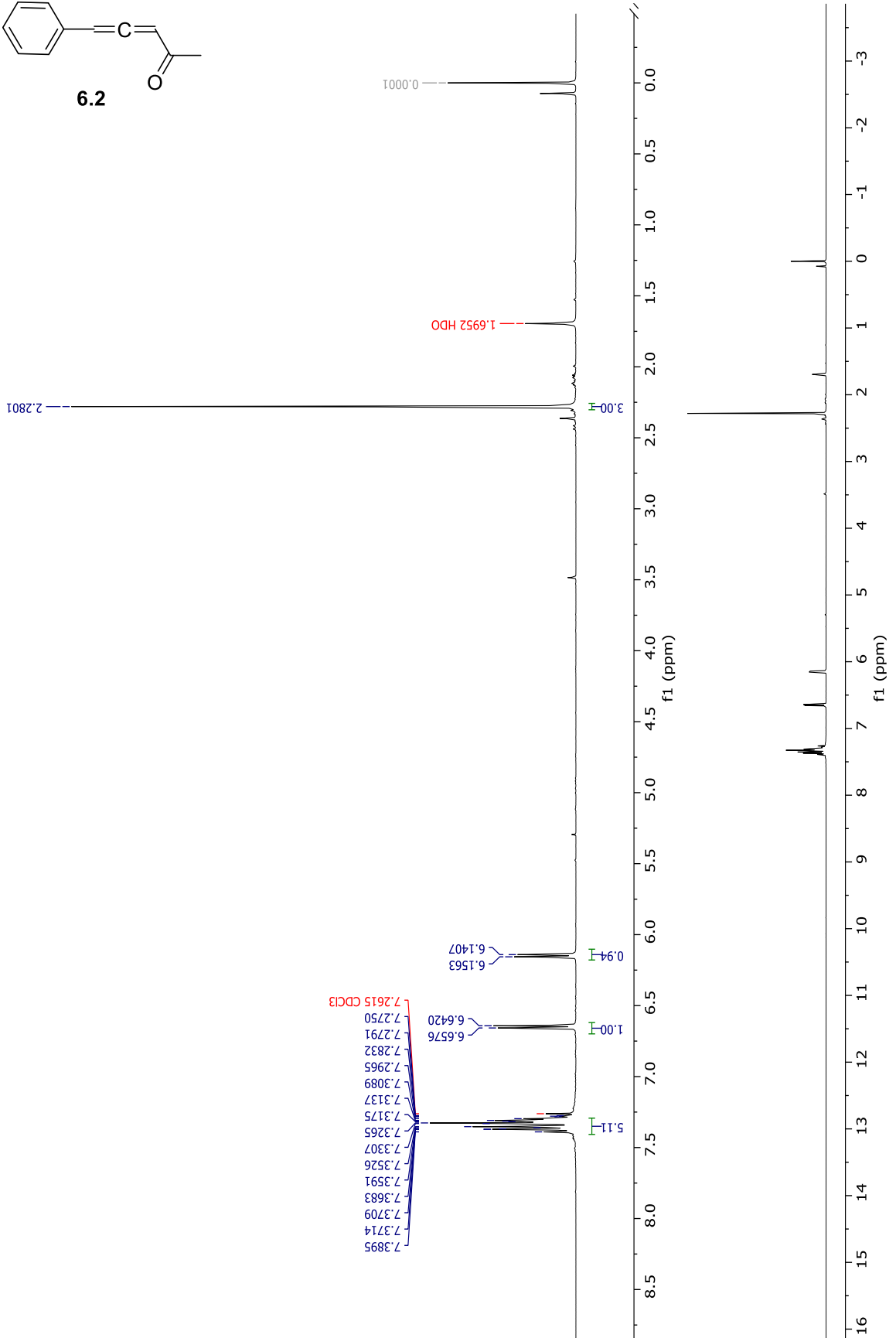
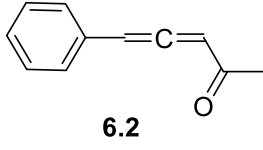


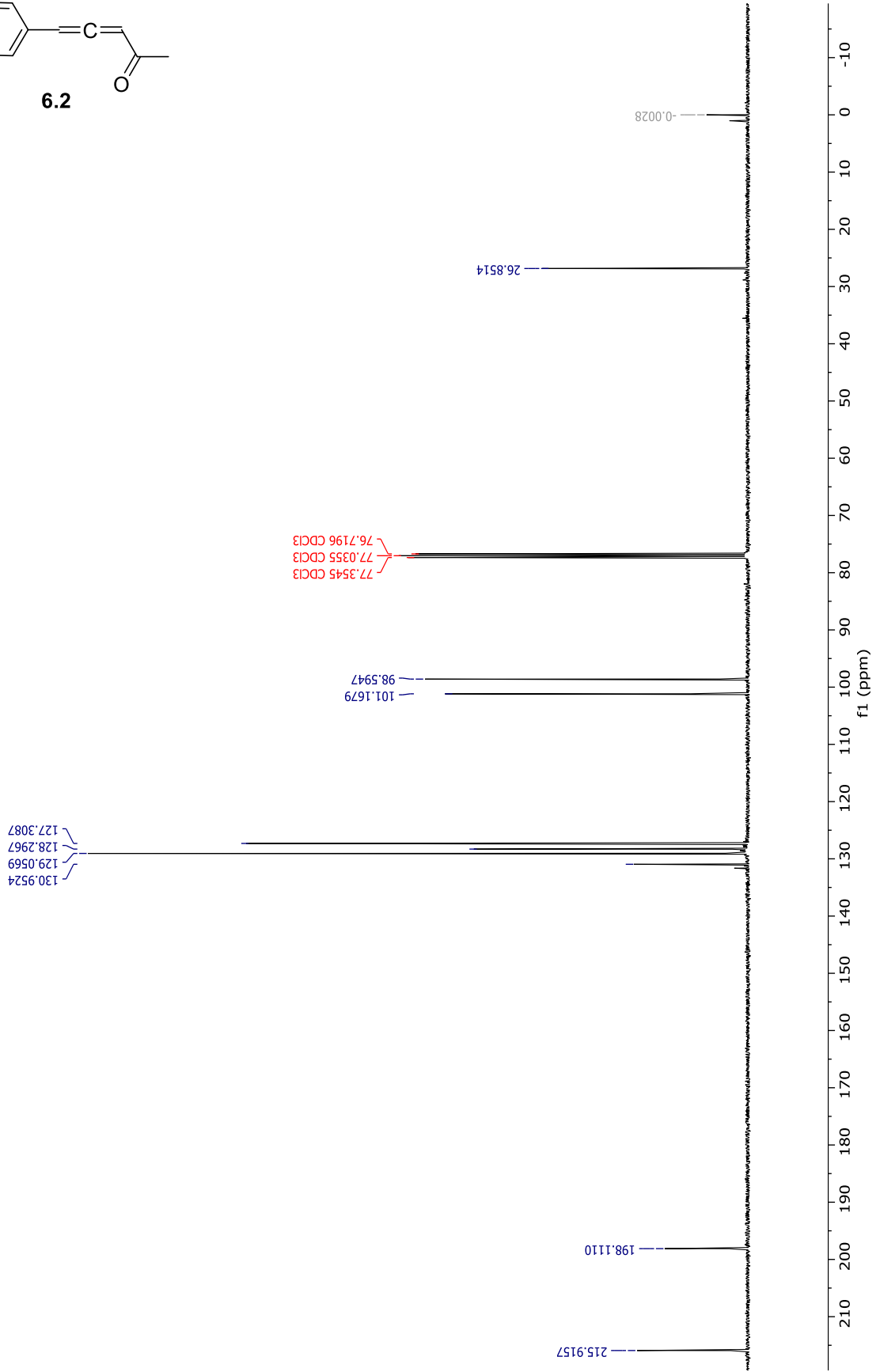
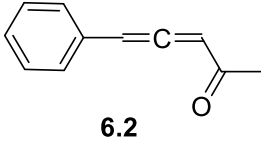


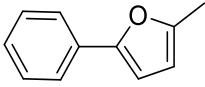












6.3

0.00

2.37

3.04

1.56 H₂O

6.06
6.05
6.05
6.05
6.05
6.05

6.54
6.53

7.64
7.64
7.63
7.62
7.62
7.61
7.37
7.37
7.35
7.34
7.33
7.26 CDCl₃
7.23
7.23
7.23
7.21
7.21
7.19

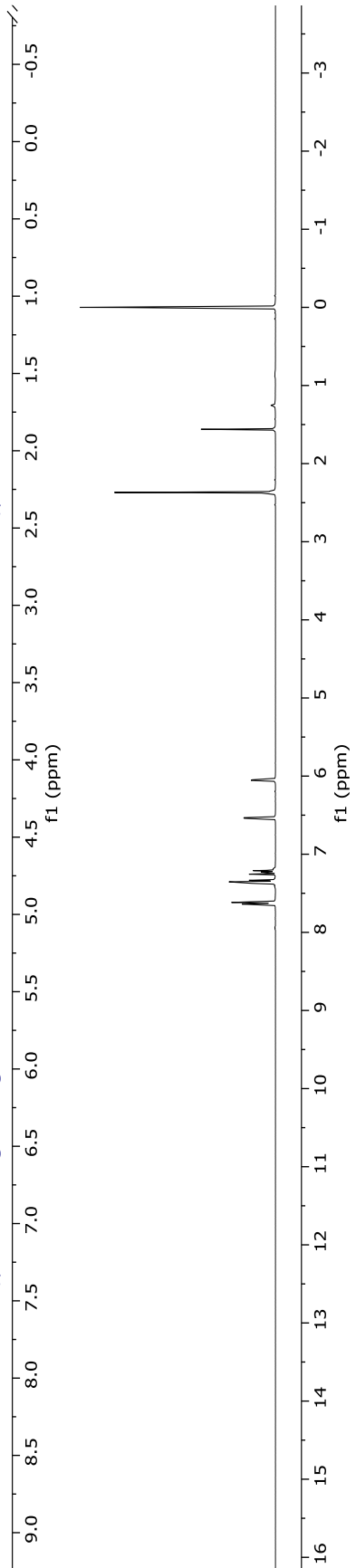
0.96

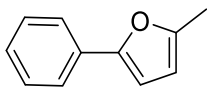
0.98

1.01

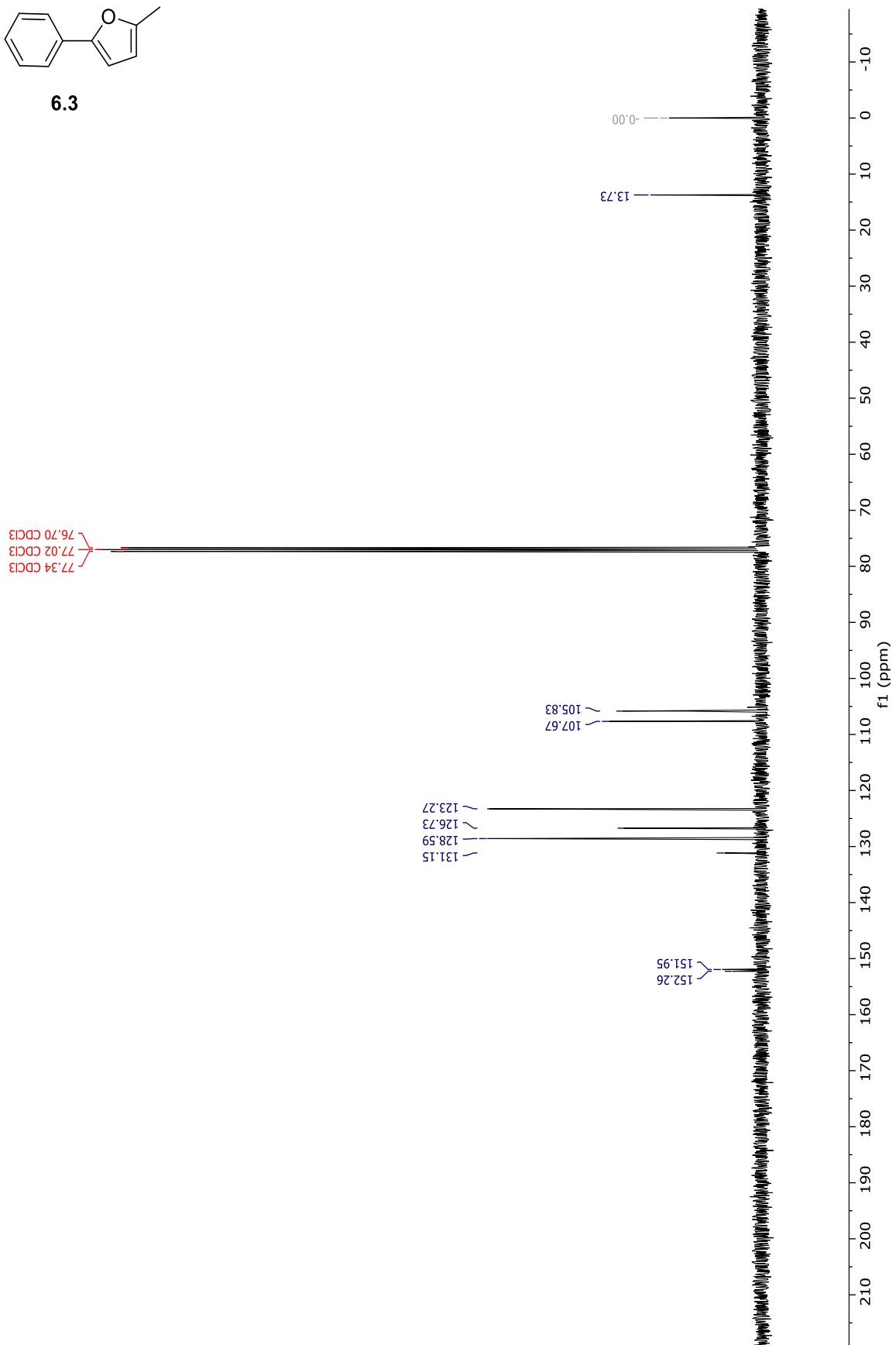
2.03

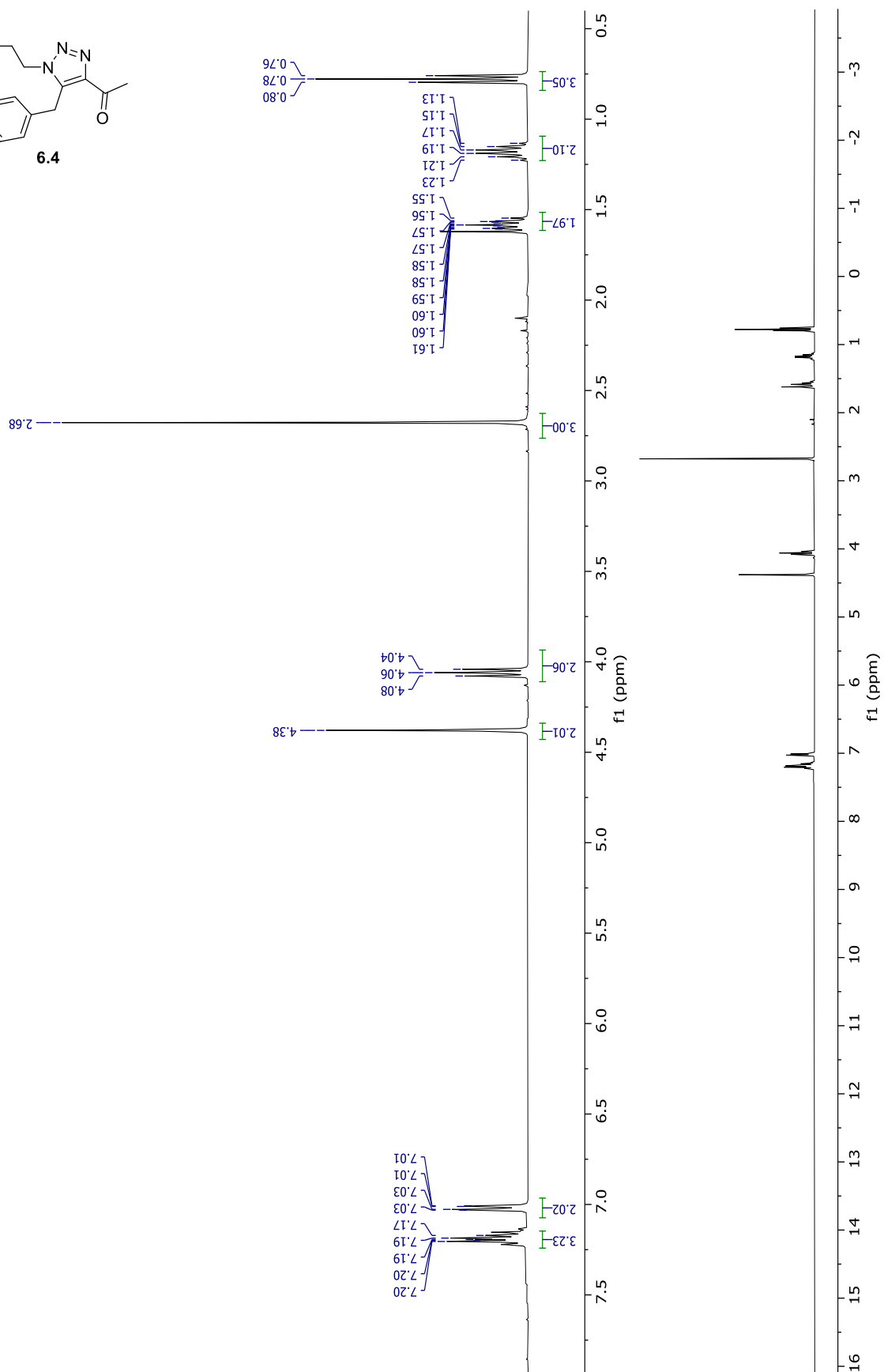
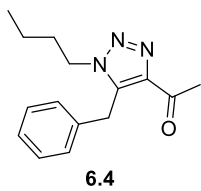
1.98

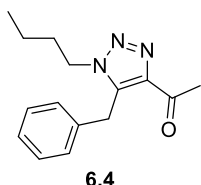




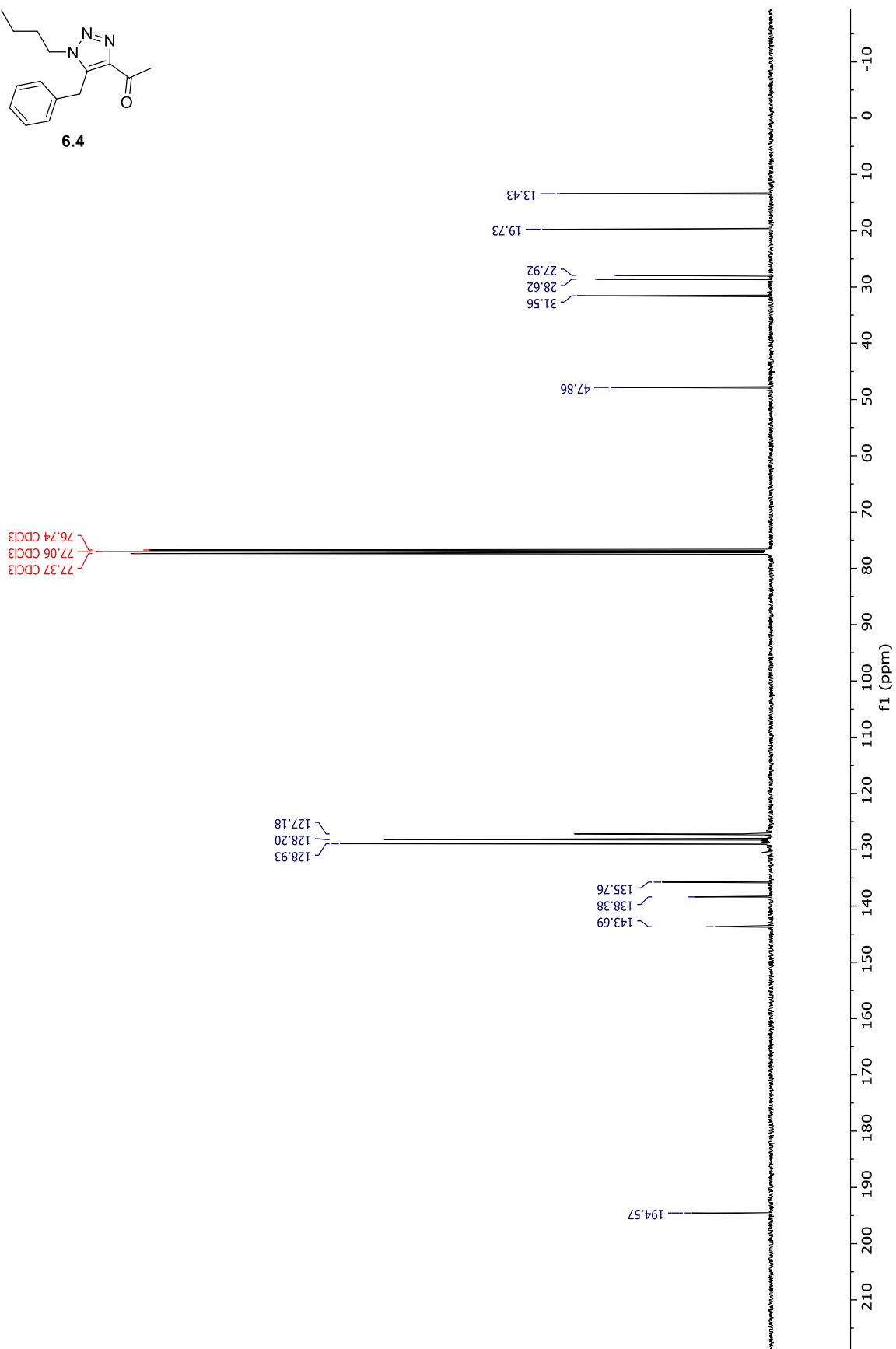
6.3

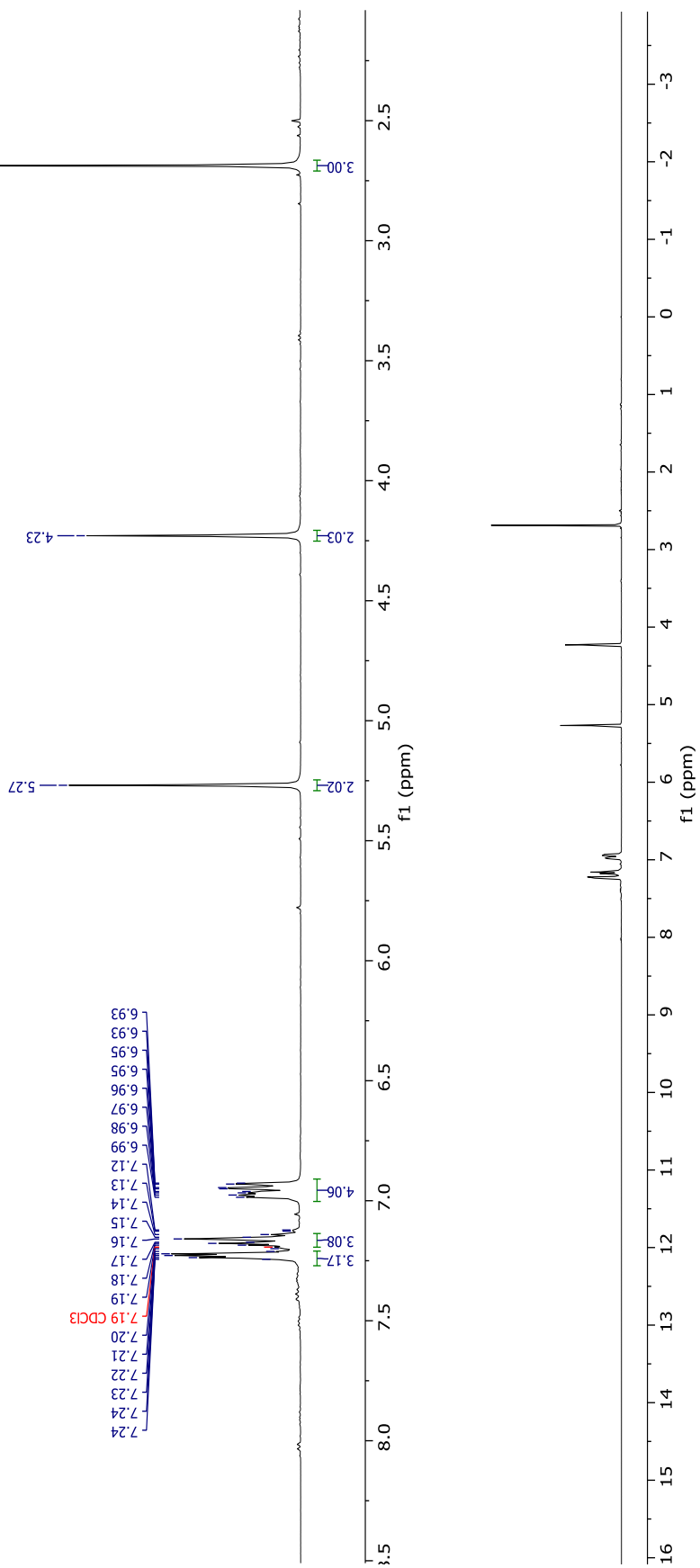
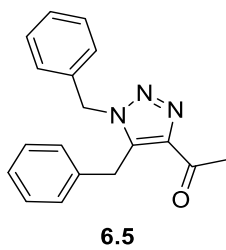


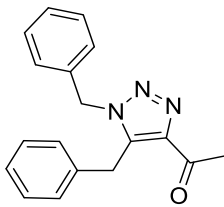




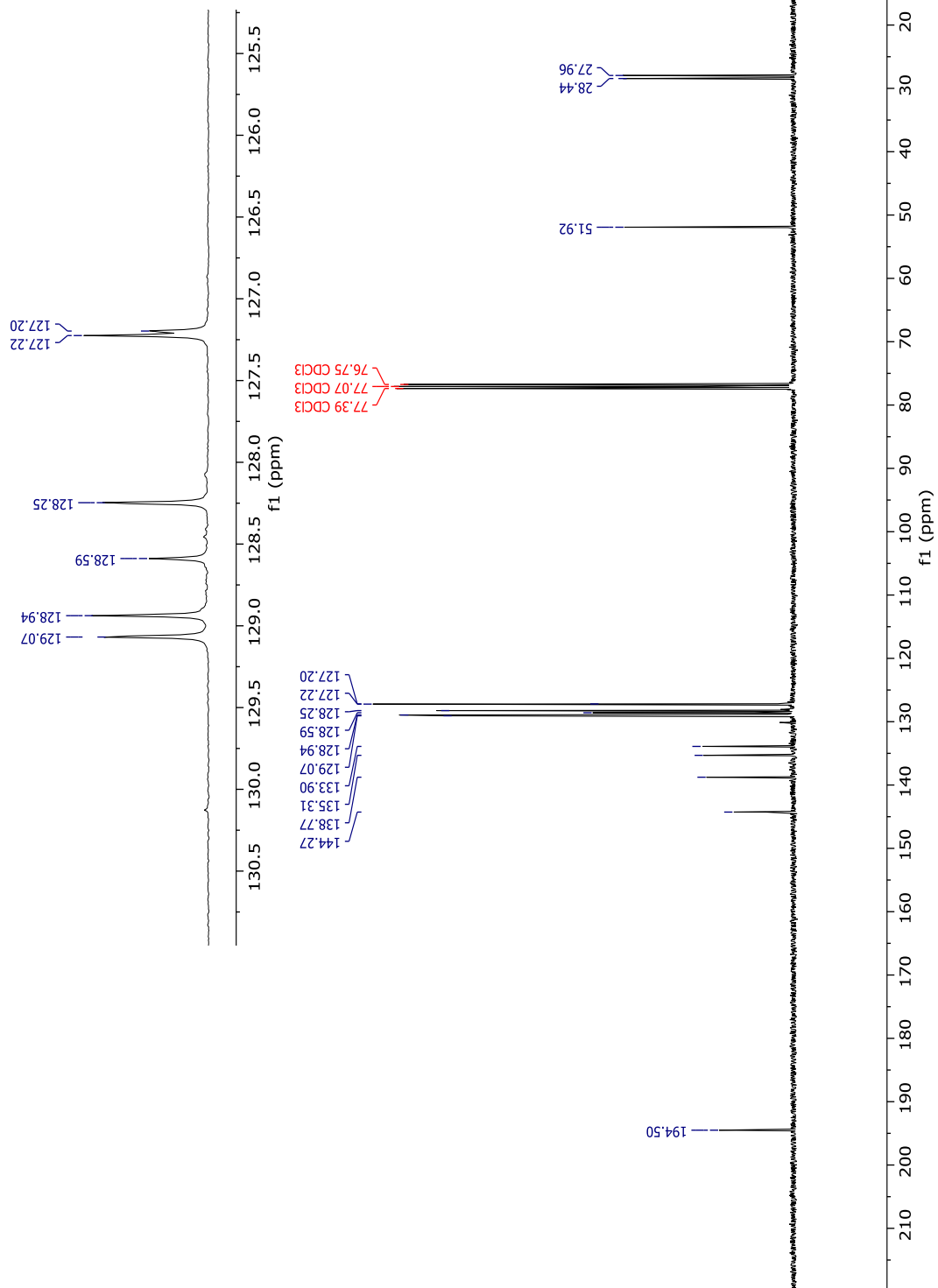
6.4

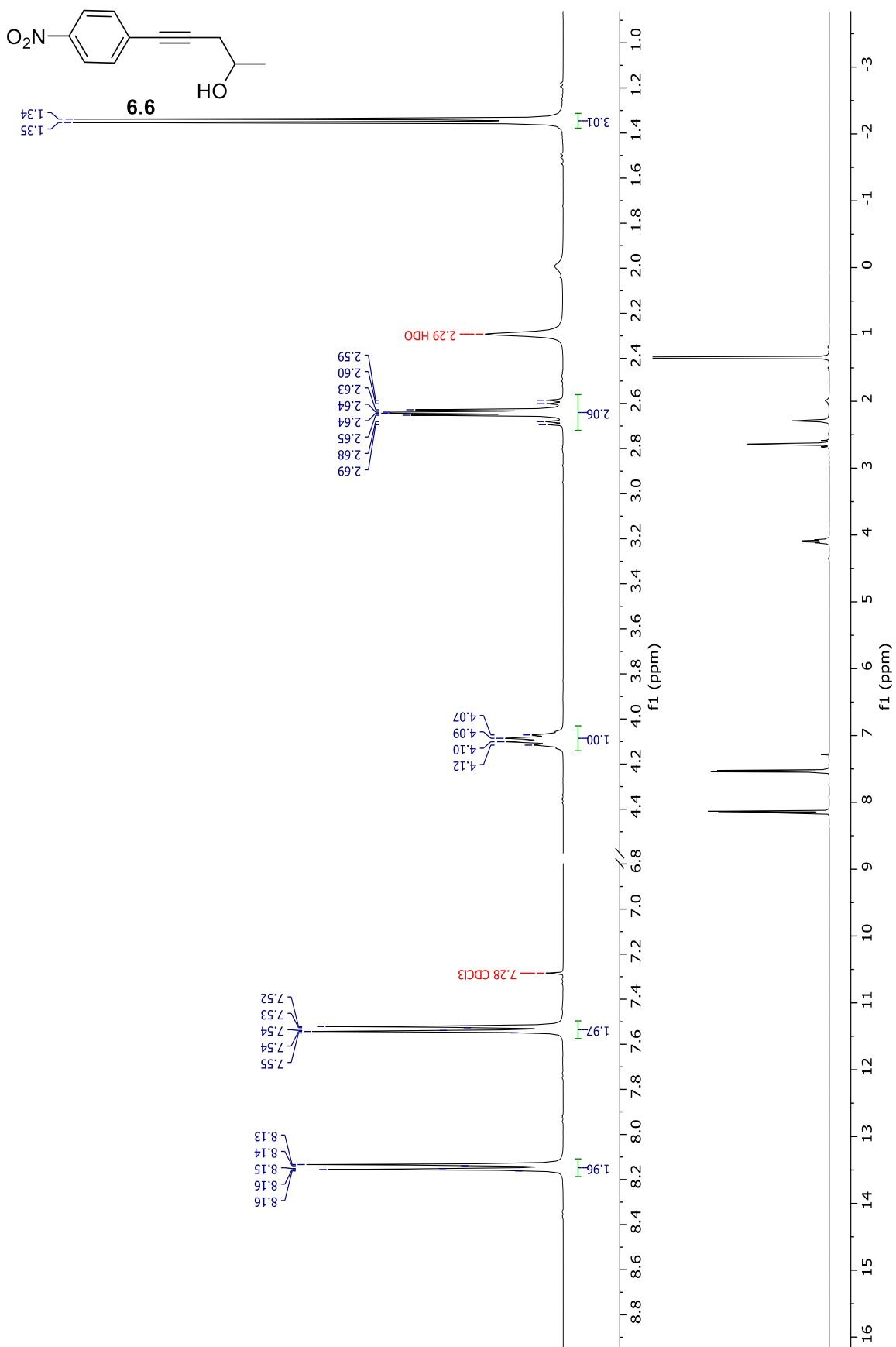


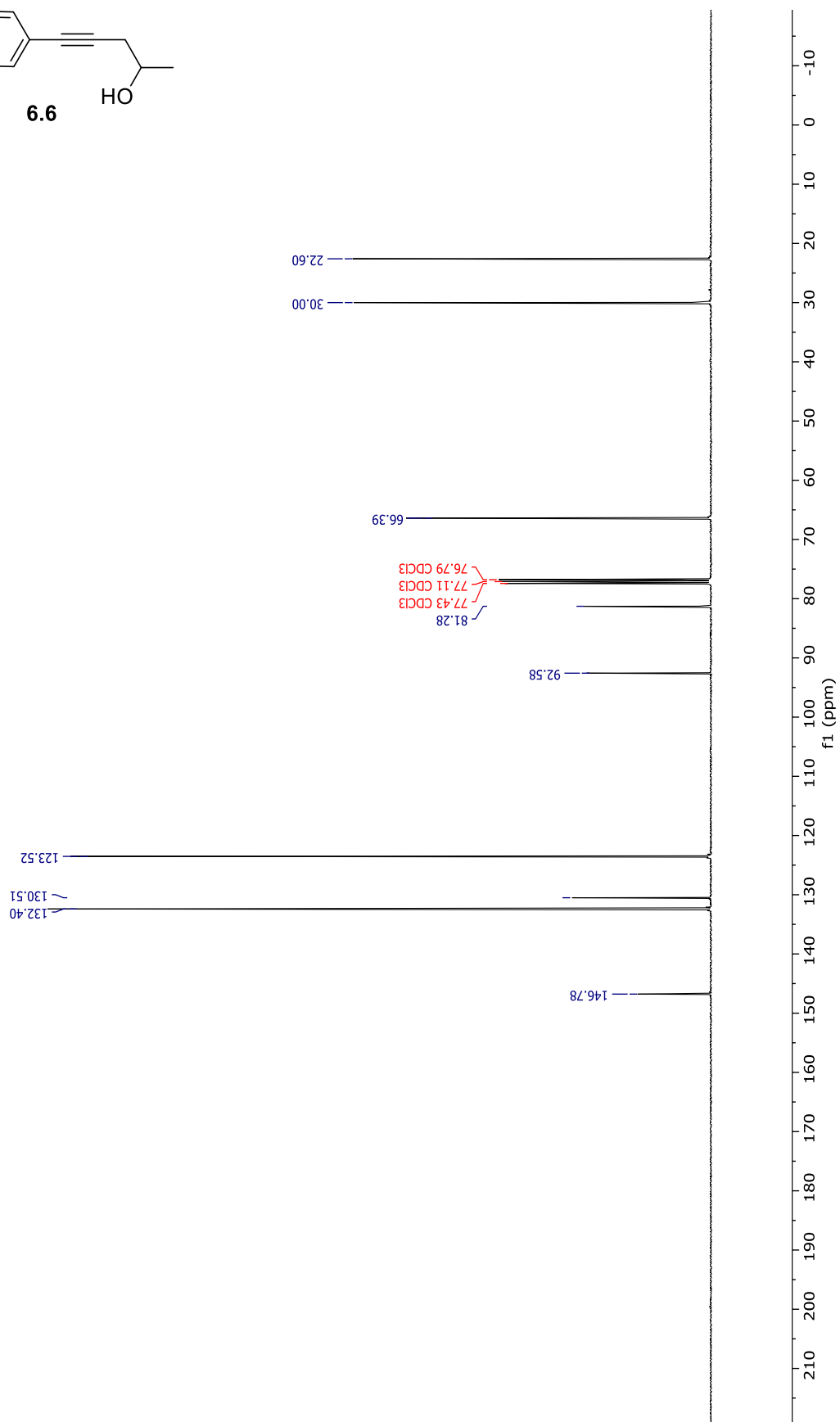
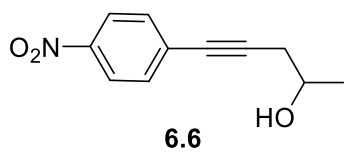


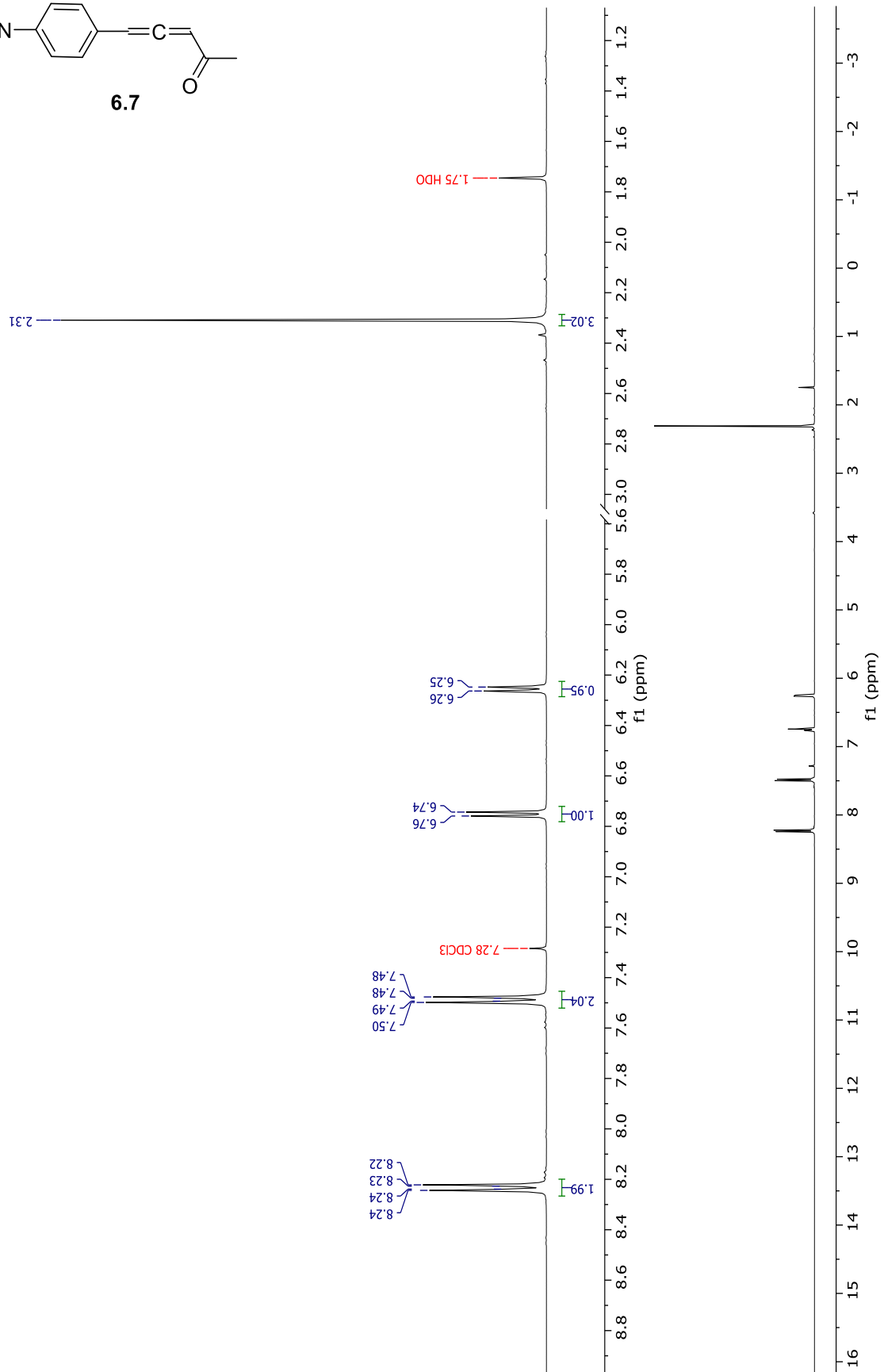
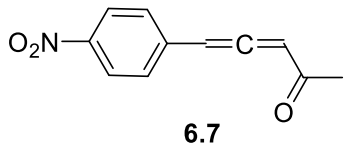


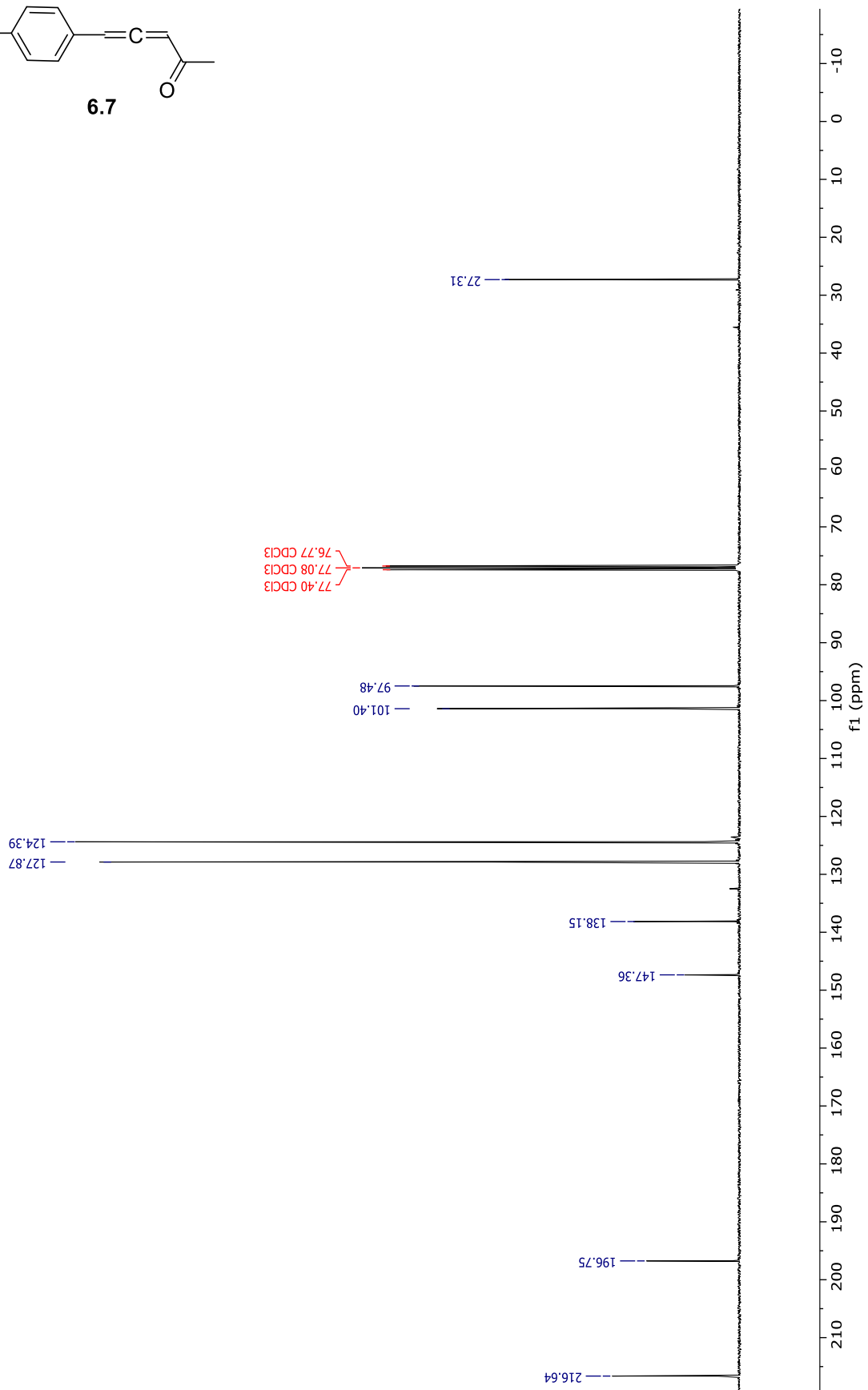
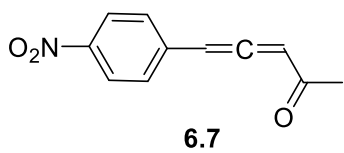
9.5

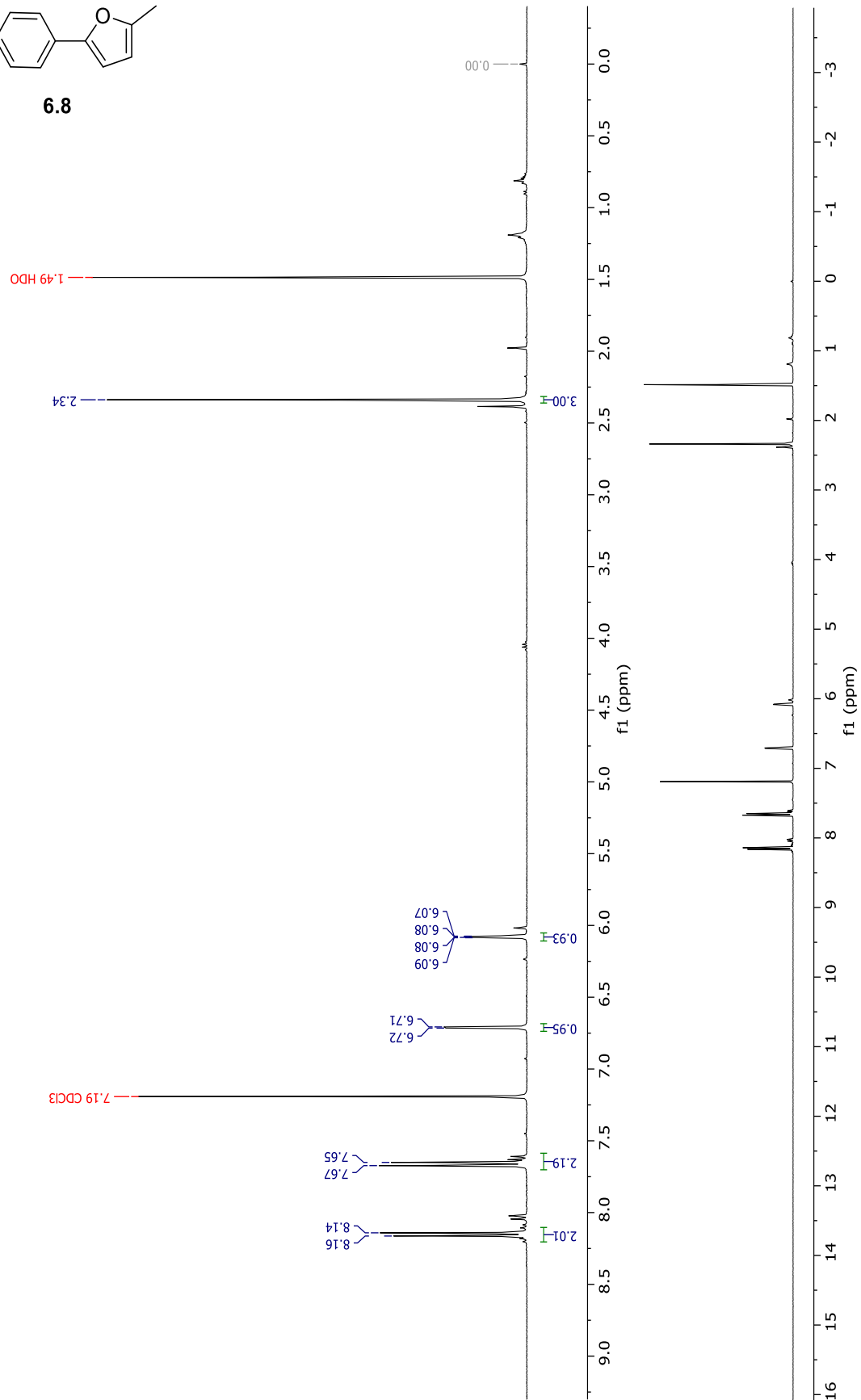
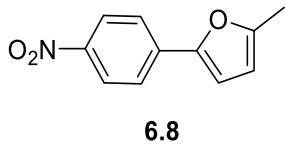


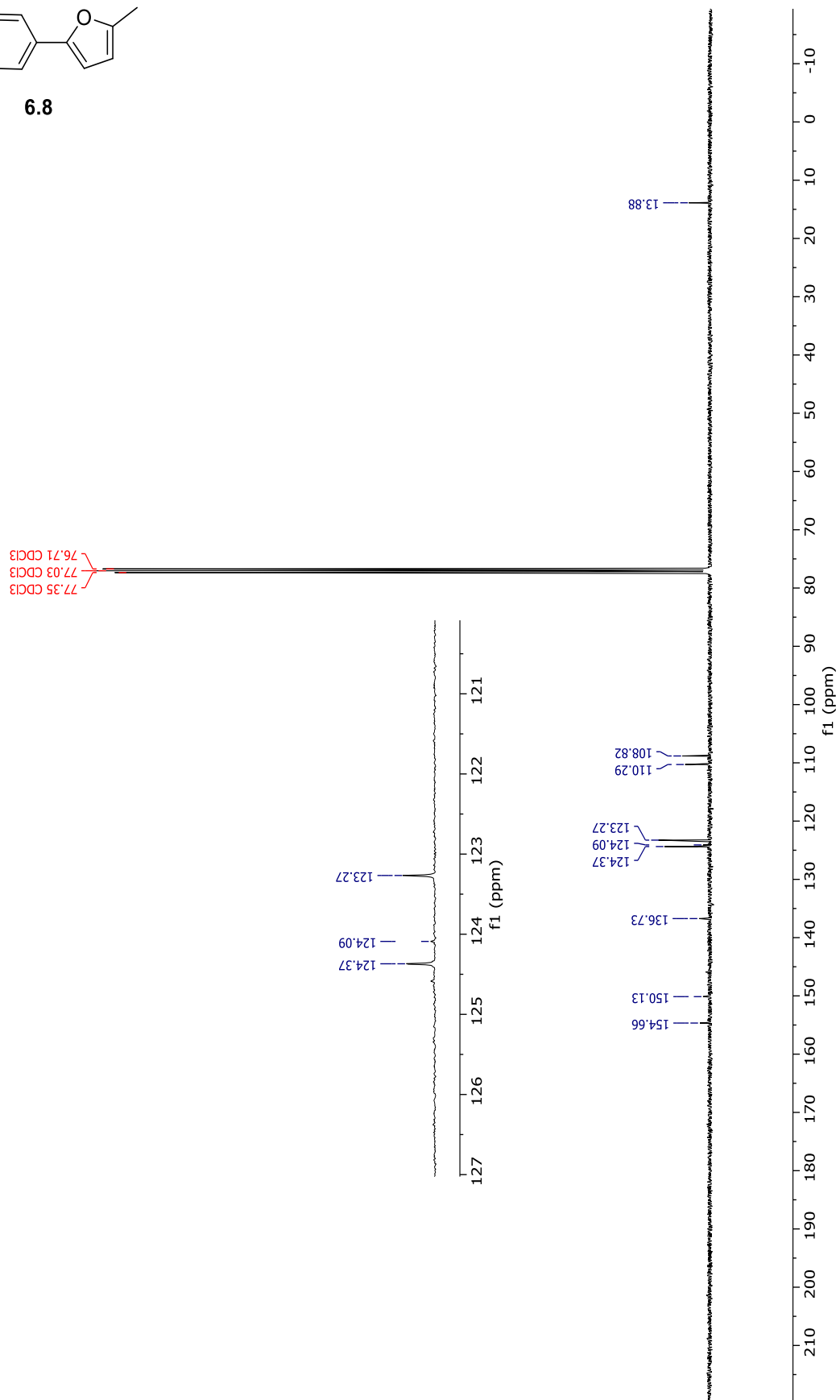
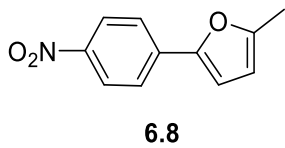


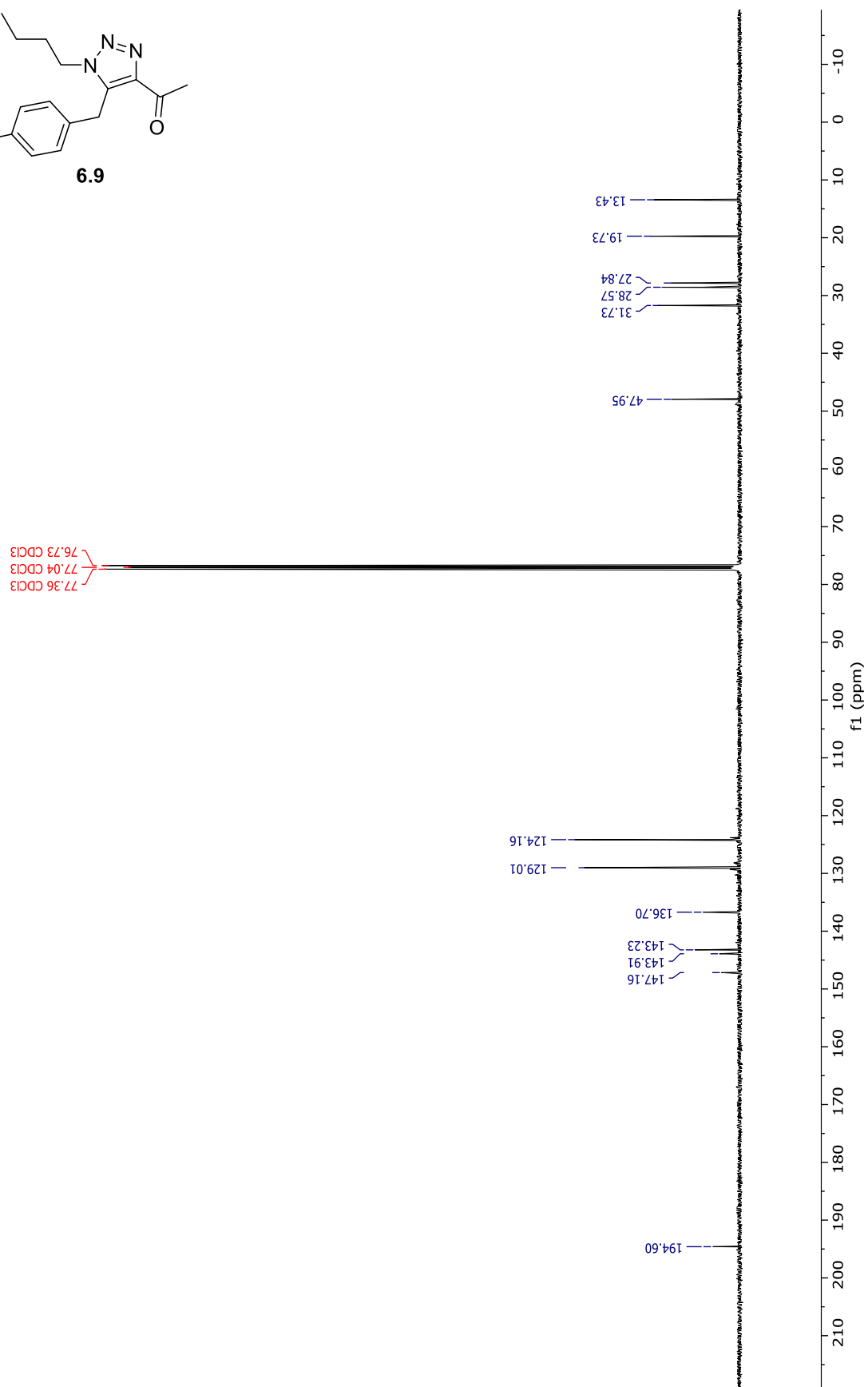
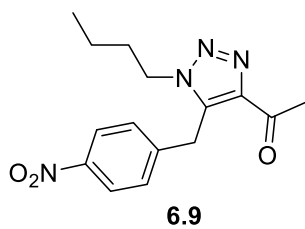


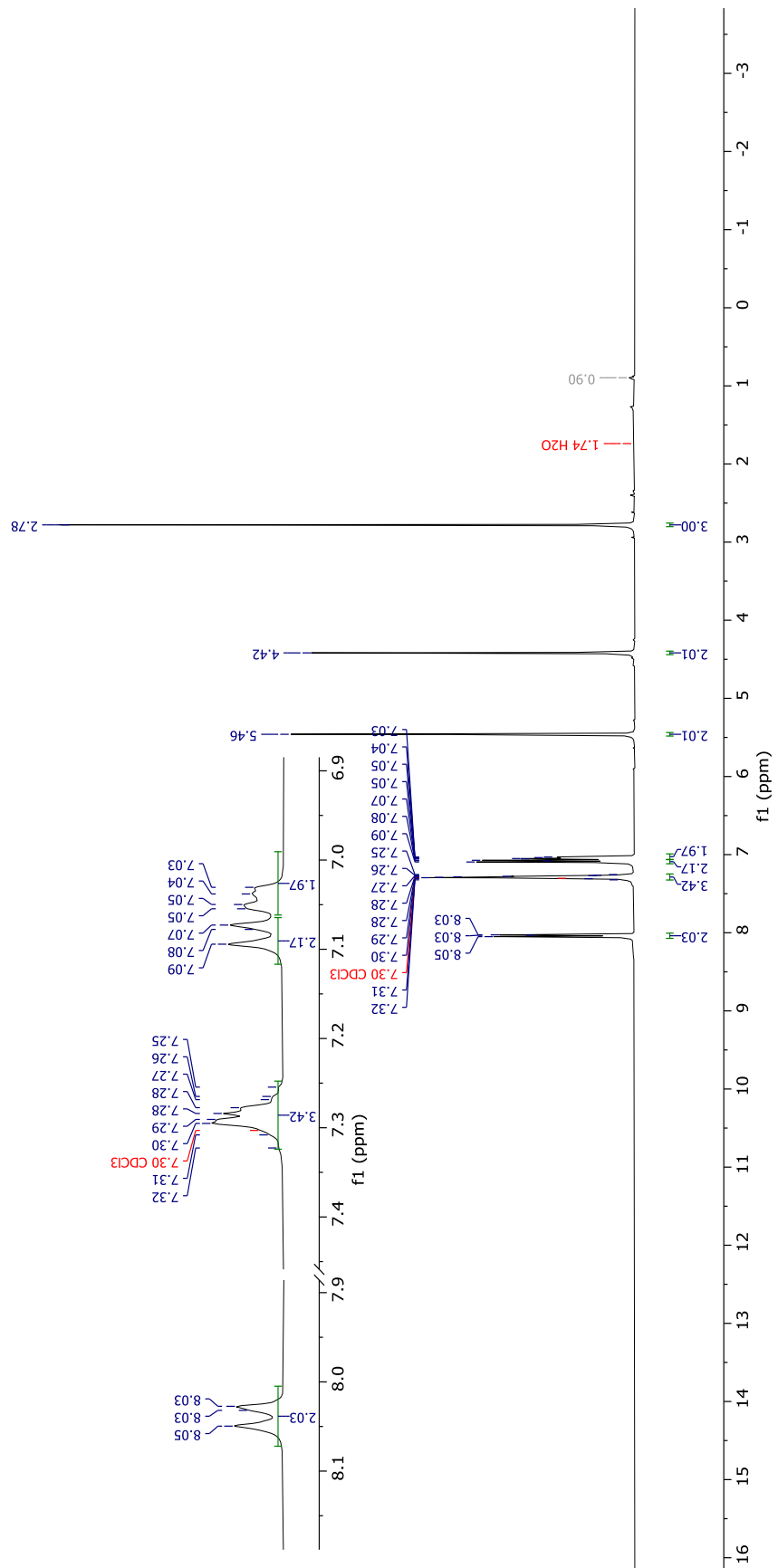
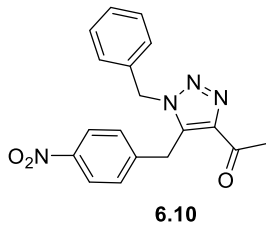




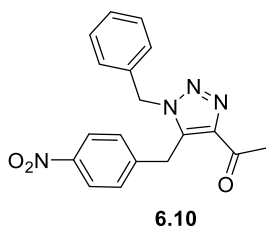








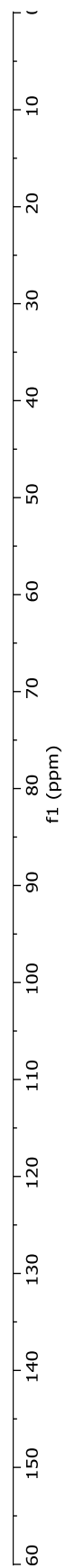
DEPT135



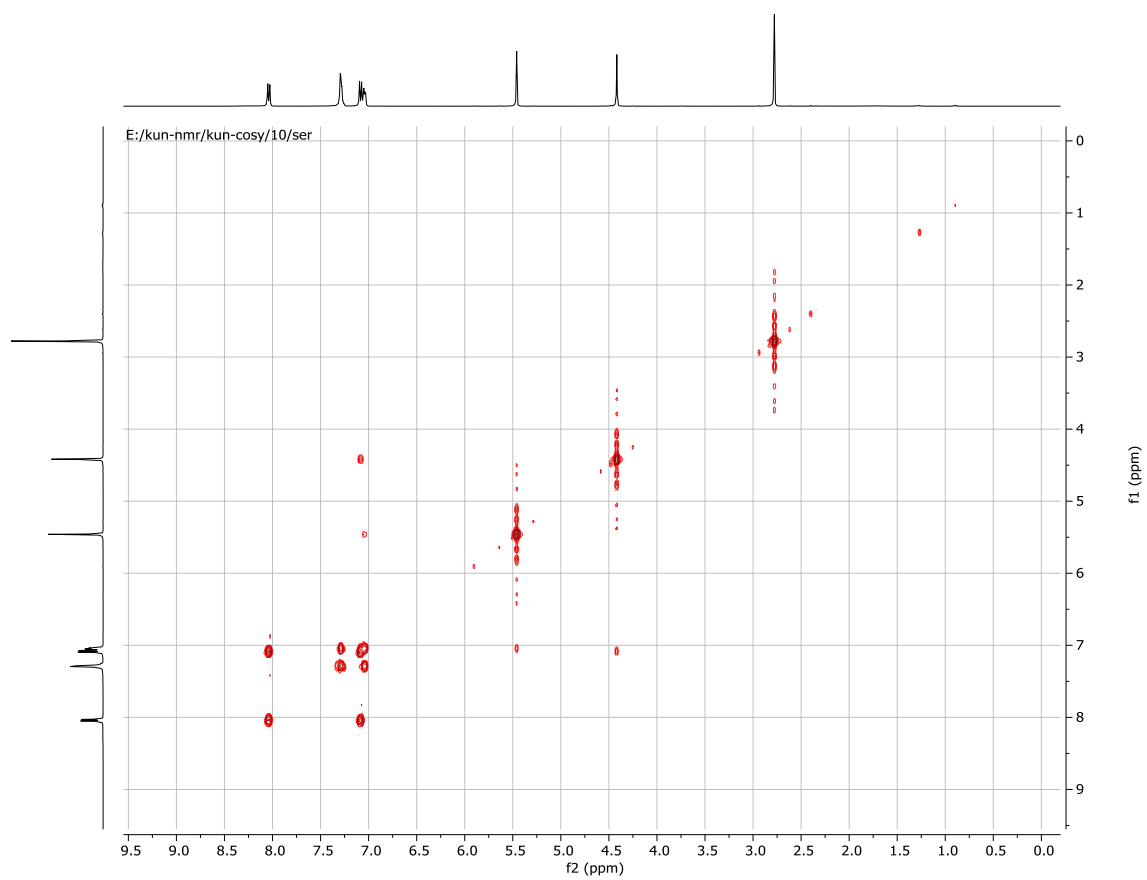
E:/kun-nmr/kun-dept135/10/ftd

129.18
128.98
128.83
127.09
123.90

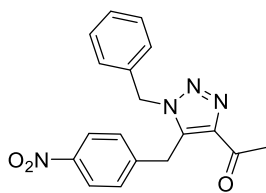
27.88



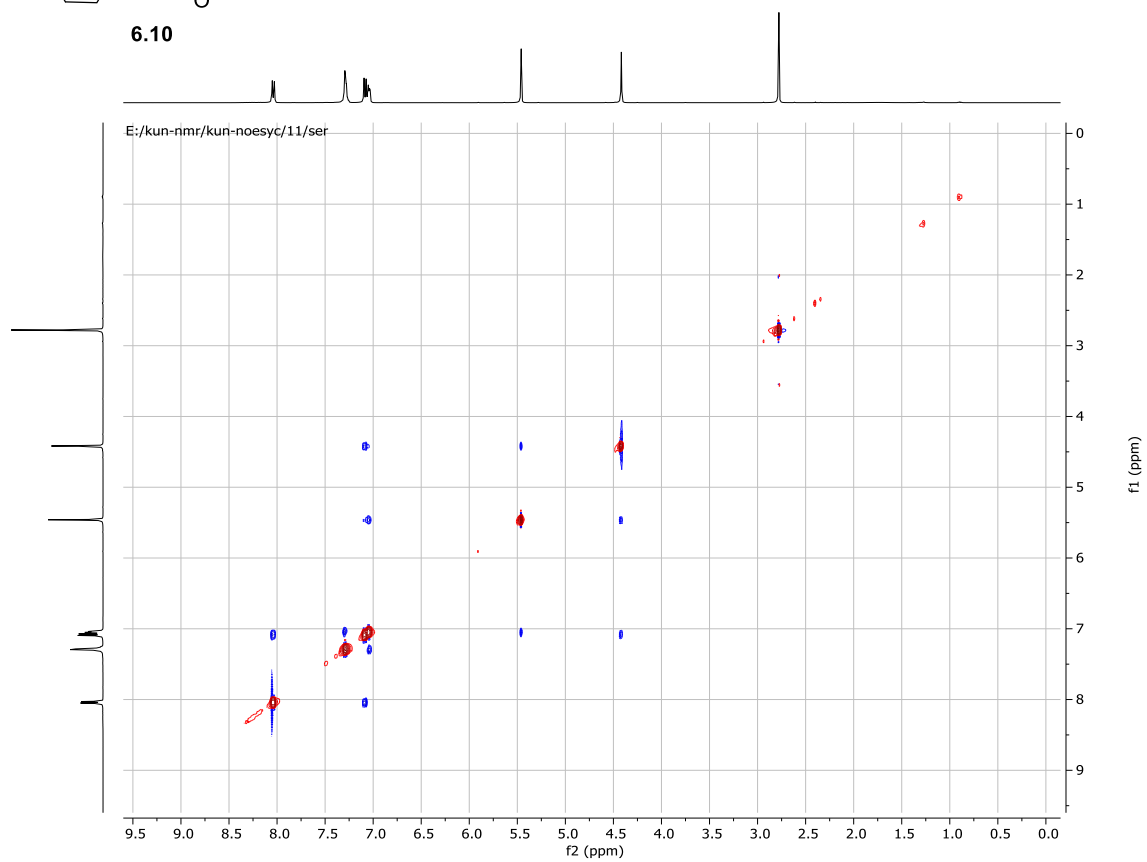
COSY



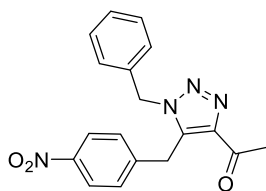
NOESY



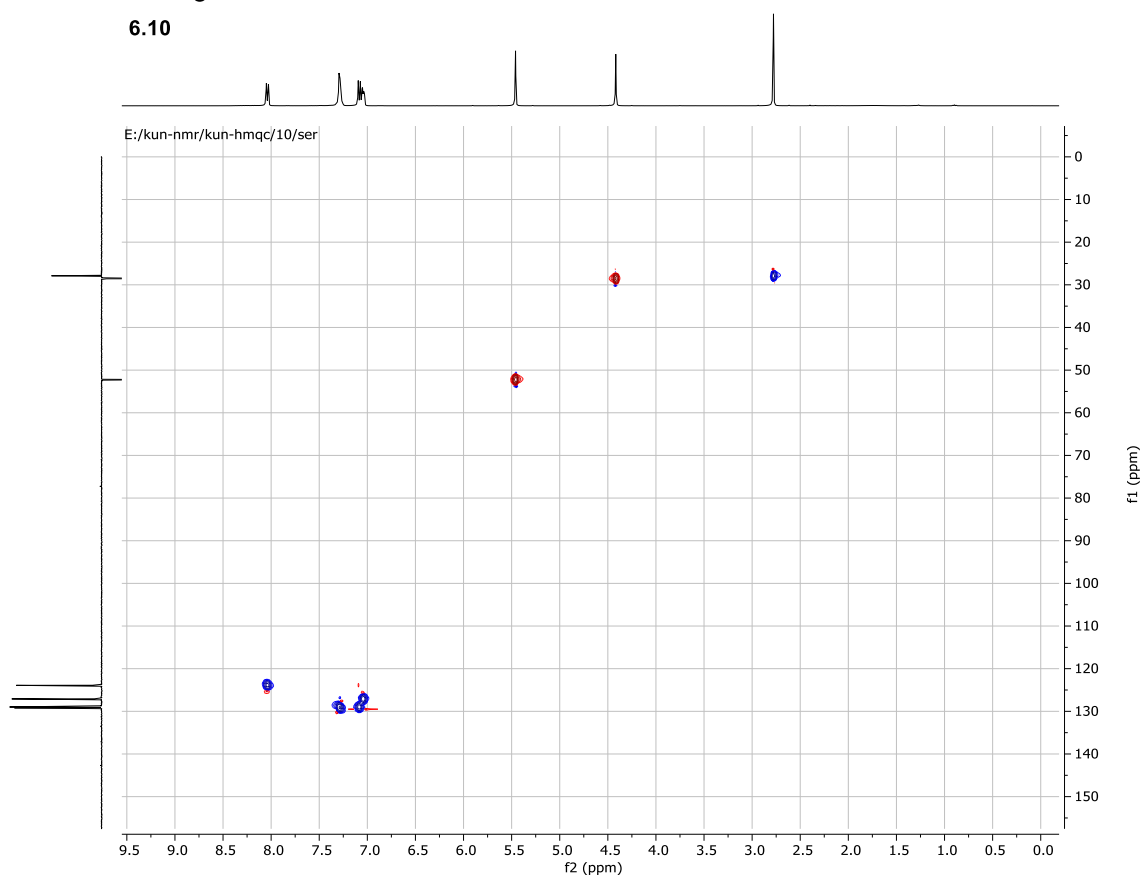
6.10



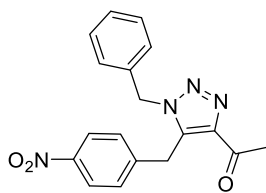
HSQC



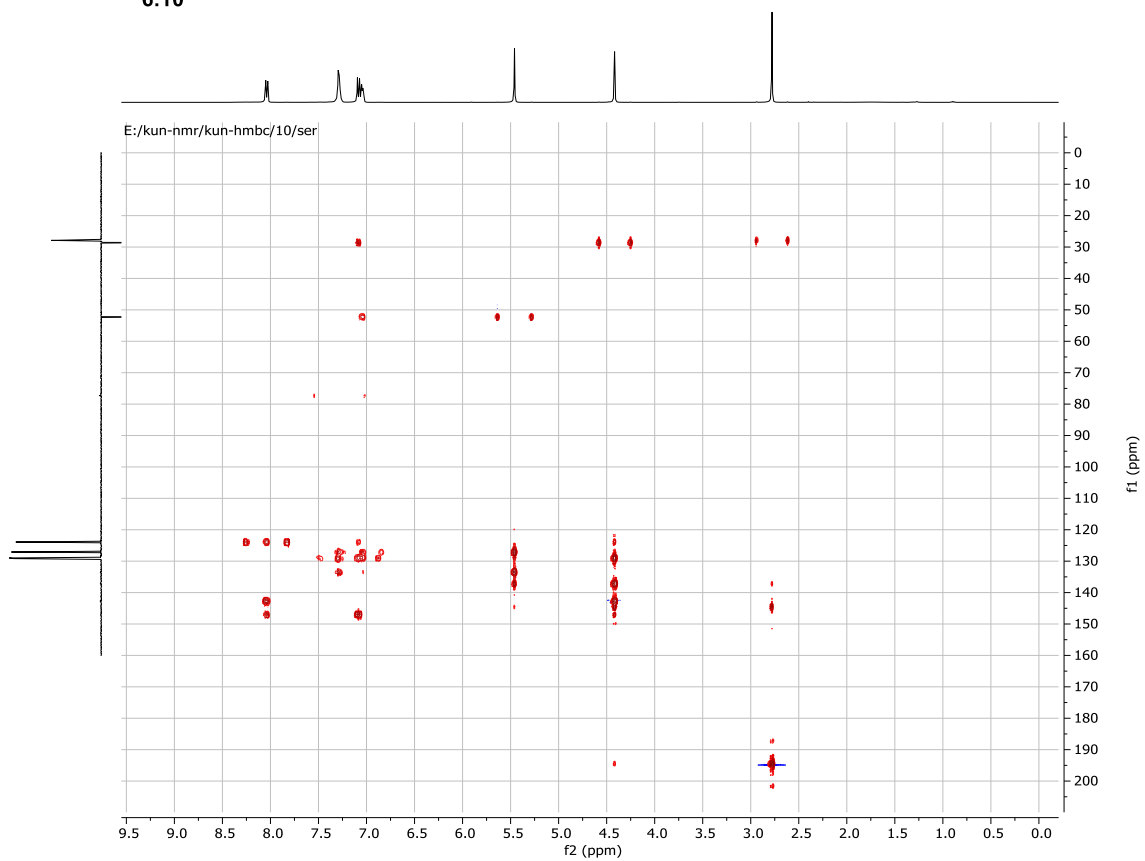
6.10

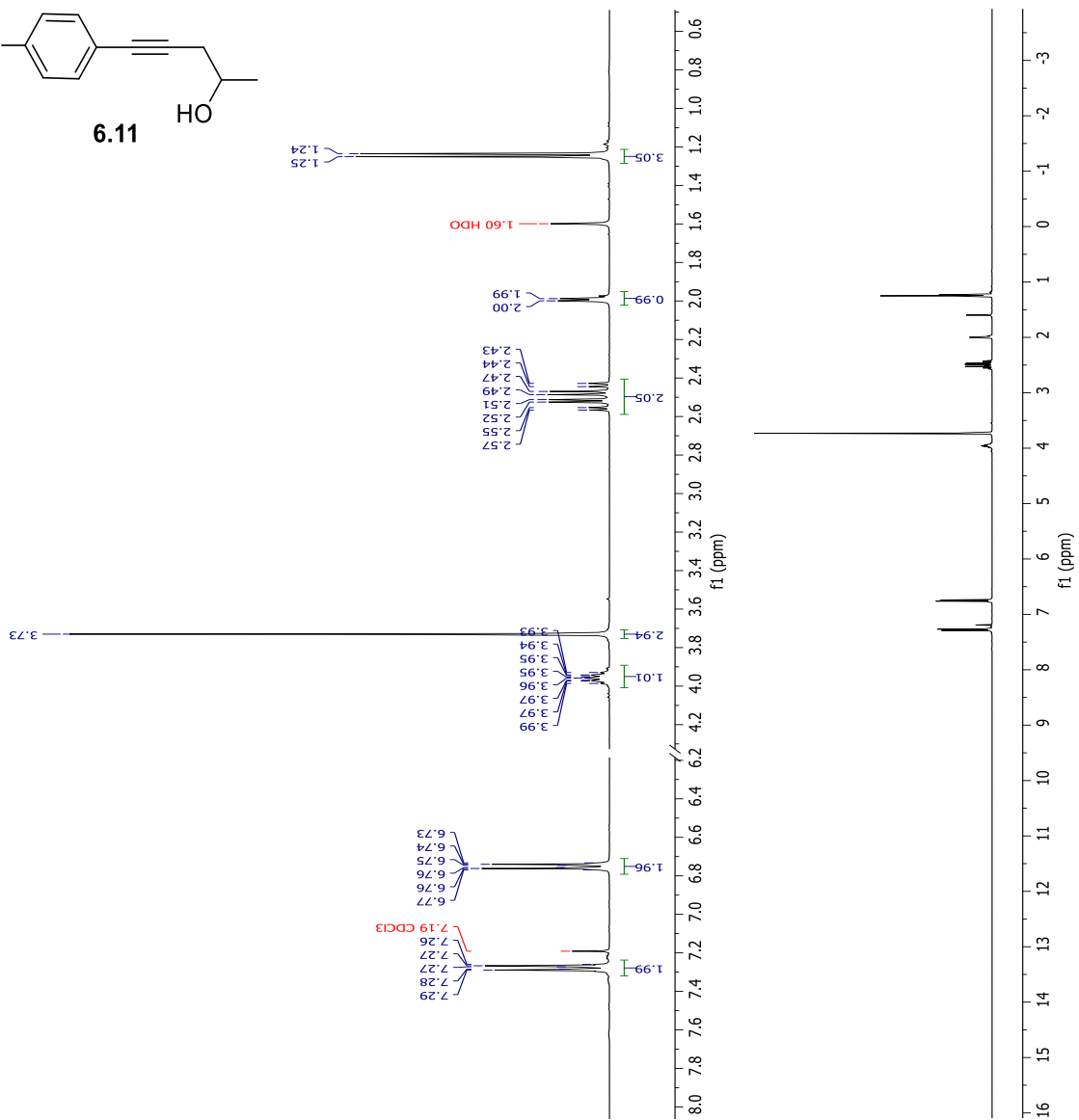
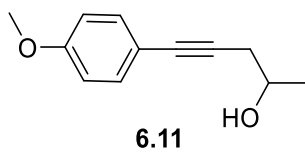


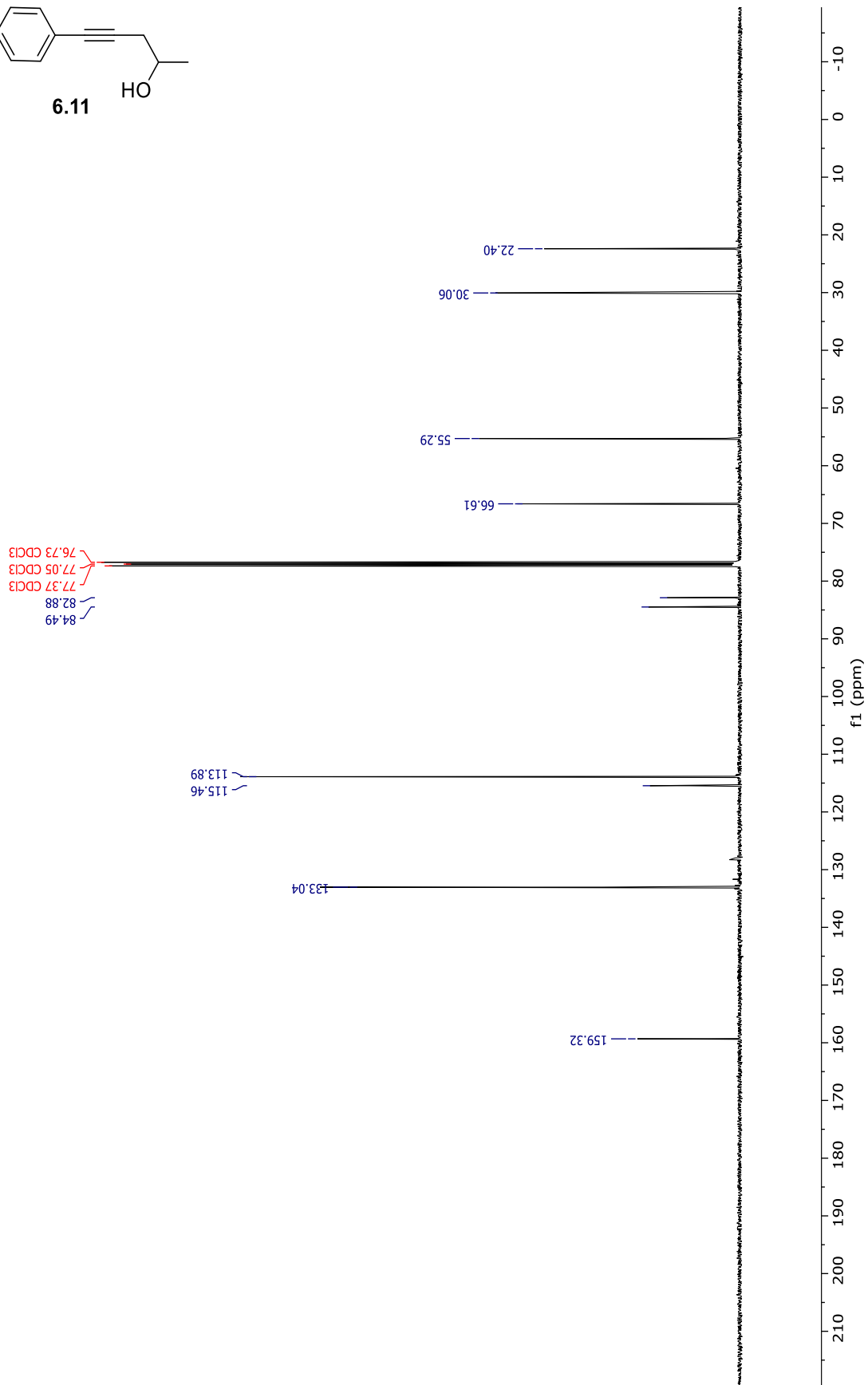
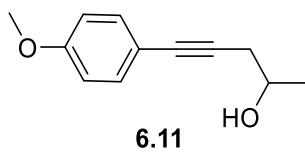
HMBC

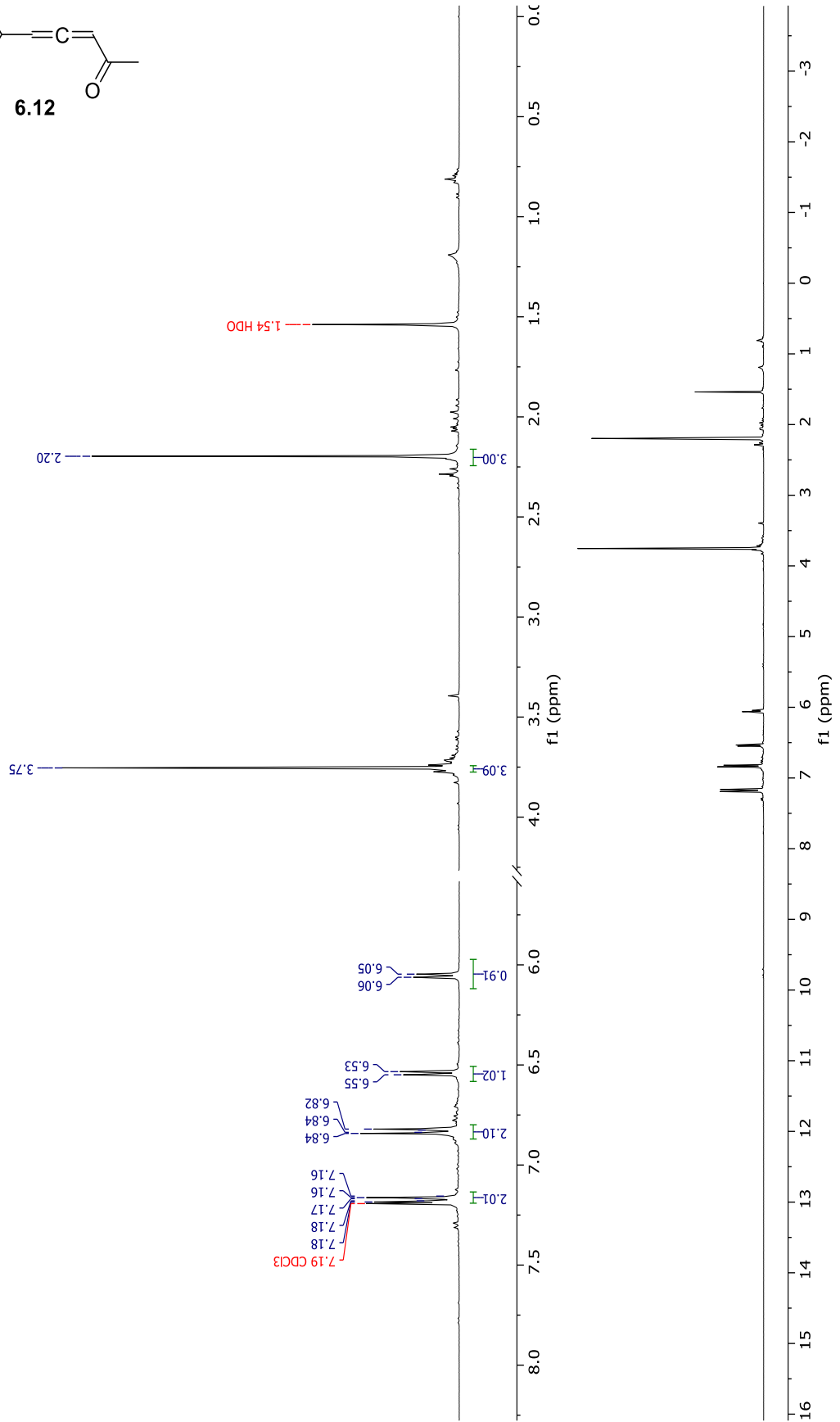
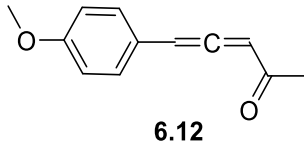


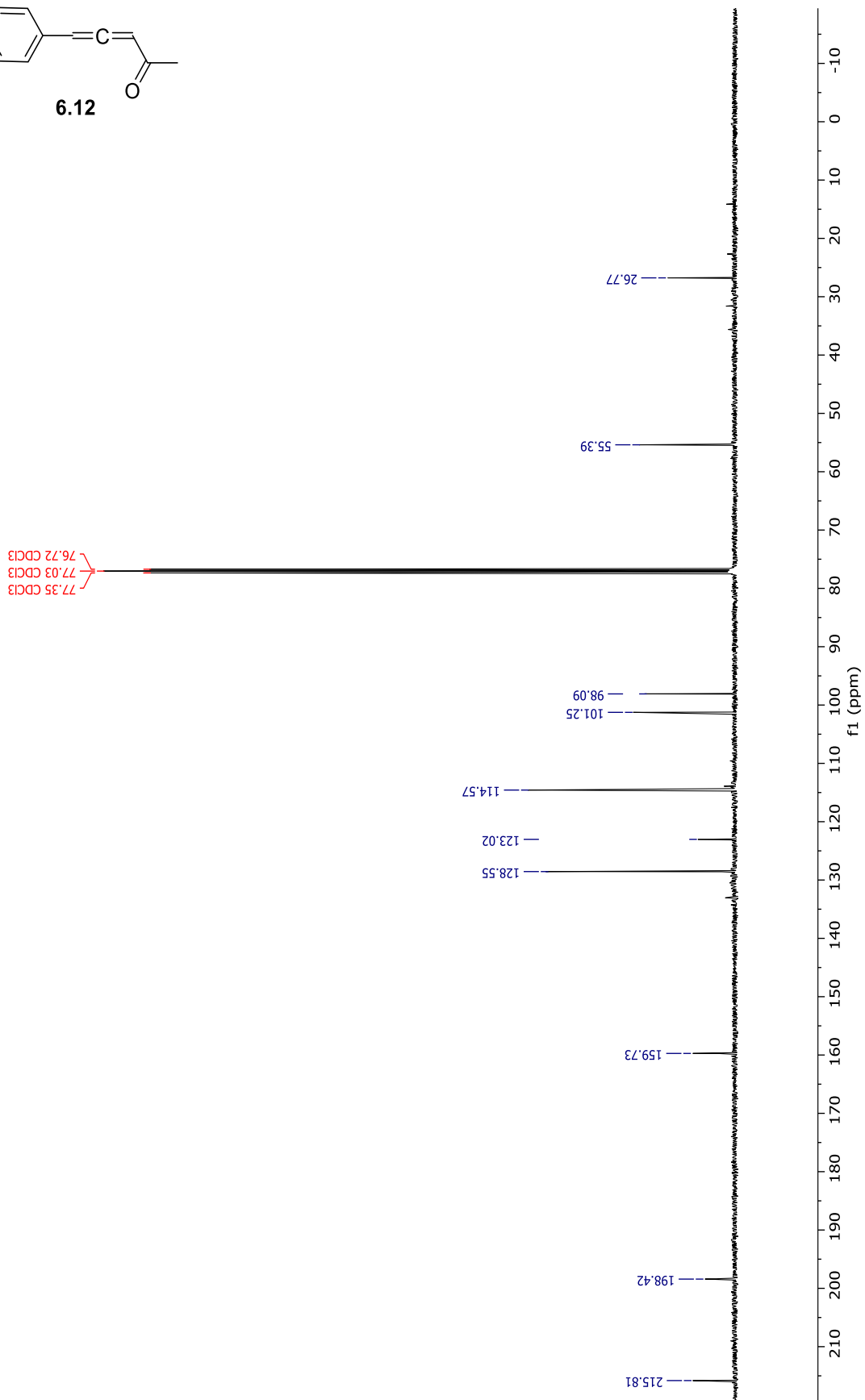
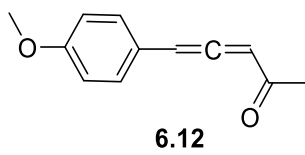
6.10

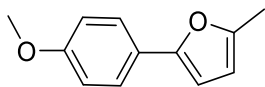




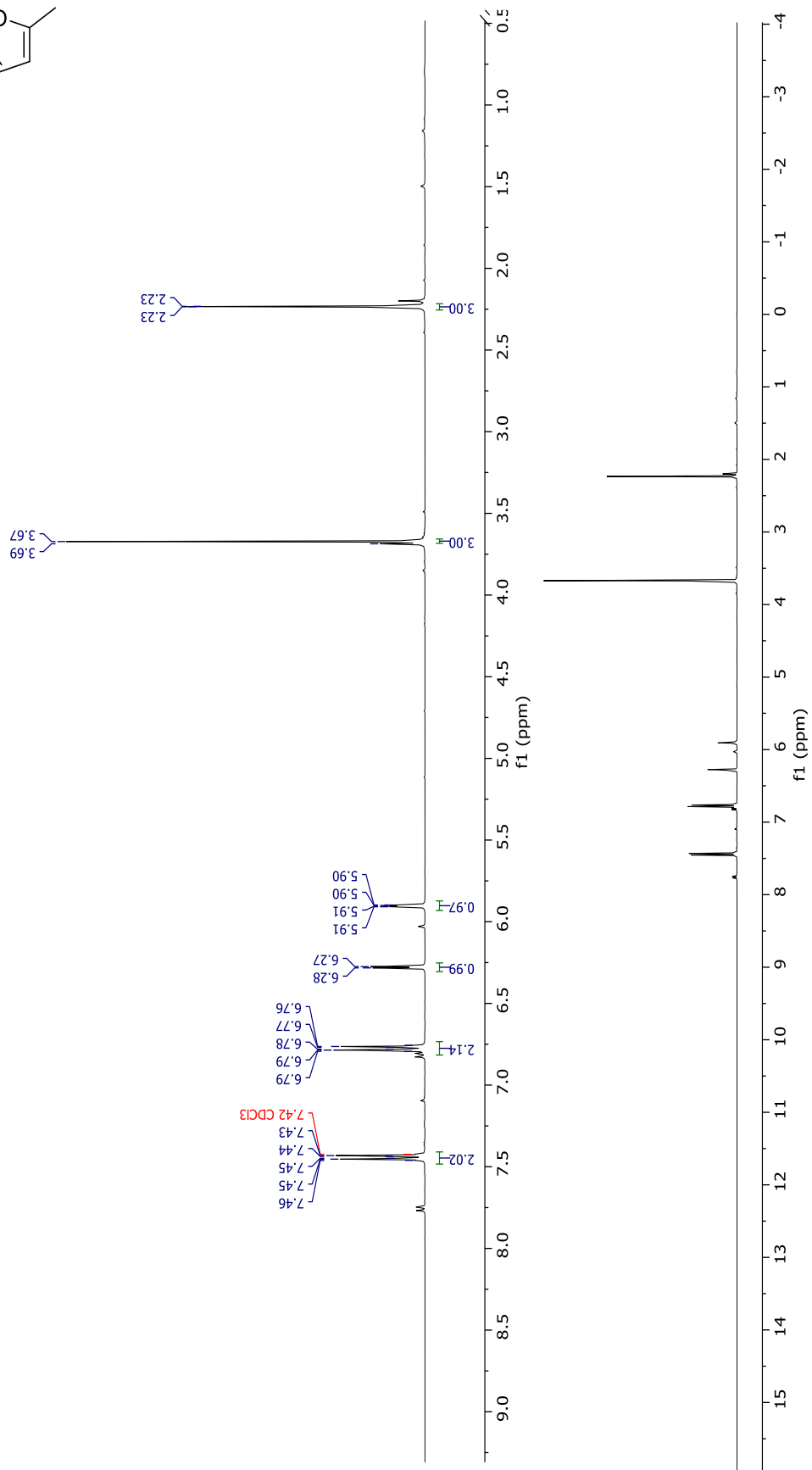


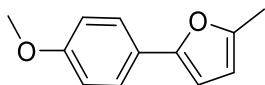




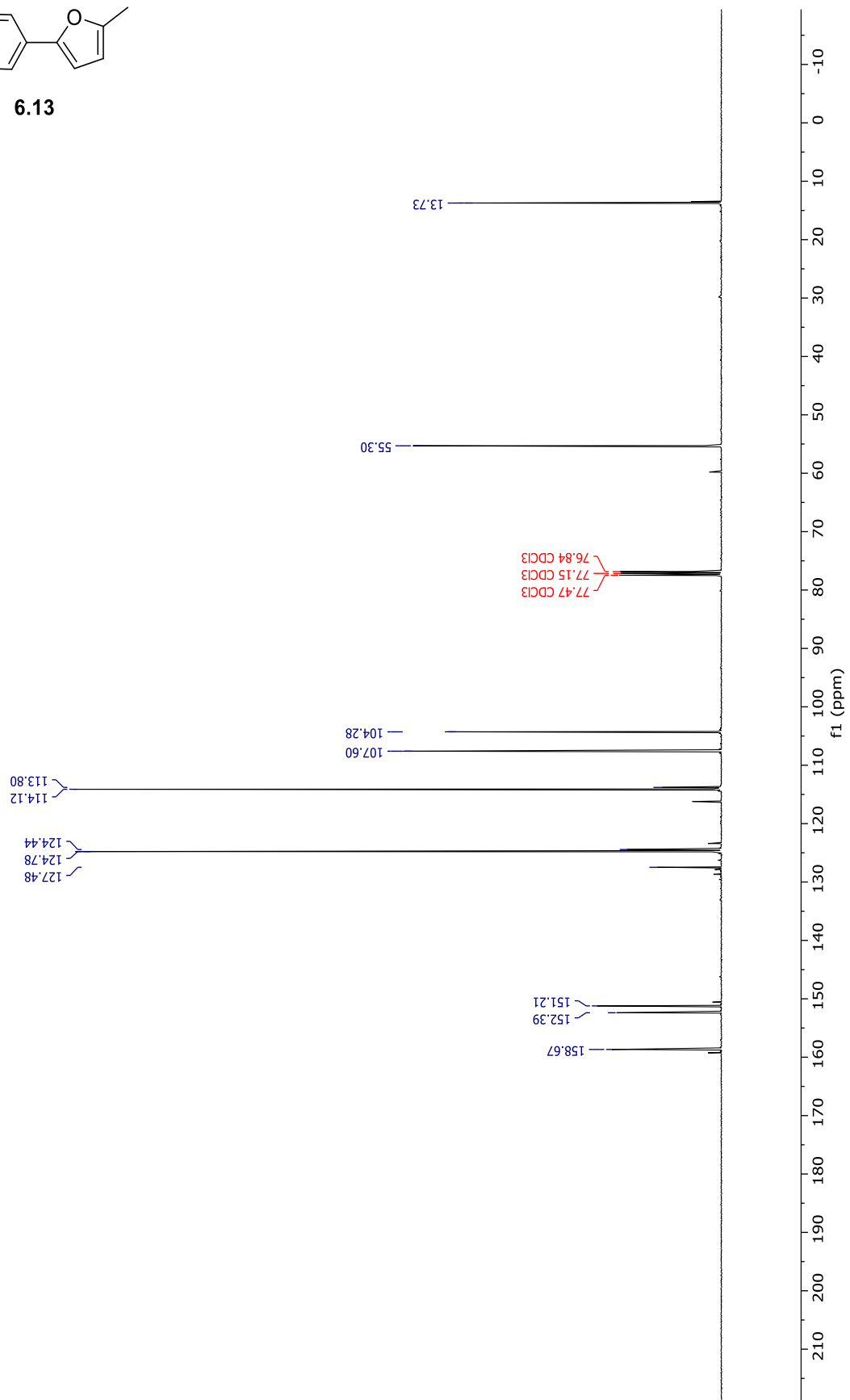


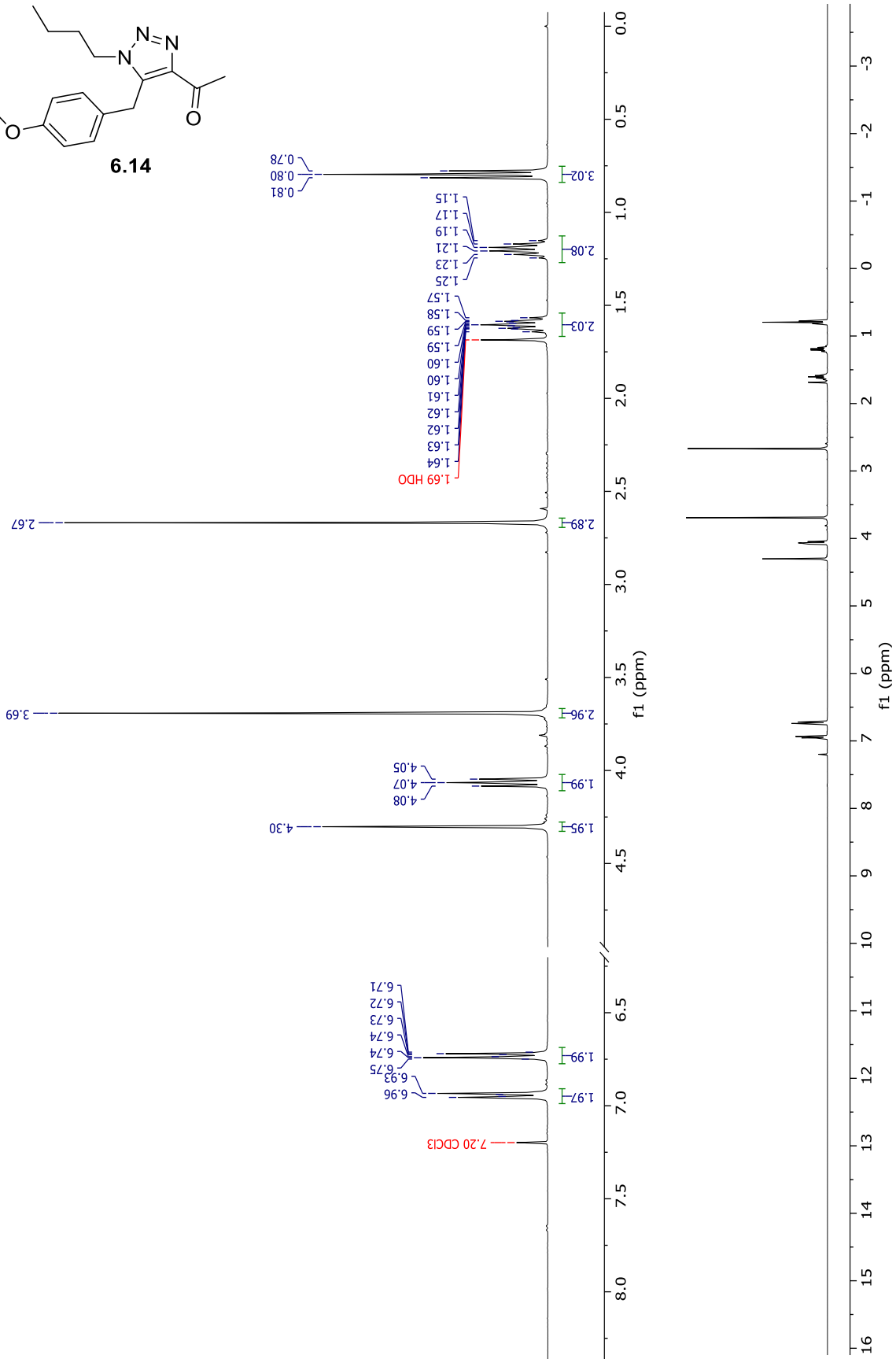
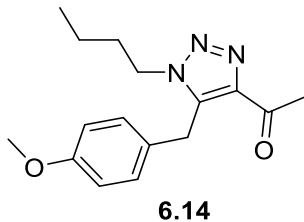
6.13

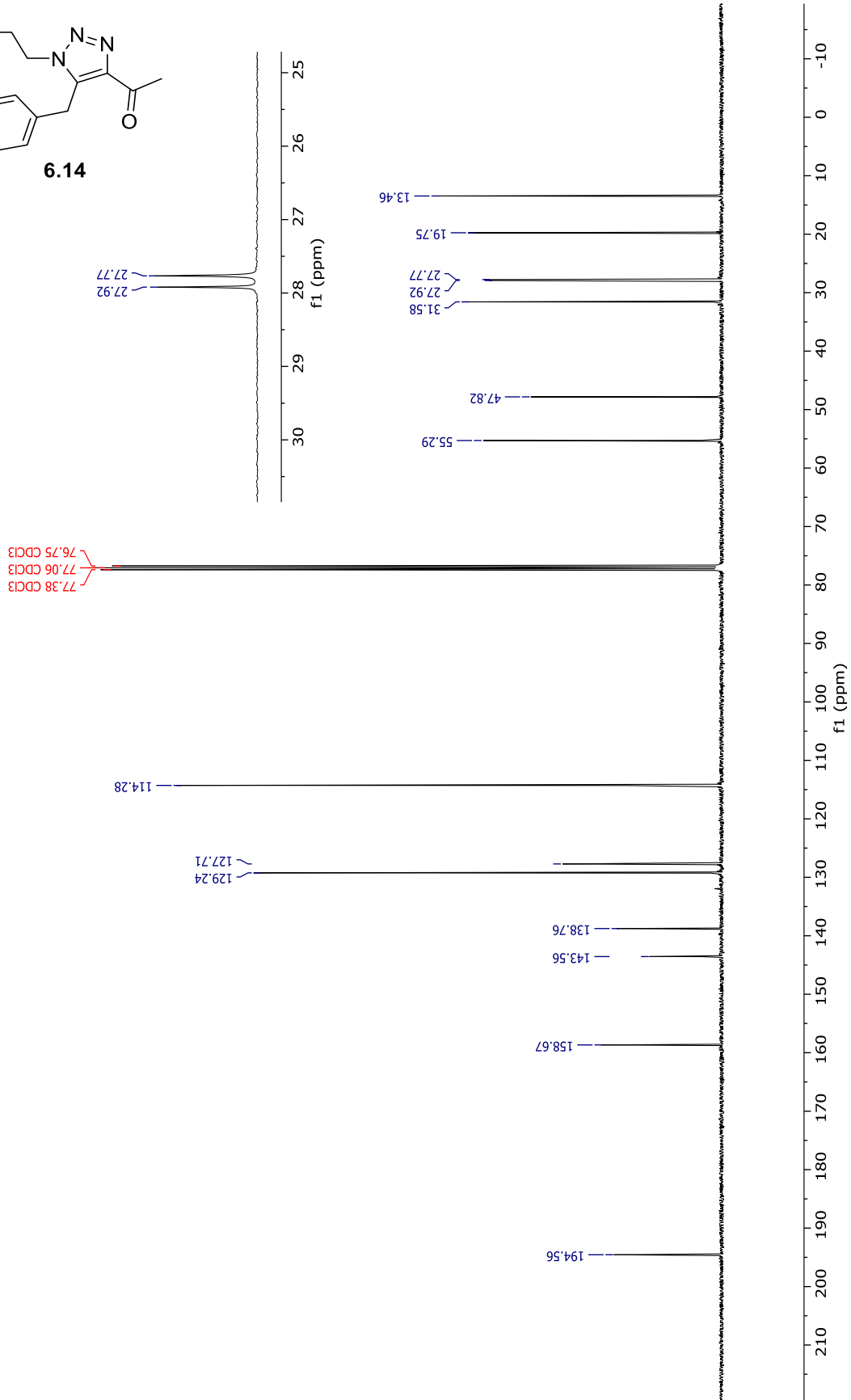
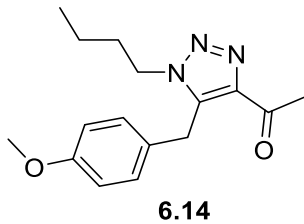


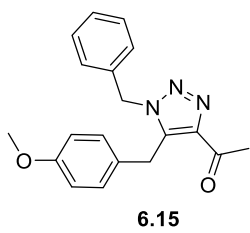


6.13

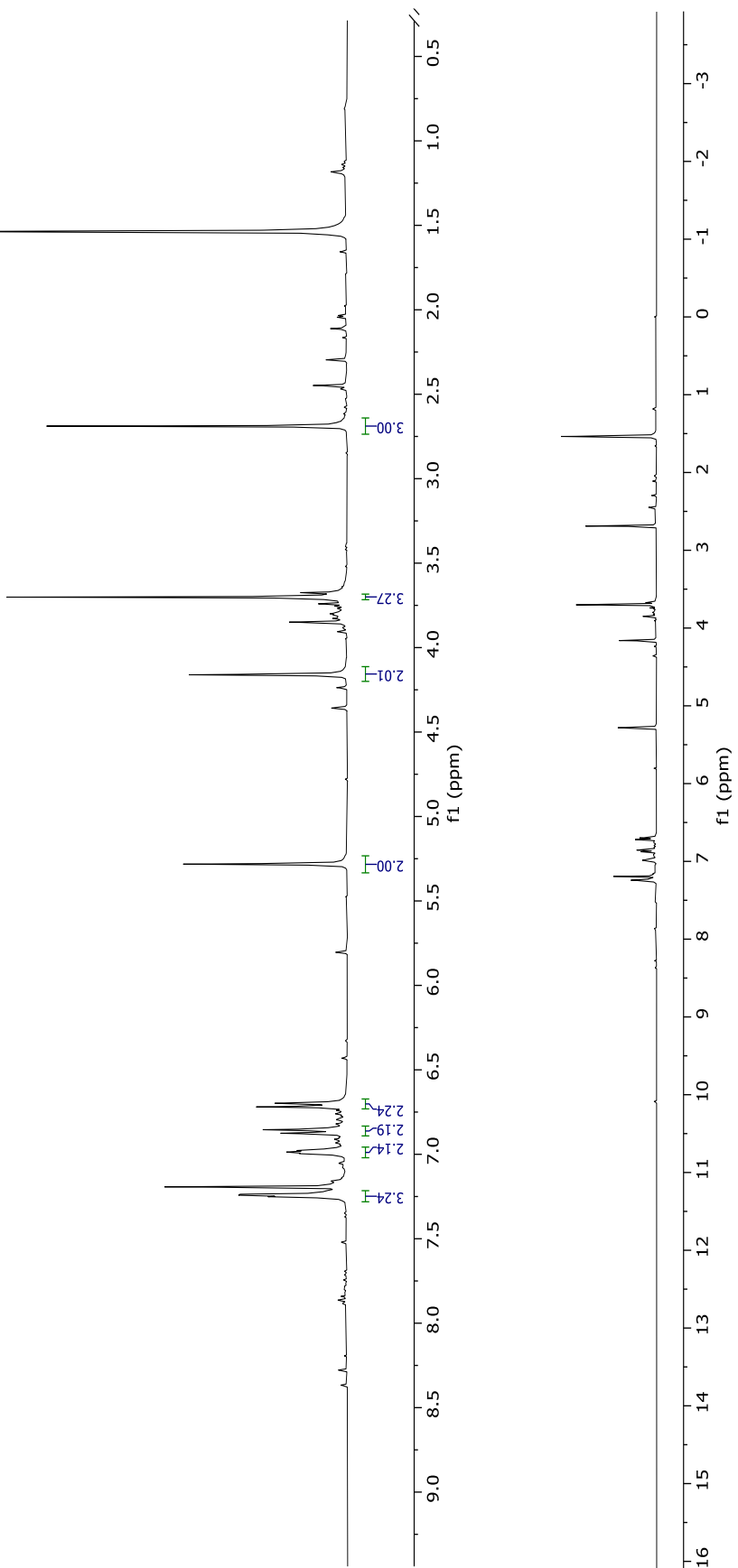


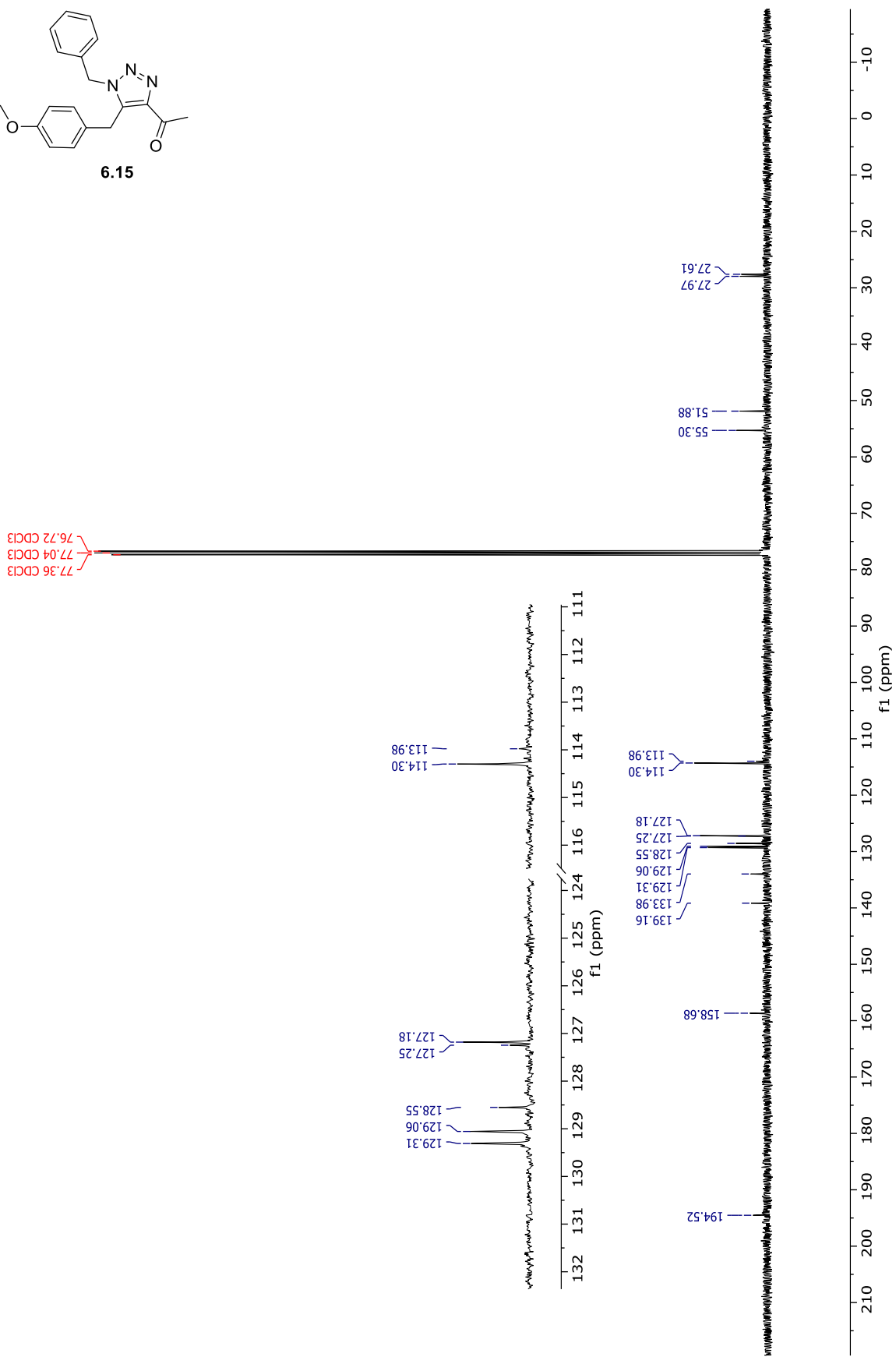
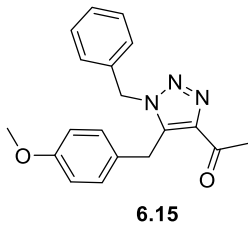


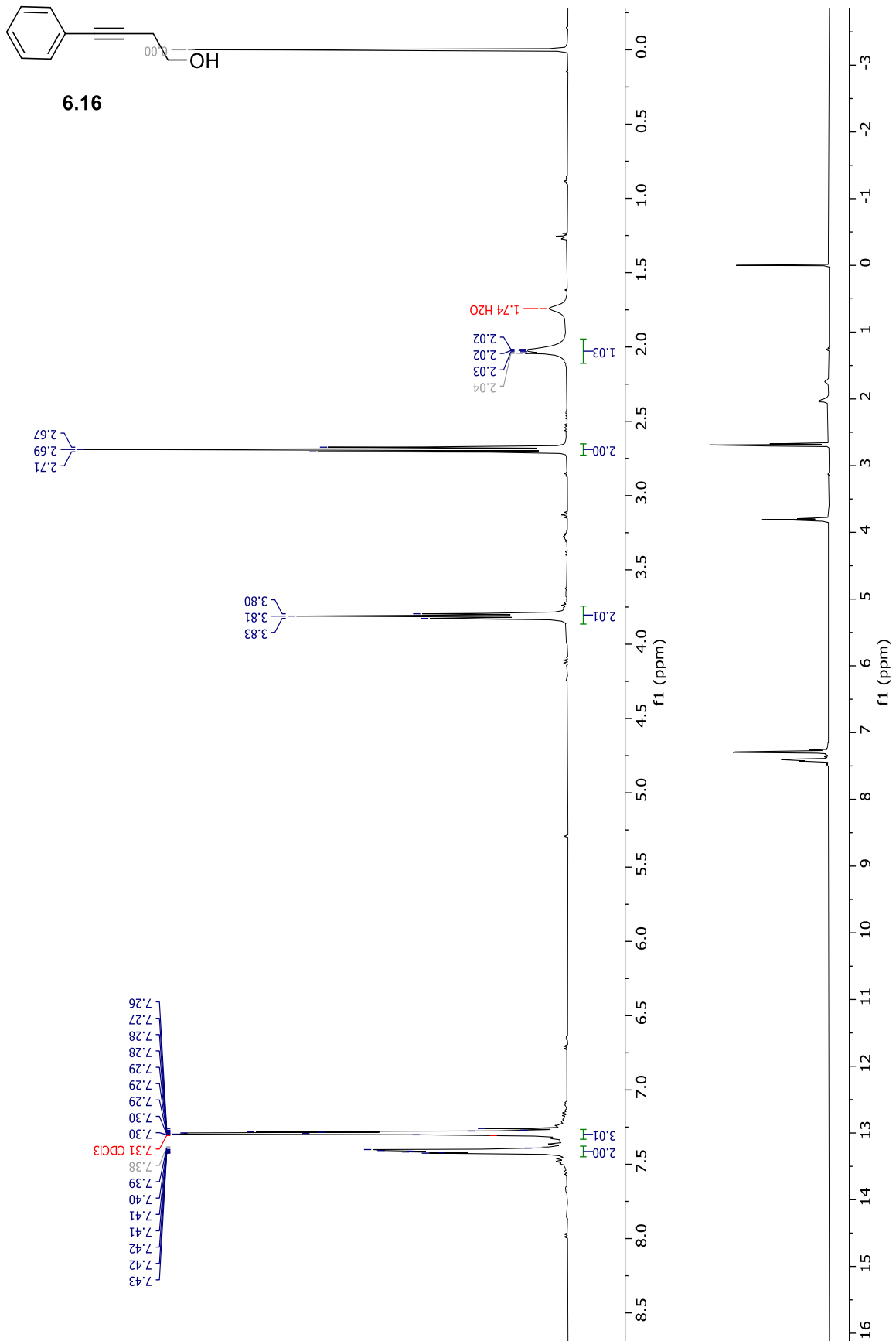


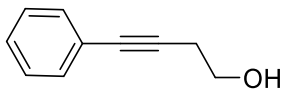


1.54 H₂O

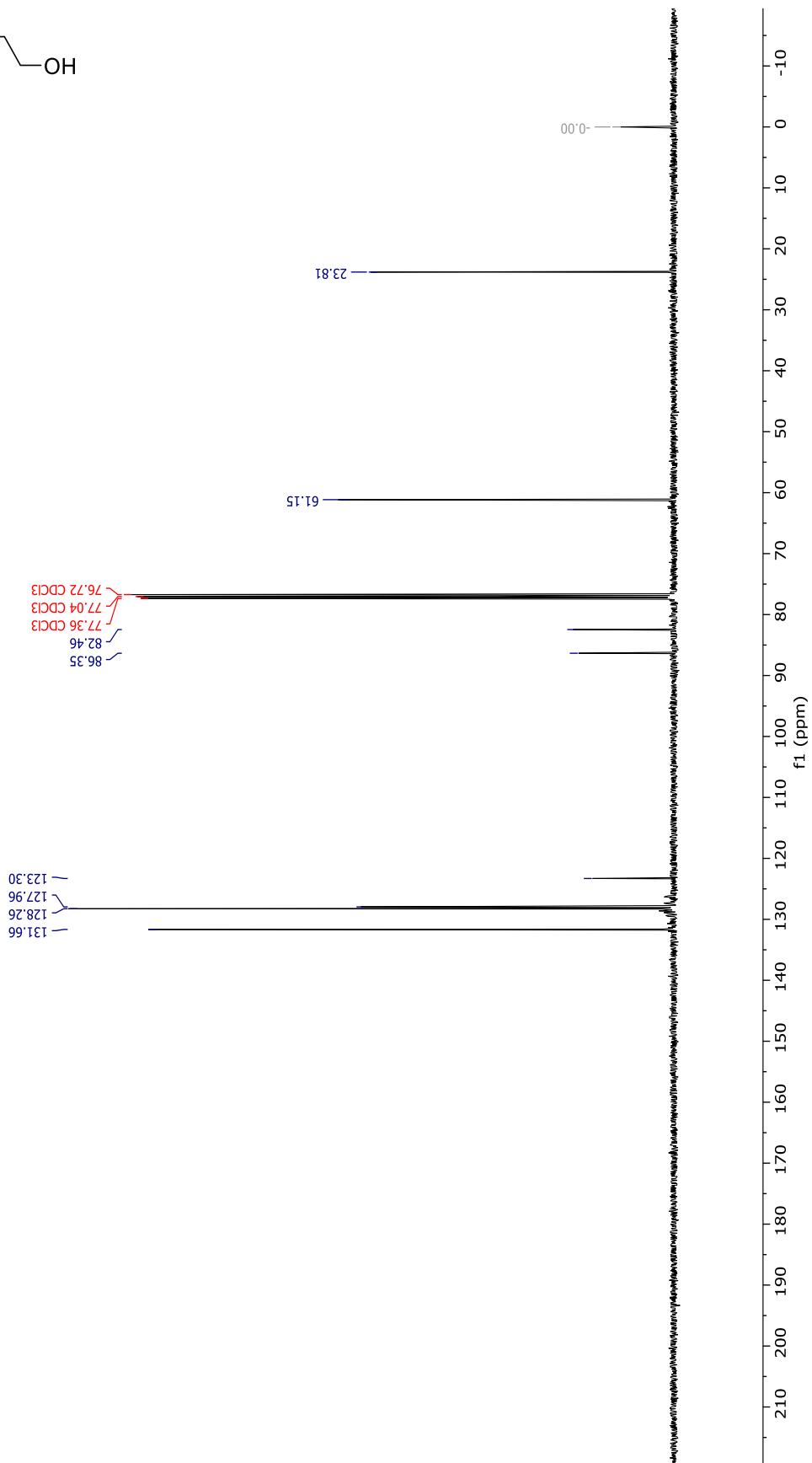


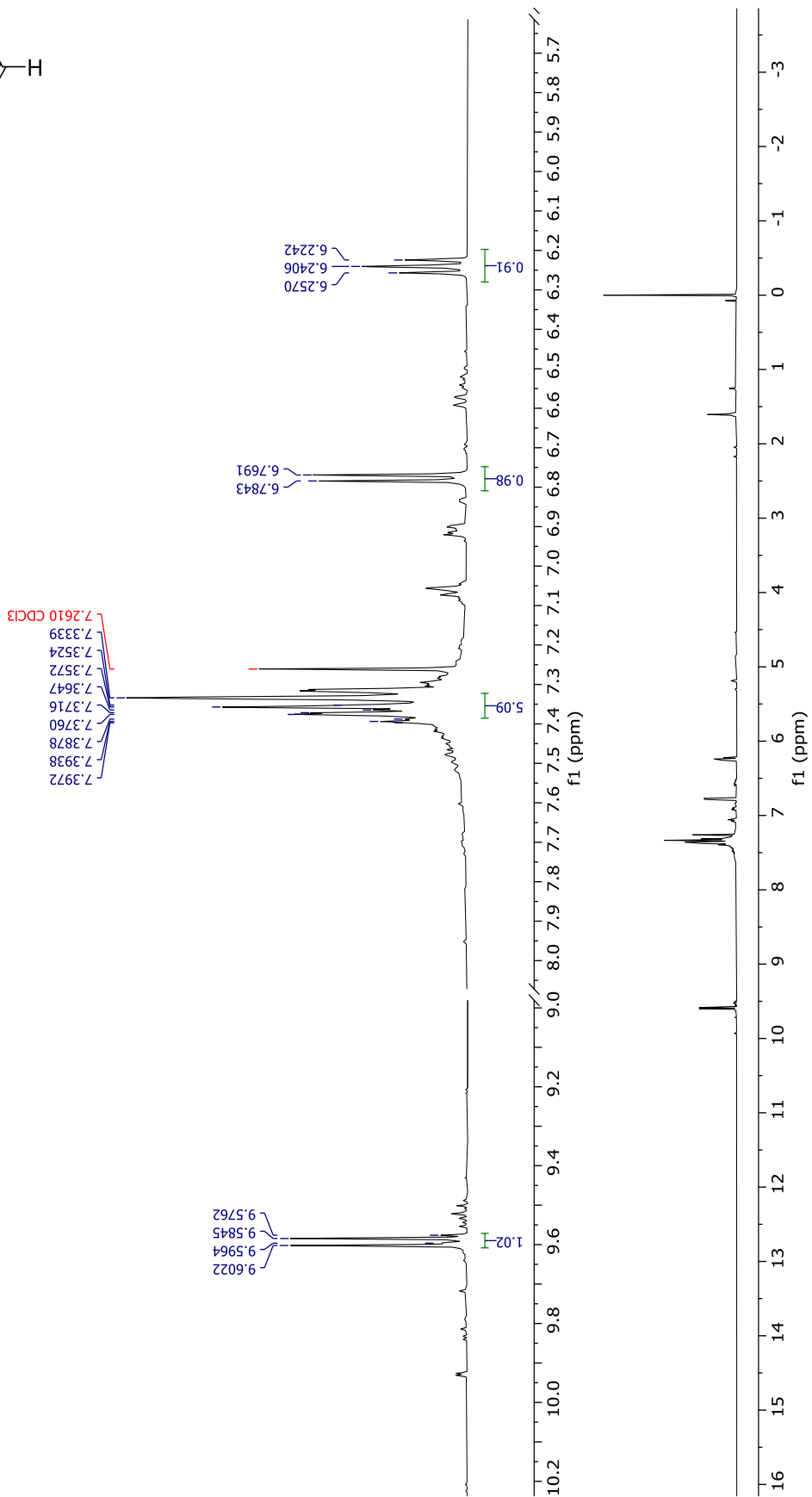
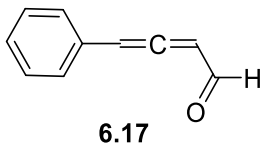


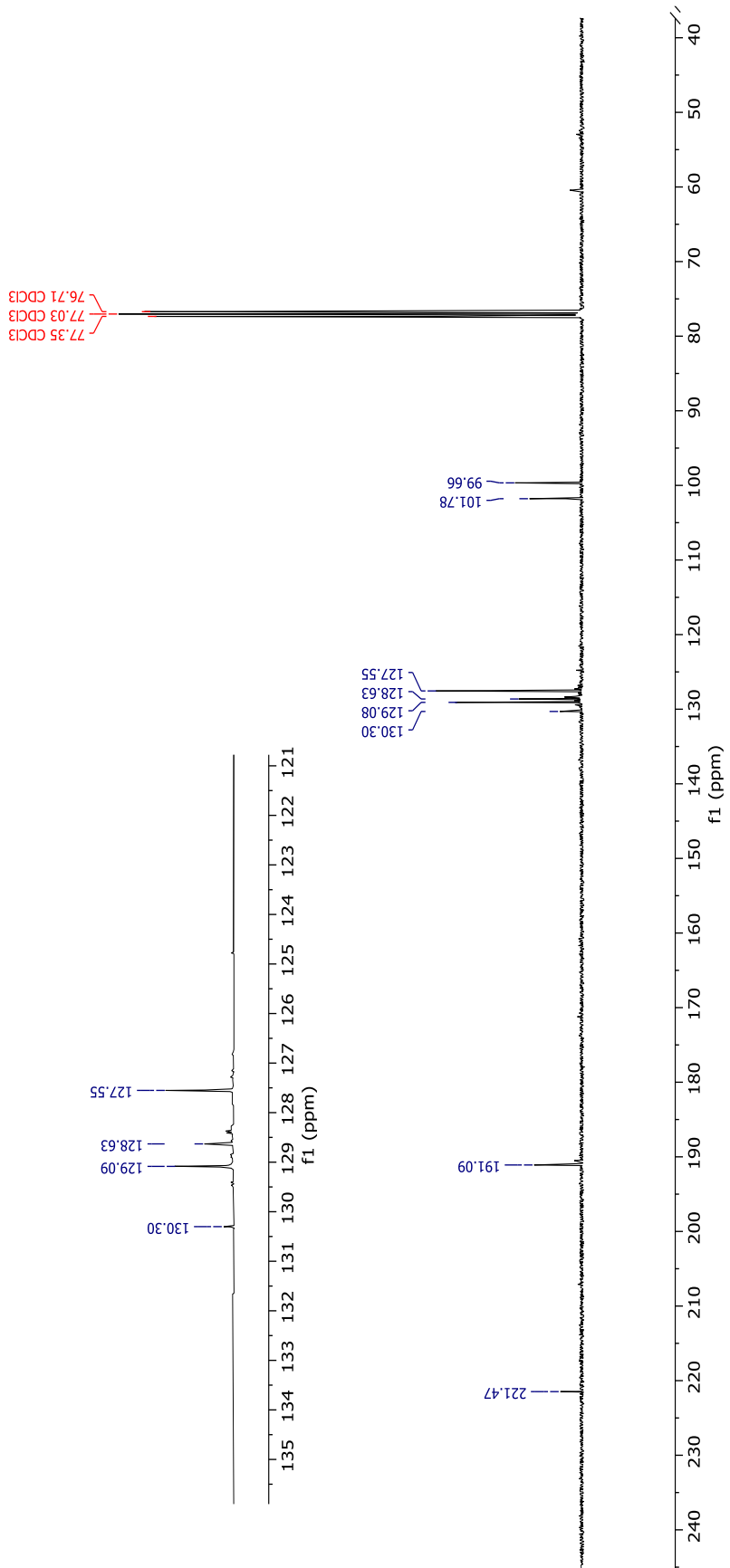
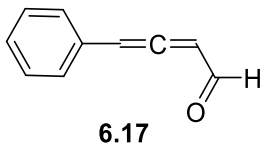


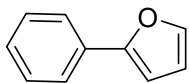


6.16

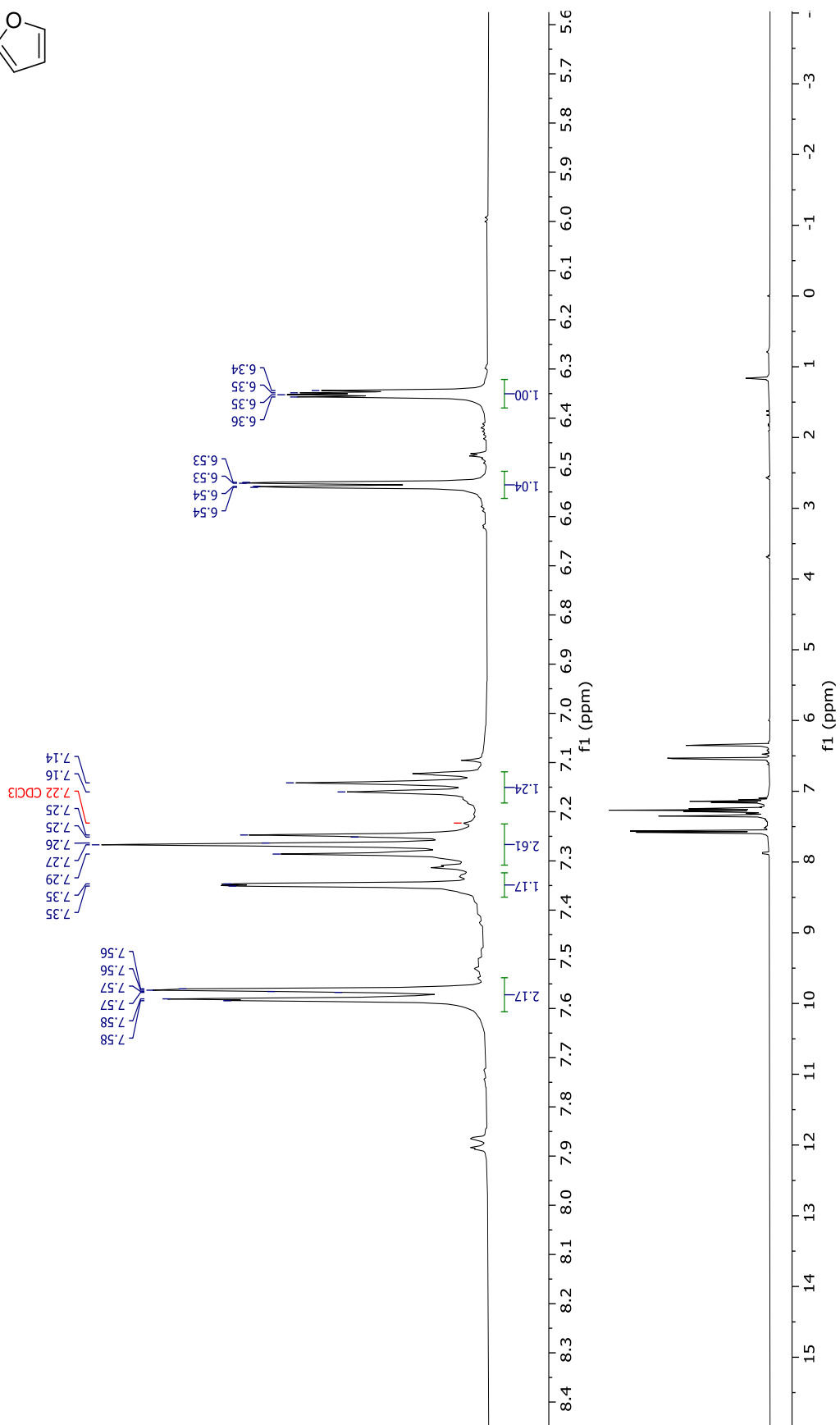


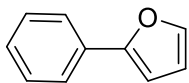




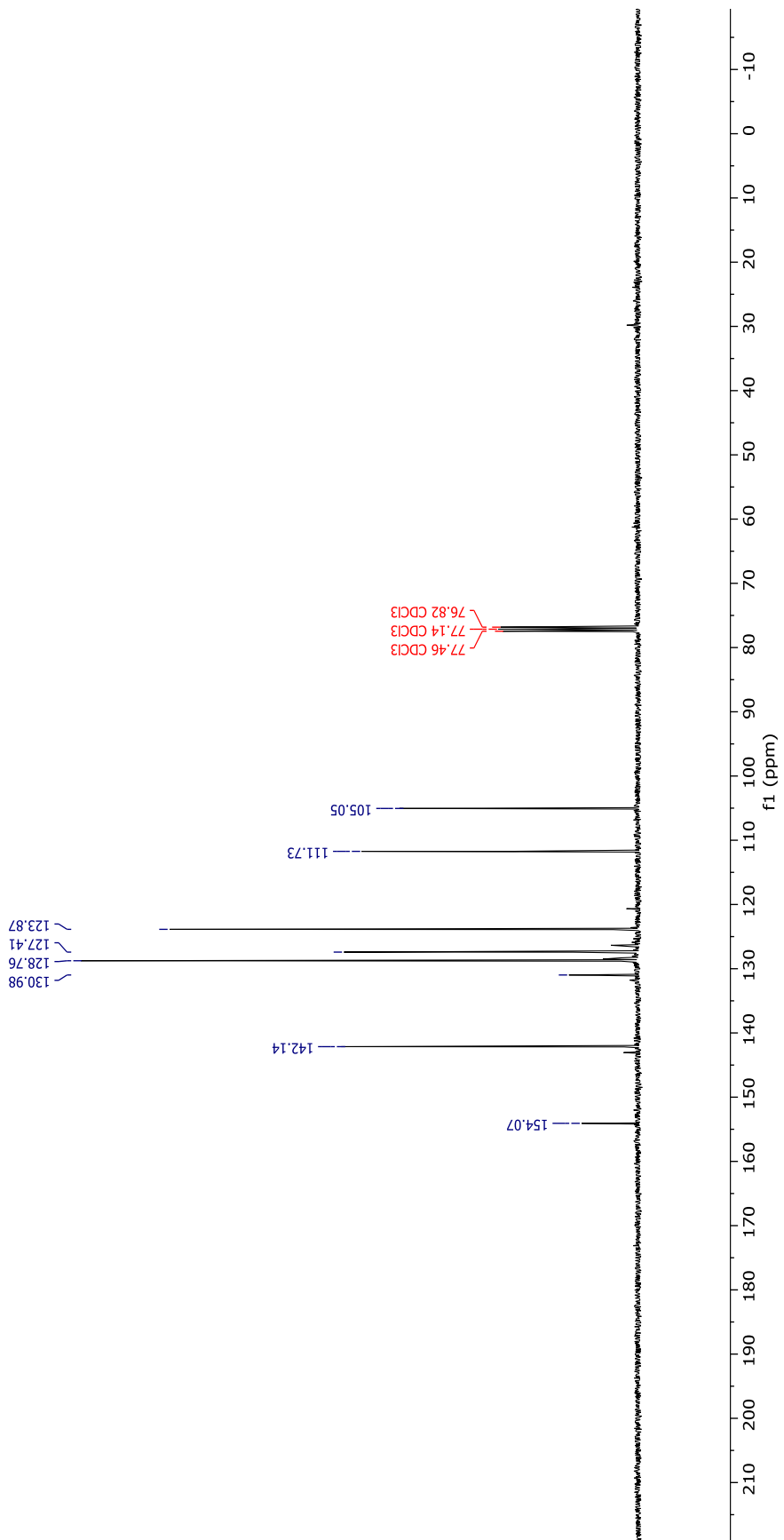


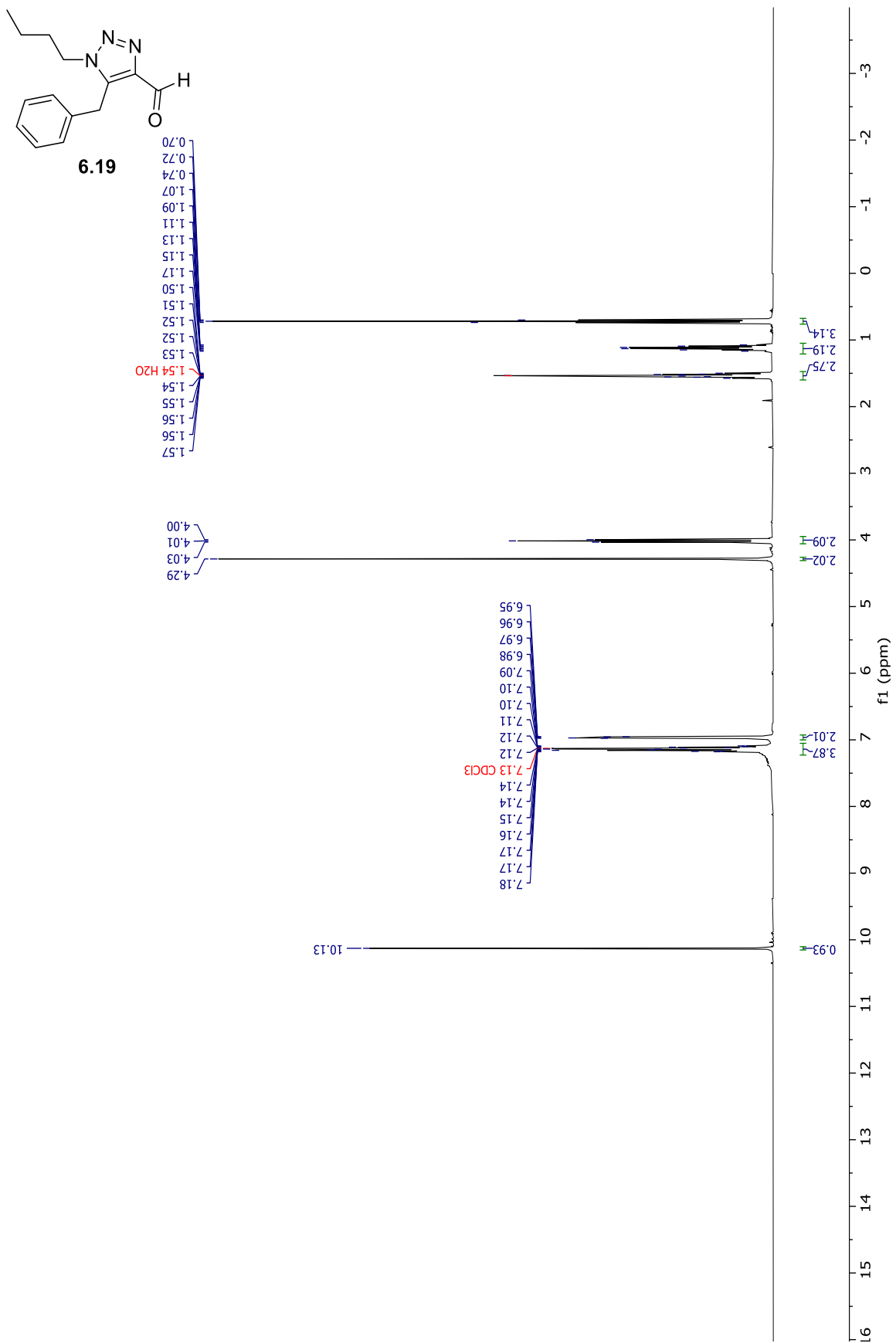
6.18

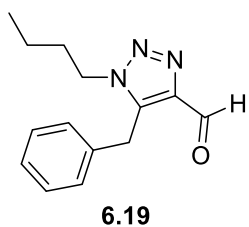




6.18

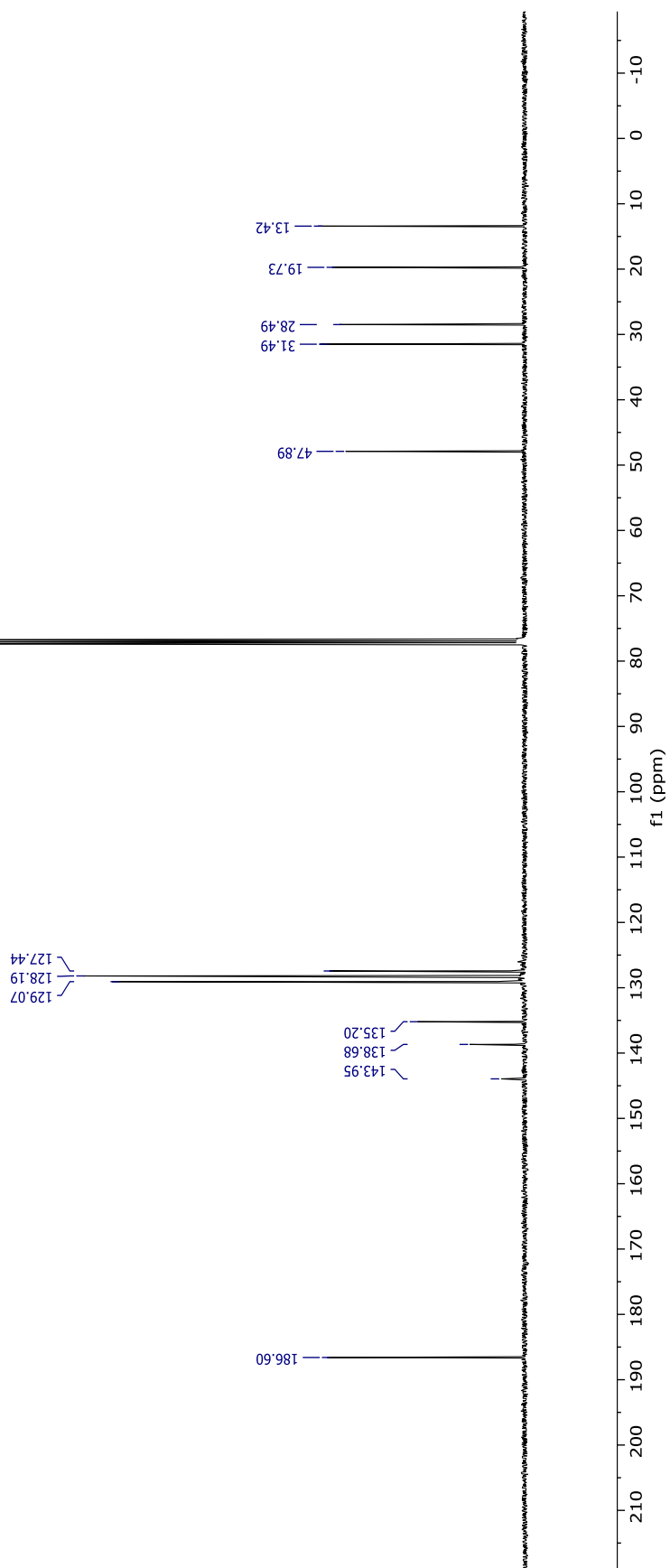


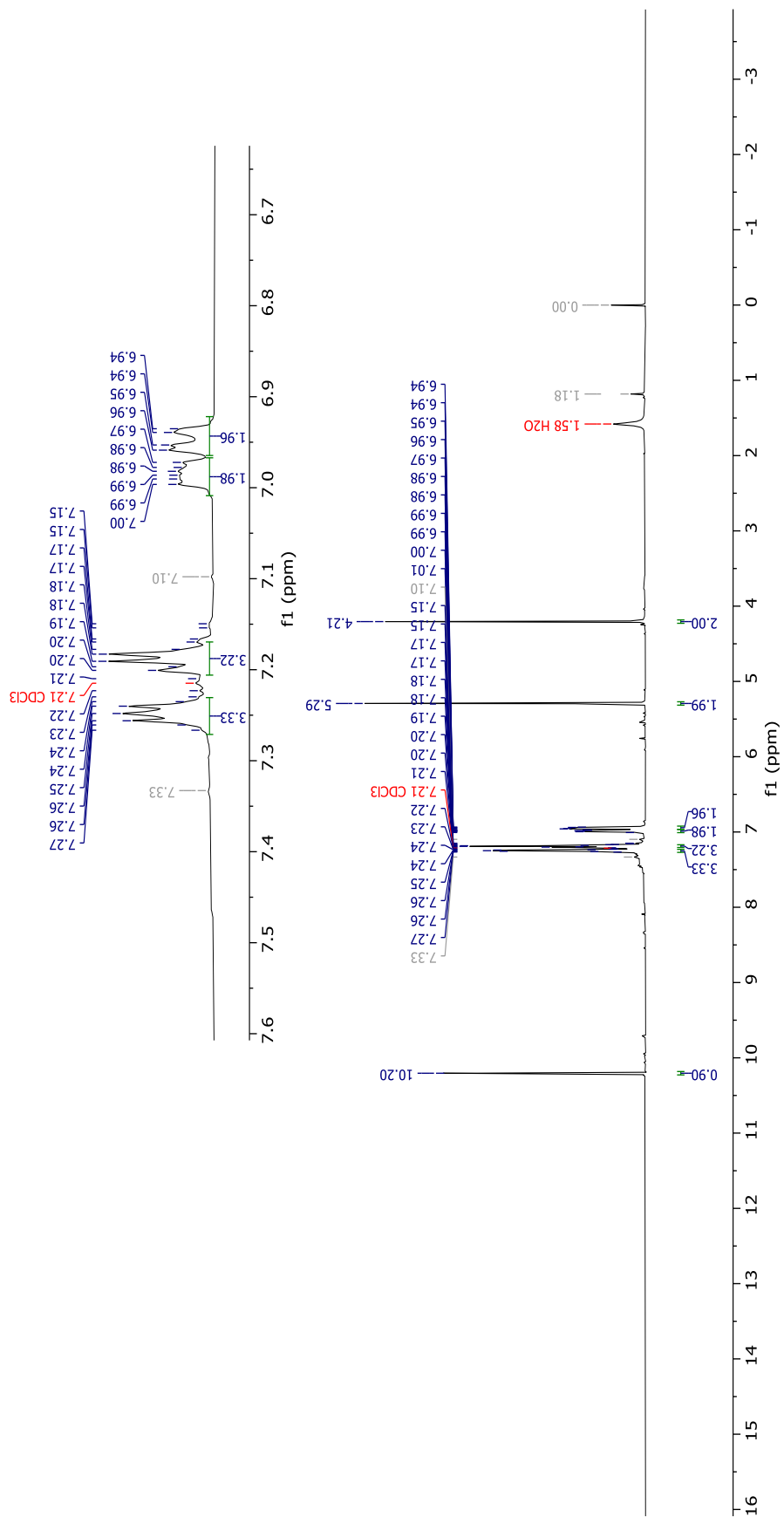
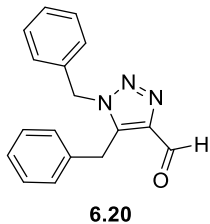


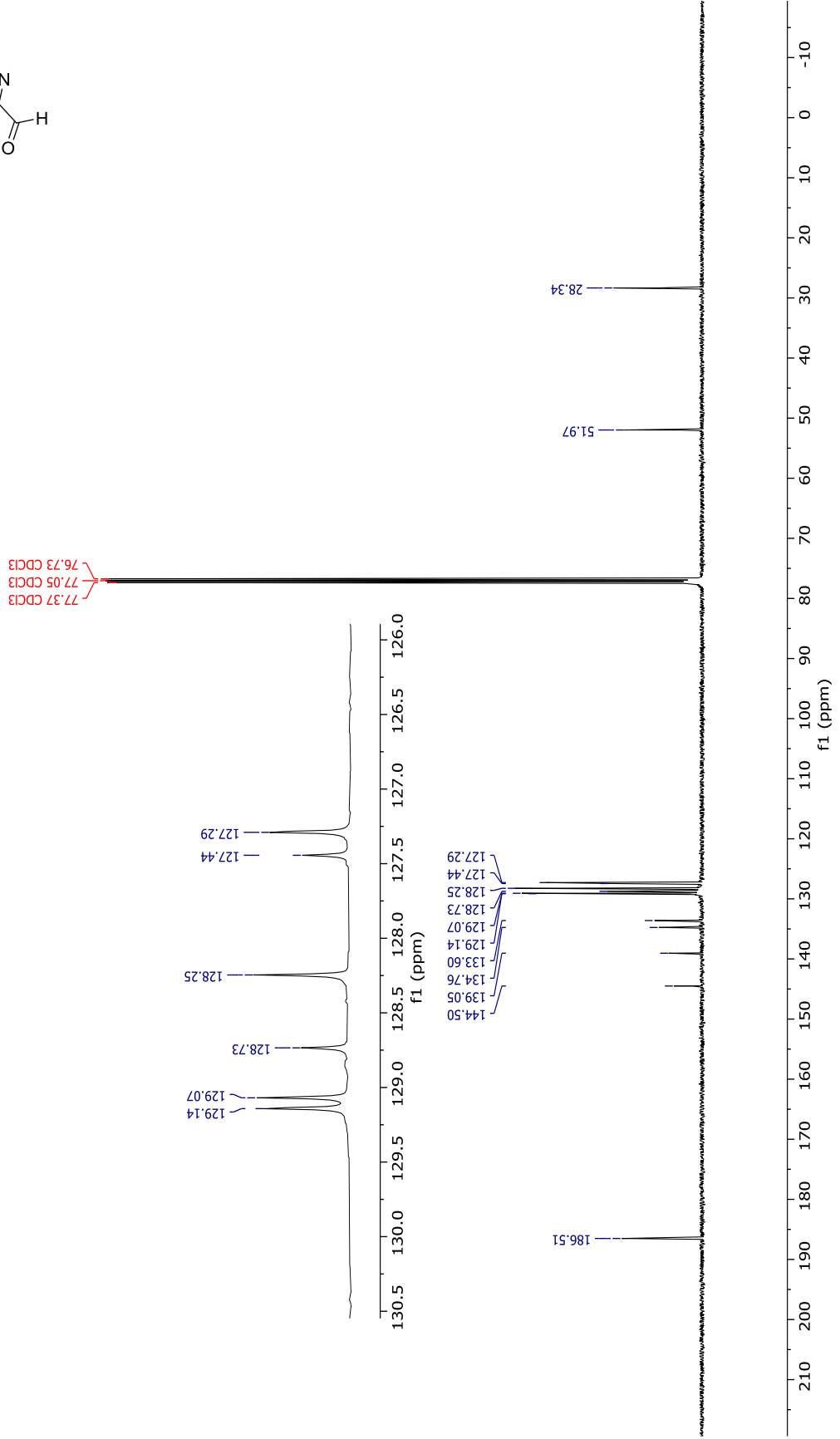
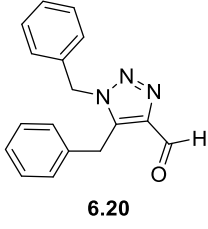


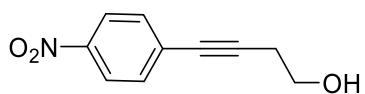
6.19

76.74 CDCl₃
77.05 CDCl₃
77.37 CDCl₃

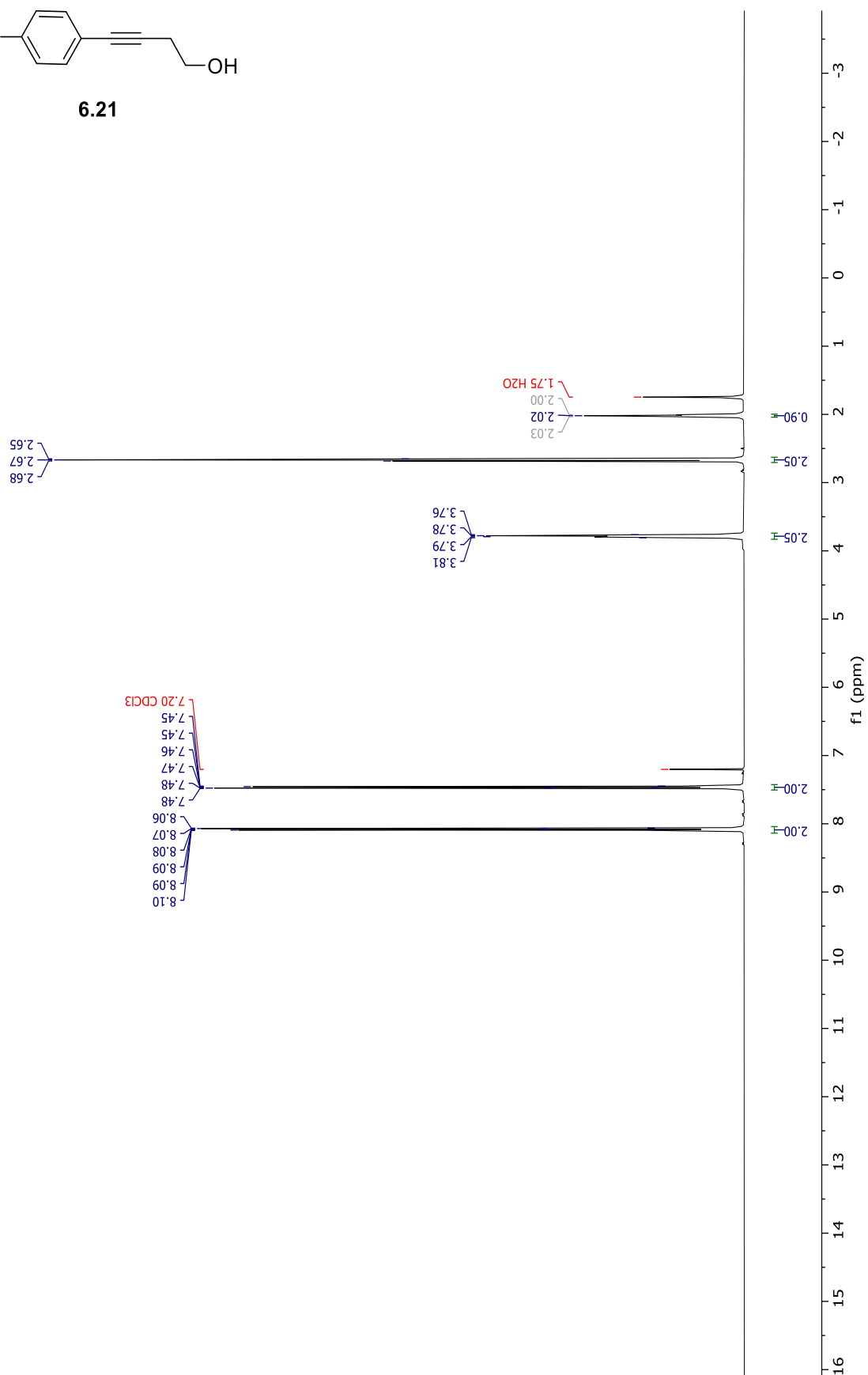


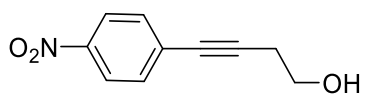




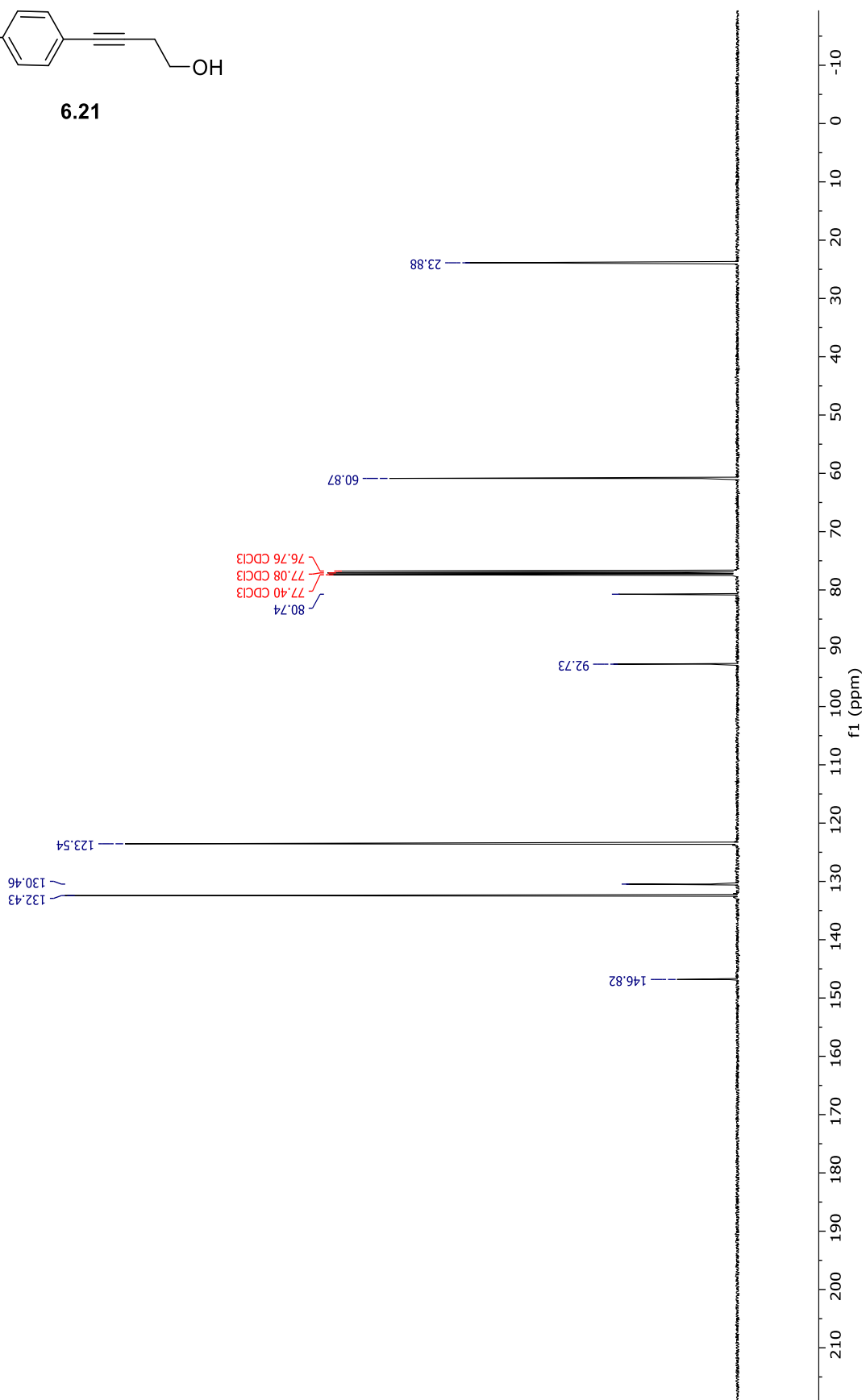


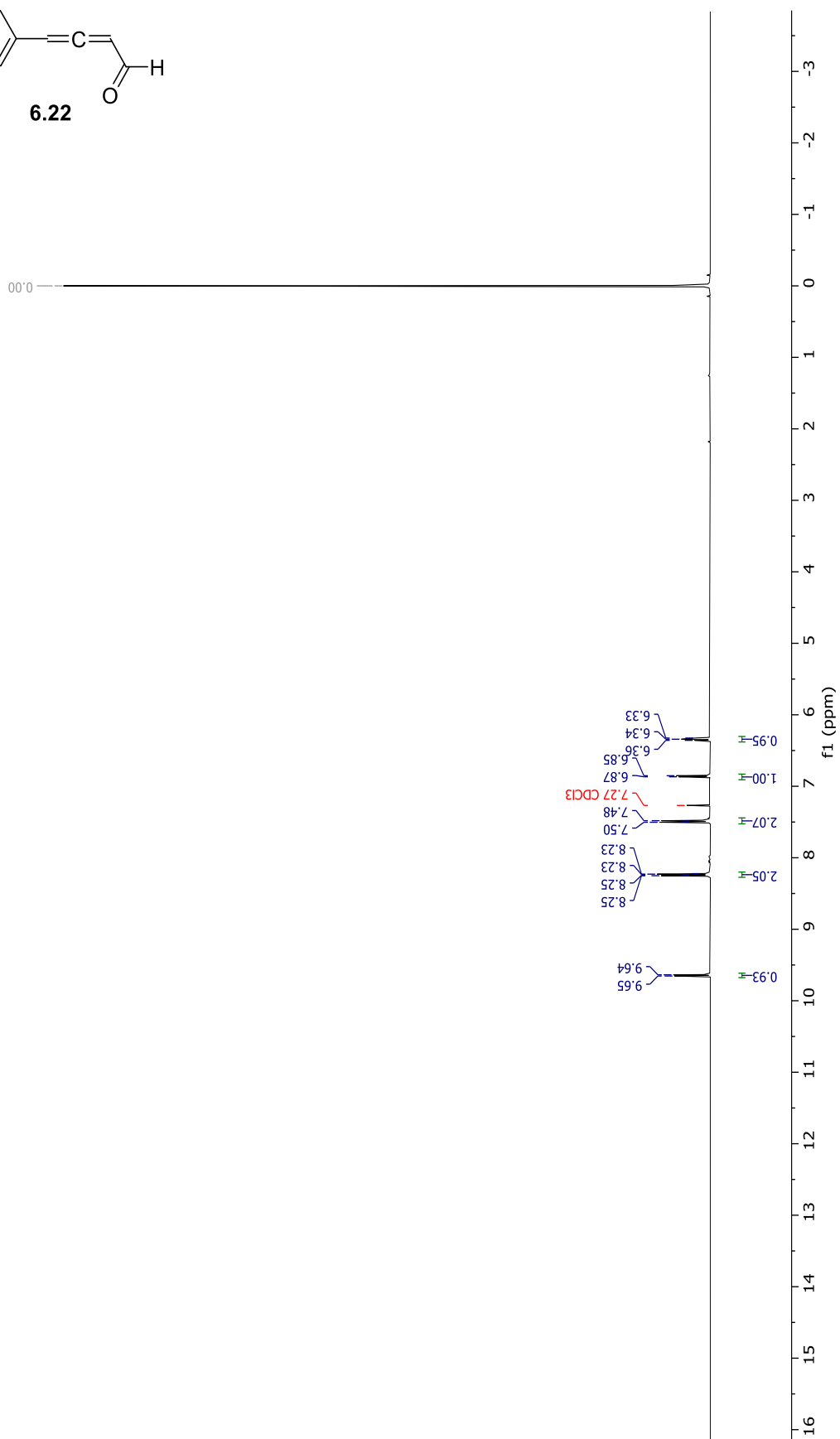
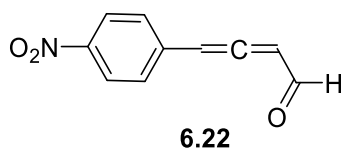
6.21

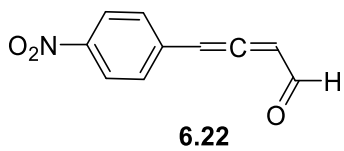




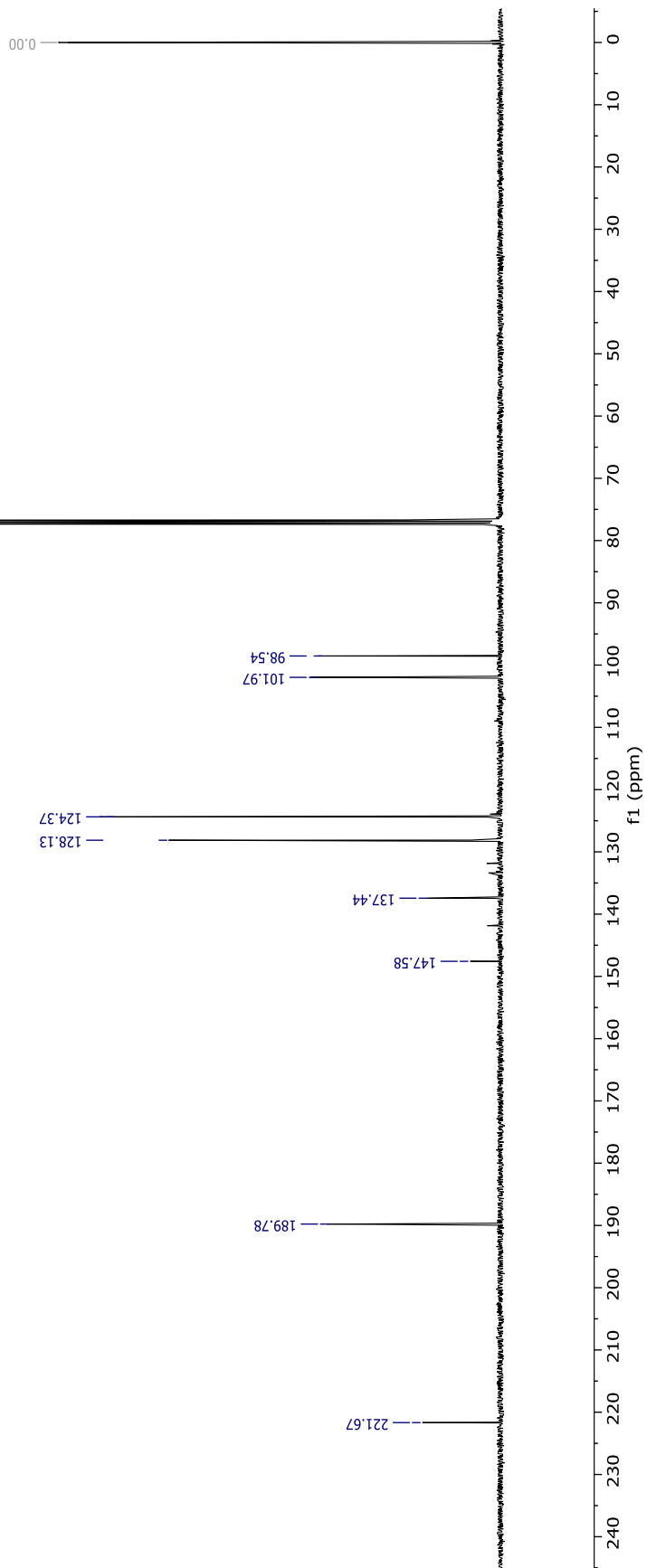
6.21

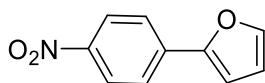






76.71 CDCl₃
77.03 CDCl₃
77.35 CDCl₃

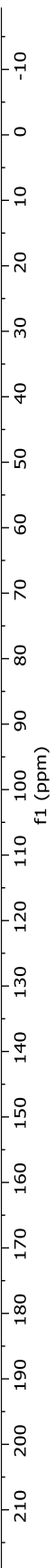


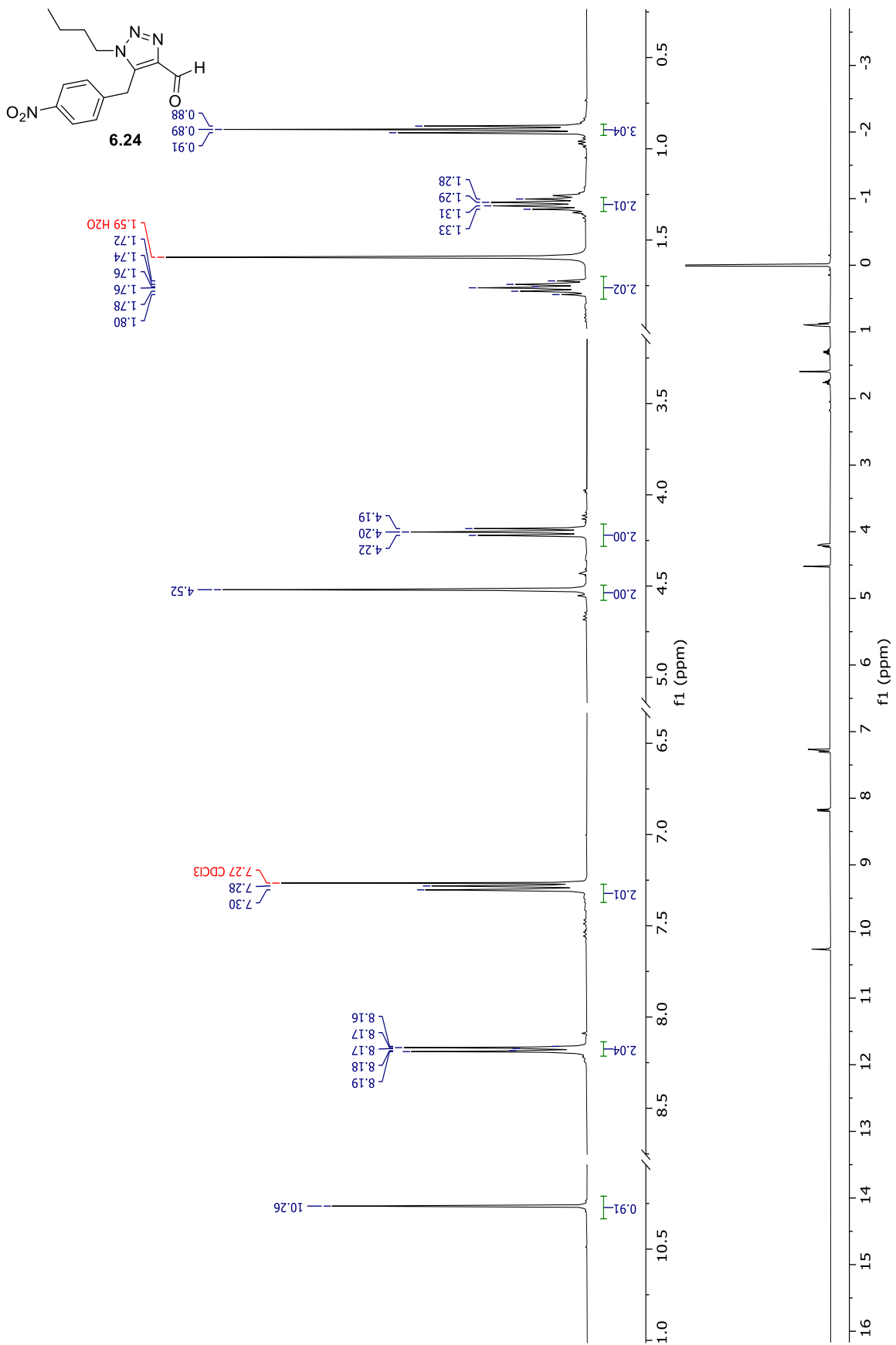


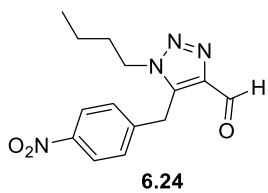
6.23

77.37 CDCl₃
77.05 CDCl₃
76.73 CDCl₃

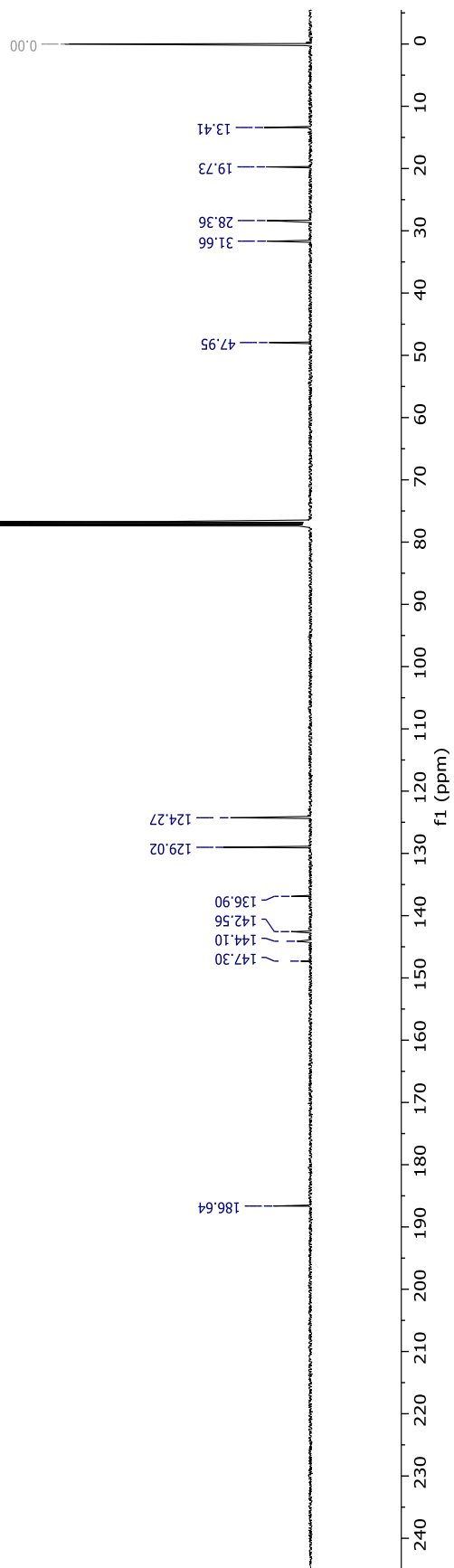
151.77
146.43
144.20
136.48
124.38
123.98
112.49
109.02

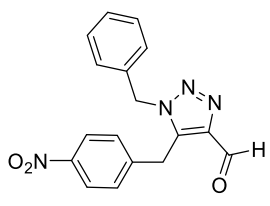




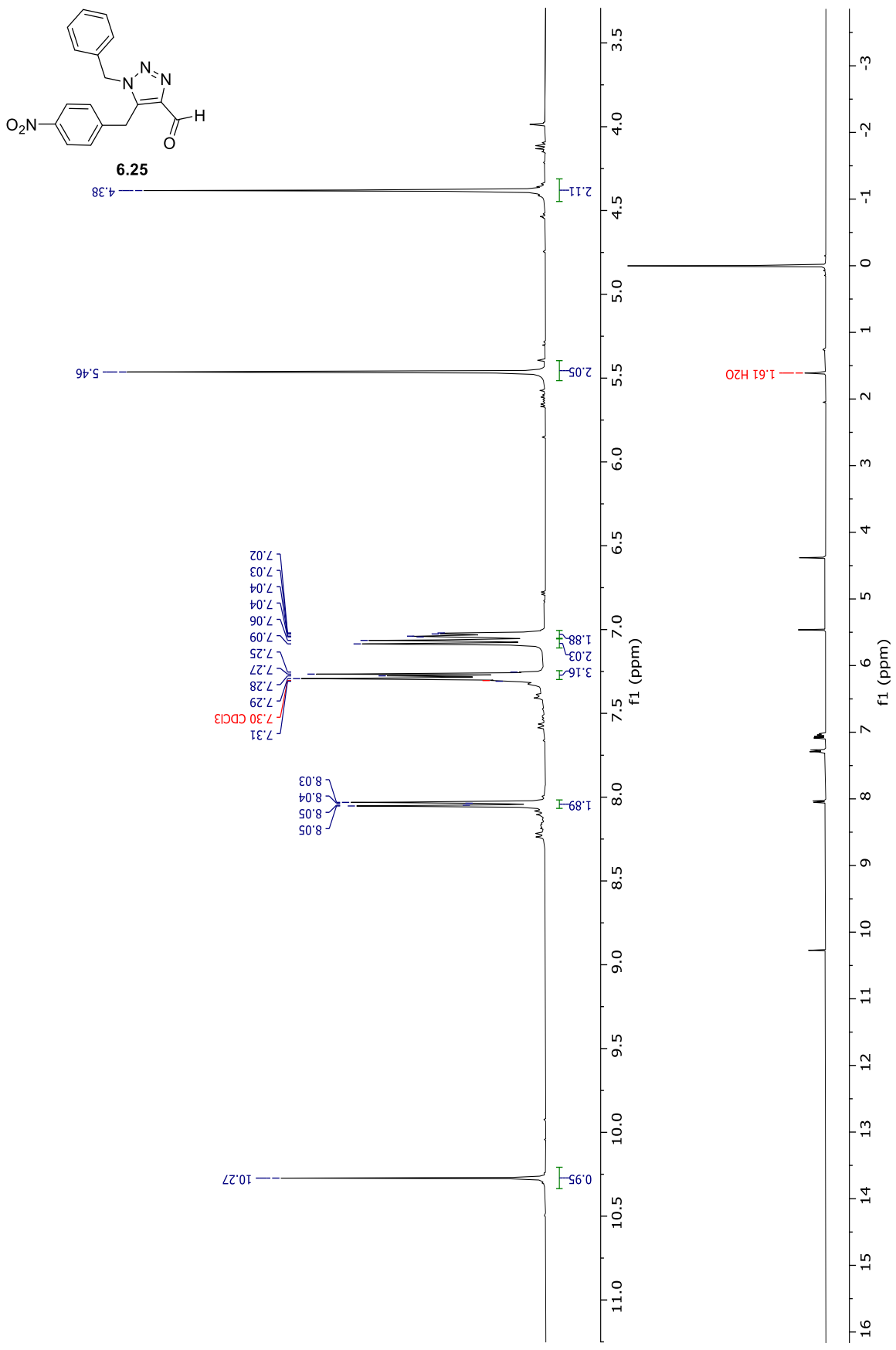


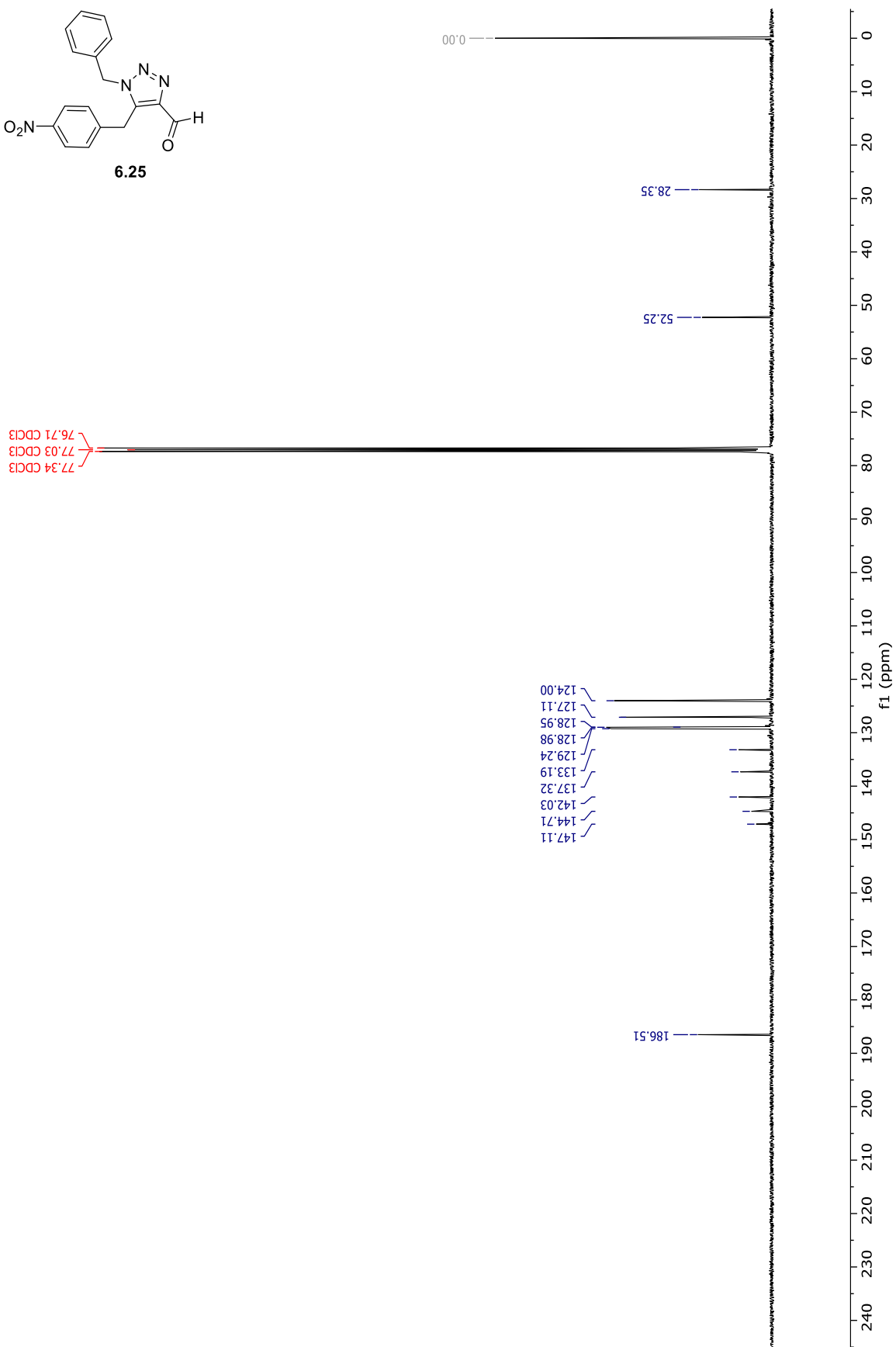
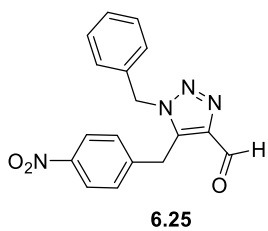
76.70 CDCl₃
77.02 CDCl₃
77.34 CDCl₃

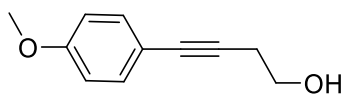




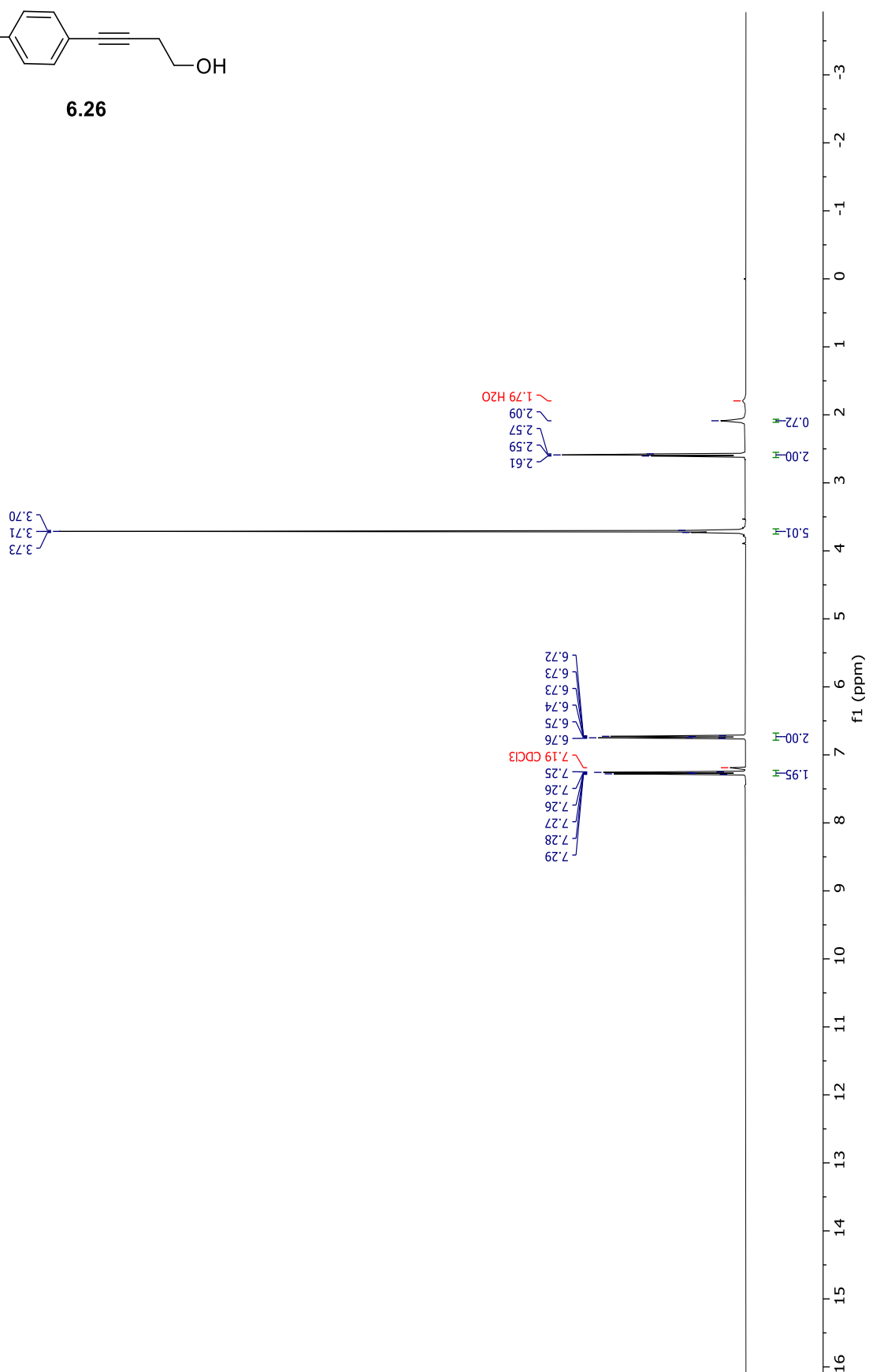
6.25

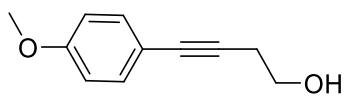




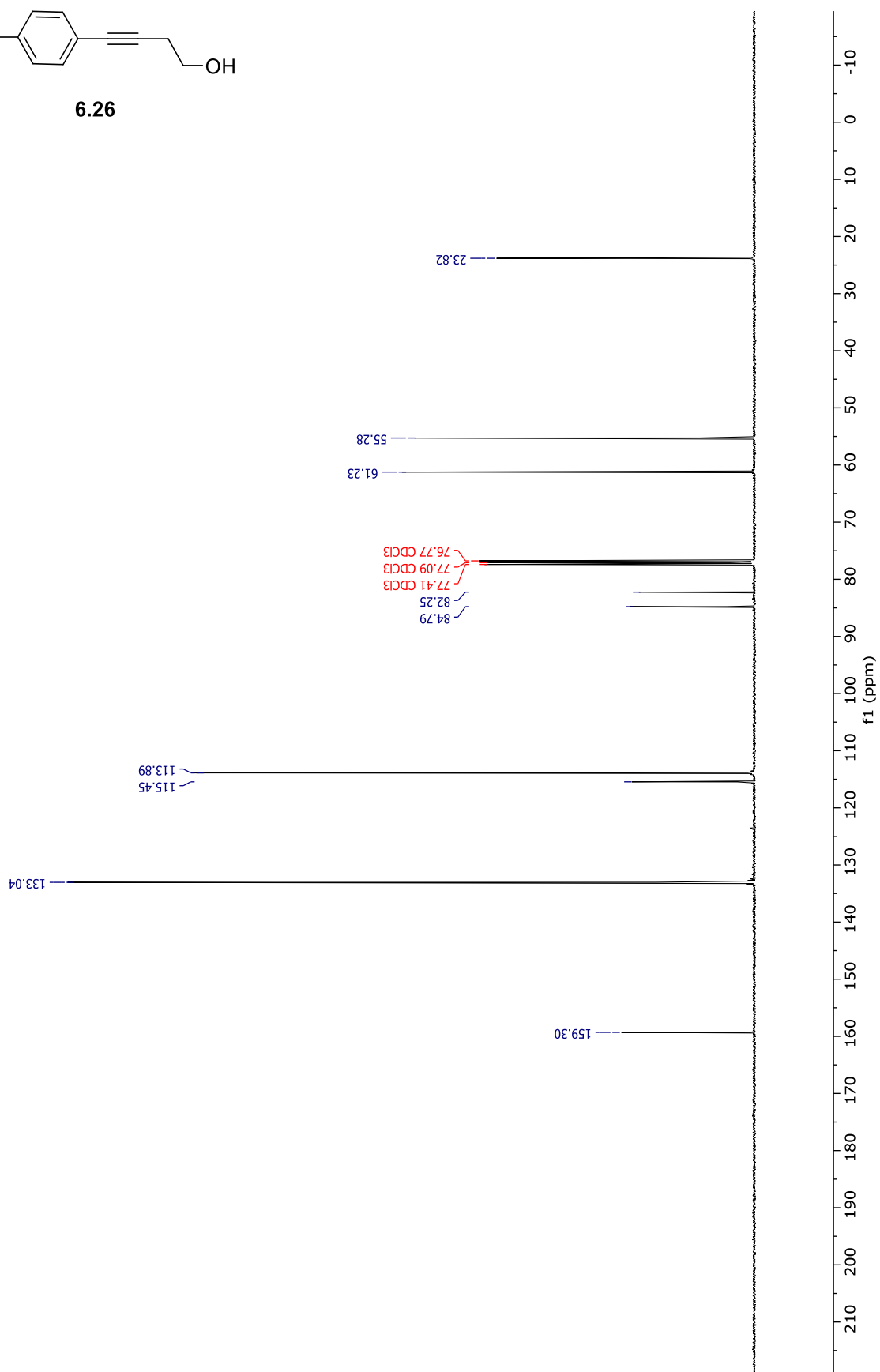


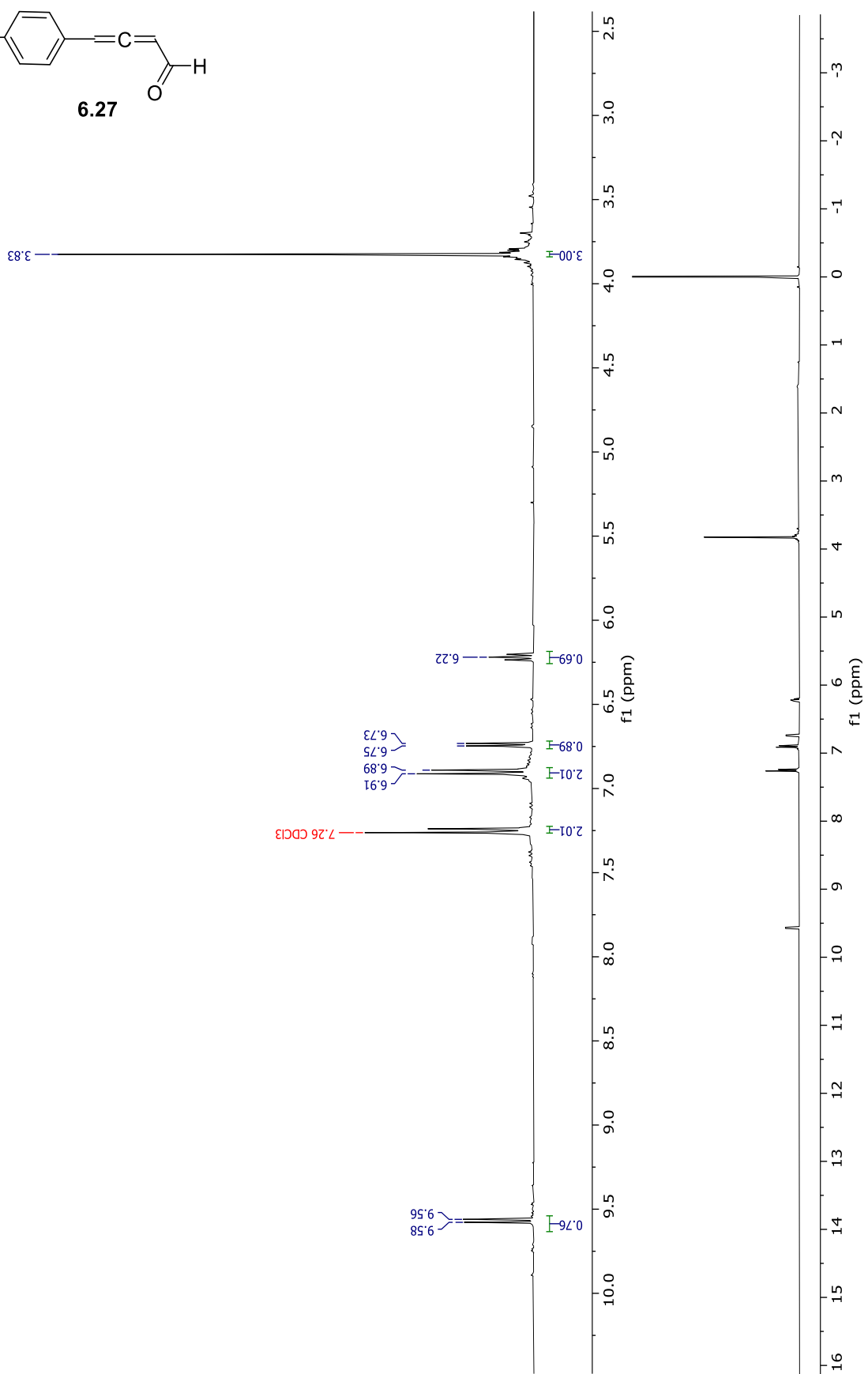
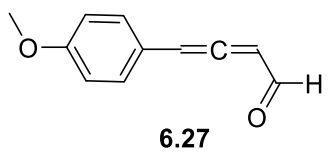
6.26

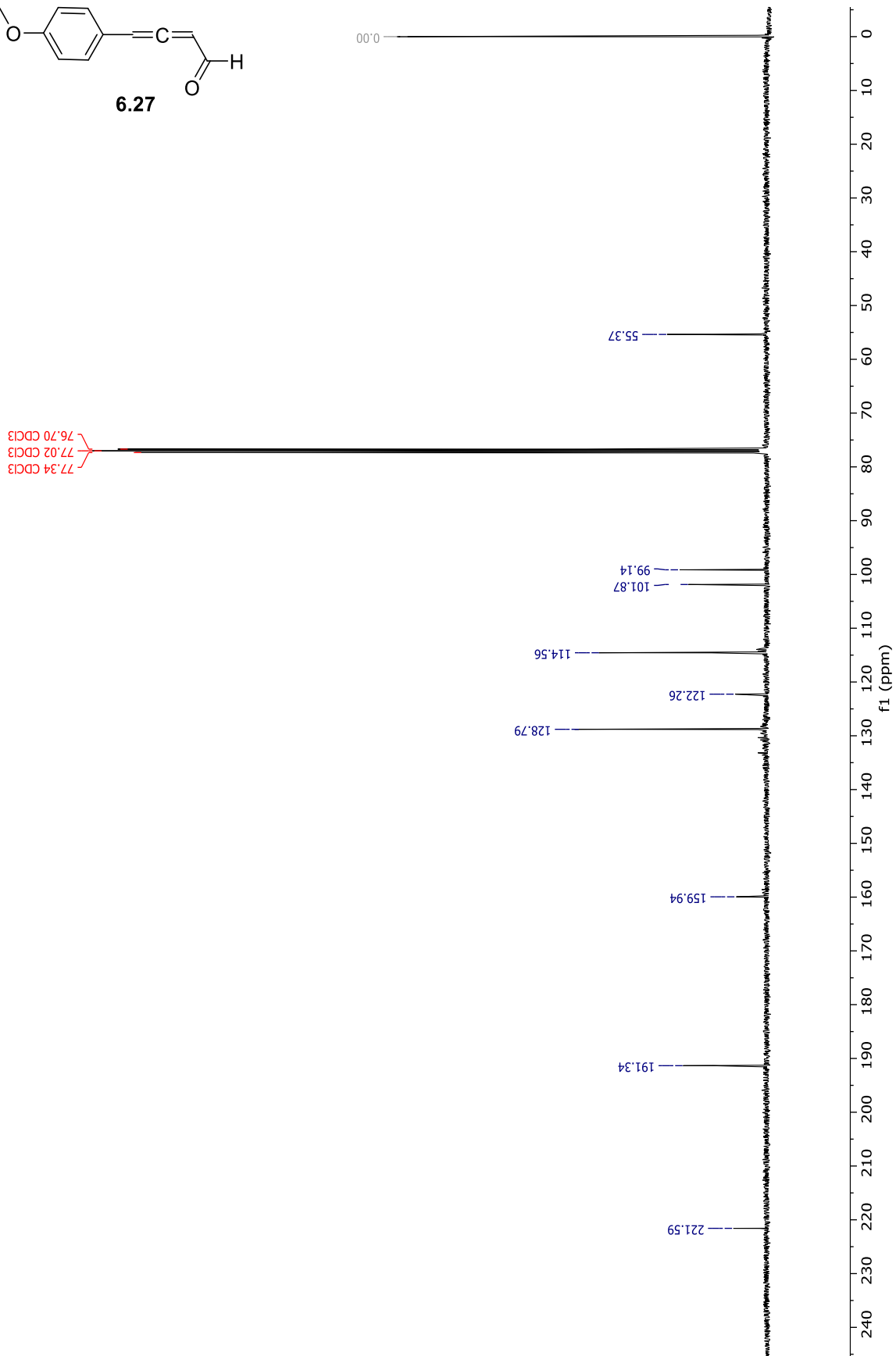
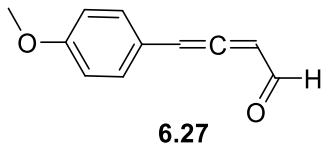


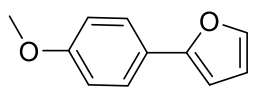


6.26

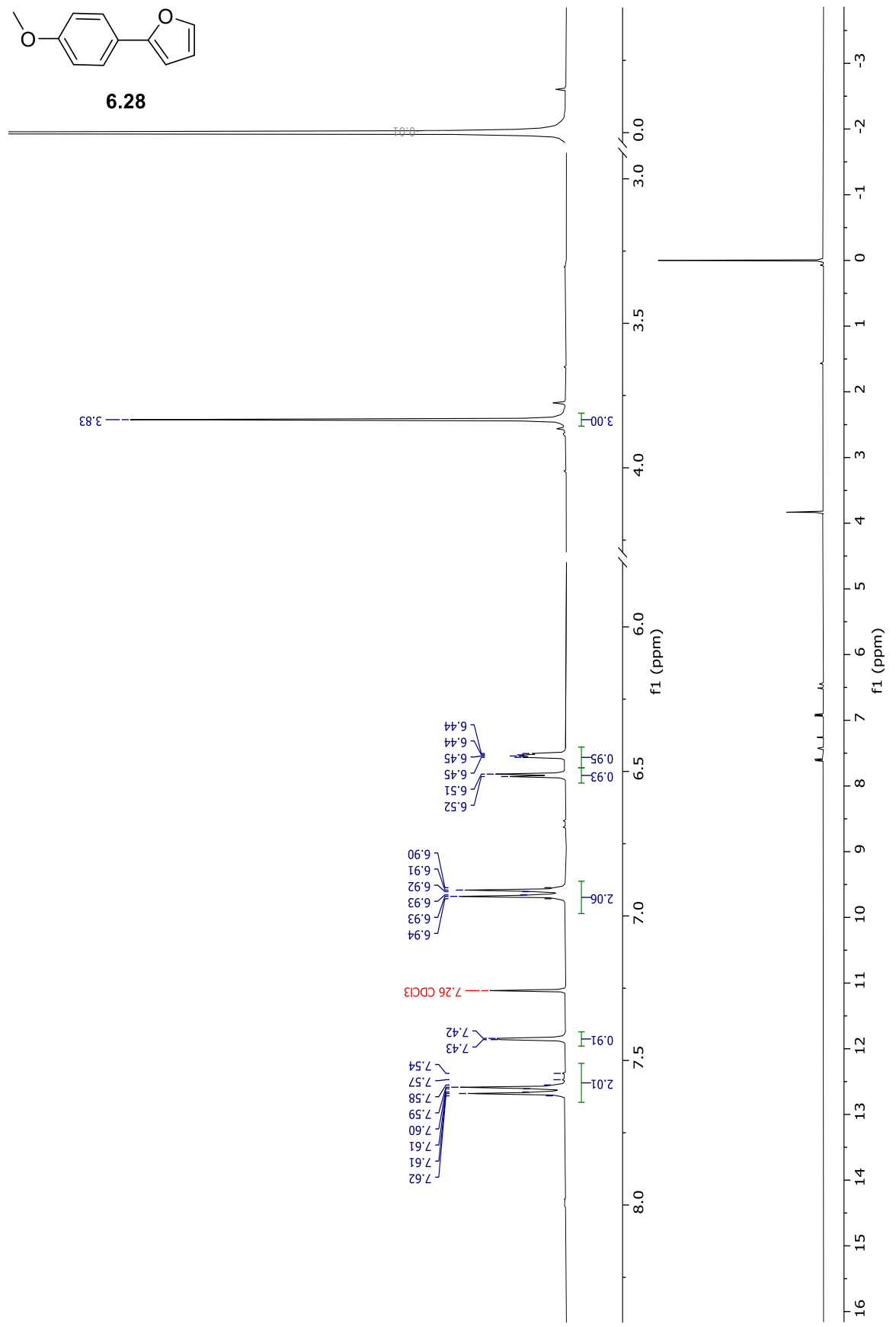


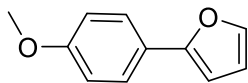




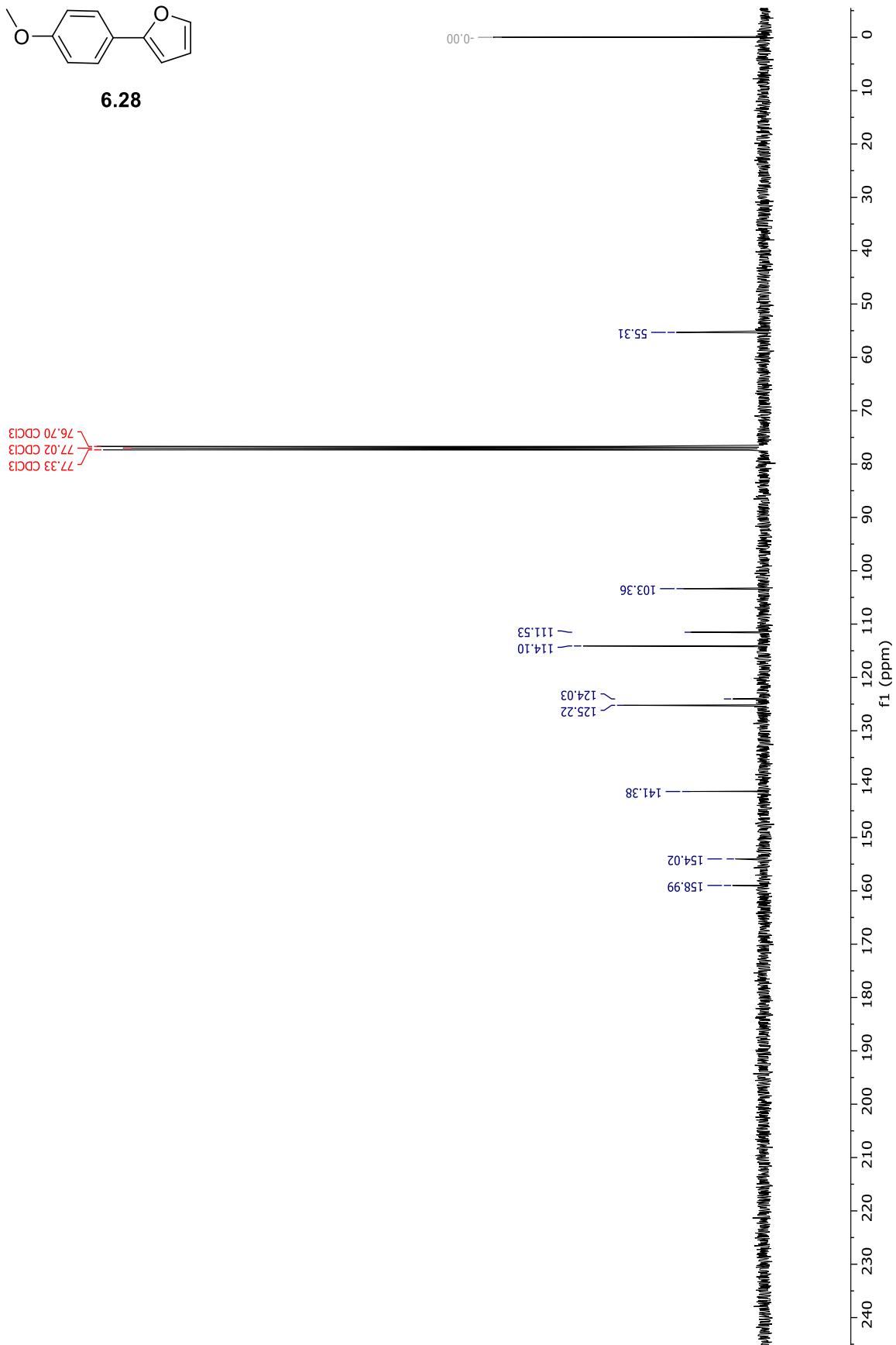


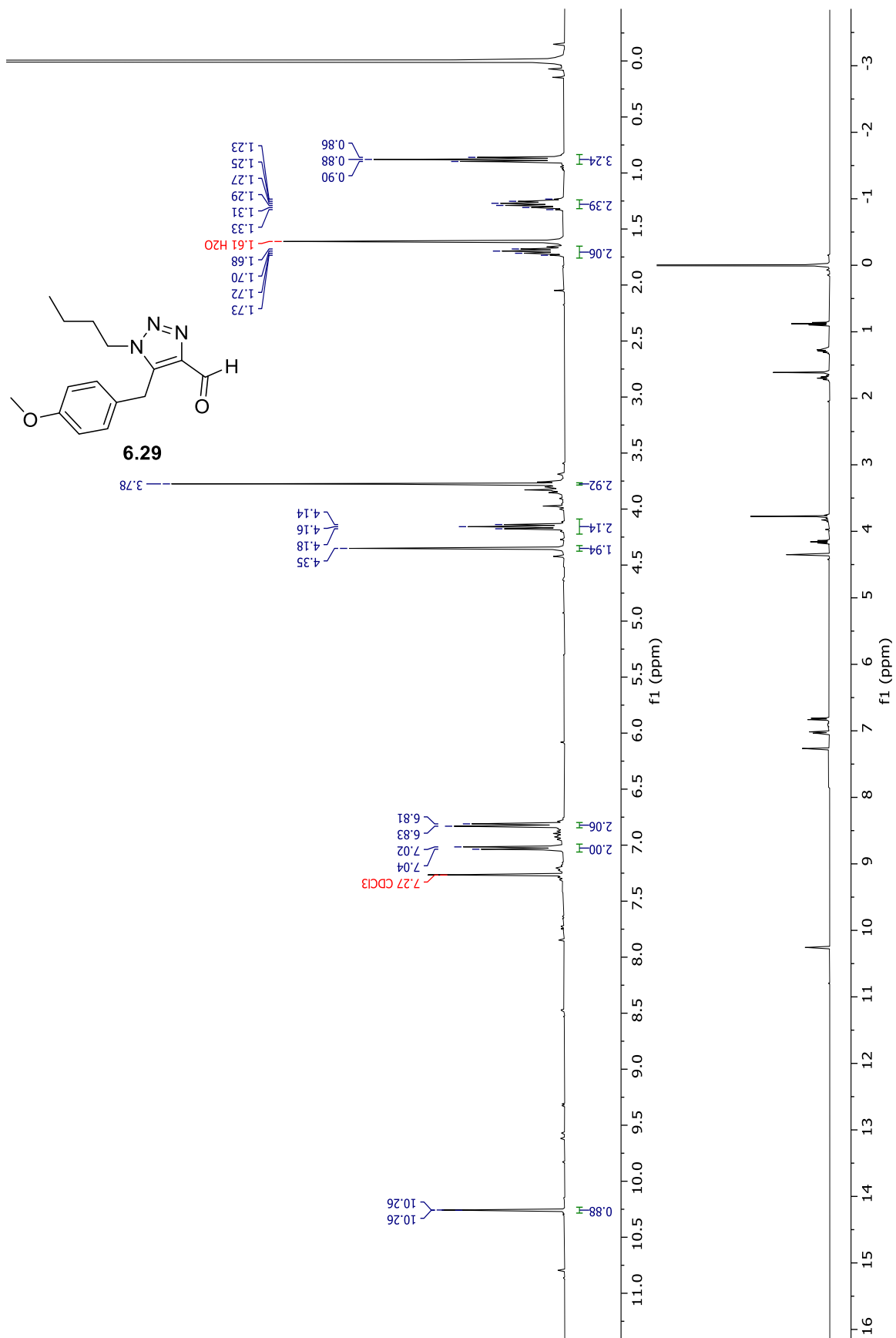
6.28

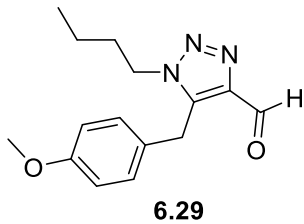




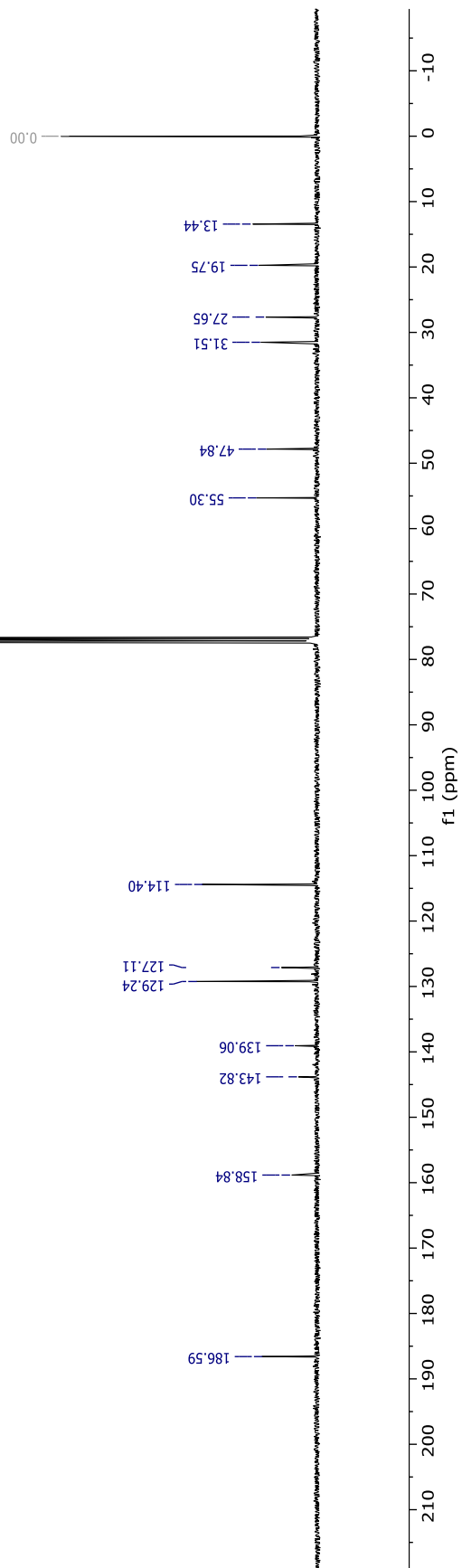
6.28

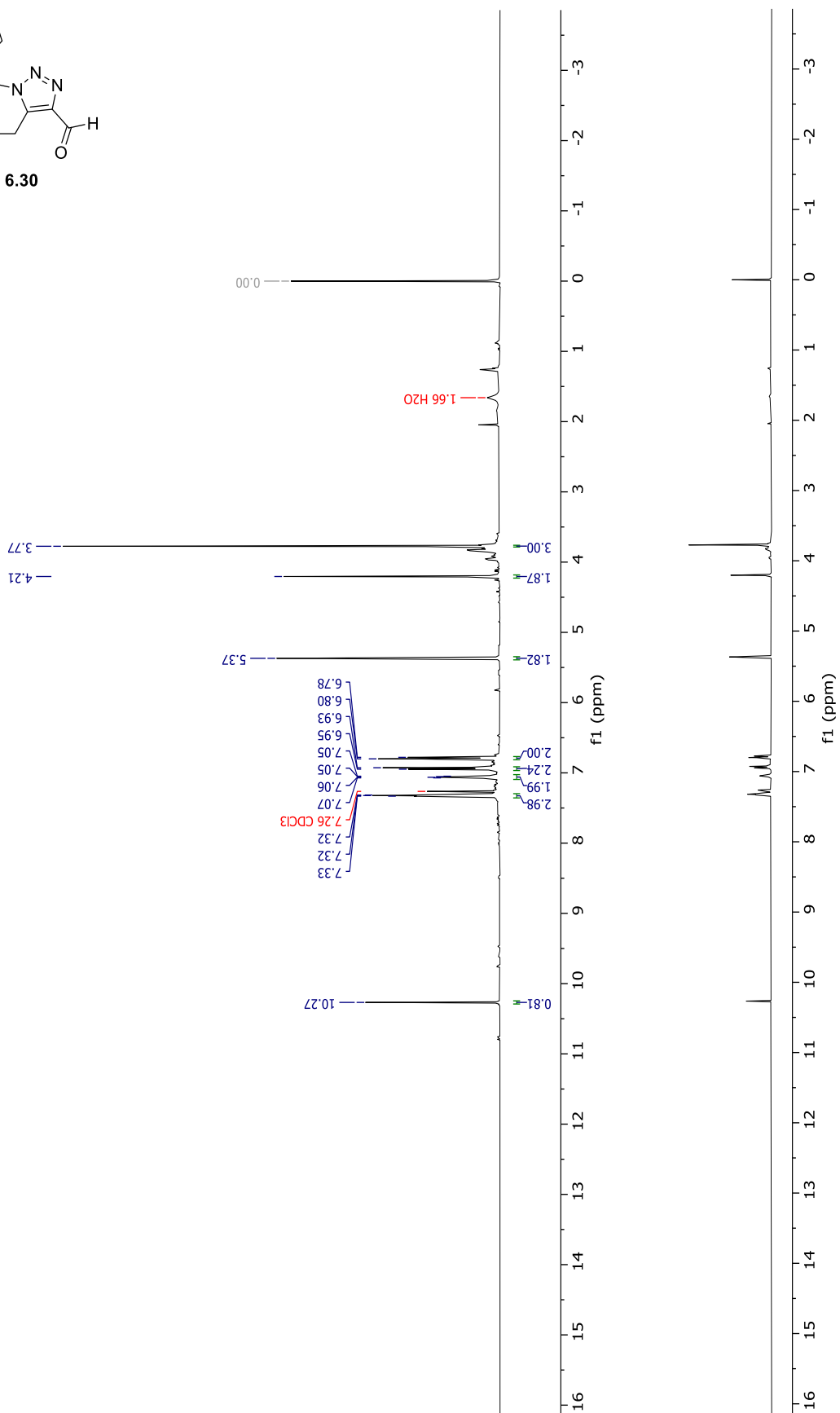
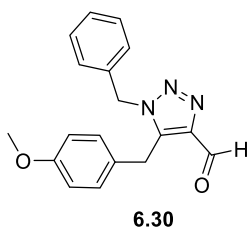


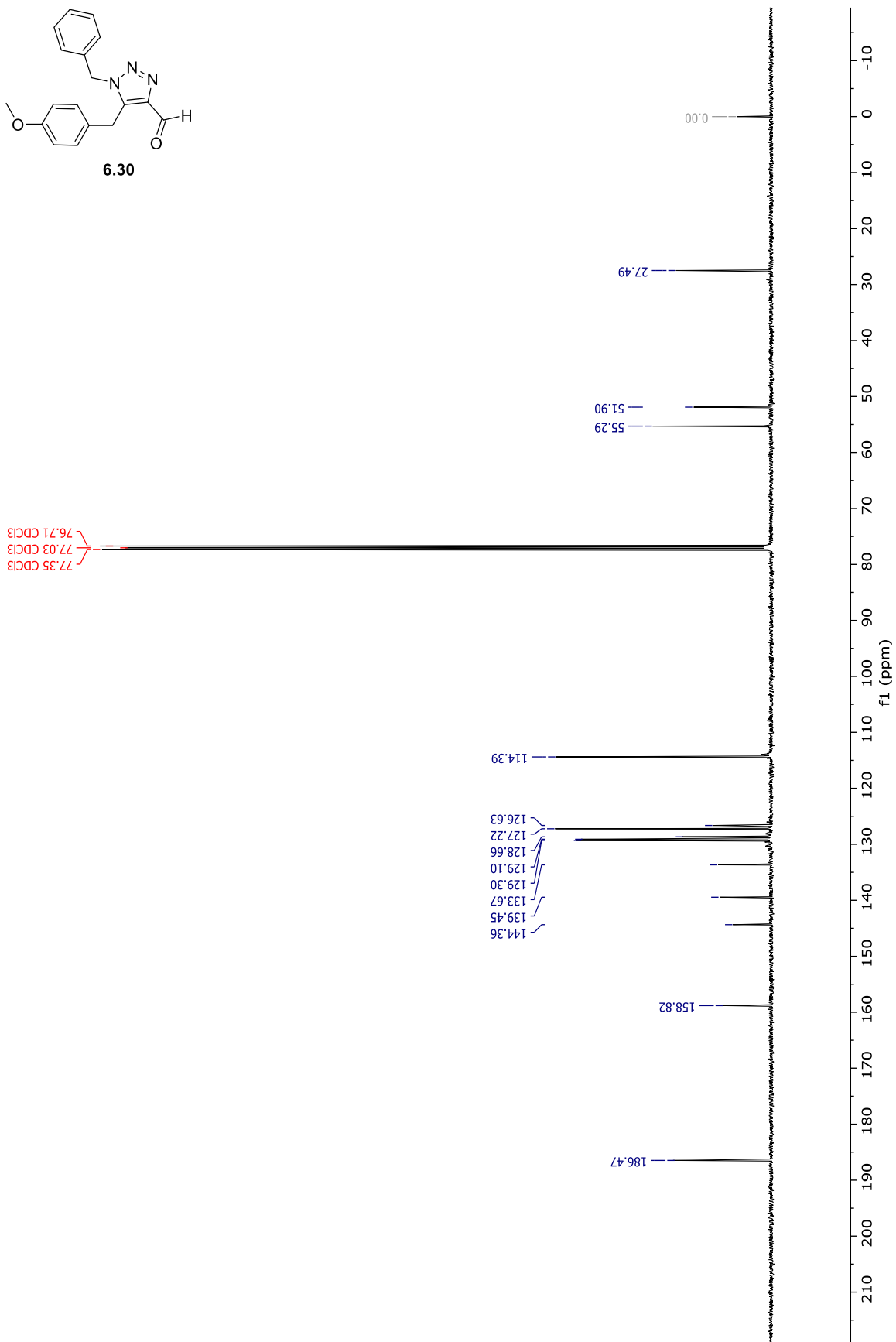
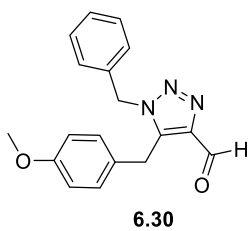


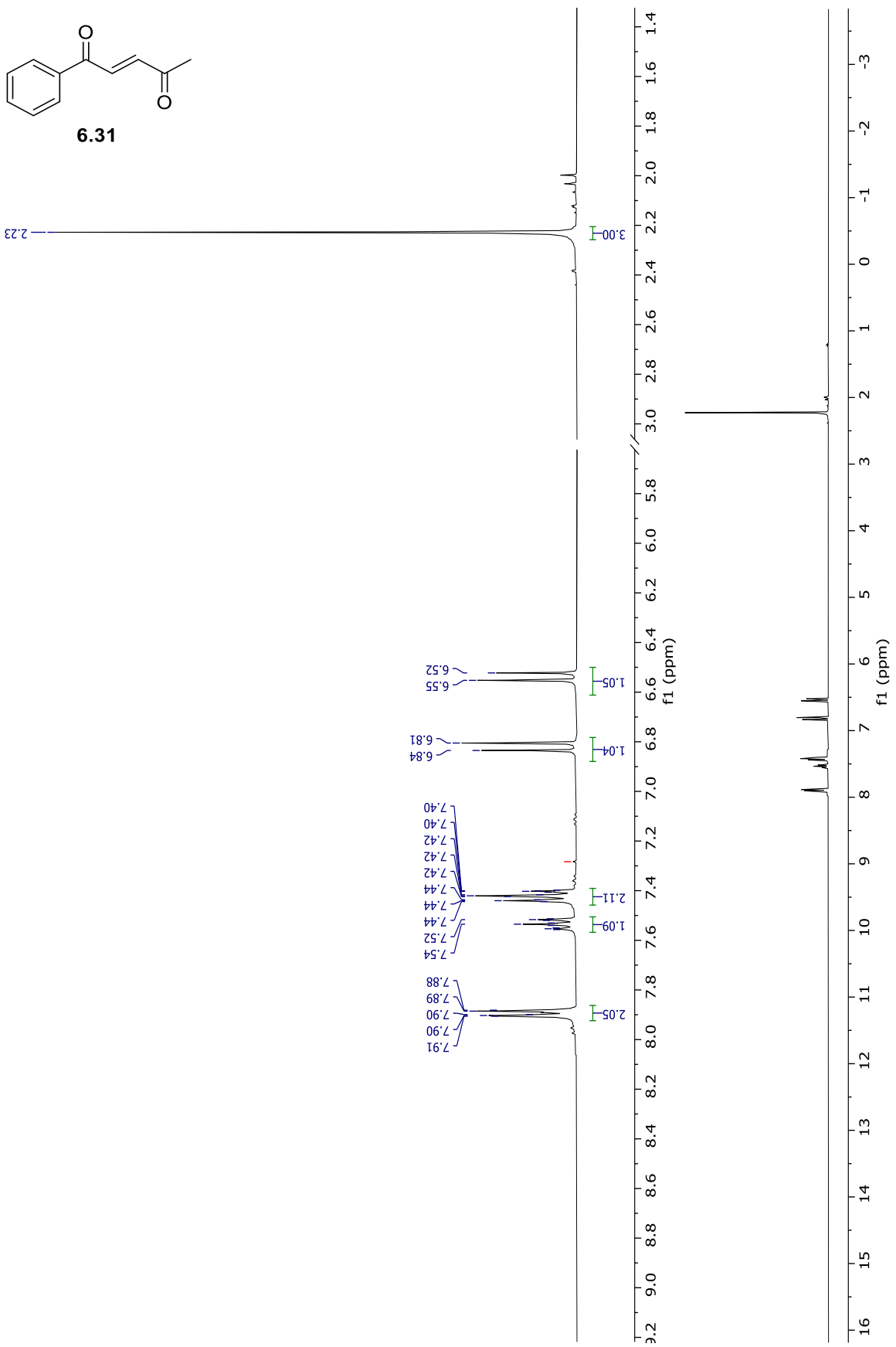
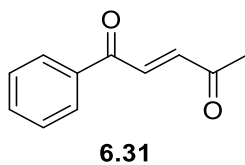


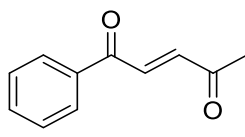
76.70 CDCl₃
77.02 CDCl₃
77.34 CDCl₃











6.31

